ICES COOPERATIVE RESEARCH REPORT

RAPPORT DES RECHERCHES COLLECTIVES

NO. 257

Proceedings of the Baltic Marine Science Conference

Rønne, Denmark, 22–26 October 1996

Edited by

Hans Dahlin
SMHI
SE-601 76 Norrköping
Sweden

Bernt Dybern
Institute of Marine Research
Box 4
SE-453 21 Lysekil
Sweden

and

Siân Petersson
EuroGOOS Office
SMHI
SE-601 76 Norrköping
Sweden

International Council for the Exploration of the Sea
Conseil International pour l'Exploration de la Mer

Palægade 2–4   DK-1261 Copenhagen K   Denmark

April 2003

Proceedings of the Baltic Marine Science Conference

Contents

Foreword

When ICES agreed to publish this collection of papers from the 1996 Baltic Marine Science Conference it had just completed devising a new structure for its Science Committees. This structure included an ecosystem-based group, the Baltic Committee, which reflected the strong interest of ICES in supporting the community of Baltic scientists, as well as its recognition that the Baltic would provide a valuable test bed for its ambition of developing ways to manage ecosystems in an integrated way. This ambition is still cherished and is manifested now, not only in a thriving Baltic Committee, but also through its active support, in its Secretariat, of the Project Office of the World Bank's GEF "Baltic Sea Regional Project (BSRP)" under the leadership of Jan Thulin. BSRP is an ambitious new project for managing the Baltic Sea ecosystem.

ICES recognised the importance of the Conference by sending the Chair of its Advisory Committee on the Marine Environment (Dr Katherine Richardson) to represent its interests there. Katherine contributed to the Conference by making a presentation on "The Baltic Sea – A Grand Challenge for ICES". In this she explained ICES interests from a Baltic perspective and how ICES supports Baltic science. In particular she noted that almost half of the Member Countries of ICES are in fact Baltic countries, which meant that ICES interests in the region had a very firm foundation. She also noted that Baltic science must be steered to address all the vital problems of the area in a multidisciplinary way, and that ICES is the organisation best suited to undertake the required steering.

This collection of papers represents an excellent cross-section of most of the current science issues pertaining to the Baltic. It is a document that will be put to good use within ICES and that will also be of great value to the whole Baltic community and anyone else interested in the scientific understanding of the Baltic Sea.

Harry Dooley

ICES Science Coordinator

1 February 2003

Preface

Marine Scientific activities in the Baltic Sea are carried out by a number of national and international organisations and groups as well as by individual researches belonging to different institutes, universities, etc. Some are concerned with applied science such as fish stock assessment and anthropogenic influence on the marine environment, others devote themselves to more basic hydrographical, marine geological or marine biological work.

It had long been a wish among many Baltic scientists to simplify and coordinate the activities of various groups to achieve better efficiency regarding work on the Baltic problems when the Baltic Marine Science Conference was arranged in Rønne on the Danish island of Bornholm on 22–26 October 1996. The organisers were the Baltic Marine Biologists (BMB), the Baltic Oceanographers (CBO), and a group consisting of Baltic Geologists. The Conference was also co-sponsored by the Baltic Marine Environment Protection Commission (HELCOM) and the International Council for the Exploration of the SEA (ICES).

The intention was to bring together people and groups working within different branches of Baltic marine research to facilitate contacts and discussions and to bring information on ongoing research and results of research projects. The outcome was a number of papers in different scientific fields, some of which are published in this volume, as well as results from fairly deep discussions on Baltic problems and the future organisation of Baltic Research. Some of the differences in opinion could not be bridged at once, but time has shown that Baltic cooperation is increasing, for example through a similar, well-visited conference in Stockholm in 2001 and the next conference planned in Helsinki in 2003. BMB and CBO also co-sponsored the Baltic Sea Science Conference in Rostock-Warnemünde in 1998.

The printing of this volume has been delayed for technical reasons. It has, however, been considered valuable to publish these papers which deal with current problems.

We thank the International Council for the Exploration of the Sea (ICES) for the valuable assistance in printing the volume.

Bernt Dybern   Hans Dahlin

For BMB   for CBO

International Steering Committee

Hans Dahlin, CBO, Chair
Ingemar Cato, BMG
Bernt Dybern, BMB
Hans Peter Hansen, CBO
Bodo v. Bodungen, CBO
Matti Perttilä, CBO
Sigurd Schultz, BMB
Serge Victorov, CBO
Erik Buch, CBO
HELCOM and ICES

Local Organising Committee

Erik Buch, Chair
Gunni Ærtebjerg
Birger Larsen
Jørn Bo Jensen
Karsten Bolding
Lars Hagerman
Lars Chresten Lund-Hansen

Statement from the Baltic Marine Science Conference

Rønne, Denmark, 22–26 October 1996

The Baltic Sea is an ecosystem with unique features and its ecological condition is of great importance for the surrounding human population. In the past years, several indications of improved environmental conditions in the Baltic Sea have been found, but the overall view on the system is that it is still severely threatened in many respects. If these threats are not met by proper management, serious environmental, economic and political problems and even conflicts may develop in the future.

Baltic marine scientists have a comprehensive knowledge and expertise in relevant research, monitoring and management programmes. The knowledge of the scientists has to be used more efficiently, and it is a challenge for both the scientists and the politicians to achieve this.

The Baltic Sea is recognised world-wide as the cradle of modern oceanography, and extraordinary test site where the implementation of measurement systems, new marine biological techniques, remotely sensed data, management processes and assessment of short– and long–term trends has led to a high degree of operationality.

Experiences gained during decades and the present socio-economic situation in Europe makes the Baltic marine scientists suggest a better usage of the multidisciplinary modern research results in the Baltic Sea Region than hitherto.

Statement discussed and adopted on 26 October 1996.

Micro-organisms in the digestive tracts of Baltic fish

Janina Šyvokiene and Liongina Mickeniene

Abstract

Investigations of the aerobic bacterial flora in the digestive tract of the following fish were carried out in 1995:

- European flounder (*Platichthys flesus*)
- burbot (*Lota lota*)
- Baltic herring (*Clupea harengus membras*)
- bullrout (*Myoxocephalus scorpius*)
- European pike-perch (*Stizostedion lucioperca*)
- European whitefish (*Coregonus lavaretus*)
- ruffe (*Gymnocephalus cernuus*)
- plaice (*Pleuronectes platessa*)
- Baltic cod (*Gadus morhua callarias*)
- European smelt (*Osmerus eperlanus*) from the Lithuanian coast (Baltic Sea).

Heterotrophic bacteria predominated in the bacteriocenosis of the digestive tract of the tested fish, proteolytic and amylolytic bacteria were isolated too. Increasing environmental pollution by various xenobiotics affects the bacteriocenosis of the digestive system of animals. Hydrocarbon-degrading bacteria were detected in great abundance in the digestive tract of the tested species, and counts were highest in autumn with a maximum of about 3×10^5 cells g^{-1} in ruffe. Hydrocarbon-degrading bacteria get into the digestive tract of fish from the environment and oil products—with food. Oil products taken up by fish may be partly degraded by enzymes of micro-organisms present in the intestines. We argue that fish with well developed intestinal microflora have a greater opportunity to assimilate food with high efficiency, and that increasing environmental pollution by xenobiotics may effect the bacteriocenosis of the digestive tract.

Introduction

The gut is sterile until hatching, but soon after hatching, the fish comes into contact with the environment and live food that leads to successive colonisation by a variety of microbes (Hansen *et al.*, 1992; Munro *et al.*, 1994; Ringø *et al.*, 1996, Ringø, Olsen, 1999). The balance of this microbiota is influenced by a variety of factors including food, animal physiology and immunological factors (Ringø, Strøm, 1994). The establishment of a normal gut flora may be regarded as complementary to the establishment of digestive enzymes and under normal conditions it serves as a barrier against invading pathogens (Sugita *et al.*, 1988; Ringø, Gastesoupe, 1998). It has been indicated, however, that the gastrointestinal microflora of aquatic animals is less abundant in both generic diversity and population number compared with that of terrestrial mammals (Sakata, 1990). Recently, these bacteria were found to be important for the physiology of such aquatic animals by producing vitamins, digestive enzymes and amino acids similar to those of mammals (Šyvokiene, 1989; Sugita *et al.*, 1991; Mickeniene, 1992). Most studies on the intestinal microbial community in fish focus on the total microbiota found in the intestinal contents or in intestinal homogenates (Sugita *et al.*, 1985; Cahill, 1990). Increasing environmental pollution has an undoubtless influence on hydrobionts, as well as fish, and on microorganisms associated with their digestive tract (Mironov, 1987, Suchanek, 1992; Leahy, Colwell, 1992). Changes in life conditions of the macroorganism cause changes in the structure of communities of intestinal microorganisms and functioning regularities of separate populations of microorganisms (Sugita *et al.*, 1987). Published data about the microorganisms of the digestive tract of Baltic fish from the Lithuanian coastal zone are scare. The aim of this study was to determine quantitative and qualitative indices of the microflora in the digestive tract of various fish species from the Baltic Sea in relation to feeding mode and season.

Material and Methods

Quantitative and qualitative compositions of the bacteriocenosis of the digestive tract of 10 species of fish were analysed under laboratory conditions. The aerobic bacterial population from the digestive tract was investigated as described by Segi (1983), Romanenko (1985), Kuznecov and Dubinina (1989).

Fish samples were taken from the Lithuanian coastal zone in spring (March and April), summer (August), and autumn (November) 1995. All fish were caught before midday according to guidelines given by Thoresson (1996). The fish were killed by a blow to the head and brought to the laboratory on ice (with a maximum 6 hours from catching to sampling). Preliminary experiments showed that the contents of cultivatable bacteria in the intestine did not change significantly during this period, neither qualitatively nor quantitatively (Onarheim *et al.*, 1994). Five specimens were analysed per species and sampling date. The fish were cleaned externally with ethanol and the intestines dissected under sterile conditions. The contents were squeezed, weighed and placed in a physiological NaCl solution, diluted in the range from 1:10 to 1:1000000. Subsamples of 0.1 ml of at least of three dilutions expected to give between 30 and 300 colony forming units were placed on four different nutrient media and incubated at $20-22\,^{o}C$. The media chosen were:

- beef agar (for isolation of heterotrophic bacteria): 1 l beef water, 10.0 g peptone, 5.0 g NaCl, 20.0 g agar;
- milk agar (for proteolytic bacteria): 1 l distilled water, 20.0 g agar and 40 ml skimmed milk;
- starch agar (for amylolytic bacteria): 1 l distilled water, 0.5 g KH_2PO_4, 0.5 g K_2HPO_4, 0.2 g $MgSO_4 \cdot 7H_2O$, 0.2 g $(NH_4)_2SO_4$, 10.0 g starch, 20.0 g agar
- Dianova and Voroshilova medium (for hydrocarbon-degrading bacteria): 1 l distilled water, 1.0 g NH_4NO_3, 1.0 g KH_2PO_4, 1.0 g $K_2HPO_4 \cdot 3H_2O$, 0.2 g $MgSO_4 \cdot 7H_2O$, 0.02 g $CaCl_2 \cdot 6H_2O$, traces of $FeCl_3 \cdot 6H_2O$, 20.0 g agar; a thin layer of black oil was spread on the agar medium as hydrocarbon source. The same medium without the hydrocarbon source was used as a control.

Bacterial colonies appearing on each plate were counted and a count of viable bacteria per g wet weight of intestinal contents was obtained accordingly. Proteolytic bacteria were identified according to zones of protein (casein) hydrolysis on milk agar, amylolytic bacteria were determined according to zones of starch hydrolysis under the action of iodine solution.

The digestive tracts of 57 fish were investigated including the following species: European flounder (*Platichthys flesus*), burbot (*Lota lota*), Baltic herring (*Clupea harengus membras*), bullrout (*Myoxocephalus scorpius*), European pike-perch (*Stizostedion lucioperca*), European whitefish (*Coregonus lavaretus*), ruffe (*Gymnocephalus cernuus*). plaice (*Pleuronectes platessa*), Baltic cod (*Gadus morhua callarias*), European smelt (*Osmerus eperlanus*).

Results

The data obtained have shown that viable counts of bacteria in the cenoses of the digestive tract of fish from Baltic Sea were mainly predominated by the populations of heterotrophic bacteria. Counts of the different types of bacteria in the digestive tract of fish varied among seasons and fish species (Figure 1, Figure 2 and Figure 3). In flounder, no microorganisms were detected in early March. Comparing all fish species considered in spring (Figure 1) heterotrophic and proteolytic bacteria dominated. Numbers of hydrocarbon-degrading bacteria fluctuated more significantly and were comparatively high in burbot, herring and bullrout. In the digestive tract of cod and plaice hydrocarbon-degrading bacteria were less abundant. Proteolytic bacteria were comparatively numerous in cod compared with other groups of bacteria. Amylolytic bacteria were not detected in any fish investigated in spring.
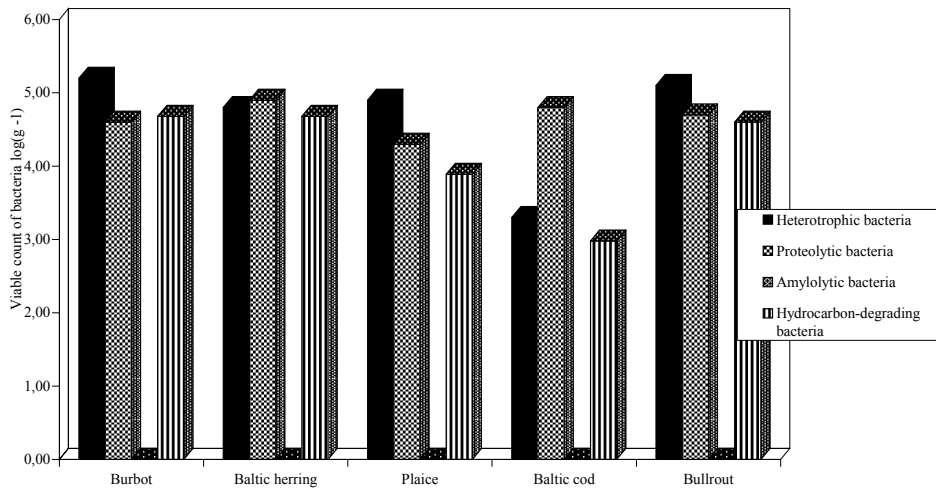
Figure 1 Viable count of bacteria in the digestive tract of fish in Spring

High counts of viable heterotrophic bacteria ($14.5 \times 10^6 \text{g}^{-1}$) were obtained in the digestive tract of flounder in summer (Figure 2), at the time of intensive feeding. Proteolytic and hydrocarbon-degrading bacteria were observed in similar numbers in flounder and were an order of magnitude less abundant than heterotrophic. The highest viable count of hydrocarbon-degrading bacteria amounting $1.6 \times 10^6 \text{g}^{-1}$ of intestine contents was isolated from the digestive tract of 2 year-old flounder.
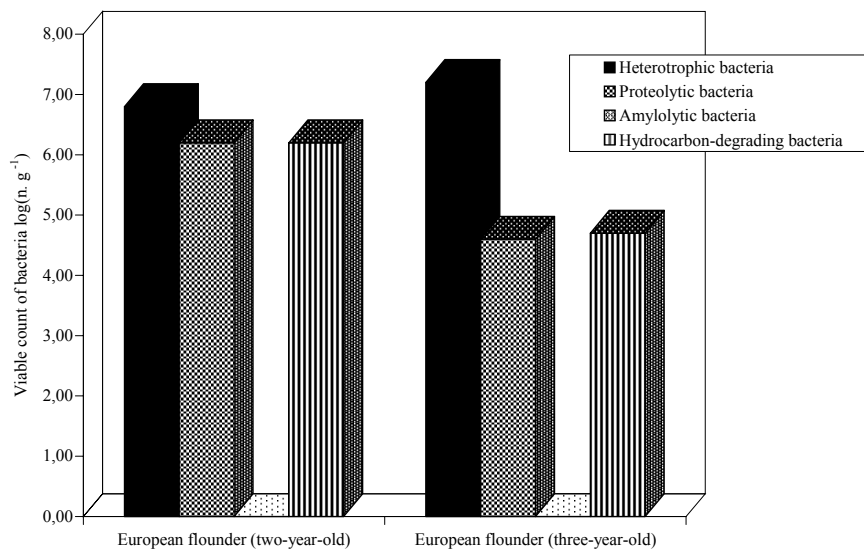
Figure 2 Viable count of bacteria in the digestive tract of fish in the summer

In autumn, the viable count of heterotrophic bacteria in the digestive tract of flounder decreased compared with summer. Heterotrophic bacteria predominated in the digestive tract of flounder and pike-perch (Figure 3). In cod, proteolytic and amylolytic bacteria were detected in similar numbers, not much less than the heterotrophic bacteria. Viable hydrocarbon-degrading bacteria were isolated in high numbers from all species, with a maximum in ruff—$0.3 \times 10^6 \text{g}^{-1}$.
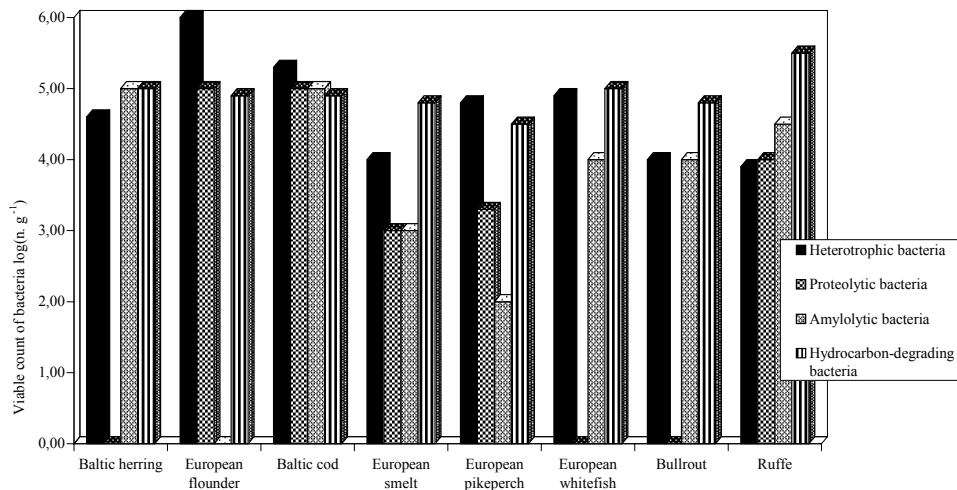
Figure 3 Viable count of bacteria in the digestive tract of fish in autumn

Discussion

Numerous studies have been carried out on the intestinal microflora of various fishes in the world (Ringø and Strøm, 1994; Ringø and Gatesoupe, 1998; Ringø and Olsen, 1999; Sakata, 1990; Sugita *et al.*, 1985, 1988, 1991). There is evidence that dense bacterial populations occur within the intestinal contents of fish indicating that the intestines provide favourable ecological niches for these organisms. The data obtained have shown that the intestinal microflora of fish, however, is influenced by endogenous and exogenous factors including the developing stage, structure of fish gastrointestinal tract, rearing conditions, handling stress, oral administration of antibiotics, diet etc. Additionally it was shown that there are daily fluctuations and inter-individual variations in the intestinal microflora of fish (Sugita *et al.*, 1982; 1988, 1988a, Ringø and Olsen, 1999).

Our studies revealed that dense bacterial populations occur in the digestive tract of the fish studied. Heterotrophic bacteria dominated in the digestive tract of the fish studied from the Baltic Sea. Counts of the different types of bacteria in the digestive tract of fishes varied between seasons and fish species. However, hydrocarbon-degrading bacteria were obtained in high numbers. Viable hydrocarbon-degrading bacteria were isolated in high numbers from all species, with a maximum in ruffe of $0.3 \times 10^6 \mathrm{g}^{-1}$. If the microflora of fish reflects that of their habitat, fish could even harbour various bacteria such as pathogens, if grown in contaminated water (Cahill, 1990). Hydrocarbons are naturally occurring organic compounds, and it is not surprising that microorganisms have evolved the ability to utilize these compounds. The most widely documented response of microbial communities to exposure to oil is the rapid increase in the size of the hydrocarbon-utilising component of the community (Leachy, Colwell, 1990). High numbers of hydrocarbon-degrading bacteria in the digestive tract of fish may be taken as an indication of high amounts of hydrocarbon in the environment, which could either been produced by other organisms or be due to a polluted environment. An understanding of the response of microflora in the digestive tract of fish to the environment may help to explain effects of pollution.

References

Cahill, M. M. 1990. Bacterial flora of fishes: a review. Microb. Ecol. 19: 21−41.

Hansen, G. H., Strum E. Olafsen J. A., 1992. Effect of different holding regimes in the intestinal microflora of herring (Clupea harengus) larvae. Appl. Environ. Microbiol. 8:461−470.

Kuznetsov, S. I., Dubinina, G. A. 1989. Methods of investigation of aquatic microorganisms (In Russian). Moscow, 285 pp.

Leahy, J. G., Colwell, R. R. 1990. Microbial degradation of hydrocarbons in the environment. Microbiol. Rev. 54(3): 305−315.

Mickeniene, L. 1992. Microflora of the digestive tract of crayfish and its relation with feeding (In Russian). Minsk, 23 pp.

Mironov, O. G. 1987. Microflora of Mytilus galloprovincialis. Microbiology, 56(1): 162−163 (In Russian).

Munro, P. D., Barbour, A., Birkbeck, T. H. 1994. Comparison of the gut bacterial flora of start-feeding turbot larvae reared under different conditions. J. Appl. Bacteriol. 77: 560−566.

Onarheim, A. M., Wiik, K. R., Burghardt, J., Stackebrandt, E. 1994. Characterization and identification of two Vibrio species indigenous to the intestine of fish in cold sea water. Description of Vibrio iliopiscarius sp. nov. System. Appl. Microbiol. 17: 370−379.

Ringø, E., Strøm, E. 1994. Microflora of Arctic char Salvelinus alpinus (L.); gastrointestinal microflora of free-living fish and effect of diet and salinity on the intestinal microflora. Aquacult. Fish. Manage. 25: 623−629.

Ringø, E., Gatesoupe, F. J. 1998. Lactic acid bacteria in fish: a review. Aquaculture. 160: 177−203.

Ringø E., Olsen, R. E. 1999. The effect of diet on aerobic bacterial flora associated with intestine of Arctic char (Salvelinus alpinus) J. Appl. Microbiol. 86(1): 22−28.

Romanenko, V. I. 1985. Microbiological processes of production and destruction of organic matter in inland water-bodies. (In Russian). Leningrad, 295 pp.

Segi, J. 1983. Methods of soil microbiology. (In Russian). Moscow, 295 pp.

Suchanek, T. H. 1992. Oil impact on marine invertebrate populations and communities. Amer. Zool. 32(5): 115A.

Sakata, T. 1990. Microflora in the digestive tract of fish and shellfish, p.171−176. In: R. Lesel (ed.) Microbiology of poecilotherms, Elsevier Science Publishers, Amsterdam.

Sugita H., Ishida Y., Deguchi Y., Kadota H. 1992. Aerobic microflora attached to wall surface in the gastrointestine of Tilapia nilotica. Bull. Coll. Agric. Vet. Med. Nihon. Univ. 39: 212−217

Sugita, H., Takuyama, K., Deguchi, Y. 1985. The intestinal microflora of carp Cyprinus carpio, grass carp Ctenopharyngodon idella and tilapia Sarotherodon niloticus. Bull. Jap. Soc. Sci. Fish. 51: 1325−1329.

Sugita, H., Takahashi, T., Kamemeoto, F., Deguchi, Y. 1987. Aerobic bacterial flora in the digestive tract of freshwater shrimp Palaemon paucidens acclimated with sea water. Bull. Jap. Soc. Sci. Fish. 53: 511−513.

Sugita, H., Tsunohara, M., Ohkoshi, T., Deguchi, Y. 1988. The establishment of an intestinal microflora in developing goldfish (Carassius auratus) of culture ponds. Microbiol. Ecol. 15: 333−344.

Sugita H., Fukumoto M., Koyama H., Deguchi Y. 1988a Changes in the fecal microflora of goldfish Carassius auratus with oral administration of oxytetracycline. Bull. Jap. Soc. Sci. Fish. 54: 2181−2187.

Sugita, H., Miyajima, C., Deguchi, Y. 1991. The vitamin B12-producing ability of the intestinal microflora of freshwater fish. Aquaculture 92: 267−276.

Šyvokiene, J. 1989. Ecological aspects of symbiotic digestion in hydrobionts. (In Russian). Moscow, 40 pp.

Šyvokiene, J. 1989[a]. Symbiotic digestion in hydrobionts and insects. Mokslas, Vilnius, 222 pp.

Thoresson G. 1996. Guidelines for coastal fish monitoring. Oregund Kustrapport Publishers. 34pp.

Fertiliser consumption in the catchment area and eutrophication of the Baltic Sea

Dietwart Nehring and Günther Nausch

Summary

The increasing use of synthetic fertilisers in the catchment areas is very often the main cause of eutrophication in shelf seas. The drastic reduction in fertiliser consumption mainly caused by the great economic changes in the countries of the former East Block bordering the Baltic Sea began in the late 1980s and is reflected in decreasing winter concentrations of phosphate in the middle of the 1990s especially in the Arkona and Bornholm Basins, whereas nitrate concentrations still remain at their high level.

Eutrophication will slowly lose its significance as a problem in the Baltic Sea due to decreasing consumption of synthetic phosphorus and nitrogen fertilisers and the creation of modern waste water treatment plants. This optimism is based on the assumption that the measures for the protection and restoration of ecological balance of the Baltic Sea are implemented consequently by the countries present in the catchment area.

Introduction

Eutrophication is one of the most serious environmental problems in the Baltic Sea. This process increases the production of organic matter and thus the microbial oxygen demand in stagnant deep waters. Due to the accumulation of organic material in the sediments, oxygen depletion and hydrogen sulphide formation are also being increasingly recorded in shallow coastal areas (10–15 m depth) during calm weather conditions in summer, thereby producing very steep redox gradients (Nehring *et al.*, 1995a). Although these unfavourable conditions continue only for a few days (<2 weeks), the consequences are dramatic for the benthic community, which needs years to recover completely (cf. Weigelt, Rumohr, 1986).

The increasing use of fertilisers in the catchment area is discussed as the main cause of eutrophication in shelf seas (Nixon, 1995). Fertilisers are applied to increase agricultural production. Consequently, waste production by livestock, the food industries and human population is also increasing.

Large amounts of fertiliser are retained by the soil or lost by denitrification. Only a small fraction of the synthetic fertilisers applied in the drainage areas reaches the coastal zone after transformation by various biogeochemical and technological processes.

Results

The catchment area of the Baltic Sea covers $1.7 \times 10^6 \, km^2$, which is four times greater than the Baltic Sea ($0.415 \times 10^6 \, km^2$). Especially in its southern and eastern parts and around the Kattegat, the catchment area drains regions with extensive crop production, intensive animal production and large foodstuffs industry (Figure 1). Additionally, large towns and numerous villages in these regions generate great amounts of communal sewage which are often not or only insufficiently cleaned by waste water treatment plants.
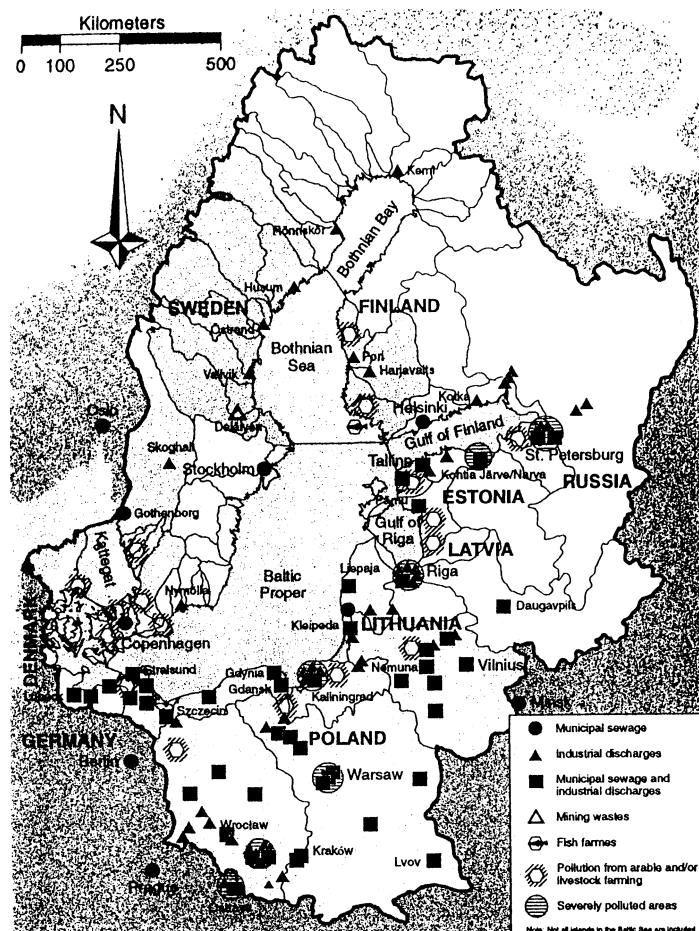
Figure 1 Hot spots identified by HELCOM (1993) in the catchment area of the Baltic Sea.

Period	1958/68	1969/73	1974/78	1979/83	1984/88	1989/93
Arkona Sea (average of Stat. 069, 109, 113)						
Phosphate (Jan–Mar)	-	0.26±0.07(5)	0.49±0.12(16)	0.48±0.11(50)	0.67±0.09(52)	0.61±0.17(155)
Nitrate (Jan–Feb)	-	2.68±0.14(4)	3.93±0.78(14)	4.61±0.83(20)	4.74±0.46(35)	4.17±0.79(84)
Bornholm Sea (average of Stat. 200, 213, 214)						
Phosphate (Jan–Mar)	0.32±0.15(22)	0.35±0.12(50)	0.56±0.14(46)	0.58±0.21(53)	0.67±0.19(88)	0.64±0.18(89)
Nitrate (Jan–Mar)	0.69±0.37(3)	2.08±0.73(34)	3.16±0.56(46)	3.89±0.94(53)	4.37±1.16(90)	3.90±0.83(89)
Eastern Gotland Sea (average of Stat. 250, 255, 259, 260, 270, 271)						
Phosphate (Feb–Mar)	0.27±0.09(24)	0.26±0.14(95)	0.54±0.09(61)	0.59±0.16(60)	0.60±0.15(125)	0.67±0.11(182)
Nitrate (Jan–Apr)	0.97±0.36(5)	2.44±0.40(75)	3.81±0.94(61)	4.15±0.93(60)	4.30±0.99(132)	4.23±1.28(200)

Table 1 Five (eleven) year averaged winter concentrations of phosphate and nitrate ($\mu mol\,dm^{-3}$) in the surface layer (0–10m) of main subregions in the Baltic Proper (exact position of stations cf. Nehring *et al.*, 1995b); number of data available in parenthesis (mainly from Germany but also from Sweden, former USSR, IBY and HELCOM)

Synthetic fertiliser consumption in the countries contributing to the nutrient load in the catchment area of the Baltic Sea began to increase rapidly in the early 1960s (FAO, 1952–1993). The phosphorus and nitrogen fertilisers applied in the various countries have been set in proportion to the respective drainage areas to give a more realistic picture (Figure 2). These amounts are compared with the winter concentrations of phosphate and nitrate in the surface layer averaged over five (eleven) year periods (Table 1). The increasing number of data available for these periods indicates the intensifi-

cation of monitoring activities initiated by HELCOM. Fertiliser consumption in the catchment area is reflected in the phosphate and nitrate winter concentrations in the surface layer of the Baltic Proper after a delay of five to ten years (Figure 2). The figures for the nutrient distributions are quite similar for all central Baltic basins (cf. Table 1).
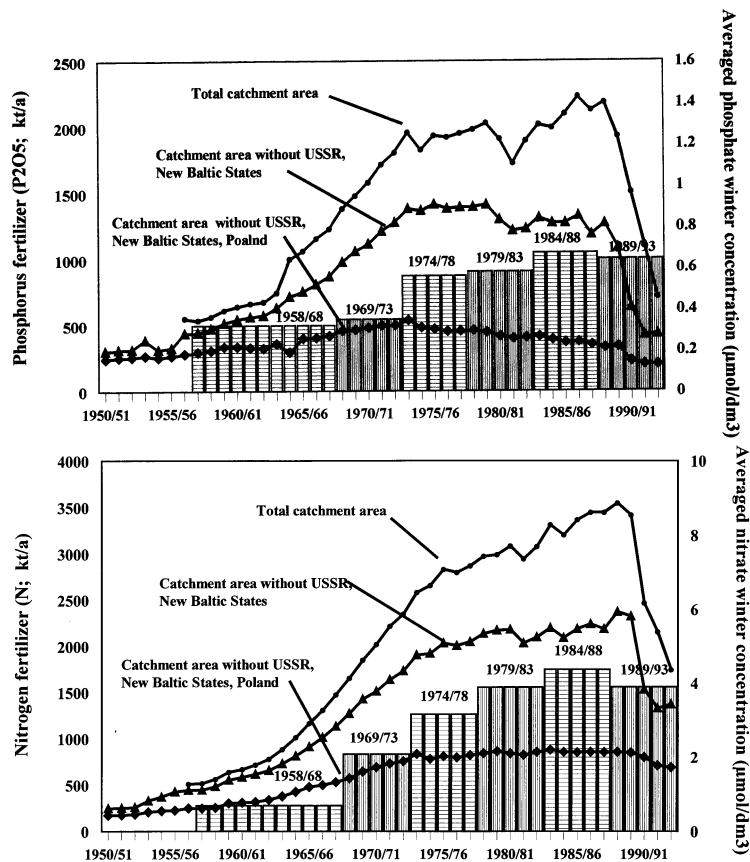
Figure 2 Consumption of synthetic phosphorus (above) and nitrogen (below) fertilisers (lines) in the drainage area of the Baltic Sea and five (eleven) year averaged phosphate and nitrate winter concentrations (columns) in the surface layer (0–10 m depth) of the Bornholm Basin (cf. Nehring *et al.*, 1995b)

A drastic reduction in fertiliser consumption, mainly caused by the great economic changes in the countries of the former East Block, began in the late 1980s and is thus not yet reflected significantly by the mean nutrient conditions in the Baltic Proper (Table 1, Figure 2). However, signs of the decrease are now becoming apparent in the figures for the long-term behaviour of phosphate (Figure 3). Winter concentrations of this nutrient, which increased on average until the mid-1980s, now show a decreasing tendency in central Baltic surface waters (Nehring *et al.*, 1995b). This phenomenon is more pronounced in the Arkona and Bornholm Basins, where the stations are located nearer to the coast, than in the Eastern Gotland Basin with its more offshore stations.
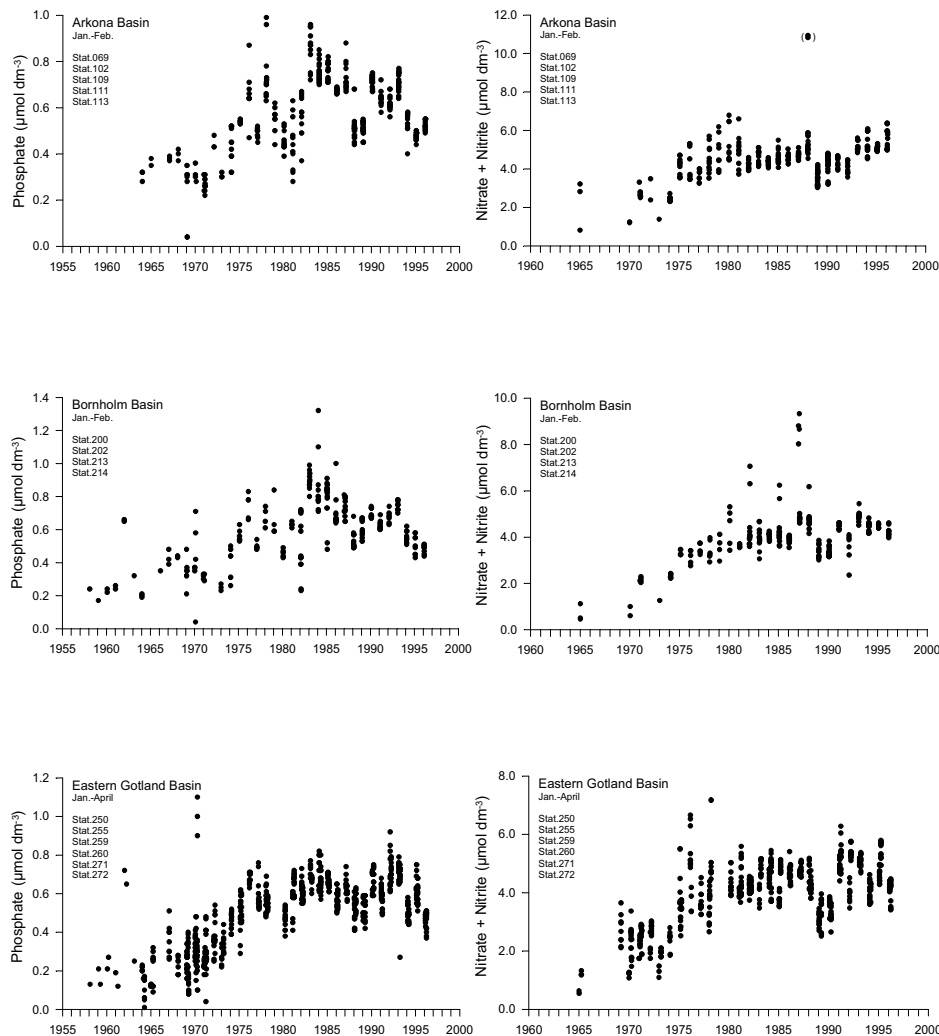
Figure 3 Long-term changes of phosphate (left side) and nitrate (right side) concentrations in the surface layer (0–10 m depth) of the Baltic Proper (position of stations cf. Nehring *et al.*, 1995b)

The situation is less clear for nitrate (Figure 3). Recent data from monthly Swedish monitoring cruises in the Baltic Sea also show lower winter concentrations for phosphate, but not for nitrate, when compared to the long-term means (Swedish cruise reports, 1995 and 1996). Similar observations have been made in the coastal waters off Mecklenburg–Vorpommern (eastern Germany), where total phosphorus and phosphate concentrations— coming to a larger percentage from point sources—are decreasing rapidly, but the decrease in total nitrogen is only moderate and nitrate concentrations have so far even remained at their former high levels (LAUN, 1994–1996; Bachor *et al.*, 1996) due to the dominance of diffuse nitrogen sources.

Low fresh water discharge in autumn correlates with low nitrate concentrations in coastal waters in winter and vice versa (Kornvang *et al.*, 1995, Bachor *et al.*, 1996). Similar correlations have been observed in internal coastal waters (Nausch, Schlungbaum 1991, 1995). This indicates that not only human activities, but also natural variations, for instance the meteorological conditions such as precipitation, influence the nutrient pool at least in inshore regions. Interannual variations in biological activity and their influence on the winter concentrations is also an open question.

Discussion

Inorganic phosphorus and nitrogen compounds are the forcing factors driving eutrophication (Vollenweider, 1992). Any reduction in inputs of these compounds will also reduce biological productivity and, consequently, oxygen demand in stagnant deep waters. Due to the decreasing nutrient load expected in the future, eutrophication will slowly lose its significance as a problem in the Baltic Sea. This optimism is based on the assumption that the measures for the protection and the restoration of the ecological balance of the Baltic Sea recommended by the Helsinki Commission (HELCOM, 1993) and accepted by the governments are implemented consequently in the countries present in the catchment area.

With respect to diffuse nutrient sources from agriculture (non-point sources), the most promising approach will be the reduction of fertiliser application to the level which meets only the most essential requirements of the plants. Point sources contain phosphorus and nitrogen compounds indirectly resulting from fertilisers after transformation via livestock, the food industry and man. Nutrients from point sources can be eliminated without difficulty by modern waste water treatment plants.

Altogether, the recovery of the Baltic sea is a lengthy process since the changes in the ecosystem caused by the nutrient loads for more than 50 years cannot be reversed within a few years. Realistic estimations of the time scale needed are difficult to obtain because for example information about accumulation in and remobilisation from the sediments is insufficient. Bearing in mind the long residence times of the Baltic Sea (Wulff *et al.*, 1990) at least several decades have to be taken into account.

References

Bachor, A., v.Weber, M., and Wiemer, R., 1996. Die Entwicklung der Wasserbeschaffenheit der Küstengewässer Mecklenburg−Vorpommerns. Wasser und Boden 48, 26−32.

FAO, 1952−1993. Yearbook Fertilizer. FAO Statistic Series, 1952−1993.

HELCOM, 1993. The joint comprehensive action programme. Baltic Sea Environment Proc. 49, 1−58.

Kornvang, B., Aertjeberg, G., Grant, R., Kristenson, P., Hovmand, M., and Kirkegaard, J., 1993. Nationwide monitoring of nutrients and ecological effects: State of the Danish aquatic environment. Ambio 22, 632−638.

LAUN, 1994−1996. Küstengewässer-Monitoring Mecklenburg−Vorpommern. Küsten-gewässerberichte 1994−1996 des Landesamtes für Umwelt und Natur Mecklenburg−Vorpommern.

Nausch, G., and Schlungbaum, G., 1991. Eutrophication and restoration measures in the Darss−Zingst Bodden chain. Int. Revues ges. Hydriobiol. 76, 451−464.

Nausch, G. and Schlungbaum, G., 1995. Nährstoffdynamik in einem flachen Brackwassersystem (Darß−Zingster Boddenkette) unter dem Einfluß variierender meteorologischer und hydrographischer Bedingungen. Bodden 2, 153−164.

Nehring, D., and Aertjeberg, G., 1996. Verteilungsmuster und Bilanzen anorganischer Nährstoffe sowie Eutrophierung. In: Lozan, J.L., Lampe, R., Matthäus, W., Rachor, E., Rumohr, H., v.Westernhagen, H. (Hrsg.), Warnsignale aus der Ostsee. Berlin, Parey 1996, 61−68.

Nehring, D., Matthäus, W., Lass, H.-U., Nausch, G., and Nagel, K., 1995a. The Baltic Sea 1994—consequences of the hot summer and inflow events. Dt. Hydrogr. Z. 47, 131−144.

Nehring, D., Matthäus, W., Lass, H.-U., Nausch, G., and Nagel, K., 1995b. The Baltic Sea 1995—beginning of a new stagnation period in its central deep waters and decreasing nutrient load in its surface layer. Dt. Hydrogr. Z. 47, 319−327.

Nixon, S.W., 1995. Coastal marine eutrophication: a definition, social causes, and future concerns. Ophelia 41, 199−219.

Vollenweider, R.A., 1992. Coastal marine eutrophication: principles and control. Sci. Of Total Environ., Suppl. 1992, 1−20.

Weigelt, M., Rumohr, H., 1986. Effects of wide-range oxygen depletion on benthic fauna and demersal fish in Kiel Bay 1981−1983. Meeereforsch 31, 124−136.

Wullf, F., Stigebrandt, A., Rahm, L., 1990. Nutrient dynamics of the Baltic Sea. Ambio 19, 126−133.

Chemical and biological interactions in mixing gradients in the Pomeranian Bight

M. Nausch and E. Kerstan

Abstract

The changes of inorganic nutrients, dissolved carbohydrates and activities of carbohydrate degrading enzymes (glucosidase, glucosaminidase) were investigated during the mixing of water from the river Oder and water from the open Pomeranian Bight from 1994 to 1996. In winter, nutrients were introduced mainly in inorganic form. Physical mixing processes dominated the changes in the salinity gradient because the biological activities were low. During the growth season, the input was mainly in organic form as can be shown by particulate organic carbon and chlorophyll. The influence of physical and biological processes on the alteration of introduced material cannot be distinguished clearly. However, the interaction between biochemical parameters and bacterial activities could be demonstrated on the example of dissolved carbohydrates and glucosidase activity. Concentrations of total dissolved carbohydrates (TCHO) and dissolved monosaccharides (MCHO) decreased if the uptake by bacteria exceeded the hydrolytic activity. In the salinity gradient ranging between 1.9 and 7.8 PSU, TCHO decreased from $15.1\,\mu$mol l^{-1} to $2.8\,\mu$mol l^{-1} and MCHO from $3.4\,\mu$mol l^{-1} to 1.1 μmol l^{-1}. The hydrolysis rate (Hr) of glucosidase and glucosaminidase (Chitinase) reduced from 13.9% h^{-1} to 0.3% h^{-1} and 9.9% h^{-1} to 0.2% h^{-1}, respectively.

Introduction

The river Oder is the largest external source of nutrients entering the Pomeranian Bight (Pastuszak *et al.*, 1996). The river load amounts to 17% of phosphate and 15% of fluvial nitrogen for the whole Baltic Sea (Rosemarin *et al.*, 1990). Beside inorganic nutrients, river load contains also organic material in large quantities (Wedborg et al,.1994). In marine systems, carbohydrates represent up to 35% of the dissolved organic carbon (DOC) (Benner *et al.*, 1992). They are the main component of DOC beside amino acids and lipids (Hellebust, 1965, 1974). Carbohydrates are products of phytoplankton photosynthesis and are released by phytoplankton exudation, cell lysis and microbial degradation. Furthermore, zooplankton excretion is a source of dissolved carbohydrates (Klok *et al.*, 1984, Mopper *et al.*, 1991, Lee & Hinrichs, 1993). Low molecular weight carbohydrates such as monosaccharides are directly released from phytoplankton into the surrounding seawater or they are released from polymeric carbohydrates after degradation by microbial enzymes. High concentrations of low molecular weight carbohydrates are produced during intensive primary production (Münster & Chrost, 1991). But in water, they remain on a low level due to high rates of bacterial uptake (Libes, 1992). In marine systems, glucose is the most important carbohydrate in monomeric form (monosaccharide) and in polymeric form (polysaccharide) such as glucanes and cellulose (Handa & Domiga, 1969, Liebezeit & Bölter, 1991).

The activity of glucosidases is often used to describe the degradation of polymeric carbohydrates (Münster, 1991, Vrba, 1992, Marxen, 1991, Hoppe *et al.*, 1998). High ß-glucosidase activity was measured during the breakdown of a plankton bloom (Chrost, 1991). Rath *et al.* (1993) and Hoppe *et al.* (1998) describe the behaviour of glucosidase activities in trophic gradients.

The main objectives of the interdisciplinary project TRUMP (transport and modification processes in the Pomeranian bight) of the Baltic Sea Research Institute Warnemünde were investigations on the distribution, modification and fate of material transported by the Oder river via the Szczecin Lagoon into the coastal ecosystem of the Pomeranian Bight. Physical transport and biochemical modification of different classes of material are described over the seasonal cycle and the salinity gradient (v. Bodungen *et al.*, 1995). During this study, the distribution of dissolved carbohydrates and glucosidase activity as a marker for carbohydrate degradation as well as the relationship between these parameters were investigated.

Investigation Area and Methods

In June/July 1994, July and September 1995 and in January 1996 several drift experiments and high resolution sampling transections in the salinity gradients were performed in the Pomeranian Bight to describe the mixing and biological and

chemical transformation of introduced river water. However, the river Oder does not enter the bight directly. A shallow lagoon, the Szczecin Lagoon (Odra Haff), is situated between the river mouth and the open bight. The Szczecin Lagoon and the Pomeranian Bight are connected via the rivers Peene and Szwina and lead to mixing of river water with water from the bight. The lagoon water with a salinity range between 0.5 and 2 PSU (practical salinity units) enters the Pomeranian Bight in a pulse like manner and in plumes of different size and is mixed with bight water within 2 or 3 days (v.Bodungen *et al.*, 1995).

Water samples were taken at depths of $1-2$, $5-6$ and $8-10$ m with a rosette sampler combined with sensors for conductivity, temperature and density (CTD) as well as a sensor for fluorescence.

Inorganic nutrients were analysed using standard colorimetric methods according to Rohde & Nehring (1979) and Grasshoff *et al.* (1983).

For the determination of dissolved carbohydrates, samples were filtered through GF/F filters. Dissolved monosaccarides were estimated according to the 3-methyl-2-benothiazolon-hydrazon (MBTH) method (Johnson & Sieburth, 1977). For the determination of total dissolved carbohydrates (TCHO), filtered water samples were hydrolysed with 0.09N HCl at 100°C for 20h followed by the application of MBTH method.

For the characterisation of the degradation of carbohydrates by bacteria, glucosidase and glucosaminidase (chitinase) activity were investigated. Glucosidase degrades preliminary oligosaccharides. Glucosaminidase acts on aminopolysaccharides like chitin. The enzyme activities were determined according to Hoppe (1993) using the model substrates 4-methylumbelliferryl (MUF)-a-glucoside, -ß-glucoside and MUF-glucosaminide. For estimation of in situ hydrolysis of natural substrates, the hydrolysis rate (Hr ($\%h^{-1}$)) was measured at final concentrations of 100 nM MUF-a-or ß-glucoside and at in situ temperatures.

Turnover rates (To ($\%h^{-1}$)) of glucose were determined with D-[U-14C] glucose at final concentrations of 80nM at in situ temperatures (Jost & Pollehne, 1998).

Results

In winter, nitrogen and phosphorus from the Oder river were introduced into the Pomeranian Bight mainly in inorganic form. Reduced primary and bacterial production (<5% of summer values for primary production, <8% of summer values for bacterial production) were indications of low biological activities. In the growth season, these nutrients were transformed already in the lagoon by phytoplankton production and entered the bight as organic material as shown by the high particulate organic carbon and nitrogen concentrations of $229.4-510.3\,\mu mol\ l^{-1}$ and $29.4-36.4\,\mu mol\ l^{-1}$, respectively (Table 1). Phytoplankton biomass is the dominating component of introduced organic material. It accounted for up to 70% of the total organic carbon. In winter, the decrease of inorganic nutrients in the salinity gradient in the Pomeranian Bight was caused by conservative dilution of lagoon water with water from the open bight. In that season, low biological activity left the inflowing nutrients without significant alteration. Figure 1 shows the behaviour of ammonia and nitrate in the salinity gradient. Phosphate and silicate had the same characteristics. In summer, inorganic nutrients were generally low. Therefore, no or only small gradients were observed. The difference before and after dilution were about $0.3\,\mu mol\ l^{-1}$ for nitrate, about $0.1\,\mu mol\ l^{-1}$ for ammonia and $0,02\,\mu mol\ l^{-1}$ for phosphate.

		Winter period	Vegetation period
salinity	(PSU)	4.6–5.5	1.9–4.2
NO3 +NO2	($\mu mol\ l^{-1}$)	30–60	0.2–0.6
NH4	($\mu mol\ l^{-1}$)	10–32	0.8–1.8
PO4	($\mu mol\ l^{-1}$)	1.5–3.0	0.05–0.36
POC	($\mu mol\ l^{-1}$)	36.7	229.4–510.3
PON	($\mu mol\ l^{-1}$)	5.5	29.4–36.4
Phytoplankton C($\mu mol\ l^{-1}$)		11.4–16.2	118.6–361.1

Table 1 Concentration of nutrients, particulate organic matter and phytoplankton biomass in the river plume entering the Pomeranian Bight
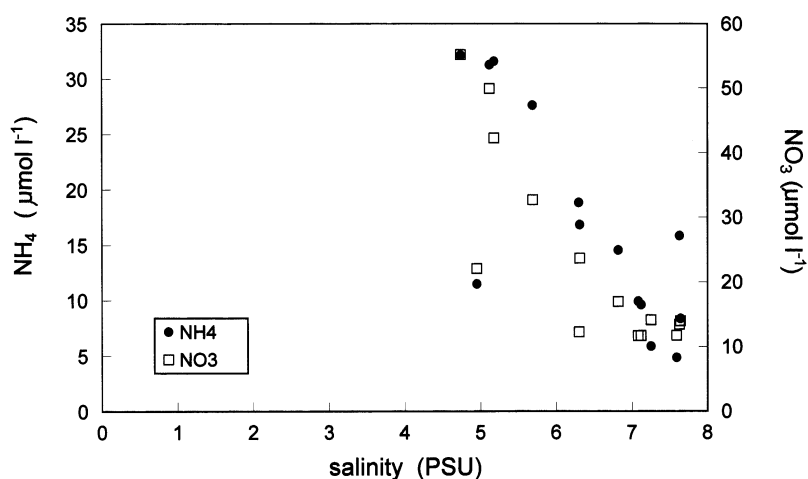
Figure 1 Ammonia and nitrate concentrations in the salinity gradient in winter 1996

The highest concentrations of dissolved carbohydrates were measured near to the Swina mouth in the growing season. Concentrations of TCHO up to 15.1 μmol l^{-1} (Figure 2) and MCHO up to 4.8 μmol l^{-1} (Figure 3) were estimated. In winter, the values were significantly lower. TCHO and MCHO concentrations of about 4 μmol l^{-1} and 1 μmol l^{-1} were determined. Dissolved carbohydrates had the same concentrations in summer and in autumn. The pattern of dissolved carbohydrates in the salinity gradient varied from year to year and from season to season. TCHO showed a significant decrease with increasing salinities in July 1994 and September 1995. During the other investigations, the TCHO concentrations remained on the same level: 3–4 μmol l^{-1} in January 1996 and about 7.3 μmol l^{-1} in July 1995. MCHO showed a clear relationship to salinity only in autumn 1995 (Figure 3). Its concentrations scattered from 1.1 to 3.4 μmol l^{-1}.
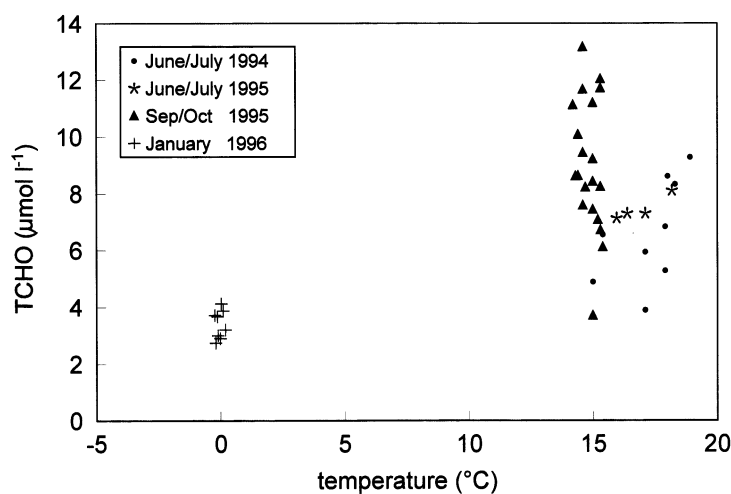
Figure 2 TCHO concentrations in the surface layer in winter and in the growth season
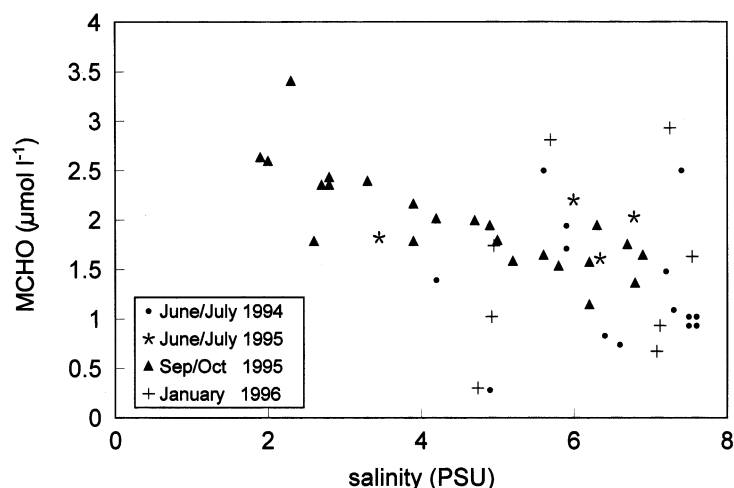
Figure 3 MCHO concentrations in salinity gradients

The hydrolysis rate of the carbohydrate degrading enzymes a-glucosidase, ß-glucosidase and glucosaminidase showed the same pattern in the salinity gradient and between the seasons. The values of these enzyme activities were in the same range and decreased linearly in the salinity gradient. In summer, glucosidase activity reduced from 13.9% h^{-1} to 0.3% h^{-1} and the glucosaminidase activity from 9.9% h^{-1} to 0.2% h^{-1} during mixing processes. Bacteria are the carrier of these enzymes. The decrease of glucosidase activities is higher (by factor 46) than the decrease of bacterial counts (by factor 2.5). From that it can be deduced that the activity per bacterial cell decreased and that the specific activity is the dominant factor influencing the pattern of glucosidase activities. In winter, glucosidase- and glucosaminidase activities amounted to only 8% of summer values (Figure 4).
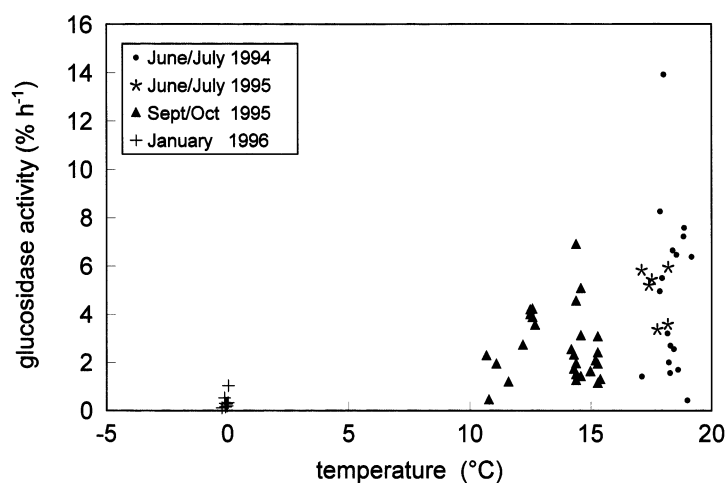
Figure 4 Glucosidase activities in winter and in the growth season

Glucosidase- and glucosaminidase activity correlated with the MCHO and TCHO (Table 2). These relationships were especially clear at low glucosidase activities up to 4.5% h^{-1} and glucosaminidase activities up to 2% h^{-1} (Figure 5). At higher glucosidase activities in the outflowing lagoon water where the highest bacterial production (Jost & Pollehne 1998) and enzyme activities were measured this relationship was not evident.

	MCHO µmol l^{-1}	TCHO µmol l^{-1}
glucosidase activity (% h^{-1})	0,38 n=36, p=0.05	0,22 n.s.
glucosaminidase activity (% h^{-1})	0,81 n=36, p=0.01	0,67 n=33, p=0.01

Table 2 Correlation coefficients between dissolved carbohydrate concentrations and glucosidase activities up to 4.5%h^{-1} and glucosaminidase activities up to 2% h^{-1}
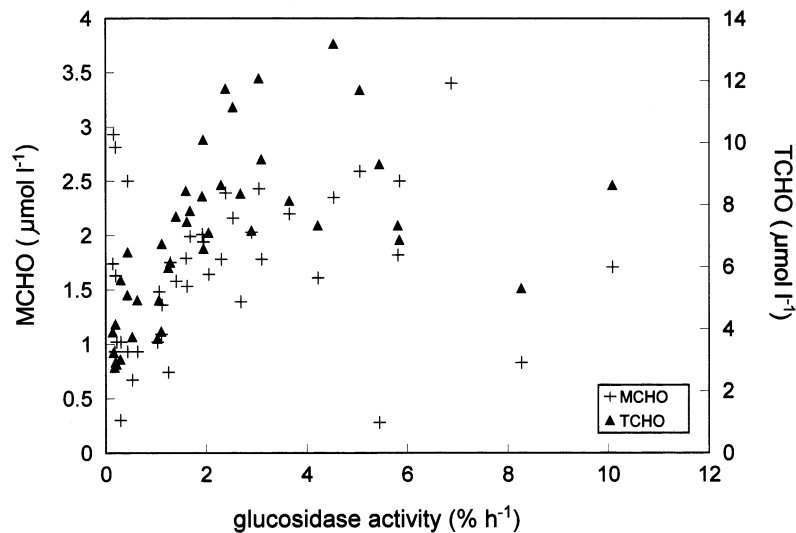
Figure 5 Relation between MCHO and TCHO concentrations and glucosidase activities

The uptake of low molecular weight substances by bacteria, determined as glucose turnover (To), was highest in summer. At this time, glucose turnover rates up to 30% h^{-1} were measured in the outflowing lagoon water. After dilution in the salinity gradient the values were reduced to $1-2$% h^{-1}. In winter, turnover rates ranged between 0.2 and 0.5% h^{-1}.

The quotient between To and Hr (To/Hr) can be used as an index for coupling of glucose uptake and release via enzymatic degradation by bacteria. In the outflowing lagoon water, a median To/Hr-ratio of 1.6 was determined in winter and a ratio of 4.2 in summer. In the growing season, the To/Hr-ratio had a relatively constant level in a salinity range between 1.9 and 7 PSU. Between 7 and 7.8 PSU, the quotient rose up to 21.4 (Figure 6). The increase is due to the fact that Hr was more (factor 4.8) reduced than To (factor 2.1). At salinities >5 PSU, the relationship between uptake of glucose and the hydrolysis rate of carbohydrates and the concentration of MCHO could be observed. In this range, the distribution of dissolved monosaccharides and the To/Hr-quotient were independent from the salinity. There was a negative correlation between the To/Hr-quotient and MCHO concentrations (Figure 7).
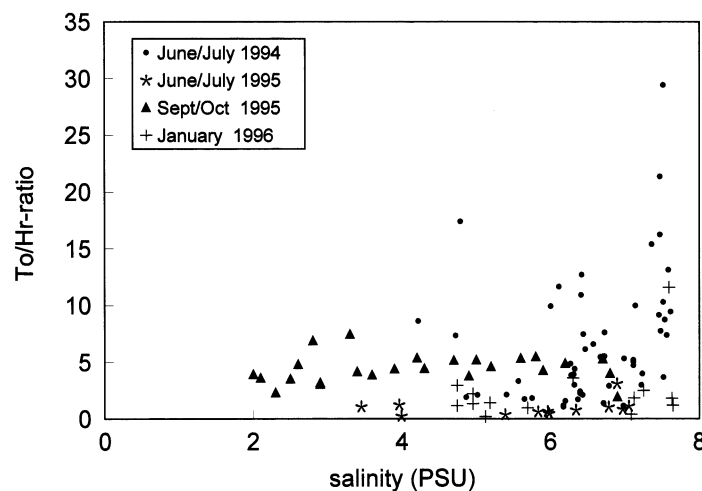
Figure 6 Relation of glucose turnover and glucosidase activity in the salinity gradient
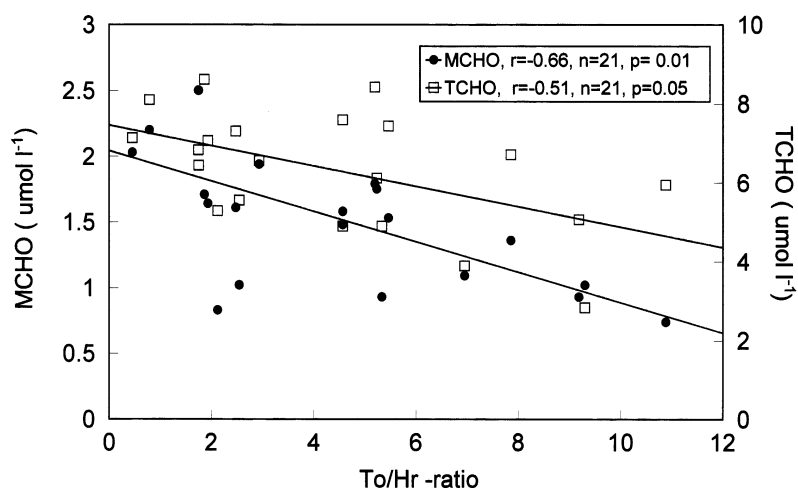
Figure 7 Relation between To/Hr-quotients and concentrations of MCHO and TCHO at salinities >5 PSU

Discussion

Organic and inorganic material introduced into the Pomeranian Bight can be modified by physical dilution or by transformation via biological processes. These processes cannot be distinguished clearly, biological processes are masked by physical dilution. However, we could show by the example of glucose turnover and enzymatic carbohydrate degradation that an interaction of different parts of planktonic community existed.

Carbohydrates are produced as a result of photosynthesis and are released into seawater by exudation from phytoplankton and cell lysis as well as sloppy feeding of zooplankton (Klok *et al.*, 1984, Mopper *et al.*, 1991, Münster & Chrost, 1991). We assume that phytoplankton was the main source of dissolved carbohydrates in the Pomeranian Bight because the highest TCHO and MCHO concentrations were found near the Swina mouth where the phytoplankton biomass was also highest (Jost & Pollehne, 1998). Zooplankton biomass in the outflowing lagoon water was not higher than in the open bight. However, there was a shift from limnetic to more marine species (Postel & Mumm, 1995).

For stock parameters (POC and chlorophyll) as well as for activity parameters (primary production, bacterial production) a linear decrease was observed in all gradients (Jost & Pollehne, 1998). In contrast to that, dissolved carbohydrates had not such a strong relationship to salinity. Especially in summer, the MCHO concentrations were not correlated with the salinity. According to Jost & Pollehne (1998), the primary production near the Swina mouth is more light-limited than in the open bight. Respiratory processes exceeded the primary production and a negative carbon balance was calculated for the whole water column. Due to the deeper light penetration, the carbon balance in the open bight was positive. These relationships between autotrophic and heterotrophic processes could have an influence on the concentrations of TCHO and MCHO.

Bacteria are the main consumers of low molecular weight substances and they possess extracellular enzymes for carbohydrate degradation. For the characterisation of extracellular enzymes the maximum enzyme activity (Vmax) is used (Hoppe, 1993). In this context, the enzyme activities at low MUF-substrate concentrations (Hr) were used for a better description of the in situ substrate hydrolysis. The distribution of Vmax of glucosidase activities in the salinity gradient of the Pomeranian Bight is shown in Nausch *et al.* (1998). Vmax and Hr correlated.

TCHO are substrates for glucosidase- and glucosaminidase activity. The mechanism of substrate stimulation can be made responsible for the correlation of these parameters. The rapid degradation of TCHO and uptake of MCHO can lead to a constant or lower level of dissolved TCHO and MCHO in this area. The relationship between glucosidase activity and MCHO was not so tight because MCHO can be directly released by phytoplankton in addition to the release after degradation of polysaccharides.

Figure 7 demonstrates the connection between glucose turnover, the hydrolysis of carbohydrates and the concentrations of MCHO and TCHO at salinities >5PSU. The To/Hr quotient correlated with MCHO as well with TCHO. The negative correlation between the To/Hr quotient and TCHO can be explained by substrate stimulation as a regulatory mechanism of extracellular enzyme activities (Münster, 1991, Rath *et al.*, 1993, Karner & Rassoulzadegan, 1995). The decrease of TCHO may cause a lower stimulation of glucosidase activity with the result that the importance of hydrolysis products for bacterial uptake is reduced. This assumption was supported by the decrease of the specific glucosidase activities in

the salinity gradient. The negative correlation between To/Hr quotients and MCHO can be attributed to the turnover which exceeded the hydrolysis and caused the decrease of MCHO-concentrations coming from other sources.

Acknowledgements

References

Benner, B., Pakulski, J. D., McCarthy, M., Hedges, J. I., Hatcher, P. G. (1992): Bulk chemical characterization of dissolved organic matter in the ocean. Science 255,1561−1564.

Chrost, R. J. (1991): Environmental control of the synthesis and activity of aquatic microbial ectoenzymes. In: Chrost, R. J. (ed.) Microbial enzymes in aquatic environments, Springer−Verlag, pp 29−59.

Grasshoff, K., Ehrhardt, M., Kremling, K. (eds.) (1983): Methods of seawater analysis, 2nd edition, Verlag Chemie, Weinheim, pp 419.

Handa, N., Tominga, H. (1969): A detailed analysis of carbohydrates in marine particulate matter. Mar. Biol. 2, 228−235.

Hellebust, J. A. (1965): Excretion of some organic compounds by marine phytoplankton. Limnol. Oceanogr. 10, 192−206.

Hellebust, J. A. (1974): Extracellular products. In Stewart, W.D.P. (ed.) Algal physiology and biochemistry. Blackwell, Oxford, pp 838−863.

Hoppe, H. G. (1993): Use of fluorogenic model substrates for extracellular enzyme activity (EEA) measurement of bacteria. In: Kemp, P.F., Sherr, B.F., Sherr, E.B., Cole J.J. (eds.) Handbook of methods in aquatic microbial ecology, Lewis Publishers, Boca Raton, pp 423−431.

Hoppe, H. G., Giesernhagen, H. C., Gocke, K. (1998): Changing patterns of bacterial substrate decomposition in a eutrophication gradient. Aquat. Microb. Ecol. 15, 1−13.

Johnson, K. M., Sieburth, J. McN. (1977): Dissolved carbohydrates in seawater I. A precise spectrophotometric analysis for monosaccharides. Mar.Chem. 5, 1−13.

Jost, G., Pollehne, F. (1998): Coupling of autotrophic and heterotrophic processes in a Baltic estuarine mixing gradient (Pomeranian Bight). Hydrobiol. 363, 107−115.

Karner, M., Rassoulzadegan, C., Rassoulzadegan, F. (1995): Extracellular enzyme activity: indications for short-term variability in a coastal marine ecosystem. Microb. Ecol. 30, 143−156.

Klok, J., Cox, H. C., Baas, M., Schuyl, P. J. W.,de Leeuw, J. W., Schenck, P. A. (1984): Carbohydrates in recent marine sediments—I. Origin and significance of deoxy- and O- methyl-monosaccharides. Org. Geochem. 7, 73−84.

Lee, C., Henrichs, S. M. (1993): How the nature of dissolved organic matter might affect the analysis of dissolved organic carbon. Mar. Chem. 41, 105−120.

Libes, S. L. (1992): An introduction to marine biogeochemistry. John Wiley & Sons, pp 394−422.

Liebezeit, G., Bölter, M. (1991): Water-extractable carbohydrates in particulate matter of the Bransfield Strait. Mar. Chem. 35, 389−398.

Mopper, K., Zhou, X., Kieber, R. J., Sirorski, D. J., Jones, R. D. (1991): Photochemical degradation of dissolved organic carbon and its impact on the oceanic carbon cycle. Nature 353, 60−62.

Münster, U., Chrost, R. J. (1990): Origin, composition, and microbial utilization of dissolved organic matter. In: Overbeck, J.,Chróst, R.J. (eds.) Aquatic microbial ecology. Biochemical and molecular approaches. Springer−Verlag, New York, pp 8−46.

Münster, U. (1991) Extracellular enzyme activity in eutrophic and polyhumic lakes. In: Chrost, R. J. (ed.) Microbial enzymes in aquatic environments, Springer–Verlag, pp 96–122.

Nausch, M., Kerstan, E., Pollehne, F. (1998): Extracellular enzyme activities in relation to hydrodynamics in the Pomeranian Bight (Southern Baltic Sea) Microb. Ecol. 36, 251–258.

Pastuszak, M., Nagel, K., Nausch, G. (1996): Variability in nutrient distribution in the Pomeranian Bay in September 1993. Oceanologia 38, 195–225.

Postel, L., Mumm, N., Krajewska-Soltys, A. (1995): Metazooplankton distribution in the Pomeranian Bay, (Southern Baltic)—Species composition, biomass, and respiration. Bull. Sea Fish. Inst. 3, 61–73.

Rath, J., Schiller, C., and Herndl, G. J. (1993): Ectoenzymatic activity and bacterial dynamics along a trophic gradient in the Caribbean Sea. Mar. Ecol. Prog. Ser. 102, 89–96.

Rohde, K. H., Nehring, D. (1979): Ausgewählte Methoden zur Bestimmung von In-halts-stoffen im Meer- und Brack-wasser. Geod. Geoph. Veröff. R.IV 27, 1–68.

Rosemarin, A., Notini, M., Soederstroem, M., Jensen, S., Landener, L. (1990): Fate and effects of pulp mill chlorophenolic 4,5,6-trichloroguaiacol in a model brackish water ecosystem. Sci. Total Environ. 92, 69–89.

Vrba, J. (1992): Seasonal extracellular enzyme activities in decomposition of polymeric organic matter in a reservoir. Ergeb. Limnol. Adv. Limnol. 37, 33–42.

v.Bodungen, Graeve, M., Kube, J., Lass, U., Meyer-Harms, B., Mumm, N., Nagel, K., Pollehne, F., Powilleit, M., Reckermann, M., Sattler, C., Siegel, H., Wodarg, D. (1995): Stoffflüsse am Grenz-fluß—Transport- und Umsatzprozesse im Übergangsbereich zwischen Oderästuar und Pommerscher Bucht (TRUMP). Geowiss. 12/13, 4–79–485.

Wedborg, M., Skoog, A., Folgeqvist, E. (1994): Organic carbon and humic substances in the Baltic Sea, the Kattegat, and the Skagerrak. In: Senesi, N., T.M. Miano (eds.) Humic substances in the global environment and implications in human health. Elsevier Pub., Amsterdam, pp 914–924.

Distribution and morphological parameters of the polychaete *Marenzelleria viridis* population in the Gulf of Riga

Vadims Jermakovs and Hans Cederwall

Introduction

In the Baltic Sea *M. viridis* was found first in 1985 in the Darss−Zingst estuary (Bick and Burckhardt, 1989) and in Polish waters (Gruszka, 1991). In 1988, this polychaete was found in the southeastern part of the Baltic Sea and near the shore region of Lithuania (Olenin and Chubarova, 1992).

Near the southern coasts of Sweden and Finland *M. viridis* was observed for the first time in 1989 and 1990 (Persson, 1990; A.-B. Andersin, unpubl.; Norrko *et al.*, 1993). Presently this species has become an important component in some Baltic coastal benthic communities (Kube *et al.*, 1996).

In the Gulf of Riga the first findings of *M. viridis* were done in 1988, near the mouth of the river Daugava (Lagzdins and Pallo, 1994). During the period 1988−1994 *M. viridis* spread all over the Gulf of Riga and became one of the dominating benthic species (Cederwall *et al.*, 1999).

The present study describes the distribution of *M. viridis* in the Gulf of Riga six years after introduction. Data on the morphological parameters of *M. viridis* in the Gulf are also presented.

The Gulf of Riga is one of the most eutrophied areas of the Baltic Sea. The annual primary production has been estimated to 4 million tons per year in 1989 (Andrushaitis *et al.*, 1992). This is about 290 $gcm^{-2}yr^{-1}$ which is approximately two times more than average for the entire Baltic proper (Elmgren, 1989). The area of the Gulf of Riga is 16330 km^2, and the drainage area is 8 times as large (Pastors, 1967). The mean and maximum depth of the Gulf is 27m and 62m, respectively.

The Gulf of Riga is seasonally (April−October) stratified thermally, with a thermocline between 20 and 30 m. Salinity varies between 4−7‰ (Yurkovskis *et al.*, 1993; Berzinsh, 1995).

Oxygen concentration in the near bottom water is usually between 4−8 mll^{-1}, but can decrease to 0.7 mll^{-1} during years of water stagnation (Botva *et al.*, 1987).

The macrozoobenthos of the Gulf of Riga has been monitored almost continuously since 1945 (Lagzdins, 1990). A clear increase in total abundance and biomass of macrozoobenthos has been observed since the beginning of the 1970s. The abundance of the dominating crustacean species, *Monoporeia affinis* and *Pontoporeia femorata*, decreased considerably, but that of *Macoma balthica* and the annelids increased (Gaumiga and Lagzdins, 1995).

Material and Methods

Samples were collected from 56 stations (Figure 1, Figure 2).

During July 1993 the sampling of sediments was done with a modified 0.05m^2 van Veen bottom-grab. During 1994 samples were taken with a BMB standard 0.1m^2 van Veen grab (Dybern *et al.*, 1976). The results of intercalibration do not show a significant difference between modified 0.05m^2 and BMB standard 0.1m^2 van Veen grabs. The sampling efficiency of these two bottom-grabs is similar (Jermakovs, unpubl.).

Five replicate samples were taken from each station in 1993 and one to three replicates were taken in 1994. A total of 162 samples have been analysed.

Sediments were sieved through a nylon net with 0.5mm mesh. The original construction of the sieves is described in "Comparisons between Soviet and Swedish methods of sampling and treating soft bottom macrofauna" (Ankar *et al.*, 1978). The residue of sediments with organisms was preserved in 4% formaldehyde solution, buffered with hexamine. The organisms were sorted under stereomicroscope. The organisms were weighed after drying on filter paper.

The specimens of *Marenzelleria viridis* were measured using a stereomicroscope, with a measuring ocular at ×16 magnification.
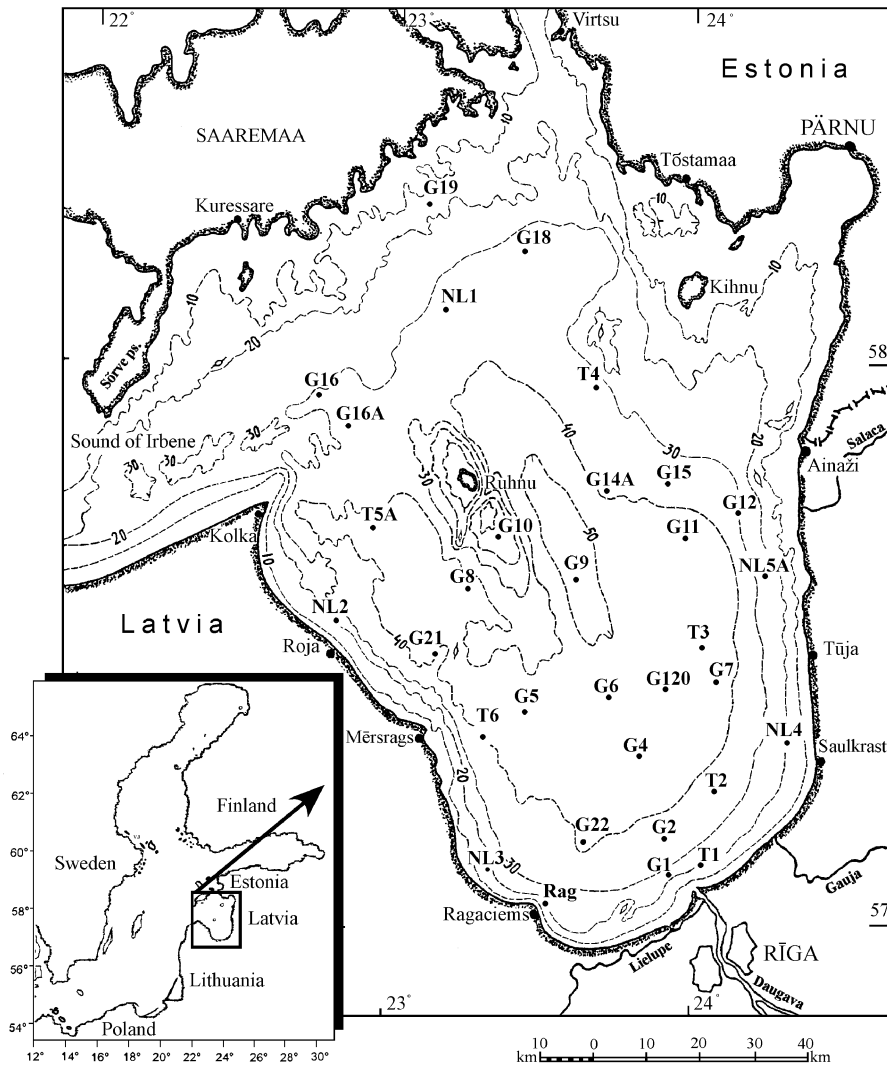
Figure 1 Map showing the location of the sampling stations in the Gulf of Riga.
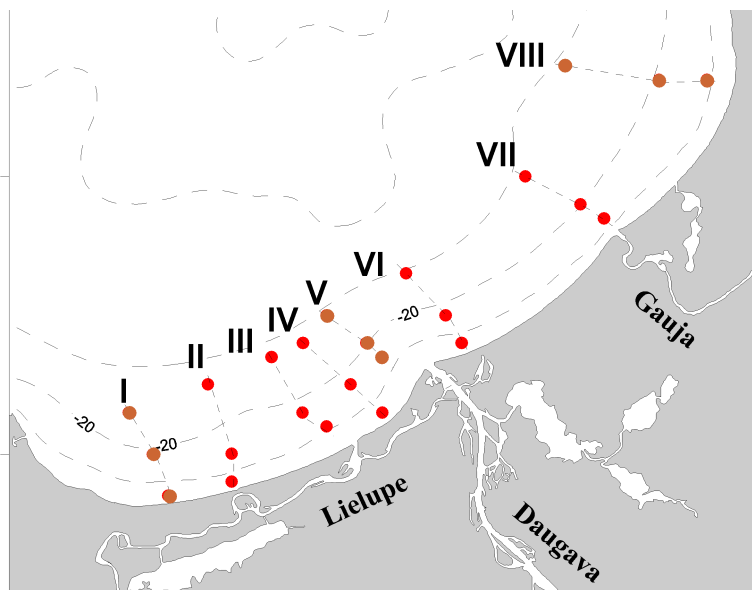
Figure 2 Map showing the location of the eight transects in the southernmost part of the Gulf of Riga. I– transect near the western coast of the Gulf of Riga; II– transect westward from the mouth of the river Lielupe; III– transect near the mouth of the river Lielupe; IV– transect between the mouths of the rivers Lielupe and Daugava; V– transect near the mouth of the river Daugava; VI– transect eastward from the mouth of the river Daugava; VII– transect near the mouth of the river Gauja; VIII– transect near the eastern coast of the Gulf of Riga.

Results and Discussion

Generally the highest concentrations of *M. viridis* were observed in the southern part of the Gulf, in the areas near the mouths of the large rivers—Lielupe, Daugava and Gauja (Figure 3). Mean densities of the polychaete ranged here between $500-3000$ ind.$\cdot$m^{-2}. Another area with high density of *M. viridis* was noticed near the mouth of Salaca river—in eastern part of the Gulf. In the central part of the Gulf the abundance of *Marenzelleria* was much lower—here densities did not exceed 150 ind.$\cdot$m^{-2}.
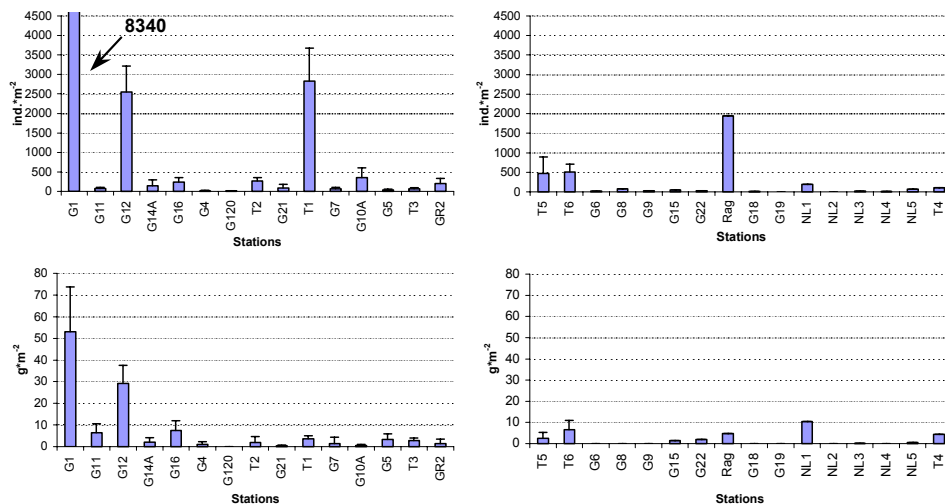
Figure 3 Average abundance and biomass of *Marenzelleria viridis* at selected stations from the Gulf of Riga. Error bars show standard deviation.

The maximum value for the Gulf of Riga, 8300 ind.$\cdot$m^{-2}, was recorded in July 1993 at site G1 near the mouth of the Daugava. One year earlier Lagzdins and Pallo (1994) reported the maximal density to be only 1380 ind.$\cdot$m^{-2} in the same area.

The density of *M. viridis* in the southwestern Baltic Sea, especially in estuaries and coastal lagoons is much higher—up to $39\,000$ ind.$\cdot$m^{-2} (Kube at al., 1996; Zettler, 1996). In these lagoons chlorophyll concentrations are $2-10$ times higher than in the Gulf of Riga (Jansone, 1995; Kube at al., 1996). Here a clear positive relationship between distribution, abundance and population dynamics of *M. viridis* and phytoplankton concentration was observed, because the water column in shallow waters is usually well mixed by wind (Kube at al., 1996). The Gulf of Riga is thermally stratified which may cause the absence of a strong positive relationship between phytoplankton concentrations and distribution of *M. viridis*.

In the southwestern Baltic Sea a high density of *Marenzelleria* was observed in the areas around the mouths of large rivers and in lagoons (Kube at al., 1996). High numbers of *M. viridis* near the mouth of the river Salaca (station G12, eastern part of the gulf) and especially in the southern part of the Gulf of Riga support the hypothesis that the river outflow has a positive influence on the distribution and density of *M. viridis* (Figure 3, Figure 4).

In the sandy sediments at 10 m depth the benthic community is dominated by polychaetes: *Pygospio elegans*, *Manayunkia aestuarina*, *Marenzelleria viridis* and *Nereis diversicolor*, which constitute about 66% of the total makrozoobenthos abundance (1650 ind.$\cdot$m^{-2}). At the same time polychaetes constitute only 7% of the benthos biomass (57.5 g$\cdot$m^{-2}) (Jermakovs, unpubl.). On average, *M. viridis* alone constitutes 25% and 1.4% of the total abundance and biomass, respectively. At a 30 m depth *Marenzelleria* constitutes 74% and 64% of the total biomass and total abundance, respectively. In comparison with other 20 m deep sites, high *M. viridis* abundance (Figure 4) was observed at a 20 m deep sampling site from the fifth transect, near the mouth of the river Daugava (Figure 2). This is probably due to deposition of large quantities of river-transported organic matter. That in turn provides plenty of fresh detritus at the surface of sandy sediment.
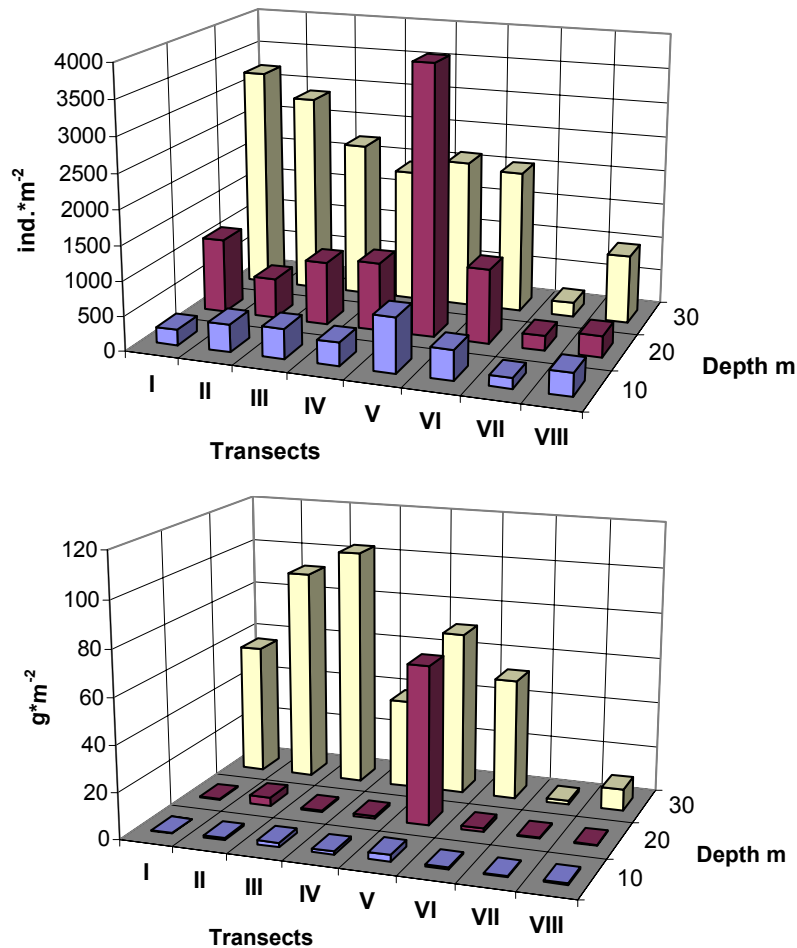
Figure 4 Average abundance and biomass of *Marenzelleria viridis* in the southernmost part of the Gulf of Riga.

In muddy sand and sandy sediments at 10 and 20m depth the population of *Marenzelleria* was dominated by juveniles (body width 0.3–0.6mm), while in muddy sediments at 30m depth adult specimens of *Marenzelleria* dominated (body width 0.9–1.8mm). It can be partly explained by young *M. viridis* avoiding high concentrations of adult individuals, as was observed in the Ems estuary (Essink and Kleef, 1993).

Animal size was measured both as their length and width, the latter since many of the animals found were broken during the sampling and sieving process. Significant correlations were found between length and weight of Marenzelleria as well as between width and weight and width and length (Figure 5). The results of regression analyses are given in Table 1.

The morphological parameters of *M. viridis* from the Gulf of Riga and other regions of the Baltic Sea are different. In Germany, in the Darss–Zingst estuary and in Oderhaff the maximum body width of *M. viridis* is 2.8–3.1mm (Zettler *et al.*, 1995; Kube *et al.*, 1996). Specimens of *M. viridis* from the Pomeranian Bay have a maximum body width of 2.5–2.6mm (Kube *et al.*, 1996). Along the East coast of North America, the native land of *M. viridis*, in Great Sippenissett salt marsh (Massachusetts, USA) the body width of *M. viridis* at 5th segments are 2.5mm (Sarda *et al.*, 1995). The greatest worms from the Gulf of Riga were recorded by Lagzdins and Pallo (1994), having more that 260 segments, body length 100mm and width at the 7–10 segments up to 2.5mm.
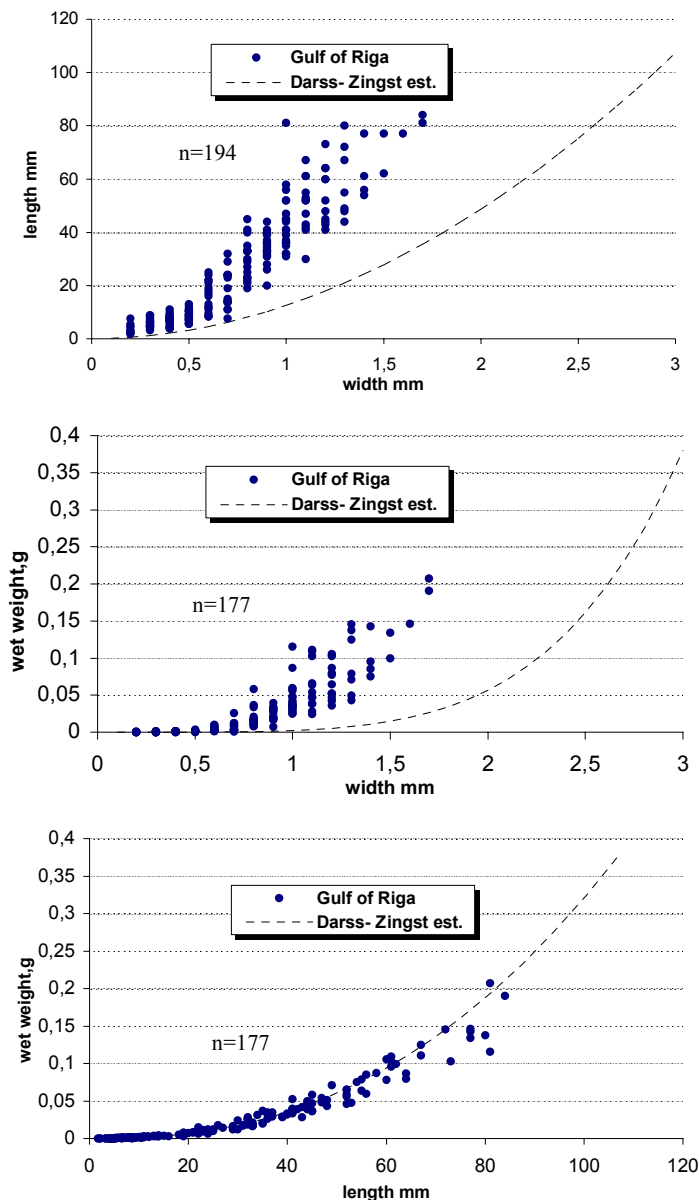
Figure 5 Relations between length, width and weight of *Marenzelleria viridis* from the Gulf of Riga in comparison with data from Darss−Zingst estuary (Zettler, 1996).

The size−weight relationship of *M. viridis* was studied more detailed in Germany, in the Darss−Zingst estuary (Zettler, 1996). The specimens of *M. viridis* from the Gulf of Riga have 0.5−1 mm less width than those of the same length from Darss−Zingst estuary. Consequently *M. viridis* from the Gulf of Riga have less width than specimens of the same weight of *M. viridis* from the Darss−Zingst estuary (Figure 5). The methods of measuring the morphological parameters of *M. viridis* in Latvia and in Germany were not intercalibrated, but they are approximately the same. If the difference in width−length−weight ratio between the Darss−Zingst estuary and the Gulf of Riga was due to incompatibility of methods, then the regression lines for the size−weight relationship should be parallel. However, that was not the case. Therefore, more probably the observed difference was due to different environmental conditions between the studied regions.

Variables	Number of measured specimens	Coefficient of determination r^2	Linear equation
Length/width	194	0.8813	$Y=36.94 \cdot X^{1.6812}$
Weight/length	177	0.9787	$Y=7.82 \cdot 10^{-6} \cdot X^{2.269}$
Weight/width	177	0.8913	$Y=0.0303 \cdot X^{3.792}$

Table 1 Results of regression analysis on size-weight relationship of *Marenzelleria viridis* from the Gulf of Riga, Baltic.

Conclusions

- *M. viridis* was the most abundant species in the soft-bottom macrozoobenthos community of the Gulf of Riga in the mid-1990s.

- The highest abundances of *M. viridis* were found near the outflow of the three largest rivers in the southern part of the Gulf.

- In the southern part of the Riga Gulf adult individuals of *M. viridis* dominate on the soft muddy sediments at depths of around 30m, while juveniles dominate in the shallow waters and on sandy sediments.

- Significant correlations between length, width and weight of *M. viridis* give a possibility to estimate the length and weight of fragmented specimens from data on body width.

Acknowledgements

References

Andrushaitis, G., Andrushaitis, A., Bitenieks, Y., Lenshs, E. and. Priede, S., 1992. Organic carbon balance of the Gulf of Riga. Proceedings of the 17th CBO Conference, Norrköping 1990, Swedish Hydrological & Meteorological Institute Report, p. 59–66.

Ankar., S., Cederwall, H., Lagzdins, G. and Norling, L., 1978. Comparison between Soviet and Swedish methods of sampling and treating soft bottom macrofauna—Final report from the Soviet–Swedish Expert Meeting on Intercalibration of Biological Methods and Analyses, Askö, July 5–12, 1975. Contrib. Askö Lab. Univ. Stockholm, 23:1–38.

Berzinsh, V., 1995. Hydrology. In: E. Ojaveer (editor), Ecosystem of the Gulf of Riga between 1920 and 1990. Estonian Academy Publishers, Tallinn: 7–31.

Bick, A. and Burckhardt, R., 1989. First record of Marenzelleria viridis (Polychaeta: Spionidae) in the Baltic Sea, with a key to the Spionidae of the Baltic Sea. Mitt. Zool. Mus. Berl. 65: 237–247.

Botva, U., Filmanovicha, R. and Alksne, M., 1987. Areal survey of hydrochemistry in the Eastern Baltic Proper, the Gulf of Riga and the Gulf of Finland. Hydrobiological and hydrochemical characteristics of the eastern part of Baltic Sea. The Gulf of Riga and the Gulf of Finland. Riga: 20–39. (in Russian).

Cederwall, H., Jermakovs, V. and Lagzdins, G., 1999. Long-term changes in the soft-bottom macrofauna of the Gulf of Riga. ICES Journal of Marine Science, 56, Suppl.: 41–48.

Dybern, B.I., Ackefors, H. and Elmgren, R., 1976. Recommendations on methods for marine biological studies in the Baltic Sea. BMB Publ. No. 1: 1–98.

Elmgren, R., 1989. Man's impact on the ecosystem of the Baltic Sea: Energy flows today and at the turn of the century. Ambio, 18: 326–332.

Essink., K., and Kleef, H. L., 1993. Distribution and life cycle of the North American Spionid Polychaete Marenzelleria viridis (Verrill, 1873) in the Ems Estuary. Neth. J. Aquat.Ecol.27:237–246.

Gaumiga, R. and Lagzdins, G., 1995. Macrozoobenthos. In: E. Ojaveer (editor), Ecosystems of the Gulf of Riga between 1920 and 1990. Estonian Acad. Publ. Tallinn: 198–211.

Gruszka, P., 1991. Marenzelleria viridis (Verill, 1873) (Polychaeta, Spionidae)—a new component of shallow water benthic community in the southern Baltic. Acta Ichtyol. Pisc. 21, Suppl.: 57–65.

Jansone, B., 1995. Concentration of chlorophyll "a" in the Gulf of Riga. In: E. Ojaveer (editor), Ecosystem of the Gulf of Riga between 1920 and 1990. Estonian Academy Publishers, Tallinn: 127–130.

Kube, J., Zettler, M. L., Gosselck, F., Ossig, S. and Powilleit, M., 1996. Distribution of Marenzelleria viridis (Verrill, 1873) (Polychaeta: Spionidae) in the southwestern Baltic Sea in 1993/94—ten years after introduction.Sarsia 81: 131–142.

Lagzdins, G., 1990. Gulf of Riga. In: HELCOM, Second periodic assessment of the State of the marine environment of the Baltic Sea, 1984–1988. Background document. Baltic Sea Environmental Proceedings 35B. Helsinki: 257–258.

Lagzdins, G., and Pallo, P., 1994. Marenzelleria viridis (Verrill) (Polychaeta, Spionidae)—a new species for the Gulf of Riga. Proc. Estonian Acad. Sci. Biol., 43(3): 184–188.

Norrko, A., Bondsdorff, E., and Boström, C., 1993. Observations of the polychaete Marenzelleria viridis (Verrill) on a shallow sandy bottom on the south coast of Finland. Memoranda Soc. Fauna Flora Fennica, 69: 112–113.

Olenin, S. and Chubarova, S., 1992. Recent introduction of the North American spionid polychaete Marenzelleria viridis (Polychaeta, Spionidae) in the coastal areas of the south-eastern part of the Baltic Sea. In: International Symp. On Functioning of Coastal Ecosystems in Various Geographical Regions.September 23–25, 1992. Gdansk University, Poland, p.20

Pastors, A., 1967. Water and heat balance in the Gulf of Riga. Morzskie zalivy kak priyomniki stochnykh vod. Riga, Zinatne: 8–20. (in Russian).

Persson, L. -E., 1990. The national Swedish environmental monitoring programme (PMK): Soft-bottom macrofauna monitoring of the south coast of Sweden—Annual Report 1990. Naturvårdsverket Rapport, 3937: 5–12.

Sarda, R., Valiela, I. and Foreman, K., 1995. Life cycle, demography, and production of Marenzelleria viridis in a salt marsh of southern New England. J. mar. biol. Ass. U.K. 75: 725–738.

Yurkovskis, A., Wulff, F., Rahm, L., Andrushaitis, A. and Rodrigues-Medina, M., 1993. A nutrient budget of Gulf of Riga, Baltic Sea. Estuarine, Coastal and Shelf Sci. 37: 113–127.

Zettler., M. L., Bick, A. and Bochert, R., 1995. Distribution and population dynamics of Marenzelleria viridis (Polychaeta: Spionidae) in a coastal water of the southern Baltic. Arch. Fish. Mar. Res. 43(3): 209–224.

Zettler, M. L., 1996. Ökologische Untersuchungen am Neozoon Marenzelleria viridis (Verrill, 1873) (Polychaeta, Spionidae) in einem Küstengewässer der südlichen Ostsee. Dissertation, Rostock University, Rostock, Germany.

The ecophysiological consequences of the underwater light climate in a shallow Baltic estuary

Hendrik Schubert, Louise Schlüter, and Peter Feuerpfeil

A series of highly eutrophic shallow water systems, locally called boddens or haffs, occur along the southern coastline of the Baltic Sea. One of these estuaries, the Darss–Zingst bodden chain (DZBC), has been the main subject of investigation at the Department of Ecology, University of Rostock for many years. The yearly succession of phytoplankton in this system typically shows a spring and autumn bloom of green algae, separated by a long period of high cyanobacterial biomass in the summer months (Figure 1). The reason for this mass algal development lies in the trophic status of the water, in other words the rich availability of nutrients. This is, however, a cause for all algal blooms, and is not specific to cyanobacteria. "Cyanobacterial blooms" describes the development of organisms which may show a wide phylogenetic separation. The factors leading to algal blooms are accordingly diverse, and may vary from water to water. The following properties of cyanobacteria have been cited in the literature as reasons for cyanobacterial blooms:

1. their high nutrient affinity (Reynolds, 1987)

2. the ability to store nutrients (Allen and Hutchinson, 1980)

3. their high temperature optimum (Foy *et al.*, 1976)

4. a low maintenance energy requirement (Zevenboom and Mur, 1984)

The summer blooms of the DZBK are unusual, in that they consist of a mixture of small unicellular cyanobacteria (picoplankton). The occurrence of a mixed bloom suggests that the causal factor is relatively unspecific. The causes listed above will now be examined for their relevance to our system. Points 1 and 2 can be discounted because nutrient concentrations in the DZBK are not low enough to be limiting (Schlungbaum and Nausch, 1994). In the light of other experiments, point 3 is also unlikely to be important (Sagert *et al.*, 1993, Zhuang *et al.*, 1993). The low metabolic requirements of cyanobacteria are also unlikely to be important, as they are advantageous only during periods of adverse environmental conditions e.g. in deeper waters with greater depths of vertical mixing. A replacement of dominant green algae by cyanobacteria on these grounds is therefore not possible.
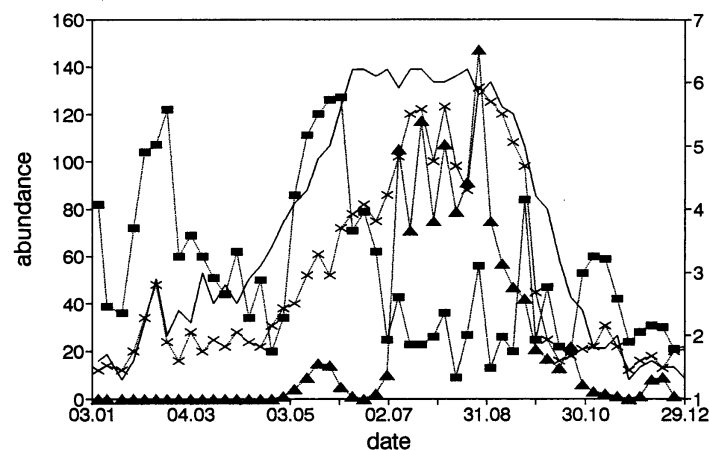
Figure 1 Annual course of phytoplankton species composition, and global irradiance at the Zingst field station (on the Darss–Zingst bodden chain). Results of weekly phytoplankton counts are presented (in millions of cells per litre), as well as the weekly sum of global irradiance (MJ/m^2)
Symbols: ■−green algae, ♦−colonial and filamentous cyanobacteria, ×−unicellular cyanobacteria, continuous line− global irradiance.

Because of the strong correlation between the annual temperature curve and cyanobacterial numbers, it may be possible that both are driven principally by the amount of irradiance reaching the system, and that the role of irradiance should be examined in more detail.

Spectrally-resolved transmission coefficients are low throughout all parts of the DZBK (Figure 2). This reduction in light penetration is due to large quantities of living and dead organic material in the water column (Schubert *et al.* 2000). The spectral range of light in the water column becomes narrower, being restricted to around 580 nm, with increasing depth. The light conditions at all depths in the water column are relevant for phytoplankton.
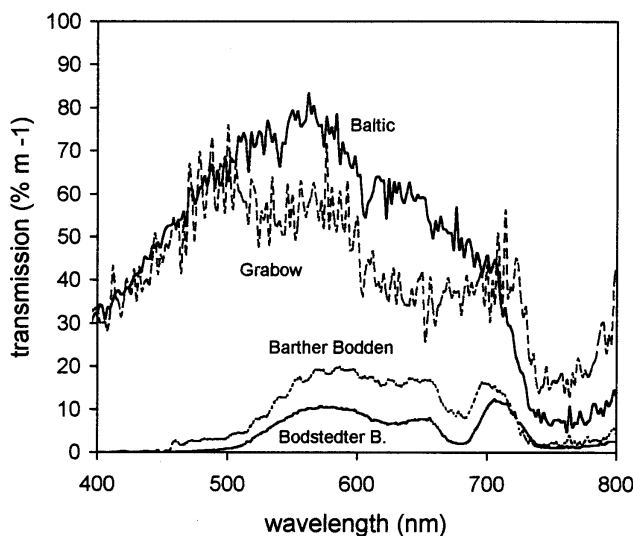
Figure 2 Spectrally-resolved transmission measurements from different areas of the DZBK. Measurements were made on 15 July 1995, with a double-monochromator spectroradiometer (Macam Photometrics Ltd., Scotland) at 5 different depth intervals.

The bodden chain lies in a west-east direction, which means that the longest reaches of open water are aligned with the direction of the prevailing wind. Even the slightest wind speeds are sufficient to cause a complete mixing of the water column, which is mostly 80–100 cm deep. The wind-dependence of this circulation shows that phytoplankton organisms are exposed either to full surface irradiance, or to total darkness on average every 20 minutes (Schubert *et al.* 1995a).
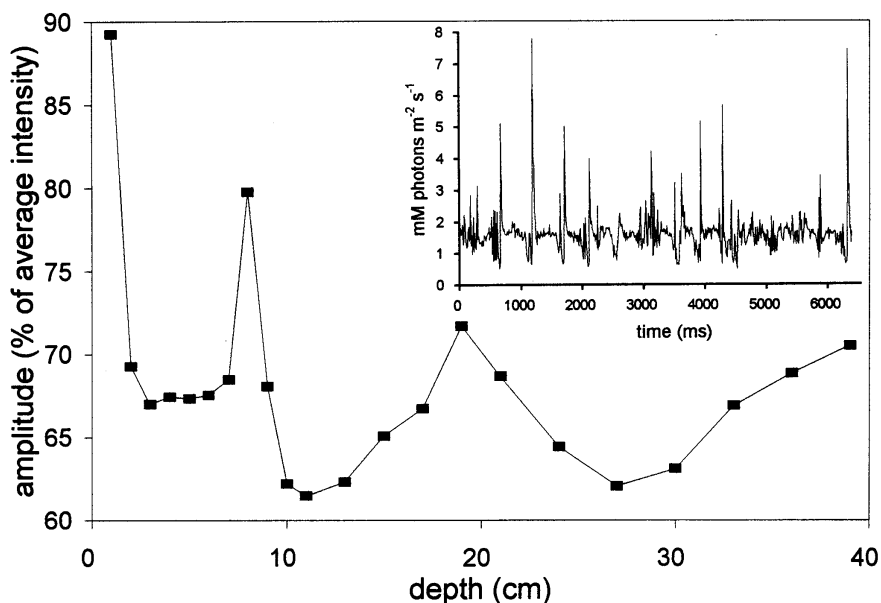
Figure 3 Depth profile of wave focusing effects in the DZBK near Zingst. The average amplitude of the wave-focusing effect is plotted as a percentage of the average irradiance. Measurements were made on 2.9.1995 between 10.45 and 15.15 with 8/8 thin stratus cloud cover. Shown in the insert is an example of a single measurement at a depth of 1 cm at the same station but with cloudless conditions (29.8.1995).

A further effect is noticeable near the surface of the water, the so-called "wave-focusing" effect. Each wave acts as a lens and focuses the light in a certain depth. Several focusing depths occur simultaneously due to the presence of different forms of surface waves. The result of the focusing is that organisms may be exposed to light intensities greater than those

at the surface (Figure 3). Irradiance is increased to 4 to 5 times the surface irradiance at the first focusing depth (1 cm, Figure 3, insert); this irradiance is clearly "oversaturating". The focusing effect is weak at 6 cm depth, but increases again at 8 cm to form a second maximum. A third, weaker maximum is seen at approx. 20 cm. Planktonic organisms are therefore exposed to extremely fast changes in the light climate, of both quantitative, and, with increasing depth, qualitative nature.

The ability to react to these changes, and to adapt to either the short, concentrated light pulses at the surface, or to make optimal photosynthetic use of the longer periods of low light availability, may give a competitive advantage.

Adaptation to high light always consists of a change in the pigmentation of the organisms, e.g. a change in the ratio of photoprotective pigments to photosynthetically-active light harvesting pigments.

Carotenoids are the main photoprotective pigments in both green algae and cyanobacteria. Photosynthesis and light harvesting are due, with the exception of the outer (PSII) antenna, to chlorophyll a (chl a). Chl a in the reaction centres is the pigment most likely to be damaged by excess light. The ratio of carotenoids to chl a give an indication of the high light tolerance. Published values for this ratio are difficult to compare because of differences in the light sources and light measuring equipment used. Therefore, an experiment was carried out in which the pigmentation of 10 species of cyanobacteria (5 unicellular, 2 filamentous and 3 colonial) and 7 green algal species were measured after culture at light intensities between 20 and 260 μmol photons $m^{-2}s^{-1}$ (Figure 4). The chl a / carotenoid ratio of cyanobacteria is always lower than that of green algae. In effect, more protective pigments are available per chl a. This type of analysis does not show the extent to which these pigments are actually active in photoprotection.
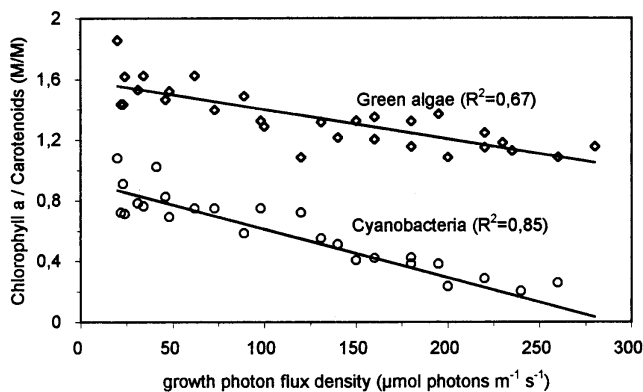
Figure 4 Chlorophyll a / carotenoid ratios (mole/mole) for 10 species of cyanobacteria (m) and 7 green algal species (7) after precultivation for 6 days at different irradiances (x-axis).

The next major difference between cyanobacteria and green algae is found in the composition of the carotenoid pigments. Green algae (and higher plants) have the three pigments of the "xanthophyll cycle", violaxanthin, antheraxanthin and zeaxanthin, which are interconvertible in the presence of light. Of the three xanthophyll cycle pigments, only zeaxanthin is detectable in cyanobacteria, which rules out the presence of a xanthophyll cycle. Cyanobacteria, however, possess a range of glycosidic carotenoids (sugar-carotene compounds), which have up to 14 conjugated double bonds, and are otherwise only known in the myxobacteria.

The simplest form of photoprotection occurs when the carotenes, because of their high molar absorption coefficients, reduce the irradiance inside the cell and act as filters. The efficiency of this form of photoprotection in cyanobacteria is only an energetic problem: sufficient quantities of carotene must be produced to form the filter. Otherwise, the blocking of the blue region of the spectrum by carotenoid pigments does not interfere with the light-harvesting process, as light-harvesting in these algae is largely due to phycobiliproteins, which absorb outside of the blue range.

A problem occurs when this type of photoprotection is used by green algae. Carotenoids absorb the complete blue part of the spectrum, to 500 nm. A carotenoid accumulation would cause shading not only of the reaction centres, but also of the main chl a / chl b light-harvesting antenna. This has important consequences under the fluctuating conditions of the DZBC. Accumulation of carotenoids to provide photoprotection at the surface will result in loss of light harvesting ability when cells leave the surface and return to low light conditions. Alternatively, a low concentration of carotenoids may cause the cells to be light-damaged during the short periods at the surface. Two mutually exclusive strategies based on fixed chl a / carotene ratios would appear to be possible, and the two extreme forms of these strategies are indeed exhibited between the mature and spore stages of some green algae. However, other possibilities may have developed

during evolution. The xanthophyll cycle offers a more flexible photoadaptive strategy. Forms of the xanthophyll cycle have been found in all eukaryotic photoautotrophs, other than those (such as the red algae) which utilise phycobiliproteins as light-harvesting pigments and avoid the antenna-shading problem altogether. There is still debate over which of the many suggested protective mechanisms is actually fulfilled by the xanthophyll cycle. Zeaxanthin is suggested to be active in the conversion of absorbed light energy to harmless heat energy. The light dependent conversion of violoxanthin to zeaxanthin results in a decreased efficiency of light energy transfer in the antenna and between the antenna and reaction centres. This reduces the excitation pressure on the reaction centre.

A simple uncoupling of the antenna from the reaction centre will also achieve this, as has been shown for cyanobacteria (Mullineaux, 1988). Why is this method not possible for green algae, or for all organisms with a chl a / chl b antenna?

Overexcitation of chl can lead to the formation of long-lasting, triplet excitation states, which can transfer their energy to oxygen molecules. The result is the formation of a highly energetic oxygen radical, capable of oxidising and destroying all biomolecules in its vicinity. An uncoupling of the antenna may save the reaction centre, but without additional mechanisms to protect itself, the antenna may be oxidised.

The energy level of the (singlet) excitation state of all carotenoids becomes lower as the number of double bonds is increased (Murasecco–Suardi et al., 1988). Carotenoids with 9 conjugated double bonds are able to transfer energy to chl a. Functionally active light harvesting carotenes with this number of bonds are common on diatoms and brown algae. The energy level of the first excited state is higher than the first excited state of chl a. In contrast, carotenes with 11 or more conjugated double bonds show both in vivo and in vitro an ability to quench excited chlorophyll and oxygen molecules (Krinsky, 1971).

The conversion of violoxanthin to zeaxanthin means that a light harvesting pigment has been converted to an "energy trap", which can reduce excitation pressure in the antenna and quench oxygen radicals. [The reaction centre, according to Telfer and Barber (1995) contains only ß-carotene, which acts as a quencher but not as energy trap due to its distance from chl a. This is undoubtedly a sensible compromise between efficiency of light use, and protection requirements.]

The production of an energy trap via enzymatic deepoxidation has a further advantage: during the quenching of oxygen radicals the zeaxanthin may be destroyed with probability of 1:1000 (Foote et al., 1970). Some of the reaction products are the epoxy-compounds, antheraxanthin and violaxanthin. These products will be immediately converted back to zeaxanthin, so that a recycling of the destroyed photoprotective pigments takes place. This explains the low carotene / chl a ratio of green algae.

Continuous shading of the light-harvesting antenna is avoided by the production of protective pigments only under stress conditions (Schubert et al., 1994). Phycobiliprotein-containing organisms which absorb light energy outside the carotenoid bands do not require this series of reactions, and can afford to have excessive concentrations of carotenoids without the danger of self-shading. There is still the consideration of overexcitation within the light-harvesting antenna itself. It appears that no antenna protection mechanisms are present in this group of organisms. The reason is that phycobiliproteins, although structurally similar to the chlorophylls, are not able to form excited triplet states (at least not in measurable quantities, pers. comm. Prof. H. Scheer, München), and will not produce oxygen radicals. The phycobiliprotein antenna system can be safely decoupled from its reaction centre. This may be the reason why cyanobacteria and red algae can "misuse" their antenna as a nitrogen-store, without the dangers of excessive overexcitation. The presence of these storage antenna are apparent in the form of increased PBS fluorescence emission in comparison to PS II fluorescence, showing that the antenna are not coupled to the reaction centre. This explains the frequent descriptions of "inverse adaptation" in the cyanobacteria (Raps et al., 1983). Increasing light intensity makes more energy available for the deposition of N stores, so that the PBS content per cell increases and the antenna size increases. Observation of the emission spectrum shows that only a small part of the pigment pool functions as an antenna. Decreasing the nitrogen supply reduces the antenna emission so that the oft-cited and astonishingly high energy-transfer value of 98% is reached (Figure 5).

On the other hand, photosynthesis is only possible in the presence of chl a, and cyanobacterial reaction centres also have this pigment.
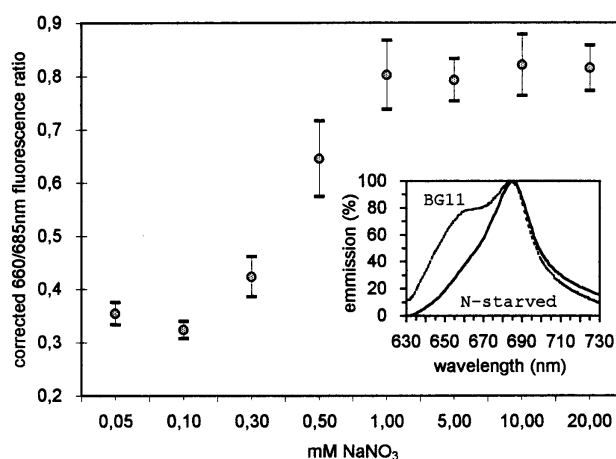
Figure 5 Absorption-corrected 660/685 nm fluorescence emission ratios of *Synechocystis* sp. 6803 cultured with different concentrations of nitrate in the medium.
The emission ration was corrected for the absorption at 625 nm. Measurements were made after 6 days growth in BG-11 medium, after replacement of all N-sources in the medium with the concentrations of $NaNO_3$ shown on the X-axis. Insert: emission spectra of *Synechocystis* sp. 6803 with 580 nm excitation light. Dashed line: final state after culture with saturating N-supply (BG11 medium), continuous line: condition after 5 generations in N-free BG-11 medium. The emission spectra consist of: a shoulder at 660 nm which is due to autoemission of the phycobilisome, a fluorescence maximum at 685 nm from PS II. The PS II peak is derived from excitation energy transferred from the phycobilisome, as PS II does not absorb at the chosen excitation wavelength of 580 nm.

The danger of an overexcitation of the reaction centre under stress conditions, with subsequent triplet formation and active oxygen formation, is reduced by decoupling of the antenna, and by shading of the reaction centre, but there is still some risk to the reaction centre under normal operating conditions. There is a need for additional protective quenching mechanisms in addition to the shading provided by carotenoids. The reaction centre itself is protected in cyanobacteria and in green algae by the internal presence of a ß-carotene molecule. Other photoprotective functions, for example for the lipids of the various membrane systems, may be performed by not by the "filter" carotenoids, but by other (membrane-bound?) carotenoids. The latter pool should have a much shorter lifetime (higher turnover). Radiocarbon-labelling experiments were performed in order to separate between the active and passive photoprotection roles of carotenoids. There were only small differences between the rates of pigment labelling in *Synechocystis* and *Chlorella* after exposure to the irradiance at which they were grown (not shown). *Synechocystis* reacted to an increase in the incident irradiance by immediately increasing the rate of carotenoid metabolism (Figure 6). The speed of the response, less than 15 min, is surprisingly fast. Equally surprising was the finding that myxothanophyll, previously thought of as having only a shading function, showed the highest turnover. Due to the speed and flexibility of its carotenoid response, *Synechocystis* appears to be able to react much faster to a light stress than *Chlorella*, in which a delay was noticed between stress and response (Figure 6). The frequency at which the irradiance changes between high light and low light is likely to determine which photoprotective strategy will be most successful. The speed at which chlorophyll-breakdown products (phaeophytins) appear is a good indicator of the damage caused by the light stress (Figure 7). The short-term photoprotective mechanisms of *Synechocystis* appear to work well, as the first breakdown products do not appear until after 45 min. Phaeophytin products are detectable in *Chlorella* soon after the start of the light stress, indicating insufficient photoprotection, but after 60 minutes the production has stabilised and there is evidence of an adaptation.

Cyanobacteria can withstand short periods of high light stress firstly because of their larger available pool of carotenoids, and secondly because of the greater flexibility of their metabolism. Green algae appear to be better adapted to withstand longer periods of light stress due to their possession of a recycling system, and their K-strategy oriented acclimation reactions.
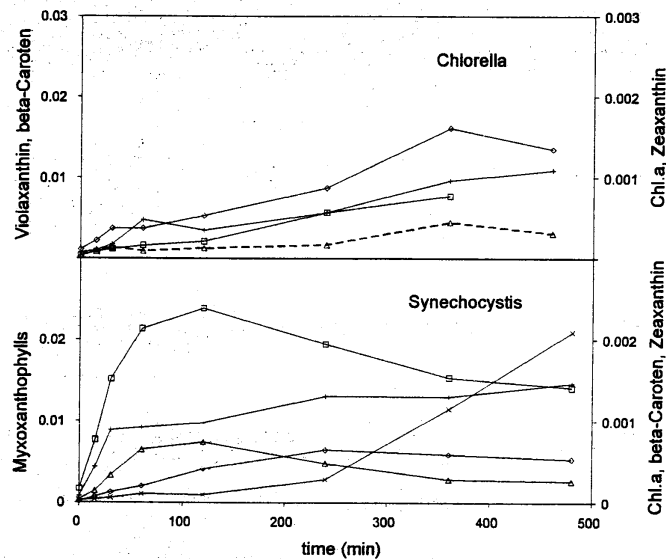
Figure 6 Kinetics of the integration of radioactive carbon into certain pigments after increase of the irradiance from 25 to 180 µmol photons $m^{-2} s^{-1}$. The radioactivity of the pigments is given as disintegrations per absorption unit. The method was to extract samples at the time points shown after the beginning of the light stress (and simultaneous supply of $Na\,H^{14}CO_3$). The pigment extracts were separated by HPLC, then the individual fractions were collected and analysed for radioactivity.

Symbols: ◇−Chl a, Δ−ß-Carotene, +−zeaxanthin, ×−myxoxanthophyll-1, ❑−myxoxanthophyll-2 (*Synechocystis*) or violaxanthin (*Chlorella*). For further details see Schubert (1996).
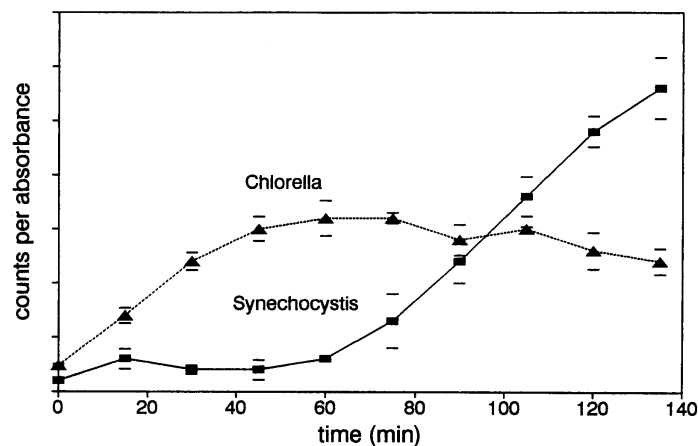
Figure 7 Kinetics of radioactively-marked phaeophytin labelling after increasing the irradiance from 25 to 260 µmol photons $m^{-2} s^{-1}$. The concentration of radioactively labelled phaeophytin at different time points after the beginning of the light stress is shown (disintegrations per absorption unit), with standard deviations for 4 samples. The algae were marked with $NaH^{14}CO_3$ 6 h before the start of the experiment. For further details see Schubert (1996).

The retention of full photosynthetic performance after exposure to light stress depends not only on the availability of photoprotective pigments. Other factors include the ability to process light energy through the electron transport chain and avoid an overloading at PSII. Many cyanobacteria have the ability to couple photosynthetic and respiratory electron transport, and thus reduce the pressure on PSII, as described more fully in Schubert *et al.* (1995b). On the other hand, this can led to a better ability to utilise the very short pulses of the wave-focusing for photosynthesis purposes, because part of the photosynthetic electron transport chain of these cyanobacterial species are activated by respiration already in darkness, so additional electrons coming from PSII can be used without delay caused by the formation of a sufficient pH-gradient prior onset of ATP-production (Figure 8).
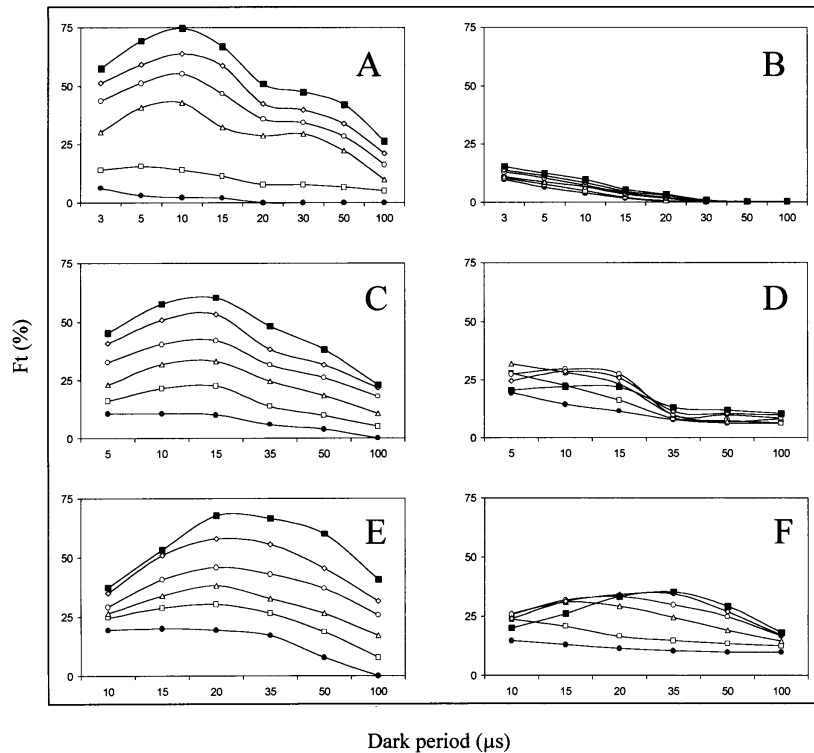
Figure 8 Dependency of PSII-fluorescence from light intensity, dark period and duration of short light pulses comparable to wave focusing events.

The values of triggered fluorescence (Ft) are shown, as a percentage of the variable fluorescence measured in the dark before switching on the pulses generated by a 660 nm LED. The x-axes indicate the length of the dark period between two successive pulses. Intensities of the pulses in μmol photons $m^{-2}s^{-1}$: ●−12, □−24, △−34, ○−50, ◈−64, ■−114. Left panels (A, C, E): *Synechocystis* spec. PCC 6803 (Cyanobacteria), right panels (B, D, F): *Chlorella vulgaris* (Chlorophyta). Duration of the individual pulses: A, B − 3μs, C, D − 5μs, E, F − 10μs. The pronounced shoulder in the left side of A and B indicate photosynthetic activity of *Synechocystis* already at very long dark intervals, whereas electron transport in *Chlorella* start much later at approx. 20–15μs dark intervals.
The experimental setup is described in detail in Schubert (1996).

A further advantage for cyanobacteria in the light conditions of the DZBC comes from their better ability to achieve an equilibration of excitation energy between the photosystems (state transition) in comparison with green algae. As described in Schubert *et al.* (1995a), cyanobacteria can react almost without delay to a change in light quality whereas the slower reaction in green algae may lead to a loss in efficiency.

In addition to all of the above factors, it can be seen that the wavelengths of light which penetrate most deeply in the DZBC (at 580 nm) are better absorbed by cyanobacteria then their green algal competitors. Therefore, the gradient in irradiance in the water column is less steep for cyanobacteria than for green algae.

The highly unstable light climate with periods of extreme high light stress do not seem to be a problem for cyanobacteria, and may even give a selective advantage, as shown in experiments where cyanobacteria were exposed to high frequency light stress (Schubert *et al.*, 1995c). If photoinhibtion occurs immediately after light stress, as in green algae, then recovery may not be fully complete before the start of the next light phase. This means that both the optimal and suboptimal irradiances occurring after the surface exposure will not be utilised efficiently, which can be a disadvantage under fluctuating light conditions. The reason for the sensitivity of cyanobacteria to continuous light stress can only be speculated. The green algal response to an increase in irradiance, namely to reduce the capacity of the light reactions, seems to be necessary in order to balance the metabolic requirements after the change from light limitation to nutrient limitation.

It could be possible that cyanobacteria under fluctuating light conditions become nutrient-limited at a later stage than green algae. This is because nutrient storage takes place under optimal conditions, the reserves may last for several generations. Limitation is most likely to be due to the CO_2 supply, in this case water movement does not increase the supply. Large changes have been observed in the cyanobacterial photosynthetic apparatus during CO_2 limitation experiments, and changes caused by this factor can not be ruled out (Reuter and Müller, 1993).

Finally, it should be mentioned again that cyanobacterial diversity is very high in comparison to green algae. Not all of the mechanisms described above will occur in every cyanobacterial species, and not all of the physiological mechanisms can be explained. The selection presented here was chosen for their relevance to the particular problems of the DZBC.

Acknowledgements

References

Allen, M.M. and Hutchinson, F, 1980, Nitrogen limitation and recovery in the cyanobacterium *Aphanocapsa* 6308. Arch Microbiol. 128, 1−7

Foote, C.S., Chang, Y.C. and Denny, R.W., 1970, Chemistry of singlet oxygen. XI. Cis-trans isomerization of carotenoids by singlet oxygen and a probable quenching mechanism. J. Am. Chem. Soc. 92, 5218−5219

Foy, R.H., Gibson, C.E. and Smith, R.V., 1976, The influence of daylength, light intensity and temperature on the growth rates of planktonic blue-green algae. Br. Phycol. J. 18, 267−273

Krinsky, N.I.: Function. In: Isler, O. (Ed.), 1971, Carotenoids. 36−92. Basel: Birkhäuser−Verlag

Mullineaux, C.W. and Allen, J.F., 1988, Fluorescence transients indicate dissociation of photosystem II from the phycobilisome during the state-2 transition in the cyanobacterium Synechococcus 6301. Biochim. Biophys. Acta 934, 96−107

Murasecco−Suardi, P., Oliveros, E., Braun, A.M. and Hansen, H., 1988, Singlet-oxygen quenching by carotenoids: steady-state luminescence experiments. Helv. Chim. Acta 71, 1005−1010

Raps, S., Wyman, K., Siegelman, H.W. and Falkowski, P.G., 1983, Adaptation of the cyanobacterium *Microcystis aeruginosa* to light intensity. Plant Physiol. 72, 829−832

Reuter,W. and Müller, C., 1993, Adaptation of the photosynthetic apparatus of cyanobacteria to light and CO2. J. Photochem. Photobiol. B. Biol. 21, 3−27

Reynolds, C.S., 1987, Cyanobacterial water-blooms. In: Callow, P. (Ed.): Advances in botanical Research 13. S. 67−143. London: Academic Press

Sagert, S., Schubert, H. and Suchau, A., 1993, Light and temperature adaptation of two picoplankton species in the bodden chain south of the Darss–Zingst peninsula. J. Plankt. Res. 15, 953−964

Schlungbaum, G. and Nausch, G., 1994, Die Darß–Zingster Boddenkette-ein typisches Flachwasserästuar an der südlichen Ostseeküste. Rostock. Meeresbiol. Beitr. 2, 5−26

Schubert, H., 1996, Ökophysiologie der Lichtanpassung des Phytoplanktons eutropher Flachgewässer. Habilitationsschrift, Univ. Rostock, Rostock, 179 pp.,

Schubert, H., Forster, R. and Sagert, S., 1995a, *In situ* measurement of state transition in cyanobacterial blooms: kinetics and extent of the change in relation to underwater light and vertical mixing. Mar. Ecol. Progr. Ser. 128, 99−108.

Schubert, H., Sagert, S. and Forster, R., 2000, Evaluation of the different levels of variability in the underwater light field of a shallow estuary. Helgoland Marine Res.

Schubert, H., Kroon, B.M.A. and Matthijs, H.C.P., 1994, *In vivo* manipulation of the Xanthophyll cycle and the role of zeaxanthin in the protection against photodamage in the green alga *Chlorella pyrenoidosa*. J. Biol. Chem. 269, 7267−7272

Schubert, H., Matthijs, H.C.P. and Mur, L.R., 1995b, *In vivo* assay of P700 redox changes in the cyanobacterium *Fremyella diplosiphon* and the role of cytochrome-c-oxidase in regulation of photosynthetic electron transfer. Photosynthetica, 31(4), 517−527

Schubert, H., Matthijs, H.C.P., Mur, L.R. and Schiewer, U., 1995c, Blooming of cyanobacteria in turbulent water with steep light gradients: the effect of intermittent light and dark periods on the oxygen evolution capacity of *Synechocystis* sp. PCC 6803. FEMS Microbiol. Ecol., 18, 237–245

Telfer, A. and Barber, J., 1995, Role of carotenoid bound to the photosystem II reaction centre. Photosynth. Res. Suppl. 1, 11

Zevenboom, W. and Mur, L.R., 1984, Growth and photosynthetic response of the cyanobacterium *Microcystis aeruginosa* in relation to photoperiodicity and irradiance. Arch. Microbiol. 139, 232–239

Zhuang, S., Schubert, H. and Schiewer, U., 1993, Influence of irradiance and temperature on the Cyanobacterium *Aphanothece stagnina* Sprengel isolated from the Darss–Zingst estuary (Southern Baltic) under continuous turbidostat culture. Arch. Hydrobiol. Algological studies 70, 51–63

Chlorinated hydrocarbons in marine biota and sediments from the Gulf of Gdansk

Grazyna Sapota

Abstract

The aim of this work was establishing the level of pollution by highly persistent polychlorinated contaminants in the Gulf of Gdansk.

Concentrations of PCBs, DDT and its metabolites, HCH-isomers and HCB were determined in stratified sediments (from 2 stations — 1 cm slices from 0 to 10 cm depth) and in marine biota (*Salmo trutta trutta, Halicryptus spinulosus, Saduria entomon, Mytilus trossulus, Macoma baltica, Mya arenaria*) from 3 sampling stations. For bivalves, toxic substances were analysed in tissue and shell.

All investigated substances were present in sediment and biota samples from the Gulf of Gdansk in concentrations above the detection limit ($0.01\,ng\cdot g^{-1}$) of the method used.

Introduction

Chlorinated hydrocarbons are some of the mostly widely distributed environmental pollutants (Dunn et. al., 1984). These synthetic substances are produce mainly for agriculture, horticulture, forestry and many branches of industry. PCBs and DDTs are especially well-known as global contaminants due to their persistency in the environment (Flower, 1990). Pollutants adsorb to suspend particles in the water and are sooner or later associated with the sediments. When concentration in the water decreases, the sediments can act as a source to the water (Rasmunson et. al., 1990).

Materials and Methods

Sampling

Fifteen 8 years old sea trout (*Salmo trutta trutta*) were caught in late autumn (October and November 1995) from station No 3 (54° 23' N, 18° 57' 5" E). Weight, length and sex of each fish were determined. For each sea trout a segment of the muscle was taken from below the dorsal fin, after which the samples were frozen (-27^oC).

The benthic animals were taken with drag from two sampling stations (station 1: 540 35' N, 180 40' E and station 2: 540 35' N, 180 44' E) in early spring (March 1996). *Saduria entomon* was grouped into length classes. The bivalves (*Macoma baltica, Mya arenaria, Mytilus trossulus*) were espoused for 24 h in filtrated sea water, then grouped into length classes. Tissue and shell were separated. All individuals from species *Halicryptus spinulosus* were similar in size and treated as one sample. *Saduria entomon* cultivated in aquatic system for half a year was analysed as comparable material. All samples were frozen (-27^oC).

The sediment samples were taken (from stations 2 and 3 in March 1996) with a Niemistö corer, separated into 1 cm slices to 10 cm depth and frozen (-27^oC).

Sample preparation

Muscle tissue of fish, tissues, shells and sediments were freeze-dried to complete dryness and divided into small pieces. A portion of about $1-2$ g was transferred to a glass extraction vial and Soxhlet-extracted in hexane and acetone at 180^oC for 2 hours. Octachloronaphtalene was used as an internal standard and added prior to the extraction. After extraction, water was added to the extract to separate the hexane (containing the fat and lipophilic pollutants) from the acetone/water phase. Concentrated H_2SO_4 was added to oxidise the fat. The hexane phase was then evaporated in a vacuum centrifuge to dryness. The remaining material was dissolved in $400\,\mu l$ hexane and eluted with hexane/dichlorometane through a column containing two layers of silica gel to which K_2CO_3 and H_2SO_4 had been added. The eluate was then evaporated to dryness and dissolved in isooctane.

Analysis

The cleaned-up extract was analysed for persistent pollutants by capillary GC/ECD on VARIAN STAR 3400. Investigated substances were separated on a 30-m DB-5 quartz capillary column. Injection technique was split/splitless. H_2 ($1.5\,ml\,min^{-1}$) was used as a carrier gas and N_2 ($50\,ml\,min^{-1}$) as a make-up gas. The oven temperature was programmed as follows:

- Initially 15 min at $80^{o}C$
- Increase by $4^{o}C$ per min to $320^{o}C$
- Hold for 15 min.
- Injection temperature—$330^{o}C$
- Detection temperature—$340^{o}C$

A pesticide mixture containing p,p'-DDE, p,p'-DDD, o,p'-DDT, p,p'-DDT, a-HCH, b-HCH, g-HCH and HCB was used as a standard. Clophen A 60 was used as a PCB standard. All substances were identified and quantified according to Mullin et. al. (1984) and Schultz et. al. (1989).

Dry weight and fat content (without shell) was determined for each sample. Fat content was determined in Soxhlet extraction (Ewald et. al., 1998).

Results and Discussion

The vertical distribution of the concentration of all investigated substances in sediments was very similar for both stations, but values at station 3 were higher than at station 2 (Figure 1). The highest concentration of all analysed substances was observed between the 3rd and 7th cm of sediment. The sediments from station 2 belong to very fine powdered sands and from station 3 to very fine organic powdered sands. Duinker and Hillebrand (1979) estimated that in organic sediments the amount of chlorinated hydrocarbons is much higher than in inorganic sands. In 1977 Trzosinska and Baumgartner reported that concentrations of SDDT for surface sediments from the Gulf of Gdansk varied from $14.6\,ng\cdot g^{-1}$ d.w. to $29.3\,ng\cdot g^{-1}$ d.w. In 1979 Andrulewicz et. al. estimated for the same area concentrations for sands: DDE $-4\,ng\cdot g^{-1}$ d.w., DDD $-1\,ng\cdot g^{-1}$ d.w., DDT $-2\,ng\cdot g^{-1}$ d.w. and for mud: DDE $-7\,ng\cdot g^{-1}$ d.w., DDD $-2\,ng\cdot g^{-1}$ d.w., DDT $-8\,ng\cdot g^{-1}$ d.w. In 1987 Slaczka *et al.* gave concentrations of SDDT for sound sediments from Southern Baltic— $5\,ng\cdot g^{-1}$ d.w. and for mud—$20\,ng\cdot g^{-1}$ d.w. In comparison to these data it could be stated that concentrations of DDT and its metabolites in the Gulf of Gdansk decrease.

Generally in all analysed samples the pattern of concentrations of investigated substances was similar. It was observed that the highest amount of DDE among DDT and its metabolites is an effect of metabolic degradation of DDT (Larsson and Okla, 1989). In analysed benthic organisms concentrations of all investigated substances increase with increase of fat content (Table 1, Figure 2, Figure 3, Figure 4, Figure 5). This statement is also valid taking into account the same species from the different stations (Figure 2, Figure 3, Figure 5). *Saduria entomon* cultivated in aquatic system shows lower concentrations than the same species from environment. Tooby and Durbin (1975) estimated that residue substances were rapidly eliminated from tissues when organisms were placed into clean water. In analysed benthic organisms concentrations increase with increase of size of animals. Comparison of concentrations calculated on wet weight in tissue and shells shows much higher concentrations in tissue (except *Mya arenaria*) (Figure 6). The highest concentrations of investigated substances were found in sea trout (Figure 4). Bremle et. al. (1995) stated that the level of fish contamination mainly depends on the food web. Sea trout is the fish at the top of the marine food web.

Station No	Species	Length class [cm]	Fat content [% w. w.]
1	*Halicryptus spinulosus*		0.78
	Macoma baltica	1.0–1.5	2.55
		1.6–2.0	1.72
	Mya arenaria	1.0–1.5	2.40
		1.6–2.0	1.27
		2.1–2.5	1.74
		2.6–3.0	1.68
	Mytilus trossulus	2.6–3.0	2.13
		3.1–3.5	2.82
	Saduria entomon	1.6–2.5	9.09
		2.6–3.5	8.40
		3.6–4.5	5.64
		4.6–5.5	5.62
		5.6–6.5	5.91
		6.6–7.5	5.94
2	*Macoma baltica*	1.0–1.5	1.56
		1.6–2.0	1.59
		2.1–2.5	1.74
	Saduria entomon	2.6–3.5	7.31
		3.6–4.5	4.63
		4.6–5.5	4.58
		6.6–7.5	4.35
3	*Salmo trutta trutta*		7.78
cultivated	*Saduria entomon*	1.6–2.5	4.44
		2.6–3.5	3.38
		3.6–4.5	1.94
		4.6–5.5	2.38
		5.6–6.5	2.35
		6.6–7.5	2.17

Table 1 Fat content (in % of wet weight) in analysed species from the Gulf of Gdansk
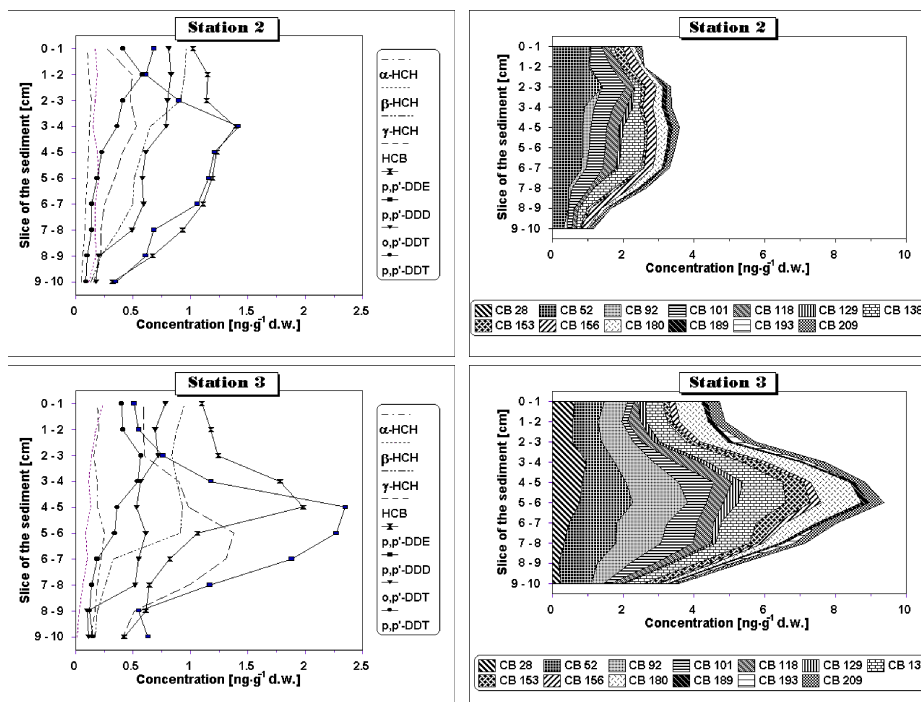
Figure 1 Concentrations of investigated substances in stratified sediments from stations 2 and 3
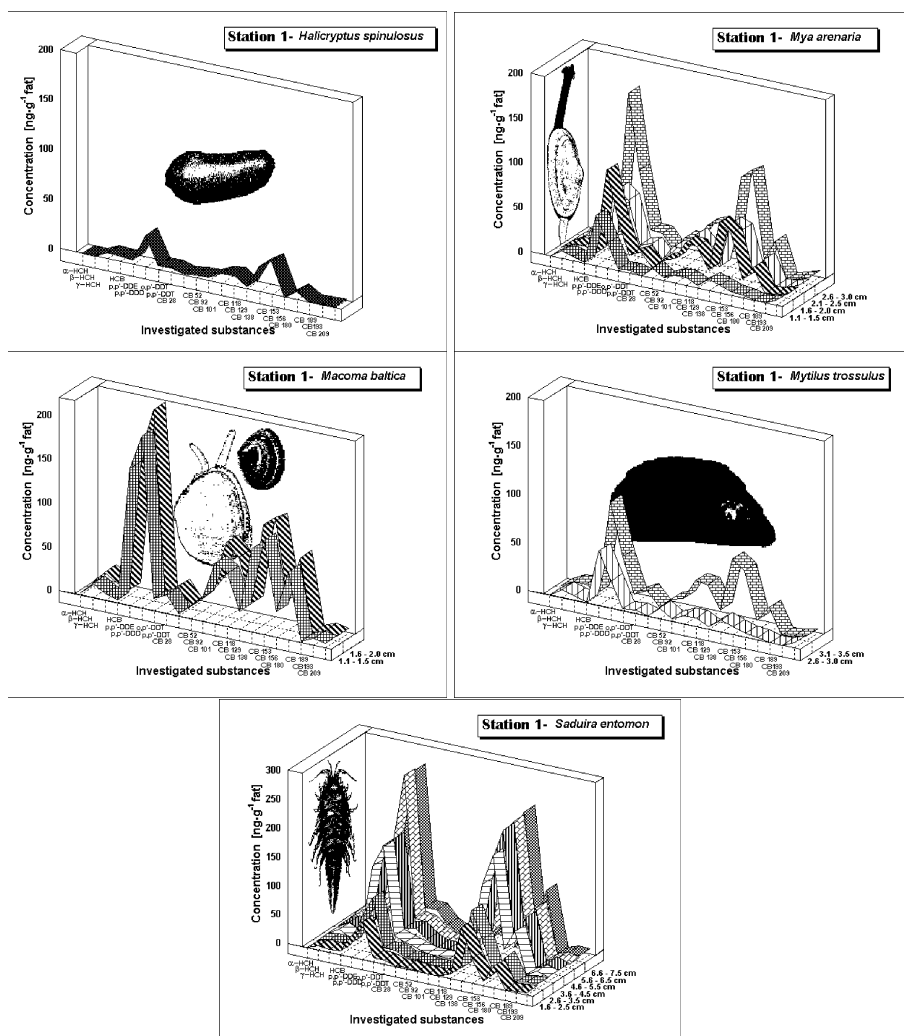
Figure 2 Concentrations of investigated substances in animals from station 1
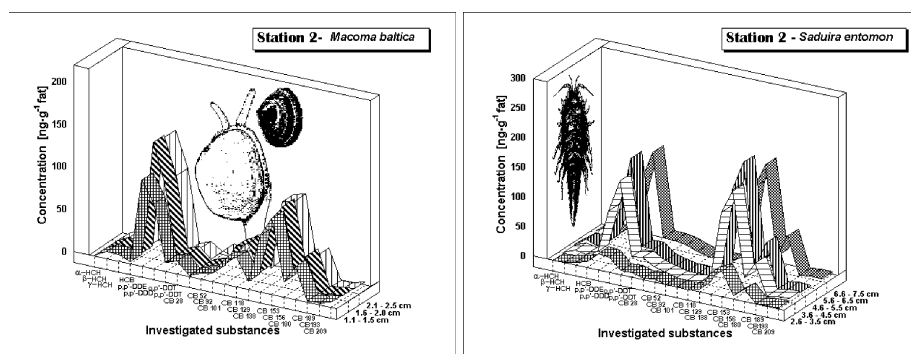
Figure 3 Concentrations of investigated substances in animals from station 2
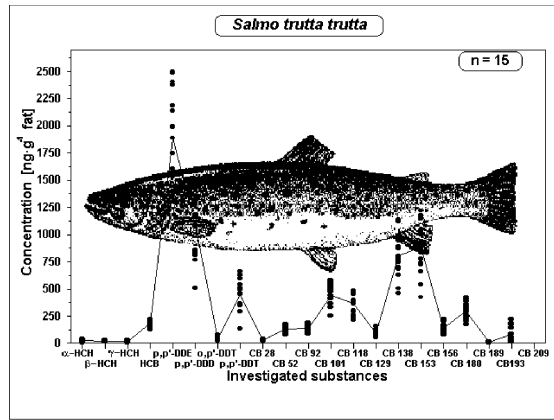
Figure 4 Concentrations of investigated substances in fish from station 3
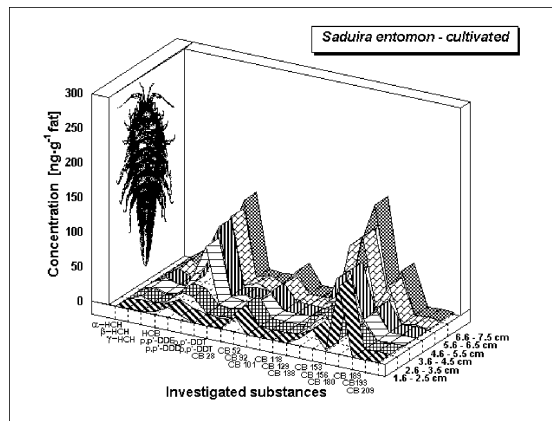
Figure 5 Concentrations of investigated substances in cultivated *Saduria entomon*
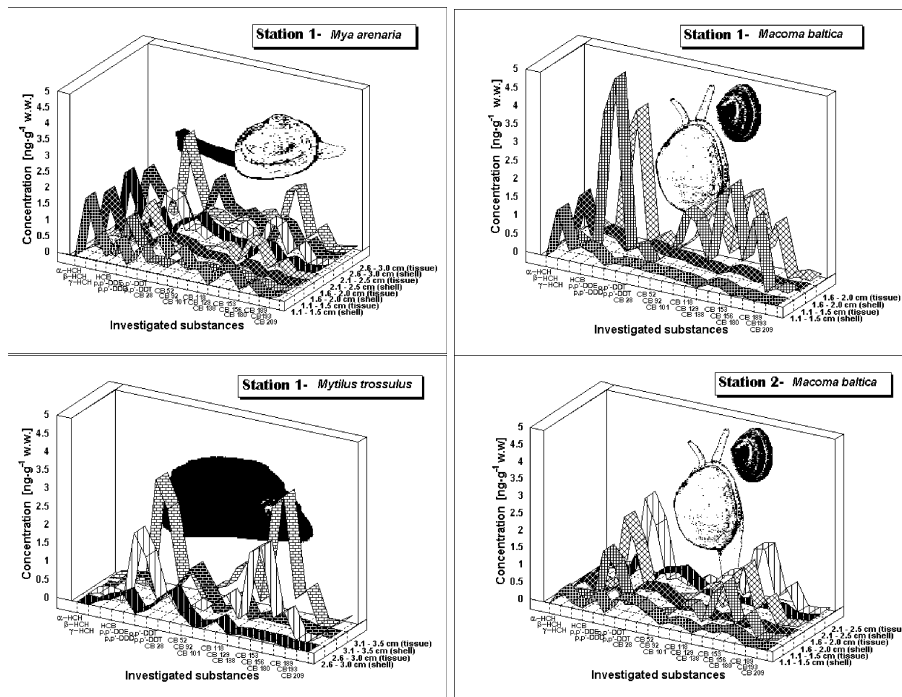
Figure 6 Concentrations of investigated substances in tissues and shells of bivalves calculated on wet weight

Conclusions

- The presence of all investigated substances in biota and sediments from the Gulf of Gdansk was confirmed.
- Fat content was the governing factor for the distribution of persistent pollutants.
- Persistent pollutant concentrations vary in marine biota in due to size.
- Concentrations of chlorinated hydrocarbons in cultivated *Saduria entomon* were lower than in *Saduria entomon* from the environment.
- Concentrations of persistent pollutants increase towards higher trophic levels.
- In bivalves, concentration of investigated substances were higher in tissue than in shell.
- The amount of analysed chlorinated hydrocarbons was higher in marine biota than in sediments.

Acknowledgements

References

Andrulewicz, E., Brzezinska, A., Trzosinska, A., 1979. Some aspects of the chemical composition of particulate matter in the Southern Baltic. Ref. Marine Environ.

Bremle, G., Okla, L., Larsson, P., 1995. Uptake of PCBs in fish in a contaminated river system: bioconcentrations factors in the field. Environ. Sci. Technol. 29 (8), 2010−2015.

Duinker, J.C., Hillebrand, M.T.J., 1979. Behaviour of PCB, hexachlorobenzene, a-HCH, b-HCH, g-HCH, dieldrin, endrin and p,p'-DDD in the Rhinemeuse Estuary and the adjacent coastal area. Neth. J. Sea Res. 13 (2), 256−281.

Dunn, W.J., Stalling, D.L., Schwartz, T.R., Hogan, J.W., Petty, J.D., Johansson, E, Wold, S., 1984. Pattern recognition for classification and determination of Polychlorinated biphenyls in environmental samples. Anal. Chem. 56 (8), 1308−1313.

Ewald, G., Bremle, G., Karlsson, A., 1998. Differences between Bligh and Dyer and Soxhlet extractions of PCB and lipids from fat and lean fish muscle: Implications for data evaluation. Mar. Pollut. Biul. 36 (3), 222−230.

Flower, S.W., 1990. Critical review of selected heavy metal and chlorinated hydrocarbon concentration in the marine environment. Mar. Environ. Res. 29, 1−64.

Larsson, P., Okla, L., 1989. Atmospheric transport of chlorinated hydrocarbons to Sweden in 1985 compared to 1973. Atmos. Environ. 23 (8), 1699−1711.

Mullin, M.D., Pochini, C.M., McCrindle, S., Romkes, M., Safe, S.H., Safe, L.M., 1984. High-resolution PCB analysis: synthesis and chromatographic properties of all 209 PCB congeners. Environ. Sci. Technol. 18 (6), 468−476.

Rasmunson, A., Lindgren, M., Jones, C., 1990. Release of contaminants from sediments as compered to remedial actions involving dredging and land disposal. Report No 3871; Swedish National Protection Board.

Schulz, D.E., Petrick, G., Duinker, J.C., 1989. Complete characterization of polychlorinated biphenyls congeners in commercial Aroclor and Clophen mixtures by multidimensional Gas Chromatography—Electron Capture Detection. Environ. Sci. Technol. 23 (7), 852−859.

Slaczka, W., Andrulewicz, E., Trzosinska, A., 1987. Harmful substances. Baltic Sea Environment Proceedings No. 17B, First Periodic Assessment of the State of Baltic Sea.

Tooby, T.E., Dubrin, F.J., 1975. Lindane residue accumulation and elimination in rainbow trout (Salmo gairdner Richardson) and roach (Rutilus rutilus Linnaeus). Environ. Pollut. (8), Applied Science Publishers Ltd., England, 79−89.

Trzosinska, A., Baumgartner, D.J., 1977. Hydrological, chemical and physical processes affecting pollution of the Baltic Sea. Final Report, Gdynia.

Polonium, uranium, and plutonium in the Southern Baltic ecosystem

Bogdan Skwarzec and Piotr Stepnowski

Introduction

^{210}Po belongs to the natural uranium decay series starting from ^{238}U and its fate depends on further members of this series such as ^{226}Ra, and most of all on ^{210}Pb. ^{222}Rn escaping from the Earth's surface constitutes the source of atmospheric ^{210}Po (Scholander *et al.*, 1961). the total amount of ^{210}Po in the air depends directly on the amount of ^{210}Pb supplied and formed in the atmosphere (Jaworowski and Kownacka, 1976). Apart from the ^{210}Po formed by the decay of ^{210}Pb contained in the air, additional quantities are emitted directly from the Earth as a result of forest fires (Moore *et al.*, 1976) and volcanic eruptions (Lambert *et al.*, 1970; Danielsen, 1981). Atmospheric precipitation of ^{210}Po and, to a smaller extent, precipitation of ^{210}Pb itself onto the surface of seas and oceans are the principal sources of ^{210}Po that enter the marine environment. A small amount of ^{210}Po is formed in situ as a result of the radioactive decay of uranium contained in sea water.

Uranium occurs naturally in the Earth's crust and is present in much higher concentrations—along with thorium and rare-earth elements—in areas where heavy mineral sands occur. The major source of uranium in the marine environment is the atmospheric precipitation of terrigenic (rock) derived material, together with river water (Ku *et al.*, 1974).

Plutonium belongs to a group of man-made radionuclides that have attracted considerable attention from the radioecological point of view due to their high radiotoxicity, long physical half-life, high chemical reactivity and long residence in biological systems. The principal source of plutonium radionuclides in the Baltic Sea is the atmospheric fallout from nuclear weapons tests (Hardy *et al.*, 1973). Other sources such as releases from nuclear power plants and the European nuclear reprocessing facilities at Sellafield (UK) and Cap de la Hague (France), while not fully documented, are often considered less important. Since 26 April 1986 another source of plutonium isotopes, from Chernobyl-originating radioactive debris, has had to be taken into account (Aarkog, 1988).

Marine plants and animals are capable of absorbing both natural and artificial radionuclides from their surroundings (Carlson, 1990; Carlson and Holm, 1990; Dahlgaard and Boelskifte, 1992) and are often used as bioindicators of radioactive pollution in the environment. For example, the brown algae *Fucus vesiculosus* has been found to preferentially accumulate radionuclides in the following order: technetium>americium>plutonium>cesium (Carlson, 1990; Carlson and Holm, 1990). Among the natural emitters of alpha radiation, ^{210}Po is often accumulated to a high degree by marine organisms. The great ability of organisms to accumulate ^{210}Po means that they are exposed to a large ionising radiation dose. The ^{210}Po and uranium isotopes are responsible for over 90% of all natural radiation to which many organisms are subjected (Cherry and Heyraud, 1982; Woodhead, 1973).

Materials and Methods

Seawater and biota were collected between 1980 and 1991 in various regions in the southern Baltic Sea.

The radioanalytical procedure for determination of polonium, uranium and plutonium in the Baltic Sea samples are presented in Figure 1. All details about activity determination of ^{210}Po, ^{234}U, ^{238}U and $^{239+240}$Pu are given by Skwarzec (1996).
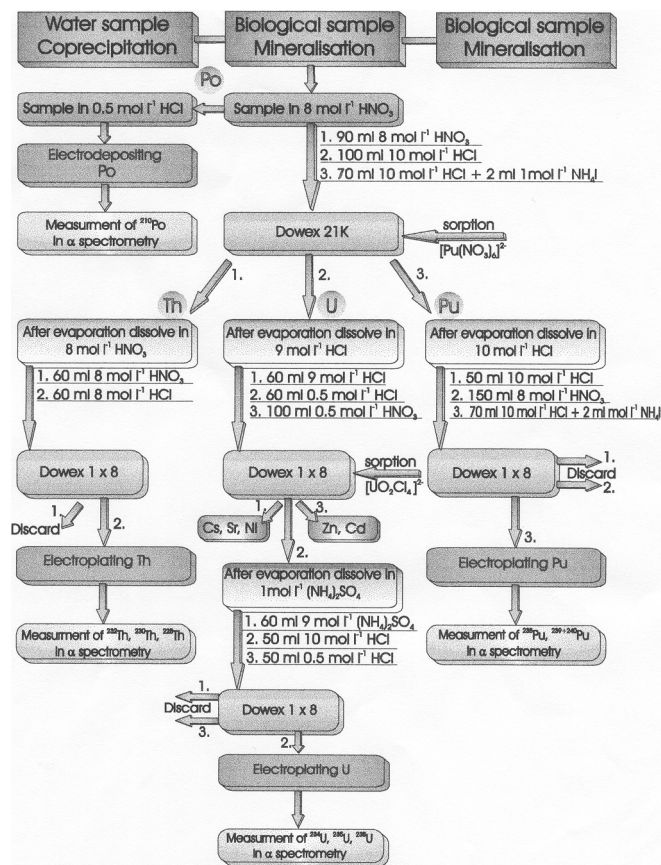
Figure 1 The radioanalytical procedure for determination of Po, U and Pu in the Baltic Sea samples

Results and Discussion

The activity concentration of ^{210}Po, ^{234}U, ^{238}U and $^{239+240}$Pu in the southern Baltic water and sediments are presented in Figure 2 and Figure 3.
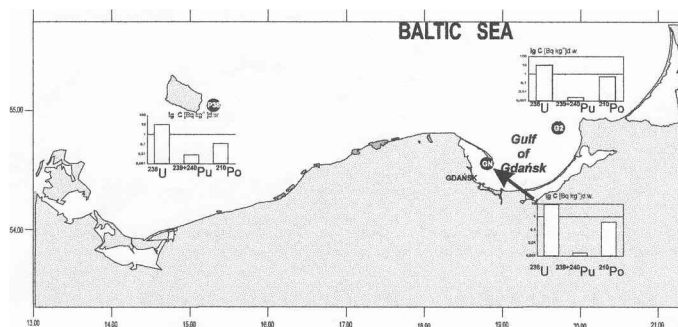
Figure 2 The activity concentration of ^{210}Po, ^{238}U and $^{239+240}$Pu in the Southern Baltic water
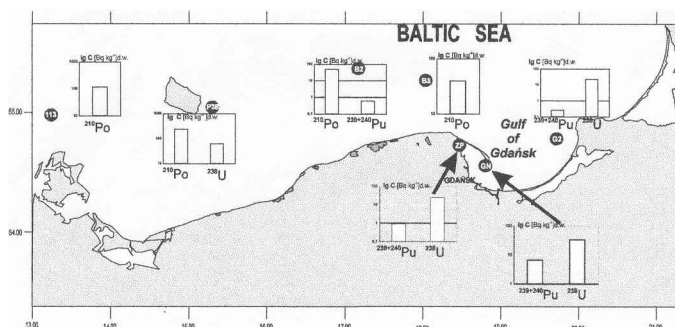
Figure 3 The activity concentration of ^{210}Po, ^{238}U and $^{239+240}$Pu in the Southern Baltic sediments

The analysis of seawater samples revealed that the mean concentration of ^{210}Po in Baltic water was 0.6 mBq dm^{-3}, 80% of which consisted of soluble forms (Skwarzec and Bojanowski, 1988). There were significant differences in the concentrations of dissolved polonium in the samples analysed. The mean concentrations of ^{210}Po in the waters of the Slupsk Furrow and Lübeck Bay (0.57 and 0.52 mBq dm^{-3} respectively) were over three times as high as the mean concentration of this nuclide in the water of the Bornholm Deep (0.17 mBq dm^{-3}).

The uranium concentrations were within the range of 0.68 to 0.85 µg dm^{-3} in surface seawater samples, but from 0.64 to 1.28 µg dm^{-3} in Vistula river water. The mean ^{234}U/^{238}U activity ratio in Baltic seawater was found to be 1.17, and in Vistula river water it was 1.31. The uranium concentration in seawater increased, while values of the ^{234}U/^{238}U activity ratio decreased with salinity (Skwarzec, 1995).

The average ^{234}U/^{238}U activity ratio in the suspended matter is about 1.0, i.e. similar to that in sediments. This indicated that terrigenic material is the source of uranium in the Baltic sediments. Since the ^{234}U/^{238}U activity ratio in Baltic organisms, in the 1.12–1.15 range, is similar to that in seawater, it can be inferred that the dissolved forms of this element in seawater are the source of uranium in Baltic biota (Skwarzec, 1995).

The average level of $^{239+240}$Pu in Baltic seawater was found to be 4.8 µBq dm^{-3}, 70% of which constituted filterable forms (<0.45 mm). The concentration of plutonium in the suspended matter was 1.5 Bq kg^{-1} dry wt., and the distribution coefficient (DC) of plutonium was of the order of $4 \cdot 10^5$ (Skwarzec and Bojanowski, 1992). These results agree well with those from for Danish, Swedish and Finnish waters (Aarkog *et al.*, 1980; Holm *et al.*, 1980; Kautsky *et al.*, 1986; Leskinen *et al.*, 1987).

The activity concentrations of ^{210}Po, ^{234}U, ^{238}U and $^{239+240}$Pu in the southern Baltic ecosystems are shown in Figure 4. Investigation of the ^{210}Po and $^{239+240}$Pu content in the Baltic biota showed that organisms display a strong affinity for them. Mean values of the bioaccumulation factor (BCF) in the Baltic organisms, calculated on the basis of the polonium content fell within the range $4.1 \cdot 10^3$–$3.5 \cdot 10^4$ (Skwarzec, 1995).

In the case of planktonic organisms the BCF values increased in the sequence: phytoplankton<macrozooplankton<mesozooplankton, while in the zoobenthos they increased in the following order: *Polychaeta<Priapulida<Malacostraca<Bivalvia* (soft tissue) (Skwarzec and Bojanowski, 1988). The data on *Saduria entomon* crustacea, and *Mya arenaria* bivalves indicated that ^{210}Po is non-uniformly distributed in their bodies. The polonium content in the internal organs of these animals decreased in the sequence: hepatopancreas>alimentary tract>gills>muscles (Skwarzec and Falkowski, 1988). It was additionally demonstrated that in the fish the organs directly connected with digestion (intestine, liver, spleen, pyloric caeca) contain much higher ^{210}Po concentrations as compared to muscle tissue (Skwarzec 1988). On the basis of the data on ^{210}Po content in fish, it is suggested that this nuclide is removed from seawater by fish.
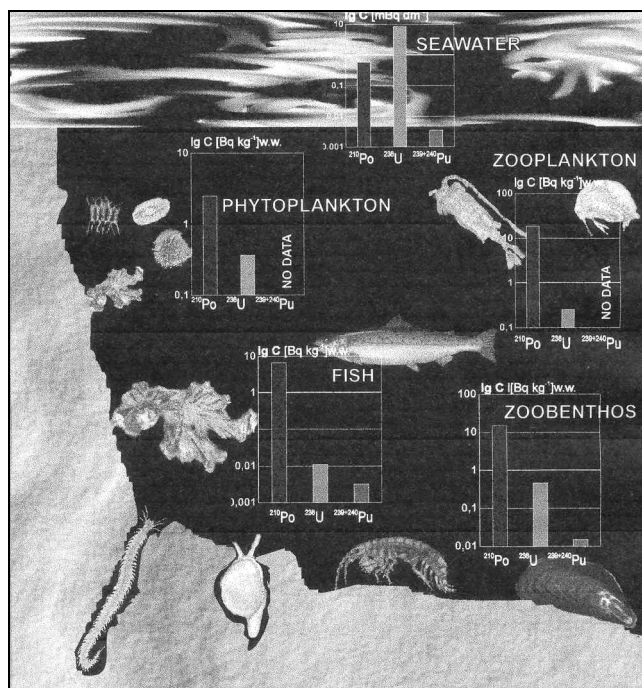
Figure 4 The activity concentration of ^{210}Po, ^{238}U and $^{239+240}$Pu in the Southern Baltic ecosystem

The $^{239+240}$Pu concentrations in the Baltic organisms ranged from 14 mBq kg^{-1} dry wt. (fish) to 957 mBq kg^{-1} dry wt. (*Priapulida*), and respective BCFs from 900 to 27000 (Skwarzec, 1995). In the seaweeds the highest plutonium concentrations were found in *Pilayella litoralis* collected in Puck Bay in 1987. In the zoobenthos, plutonium concentrations were higher in *Priapulida* and *Polychaeta* and lower in *Entomostraca*, *Malacostraca* and *Bivalvia* (soft tissue) (Skwarzec and Bojanowski, 1992).

The average ^{238}Pu/($^{239+240}$Pu) activity ratio in seaweeds was 0.032 i.e. not very different from that in typical fallout (Perkins and Thomas, 1980). This means that the impact of the Chernobyl-derived plutonium [^{238}Pu/($^{239+240}$Pu) activity ratio was about 0.60] on the Baltic plants was small (a few percent).

The mean ^{238}Pu/($^{239+240}$Pu) activity ratio in some benthic animals was found to be 0.093, which is generally higher than in marine plants as a whole. The impact of the Chernobyl-derived plutonium on the benthic organisms was calculated to be about 10%. It appears that benthic organisms have responded to the increased level of plutonium faster and more noticeably than seaweeds have. It can therefore be concluded that the impact of Chernobyl-derived plutonium on the southern Baltic ecosystem was not of great significance (Skwarzec, 1995).

Marine algae and benthic animals concentrated uranium isotopes to a small extent only. The BCF ranged from 30 to 55 (Skwarzec, 1995). The mean uranium concentration in phytoplankton was about twice as high as in zooplankton. Only small differences were observed between the uranium levels in benthic organisms. The higher values were found in the Bivalvia, the lower ones in the Crustacea. Investigations on fish showed that uranium is non-uniformly distributed in their bodies, its concentration increasing in the sequence: muscle<skeleton<viscera.

On the basis of the content of the radionuclides analysed in the Baltic samples, it can be concluded that polonium probably circulates in the southern Baltic ecosystem in the same way as organic matter does. On the other hand, sedimentation and diffusion from sediments to deep seawater are important ways in which uranium and plutonium migrate within this ecosystem (Skwarzec, 1995).

References and Notes

Aarkrog, A. 1988. The radiological impact of the Chernobyl debris compared with that from nuclear weapon fallout. J. Environ. Radioactivity, 6, 151–162.

Aarkrog, A., Dahlgaard, H. and Nilsson, K. 1980. Studies on the distribution of transuranics in the Baltic Sea, the Danish Belts, the Kattegat and the North Sea. In: Transuranic Cycling in the Marine Environment. IAEA-TECDOC-265, Vienna, 23–29.

Carlson, L. 1990. Effects of biotic and abiotic factors on the accumulation of radionuclides in Fucus vesiculosus L., Ph.D. Thesis, Department of Ecology, Marine Ecology, University of Lund. Sweden.

Carlson, L. and Holm, E. 1990. Radioactivity in the Baltic Sea following the Chernobyl accident, SSI project 393–86, University of Lund, Sweden.

Cherry, R.D. and Heyraud, M. 1982. Evidence of high natural radiation doses in certain mid-water oceanic organisms, Science, 218, 54–56.

Dahlgaard, H. and Boelskifte, S. 1992. "SENSI", A Model describing the Accumulation and Time-Integration of Radioactive Discharges in the Bioindicator Fucus vesiculosus, J.Environ. Radioactivity, 16, 49–63.

Danielsen, E.F. 1981. Trajectories of the Mount St. Helens plume, Science, 221, 819–921.

Hardy E. P, Krey P. W., Volchak H. L., 1973. Global inventory and distribution of fallout plutonium, Nature, 241, 444–445.

Holm, E., Persson, B.B., and Mattsson, S. 1980. Studies of concentration and transfer factors of natural and artificial actinide elements in a marine environment. In: Proc. 5th Int. Congress of the International Radiation Protection Association, Vol III, Jerusalem, 9–14 March, 311.

Jaworowski, Z. and Kownacka, L. 1976. Lead and radium in the lower stratosphere. Nature, 263, 303–304.

Kautsky, H., Wedekind, C. and Eicke, H.F. 1986. Radiological investigations in the Baltic Sea. Including the Danish Strains and the Kattegat during 1982 and 1983. In: Study of Radioactive Materials in the Baltic Sea. IAEA-TECDOC-362, Vienna, 110–117.

Ku T. L., Knauss K. G. and Mathien G. G., 1977. Uranium in open ocean: concentration and isotopic composition, Deep-Sea Res., 24, 1005–1017.

Lambert, G., Buisson, A., Sanak, J. and Ardonin, B. 1979. Modification of the atmospheric polonium-210 to lead-210 ratio by volcanic emissions. J. Geophys. Res., 84, 6980–6986.

Leskinen, S., Miettinen, J.K. and Jaakkola T. 1987. Behaviour of 239,240Pu and 241Am in the Baltic Sea; Measurements and interpretations in 1980–1984, J. Radioanal. Nucl. Chem., 115, 289–298.

Moore, H.E., Martell, E.A. and Poet, S.E. 1976. Sources of polonium-210 in the atmosphere. Envir. Sci. Technol., 10, 586–591.

Perkins, R.W. and Thomas, C.W. 1980. Worldwide fallout. In: Transuranic elements in the environment, Hanson, W.C. (ed.). Technical Information Center/US Department of Energy, USA, 53–82.

Scholander, P.F., Hemmingsen, E.A., Coachman, L.K. and Nutt, D.C. 1961. Composition of gas bubbles in Greenland icebergs, J. Glacial., 3, 813–822.

Skwarzec B. 1988, Accumulation of ^{210}Po in selected species of Baltic fish, J. Environ. Radioactivity, 8, 111–118.

Skwarzec, B. 1995. Polonium, uranium and plutonium in the southern Baltic ecosystem, Rozprawy i monografie KBM PAN, 6, (in Polish, summary in English).

Skwarzec, B. 1996. Radiochemical methods for determination of polonium, radiolead uranium and plutonium in environmental samples, Chem. Anal. (in press).

Skwarzec, B. and Bojanowski, R. 1988. The ^{210}Po content in sea water and its accumulation in southern Baltic plankton, Mar.Biol., 97, 301–307.

Skwarzec B. and Bojanowski R., 1992. Distribution of plutonium in selected components of the Baltic ecosystem within the Polish economic zone, J. Envir. Radioactivity, 15, 249–263.

Skwarzec, B. and Falkowski, L. 1988. Accumulation of ^{210}Po in Baltic invertebrates, J.Environ.Radioactivity, 8, 99–109.

Woodhead, D.S. 1973. Levels of radioactivity in the marine environment and the dose commitment to marine organisms, In: Radioactive contamination of the marine environment. IAEA, Vienna, STI/PUB/313, 499–525.

The application of dynamic segmentation in coastal vulnerability mapping

Jacek Urbanski

Abstract

This paper discusses the application of a dynamic segmentation data model in the development of a coastal GIS. The discussion presents a hybrid data model of the coast, which combines a raster data model with dynamic segmentation. Several cartographic modelling methods are presented for working with this data model. The model was used to develop an oil spill vulnerability map for the Bay of Gdansk coastline. The following factors were evaluated: probability of an oil spill occurrence, oil residence time, degree of exposure to wind and wave action, fish potential and seabird potential. The Multi-Criteria/Single-Objective decision making technique was used to calculate the vulnerability index.

Introduction

The coastal zone, which is defined as the space in which terrestrial environments influence marine environments and vice versa (Carter 1988), is a complex dynamic system. Because of the strong, diverse and often uncoordinated human activity in this zone, its living resources and environment are sensitive to many factors created by man. The state of the Marine Environment (GESAMP, 1990) report concluded that "In contrast to the open ocean, the margins of the sea are affected by man almost everywhere, and encroachment on coastal areas continues worldwide...". Coastal Zone Management is used to find a wise balance between the many conflicting elements exerting their influence on the coastal environment, ensuring that its limits of tolerance and its capacity for sustainability are not exceeded (Tortell, 1992). This process needs reliable and accurate data about different environmental factors and human activities.

One of the basic methods for representing and evaluating this type of data is the use of thematic maps of the coastal zone. Table 1, adopted partially from Tortell (1992), illustrates resources, demands and issues that can be featured in such a map.

Resources, demands and issues that can be featured in thematic maps of a coastal zone
Maritime shipping operations and navigation lanes
Ecological sanctuaries and other protective measures
Tourism and recreational facilities and uses
Administrative boundaries and zones
Solid wastes dumping sites
Discharge points for liquid wastes
Fisheries activity and methods used
Land cover
Bottom cover
Bottom sediments
Fish potential
Bird potential
Wave conditions
Bathymetry and elevation
Water pollution
Coastline types
Probability map of oil spill accidents
Commercial port facilities
Temperature of water
Sediment transport
Sea level variation
Salinity of water

Table 1 Resources, demands and issues that can be featured in thematic maps of a coastal zone

In order to convert data to useful information, different kinds of spatial data processing techniques are used. One of the techniques is to create vulnerability maps which describe the sensitivity of the coast to threats of different kinds using an undimensional sensitivity index. These maps are produced by overlaying thematic maps of processes or issues which are

important factors in sensitivity evaluation. Vulnerability maps were successfully used to evaluate the vulnerability of the coast to oil spill impact (Jansen *et al.*, 1990, Populus *et al.*, 1995) and sea level rise (McCall and Devoy, 1995). GIS constitutes the best method for data processing using the cartographic modelling concept, since all processed data are spatial data. The cartographic modelling is the processing of spatial data via a sequence of transformations. The spatial data are organised in a data model which represents reality.

Data model

There are two data models—the raster data model and the vector data model—which are most often implemented in contemporary GIS systems. Testing of these models for coastal applications to solve problems in the coastal zone, especially for creating vulnerability maps, shows that they are generally poor at representing the distinctive nature of the coastal system, for reasons given below.

The coastal waters are an essential area of the geographic space covered by a Coastal Geographic Information System included in the vulnerability analyses. The main problem in the development of successful coastal waters applications is the lack of a well-suited data model for this area. Although raster and vector data models may be used to represent nearly all the elements of the terrestrial part of the coast, only a few elements of coastal waters like bottom elevation or bottom cover may be described using these models. The main reason for this is the variability in time of the many parameters used to describe coastal waters like temperature, salinity, amount of nutrients or wave heights (Langran, 1993). An additional difficulty in designing the new model is posed by the necessity to retain compatibility with existing GIS systems to facilitate their utilisation in the analysis process. One of the possible solutions is to replace the attributes with the probability of occurrence of a particular range of attributes, for example we would use a map of the probability that salinity would be below some threshold value instead of mean salinity map.

The area "near the waterline" is especially essential in vulnerability analyses of the coastal zone. At the same time it is very difficult to model this area using raster or vector data models. Firstly, most of the entities within the coastal zone lack clear boundaries. For example, a sandy beach may gradually change into a cobble or gravel beach. A second problem emerges out of the very great range of spatial scales of coastal phenomena, which range from centimetres to tens of kilometres. Many coastal objects have a strongly shaped anisotropy, a beach which is a few meters wide may be several kilometres long. Objects are often overlaid, for example seabird breeding areas are placed on the beach. Another problem is created by the variability of some objects in time, which necessitates the additional inclusion of the temporal dimension (Bartlett 1994). A solution which has been proposed recently to overcome some of disadvantages of raster and vector models is the dynamic segmentation model. The dynamic segmentation (Figure 1) is the line data model in which spatial objects are referenced based on the distance along the polyline. The polyline consists of arcs defined by nodes. Localisation of the object is described by the start and end point position using the percentage of arcs as a units. Because all objects are referenced based on their distance along the polyline, attributes may be connected to any segment of this polyline. Closely linked to the application of the model is the development of a comprehensive coastal classification scheme (McCall and Devoy, 1995). This model was successfully used by McCall and Devoy (1995) in sensitivity analyses of the coast of Ireland to the threat posed by rising sea level. They classified the coastal zone using weighted combinations of the attributes at each location. The main problem in using the dynamic segmentation model for vulnerability analyses is how to integrate this model with a raster data model in which many factors are represented. The fact that many decision making techniques are implemented using raster data models is also important.

	start node	%	end node	%
object 1	n+1	7	n+1	40
object 2	n+1	30	n+2	10
object 3	n+3	58	n+3	62
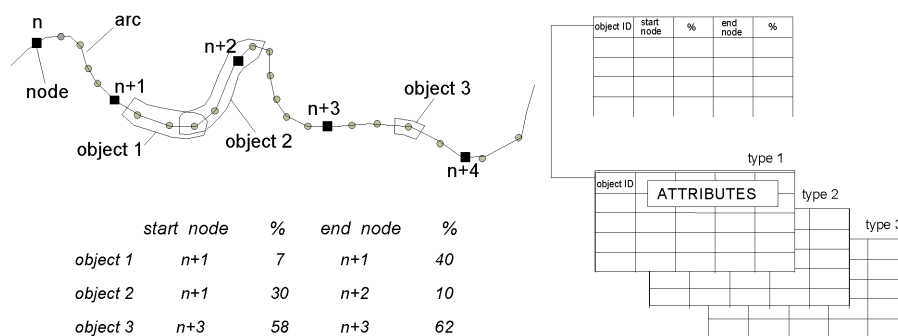
Figure 1 The dynamic segmentation data model

To enable cartographic modelling of a wide spectrum of coastal zone problems and use different models for different factors in vulnerability analyses, all the data models presented above should be combined together to form one hybrid data model to represent the complex nature of the coast. It should be emphasised that the term data modelling refers to a comprehensive set of conceptual tools for organising data and the creation of this data model (Bartlett, 1994).

The hybrid data model (Figure 2) is centred around the raster data model which offers considerably greater potential for incorporating fuzzy techniques, uncertainty and decision making techniques. The raster data model format is also the output format of many simulation models and satellite images. The second block in the raster column of the model is the dynamic raster data model which is used to create the raster maps of probability using time variable data from a typical oceanographic relational database or from modelling. A separate column in the model is created by a vector data model for typical vector data like the coastline, roads, rivers and the dynamic segmentation model. All data processed in the dynamic segmentation model may be converted into a vector format. The link between the two columns of the model is made possible via the conversion of vector data to raster form. The typical data sources for particular blocks of the model are also represented on the figure.
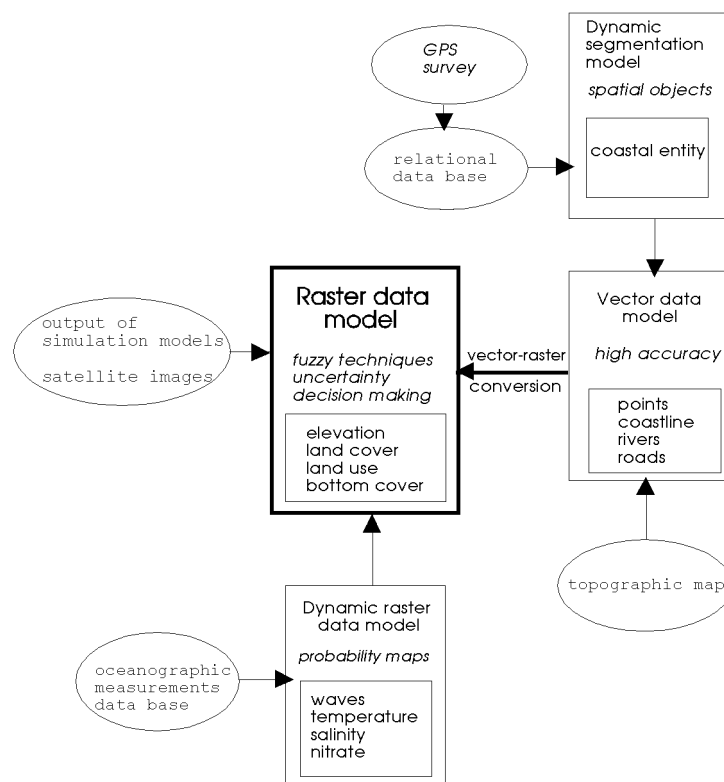
Figure 2 The hybrid data model

Oil spill vulnerability mapping

Oil spills are one of the major threats to coastal areas throughout the world. The potential damage to economic activities and the natural environment requires some planning and preparation. One of the aims of this process is to establish in quantitative terms the sensitivity or vulnerability of the surrounding environment to an oil spill (Populus *et al.*, 1995). An example of a hybrid data model application is provided by the oil spill vulnerability map of the Gdansk Bay Coast. The Multi-Criteria/Single-Objective decision making technique was used (Eastman *et al.*, 1995).

The area of Gdansk Bay is presented in Figure 3. Three big ports are located on the coast of the bay, including oil discharge facilities. Several shipping lanes cross this area which increases the probability of an oil spill. The coastal zone of the Gdansk Bay is a very diverse environment. There are four wildlife sanctuaries, several recreational areas, city water fronts, ports, marinas and industrial facilities along the 150 kilometres long coastline. The waters of the bay are also an area of intensive commercial fishing and spawning.
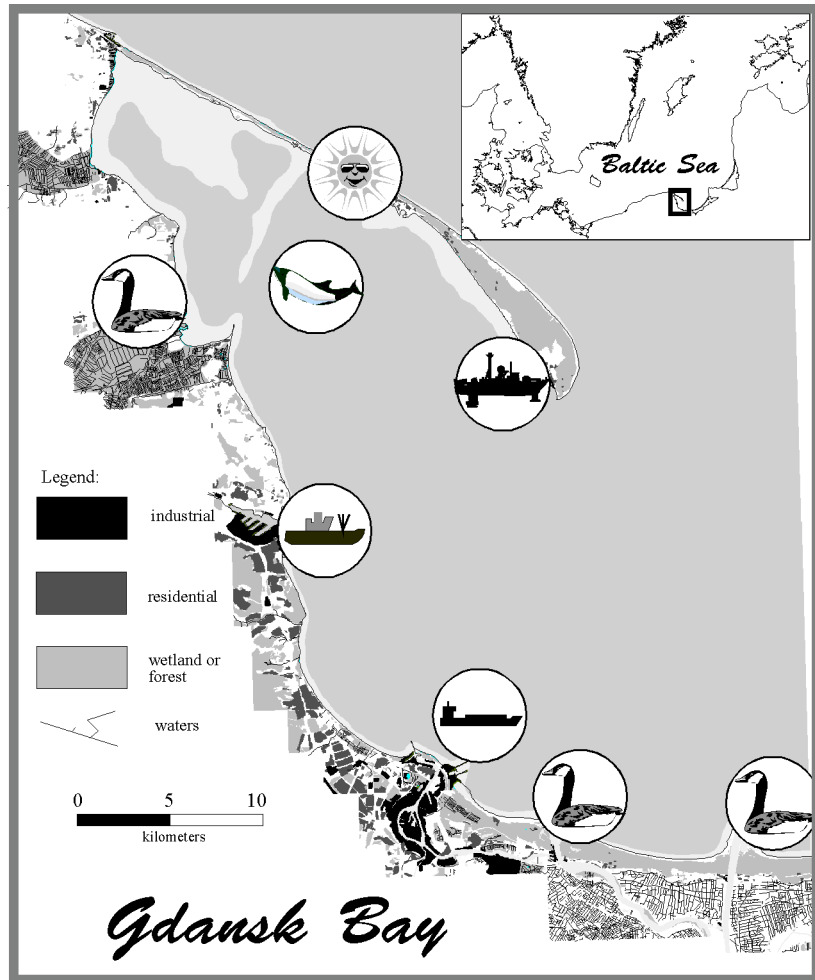
Figure 3 The Gdansk Bay
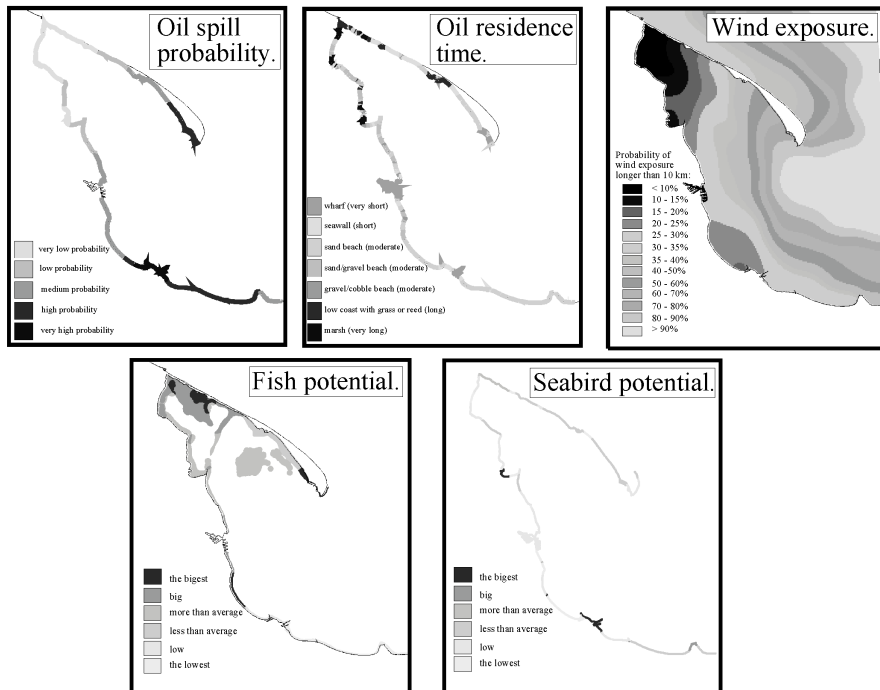
Figure 4 The factor maps used in the oil spill vulnerability modelling of Gdansk Bay coast

The application of dynamic segmentation in coastal vulnerability mapping

It was decided in this project that the coast sensitivity depends on five factors: probability of an oil spill, oil residence time, degree of exposure to wind and wave action, fish potential and seabird potential. These factors with minor modifications have been used for a number of coastal environments from the Arctic to the tropics (Tortell 1992). The first stage was to create the maps for the particular factors (Figure 4).

The vector map of the probability of an oil spill was created from the results of 120 numerical oil spill experiments using the numerical model (Gajewski *et al.*, 1991). The location of accidents and wind scenarios were included using a frequency distribution of both parameters. The map was transformed to a raster map of the probability which was reclassified to 5 classes where the probability ranged from very low to very high.

Entity	Description
Beach	Accumulation of sand/gravel/cobbles near the water line.
Dune	Ridge of loose well-sorted sand shaped by wind and water.
Cliff or undercut dune	Sediment near vertical wall maintained by erosion.
Sand spit	Local sediment forms build above water level by littoral drift and wave action.
Marsh	Poorly drained area of mixed vegetation.
River mouth	Mouth of river or canal.
Low coast	Low coast without beach, dune or marsh.
Artificial	Man-made structures on coast.

Table 2 Types of objects on the coast of Gdansk Bay

Oil residence time depends on the type of the coastline. For example seawalls and exposed sand beaches are less sensitive because they are usually cleaned by natural forces or can be effectively cleaned by man (Jansen *et al.*, 1990). To map the types of coastline a dynamic segmentation data model was used. The classification scheme for the coast of the Gdansk Bay had to be created. The 9 types of objects on the shore were defined (Table 2) each with 3 to 9 attributes. The DGPS—Global Positioning System with differential correction—was used to prepare an inventory of all objects of the Gdansk Bay coast. All data was stored in a relational database. The implementation of the model required new custom software for input data, reclassification, overlay, length calculation and appending sets of data. The type of coast was classified for 7 classes according to oil residence time. The classified segments were saved in vector format and then transformed to a raster data model.

The map of the degree of exposure to wind and wave action was created as a map of the probability that wind exposure would be greater than 10km. Custom software was written to combine the coastal geometry and wind direction statistic information. The map used 6 classes of probability of wind exposure greater than 10km.

The map of fish potential was created as a raster map. The biomass and biodiversity of 15 species (fish and shrimp) and additionally intensive fishing areas were considered (Sapota and Skora, 1996). The map used 5 classes.

The sea bird potential map is a result of a 3-year investigation of sea bird appearance along the coast (Meissner 1996). The average amount of birds, biodiversity and appearance of threatened birds were considered. The map was created using a dynamic segmentation model then saved in vector format and transformed to a raster data model. The map used 5 classes.

The criteria for creating the map of the sensitivity index were combined by means of cartographic modelling according to the formula

$$S = \sum w_i x_i \prod c_j$$

where:

x_i = criterion score of factor i (normalised to 0–255)

w_i = weight of factor i

c_j = criterion score of constraint j (1 for coast, 0 for the rest)

Weights of factors were calculated using Saaty's technique by taking the principal eigenvector of a square reciprocal matrix of pairwise comparisons between the criteria. All calculations were made using Idrisi for Windows GIS software. The final result of modelling is shown on Figure 5A.

The main source of uncertainty of the method is a subjective process of weights evaluation. To determine the degree of consensus the coefficient of variation ν of the oil spill vulnerability index calculated for each cell for 8 independent evaluations was used. The coefficient was calculated according the formula

$$\sigma = \sqrt{\frac{\sum (x_i - x_s)^2}{n}}$$

$$\nu = \frac{\sigma}{x_i}$$

where:

$$x_i = x_{1,2,3,4,5,6,7,8}$$
$$n = 8$$

$$x_s = \frac{\sum x_i}{n}$$

Figure 5B presents the coefficients of variation of oil spill vulnerability index of the created map.
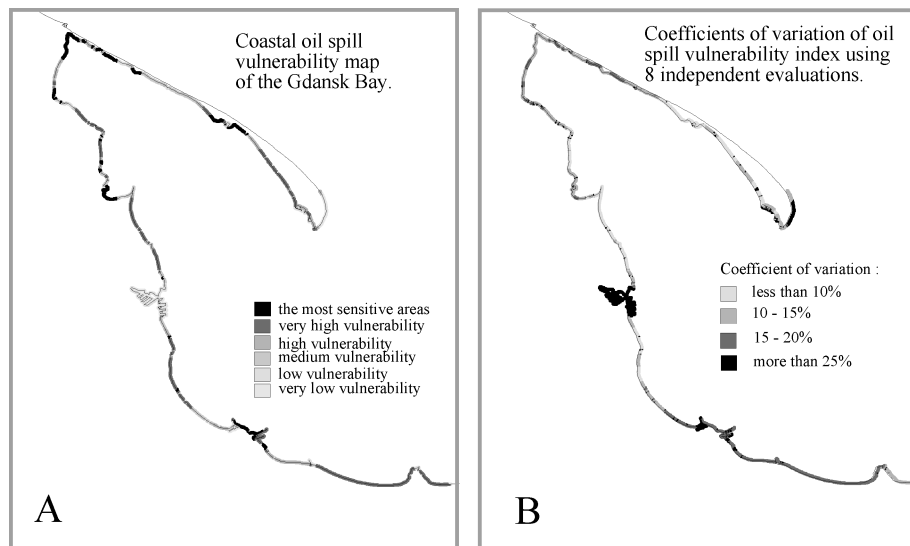
Figure 5 Coastal oil spill vulnerability map (A) and map of coefficients of variation of vulnerability index (B)

Conclusion

The aim of this paper was to present the work undertaken in the development of a decision support system for the coastal zone management operations. The database of the system was designed using the hybrid data model which allowed us to combine the raster data model and the dynamic segmentation model. The Multi-Criteria/Single-Objective technique implemented for the raster data model was used to create an oil spill vulnerability map. The uncertainty of this map was evaluated using different weights derived from a group of individuals.

References

Bartlett, D. (1994). GIS and coastal zone: Past, present and future. AGI Publication 3/94.

Carter, R. (1988). Coastal Environment. Academic Press, London.

Eastman, J., Kyem, P., Toledano, J., and Weigen, J. (1995). GIS and Decision Making. Explorations in GIS Technology. vol.4, UNITAR, Geneva.

Gajewski, L., Krezel, A., and Urbanski, J. (1991). System symulacji rozlewow olejowych w Zatoce Gdanskiej. Budownictwo okretowe i gospodarka morska. nr 2, pp.23–27.

GESAMP (1990). The State of the Marine Environment. GESAMP Reports & Studies. No. 39. UNEP, Nairobi.

Jansen, J., Ramsey, E., Holmes, J., Michel, J., Savitsky, B. and Davis, B. (1990). Environmental sensitivity index (ESI) mapping for oil spills using remote sensing and geographic information system technology. Int. J. Geographical Information Systems, vol.4, no.2.

Langran, G. (1993). Time in Geographic Information Systems. Taylor & Francis, London.

McCall, S., and Devoy, R. (1995). Applications of Geographic Information Systems to Coastal Management Approaches in Ireland. Directions in European Coastal Management. Healy and Doody (eds), Samara Publishing Limited, Cardigan.

Meissner, W. (1996). Database of birds—Gdansk Bay. (personal communication).

Populus, J., Moreau, F., Coquelet, D., and Xavier, J. (1995). An assessment of environmental sensitivity to marine pollutions: solutions with remote sensing and Geographical Information Systems (GIS). Int. J. Remote Sensing, vol. 16, no. 1, 3–15.

Sapota, M., and Dkora, K. (1996). Database—Gdansk Bay. (personal communication)

Tortell, P. (1992). Coastal Zone Sensitivity Mapping and its Role in Marine Environmental Management. Marine Pollution Bulletin, Volume 25, 1–4, pp 88–89.

Variability of the chemical composition of interstitial water of surficial bottom sediments in the region of the Gdansk Deep, Gdansk Bay, and Puck Bay

Teresa Szczepanska and Krzysztof Sokolowski

Introduction

The Gdansk Bay and Gdansk Deep are reported to be one of the most polluted regions of the Baltic Sea (Pempkowiak, 1994, Szczepanska and Uscinowicz 1994, Szczepanska 1995) and it is the most international part of the Baltic Sea catchment area. The sources of pollutants are rivers, domestic and industrial waste-waters and atmospheric dust. Pollutants accumulate in suspended matter which become bottom sediments. Heavy metals occurring in surficial sediments and in interstitial water play a important role in disturbing the ecological equilibrium of the marine environment. They have a toxic influence on marine organisms, especially "filtering" organisms, which live in constant contact with interstitial water in the pore spaces in the uppermost levels of the sediments.

According to definition, the interstitial water (pore water) fills pores and gaps in sediments independently of the degree of connection with the mineral skeleton. It consists of free water, water imprisoned in pores, capillary water and virtually connected water (Szczepanska *et al.*, 1980).

Interstitial water contains from a few to about a dozen times higher concentration of elements than sea water (Shiskhina, 1972, Lisitzin and Emelianov, 1981, Bolalek and Szczepanska, 1986, and Golimowski and Szczepanska, 1996). This is due to several factors, e.g. the limited circulation of water at high rates of sedimentation, desorption and dissolution of chemical compounds occurring in sediments in specific conditions of pH and Eh and the ion exchange processes.

The special interest in the water/deposit contact zone is connected with intense processes of translocation of elements. Bottom surface sediments are the habitat of over a dozen species of sea bottom fauna, living mainly in the 0–3 cm layer. Many of these species have adapted themselves to anaerobic conditions, however the presence of some chemical components, including certain metals and non-metals, can result in protracted illnesses. In addition, elements that were thought for a long time to be nontoxic, such as Al or Be, can also exert a negative influence when their concentrations exceed the level tolerated by marine organisms.

The objective of the investigations was to present the distribution of typical toxic metals Pb, Cu, Co, Cr and Ni, and also of elements which when appearing in higher concentrations have a negative influence on marine flora and fauna (Al, Fe, Mn, Sr, Li, B and Ba) in interstitial waters of mud/clay bottom surface deposits in the 0–25 cm layer.

The degree of enrichment of interstitial waters with these elements in comparison with sea water is given. The layer of deposits with interstitial waters containing concentrations of elements exceeding levels of tolerance of marine organisms is determined. This information is very important since concentrations of elements become many times higher as they pass through the food chain.

Materials and Methods

Investigations were carried out in two areas of the Gdansk Deep, part VII (central) located between 18°40' to 18°57' E and 54°43' to 55°07' N and part VIII (eastern) located between 19°03' to 19°20' E and 54°43' to 55°07' N (Figure 1 and Figure 2). These areas cover a part of the Gdansk Bay, defined by Majewski (1990). However, part VII of Gdansk Deep reaches westward outside the boundary of the Deep given by that author.

The sea-floor of the Gdansk Deep is covered by clayey mud, on the surface of dark grey or grey-olive colour, passing, generally below 1.5–2 cm, to black mud. In the ceiling parts of the cores there is a slight smell of H_2S, in the middle parts the smell is very strong. The deposits are generally semi-liquid (the water content is 92–98%), homogeneous, in places of gel-like consistency, saturated with diagenetic gasses. At contact with water there is a 2–4 mm thick minilayer of flocculent deposit. These are fragments of the brown algae *Pylaiella litoralis*, which change their colour with periods of vegetation (in Summer from creamy to dark yellow, in the Autumn from brown to black). The values of the physical and chemical parameters of the deposits change in vertical as follows: pH increases from 6.50 to 6.90 and Eh decreases from

+64 to −110mV (point 30/91) (Figure 3). Contemporary deposits in the Southern Baltic show typical pH and Eh values, depending on the stage of early diagenesis. Generally, in the 0–2cm layer pH is 6.8–7.2 and Eh ranges from small positive values, ca. +50mV, to negative values of −150 to −180mV (Szczepanska, 1993). The rate of sedimentation of the deposits, as determined by the Pb210 method is 1.65±0.16mm year^{-1} at point 34/91 and 1.85±0.18mm year^{-1} at point 2 El 96/92 (Szczepanska and Uscinowicz, 1994).

In the Gdansk Bay the investigated area was located between the coordinates 18°53' to 19°27' E and 54°27' to 54°37' N. The surface of the muddy deposits was covered with flocculent fragments of decayed *Pylaiella litoralis*. Down to a depth of 15cm, in places even to 30cm, black mud with a strong H$_2$S smell was present, and below dark grey mud occurred. In this last layer numerous *Macoma baltica* shells were found. The pH value of the deposits changed vertically from 6.70 to 7.10, and the redox potential from −12 to −160mV (point 1/92). Besides, in the shallow water zones marked by the 70m depth contour bottom dwelling molluscs occurred such as *Mesidotea entomon*, *Pontoporeia femorata* and *Mysis mixta*. A large concentration of shells was found at point 15/91. They were unbroken, well preserved but coloured black. At this point pH variability in the profile is quite large and changes from 7.14 to 7.59, and Eh from +13 to −324mV, which is the lowest recorded value of Eh for this part of the sea. The rate of sedimentation is 1.86±0.16mm year^{-1} (point 8/93). The surface area of the investigated area of the Gdansk Deep and Gdansk Bay is about 4700km^2.
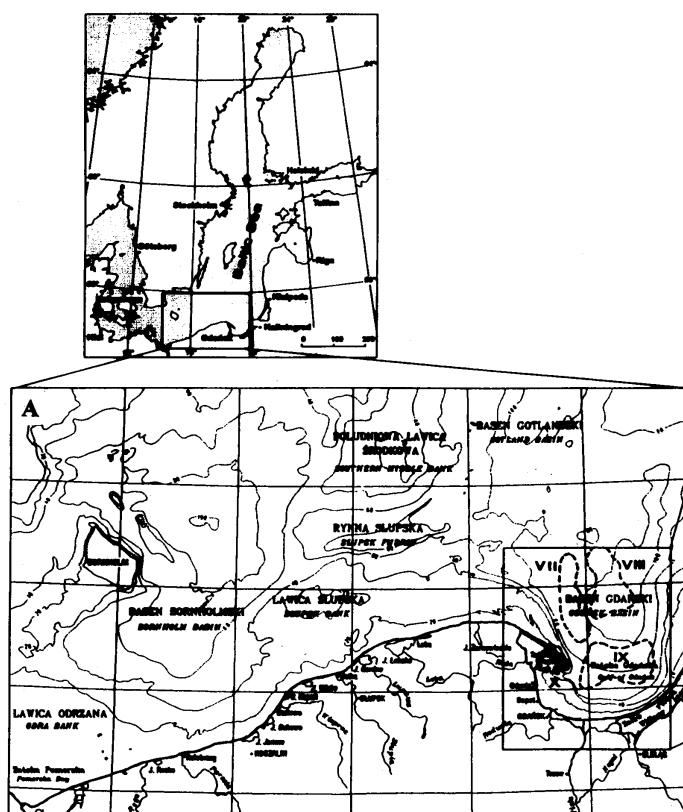
Figure 1 The investigation area. Area with geochemically differing deposits in the Gdansk Basin according to the Geological Atlas of the Baltic Sea 1:500 000, tab.XIX.
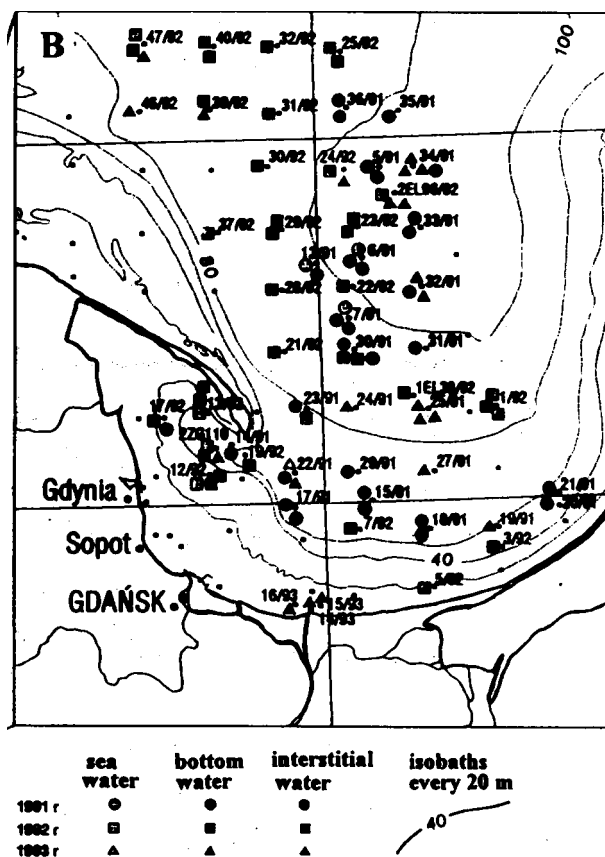
Figure 2 Location of research stations
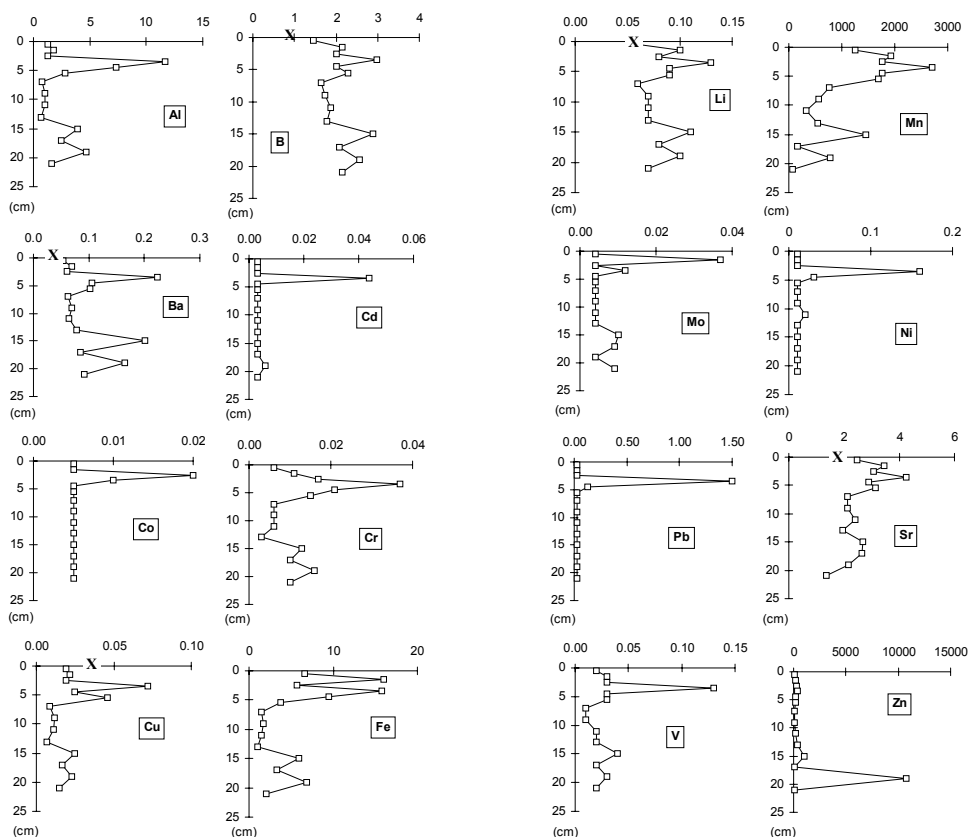
Figure 3 Vertical profiles pH and Eh in sediment and metals concentration in interstitial water (□) and bottom water (X)

The area investigated in the Puck Bay lies within 18°37' to 18°50' E and 54°33' to 54°38' N. Mud/clay deposits here cover about 100km^2 of the sea-floor. They are granulometrically differentiated, though their composition is quite similar

to the muds of the Gdansk Bay. At the surface, in the zone of contact of sea water and sediments, there is a 4mm thick layer of brown, flocculent deposits. In the part nearest to the Hel Peninsula homogenous clayey mud occurs, with light grey nests, with a strong H_2S smell. West and south of the Peninsula there is a 2–3cm layer of light brown sandy mud. Deeper, there is about a dozen centimetres of black mud with gel-like consistency and H_2S smell. Dark grey mud is present to a depth of about 40cm. Vertically, from the ceiling downwards, pH increases from 6.85 to 7.19 at the 16cm horizon, and the redox potential Eh from +34 to –90mV (points 12/92, 2 ZG/92). The highest saturation with diagenetic gasses such as H_2S, CH_4, CO_2 is observed in the central part of the investigated area, which causes sponginess in the deposit. pH values there change vertically from 7.19 to 7.39 and Eh decreases from –15 to –200mV. This indicates a significant diagenetic processing of the deposits. Muds in the eastern part are most strongly diagenesed, pH changes significantly vertically from 6.90 to 7.62, and Eh from +24 to –290mV (point 12/91).

Clayey silts containing over 75% of the fine fraction <0.063mm cover central parts of this region. The content of total organic carbon is 1.46–8.77% (mean 5.59%), cadmium 0.5–2.3ppm (mean 1.4ppm), lead 8–92ppm (mean 66ppm), zinc 65–259ppm (mean 169ppm) and copper 21–57ppm (mean 41ppm) (Szczepanska and Uscinowicz, 1994).

In the investigated region 28 research stations are located, 24 in the Gdansk Deep and Gdansk Bay and 4 in the Puck Bay. 190 samples of interstitial water (140 samples from the Gdansk Deep and Gdansk Bay and 50 from the Puck Bay) were analysed.

Interstitial waters were obtained from sediment samples taken in 1991–1993 on board r/v "Oceania" and "Dr Lubecki" using Kajak and Niemistö corers. After dividing into 2cm thick slices and measuring pH and Eh, the samples were centrifuged for 20 min. at 5000rpm at a temperature of 4°C. The obtained interstitial water was divided into two parts—one for determination of chloride ions and alkalinity and the other to determine the content of metals. The second part of the interstitial water sample was acidified by concentrated HCl ultrapure in proportion 2.5cm^3 acid to 100cm^3 of investigated water. Nalge polyethylene bottles were used for storing the water samples at a temperature of 4°C.

The content of heavy metals in the water was determined by the ICP method (Table 1).

	Element	Wave length (nm)	Detection limit (mgdm^{-3})
1	Al	308.215	0.1
2	B	208.893	0.02
3	Ba	233.527	0.005
4	Ca	317.933	0.1
5	Cd	226.502	0.006
6	Co	228.616	0.005
7	Cr	267.716	0.01
8	Cu	324.754	0.005
9	Fe	259.940	0.01
10	Li	670.776	0.02
11	Mn	257.610	0.005
12	Ni	231.604	0.02
13	Pb	220.353	0.04
14	Sr	407.771	0.002
15	Zn	213.856	0.005

Table 1 Detection limits and analytical conditions of determination of metals by ICP method.

The acidified sample was filtered by hard filter in order to separate accidental grains. The filter was produced in Germany. The sample's volume for analysis was usually 20cm^3. Standard curves were prepared on the ground of our own standard. A blank test was analysed simultaneously. The conditions of measurements and detection limits are given in Table 1.

Each result is the average value of 5 measurements. Precision of determination is specified by relative standard deviation (RSD). For concentrations near detection limit RSD= <20%, for concentrations 10 times larger, RSD = 10% and for concentrations 100 times larger, RSD = 1%. Accuracy for the 95% confidence level is confidence interval (m) for the arithmetic mean (the result for five measurements).

We can define it as: m = average result ± result·RSD/100.

For example Zn, which was measured on the level near detection limit i.e. $0.005\,\text{mg}\,\text{dm}^{-3}$ with precision RSD < 20%, has $m = 0.005 \pm 0.005 \cdot 20/100 = 0.005 \pm 0.001$; and for concentration Zn 10 times larger i.e. $0.050\,\text{mg}\,\text{dm}^{-3}$ and RSD < 3%, $m = 0.050 \pm 0,05 \cdot 3/100 = 0.05 \pm 0.0015$.

The total organic carbon content by modified coulometric titration was determined in the Central Chemical Laboratory of the Polish Geological Institute in Warsaw.

Results and Discussion

The results obtained were analysed statistically. The analysis comprised:

- calculation of geometric and arithmetic means of content of elements in interstitial water in analysed layers in the Puck Bay and Gdansk Bay and in two areas of the Gdansk Basin (Table 2)
- calculation of correlation coefficients between concentrations of elements (Table 3)
- linear regression on element concentration (Figure 4)

Vertical profiles of metal concentrations are shown in Figure 3. Cadmium, lead, zinc and copper concentrations in interstitial water 2–8 cm layer and concentrations harmful to marine organisms are shown in Figure 5.

Interstitial waters of Gdansk Deep deposits, part VII, contain more chlorides (mean from 5.24 to $6.11\,\text{g}\,\text{dm}^{-3}$) than part VIII of that basin (mean from 4.87 to $5.24\,\text{g}\,\text{dm}^{-3}$). Alkalinity is comparable in both areas and the vertical mean increases from 1.59 to $4.75\,\text{mval}\,\text{dm}^{-3}$ (Szczepanska, 1996). In the interstitial waters, 2–8 cm layer, of Gdansk Deep deposits, aluminium is nonuniformly distributed, in part VII the mean is $1.11\,\text{mg}\,\text{dm}^{-3}$, less than half of the amounts found in part VIII, where its content is $3.10\,\text{mg}\,\text{dm}^{-3}$.

Only four elements occur in comparable amounts in interstitial waters, 2–8 cm layer, in both parts of the Gdansk Deep, and the ranges of values are rather narrow: boron 1.96–2.01; barium 0.090–0.108; strontium 2.45–2.68 and calcium 131–$149\,\text{mg}\,\text{dm}^{-3}$. Cadmium, cobalt, chromium, nickel and lead occur in concentrations equal or lower than the limit concentrations measurable by the ICP method (Table 1). This makes comparative analyses of distribution of these metals rather difficult.

In part VII of Gdansk Deep, interstitial waters 2–8 cm layer contain significant amounts of iron (mean $16.22\,\text{mg} \cdot \text{dm}^{-3}$) and manganese (mean $6828\,\text{mg}\,\text{dm}^{-3}$). In part VIII the content of these metals in interstitial waters is much lower: iron mean $8.83\,\text{mg}\,\text{dm}^{-3}$ and manganese mean $2429\,\text{mg}\,\text{dm}^{-3}$. On the other hand, there is more copper (mean $18\,\text{mg}\,\text{dm}^{-3}$) and zinc (mean $147\,\text{mg}\,\text{dm}^{-3}$). Concentrations of lithium are nearly constant (0.07–$0.08\,\text{mg}\,\text{dm}^{-3}$) and moreover an increase of concentration with depth was observed only in interstitial waters of deposits of part VIII of Gdansk Deep.

In the Gdansk Bay, part IX, amounts of chlorides in interstitial waters are lower (3.62–$5.10\,\text{g}\,\text{dm}^{-3}$) than in the Gdansk Deep, but alkalinity is higher. Alkalinity increases vertically to $6.05\,\text{mval}\,\text{dm}^{-3}$ in the 8–20 cm layer (Szczepanska, 1996). As in the Gdansk Deep, most of the elements accumulate in interstitial waters of the 2–8 cm layer, though in lower concentrations. Only calcium and zinc occur in comparable amounts. In the coastal zone of the Gdansk Bay (points 14/93, 15/93, 16/93) the content of iron, manganese and zinc were several times 1/3 higher than in the central part of the Bay.

Layer (cm)	Para-meters	Al	B	Ba	Ca	Cd	Co	Cr	Cu	Fe	Li	Mn	Ni	Pb	Sr	Zn
		(mg·dm^{-3})				(µg·dm^{-3})				(mg·dm^{-3})		(µg·dm^{-3})		(mg·dm^{-3})	(µg·dm^{-3})	
Gdansk Deep, area VII																
0–2	Xg	0.98		0.060	123				7	7.34		3768			2.42	99
	X	1.02		0.062	124	<6		<10	9	9.33		3956	<20	<0.04	2.44	248
	min	0.71	-	0.049	111		-		<5	2.62	-	2380			2.07	35
	max	1.60		0.076	142				17	18.70		5633	20		2.85	1160
	n	6		6	4	6		6	6	6		6	6	6	6	6
2–8	Xg	1.11	1.96	0.090	147				14	16.22	0.07	6828			2.68	111
	X	1.30	1.97	0.093	148	<6	<10	<10	16	21.32	0.07	8289	<20	<0.04	2.69	127
	min	0.55	1.70	0.046	138				6	3.75	0.06	2077			2.43	56
	max	3.70	2.29	0.146	171	8		12	38	43.50	0.08	30653	20	0.07	3.28	283
	n	15	4	15	11	15	4	15	15	15	4	15	15	15	15	15
Gdansk Deep, area VIII																
0–2	Xg	1.96	1.71	0.074	118			<10	16	7.42	0.07	2081	<20	z0.04	2.34	103
	X	3.66	1.73	0.087	122	<6	<10	10	25	12.69	0.07	2248	20	0.05	2.41	130
	min	0.46	1.39	0.032	79			<10	<5	0.76	0.05	1240	<20	<0.04	1.28	42
	max	25.8	2.15	0.238	174	6	10	70	130	49.20	0.10	4371	70	0.28	3.46	472
	n	16	9	16	7	16	9	16	16	16	9	16	16	16	16	16
2–8	Xg	3.10	2.01	0.108	131			11	18	8.83	0.08	2429	20	0.04	2.45	147
	X	9.09	2.03	0.131	134	<6	<10	27	44	22.1	0.08	3001	30	0.13	2.53	263
	min	0.56	1.55	0.030	67			<10	<5	0.88	0.06	313	<20	<0.04	1.12	25
	max	84.1	2.99	0.360	163	44	20	240	400	167	0.13	12466	240	1.50	4.26	1600
	n	38	18	38	20	38	18	38	38	38	18	38	38	38	38	38
Gdansk Bay, area IX																
0–2	Xg	1.60	1.62	0.078	139			<10	17	4.73	0.06	671		<0.04	2.24	101
	X	2.50	1.68	0.093	140	<6	<10	10	20	6.51	0.06	762	<20	0.04	2.27	130
	min	0.37	1.25	0.041	119			<10	<5	1.25	0.05	222		<0.04	1.70	15
	max	12.70	2.92	0.263	152			50	52	24.10	0.07	1558	40	0.11	3.21	329
	n	13	9	13	4	13	9	13	13	13	9	13	13	13	13	13
2–8	Xg	1.86	1.64	0.101	142			<10	19	3.24	0.06	808	<20	0.04	1.86	147
	X	3.20	1.69	0.114	143	<6	<10	12	27	5.51	0.06	973	20	0.05	1.97	198
	min	0.52	1.22	0.044	127			<10	5	1.04	0.05	281	20	0.04	0.63	42
	max	15.8	2.69	0.259	153	6	10	50	182	29.9	0.08	3088	50	0.42	2.80	924
	n	30	22	30	8	30	22	30	30	30	22	30	30	30	22	30
Puck Bay, area X																
0–2	Xg	0.93		0.113	106				7	4.08		859			1.66	73
	X	1.25		0.148	108	<6		<10	8	4.85		2007	<20	<0.04	1.70	80
	min	0.17	-	0.028	83		-		<5	1.78	-	132			1.16	37
	max	3.43		0.346	136			10	19	9.52		8370		0.05	2.51	138
	n	7		7	7	7		7	7	7		7	7	7	7	7
2–8	Xg	6.43		0.251	130.7	<6		28	42	17.96		1128	40	0.08	1.69	310
	X	49.59		0.371	154.2	11		239	231	130.1		1857	180	0.42	1.82	267
	min	0.37	-	0.063	55.5	<6	-	<10	<5	0.81	-	181	<20	<0.04	0.82	38
	max	334		1.280	499	87		1820	1420	951		10300	1410	2.94	4.21	8640
	n	17		17	17	17		17	17	17		17	17	17	17	17

Table 2 Content of metals in interstitial water in selected enrichment layers of bottom surface sediments, where;

Xg is the geometric mean concentration,

X is the arithmetic mean concentration,

min is the minimum value of concentration

max is the maximum value of concentration

n is the number of water samples

| **Gdansk Deep, area VII** | | | | | | | | | | | | |
	Al	**B**	**Ba**	**Ca**	**Cr**	**Cu**	**Fe**	**Li**	**Mn**	**Ni**	**Pb**	**Sr**	**Zn**
Al	X	0.36	-0.32	-0.43	0.62	0.65	-0.49	0.70	0.55	0.54	0.76	0.46	0.72
B		X	0.94	-	0.45	0.15	0.49	0.92	0.35	-0.32	0.98	0.99	0.59
Ba			X	0.44	-0.15	-0.25	0.38	0.98	0.20	-0.42	-0.23	0.21	-0.51
Ca				X	0.00	-0.10	-0.28	-	0.72	0.00	0.00	0.86	-0.05
Cr					X	0.66	-0.41	0.40	0.70	0.82	0.77	0.45	0.79
Cu						X	-0.08	0.24	0.47	0.66	0.55	0.19	0.73
Fe							X	0.78	-0.05	-0.47	-0.57	-0.42	-0.48
Li								X	0.57	-0.30	0.89	0.95	0.49
Mn									X	0.50	0.38	0.32	0.38
Ni										X	0.45	0.06	0.69
Pb											X	0.73	0.81
Sr												X	0.47
Zn													X

| **Puck Bay, area X** | | | | | | | | | | | | |
	Al	**Ba**	**Ca**	**Cd**	**Cr**	**Cu**	**Fe**	**Mn**	**Ni**	**Pb**	**Sr**	**Zn**
Al	X	0.54	0.96	0.93	0.99	1.00	1.00	0.94	0.98	0.99	0.86	0.99
Ba		X	0.52	0.50	0.53	0.55	0.53	0.52	0.52	0.54	0.37	0.54
Ca			X	0.91	0.95	0.95	0.96	0.92	0.95	0.95	0.95	0.96
Cd				X	0.97	0.92	0.95	0.96	0.98	0.96	0.84	0.96
Cr					X	0.98	1.00	0.97	1.00	1.00	0.86	1.00
Cu						X	0.99	0.92	0.97	0.99	0.85	0.99
Fe							X	0.97	0.99	1.00	0.87	1.00
Mn								X	0.98	0.97	0.86	0.96
Ni									X	0.99	0.87	0.99
Pb										X	0.85	1.00
Sr											X	0.87
Zn												X

Table 3 Correlation coefficients of concentrations of metals occurring in interstitial water.
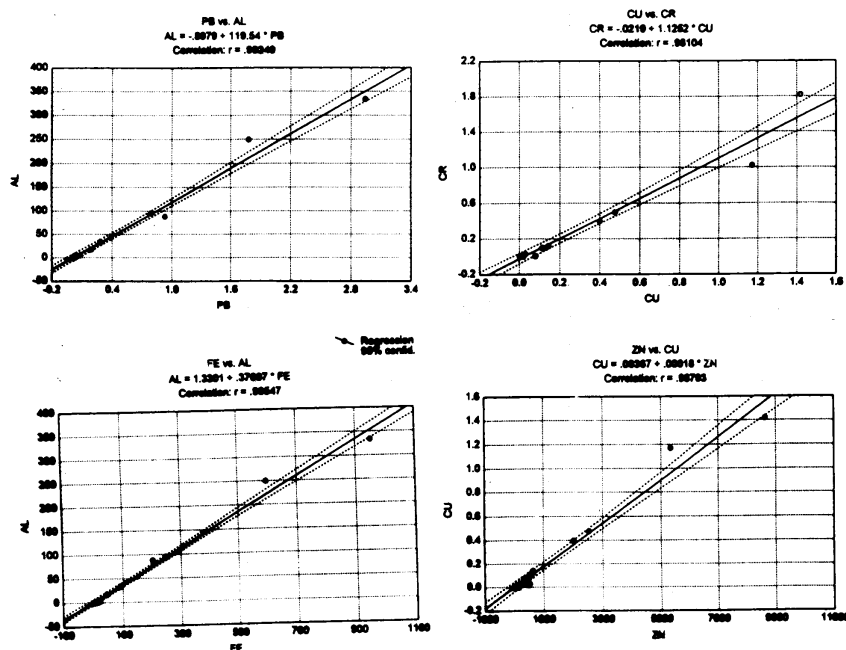
Figure 4 Linear regression on element concentration in interstitial water 2–8 cm layer in the Puck Bay.

● Gdañsk Deep,   ◇ Gdañsk Bay,   ✦ Puck Bay

Vertical lines ⌶ show the ranges of concentration harmful
to marine organisms (vide Pempkowiak, 1994)
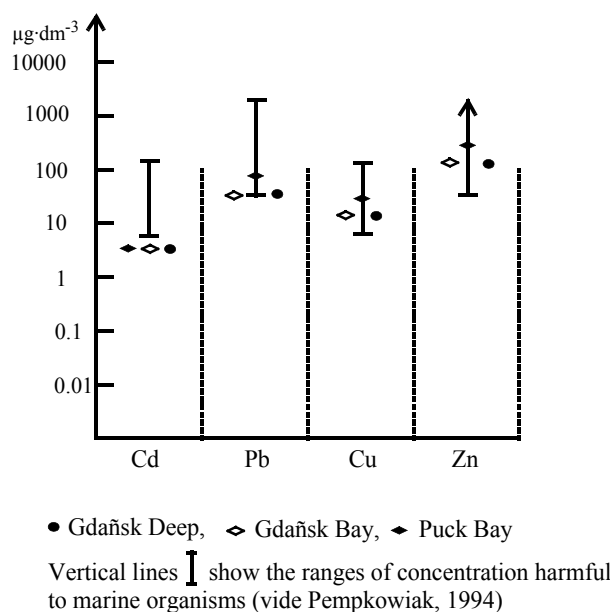
Figure 5 Metal concentration occurring in interstitial water 2–8 cm layer

In the Puck Bay, part X, interstitial waters of sea bottom deposits are characterised by the lowest content of chlorides (1.66–3.97 g dm^{-3}) and low alkalinity (below 3.6 mval dm^{-3}; Szczepanska, 1996). In the 2–8 cm layer of these waters there are higher concentrations with mean values of aluminium 6.43; barium 0.251; calcium 130.7; iron 17.96 mg dm^{-3}, and chromium 28, manganese 1128, nickel 40, lead 80 and zinc 310 mg dm^{-3}. Concentration peaks at the 3–4 cm horizon were observed (Figure 3). It is characteristic that in this water area there is twice or even three times as much aluminium, barium, chromium, copper, nickel, lead and zinc then in interstitial waters of the Gdansk Deep and Gdansk Bay. The exceptions are iron in part VII of the Gdansk Deep and manganese in both parts of the Gdansk Deep occurring in highest concentrations. Concentrations of calcium in interstitial waters are comparable in all the investigated areas, while the concentration of strontium is significantly lower in interstitial waters of the Puck Bay (Table 2).

Conclusions

The presented distribution of elements in deposits and in interstitial waters shows that processes of sedimentation are closely related with the circulation of waters in the Southern Baltic. This circulation is rather well documented for the area of the Gdansk Bay (Jankowski and Staskiewicz, 1994). In the Puck Bay this circulation periodically reaches only to the eastern part of the Bay.

The chemical composition of interstitial waters is formed appropriately to the degree of enrichment of the deposits with various elements. The higher coefficient of anthropogenic enrichment, the higher the content of chemical elements in the interstitial waters. The best example supporting this conclusion is the area of the Puck Bay, where the bottom is covered by muds characterised by coefficients of anthropogenic enrichment nearly twice as high as the mean values for the Southern Baltic (Szczepanska and Uscinowicz, 1994, Szczepanska, 1996) and interstitial water contains the elements in highest concentrations.

Maximum concentrations of elements in interstitial water are observed most often in the 5–6 and 6–8 cm layers (Suess, 1976, Lisicyn and Emelianow, 1981, Brügmann, 1988), and this confirms the data obtained in this work. In our opinion, the 2–8 cm range is more adequate.

The chemical composition of interstitial waters depends on a number of competing processes such as precipitation, sorption by clayey minerals, organic matter, formation of organic complexes and various diagenetic reactions leading to the change of physical and chemical properties.

The redox potential decides about the spatial distribution of metals easily changing valency, such as iron and manganese. In deposits of the 0 to 2 cm, and in places to 3.5 cm, there are oxidising conditions, and rather insoluble hydrated oxides Fe^{3+}, Mn^{3+} and Mn^{4+} predominate. These compounds absorb in turn other elements. In the lower lying deposits reduction conditions rule (Eh ranges from about −50 to about −300 mV), and processes of metal sulphide generation (precipitation) at a lower level of oxidation, such as Fe^{2+} and Mn^{2+} predominate. The zero potential line (redoxline) lies

as a rule in the layer of higher concentrations—ions of Fe^{2+} and Mn^{2+} and metals forming organic complexes collect here.

In the coastal zone of the Gdansk Bay, where muddy deposits are chemically enriched due to the influence of the Vistula, interstitial waters also contain more components. The distribution of calcium in the interstitial water is limited by cation exchange, Ca^{2+} and K^+ ions are freed into the water, while Mg^{2+} and Na^+ ions pass into the deposit.

In part VIII of the Gdansk Deep significant amounts of chemical components collect, mainly for two reasons: higher supply caused by typical circulation of waters from the north-east and east, and because of the higher percentage of clayey fractions in sea bottom deposits. This last factor is connected with bathymetry: 2/3 of the area VIII lies below the 100 m water depth, which forms better conditions for sedimentation. Accumulation is also facilitated in this region by the higher reduction potential of the deposits.

Elements such as Ba, Cd, Co, Cu, Cr, Fe, Ni, Pb and Zn are quickly bioaccumulated in the phyto- and zooplankton (Kabata-Pendias, Pendias 1993) and then get into the food chain. In chemical compounds most of these metals are strong poisons. Their negative influence on marine organisms becomes visible when concentrations of Cd and Cu exceed $6.8\,\mathrm{mg\,dm}^{-3}$, Pb exceeds $11\,\mathrm{mg\,dm}^{-3}$ and Zn exceeds $45\,\mathrm{mg\,dm}^{-3}$ (see Pempkowiak, 1994). The obtained results indicate that in the investigated areas concentrations of Cu and Zn in interstitial waters have exceeded these levels, in the Puck Bay also the permissible concentration of Pb is exceeded. Only Cd occurs in below-toxic concentrations.

Because of the mobility of Al, Cu, Cr, Fe, Mn, Ni, Pb and Zn ions and the possibility of their remobilisation from deposits into the nearbottom water, the existence of marine organisms is strongly endangered. Because of this, concentrations of the elements in deposits and interstitial waters should be periodically monitored.

Al, Ba, Ca and Sr show small variability in the vertical profile. The quotients of mean concentrations of elements is 1.5–16 (Table 4). Manganese shows both smallest and highest accumulation of strontium. Significant local differences in the distribution of metals in interstitial water in areas with differing geochemical characteristics were observed.

Al	B	Ba	Ca	Cr	Cu	Fe	Li	Mn	Ni	Pb	Sr	Zn	Al
Gdansk Deep, area VII													
a	1.3	1.3	2.3	1.4	-	1.3	8.8	-	37	-	-	1.5	3.8
Gdansk Deep, area VIII													
a	5.4	3.2	2.9	1.5	2.5	6.0	5.9	2.7	12.7	~2.0	~2.0	1.7	5.1
b	22.2	2.0	3.9	2.3	-	5.0	232	1.8	427	~2.0	~2.0	1.6	10.5
Gdansk Bay, area IX													
a	2.8	2.5	4.0	1.7	-	4.0	2.1	3.0	10.5	-	-	1.5	4.6
b	23.3	1.6	4.0	1.3	-	3.0	32.4	1.5	80.8	-	~2.0	1.1	7.0
Puck Bay, area X													
a	5.6	-	4.8	1.8	5.6	14.0	6.8	-	16.1	4.0	4.0	1.6	8.9
b	-	-	7.4	1.9	5.6	14.0	600	-	125	2.0	4.0	1.6	38.8

Table 4 Quotients of mean concentrations values of elements in interstitial water 2–8 cm layer versus mean concentration in bottom water 0–10 cm layer (a) and sea water (b).

Interstitial water obtained from the 2–8 cm layer of sediments contains the highest concentration of metals due to remobilisation of these metals under reduced conditions and limited possibly migration of elements at high rate of sedimentation of deposits.

Vertical variability of elements in interstitial water is a characteristic of the Puck Bay deposits. Maximum values were observed in the 2–4 cm layer.

In most of investigated profiles in the Gdansk Deep and Gdansk Bay area, maximum concentrations are strongly marked in the 2–8 cm layer, but sometimes the distribution of elements in interstitial water can be irregular.

The similarity of data obtained in consecutive years and similar vertical profiles of concentration of elements testify to a steady state of balance between dissolved forms of metals and forms deposited in the bottom sediments.

Pb, Cu and Zn occur in interstitial water in the sediments of the Gdansk Basin and Puck Bay in concentrations higher than are harmful to marine organisms.

Statistical analysis was carried out using the STATISTICA 5.0 program. Partial values of linear correlation coefficients r for probability $p < 0.05$ and 95% confidence level were calculated. The obtained high correlation coefficients for vapours of elements result from the similar chemical properties and similar role in the geochemical circulation. An exception is the good correlation with aluminium, which has a different geochemical characteristic. This may be explained by precipitation of this element in interstitial water with high alkalinity caused by diagenetic processes. Significant correlation between concentrations of metals in interstitial waters 2–8 cm layer ($r > 0.9$, $n > 16$) was obtained for the following pairs:

Al and Ca, Sr; Sr and Li, Ca in the Gdansk Deep (area VII),

Al and Mn, Cr, Cu; Ba–Sr; Cr and Cu, Pb, Zn in the Gdansk Deep (area VIII),

Ca and Sr, Cu and Cd, Cr, Fe, Ni, Pb, Zn in the Puck Bay (area X).

References

Bolalek J., and Szczepanska T., 1986. The distribution of Cu, Zn, Pb, Cd on Gotland Deep sea bottom in the area of sea water-sediment-pore water contact. 15th CBO, Copenhagen.

Brügmann L., 1988. Some peculiarities of the trace metal distribution in Baltic waters and sediments. Mar. Poll. Bull. 12, no. 6.

Golimowski J., and Szczepanska T., 1996. Voltammetric method for the determination of Zn, Cd, Pb, Cu and Ni in interstitial water. Fres. J. Anal. Chem., 354. Springer Verlag. Berlin.

Jankowski A., and Staskiewicz A.,1994. Currents in: Atlas of the Baltic Sea. IMWM Warsaw (in Polish).

Kabata-Pendias A., and Pendias H., 1993. Biogeochemistry of the trace elements. PWN Warsaw (in Polish).

Lisitzin A. P., and Emelianov E.M., 1981. Sedimentation processes in the Baltic Sea. Science. Moscow (in Russian).

Majewski A., 1990. Gdansk Bay. General morphometric character of the Gdansk Bay. IMWM. PGI. Warsaw (in Polish).

Pempkowiak J., 1994. Assessment of the degree of heavy metals threat of natural environment of the Inner Puck Bay in: Puck Bay, possibilities of renovation. IEP, Warsaw (in Polish).

Shiskhina V., 1972. Geochemistry of marine and oceanic interstitial waters. Science. Moscow (in Russian).

Suess E., 1976. Porenlösungen mariner Sedimente ihre Zusammensetzung als Ausdruck Frühddiagenetissssscher vorgänge. Arch. Univ. Kiel.

Szczepanska T., 1993. Geochemical properties of the quaternary sediments and chemical composition of the interstitial waters of the South Baltic Sea in relation to stratigraphy. Works PIG CXLI. Warsaw (in Polish).

Szczepanska T., 1995. Geochemistry of surficial bottom sediments. Plate XXIX, in: Geological atlas of the Southern Baltic 1:500 000. PGI. Warsaw.

Szczepanska J., Szczepanski A., and Vu Ngock Ky, 1980. On the influence of pressures on results of studies on pore water chemistry. Quart. Geol., V. 24, 4.

Szczepanska T., and Uscinowicz S., 1994. Geochemical atlas of the Southern Baltic 1:500 000. PGI. Warsaw.

Szczepanska T., 1996. Variability of the chemical composition of the sea water and interstitial water in area of the Gdansk Basin. Arch. PGI Sopot-Warsaw (in Polish).

Geological conditions in the artificial pits of the western part of the Gulf of Gdansk

Dorota Maksymowska, Halina Jankowska and Bogdan Oldakowski

Abstract

This paper deals with the study of sedimentological conditions in 2 post-dredging pits in the Puck Bay (western part of the Gulf of Gdansk), in order to determine the rate of deposition of recent sediment based on lithological analysis of sediment and modelling of sediment transport.

The post dredging pits make up two individual sedimentational environments. Kuznica B pit is characterised as having weak water dynamics. Sediments deposited in this pit are formed from suspended organic and fine grained mineral matter, as well as materials slumping due to gravity. Lithological variability occurred throughout the vertical profile of core samples; the surface sediment layer is comprised of a higher percentage of silt than that of deep original sediment exposed following dredging. A high concentration of organic matter (up to 47%) was also observed in these sediment. The Kuznica A pit is characterised as having a strong water dynamic. Consequently, erosion, traction, and to a lesser extent slumping were determined to be the predominant processes of sedimentation.

The geometry of deep pits may affect the propagation of current field throughout the surrounding area.

The rate of deposition of recent sediment varied between post dredging pits, with estimated values ranging between 0.5 and 4 cm per year.

Introduction

Human interference in the environment of the marine bottom sediments, such as dredging activities, may result in some changes to the sea floor morphology and sedimentation conditions. These changes are not irrelevant to the other components of the ecosystem and their impact is usually disadvantageous to the environment. Research to determine the influence of artificial pits after dredging in the sea environment has been carried out by many authors, among others Nichols *et al.* (1990) and Wolanski *et al.* (1992). In the Polish coastal zone the underwater work was carried out by the suction method. As a result, five deep post dredging pits were formed in the bottom of the western part of the Gulf of Gdansk–Puck Bay.

These deep artificial pits have been determined to affect the bay's geometry (Figure 2), hydrodynamic conditions, biological life and sedimentological processes.

This paper deals with the study of sedimentological conditions in post dredging pits, including the lithological character of recent deposits and the rate of deposition of recent sediment.

1 — Post dredging pits
2 — Investigated post dredging pits
A — Kuznica A pit
B — Kuznica B pit
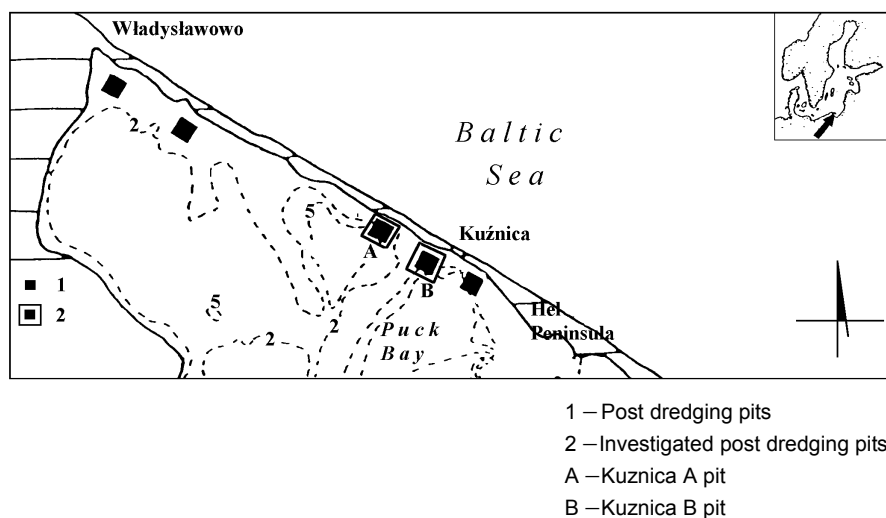
Figure 1 Bathymetry of the Puck Bay
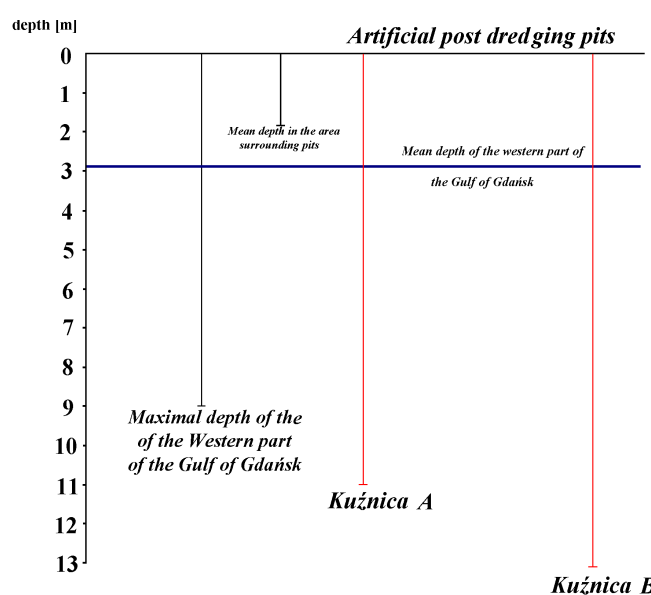
Figure 2 Comparison of natural depth of the Western part of the Gulf of Gdansk–Puck Bay and depth of post-dredging pits.

Study Area

Research work has been carried out in the western part of the Gulf of Gdansk–Puck Bay, in two of the post-dredging pits: Kuznica A and Kuznica B (Figure 1). In this area the natural depth of the bay varies between 0.8 and 1.9m (Figure 2), medium sand was the predominant type of sediment, and organic matter content varied between 0.5 to 3%.

Kuznica A pit is located 10.6km from the root of the Hel Peninsula, at a distance of 220–440m from the peninsula coast line (Figure 3). The pit is nearly parallel to the coast line, and it length is about 1000m and width is 50–250m. The maximum pit depth is 11m. The total dredged material taken from this pit between 1990 and 1992 was $1.108 \cdot 10^3 \, \text{m}^3$ (Cieslak, 1990, 1991, 1992).

Kuznica B pit is located 13.6km from the root of the Hel Peninsula (Figure 4). A large portion of this pit covers the Kuznica fairway. The distance between the Hel Peninsula coast line and the pit edge is 420–850m. The pit is 1100m long and 100–250m wide. The maximum depth reached 13m. The amount of all dredged material (between 1989 and 1991) was 1.437 thousand cubic meters (Cieslak; 1989, 1990, 1991).

The bathymetry of artificial post dredging pits stand in distinct contrast with the natural bathymetry of the Puck Bay. They are the deepest parts of the shallow part of the Puck Bay, where the average depth is 3.5m (Figure 2).
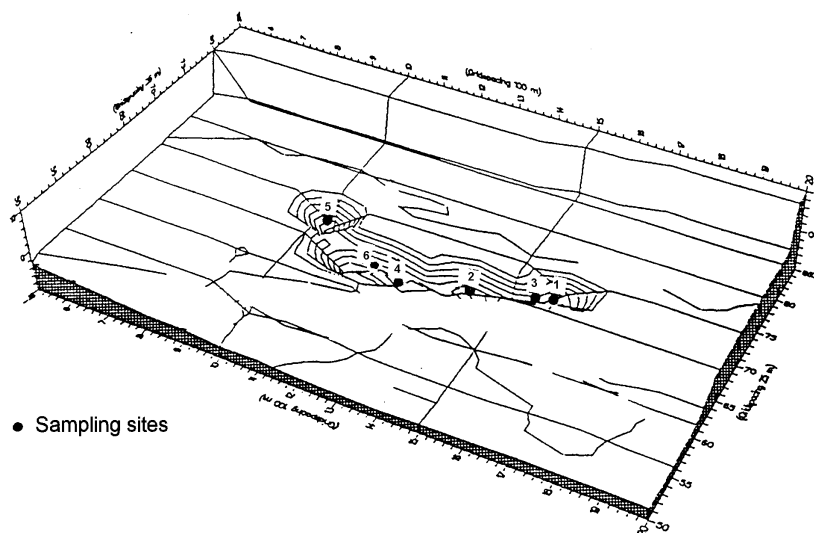
Figure 3 Bottom bathymetry of the Kuznica A pit (1990).
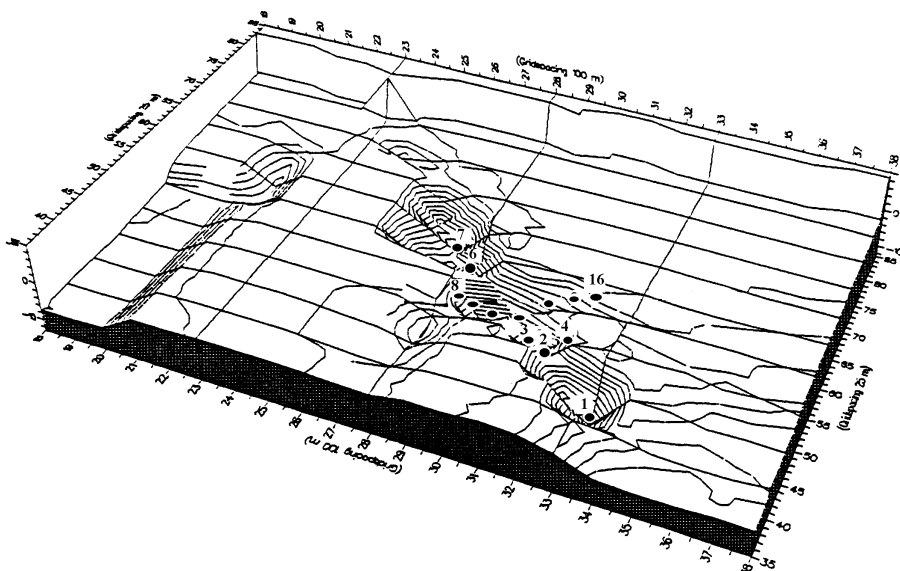
Figure 4 Bottom bathymetry of the Kuznica B pit (1990)

Materials and Methods

Sediment samples were collected by scuba divers in May, August and November 1992, using a plexiglas sediment sampler and gravitation sampler. Both sampling methods obtained undisturbed sediment cores. The length of sediment cores varied between 10 cm and 1 m.

In the Kuznica A pit, 6 cores were collected, from depths of 6, 6.7, 8, 9 and 10 m (Figure 3).

In the Kuznica B pit, 17 cores were collected, from depths of 4, 5, 6, 7, 8, 9, 10, 11.5, 12 and 13 m (Figure 4).

Immediately following their collection the sediment cores were divided into segments according to lithological variability, or into 1 cm segments.

Laboratory analyses on the segmented samples included grain-size analysis and organic matter content.

Sediment analyses included:

- granulometric composition:
  - by sieve method (sandy fraction, on calibrated strainers: 2.0; 1.0; 0.5; 0.25; 0.16; 0.125; 0.09; 0.063 mm)
  - by laser sedimentograph (silt and clay fractions (0.0015 mm–0.063 mm)

- organic matter content was determined as the ignition loss at a temperature of $550^{\circ}C$.

Sediment types were distinguished according to Shepard (1954). The statistical parameters of the sediments were calculated using equations proposed by Folk and Ward (1957) in addition to the Task's (1939) sorting coefficient. The dynamic of the sedimentological environment was determined by the method proposed by Passega and Byramjee (1969).

Surface sediment layer deposited after completion of dredging works were distinguished based on changes of lithology, statistical parameters of sediment, organic matter content and Passega and Byramjee's (1969) types along depth in cores.

Modelling of sediment transport was done using the MIKE 21 program (Danish Hydraulic Institute, 1992). The sediment transport model was based on a two-dimensional hydrodynamic model for stationary conditions; constant direction and velocity of wind were used. The influence of wave action on sediment transport was not taken into consideration and a non-cohesive character of the sediment was assumed because most of bottom sediments in the modelled area were sandy. A mean size of 0.23 mm (Cieslak, 1991, 1992) was used for model calculation for sediment of Kuznica A and Kuznica B pits area.

Only transport of bottom sediment was considered, suspended material was not taken into consideration during modelling.

The modelling areas covered the post dredging pits (Kuznica A, Kuznica B) along with a 1 km area surrounding each pit. Modelling was set at 100 and 25 m gridspacing for X and Y axis, respectively. The X axis was set perpendicular to the Hel Peninsula axis.

Extended bathymetry was used in the pit areas. Simplifications of boundary conditions were introduced.

As a result of modelling, the sediment transport value was obtained as bottom divergence in $cm\,year^{-1}$.

Results and Discussion

Results from this work revealed that there is a considerable differentiation in lithological types of recent sediments in each pit, and in addition, estimated rates of deposition of recent sediment were also different. This implied that each pit forms an individual specific sedimentary environment.

Kuznica A Pit

Based on changes of granulometric composition, statistical parameters and organic matter distribution through vertical profiles of sediment cores, a clear contact between the surface layer of fresh deposits and the lower layer of middle sand was distinguished. This contact was observed at a depth of 4–5 cm in the deeper pit area and at 3 cm depth of sediment in the shallow one (Figure 5).

The surface 3–5 cm sediment layer of Kuznica A pit is characterised by fine grained material: silty sand, sandy silt, and silt; with a mean size ranging from 3.74 to 5.97 Ø and an average of 4.66 Ø (Figure 5). In this surface sediment layer an enrichment with silty fraction compared to the surrounding area took place.

Depth in core [cm]	1	2	3	4	5	6
0 - 1	V s.s. 3.34	VII s. 5.60	VII s.s. 4.11	VII s.s. 4.65	VII s.s. 3.82	V s.s. 3.81
1 - 2	V f.s. 2.99	VII s. 5.90	VII s.s. 4.70	VII s.s. 5.78	V s.s. 3.77	VII s.s. 4.51
2 - 3	VII s.s. 3.76	VII s. 5.94	VII f.s. 3.79	VII s. 5.91	VII s.s. 3.92	VII s.s. 5.00
3 - 4	VII f.s. 3.53	VII s.s. 4.72	VII f.s. 3.74	VII s. 5.87	VII s.s. 4.22	V 2.81
4 - 5	V f.s. 3.38	VII s.s. 3.89	VII f.s. 4.14	V f.s. 2.95	V f.s. 3.15	V f.s. 2.82
5 - 6		V f.s. 3.34	V f.s. 3.42	V f.s. 2.79	V f.s. 2.74	V f.s. 3.02
6 - 7			V f.s. 3.05	V f.s. 2.78	V f.s. 2.75	V f.s. 2.80
7 - 8			V f.s. 2.70	V f.s. 2.75	V f.s. 2.68	V f.s. 2.68
8 - 9			V f.s 2.70	V f.s. 2.68		V f.s. 2.68

f.s. — fine sand
s.s. — silty sand
s. — silt and sandy silt
V — Passega type
2.05 — mediana

Figure 5 Lithological profiles of sediment of the Kuznica A pit.

The TRASK sorting coefficient (S_o) varied from 1.23 to 3.60 (Figure 6) and was considerably greater then in deeper layers. This upper 3–5 cm sediment layer is poorly sorted, indicating that it was formed during dynamic changes of sedimentary environment (Trask, 1939).
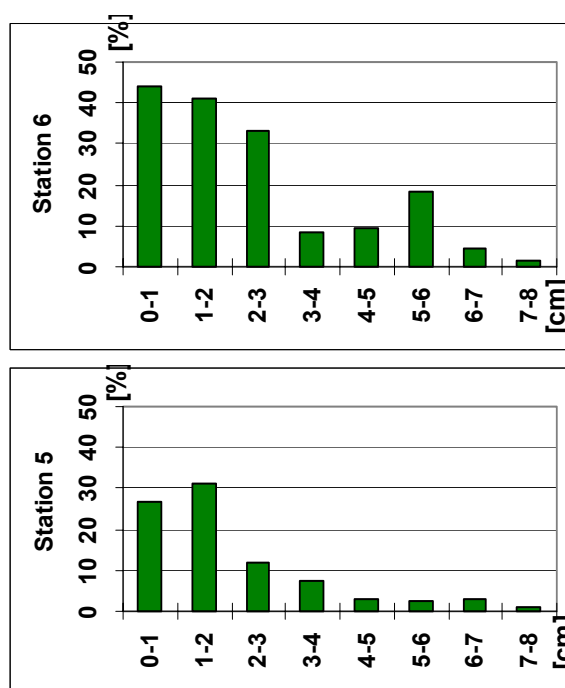
Figure 6 Organic matter in sediment profiles of Kuznica A pit.

The skewness coefficient (S_{KI}) varied from –0.001 to +0.75 in sediment cores from the Kuznica B pit, with a majority of values from +0.30 to +0.55 (Table 1). Such skewness coefficient values indicated that the sediment rubble was supplied constantly with fine material by low velocity currents (Folk and Ward, 1957). The S_{KI} coefficient did not change in the vertical sediment profile. This does not allow for a distinction of the border between in-situ sediment and these deposited after the conclusion of dredging works in this area.

In the surface sediment layer (2–4 cm) the kurtosis (K_G) was usually below 1.5 (Table 1). Low values of K_G coefficient indicated fast deposition of rubble and pulsative dynamic changes of the sedimentary environment (Folk and Ward, 1957; Racinowski and Szczypek, 1985).

According to Passega and Byramjee (1969) classification (Figure 5) the surface sediment layer (type VII), was deposited mostly from homogeneous suspended matter without density changes throughout the vertical profile of the water column. Passega and Byramjee (1969) classification indicated that the Kuznica A pit was a low dynamic sedimentational area.

Organic matter content for the surface 3–5 cm sediment layer of Kuznica B pit varied from 3.8 to 47% (Figure 7) and usually reached maximum at the depth of 1–2 cm, decreasing with increasing depth of sediment.
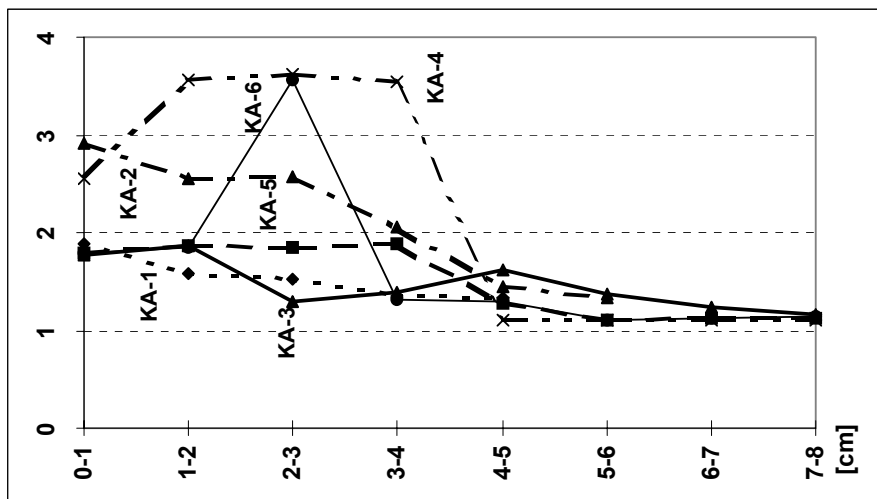
Figure 7 Trask's sorting coefficient in sediment profiles of Kuznica A pit

Such a high organic matter content is only found in areas of peat formation and in deep clay sediment in the Puck Bay (Jankowska, 1993).

A high content of organic matter in the 0–5 cm sediment layer, shows a slow mineralisation ratio in anoxic condition (H_2S was present in most samples).

In contrast to the surface sediment layer, the layer below the 3–5 cm depth, depending on the area of pit, is composed of fine sand with a mean diameter ranging from 2.68 to 3.42 Ø.

The Trask Sorting coefficient (S_o) (Figure 6), as well as a high kurtosis coefficient (K_G) (Table 1) indicate that it was deposited during homogenous dynamical conditions (Trask, 1939; Folk and Ward, 1957).

According to Passega and Byramjee (1969) classification, deeper sediment layer was formed from fractional suspended matter differentiated in respect towards density and grain size throughout the vertical profile of the water column, as well as rolling material by low turbulent currents (type V, Figure 5).

Sandy sediment was characterised by low organic matter content varied from 0.35 to 1.02% (Figure 7).

Such lithological characteristic of the deeper sediment layer allow to suppose that these are original, older sediment—typical for Puck Bay.

As a result of above analysis, the silt, sandy silt and silty sand surface sediment of Kuznica A pit have an estimated average rate of deposition of recent sediment from 2–4 cm year^{-1}.

Sample	Mean Size	Standard deviation	Skewness coefficient	Kurtosis coefficient	Trask's sorting coefficient	Passega classifi-cation
1KA– 0-1	3.34	1.65	0.48	1.42	1.89	V
1KA– 1-2	2.99	1.15	0.33	1.38	1.58	V
1KA– 2-3	3.76	1.41	0.47	2.01	1.52	VII
1KA– 3-4	3.53	0.98	0.39	1.95	1.35	VII
1KA– 4-5	3.38	0.81	0.39	1.76	1.33	V
2KA– 0-1	5.59	2.17	0.56	0.82	2.91	VII
2KA– 1-2	5.97	2.16	0.47	0.65	2.55	VII
2KA– 2-3	5.94	2.16	0.49	0.64	2.57	VII
2KA– 3-4	4.72	1.96	0.65	1.25	2.05	VII
2KA –4-5	3.89	1.55	0.58	2.46	1.44	VII
2KA– 5-6	3.34	1.06	0.49	2.47	1.34	V
3KA– 0-1	4.11	1.98	0.56	1.93	1.78	VII
3KA– 1-2	4.7	2.11	0.59	2.15	1.86	VII
3KA– 2-3	3.79	1.21	0.45	2.82	1.29	VII
3KA– 3-4	3.74	1.26	0.51	2.26	1.39	VII
3KA– 4-5	4.14	1.56	0.54	1.85	1.61	VII
3KA– 5-6	3.42	0.99	0.54	1.88	1.37	V
3KA– 6-7	3.05	0.54	0.37	1.22	1.24	V
3KA– 7-9	2.69	0.39	-0.01	1.47	1.16	V
4KA– 0-1	4.65	2.11	0.61	0.99	2.55	VII
4KA– 1-2	5.78	2.36	0.39	0.71	3.56	VII
4KA– 2-3	5.91	2.32	0.34	0.71	3.61	VII
4KA– 3-4	5.87	2.27	0.44	0.69	3.54	VII
4KA– 4-5	2.95	0.91	0.66	6.01	1.11	V
4KA– 5-6	2.79	0.37	0.31	2.35	1.11	V
4KA– 6-7	2.78	0.36	0.29	2.33	1.11	V
4KA– 7-8	2.75	0.35	0.29	2.34	1.11	V
4KA– 8-9	2.68	0.19	0	0.99	1.09	V
5KA –0-1	3.82	1.59	0.65	1.52	1.79	VII
5KA– 1-2	3.77	1.65	0.75	1.47	1.86	V
5KA– 2-3	3.92	1.64	0.59	1.49	1.84	VII
5KA– 3-4	4.22	1.71	0.51	1.42	1.89	VII
5KA– 4-5	3.15	0.81	0.66	1.86	1.28	V
5KA– 5-6	2.74	0.28	0.19	1.63	1.11	V
5KA– 6-7	2.95	0.44	0.46	2.07	1.12	V
5KA– 7-8	2.94	0.44	0.45	1.94	1.12	V
6KA– 0-1	3.81	1.59	0.65	1.53	1.79	V
6KA– 1-2	4.51	1.76	0.51	1.49	1.84	VII
6KA– 2-3	5.57	2.36	0.39	1.73	3.56	VII
6KA– 3-4	2.82	0.81	0.59	1.87	1.31	V
6KA– 4-5	2.82	0.85	0.63	1.85	1.29	V
6KA– 5-6	3.02	0.26	0.21	1.64	1.11	V
6KA– 6-7	2.81	0.43	0.44	2.19	1.13	V
6KA– 7-9	2.68	0.37	0.19	1.62	1.14	V

Table 1 Grain size distribution coefficients of geological profiles from Kuznica A pit.

Kuznica B Pit

In Kuznica B pit medium sand and fine sand are deposited, however in some places, sandy silt, silty sand, and clay sand occurred (Figure 8).

The mean size (M_z) of sandy sediment ranged from 1.80 to 3.38 with an average of 2.5Ø (Figure 8), while in fine grained sediment it ranged from 3.73 to 4.74Ø.

The trask sorting coefficient (S_o) varied from 1.17 to 3.21, with an average of 2.20 (Table 2), and indicated that sandy sediment from Kuznica B pit were well sorted.

The skewness coefficient (S_{KI}) varied from –0.05 to +0.62 in sediment cores. The majority of sediment samples had positively skewed grain size distribution (+0.01–+0.30) (Table 2).

The kurtosis coefficient (K_G) varied from 0.82 to 2.24. Values most often ranged between 1.00 and 1.50 (Table 2).
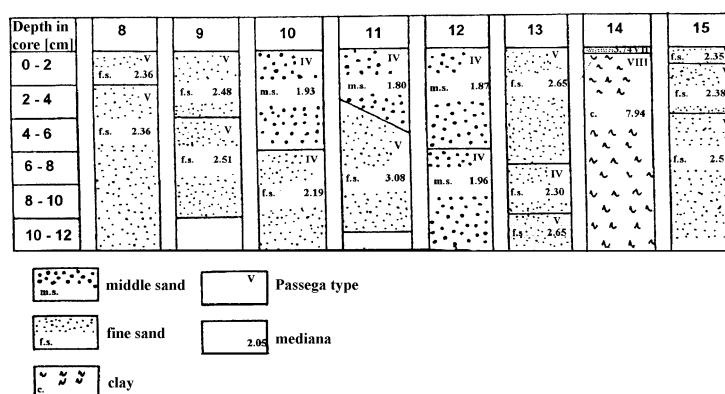
Figure 8 Chosen lithological profiles of sediment of the Kuznica B pit.

Sample	Mean Size	Standard deviation	Skewness coefficient	Kurtosis coefficient	Trask's sorting coefficient	Passega classifi-cation
1KB– 0-2	1.99	0.42	0.01	1.02	1.22	IV
2KB– 0-1	3.38	1.58	0.33	1.69	1.68	V
2KB– 1-2	3.73	1.73	0.37	1.69	1.77	VII
2KB– 2-3	4.01	1.91	0.35	1.53	1.94	VII
2KB– 3-4	4.29	1.93	0.37	1.44	1.99	VII
2KB– 4-5	4.74	1.32	0.36	1.32	2.04	VII
2KB– 5-6	4.02	1.49	0.53	1.85	1.59	VII
3KB– 0-5	2.32	0.72	0.33	1.44	1.32	V
6KB– 0-9	2.71	0.64	0.41	1.12	1.32	V
7KB– 0-9	3.11	0.89	0.32	1.14	1.49	V
7KB–9-19	4.96	2.21	0.44	0.94	2.81	VII
7KB– 19-24	5.42	2.29	0.33	0.82	3.21	VII
8KB– 0-2	2.36	0.99	0.01	1.08	1.55	V
8KB– 2-12	2.36	1.02	0.11	0.98	1.62	IV
8KB– 12-24	1.32	1.61	-0.04	1.11	1.31	I
9KB– 0-4	2.48	0.47	0.04	1.29	1.21	V
9KB– 4-10	2.51	0.51	0.13	1.46	1.21	V
10KB– 0-6	1.93	2.56	0.21	1.22	1.26	IV
10KB– 6-13	2.19	2.56	0.19	1.23	1.27	IV
10KB–13-19	2.72	2.57	0.21	1.29	1.25	V
11KB– 0-3-5	1.81	0.44	0.13	1.17	1.19	IV
11KB–3-5-9	3.07	0.83	0.09	0.84	1.53	V
12KB– 0-6	1.87	0.46	0.09	1.05	1.23	IV
12KB– 6-12	1.96	0.56	0.06	1.06	1.29	IV
12KB–12-20	2.39	0.59	0.11	1.26	1.27	V
13KB– 0-5	2.65	0.79	0.24	1.19	1.39	V
13KB– 5-8	2.29	0.48	0.09	1.26	1.21	IV
13KB– 8-9	2.65	0.62	0.09	1.22	1.29	V
15KB– 0-1	2.35	0.43	0.01	1.14	1.21	V
15KB– 1-4	2.38	0.41	0.02	1.19	1.89	V
15KB– 4-12	2.51	0.39	0.15	1.29	1.17	V
15BI– 12-27	2.96	0.68	0.29	1.21	1.32	V
16KB– 0-2	2.36	0.46	0.12	1.32	1.19	V
16KB– 2-7	2.42	0.38	0.05	1.23	1.17	V
16KB– 7-18	2.58	0.39	0.07	1.19	1.18	V
16KB–18-24	2.61	0.45	0.04	1.24	1.21	V

Table 2 Grain size distribution coefficients of geological profiles from Kuznica B pit.

Based on the Passega and Byramjee (1969) classification, collected surface sediment layer represented IV and V types, which indicates that they were formed from fractional suspended matter, as well as bottom rolling of material by turbulent currents.

The above data indicates that there are no essential differences between the lithological character of the surface sediment layer and deeper sediment layers in Kuznica B pit. This conclusion allows us to suppose that the bottom and slopes of Kuznica B pit are formed from original sediment exposed by dredging works.

Kuznica B pit is not conductive to sedimentation of material as a result of a highly dynamic sedimentary environment and a rather high current field (Nowacki, 1984; Jankowski, 1984). The Kuznica B post dredging pit is located on the site of the Kuznica marine fairway. This fairway is a place of water exchange between eastern and western parts of the Puck Bay (Nowacki, 1984). Also Passega and Byramjee (1969) classification indicates that water currents in the Kuznica B pit are rather strong, which has caused the traction of bottom material.

There was only one valid example found of on-going sedimentation in Kuznica B pit: sediment collected from the slope area of the pit at a depth of 10m (14KB). On the surface of the pleistocene clay bad, exposed during dredging works, a 0.5cm layer of very fine sands is present, with sorting coefficient equal to 1.32, S_{KI} coefficient 0.39 and K_G coefficient 1.76. This sediment was characterised by the VII Passega type. Moreover, surface sediment (1cm) in the deepest parts of Kuznica B pit were enriched with silt and fine sand fractions.

In some of the cores, clear abnormal contact was observed, revealing that under-water slides formed on the steep slopes of the pit cause displacement of the material from the slopes down to the bottom.

The organic matter content in collected sediment samples varied from 0.2 to 3.5% (Figure 9).

The distribution of organic matter throughout the vertical profile of Kuznica B sediments are typical for sediments of the Puck Bay (Jankowska, 1993). Organic matter content in sediment were highest in the deepest parts of Kuznica B pit.

In conclusion, deposition of recent sediment in the Kuznica B pit, occurring between autumn 1991 and May 1992, was observed only as a locally thin sediment layer (0.5–1.0cm).
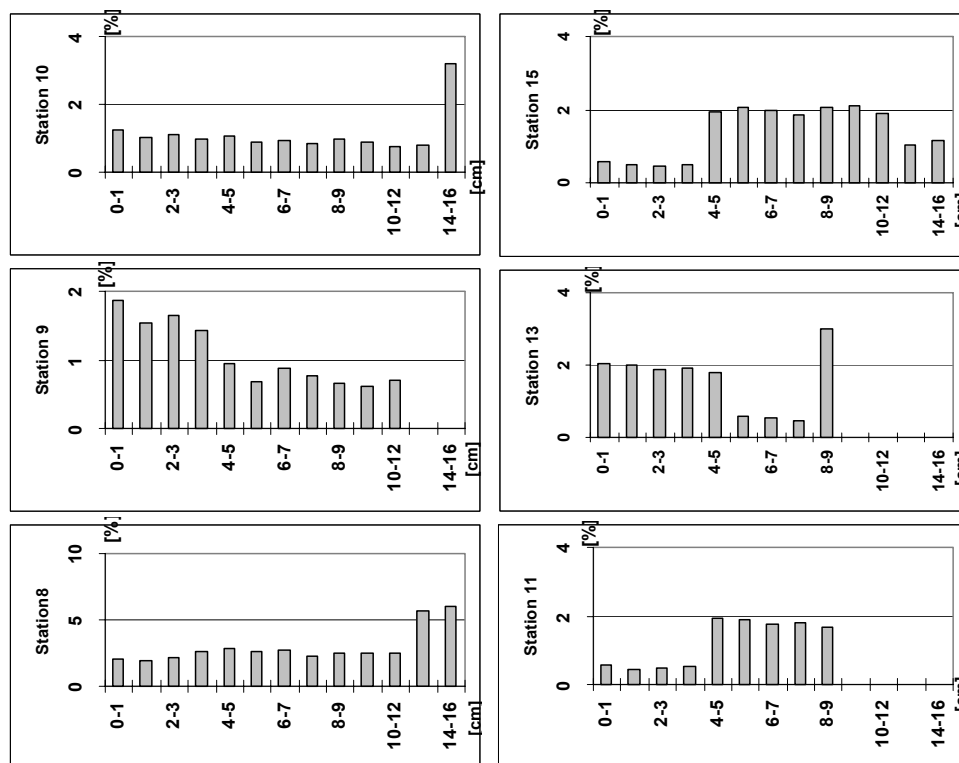
Figure 9 Organic matter in chosen sediment profiles of Kuznica B pit.

Results of Sediment Transport Modelling

Sediment transport calculations have been made for the most probable wind directions: N, NW, W, SW blowing with velocities of 5ms^{-1} and 15ms^{-1}. The first value corresponds to the mean wind velocity over the Puck Bay, while the 15ms^{-1} wind velocity equals to the strongest wind velocity for the Puck Bay region, causing the strongest movement of water and bottom sediment.

Modelling of the current pattern, derived by the wind field clearly shows the near shore flow, from the base of Hel Peninsula to its promontory. Similar characteristic current directions have also been observed by Jankowski (1984). In the post dredging pits areas, the current direction and velocity are changed (Figure 10).
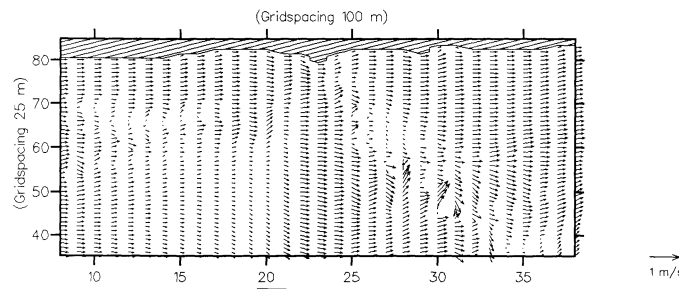
Figure 10 Depth integrated current field in Kuznica A and Kuznica B pits area, wind NW 15ms^{-1}.

Prevailing 5ms^{-1} winds has a little influence on the transport of bottom sediment. For such wind conditions, results of modelling of current pattern show that the depth integrated current speed has a value ranging from 0.02 to 0.1ms^{-1}, and does not cause an intensive sediment movement. Bottom divergence varies from –0.1 to 0.1cmyear^{-1}, which indicates that erosional-depositional processes are almost in a state of equilibrium.

The model results for the Kuznica A pit indicate that there are no significant differences in current pattern and sediment transport for winds: NE, SW and W blowing with a velocity of 15ms^{-1}. Sediment movement occurred in the largest area of the bottom with a modelled NW wind.
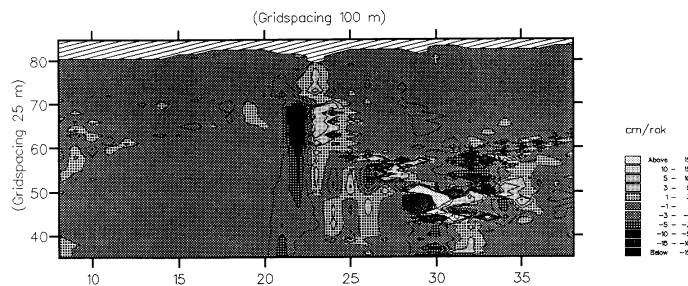
Figure 11 Bottom divergence (cm year^{-1}) in Kuznica A and Kuznica B pits area, wind NW 15ms^{-1}.

In the edge area of the pit sediment is being resuspended and then deposited in the surrounding area. The calculated bottom divergence in the edge area of the pit varied from –5 to 5cmyear^{-1}. Stronger bottom divergence occurred in the eastern part of the pit, due to higher current speed affected by smaller water depth (Figure 10). Bottom divergence in this area reaches values of up to –3cmyear^{-1}. The deposition of the sediment occurs in the eastern edge of the pit and in the northern edge region, and has a value of +3cmyear^{-1}. In deeper parts of the Kuznica A pit, calculated bottom divergence varies from –1 to 1cmyear^{-1} (Figure 11).

From sedimentological analysis the rate of sedimentation in Kuznica A pit is estimated at 2–4cm per year. It must be noted that a vertical element like suspended matter, which has not been included in the model, plays an important role in the sediment deposition.

The decreasing velocity of the current in the pit area does not affect the movement of sand fraction sediments in the deeper parts of the pit.

From the model results, it has been observed than in Kuznica B pit the current velocity is a little greater than in the other pit. The bottom erosion occurs in the eastern and south-eastern edges of the pit (up to –10cm year^{-1}) for calculated wind conditions. At the south-western pit edge erosion of the sediments occurred with a subsequent fast deposition of the material (Figure 11).

Erosion of the sandy Seagull Reef (which is very close to Kuznica B pit) is shown very clearly. Material from Seagull Reef is then deposited in the surrounding area and does not enter Kuznica B pit (Figure 11).

In this post-dredging pit bottom divergence varies from -1 to $1\,\mathrm{cm\,year}^{-1}$, which indicates that erosional-depositional processes are almost in equilibrium. This value is similar to the sedimentation rate estimated from sedimentological analysis, which means that there is almost no accumulation of recent sediment in Kuznica B pit. The calm sedimentation of suspended material in the Kuznica A pit is impossible because of a strong water dynamic.

Conclusions

From the above discussion the following conclusion are reached:

- the geometry of deep post dredging pits in the Puck Bay may affect propagation of current fields throughout surrounding area
- in the edge area of post dredging pits erosion and subsequent fast deposition occur
- suspended fine sand, silt, as well as suspended organic matter, are accumulated in pits; materials shifted by traction has only a slight influence on the sedimentation processes
- each of the post dredging pits forms an individual sedimentary environment according to different hydrodynamic conditions, flow of sedimentary material and mode of transportation
- Kuznica A pit is characterised by a weak water dynamic, and forms a kind of sedimentation trap for organic matter and fine-grained mineral suspended matter; the geometry of this pit stabilises sediment and does not allow for its redeposition
- in Kuznica A pit sedimentation of suspended organic and fine grained mineral matter as well as slumping occur
- Kuznica B pit is not conductive to sedimentation, mainly erosion, traction and to some extent slumping occur; only in the deepest parts of the pit slow sedimentation of suspended matter takes place
- the rate of deposition of recent sediment (fresh and uncompacted material) varies with respect to post dredging pit, and has an estimated values ranges between 0.5 and 4 cm per year.

References

Byers S.C., Mills E.L., Stewart P.L., 1978, A comparison of method of determining organic carbon in marine sediments, with suggestion for a standard method, Hydrobiologia 58, 43–47.

Cieslak A., red., 1990, 1991, 1992, Kompleksowa Ochrona Pólwyspu Helskiego (Comprehensive protection of the Hel Peninsula), Mimeo. Instytut Morski, Gdansk (in Polish).

Danish Hydraulic Institute, 1992, Mike 21, Sedimental Processes—Release Module, Total Transport, Pure Current, 1–40.

Folk R.L., Ward W. C.,1957, Brazos River bar; a study in the significance of grain size parameters, Journ. Sed. Petrol., vol.27, no.1, 3–26.

Jankowska H., 1993, The bottom deposits of the Puck Bay, Stud. Mater. Oceanolog., Marine Pollution 3, KBN PAN, Sopot, 64, 163–172.

Jankowski A., 1984, Przeplywy wiatrowe w Zatoce Gdanskiej (Current field in the Gulf of Gdansk), Stud. Mater. Oceanolog., KBN PAN, Sopot, 43, 5–80, (in Polish).

Musielak S., 1984, Osady denne Zalewu Puckiego (Sediment of the Puck Lagoon), Zesz. Nauk., Wydz. BiNOZ Uniw. Gdanski, Oceanografia, 10, 35–56, (in Polish).

Nichols M.M., Diaz R.J., Schaffner L.C., 1990, Effects of Hopper Dredging and sediment deposition, Chesapeake Bay, Environ. Geol. Water Sci., vol.15, no.1, 31–43.

Nowacki J., 1993, Cyrkulacja i wymiana wód, [in:] Zatoka Pucka (Puck Bay), Korzeniewski K. (Ed.), Fundacja Rozwoju Uniwersytetu Gdanskiego, Gdansk, 416–421, (in Polish).

Passega R., Byramjee R., 1969, Grain-size image of clastic deposits, Sedimentology, 13, 233–252.

Racinowski R., Szczypek T., 1985, Prezentacja i interpretacja wyników badan uziarnienia osadów czwartorzedowych (Presentation and interpretation of grain size analyses of Quantetary deposits), Katowice, Uniw. Slaski, Skrypty nr 3598, 143, (in Polish).

Shepard F.P., 1954, Nomenclature based on sand–silt–clay ratio, Journ. of Sed. Petrol., vol.24.

Trask P.D., 1939, Origin and environment of source sediments of petroleum, Gulf Publ., Houston, Texas, 323.

Wolanski E., Gibbs R., Ridd P., Mehta A., 1992, Settling of Ocean-dumped dredged material, Towsville, Australia, Estuarine, Coastal and Shelf Science, 35, 473–489.

Seabed sediments and current-induced bedforms in the Fehmarn Belt—Arkona Basin

Jørn Bo Jensen, Antoon Kuijpers and Wolfram Lemke

Abstract

The sediment map "Map sheet Fehmarn Belt—Arkona Basin, Late Quaternary sediments" is based on marine-geological investigations including shallow-seismic profiling and coring data. In addition to lithology, information on sediment ages, deposition environments and recent sediment dynamics is given. Due to the resolution of the seismic and coring data the sediment map represents an average sediment type of the uppermost 0.5 m.

Glacial till deposits form the eldest Pleistocene unit exposed in the shallow marginal parts of the survey area. At water-depths above 20 m, in the Fehmarn Belt–Mecklenburg Bucht–Arkona Basin areas, the till deposits are covered by varved clay bottomsets and in the Darss Sill area by sandy deltaic sediments. These sediments were deposited in the western part of the dammed, late-glacial Baltic Ice Lake. Oscillating Holocene lake levels and the Littorina Sea transgression resulted in deposition of Holocene freshwater and marine fine-grained sediments and sandy palaeo coastal sediments, respectively.

The marine transgression of the Darss Sill and subsequent current activity are responsible for strong erosion in the western Fehmarn Belt area, where late-glacial clay is exposed and only a few remains of Holocene sediments exist along the margin of the basin. Eastward, the erosive effect diminishes and in the central parts of Mecklenburg Bay no current-induced erosion is inferred.

Besides the removal of sediments, current-induced bedforms such as sandwaves and comet marks prove periodic, eastward inflow of saline bottom waters at water-depths of more than 15 m, while westward outflow of low-salinity Baltic water influences the seafloor in the northern part of Fehmarn Belt at water-depths of less than 15 m.

The characteristic sediment distribution and current-induced bedforms indicated on the map clearly reflect the postglacial development, whereas trawl tracks reveal recent human activity in the area.

Introduction

The map discussed in this publication deals with the Late Quaternary seabed sediments of the Fehmarn Belt and western part of the Arkona Basin. The extent of Danish and German territory covered by this map is roughly the same.

The actual bathymetry shows water depths of up to more than 40 m in the Arkona Basin and around 30 m in large parts of the Fehmarn Belt and Mecklenburg Bucht. A threshold, i.e. the Darsser Schwelle, separates the two basins for the largest part. A connection between the deeper basins is formed by the Kadet Channel with a maximum water depth of about 30 m. This erosional feature extends in a NE-SW direction just south of Gedser Rev. The prevailing water depth elsewhere in the Darsser Schwelle area is less than 20 m.

The map was made within the framework of the Danish program for mapping of offshore sand and gravel resources, which since 1990 was carried out in this area in close co-operation with the "Institut für Ostseeforschung" (IOW) in Warnemünde. The data used for the map were collected partly through individual investigations of respective institutes, partly through joint cruises of the R/Vs "Alexander von Humboldt", "Professor A. Penck", "Marie Miljø" and "Mette Miljø", during which shallow seismic investigations and sediment coring was carried out.

Methods

General

This map, which shows the area distribution of Late quaternary seabed sediments in the Fehmarn Belt and western Arkona Basin, is based on shallow seismic data and results from vibrocoring. Due to limitations of seismic resolution, characterisation of the seabed sediments applies to the sediment type found at about 0.5 m subbottom depth. It is stressed that the map not only provides lithological information, but also illustrates the regional Late quaternary stratigraphy with a [14]C-

based chronology and it includes information on the depositional environment as well. Various surveying techniques could not be applied at water depths of less than about 4 m, which implies that information from the coastal zone is not included in the map.

Apart from the sediment distribution, this publication also shows the occurrence of current-induced bedforms and evidence of direct human impact on the seafloor present in the form of trawl marks. Information from this map thus may help to distinguish between erosional, non-depositional and sediment accumulation areas, while also indicating bottom current transport directions.

Notwithstanding the restrictions referred to above, the data presented in this publication may significantly add to knowledge of the seabed conditions in the Fehmarn Belt and western Arkona Basin.

Shallow Seismics

Shallow seismic data were collected using an Elac 30 kHz echosounder, an ORE 3.5 kHz pinger system and Datasonics CHIRP (1–10 kHz) subbottom profiler system, a Uniboom (0.8–16 kHz) and an Edo Western and EG&G 100 kHz side scan sonar. The total track length is about 3000 km. The analogue data were recorded on an EPC/Klein graphic printer and stored either on analogue tape or in digital form.

Positioning was carried out using differential GPS and the Sercel Syledis precision navigational system with an accuracy of within 10 m.

The echosounder information was used to determine the water depth, whereas interpretation of the data from the subbottom profiler and Uniboom systems enabled a regional seismostratigraphic model to be established. This was done following seismostratigraphic principles introduced by Vail *et al.* (1977). These principles have previously been shown to be a useful tool in connection with the exploration of marine raw materials (Jensen 1992). When applying these seismostratigraphic analyses, depositional sequences are being defined by nonconformities as they cut off the various reflectors. In addition, the internal reflector pattern of the sequences is described.

A characterisation of the depositional environment was inferred from this seismic information and used for the selection of the coring sites.

Sediment investigations

A lithological description of about 300 vibrocores was made, whereas selected cores were subsampled for the purpose of grain size determination, loss on ignition and determination of the carbonate content. Moreover, a larger number of cores were subsampled at selected subbottom levels for ^{14}C-dating and the study of macroflora remains in order to obtain further information on the age and depositional environment of the cores. The selection of these samples was made by Ole Bennike, GEUS. The samples were dated either by conventional ^{14}C-dating at the Dating Laboratory of the National Museum and GEUS, or by Accelerator Mass Spectrometry (AMS) ^{14}C-dating at the Institute of Physics, Aarhus University, following the method described by Heinemeier and Andersen (1983). The stratigraphy used in the present publication is based on these dating results. Further and more detailed information on the ^{14}C-dating is beyond the scope of the description of this map.

Postglacial geological development

The data referred to forms the base of the interpretation of the late- and postglacial geological development of the area.

During deglaciation, ground moraines were formed, whereas flow tills and esker ice marginal deposits were also left behind by the retreating ice. Ice lake deposits accumulated in front of the melting ice masses. These deposits can be related to the earliest stage of the Baltic Ice Lake. After further retreat of the ice, changes of the lake water level resulted in various episodes (Baltic Ice Lake, Ancylus Lake) during which, amongst others, a series of littoral sediments and coastal deposits were formed in the area. Finally around 7000 years ago, the Littorina transgression occurred and marine conditions were established. In the course of this transgression, another series of (marine) coastal deposits was formed.

The development described here has resulted in the typical sediment distribution as can be observed on the map. The occurrence and area distribution of current-induced bedforms reflects actual sediment transport and bottom current conditions. A direct human impact on the seabed is seen for example by virtue of trawl marks.

Sediments

The seabed sediments found include glacial till mostly with a thin cover of sandy or gravely lag sediments, late glacial freshwater clay, silt or sand, Holocene freshwater and brackish (muddy) sand and sandy mud, and Holocene marine sand and mud.

Moraine–Glacial till

The oldest deposits exposed in the area are moraine deposits dominating along the basin margins where water depth is less than 15–20m. Two different moraine deposits can be distinguished, i.e. a consolidated ground moraine generally with a rough surface topography and an unconsolidated flow till with a smooth surface topography. Both moraine deposits are characterised by the occurrence of a thin (approx. 0.10m) layer of lag sediments of mainly gravel and coarser material.

Late glacial freshwater clay–sand

The late glacial deposits consist of ice lake sediments exposed in the central part of Fehmarn Belt, along the northern and eastern margin of Mecklenburg Bucht, and in large parts of the area between the Darsser Schwelle and Arkona Basin. Clayey and typically varved distal ice lake deposits are the most widespread late glacial surface sediments found in the Fehmarn Belt and in the area immediately south-east of Møn. Late glacial sandy deposits predominate, however, in the area south of Gedser Rev and along the south-western margin of the Arkona Basin. These sandy deposits reflect sediment input from a late glacial Warnow river system discharging in this area.

Holocene freshwater–brackish (muddy) sand and sandy mud

During the early Holocene, organic-rich fine-grained sediments were deposited in the deeper parts of the Fehmarn Belt area. These sediments were deposited during the development of the Ancylus Lake and partly also during the following beginning marine transgression (Mastogloia Sea). The sandy littoral faces of these sediments in the northern part of Fehmarn Belt have been eroded in a narrow zone at a depth of around 20m. The Ancylus sediments were also deposited south and north-east of Gedser Rev filling the older channel system and deeper parts of this area. Erosional remnants of these deposits are locally exposed on the seafloor here.

Holocene marine sand

Marine sand overlying moraine deposits is locally found at water depths of less than 20m.

This sand originates for a large part from former coastal deposits formed during the Littorina Transgression. Subsequently, reworking of the sandy deposits may have occurred locally.

Furthermore, at the Darsser Schwelle in the vicinity of Gedser Rev and more to the east larger areas are found, covered by up to 4m of sand. The water depth in these areas is around 20m. The thickness of the sand layer gradually decreases in an easterly direction.

Holocene marine mud

Areas where marine mud has been accumulating are found in the central part of the Mecklenburg Bucht, in the Arkona Basin and in the south-western part of Fehmarn Belt. In addition, a smaller mud basin is present immediately east of Møn. A characteristic feature of the mud depositional area in the Fehmarn Belt is the evidence of erosion found in the northern and western part of this area. This is indicated by an erosional inconformity and the occurrence of sediment waves. Thus, a record of continuous accumulation of recent sediments can be expected to be found only in the central parts of the Mecklenburg Bucht and Arkona Basin.

However, large-scale reworking of recent sediments may still occur here, as is suggested by the widespread occurrence of trawling marks in these areas.

Current-induced bedforms

The actual circulation pattern of the Fehmarn Belt is responsible for modifying older deposits and for the generation of specific current-induced bedforms. As outlined before, the non-tidal current system in this area is controlled by the large-scale weather pattern over NW Europe, and in particular, by wind-induced sea-level changes in the Kattegat and Baltic. Another factor to be taken into consideration is the layering of the water column with a general inflow of saline waters in the lower part of the water column and outflow of low-salinity Baltic water at the surface. The effect of the earth rotation (Coriolis force) further complicates this two-layer flow pattern.

A general conclusion is that the seabed in the southern part of the investigated area is mainly affected by inflowing saline waters from the Great Belt and Kattegat, whereas Baltic outflow affects the seafloor at shallower (<15 m) depths in the northern part of the area.

Typical current-induced bedforms are described below, illustrated by seismic examples from the Fehmarn Belt area (Figure 1 to Figure 5).
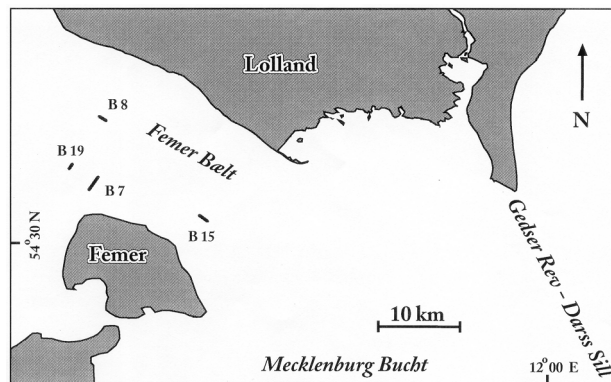
Figure 1 Location of seismic examples presented.

Sandwaves and megaripples

These transverse bedforms clearly indicate current-induced sediment transport (Figure 2). Sandwave and megaripple fields occur in various parts of the investigated area and are often found in relation to fossil sandy coastal deposits. In such areas they originate from erosional processes affecting the fossil deposits upstream, whereas downstream they are formed by accumulation processes (Figure 3).
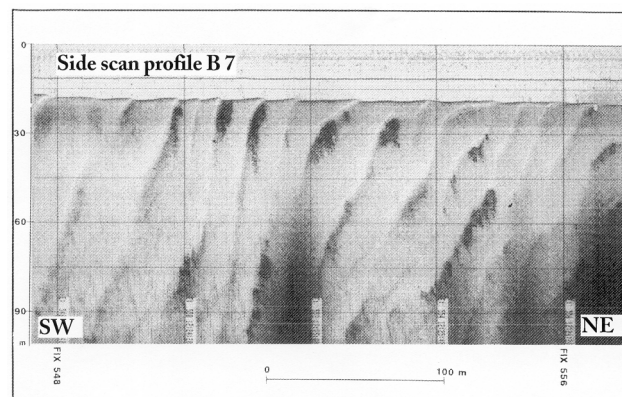
Figure 2 Side scan sonar image (B7) of sandwaves in the south-western part of Fehmarn Belt. Location indicated on Figure 1.
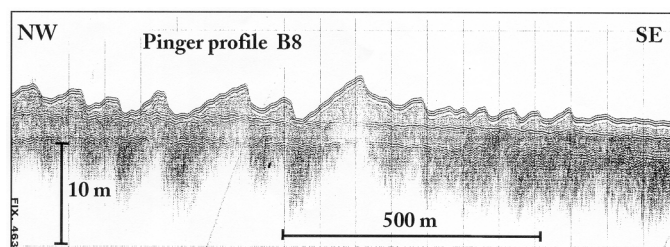
Figure 3 Pinger profile (B8) of sandwaves in the western part of Fehmarn Belt. Location indicated on Figure 1.

Investigations have previously been made of a sandwave field found between 12 and 22 m water depth north of Fehmarn (Werner and Newton, 1970; Werner and Wolf, 1974). The wavelength of these sandwaves is between 40 and 70 m, their height is 1–2 m, and they consist of medium to coarse sand (Figure 2 and Figure 3) (Werner and Wolf, 1974). The

sandwaves have a markedly asymmetric appearance with the steep sides facing east, which is indicative of an easterly current direction. The current speed required for the formation of such sand waves is in the range of 0.70 to $1.00\,\mathrm{ms}^{-1}$ (Rubin and McCulloch, 1980; Kuijpers, 1980). Current measurements demonstrate that in the area of investigation bottom current velocities are normally below this critical range; extreme bottom current events with the speed required occur at a time-scale of months or years (Wyrtki, 1953, 1954; Kuijpers, 1980). This is supported by seabed observations showing that the surface of the sandwaves can be covered by small-scale current marks and a Mya arenaria fauna indicative of long-term conditions with a largely inactive sand bed (Werner and Wolf, 1974).

Investigations of the Gedser Rev area (Lemke *et al.*, 1995) have shown the occurrence of sandwaves indicative of both inflow and outflow. Moreover, repeated observations indicated a change of bedform configurations in this area, i.e. a reversal of large sandwaves as well as the disappearance of a megaripple field (Kuijpers, 1991). The present study shows that sandwave fields also occur in the north-western part of Fehmarn Belt. These sandwaves are mainly found at water depths in excess of 15m, which correspond to the depth range of the sandwave field present in the vicinity of Fehmarn.

Isolated sediment (sand-silt) waves

The seismic data demonstrate the presence of isolated sediment waves of presumably sand or silt in the central parts of the Fehmarn Belt at water depths in excess of 20m (Figure 4).
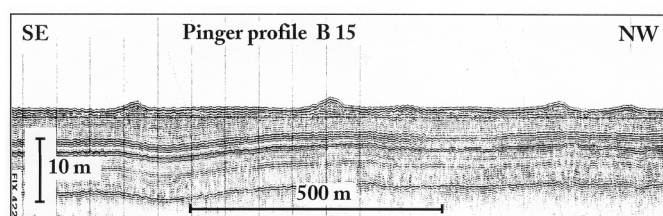
Figure 4 Pinger profile (B15) of isolated sand-silt waves in the central part of Fehmarn Belt. Location indicated on Figure 1.

These features are transverse bedforms and appear as NE-SW striking ridges of considerable length. The distance between the individual sediment waves is up to 500m. Their height is 0.5–1.0m, whereas they are about 50m wide. The single occurrence of these bedforms is ascribed to sparse sediment supply preventing a more widespread occurrence. A characteristic feature is that they occur on various substrates ranging from late glacial clay in the western part of the Fehmarn Belt to Holocene marine mud in the eastern part of this strait. In contrast to the sandwaves referred to above, these isolated sediment waves do not display a clear asymmetry or preferred orientation with regard to bottom current directions.

Comet marks

These longitudinal structures have been defined as obstacle marks characterised by a downstream erosional area of which the length is much larger than its width (Werner and Newton 1974). In the Fehmarn Belt they are preferably formed in areas where moraine deposits are locally covered by a thin layer of fine sand (Figure 5). Erratics from the moraine provide the obstacle required to form these erosional features developed in the fine sand layer. Often, however, a minor sand shadow is present downstream immediately behind the obstacle. The comet marks can be classified into various types depending on the hydrodynamic environment in which they are formed (Werner *et al.,* 1980). The comet marks observed in the Fehmarn Belt mostly have a parabolic appearance typically reflecting bottom current conditions comparable to those required for the formation of sandwaves. The areas with comet marks are found in the northern sector of the Fehmarn Belt and, more generally, along the northern margin of the deeper parts of the strait at water depths between 15 and 20m. Without exception, they all display an easterly tail direction indicative of the inflow of saline bottom water from the Great Belt.
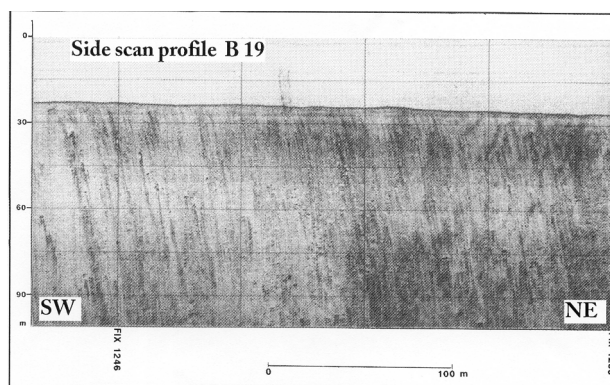
Figure 5 Side scan sonar image (B19) of comet marks in the western part of Fehmarn Belt. Location indicated on Figure 1.

Sand ribbons

Small sand ribbons are widespread at a shallow (<15 m) depth over the entire area in the northern part of the Fehmarn Belt. In just a few cases it was possible to determine the current direction from these longitudinal bedforms.

Bottom current conditions

Initially, the deeper parts of the Fehmarn Belt and Mecklenburg Bucht had been covered by freshwater and marine deposits from the earlier part of the Holocene. After the marine transgression of the Darsser Schwelle, current intensities increased and erosion started to prevail in particular in the western narrow part of the Fehmarn Belt. Presently, late glacial ice lake clay deposits are exposed widespread on the seabed in this area. Remnants from the Holocene freshwater and marine deposits referred to above still occur locally, however, along the margin of the Fehmarn Belt. Generally, erosion is less towards the Mecklenburg Bucht. Current-induced erosion is probably negligible only in the central parts of this bay.

The occurrence of strong bottom currents is not only evident from widespread erosion as described above, but is also demonstrated by the various current-induced bedform types observed in the area. Both the occurrence of sandwave fields and comet marks correspondingly indicate a prevailing easterly bottom current with maximum speeds of up to $1.0 \mathrm{ms}^{-1}$. These extreme current events are concluded to be relatively rare, normally occurring for a time scale of months or years (Wyrtki, 1954; Kuijpers, 1985). Also the isolated sediment waves in the deepest part of Fehmarn Belt suggest a relatively high-energy hydrodynamic environment. Thus it can be shown that bottom currents at water depths in excess of 15 m reach their maximum speed during inflow conditions. An easterly sediment transport direction is also found north-east of Gedser Rev in the area characterised by the presence of an up to 4 m thick marine sand layer getting thinner towards the east.

A more complicated bottom current pattern is observed around Gedser Rev, where both inflow- and outflow-induced bedforms occur. Previous investigations by Lemke *et al.* (1994) demonstrate that inflow of saline bottom water prevails in the Kadet Channel and in the area to the south, whereas outflow affects the seabed at water depths of less than 15 m north of the Kadet Channel. The bedform pattern around Gedser Rev suggest that in a situation of strong outflow an anticyclonic gyre will develop on the (western) leeside of Gedser Rev.

Finally, it can be concluded that, generally, outflow is the dominating sediment transport agent at shallow (<15 m) depth in the northern sector of the Fehmarn Belt off Lolland as well as in the coastal zone of Falster just north of Gedser Rev.

Acknowledgements

References

Björck, S. 1995. A review of the history of the Baltic Sea, 13.0–8.0 ka BP. Quaternary International, 27, 19–40.

Heinemeier, J & Andersen, H.H. 1983. Production of C directly from CO2 using the anis sputter source. Radiocarbon, 25, No. 2, 761–769.

Jensen, J.B. 1992. Råstofgeologiske undersøgelser i Østersøen. Fakse Bugt, område 520. DGU kunderapport nr. 51. 1992. 41 p.

Jensen, J.B., Bennike, O., Witkowski, A., Lemke W. & Kuijpers, A. in prep. The Baltic Ice Lake in the southwestern Baltic: Mecklenburg Bay–Arkona Basin.

Kolp, O. 1965. Paläogeographische Ergebnisse der Kartierung des Meeresgrundes der westlichen Ostsee zwischen Fehmarn und Arkona. Beiträge zur Meereskunde, 12–14, 1–59.

Kuijpers, A. 1980. Sediment patterns and bedforms, and their relationship to the flow regime in the Belt Sea and the Sound. Unveröffentlicht Dissertation, Geologich-Paläontologiches Institut. Universitet Kiel, 138 p.

Kuijpers, A. 1985. Current-induced Bedforms in the Danish straits between Kattegat and Baltic Sea. Meyniana, 37, 97–127.

Kuijpers, A. 1991. Råstofgeologiske undersøgelser i Østersøen: Gedser, område 560. DGU Kunderapport nr. 21. 1991. 67 p.

Lemke, W., Kuijpers. A., Hoffmann, G., Milkert, D. and Atzler, R. 1995. The Darss Sill, hydrographic threshold in the south-western Baltic: Late Quaternary geology and recent sediment dynamics. Continental Shelf Research, 14, 47–70.

Lemke, W., Jensen, J.B., Bennike, O. & Witkowski, A. in prep. Sequence stratigraphy of submarine Late Pleistocene and Holocene deposits in Mecklenburg Bay, south-western Baltic Sea. Sveriges Geologiska Undersökning, Ser Ca

Mörner, N.-A. 1983. The Fennoscandian Uplift: Geological data and their Geodynamical Implication. In: (eds.) D.E. Smith and A.G. Dawson. Shorelines and isostasy Academic Press, Institute of British Geographers special publication, no. 16, 251–284.

Rubin, D.M. and McCulloch, D.S. 1980. Single and superimposed bedforms: a synthesis of San Francisco Bay and flume observations. Sedimentary Geology, 26, 207–231.

Rørbeck, D.M. 1995. Late Quaternary sedimentology and seismic stratigraphy of the northern Storebælt, Denmark. Unpublished Ph.D. thesis. Geologisk Institut, Københavns Universitet. 202 p.

Svensson, N.O. 1989. Late Weichselian and Early Holocene shore displacement in the central Baltic, based on stratigraphical and morphological records from eastern Småland and Gotland, Sweden. Lundqua Thesis, 25, Lund Universitet, 195 p.

Vail, P.R., Mitchum, R.M., Jr, Todd, R.G., Widmier, J.M., Thompson, S., III, Sangree, J.B., Bubb, J.N., and Hatlelid, W.G., 1977. Seismic stratigraphy and global changes of sea level. In: Clayton, C.E., (Ed.), Seismic stratigraphy—Applications to Hydrocarbon Exploration. American. Association of Petroleum Geologists Memoir, 26, 49–212.

Werner, F. And Newton, R.S., 1970. Riesenrippeln im Fehmarnbelt (westliche Ostsee). Meyniana, 20, 83–90.

Werner, F., Wolf, E.A. and Tauchgruppe Kiel 1974. Sedimentologi und Ökologie eines ruhenden Riesenrippelfeldes. Meynianna, 26, 39–62.

Werner, F., Unsöld, G., Koopmann, B. and Stefano, A. 1980. Field observations and flume experiments on the nature of comet marks. Sedimentary Geology, 26, 133–262.

Winn, K., Averdieck, F.R., Erlemkeuser, H. & Werner, F. 1986. Holocene Sea Level Rise in the Western Baltic and the Question of Isostatic Subsidence. Meyniana, 38, 61–80.

Wyrtki, K. 1954. Die Dynamik der Wasserbewegungen im Fehmarn-belt II. Kieler Meeresforschung, 10, 162–181.

Penetration of Caesium-137 into sandy sediments of the Baltic Sea

R. Bojanowski, Z. Radecki, S. Uscinowicz and D. Knapinska-Skiba

Abstract

Large areas of the Southern Baltic floor are covered by sand and gravel. It is a common belief that such materials do not hold appreciable amounts of pollutants because their sorption capacity is low. Our measurements have shown, however, that the activities of caesium and Pu radionuclides locked in these loose sedimentary structures are not negligible. Actually, half of the total Cs-137 inventory was found to be associated with hard bottom, which occupies 64 per cent of the Polish Economic Zone.

Although activity concentrations of Cs-137 and Pu-239+240 are an order of magnitude lower in sands, compared to muddy sediments, their cumulative deposition, expressed in total amounts per unit area, differs only by a factor of two.

A relatively large accumulation of these radionuclides in coarse-grained deposits is made possible by incorporation of radioactive particles within the bottom material and the particles' downward displacement by mechanical forces. The penetration depth depends on hydrodynamical conditions prevailing at the sampling sites, and can vary from several centimetres to a few meters. The knowledge of this parameter is prerequisite for reliable assessment of radionuclide inventories in marine sediments.

Introduction

Monitoring of hazardous substances in the marine environment requires sampling of various materials for analytical purposes. Bottom sediments represent an important part of the marine realm because it is there where many pollutants accumulate. By studying vertical distribution of substances in sediment cores it is possible to reconstruct pollution history of aquatic basins, trace sources of pollutants and estimate their inventories.

Polluting substances combine frequently with fine-grained particles which carry them away to areas where they can settle. Sandy deposits, which normally occur in areas of high hydrodynamic activity, are considered free of these contaminants and are given little attention. However, our studies of the behaviour of Cs-137 in the Baltic Sea have shown, that the amounts of this radionuclide in sandy sediments are not negligible (Bojanowski *et al.*, 1995a).
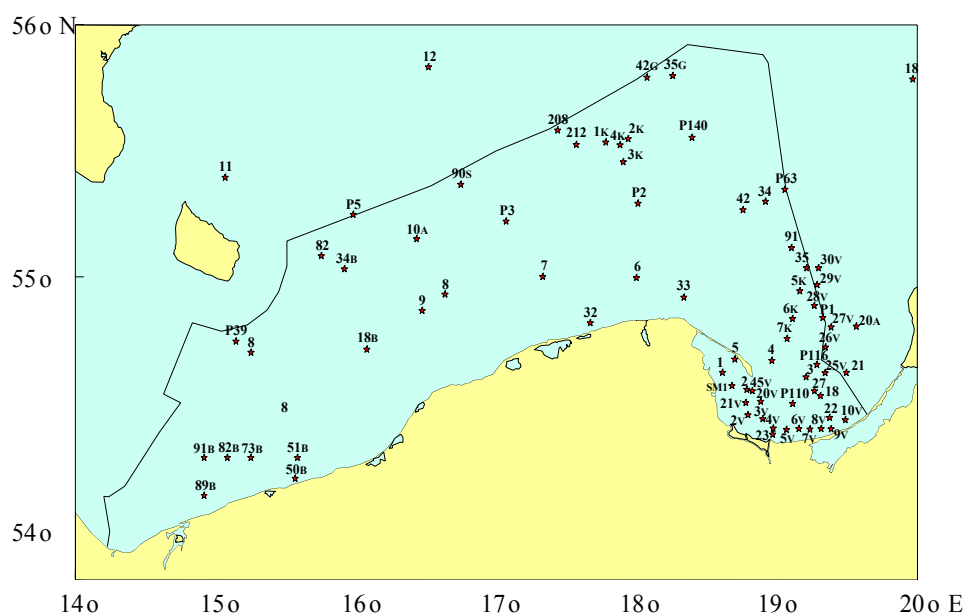
Figure 1 Sampling stations of the bottom sediments in the Southern Baltic

Sandy bottom is difficult to sample. The reaching depth of popular devices such as Van Veen and Pettersen grab samplers rarely exceeds 20 cm and the retrieved material does not preserve undisturbed structure. Box cores are more suitable, but are difficult to operate due to their weight. As a result, the depth distribution of pollutants in such sediments is poorly known. This is a serious drawback for inventory studies, which must rely on correct assessment of all input/output components.

Part of our laboratory's activity is devoted to studying the behaviour of radioactive elements in the Baltic Sea. Most of our work is confined to the Polish Exclusive Zone (Figure 1). It is a shallow water body which occupies an area of about 30.5 thousand square kilometres. Two thirds of the bottom area is covered by sand and gravel (Table 1).

	Gdansk Bay	Southern Baltic	Total
Area of mixed bottom [km^2]	-	2 147 (8%)	2 147 (7%)
Area of soft bottom [km^2]	1 733 (58%)	7 080 (26%)	8 813 (29%)
Area of hard bottom [km^2]	1 266 (42%)	18 307 (66%)	19 573 (64%)
Total area [km^2]	2 999	27 534	30 533

Table 1 Area of soft and hard sediments within the Polish Economic Zone.

Our earlier studies showed that Cs-137 is present in the southern Baltic in appreciable amounts and that its occurrence is not limited to soft sediments only. In 1986, before the Chernobyl accident, typical levels of Cs-137 were 0.2 and 0.5 kBq m^{-2} for sandy and muddy bottoms, respectively, but during 1991–93 they increased respectively to 1 and 2 kBq m^{-2}, on average. The total inventory of this radionuclide was divided between hard and soft type bottoms in the proportion 3:2.

Our inventory estimations were based on the belief, that the sampling depth of our device (which was then about 15±5 cm on average) was sufficient for this purpose. At that time we had no technical means to prove it. It is only recently that we have gained access to longer, undisturbed cores, which allowed us to test that assumption.

Methods

Cores of sandy deposits were collected at the stations shown in Figure 2 with a vibration corer 10 cm in diameter. It collected relatively undisturbed cores up to 3 m long. The material was cut into segments and kept in plastic bags until analysis.
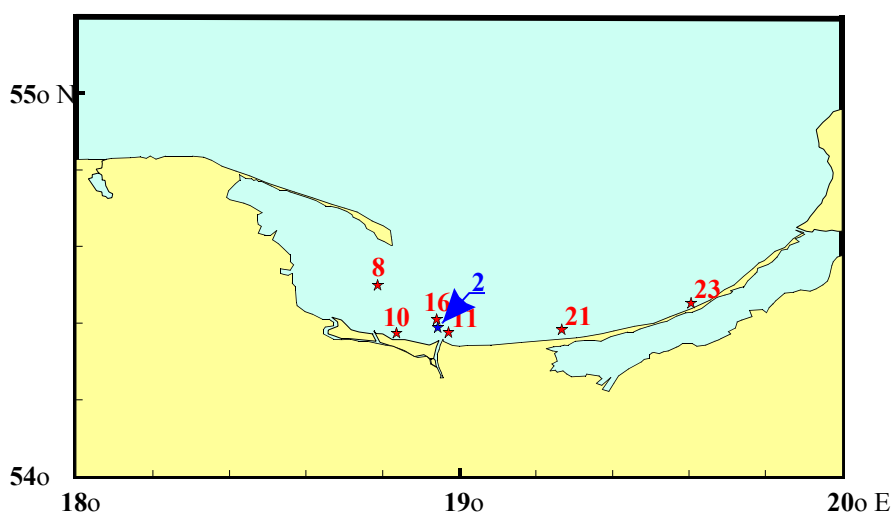
Figure 2 Location of sampling stations

Each segment was homogenised and transferred to counting vessels of the Marinelli type. The measurements were made by a gamma spectrometer equipped with a HPGe detector (20% rel. eff. and 1.8 keV FWHM resolution for a 1.33 MeV 60C^o line) and the standard S100 Canberra electronics. The counting efficiency was determined using a standardised mixture of radionuclides provided by the PTB Braunschweig (Germany). Analytical quality control was assured by using the reference materials IAEA-300 (Baltic sediment) and IAEA-375 (soil). Stability of counting efficiency and

background variation was monitored throughout the whole period of measurements. During the applied conditions (about 1 kg sample and 80.000 s. counting time) the minimum detectable activity was close to $0.2\,\mathrm{Bq\,kg^{-1}}$ d.w.

Results and Discussion

In this paper we present results for the first seven cores which were collected in the shallow parts, of the Gulf of Gdansk. This region is known for the relatively high Cs-137 levels in sediments, so the chance of observing any activity gradients in the sandy bottom seemed promising.

Station	Coordinates		Depth [m]	Segment [cm]	Activity [Bq.m^{-2}±1 σ]	
	E	N			Cs-137	Cs-134
2	18°56.77'	54°23.61'	22	0.00−0.11	480±13	8±3
				0.11−0.21	1230±28	23±5
				0.21−0.32	2630±43	39±6
				0.32−0.40	1990±23	26±4
				0.40−0.48	770±13	20±4
				0.48−0.60	1110±19	17±3
				0.60−0.70	1200±22	17±3
				0.70−0.83	1210±23	22±5
				0.83−0.90	154±7	<8
				0.90−1.00	50±6	<9
				1.00−1.10	23±6	<8
				1.10−1.20	<16	<9
				1.20−1.30	<17	<10
10	18°50.29'	54°22.64'	13	0.00−0.05	1332±25	14±5
				0.05−0.19	1150±23	18±3
				0.19−0.24	55±6	<7
				0.24−0.36	42±6	<8
				0.36−0.45	<12	<8
23	19°36.31'	54°27.27'	16	0.00−0.10	2460±45	36±6
				0.10−0.20	980±25	15±3
				0.20−0.31	260±12	<8
				0.31−0.40	130±10	<7
				0.40−0.50	59±6	<8
				0.50−0.60	23±3	<5
				0.60−0.70	<17	<8

Table 2 Vertical distribution of Cs-137 and Cs-134 in the analysed cores at the stations 2, 10 and 23.

Table 2, Figure 3 and Figure 4 shows typical vertical distribution of this radionuclide in the selected analysed cores. With the exception of core 2 (Figure 5) all other cores display the same distribution pattern, i.e. the highest activity is in the uppermost segment and then steadily decreases. The shape of the distribution curves differs from one core to another but the differences are small, considering the variable hydrodynamic conditions in this area and different depths. Some 80 to 90 percent of the total inventory resides in the layer that is 15–20cm thick, but here the activity gradients are the steepest. It seems that the action of waves and currents affect the surficial sandy sediment structure not much deeper than that in the study area.
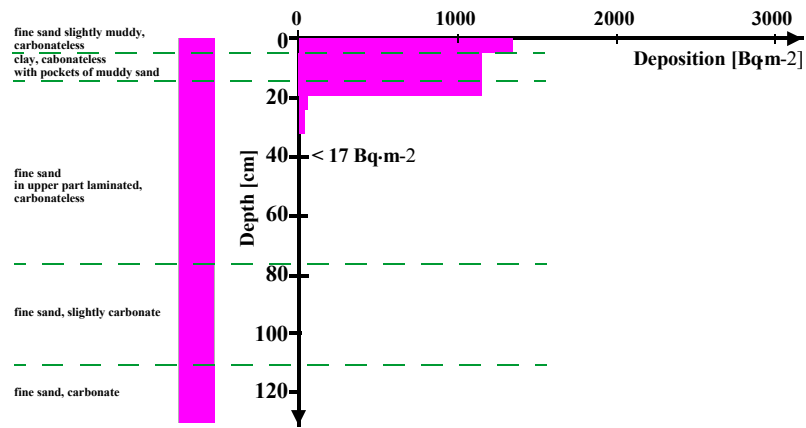
Figure 3 Vertical deposition of Cs-137 at station 10 (54°22.64'; 18°50.29')
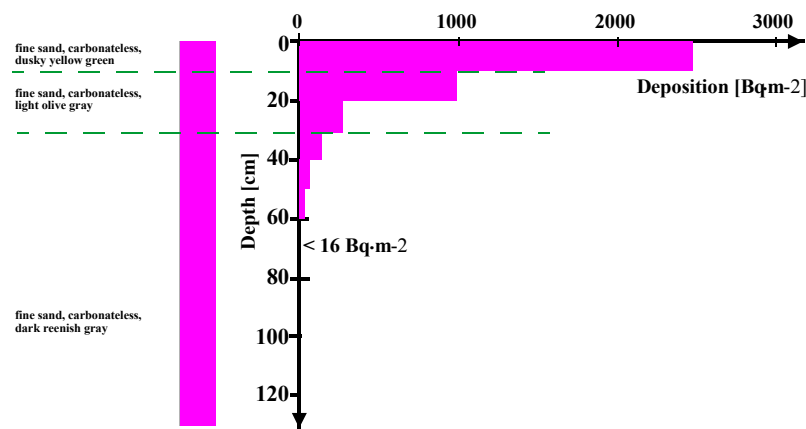
Figure 4 Vertical deposition of Cs-137 at station 23 (54°27.27'; 19°36.31')
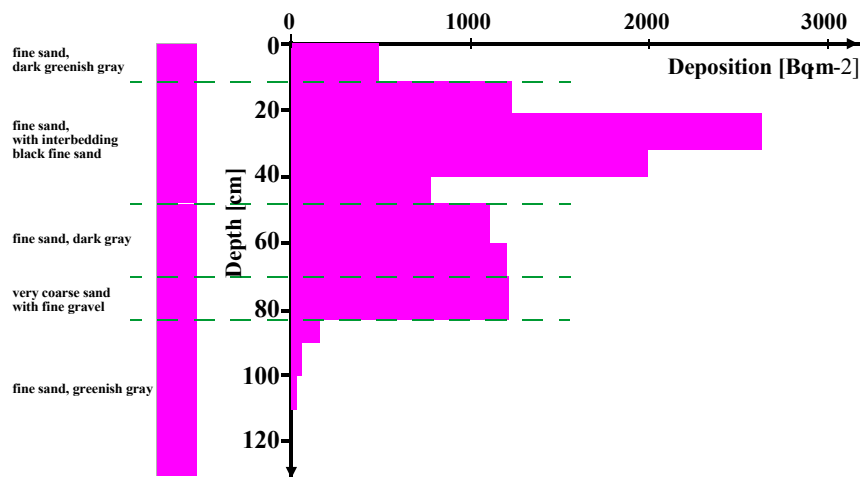
Figure 5 Vertical deposition of Cs-137 at station 2 (54°23.61'; 18°56.77')

In Table 3 the characteristic features of the Cs-137 distribution in the examined cores are summarised. We have defined the penetration depth of Cs-137 as the depth in the sea floor, below which less than 5 percent of the integral total inventory remains. In most cases this depth does not exceed 30 cm and it does not appear to be related to the water depth nor to the magnitude of total deposition. The latter varies by an order of magnitude and is much higher on average than in other parts of the Southern Baltic (Bojanowski *et al.*, 1995a and 1995b). That attests to the Vistula river as a major source of Cs-137 in the Gdansk Bay.

Station	Water depth [m]	Total deposition [kBq.m⁻²]	Sediment thickness [cm]	Percent Cs-137 in this layer	Next segment		
					Horizon [cm]	Percent deposition	Activity [Bq kg⁻¹ d.w.]
2	22	10.8	83	98	83–90	1.5	1.5
8	30	1.27	40	98	40–50	1.3	<0.2
10	13	2.58	19	96	19–24	2.2	0.9
11	15	9.58	23	99	23–32	0.5	0.4
16	27	5.36	29	96	29–40	2.0	0.8
21	24	4.14	25	96	25–35	2.6	0.7
23	16	3.92	31	95	31–40	3.3	1.3

Table 3 Summary of Cs-137 deposition characteristics in sandy deposits of the Baltic Sea.

Presenting Cs-137 activities in activity concentrations units ($Bq kg^{-1}$ of sediment) has little meaning because such values depend, to a large extent, on how the sample was taken. It is however, interesting to note, that in the uppermost layer the concentrations varied a lot with ranges of 6 to 101 $Bq kg^{-1}$ d.w., whereas below the penetration depths they in some cases approached detection limits.

The observed features are not claimed to be applicable to sandy sediments as a whole. The distribution at station 2 is at present difficult to explain but it demonstrates that such cases do exist. Some records also have evidence of homogeneous distribution of Cs-137 down to 15 cm sampling limit in Pomeranian Bay sediments (Bojanowski *et al.*, 1995b). Clearly, more information is needed on this subject, and measurements on cores from other regions are underway.

Conclusions

The most important conclusion resulting from our measurements is that the Cs-137 occurs down to about 30 cm in some Baltic near-shore sandy sediments. This observation can be extended to include other pollutants that are bound to particulate matter and are of recent origin, such as the Chernobyl fallout. Sampling to that depth is thus a prerequisite for quantitative inventory assessment of such substances.

References

R. Bojanowski, D. Knapinska-Skiba, Z. Radecki, J. Tomczak, T. Szczepanska, 1995a: Accumulation of radioactive Caesium (^{137}Cs) in Southern Baltic Sediments. *Prace Panstwowego Instytutu Geologicznego CXLJX*, 145–150

R. Bojanowski, Z. Radecki, D. Knapinska-Skiba. 1995b: Distribution of ^{137}Cs, $^{239+240}$Pu and ^{210}Po in the Pomeranian Bight ecosystem. *Bulletin of the Sea Fisheries Institute*, 3 (136)

Organochlorines in surface sediments and cores of the Western Baltic and inner coastal waters of Mecklenburg-West Pomerania

Dirk Dannenberger and Astrid Lerz

Introduction

Organochlorine compounds, e.g. chlorobiphenyls (CBs) and organochlorine pesticides, are among the most widespread and persistent environmental contaminants. Also, these substances enter the Baltic Sea via rivers, atmospheric deposition, spills and dumping of dredging material. Most of them have only short residence times in the water column, due to their hydrophobic character (low water solubility) which leads to bioaccumulation and strong sorption onto suspended particulate matter (SPM). They are carried to the bottom water and are finally trapped in marine sediments (Tolosa *et al.*, 1995; van Bavel *et al.*, 1996).

The area under investigation covered the western Baltic Sea (Beltsea, Arkona Sea, Pomeranian Bight) and the inner-coastal waters of Mecklenburg-Vorpommern (Germany). The sediment structures in the western Baltic differ widely. There are large regions with a high content of mud or clay in the sediments of the innercoastal waters (Brügmann and Bachor 1990; Schlungbaum *et al.*, 1994) and of the accumulation area of the Lübeck Bight and the Arkona Basin (Brügmann and Lange, 1990). The sedimentation rates in these areas are on average $1–2\,\mathrm{mm\,yr^{-1}}$ (Perttilä and Brügmann, 1992). Other regions in the western Baltic are dominated by fine and mixed sand with gravel and stones, e.g. the Darß Sill and the central parts of the Pomeranian Bight.

The present state of knowledge of organochlorines in Baltic Sea sediments is fragmentary and there is a lack of information for some regions (Perttilä and Brügmann, 1992; HELCOM, 1993). Recent data on organic micropollutants in Baltic Sea sediments were reported by Broman (1992, 1993), Nyland *et al.* (1992), Kjeller and Rappe (1995), Witt (1995), and Dannenberger (1996). Until now, no data about the distribution of organochlorines in the innercoastal waters of Mecklenburg-Vorpommern have been available.

Methods and Materials

Sampling and sample preparation
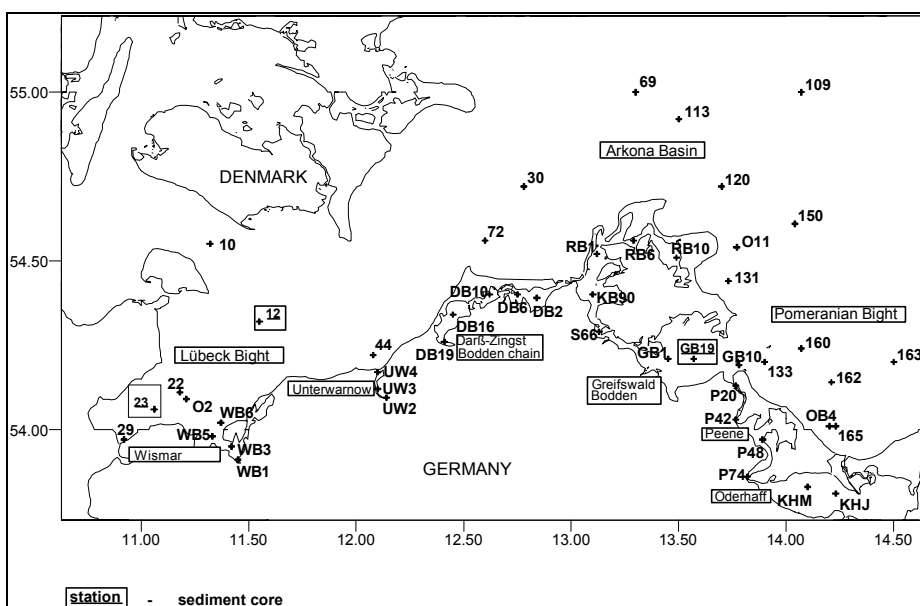
Figure 1 Locations and sediment characteristics of the samples

Surface sediment samples were taken by a corer and Van Veen-grab during cruises with R/V "A.v. Humboldt" and R/V "Strelasund" in October/November 1993 and 1994. The sediment cores were taken by a Nimistö-corer. The sampling sites are shown in the map in Figure 1.

The surface sediment samples (0–3 cm) and sediment layers of the cores were separated with a stainless steel spoon stored in precleaned (acetone, n-hexane) aluminium boxes and frozen at –20°C until sample preparation.

For the determination of dry weights and total organic carbon contents (TOC), a part of each sediment sample was freeze-dried. The carbon measurements were carried out with a CS-analyser (Metralyt CS100/100, ELTRA).

We used the extraction method in the ultrasonic bath suggested by Perttilä and Haahti (1984) and Fucco *et al.* (1993). After thawing and thorough mixing of the sample, 20 g of the moist sediment were ground with anhydrous sodium sulphate. The resulting powder was extracted in a glass flask for 2 hours in an ultrasonic bath with n-hexane/acetone (3:1/v:v) at 45°C. As a first step for sample clean up a solid phase extraction (SPE) on deactivated Al_2O_3 (2 g)/Florisil (3 g) was performed. Elemental sulphur and sulphur compounds, which were also partly extracted, were removed with precleaned metallic mercury (extraction with n-hexane) in an ultrasonic bath. After this procedure an HPLC clean up followed by a fractionation of the organochlorines on silicagel (Merck, Germany) was performed. A modification of the method suggested by Petrick *et al.* (1988) was applied and further details of the whole clean up have been described by Dannenberger (1995, 1996).

The concentrations of organochlorine compounds in the extracts were quantified by high resolution gas chromatography (HRGC) on two capillary columns of different polarity (DB-5, 60 m × 0.25 mm, film thickness 0.25 µm; DB-17, 30 m × 0.25 mm, film thickness 0.25 µm; J&W Scientific, USA). We used an HP 5890 gaschromatograph with electronic pressure control (EPC) and software HP 3365 (Hewlett Packard, USA). Conditions: Injector (splitless), temperature 250°C, detector temperature (ECD) 320°C, oven temperature programme: 60°C-1min-50°C/min-170°C-3°C/min-200°C-4°C/min-250°C-10min. Blank investigations of the applied method, recovery rates with certificated marine sediments (HS-1, HS-2; National Research Council, Institute of Biosciences, Canada) and microcontaminant spiked n-hexane solutions were carried out. The limit of detection of organochlorines using the present method is about 10 pg g^{-1} d.w. (Dannenberger, 1996).

Results

Surface sediments

Chlorobiphenyls (CBs)

The distribution of CBs (sum of 23 congeners) is presented in Figure 2. The concentrations ranged from <100 to 214000 pg g^{-1} d.w. (dry weight). In some sandy samples the concentrations of CBs were below the detection limit of 100 pg g^{-1} d.w. The highest values were detected in innercoastal areas (Warnow estuary, Wismar Bight) and in the accumulation areas of the western Baltic–Lübeck Bight (station 12 and 22) and the Arkona Sea (station 69, 113 and 109). Accumulation and deposition of suspended particulate matter (SPM) occurs predominantly in these areas of the western Baltic Sea.

One method for comparing micropollutant concentrations in a large area with different sediment structure is the normalisation to TOC. After TOC-normalisation no significant variations of the CB distribution in the western Baltic were observed. The distribution of CBs in the sedimentation areas of the Lübeck Bight, the Arkona Sea and the Pomeranian Bight was more homogeneous after normalisation to TOC, caused by high sediment dynamics in the area under investigation. The concentrations ranged between 50 and 800 ng g^{-1} C, with higher values in the Fehmarnbelt and the Arkona Sea. The local influence of the river Oder via the Oderhaff into the Pomeranian Bight was detected. It can be assumed that most of the particle-bound CBs are deposited in the Oder estuary (Oderhaff), which act as trap and filtration basin for particulate matter. A part of it will be transported as well, through the narrow mouth of the Oderhaff and via the Peenestrom to reach the Pomeranian Bight. In the small sedimentation strip along the Islands of Usedom and Rügen there were higher CB concentrations than the central part of the Pomeranian Bight. The CB values in the Bodden chain of Darß-Zingst and Rügen were low.

sum CBs -31, -28, -52, -101, -90, -110, -77, -118, -123, -149, -153, -105, -132,- 138,-163, -164, -158, -160, -126, -178, -129, -180, -169
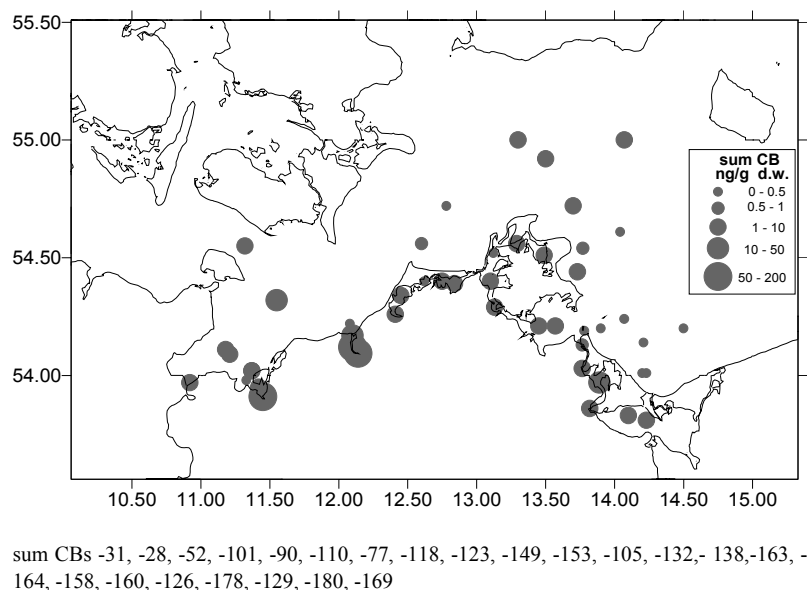
Figure 2 CB concentrations in surface sediments in the western Baltic and innercoastal waters of Mecklenburg-Vorpommern, on dry weight basis

Higher chlorinated Chlorobiphenyl congeners (CBs -138, -153, -180) were detected at elevated concentrations in almost all samples, due to their relatively low water solubility. Vice versa, the congeners with a lower chlorination degree (CBs 31, 28, 52) and higher solubility occurred at lower concentration levels. The non-ortho substituted CB congeners (CB -126, -169), characterised as the most toxic compounds as compared to 2,3,7,8-TCDD (SAFE, 1990), were below the detection limit of $10 \, \mathrm{pg\,g^{-1}}$ in all sediment samples studied in the area under investigation.

DDT and metabolites

The distribution of DDTs (sum of p,p'-DDT, o,p'-DDT, p,p'-DDE and p,p'-DDD) is presented in Figure 3. The values varied between $<500 \, \mathrm{pg\,g^{-1}}$ d.w. in areas with a fine and mixed sand structure and $85000 \, \mathrm{pg\,g^{-1}}$ d.w. in the muddy sediments of the Warnow estuary and the sedimentation areas of the Lübeck Bight and the Arkona Sea.

sum of p,p'-DDT, o,p'-DDT, p,p'-DDE and p,p'-DDD
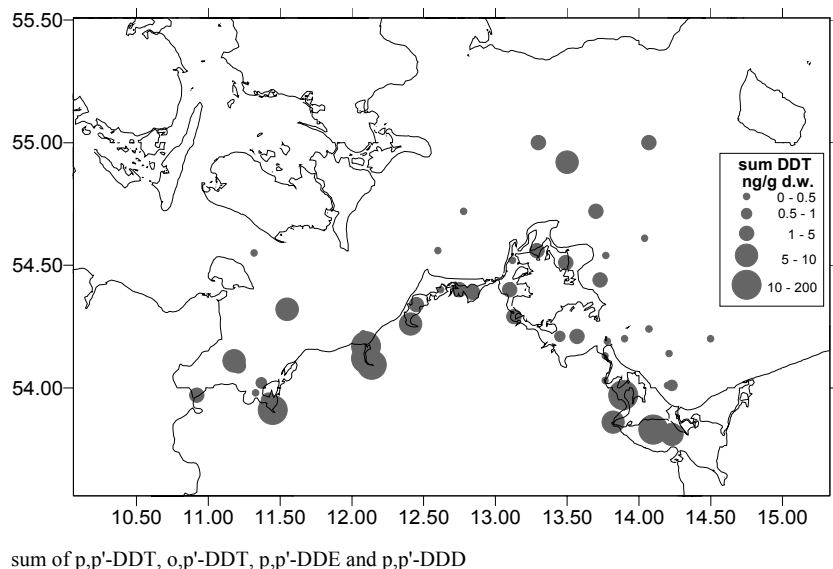
Figure 3 DDT concentrations in surface sediments of the western Baltic and innercoastal waters of Mecklenburg-Vorpommern, on dry weight basis

After TOC normalisation higher DDT values also occurred in the western part of the Pomeranian Bight (10–$500 \, \mathrm{ng\,g^{-1}}$ TOC). These higher values for DDTs are not surprising, bearing in mind that DDT was used in the former G.D.R. (German Democratic Republic) as an insecticide until the end of 1988, especially in forestry (Röber, pers. comm.).

Unfortunately, no data about the use of DDT and other chlorinated pesticides in Poland, predominantly in the area near the river Oder are available so far. Similar to the CBs, higher concentrations up to 200 ng g^{-1} on TOC basis were detected in the sedimentation areas of the Lübeck Bight and the Arkona Sea.

The DDT molecule slowly decomposes in the marine environment into DDE and DDD, with a half-life of DDT in the marine environment of several years (Jensen *et al.*, 1976). Thus the relation of these three compounds can be used to indicate the age of DDT pollution (Perttilä *et al.*, 1986). Our investigations showed that the contribution of p,p'-DDT to the entire DDT concentrations (sum of p,p'-DDT, o,p'-DDT, p,p'-DDE and p,p'-DDD) was low, indicating a high DDT decomposition level. O,p'-DDT was found with values up to 130 pg g^{-1} d.w.

Isomers of hexachlorocyclohexane (HCH)

Due to the relatively high water solubility of HCH isomers, only low concentrations were detected in sediment samples of the western Baltic and innercoastal waters of Mecklenburg-Vorpommern (Germany), when compared to other organochlorines. Concentrations were found up to 2900 pg g^{-1} d.w. (for ß-HCH, Warnow estuary). Of the investigated α-, β-, γ- and δ-HCH isomers only lindane (γ-HCH) and ß-HCH occurred in higher concentrations. The values of α- and δ-HCH with a higher water solubility were below 100 pg g^{-1} d.w. in all samples. The ß-HCH was the major isomer in the sediment. Other authors have also found higher ß-HCH values in the sediment of the lakes Ontario and Garda (Eisenreich *et al.*, 1989, Bossi *et al.*, 1992). Among the HCHs the ß-isomer is a compound which is very resistant to biodegradation. The α- and δ-HCH show a tendency to metabolise after some years to Penta-chlorocyclohexane (PCCH), Tetrachlorobenzene (TeCB) and other unpolar compounds.

Sediment Cores

Two sediment cores were collected in the accumulation area of the Lübeck Bight (station 12, 23; see Figure 1) and one core was taken in the Greifswald Bodden (station GB 19). The length of the cores were between 40 and 45 cm. The TOC profiles are rather constant over the cores in the Lübeck Bight, varying between 3.5 and 5.4% (Figure 4).
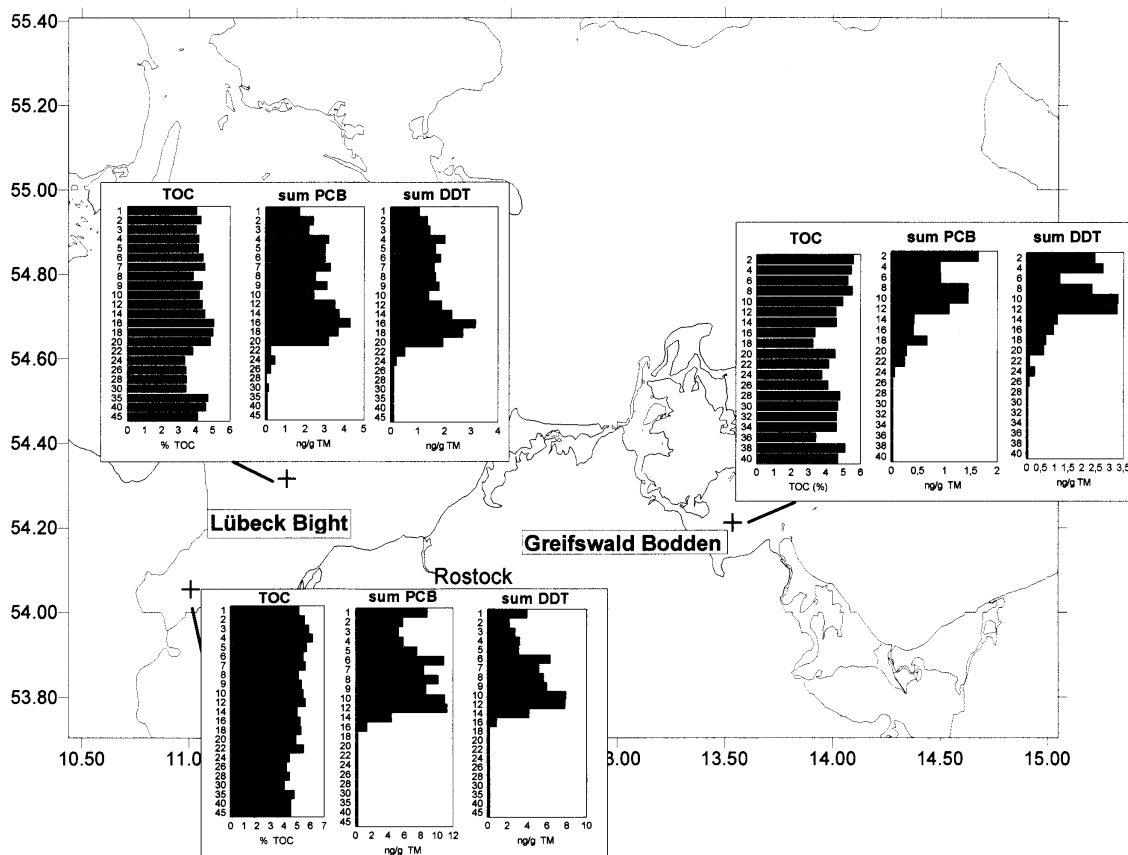
Figure 4 Vertical distribution of TOC, CBs and DDTs in sediment cores of the Lübeck Bight and the Greifswald Bodden

The vertical distribution of CBs (sum 23 congeners) and DDTs (sum of p,p'-DDT, o,p'-DDT, p,p'-DDE and p,p'-DDD) showed a similar pattern. Generally, an approximately uniform CB and DDT distribution was found in both cores down to 15 and 20 cm, without detection of great maxima.

This fact may be explained by advective processes (postdepositional mobilisation and bioturbation) and high sediment dynamics combined with mix thorough of the sediment layers down to 20 cm and 15 cm. Because of sedimentation rates between 1–2 mm yr^{-1} (Perttilä and Brügmann, 1992) CB or DDT maxima should occur at upper sediment layers. In these cases it is impossible to detect correct historical inputs of organic microcontaminants.

On the contrary, the vertical CB and DDT distributions of the core from the Greifswald Bodden show a decrease of concentrations with increase of sediment depth. The CB- and DDT maxima occurred between 10 and 12 cm, due to higher discharges of PCBs and DDTs between 1945 and 1955.

Summary

Organochlorines were investigated in surface sediments and three different sediment cores of the western Baltic, the Arkona Sea, the Pomeranian Bight and inner coastal waters of Mecklenburg-Vorpommern (Germany). Chlorinated biphenyls (CBs), isomers of hexachlorocyclohexane (HCH), dichlorodiphenyltrichloroethane (DDT) and some of its metabolites were analysed by gaschromatographic techniques (HRGC-ECD/ECD).

The organochlorine concentrations varied due to differences in the sediment structure and showed strong correlations to the TOC contents. The highest concentrations up to 220000 pg g^{-1} d.w. were measured for CBs (sum of 23 congeners) and DDTs (sum of p,p'-DDT, o,p'-DDT, p,p'-DDE and p,p'-DDD) in innercoastal waters (Warnow-Estuary, Oderhaff). In the sedimentation areas of the Lübeck Bight and Arkona Basin, the CB concentrations ranged between 2200 and 11400 pg g^{-1} d.w. The more hydrophilic HCHs were found between 10 to 2900 pg g^{-1} d.w., with higher values for the ß-isomer. In the sandy areas of the Pomeranian Bight all compounds investigated remained below the detection limit of 10 pg g^{-1} d.w. Inputs via rivers (Oder, Peene) into the Baltic Sea and discharges of industrial point sources were identified.

The distribution of organochlorines in surface sediments in the western Baltic was approximately homogenous after TOC-normalisation.

Sediment cores from the Lübeck Bight showed uniform CB- and DDT distribution down to 15 or 20 cm. By contrast, for the vertical CB- and DDT distribution in the core from the Greifswald Bodden, maxima in the upper layers (0–2 cm) and at 10 cm depth were measured. The historical inputs of organochlorines via the Peene river and from industrial sources were detected.

References

van Bavel, Näf, C., Bergquist, C.A., Broman, D., Lundgren, K. Papakosta, O., Rollf, K., Strandberg, B., Zebühr, I., Zook, D., and Rappe, C., 1996. Levels of PCBs in the aquatic environment of the Gulf of Bothnia: benthic species and sediments. Mar Poll. Bull. 32, 210–218

Brügmann, L., and Bachor, A., 1990. Present state of the Baltic Coastal Waters of Mecklenburg-Vorpommern, Germany. Geo-Journal 22.2, 185–194

Brügmann, L. and Lange, D., 1990. Metal distribution in sediments of the Baltic Sea. Limnologica 20, 15–28

Broman, D., Bandh, C., Ishaq, R., Näf, C., Pettersen, H., and Zebühr, Y., 1992. Sediment trap fluxes, residence times and surface sediment concentration variability of PCBs, PCDD/Fs and PAH in the Baltic. Organohalogen Compounds 9, 43–46

Broman, D., Näf, C., Zebühr, Y., Bandh, C., Ishaq, R., and Pettersen, H., 1993. Occurrence, distribution and turnover of some toxic substances in the water mass and sediments in the Baltic Sea. Baltic News 4, 6–10

Bossi, R., Larsen, B., and Premazzi, G., 1992. Polychlorinated biphenyl congeners and other chlorinated hydrocarbons in bottom sediment cores of lake Garda (Italy). The Science of Total Environment 121, 77–93

Dannenberger, D., 1995. Ostseewasser—Analytik im Subspurenbereich (Teil 1). CLB—Chemie in Labor und Biotechnik 46, 589–592

Dannenberger, D., 1996. Chlorinated microcontaminants in surface sediments of the Baltic Sea—investigations in the Belt Sea, the Arkona Sea and Pomeranian Bight. Mar. Poll. Bull., in press

Eisenreich, S.J., Capel, P.D., Robbins, J.A. and Bourbonniere, R., 1989. Accumulation and diagenesis of chlorinated hydrocarbons in lacustrine sediments. Environ. Sci. Technol. 23, 1116–1126

Fucco, R., Colombini, M. P., and Samcova, E., 1993. Individual determination of ortho and non-ortho substituted polychlorophenyls (PCBs) in sediments by high performance liquid chromatographic pre-separation and gaschromatography-ECD detection. Chromatographia 36, 65–70

HELCOM, 1993. First assessment of the state of the coastal waters of the Baltic Sea. Baltic Sea Environ. Proc. 54, 160 pp

Jensen, S. and Olsson, M., 1976. AMBIO Sp. Rep., 4:111

Kjeller, L.-O. and Rappe, C., 1995. Time trends in levels, pattern and profiles for polychlorinated dibenzo-p-dioxins, dibenzofurans and biphenyls in a sediment core from the Baltic Proper. Environ. Sci. Technol. 29, 346–355

Nylund, K., Asplund, L., Jansson, B., Jonsson, P., Litzen, K., and Sellström, U., 1992. Analysis of some polychlorinated pollutants in sediment and sewage sludge. Chemosphere 24, 1721–1730

Perttilä, M., and Haahti, H., 1986. Chlorinated hydrocarbons in the water and sediments of the seas around Finland. Publ. Water Res. Inst. 68, 197–200

Perttilä, M., and Brügmann, L., 1992. Review of contaminants in Baltic sediments, ICES Coop. Res. Rep. 180, 135 pp

Petrick, G., Schulz, D. and Duinker, J.C., 1988. Clean up of environmental samples by HPLC for analysis of organochlorine compounds by GC with ECD. J. Chromatogr. 435, 241–248

Safe, S., 1990. PCBs, PCDDs, PCDFs and related compounds: Environmental and mechanistic considerations which support the development of toxic equivalency factors (TEF). Critical Reviews in Toxicology 21, 51–88

Schlungbaum, G., Nausch, G., and Baudler, H., 1994. Sedimentstruktur und Sedimentdynamik in der Darß-Zingster-Boddenkette. Rostock. Meeresbiolog. Beitr. 2, 27–40

Tolosa, I., Bayona, J.M., and Albaiges, K., 1995. Spatial and temporal distribution, fluxes and budgets of organochlorinated compounds in northwest Mediterranean sediments. Environ. Sci. Technol. 29, 2519–2527

Witt, G., 1995. Polycyclic aromatic hydrocarbons in water and sediment of the Baltic Sea. Mar. Poll. Bull. 31, 237–248

Lithology and stratigraphy of glacial deposits in the Sambian-Kura area of the Baltic Sea

N. Kuten, B. Klagish and Y. Goldfarb

Abstract

This paper considers the lithological features of the glacial formation sediments for one of the most interesting oil fields of the SE Baltic sea—the Sambian-Kura high. It is well known that the different ages of glacial deposits are relatively similar to each other in that they inherit some common peculiarities regarding mineral composition and texture, none the less detailed by sequential studies of mineral typomorphism and clay mineral assemblages. The upper Pleistocene till is characterised by abundant hydromicas, which range up to 80%, with some caolinite-chlorite. The middle and Lower Pleistocene tills differ from the latter by having an essential content of swelling phases (mainly montmorillonite), which reaches 40%, but in the underlying Cretaceous glauconite sands and sandstones they increase to $39-85\%$. This fact allows us to suppose that pertinent increase of swelling clayey phases in the Middle and Lower ones are connected to local bed rock erosion and redeposition by the glaciers. The criteria for different ages of till separation have been specified as hornblende roundness, clay mineral composition, granulometric composition and physical-mechanical properties.

Boundaries
1−engineering-geological region
2−engineering-geological area
A−SE part of Baltic shield
C−southern slope of Baltic shield
C_I−southern part of Finnish Gulf
C_{II}−High of Estonian archipelago
and Western-Saaremaas step
B−Baltic syneclise
B_I−low of Riga Gulf
B_{II}−Gotland low
B_{III}−Liepaja-Klaipeda's high with
Ventspils step
B_{IV}−Neman's low
B_V−Kura high
B_{VI}−Gdansk low
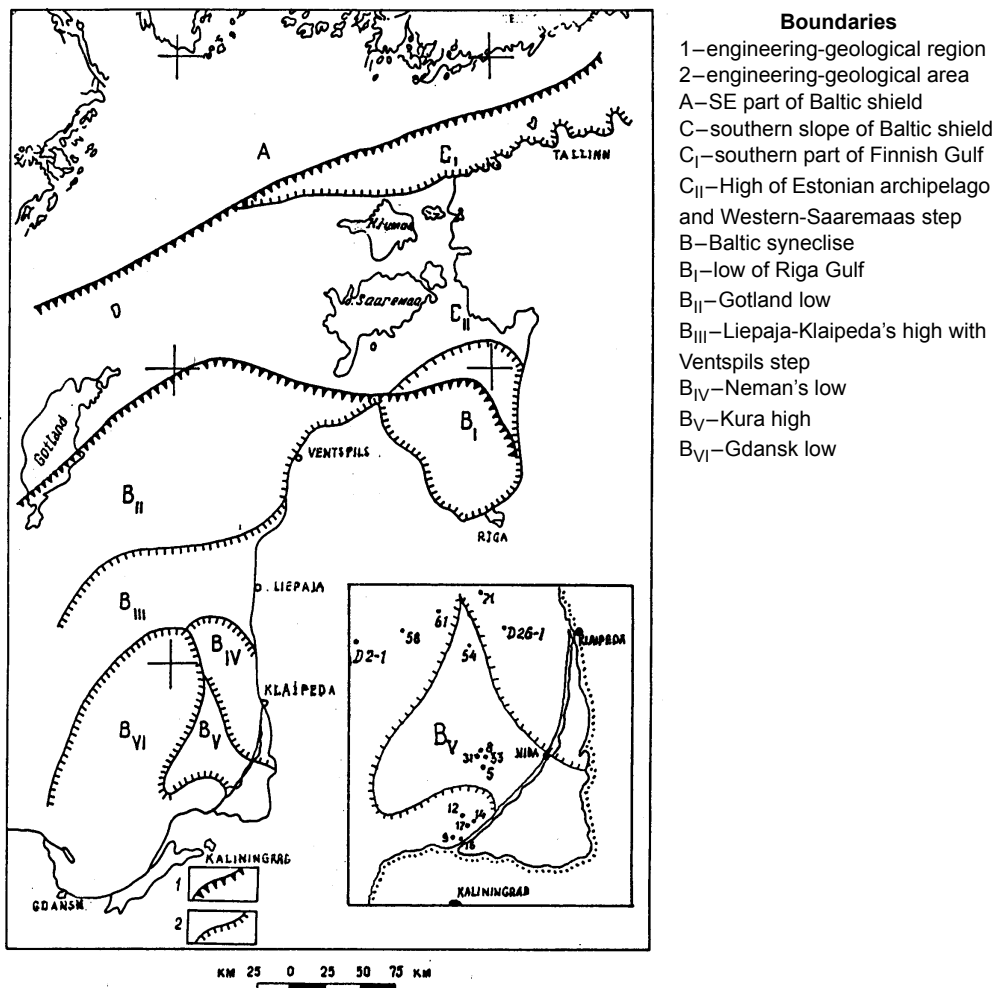
Figure 1 Chart of engineering-geological zonation of the Baltic sea (I. Dzilna [5]).
(· 21) shows the position of a bore hole and its number.

Introduction

The Sambian-Kura structural high area is the most interesting oil field in the SE Baltic sea. Extensive seismic-acoustic and geological investigations have been carried out in the SE Baltic region during the last few decades in order to solve some problems associated with geotechnical research on the sea floor. This morphostructure borders with the Gdansk low in the west and the Neman paleovalley in the north (Figure 1).

Recent marine deposits are fully abraded there or possess insignificant thickness and as a result various ancient rocks (Pleistocene and Cretaceous sediments) are exposed on the sea floor.

The Pleistocene cover has been formed mostly by glacial complexes and more rarely by interstadial ones. The latter are distributed locally as a rule, characterised by insignificant thickness.

Study

We have studied glacial and glacial-lacustrine deposits sampled from bore holes 8, 9, 12, 14, 16, 17, 31 etc. (Figure 1).

Special attention was paid to clayey and clastic materials in microsection studies because these ingredients control some important physical-mechanical properties of the sea bed deposits. Attention has been directed towards establishing the influence of external factors, which took place in a current process of sedimentation, diagenesis and retrodiagenesis [7]. We have made an attempt to investigate the effect of the mineralogical processes' influence of early diagenesis (including factors such as temperature gradients and activity of the regelation or multigelation processes). These processes may cause essential reorganisation of clay minerals and texture transfiguration.

In this situation many authors emphasise the possibility of a wide development of the aggradation processes in clay minerals, but some even admit an appearance of new mineral phases, such as montmorillonite as a result of long term repeated freezing [14]. The Lower and Middle Pleistocene glacial complexes sediments include many swelling minerals [7] and this fact is predominant for the Sambian-Kura high from the geotechnical point of view.

Bore hole no.	Sample depth in m	Fraction 0.1–0.25 mm content	Heavy fraction content,%	Hornblende roundness degree, marks				Average of rounded grains	Geologi-cal index
				1m	2m	3m	4m		
9	4.3	9	1.1	2	38	16	44	18	gl Q_{III}
9	4.7	10	0.8	2	41	14	43	16	gl Q_{III}
9	11.2	10	0.6	5	38	11	46	16	gl Q_{I}
9	11.5	14	0.9	4	38	11	43	15	gl Q_{I}
9	11.7	7	0.9	3	32	7	38	10	gl Q_{I}
14	7.0	3	1.2	2	35	10	52	12	gl Q_{III}
14	8.6	10	1.0	4	33	12	51	16	gl Q_{III}
14	9.2	10	1.2	8	32	12	48	20	gl Q_{III}
17	6.0	15	1.3	4	33	14	49	18	gl Q_{III}
17	10.5	12	0.8	8	30	17	45	25	gl Q_{II}
17	11.5	15	0.9	8	32	15	45	23	gl Q_{II}
17	13.0	14	0.8	0	31	17	42	22	gl Q_{II}
17	14.0	16	1.2	9	34	19	38	28	gl Q_{II}
19	5.3	10	0.9	5	34	12	49	17	gl Q_{III}
19	6.0	11	0.6	5	30	16	49	21	gl Q_{III}
19	6.7	11	0.6	8	33	18	41	26	gl Q_{II}
19	7.4	10	0.9	8	34	16	44	24	gl Q_{II}
19	9.2	10	1.0	5	40	15	40	20	gl Q_{II}

Table 1 Glacial formation hornblende roundness from the SE Baltic sea Sambian-Kura area (by Mayore [7])

Gaigalas *et al.* described a weathering crust of the Riss till with deep subaerial substitution replacing primary mineral associations [4]. They have distinguished ancient and recent supergenic remarkable mineralogical and chemical transfor-mations of the tills. Summing up the above mentioned genetic and histerogenus factors it is important to carry out litho-logical studies, including typomorphic descriptions of a concrete mineralogical phase in elementary grains of different

till faces. In connection with the well known close genetic relationship and lithological similarity of the different age tills, this has caused difficulties in studying the Quaternary deposits.

Separation of different age tills has been carried out using the following methods: typomorphic examination of the same predominant minerals including hornblendes from grain-size fraction for estimation of roundness, study of clay mineral composition and fabric peculiarities, mutual surface ions' absorption capacity and physical-mechanical properties [4, 5, 6, 7, 13] (Table 1, Table 2 and Table 3).

Bore hole numbers	Depth of sampling, m	Geological index	Lithological description	Approximate content,%		
				Hydrom-ica, %	Kaolinite & chlorite, %	Montmo-rillonite, %
8	1.0	gl Q$_{III}$	Red-brown, yellow-grey tight carbon-ateferous clay till with appreciable amount silty sand content & irregular distributed psephite presented the main various carbonates, quarzites, markedly weathered, often decomposed granite, migmatites, typical minor content glauconite sandstone, chert, phosphorite.	80	20	-
8	6.5	gl Q$_{III}$		80	20	-
8	8.5	gl Q$_{III}$		81	20	-
8	10.0	gl Q$_{III}$		77	23	-
12	5.5	gl Q$_{III}$		79	21	-
12	7.0	gl Q$_{III}$		66	23	11
31	3.9	gl Q$_{III}$		76	24	-
31	5.0	gl Q$_{III}$		78	22	-
31	6.0	gl Q$_{III}$		67	18	15
31	10.0	gl Q$_{III}$		64	24	12
31	13.0	gl Q$_{III}$		76	24	-
16	16.0	gl Q$_{III}$		72	28	-
14	7.5	gl Q$_{II}$	Grey hard clay till with admixture of various psephite−boulders, rare pebbles, abundant gravel presented carbonates, glauconite, granites, gabbros.	48	18	34
14	10.0	gl Q$_{II}$		48	20	32
14	12.0	gl Q$_{II}$		45	20	35
17	1.0	gl Q$_{II}$		58	14	28
17	6.5	gl Q$_{II}$		57	17	26
17	11.0	gl Q$_{II}$		45	15	40
9	10.7	gl Q$_{II}$	Deep grey hard sandy till with carbonates, sandstone boulders, pebbles with mainly decomposed granites.	70	20	10
9	13.5	gl Q$_{I}$		63	22	15
9	15.0	gl Q$_{I}$		60	21	19
9	17.0	gl Q$_{I}$		56	20	24
D26−1	17.0	K$_2$	Glauconite-quarts clayey sand with sandstone of the same mineralogy & composition with subordered quantity of hydromuscovite locally replaced by autogenetic kaolinite. In same layers it is also noted disseminated fine secondary pyrite and magnetite.	23	-	77
D26−1	17.2	K$_2$		20	-	80
D26−1	18.4	K$_2$		29	-	71
D26−1	20.2	K$_2$		15	-	85
D26−1	21.6	K$_2$		48	-	52
D2−1	22.7	K$_2$		17	7	76
D2−1	24.0	K$_2$		25	10	65
D2−1	25.4	K$_2$		50	10	39
D2−1	26.5	K$_2$		99	-	–
D2−1	29.8	K$_2$		50	10	40

Table 2 The clay mineral composition of glacial and underlying Cretaceous sediments from the SE Baltic sea (X-ray difractometric analyses of the fraction <0.002 mm) [7]

Geological index	Total granulometric composition, per cent, mm				Mineral composition, %			Mutual surface ions complex					Moisture content	Liquid limit	Plasticity index	Liquidity index	Bulk density	Skeleton density	Porosity coefficient	Shear tests		Oedometer	Triaxial tests	
	>2.0	2.0–0.05	0.05–0.005	<0.005	Hydromica	Caolinite + chlorite	Montmorillonite	Absorption capacity	Ca²⁺ + Mg²⁺	Ca²⁺	K⁺	Na⁺								Angle of internal friction	Cohesion	Modulus of deformation	Cohesion	Angle of internal friction
								mgr-eq/100 s. gr					per cent			part unit	gcm⁻¹		part unit	o	KPa	MPa	KPa	o
gl Q_III	6	44	21	29	74	22	4	13.9	8.0	4.8	1.2	4.6	15	24	9	0–0.2	2.18	1.90	0.425	23°	60	9.0	20	25
*t gl Q_II **/	7	59	18	16	-	-	-	21.8	12.4	6.4	2.2	7.7	13	20	5	<0	2.24	1.99	0.350	28°	30	17	-	-
	1	17	39	43	52	18	33	-	-	-	-	-	19	29	10	<0	2.06	1.77	0.320	23°	65	8.5	-	-
m Q_I-II	-	14	12	74	69	25	6	-	-	-	-	-	27	47	22	0.1	1.96	1.54	0.730	25°	51	3.4	-	-
gl Q_I	4	52	25	21	63	22	15	14.3	8.0	5.5	1.2	4.4	11	19	5	<0	2.28	2.05	0.320	30°	70	17.5	-	33°

Note: (*) and (**) mean "gravelly" and "ungravelly".

Table 3 The midrange data of granulometric and clay mineral compositions, surface ions' absorption capacity, physical and mechanical properties of the SE Baltic sea glacial formation sediments [7].

The Upper Pleistocene complex is widespread throughout the Sambian-Kura neotectonic structural high with a maximum thickness of 25m. The upper complex part has been formed by glacial-lacustrine deposits (lg_III) with a thickness reaching 10m. These sediments represent yellow-brown calcerous sandy clay and clay with interlaying silty sand and insignificant quantities of irregularly distributed psephite material.

The lower complex part was formed by red-brown and grey morainic sandy clay, so called "till" (g_III) with a remarkable content of psephite contributed by glacier and passing over in clay sand and glacial-fluvial sediments facially altered laterally (Figure 2 and Figure 3).
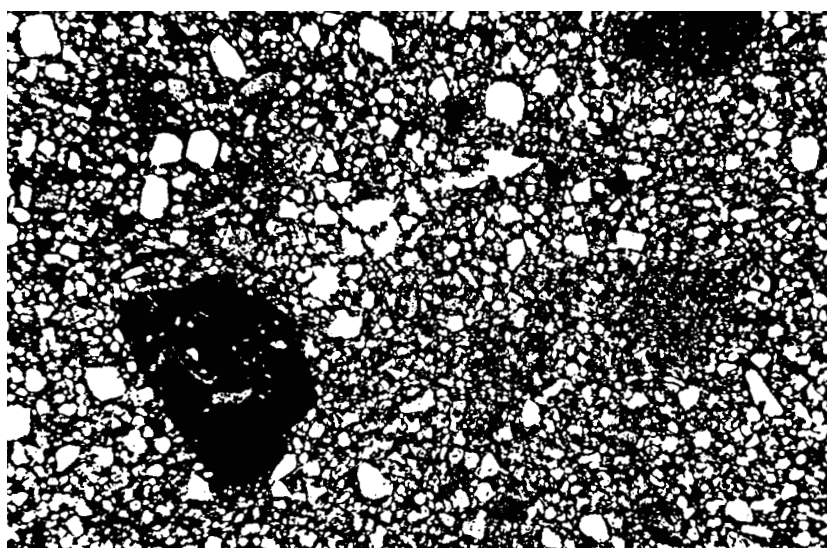
Figure 2 Silty till (gl Q_III) with admixture of rounded fine sand grains and gravel size black angular limestone fragments. The clayey matrix (dark) contains dispersed quartz, carbonates, feldspars and other mineral debris. The Baltic sea, Sambian-Kura high, bore hole 12, depth 5.5m. Photomicrograph of the thin section in transmitted light, magn. 40 X.
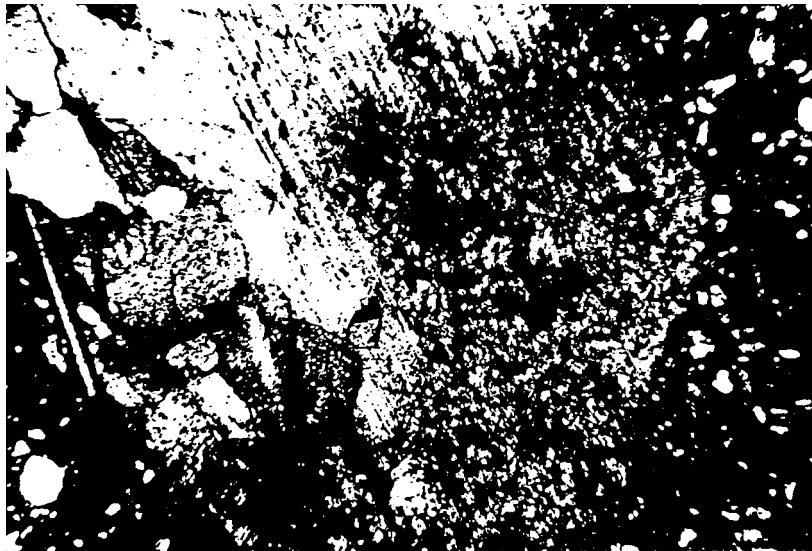
Figure 3 Calcerous silty till (gl Q_{III}) with incorporated weathered plagioclase, markedly altered by the fine flakes of hydromica. Baltic sea, Sambian-Kura high, bore hole 12, depth 5.5 m. Photomicrograph of the thin section between crossed nicols, magn. 32 X.

The glacial-lacustrine complex sediments (lg_{III}) have been studied at their maximal thickness (in depth interval 0.0–9.5 m) by profile of bore hole 16. They have been formed during a single glacier oscillation and are characterised by varved clayey deposits of low and upper parts of the sequence appearing more sandy and crudely bonded. Clastic material consists essentially of quartz, which inherits typomorphical peculiarities compared to those of the till: well-rounded, slightly-rounded angular and sharp-edged grains.

The largest part of silty-size particles was carried from the melting glacier and shows elements of typical relics due to rather delicate differentiation, transit in a liquid medium and resedimentation of detrital material. The longer axis of coarse clastic grains, as a rule, are oriented perpendicular to the top base plane of a bedding as a result of the gravitational precipitation from floating glacons.

There are a large amount of pelitic (0.001−0.006 mm) not usually fine grained (size up to 0.01 mm) carbonate particles in the clayey matrix, resedimented from the till, which causes high carbonatisation of this sediment type. Observations in thin sections below show that fine dispersional carbonates mainly represent "glacier flour" although they may partly be chemogenically sedimented in melt water lacustrine sediments in glacier lakes.

Glacial complex sediments, till (g_{III}) are represented by red-brown coarse-grained stiff morainic sandy clay and grey hard clayey sand. The clastic material includes rounded pebbles and fine-medium gravel particles consisting essentially of carbonates (total psephite content exceeds 10%). There are organogenic and chemogenic fine-grained limestones, dolomite, siderite and unusual clots of argillite in psephite. Some carbonate grains are encircled by a cover of crushed material with a grain size of about 0.06 mm.

The erratic material e.g. boulders, various rock fragments, pebbles and gravel grains represent slightly weathered unrounded granite fragments, typomorphic glacial rock debris, scale-form grains and blocks of acid plagioclase, often with alteration marks of sericite. Also it consists of specific lode quartz grains with remains of shelly fractures, that testify to the conditioning of originally outlined glacial forms (Figure 4).

Figure 4 Silty carbonateferous till (gl Q$_I$) with subparallel elongated grain arrangement. The top right corner shows displaced weathered plagioclase grain and below it—typomorphical for glacial sediments—coarse quartz grain with undulated outlines (fish-shaped). Baltic sea, Sambian-Kura high, bore hole 9, depth 10.7 m. Photomicrograph of the thin section between cross nicols, magn, 32 X.

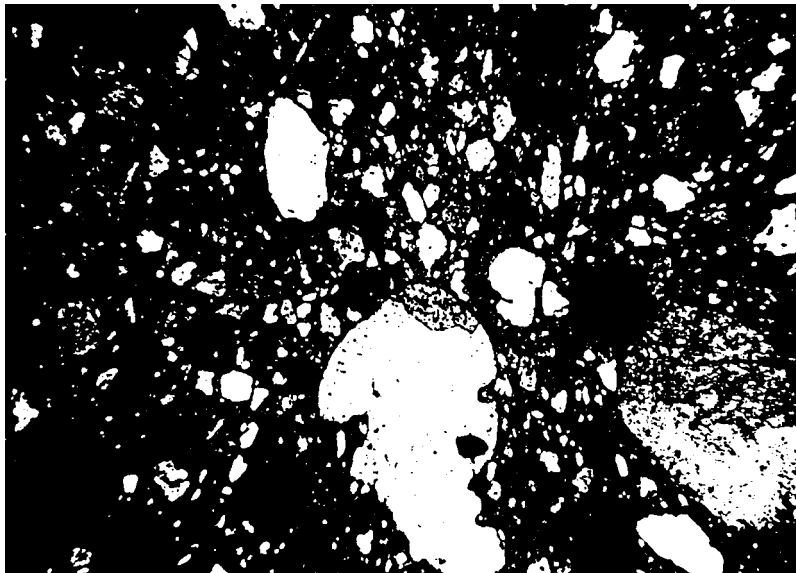Severely weathered granitoid psephite is characteristic for the Lower Pleistocene till, less for the Middle Pleistocene ones, and only the single bore holes (17,18) of the Upper Pleistocene till registered more intensively weathered samples than the Middle Pleistocene ones. The significant parts of the psephite are transitive carbonatic rocks, quarzite, argillite and local glauconitic sandstones, aleurolite, phosphorite and flint. A distinctive glauconite content in glauconitic bearing sandstones reaches 20%. The cementing matrix of the till contains about 40–50% of psammite fraction including a remarkable admixture of glauconite (up to 3−5%), phosphorite and flint (up to 1%). This testifies that material has been incorporated from underlying Cretaceous rocks (Table 3).

In the composition of a psammite fraction, quartz dominates with about 60−70%, plagioclase content is about 7%, microcline (12%), carbonate (up to 7−10%) more often represented by monocrystalline forms, glauconite (1−4%), garnet (up to 1%), hornblende (up to 1%).

A sand fraction quartz is composed of some morphologic types: the isometric subrounded grains (roundness 0.55−0.62) and angular grains (roundness 0.1−0.30). The first ones are obviously incorporated from underlying Mezozoic and Paleozoic and are likely to have endured some cycles of resedimentation, whereas the latter ones represent the erratic clastic rock debris delivered by the glaciers from the Baltic Shield.

Some grains of acid plagioclase show peripheral retrodiagenetic replacement cover of hydromica (Figure 6). This alteration changes processes obviously started in outcrops of bed-rock, continued during the process of their transportation and even "in situ" after their deposition and burying.

We agree with S. Astapova, that the till is in principle formed in a zone of supergenesis, where soil formation took place, biogeochemical processes and all weathering factors alongside with disintegration, new mineral creation and extensive migration of chemical elements [1]. The correlation ratio of the potash feldspars and plagioclases vary widely, which can be explained by the erosion of different weathering crust zones on the Precambrian Shield, leading to retrodiagenetic disintegration and glacial resedimentation too. These transformations might also occur as a result of condense intrusion between strata from deep oil structures [9].

The pelitic fraction is characterised by an abundance of illite and clastic hydromuscovite mixed with a fine dispersional carbonate, silty feldspar and quartz. The Upper Pleistocene till (g$_{III}$) clay mineral matrix contains extremely high percentages of hydromica, about 74%. Its maximal content has been marked in an upper profile part of bore hole 8 (reaching 80%) and contains a negligible admixture of montmorillonite (4%) and some kaolinite-chlorite (7−14%).

The Middle Pleistocene glacial complex (g$_{II}$) in cores of bore holes 14,16 and 17 is represented mainly by grey-green cobbled clayey sand, which is laid directly over the exarated Cretaceous rocks (Figure 5). These sediments include about 5 layers of so called "ungravelly" sandy clay (bore hole 14, interval 1.8−12.8 m from sea bed) with a negligible quantity

of psephite (about 1−2%) and psammite (up to 17%). The pelite and silty fractions dominate (on average more than 80%) and define specific physical-mechanical properties of these sediments (Table 2).
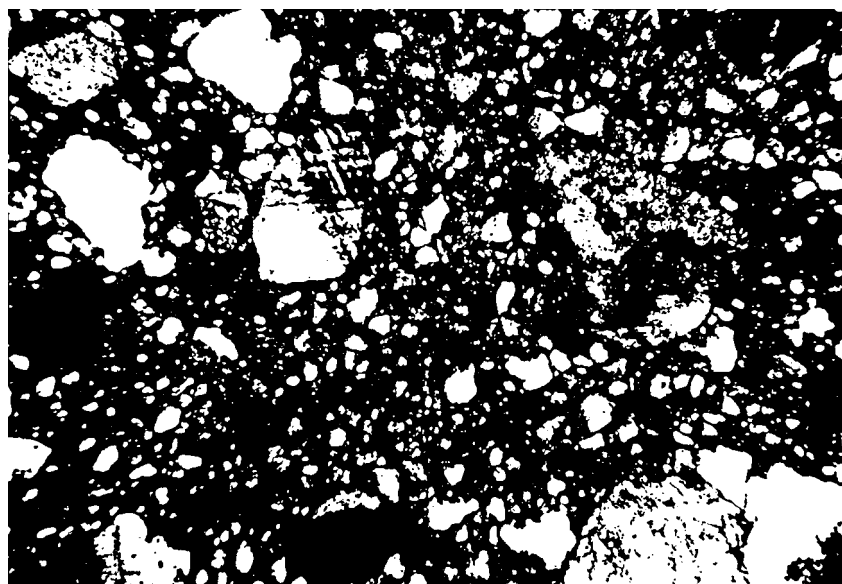
Figure 5 Silty carbonateferous till (gl Q_{II}) with sand and gravel admixture containing quartz, feldspars, granite and carbonate rock fragments incorporated in a dark clayey matrix, which is full of dusty sharp-edged clastic. Baltic sea, Sambian-Kura high, bore hole 14, depth 2.5m. Photomicrograph of the thin section between cross nicols, magn. 32 X.

The psephite material of the till (about 7%) is composed of limestones monomineralic quartzite, glauconitic sandstone, fragments of leucocratic and hornblende granites, blocks of plagioclase, rounded grains of microcline and debris of hornblende, gabbro and amphibolite (Figure 5).

The psammite and aleurite materials generally include quartz with a little admixture of feldspar (generally acid plagioclase) and calcite, glauconite (up to 3%, which coloured sediments with a green hue). The psammite grains are commonly more rounded than the silty (aleurite) ones.

A pelite matrix of the till has been formed mainly of clay minerals, silty carbonates, quartz and feldspar. It is interesting to note that there is a greater content of montmorillonite, less illite and invariably a low percentage of caolinite and chlorite in the matrix. The Middle Pleistocene till differs from the Upper one by having a greater montmorillonite content with a maximum of about 40% (Table 2).

Similar peculiarities of the tills have been reported by A. Vvedenskaya *et al.* [2] and G. Nemtsova [10] for the Russian platform, where they interpreted the till's clay minerals as an allogenic glacial material assimilated from bedrock. H.B.Willman *et al.* [15] received excellent data in their exhaustive study of the Illinois state glacial tills.

The Lower Pleistocene glacial complex sediments (g_I) have been discovered by a profile of bore hole 9 for an interval of 10.7−17.0m under the Upper Pleistocene limnetic glacial sediments. This till is represented by dark-grey hard clayey sand uncommon in the lower profile part—sandy clay (Figure 6 and Figure 7).
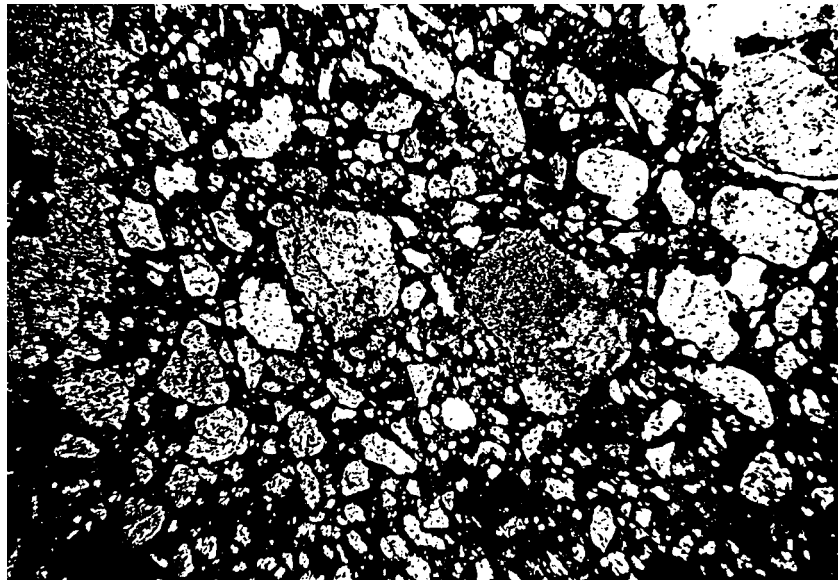
Figure 6 Sandy carbonateferous till (gl Q$_I$) with deeply weathered detrital feldspar grains. In the centre, dark feldspar grains occur, replaced by clay minerals with plagioclase relics (little white spots) and nearby coarse angular and markedly decomposed quartz grain with microcracks and fine crioclastic. The elongated grains are spaced subparallely along the long axis thus recording fluidal sediment texture. Baltic sea, Sambian-Kura high, bore hole 9, depth 10.7 m, magn. 40 X.
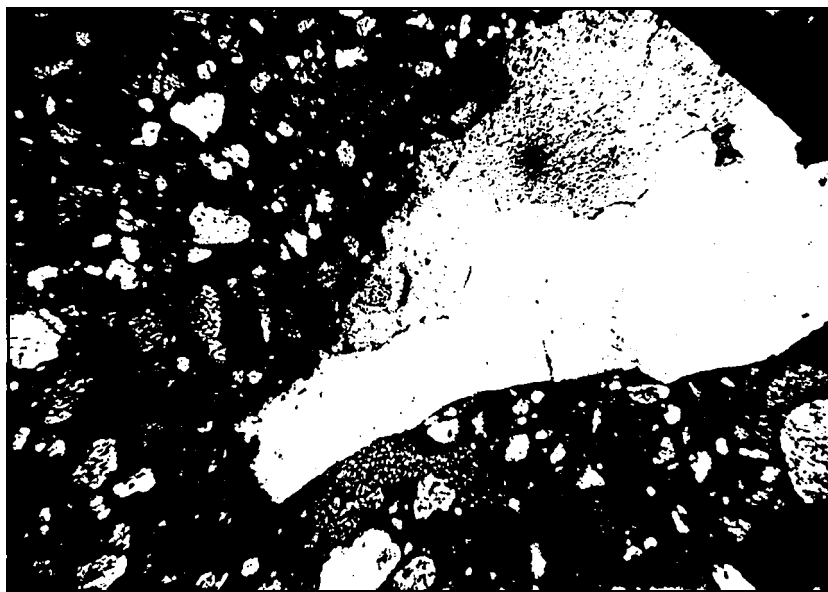
Figure 7 Clayey carbonateferous till (gl Q$_I$) with admixture of silt sand and coarse inclusions of erratic (Precambrian) quartz fragment typomorphical for the till. The specific shape of this grain is determined by crack systems and inherited shell fracture. There is a dark cementing matrix consisting of very fine clay mineral particles and sharp-edged dusty debris. Baltic sea, Sambian-Kura high, bore hole 9, depth 17.0 m. Photomicrograph of the thin section between cross nicols, magn. 20 X.

These sediments are characterised by comparatively less content of psephite, averaging about 4%. The psephite material is presented as erratic, fully weathered granite and migmatite fragments with deep alterated feldspar and dark-coloured minerals, transit gravely fine-grained and rounded carbonatic rocks and organogenic detrital limestones.

Some constituents of the granitic rubble such as a dark coloured minerals and feldspars are the most unstable in supergene conditions and they break down. So, the first ones frequently have been substituted by hydrochlorite, and the second ones by hydromica and more rarely by caolinite.

The acid and intermediate plagioclases from the till psephite are much more weathered than microcline. The marks of mineral degradation display themselves in local changes of the plagioclase blocks by their transformation and

replacement by fine-scaled hydromica, which, as a rule, contains more or less fresh relics (Figure 7). At the initial phase, cementing bonds are essentially weakened as a result of these processes, and it causes a partial or complete rock decomposition. The marked content of granitoide debris is abundant in all described stratigraphic units, though its quantity somehow varies in some stratigraphic ones. The observations confirmed that the rocks in their Prequaternary history endured influences of the supergene processes in exposure on the adjacent Scandinavian Shield.

A fine gravel fraction contains rounded magmatic and hydrothermal quartz grains and typomorphic clastic chips of the quartz with a characteristic lower content of monocrystalline grains of feldspars and limestones. (Figure 4, Figure 6 and Figure 7).

The psammite material (about 50%) can be compared to gravel due to its mineral composition, but differs in grain roundness, which evidently decreases according to its reducing tendency of grain size (Figure 6). For example, if the psammite fraction is characterised by middle roundness, then for the aleuritic (silty) fractions minor roundness coefficient is typical and the fine silty fraction, as a rule, is represented by unrounded clasts with wedge shaped particles. Its mineral assemblage, except dominated quartz, feldspars and carbonates, includes some mixture of glauconite (2%), muscovite (2%) and an insignificant quantity of biotite, green hornblende, pyroxene, garnet, etc.

The cementing clayey matrix is filled up with the mentioned detrital minerals and finely dispersed carbonatic silty grains. The clay mineral association reveals a similarity to the Middle Pleistocene one, though analyses show a distinctive decreasing of montmorillonite to 10−24% and increasing of illite (by invariable minor content of kaolinite and chlorite). If the stable montmorillonite increases in the vertical profile of glacial sediments it clearly shows their relation to bedrock and allows us to conclude that they had been derived from the underlying Cretaceous rocks (which were redeposited by the glacier; Table 2). This fact has been confirmed by a comparatively high content of glauconite in the till psammite fraction, which may be incorporated from the basement rocks.

To consider the Lower Pleistocene complex it should be noted that it remained on the Cretaceous eroded bedrock surface mostly in depressions, paleovalleys and incisions. This till possesses unique peculiarities of mineral composition, texture and physical-mechanical properties. In particular, it contains significantly more severely weathered disintegrated detrital material in coarse and sandy fractions (Figure 6), than has been revealed in overlapped younger tills. This indicates the presence in the alimentary area of the Prequaternary weathering cover.

The second Lower till peculiarity related to its physical-mechanical properties is mainly caused by its compact texture. This is confirmed by some indexes summarised in Table 3, i.e. characteristic minimal values of porosity, moisture, plasticity and maximal mean value of density. Ascertaining these data we came to the conclusion that this was caused by the gravity effect of successive glaciers, which overlapped the area at least twice and thus altered the till's texture and properties.

Hence, the characteristics of different stratigraphical units show that geotechnical properties are the result of origin of local facial conditions including alimentary and depositional areas as well as gravity effect of subsequent glaciers.

Summary

Summing up the above information we can visualise different age characteristics of lithostratigraphical types of moraines, which differ in their granulometric and mineral composition and as a degree of their supergenic and possibly retrodiagenetic transformations. The lithological factors stated above determined the peculiarities of their physical-mechanical properties too (Table 3). This is characteristic for all tills related to the Middle Pleistocene, which have comparatively high clay content (about 43%) of a specific mineral composition. There are 33% of swelling phases in the clayey matrix (Table 3).

Montmorillonite is more dispersed and hydrophilic than the hydromica and this is characterised by the much higher surface adsorption capability of the clay particles, manifested in the high surface mutual ions adsorption capacity—21.8 milligram-equivalent/100 soil grams (Table 3). Easily hydrated ions, previously Na-ion (7.7mg-eq/100 s.g.) significantly increase the hydrophilicity of clayey matrix and, as a result, it decreases the soil stability during mechanical influence [8]. It becomes clear that the tendency of cohesion increasing (65 KPa) with comparatively low data on the angle of internal friction (23°) independently of the relatively high moisture (19%) and porosity coefficient (0.520) manifests itself much more clearly (Table 3).

Special attention has been paid to till fabric studies, using the oriented thin section (with undisturbed samples) applying optical microscopy methods with polarised light at about 200−600 power magnification. The term "fabric" is used to characterise the geometrical arrangement (spacing and orientation) of clay and associated mineral particles.

The summarised results gained from microscopic examinations led us to the conclusion that two microfabric types dominate the till studied. The most common in morainic deposits is dense, isotropic cement filled with the finest grains of carbonate, quartz, feldspars and other debris, as well as the originally dispersed calcite grains inherited from marls. This phenomena considerably increases the markedly raised matrix density.

E.Sergeev *et al*. [12] calls this cement microfabric a "matrix" type fabric with continuous highly disoriented clay mass, containing the irregular tightly interlocked fine mineral grains mentioned above. Due to an interaction in the clay matrix the aggregates have been formed in the arrangements "face-to-face", "face-to-edge" and "edge-to-edge". It is characteristic that this type of fabric lacks any observed preferred clay particle orientation, and, on the contrary, the so called "turbulent" fabric oriented clay aggregates arrangement with "face-to-face", and, more rarely, "face-to-edge" prevails. Flat multiparticle aggregate streamline the incorporated grains, forming a structure pattern according to till stratification.

The mode of the till origin allows us to suggest that the retention of terrigenous material inherited multiparticle aggregates with steady arrangement, had been formed in the Prequaternary periods.

A.Larionov [8] and E.Sergeev *et al*. [13] regard that the units with the montmorillonite-hydromica clayey matrix assemblage are characterised by the "face-to-face" arrangement type interaction during clay aggregates for motion. The microscopic flake-shaped particles of the montmorillonite with uncertainly outlined, undulating edges, partially interlay each other and have a tendency to "coalescence" in their contact zones. As a result, we can not outline their boundaries. The cohesion of clayey microaggregates segregately increase and also improve the soil cohesion.

The hydromica matrix characterises another type of the clay particle and aggregates "edge-to-face" interaction. The particles of hydromica with well-traced borders have an insignificant cohesion with each other and, as a result, tend to decrease the soil cohesion. Our microscopic studies of the cemented thin section show that the hydromica cement is less organised and forms a chaotic, disordered clayey matrix texture, increasing the angle of internal friction (Table 3) [6,7,9].

From the other side, the high hydrophilicity of montmorillonite determines the lesser modulus of deformation of the Middle Pleistocene till (8.5 MPa) in comparison to the younger ones and especially to hydromica's composition of the Upper Pleistocene till (9 MPa, Table 3). The tills of different ages are alike with regard to the angle of internal friction, due to the similar contents of psephite and psammite fractions.

There is a tendency that sequential increasing of physical-mechanical properties of the till are caused by their age according to inherited minerallic and granulometric composition. The obvious exception displays the properties of the Middle Pleistocene till, whose decrease of "ungravelly" sediment layers is explained by a specific glacial-marine origin [7]. Distinctive differences in physical-mechanical properties for these stratigraphic units can be associated with the specific clay mineral composition, which formed due to the local glacial erosion plane, exchanged on the Low and Middle Pleistocene boundary.

References

1. Астапова С.Д. О методике изучения гипергенеза морен. Тр.:Компл. изучение опорн. разрезов ниж.и сред. Плейстоцена Европейской. части СССР.М.,1981, с.98-100.

2. Введенская А.И. и др.Использование показателей физ.-мех. свойств для стратигр. и фац. генет. расчленения морен. Тр. Компл. изучен. опорн. разрезов ниж. и сред. Плейстоцена Европейской части СССР. М.,1981, с.117-124.

3. Willman H.B., Glass H.D., Frye J.C. Glacial tills Part 1. Illinois state geological survey circular 347, Urbana, 1963.- 28p.

4. Гайгалас А.И. Петрографический состав, морфология и ориен. галек осн. стратигрфич. горизонтов морен Плейстоцена ЛССР. Авто-реферат. Вильнюс,- 1962, 28 с.

5. Goldfarb Y.I., Savvaitov A.S., StelleV.Y. Structure & stratigraphy of quarternary deposits of the SE Baltic. The second marine geologic confer. The Baltic. Rostock-Warnemunde, 1991.

6. Кутень Н.А., Клагиш Б.Д. Вещественный состав и физико-механические свойства моренных (мореноподобных) отложений регионов континен. шельфа.Рига,1989,с.24-30.

7. Кутень Н.А. Закономерности формирования состава и свойств новейших отложений южной части шельфа Баренцева и Балтийского морей. Диссерт.на соис.уч.ст.к.г-м.наук ВНИИМорГео, Рига, 1991.-214 с.

8. Ларионов А.К. Инженерно-геологич. изучен. структуры рыхл. осад. п.-М.:Недра,1966.-326 с.

9. Литогеохимические исследования при поиск. месторождений нефти,газа.М.-Недра,1987-184с

10. Немцова Г.М. Палеогеограф. аспект исследования гл. материала морен Центра и СевераРусской равнины.В кн:Воп. палеогеогр. плейст. и общей физ. Географии. Ч.1.М.,1986, с.69-77.

11. Немцова Г.М. Использование данных глин. минерал. в цел. корреляции ледник. отложений Тр. Компл. изучен. опор. разрезов ниж. и сред. Плейст. Евр. ч. СССР. к XI конгр. М.1981,с.153.

12. Сеглиньш В.Э. Стратиграфия плейстоцена Зап. Латвии. Автореф. диссер. Рига,1987. с.120.

13. Сергеев Е.М, Грабовска-Ольшевская Б, Осипов В.И. и др. Типы микроструктур глин. Пород ìИнженерная геологияîN 2, 1979.- с. 48-58.

14. Ульст В.Г.,Майоре Я.Я. Стратиграфическое расчленение ледн. отлож. запада Евр. ч. СССР по окатанн. зерен роговой обманки// Вопросы четвертичной геологии.-Рига, N5, 1964.-с.33-61.

15. Усков Н.М. Глинистые минералы многолетнемерзл. плейстоценов. и совр. донных отложений Центральн. Якутии. Якутск, 1988, с.88-92.

Particle size distributions in the Gulf of Gdansk

Katarzyna Bradtke and Adam Latala

Abstract

Suspended matter concentrations were measured in the Gulf of Gdansk in the years 1992-1993. Water samples were collected every month. The size and concentration of particles were analysed with Multisizer-II Coulter Counter. Against a background of corresponding hydrological conditions seasonal variability of suspended particles size distributions was studied.

The results show strong spatial and temporal variations of the particle size distributions. In space the horizontal variation of the PSDs appear to be stronger than the vertical. The Vistula River input seems to be reason of this variability. In time, particle size concentration distribution shows variations according to cycles of the biological activity and dynamical processes in the Gulf of Gdansk.

Introduction

The characteristics of suspended particulate material are related to basic biological, chemical and physical processes in the seas, for example scattering and absorption of light by sea water or transport of substances in the sea. As a consequence, knowledge about the properties and distribution of suspended particles can provide valuable information about the oceanographic processes affected by these particles.

The extent to which suspended particles influence these processes depends strongly on their size distribution, i.e. the number of particles in a volume of water as a function of their diameters. For quantitative characterisation of these influence and for purposes of the modelling of marine environment processes, it is important to find an approximation of particle size distribution by a simple arithmetic function with not too many parameters whose variability range needs to be evaluated.

In oceans, particle size distributions are predictable and described in detail (Carder *et al.*, 1971, Zalewski, 1977, Jonasz, 1983), but in coastal regions, like the Gdansk Bay, they vary due to large input of different materials from rivers or sewage, and require careful study (Jonasz, 1983).

The aim of this paper is to characterise the particle size distributions in the Gdansk Bay and to outline their spatial and temporal variability.

Materials and Methods

The data discussed here were collected during 1992 and 1993 at locations shown in Figure 1 and analysed with a Multisizer II Coulter Counter. If measurements couldn't be completed within a few hours after collection of the samples, they were frozen (volume ~100ml) onboard the ship and analysed later. A Coulter counter with a 200µm orifice and 2000µl sample volume was used to measure number of particles per unit volume for at least 50 size classes of equivalent spherical diameter in the range of 4 to 30µm. The equivalent spherical diameter is used to characterise the size of the irregularly shaped particles and means the diameter of a sphere having a volume equal to that of the particle. To limit errors resulting from inhomogenity of distribution of particles in water sample, average values of the particle concentration in every size class of at least 3 measurements were used to determine particle size distribution (PSD).
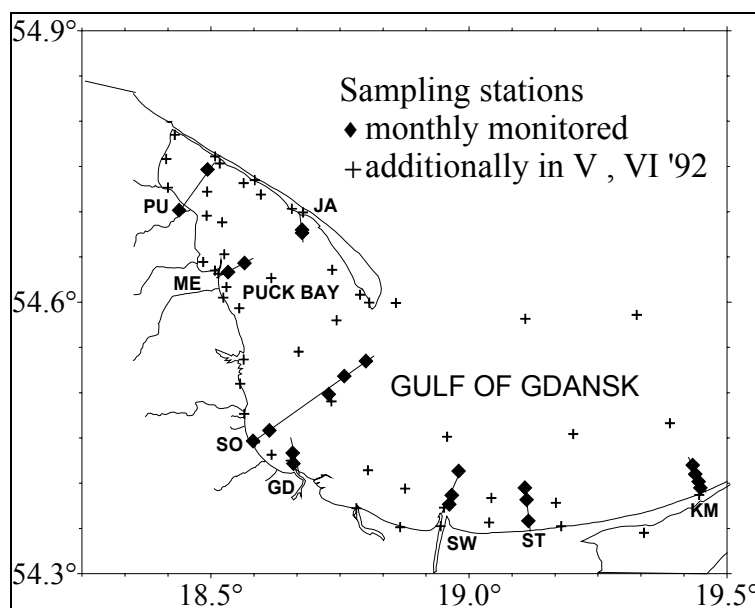
Figure 1 Location of sampling stations. Capital letters denote names of sampling profiles as follows: PU–Puck, ME–Mechelinki, JA–Jastarnia, SO–Sopot, GD–Gdansk, SW–Swibno, ST–Stegna, KM–Krynica Morska.

The particle size distribution function $FD(D)$ is defined by the equation

$$dN = FD(D)dD$$

where dN is the number of particles per unit volume of sea water with diameters D in the range of ($D,D+dD$).

The particle size distribution $FD(D)$ was determined by differentiation of the cumulative distribution, $CD(D)$, of particle sizes, defined by the equation

$$CD(D) = \int_{D}^{\infty} FD(D')dD'$$

where $CD(D)$ is simply the number of particles per unit volume having diameter greater than D. To evaluation, simplified procedure described by Jonasz (1983) was used. In this procedure, to convert $CD(D_i)$ into $FD(D_i)$ the least squares approximation to $CD(D)$ by the function KD^{-m} was constructed at three points: D_{i-1}, D_i, D_{i+1} and its derivative at $D=D_i$ was evaluated. In the first and last step additionally its value at $D=D_1$ and D_n respectively was assigned to $FD(D_1)$ and $FD(D_n)$.
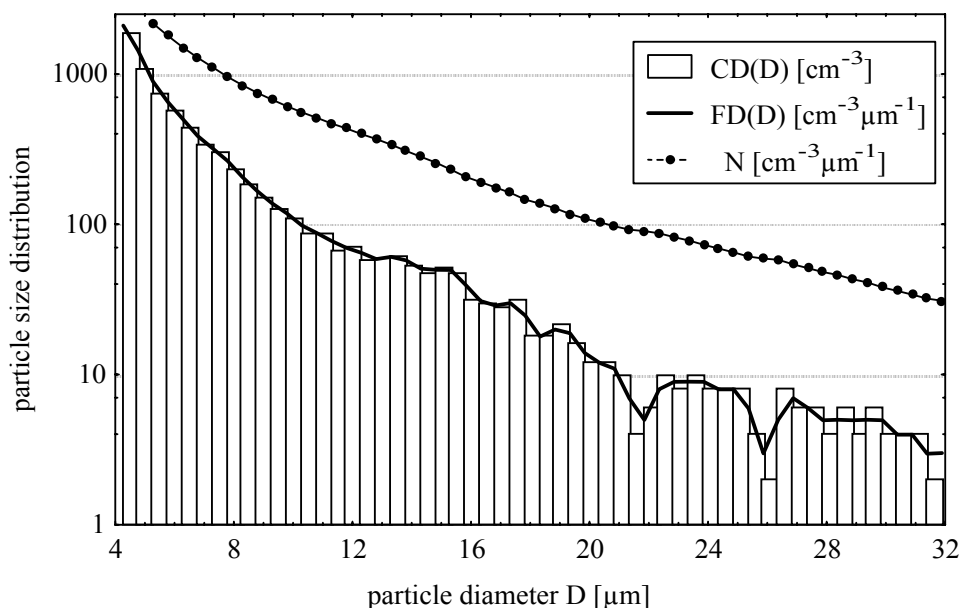
Figure 2 Particle size distribution characteristic for the Gulf of Gdansk presented in various manners.

$FD(D)$ computed in this procedure and the histogram $\Delta N(D,D+\Delta D)$ show a high goodness of fit (Figure 2). The relative error of $CD(D=4\mu m)$ in all computed PSDs was smaller then 5%.

Results and Discussion

Distribution of particle concentration

Results of measurements show differences between two main seasons, e.g. spring–summer and autumn–winter, characterised respectively by high ($1.7\times10^3<CD(4\mu m)<55\times10^3\,cm^{-3}$) and low ($0.6\times10^3<CD(4\mu m)<26\times10^3\,cm^{-3}$) concentration of particles suspended in water. This fact is thought to be a direct consequence of an autumn–winter minimum in biological activity and land runoff of suspended matter.
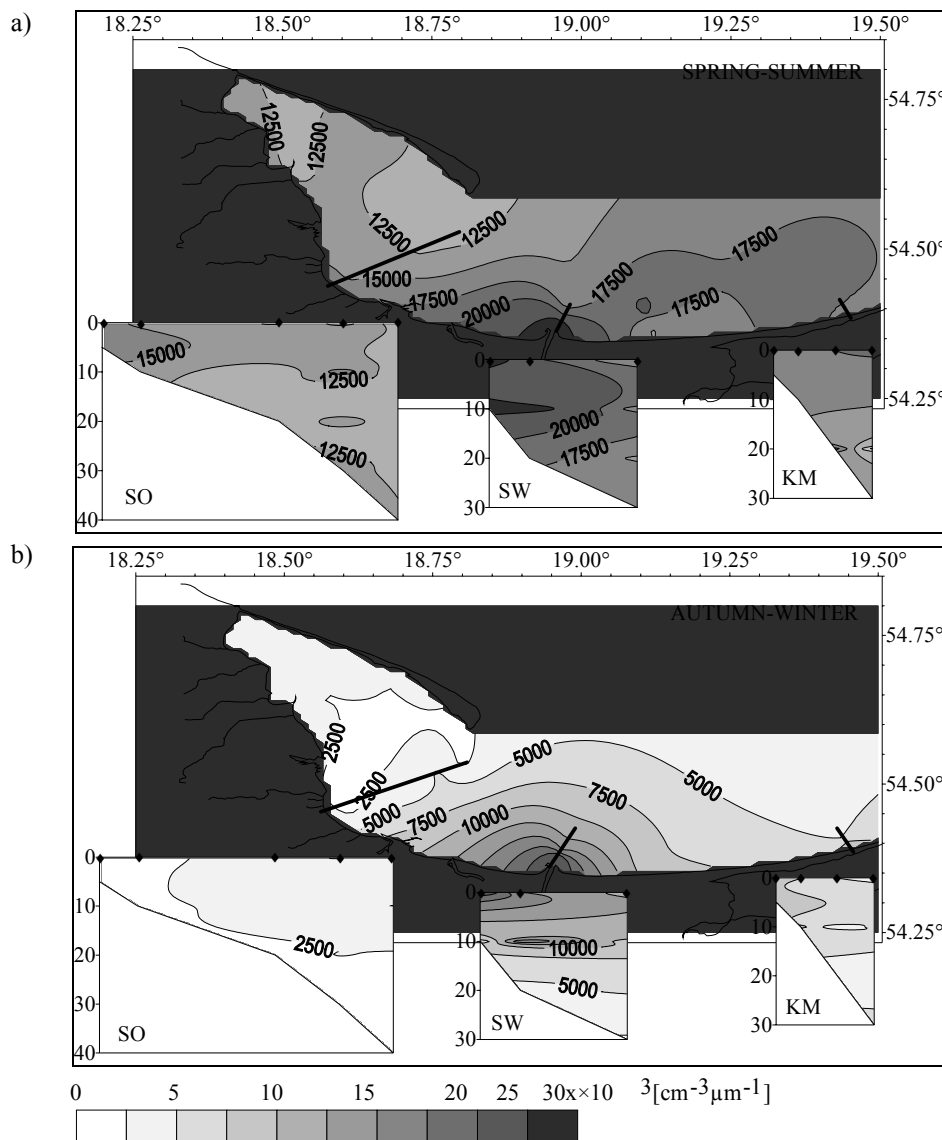
Figure 3 Surface distributions and vertical profiles of particle concentration ($CD(4\mu m)$) characteristic for the Gulf of Gdansk in a) spring and summer, b) autumn and winter months

Figure 3 shows representative surface distributions and vertical profiles of particle concentrations ($CD(4\mu m)$) found for spring–summer and for autumn–winter seasons. The most characteristic feature of these distributions are the division of the Gulf of Gdansk into two parts: eastern, that is strongly influenced by the Vistula river waters, rich in suspended matter, and western (called Puck Bay) with a relative lower concentration of particles.

The vertical distributions of suspended particle concentration differ in these regions and are time-dependent too, however, this variability is much smaller than the spatial variability. Puck Bay is characterised by rather uniform particle concentration, particularly in the autumn–winter season. In regions with higher amounts of particles the concentration

was generally found to decrease with depth. An increase in particle concentration has been observed near the bottom due to resuspension of bottom sediments and in the layer just above the seasonal thermocline (in summer). The concentration of larger particles ($D>20\mu m$) was not found to vary as strongly as that of all particles ($D>4\mu m$). The concentration of larger particles appeared to stay approximately the same in the entire water column, except the thin surface layer when amounts of larger particles resulting from biological activity were found (Figure 4).
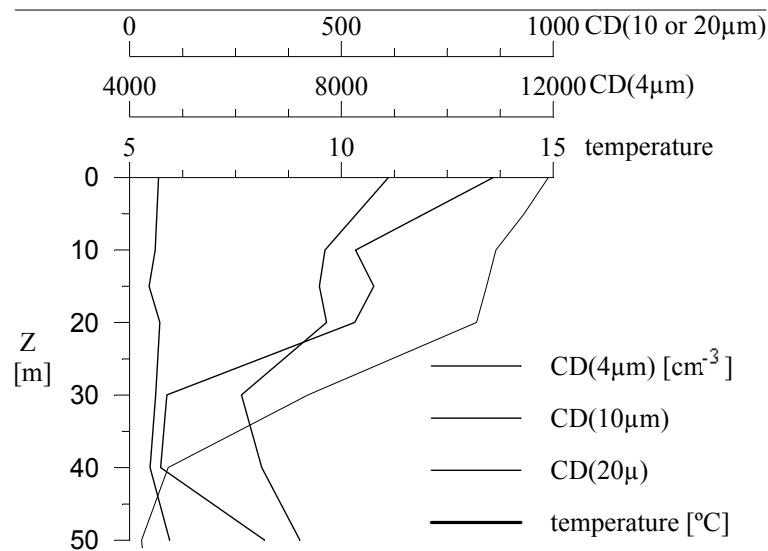
Figure 4 Vertical profiles of particles concentration for different size ranges, typical for deeper stations in summer, when seasonal thermocline occurs (June, 1992, 54°34'N 18°45'E)

Particle size distributions

Analysed particle size distributions from the Gulf of Gdansk show in most cases a regular shape with concentrations quickly decreasing with increasing particle diameter. The particle size distributions may be approximated using a hyperbolic function (Figure 5).
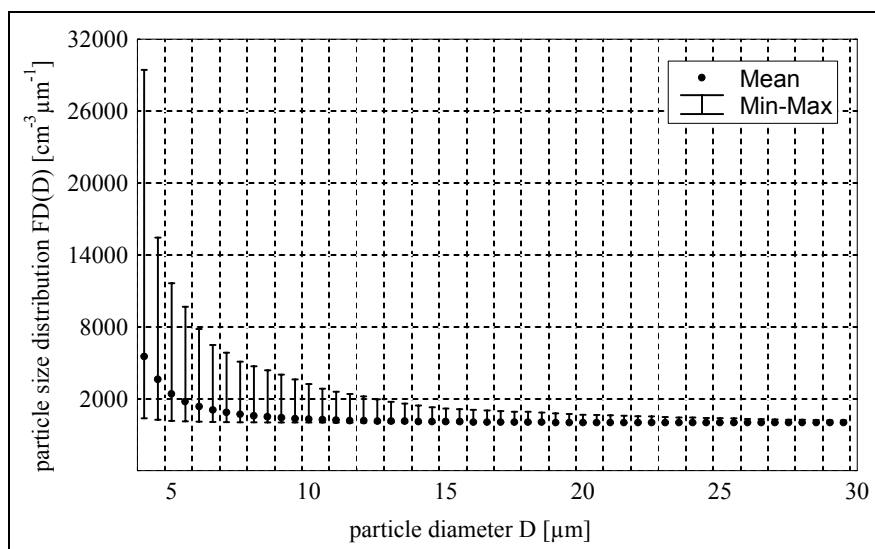
Figure 5 Mean particle size distribution function $\overline{FD}(D)$ in the Gulf of Gdansk. Vertical bars show the minimum and maximum values for diameter D.

For parametrisation of the PSD a hyperbolic function with two segments was used:

$$FD(D) = \begin{cases} k_1 D^{-m_1} (2\mu m \le D \le D_b) \\ k_2 D^{-m_2} (D_b < D \le 32\mu m) \end{cases}$$

In this equation k_1, m_1, m_2, D_b are parameters of the best fit and $k_2 = k_1 D_b^{-m_1 + m_2}$ (Jonasz, 1983). Parameters m_1 and m_2 characterise slope of the particle size distribution in log-log scale. The relative square error of the approximation, ε, was less than 2% in about 80% of the measured PSDs. Only PSDs from water rich in suspended matter e.g. sampled during phytoplankton bloom or in regions closed to the land sources of particles, have shown deviations from that described by this function. They should be approximate rather by the sum of this function and a Gaussian function or by some statistical methods (Jonasz, 1983).

Parameter	min	max	mean	standard deviation	number of data
D_b	4.63	9.58	7.38	1.87	1276
m_1	0.20	9.19	3.64	0.78	864
m_2	1.35	5.37	3.47	0.57	864
k_1	3.7 E3	21.3 E6	26.8 E6	726 E6	864

Table 1 The values of parameters of the best fit found for Gdansk Bay particle size distributions

Since D_b has been found to be close to the lower limit of the analysed diameter range, only PSDs with at least 5 size classes of diameter in the range $(4\mu m, D_b)$ were included for further consideration.

The slopes m_1 and m_2 differ negligibly, and m_1 varies in a wider range than m_2. A correlation between m_1 and m_2 was not found, but m_1 shows a slight relation (correlation coefficient $r=-0.46$) to the mass concentration of suspended matter in [mg×dm^{-3}] (Figure 6). It may suggest that the mass of suspended matter is determined mostly by the amount of particles with diameter $D<10\mu m$. The seasonal variations of m_1 and m_2 are shown in Figure 7. It is worthwhile noting that the relation between m_1 and m_2 is different for water with high and with low particle concentration. Generally $m_1>m_2$ when $CD(4\mu m)<10^4 cm^{-3}\mu m^{-1}$ and $m_1<m_2$ when $CD(4\mu m)>10^4 cm^{-3}mm^{-1}$. The slopes m_1 and m_2 of the particle size distribution differ negligibly whereas k_1 is up to 10 times higher then k_2.

$$m_1=4.96-0.25\cdot C \text{ [mg·dm}^{-3}\text{]}, \quad r=-0.46$$
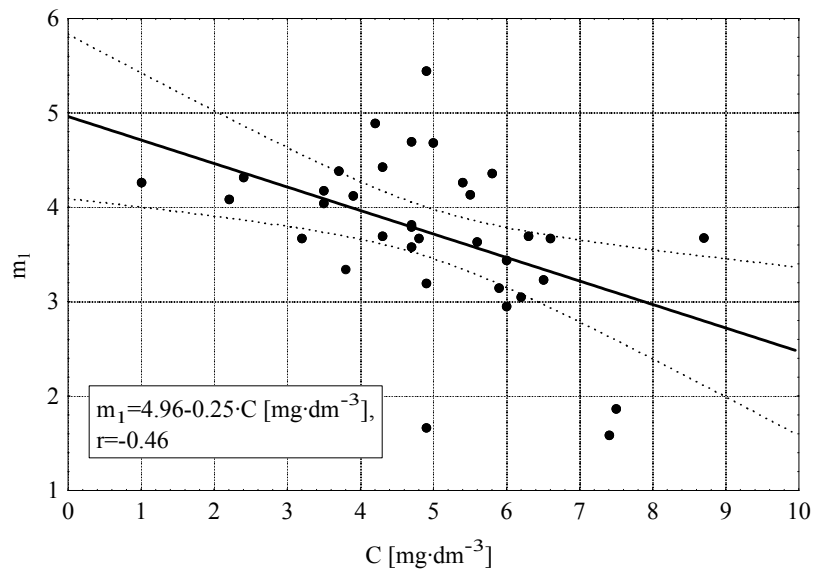
Figure 6 Relationship between the slope of the first segment of particle size distribution function m_1 and the dry mass concentration of suspended matter
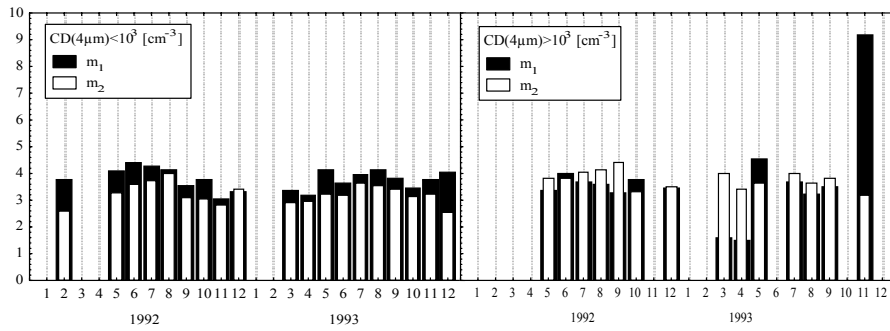
Figure 7 Temporal variations of parameters m_1 and m_2 during the analysed period for low (left) and high (right) amounts of particles in water volume

In space the vertical variation of the PSD appears to be weaker than the horizontal. The horizontal variability is wider for the first segment resulting from the variability of particle concentration connecting with land source activity. Figure 8 shows the evolution of the particle size distribution with depth in the spring–summer and in the winter–autumn seasons. The vertical variability occurs here rather than in the second segment and is evident only in the subsurface layer (deeper shape of PSD remains stable). This fact may suggest a biological reason for this variability.
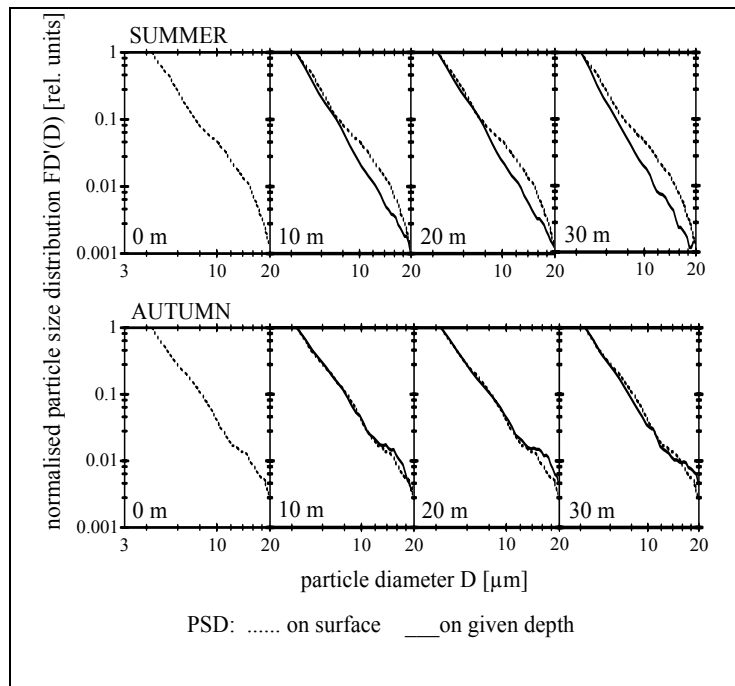
Figure 8 The evolution of the normalised particle size distribution with depth

Conclusions

Distributions of particle concentration in Gdansk Bay vary between the two main seasons: the spring–summer with higher and the autumn–winter with lower particle concentration, due to variation in biological activity and land runoff of suspended matter cycles.

The Vistula river waters, rich in suspended matter, influence the distribution of particle concentrations resulting in higher values in areas close to the river mouth during the whole year.

The vertical variability of the suspended particle concentration is much smaller than the spatial. The concentrations generally decrease with depth.

The particle size distributions measured in the Gulf of Gdansk can be described fairly well using hyperbolic functions with two segments. The parameters in the Gulf of Gdansk do not correlate between segments and the limiting diameter D_b is about 7μm.

Parameters of the particle size distribution best fit vary in time and space. The variability of the first segment of the particle size distribution can be attributed to variations in particle concentrations due to presence of the land sources of water rich in suspended matter while the second segment is due to the biological activity in surface layer. In the vertical the amount of particles relate to the density distributions and the concentrations of particles with $D>20$μm vary only in the surface layer due to biological activity.

References

Carder K. L., Beardsley Jr. G.F., Pak H., 1971. Particle Size Distributions in the Eastern Equatorial Pacific, J. Geophys. Res., vol. 76, 21.

Jonasz M., 1983. Particle size distributions in the Baltic, Tellus, 35B, 346−358.

Zalewski S. M., 1977. Analysis of the size spectrum of the marine suspended particles, Doctor thesis, PAS, Sopot.

Sediment monitoring in the Baltic Sea: results of the Baltic Sea Sediment Baseline Study

Birger Larsen, Matti Pertillä and research group

Introduction

In the mid 80s the Scientific Technological Committee of the Helsinki Commission discussed whether monitoring of sediments of the Baltic Sea should be included in the Baltic Pollution Assessments every 5 years. In order to address this question the Sediment Baseline Study was planned and organised by a group within the ICES Working group on the Baltic Marine Environment. It was agreed to first carry out a review of the existing investigations of contaminants in the Baltic Sea sediments and the relevant methods. The review was published as (Pertillä and Brügmann 1992). A multitude of interesting investigations were identified. However one of the conclusions was that sampling, positioning or analysis methods of previous data obtained from different laboratories were seldom comparable. This is due to the different objectives, the use of different methods or lack of documentation. It was recommended that a baseline study was carried out. It was not expected that the baseline study should result in major new information on the distribution of trace metals and other contaminants, but it was intended to produce a reliable set of data which may serve as reference for further studies, and to identify and evaluate the suitability of sediment stations for regional types of trend monitoring of contaminants in the major Baltic basins. With this as a starting point, the requirements have been tested in regard to procedures and quality assurance of all elements of a reliable sediment monitoring system for all the Baltic Basins. In this contribution we briefly report the general conduct of the study, review the experiences gained with respect to selection of sampling sites and the necessary quality assurance procedures and mention a few results.

What is sediment monitoring?

Sediment monitoring is the repeated measurement of concentrations of contaminants in surface sediments in order to detect changes. The reason for the monitoring can be a periodic health check of the local benthic environment or it can be to detect changes in the flux (e.g. $mg\,m^{-2}\,yr^{-1}$) through time "pollution historical records". A first requirement is that the chemical determinations have the detection limits and the stability through time to produce comparable and significant results.

The sediment trend monitoring can be based on at least two different methods. A statistic evaluation of many samples or the development in few stations in areas of little disturbance of the accumulation of sediments. The first is based on a statistical comparison of a large number of determinations made on whole bottom samples or their fine grained component from the same general area through time. This is useful where the top few centimetres of sediment move about frequently and where the areal variations in concentrations of metals and other contaminants to a large extent are governed by variation in grainsize and associated mineralogical composition and organic contents. Measurements on the fine grained component in the mostly sandy sediments in the Southern North Sea area provides an example of this approach (North Sea Task Force 1993, Rowlatt 1996, Albrecht personal communication).

The second approach—which was selected for the Baltic Baseline investigation—is based on one or a small number of stations. It is assumed that the sediment type and the sedimentation rate ($mm\,yr^{-1}$) is reasonably stable through time. For a health check it is sufficient to know that the monitored sediment types are comparable. In trend monitoring, focusing on the time variation in fluxes, it is important to analyse each time those sediments, which corresponds to the "recent" state of pollution load. It is necessary to know the time interval represented by the individual samples.

The response to a given change in flux of a substance measured as change in concentrations of a surface sample (say 0–1 cm) of a sediment monitoring station is according to (Larsen and Jensen 1989) a function of:

- the accumulation rate of the sediment
- intensity of mixing and thickness of involved layer (bioturbation)
- the thickness of sample slice and time between samplings and the chemical reproducibility.

The two first factors can be assessed using Pb210, the last are technical choices. A factor which has to be fulfilled is that the spatial variability is low compared with the precision obtainable in refinding the sampling station.

Selection and documentation of sample stations

One or a few areas for sampling were selected in each of the major Baltic basins based on previous marine-geological experience. Areas with presumed continuous and high net mud sedimentation were sought. In this context continuous deposition only implies that the average mean net deposition over the 1–5 years it takes to deposit the 1 cm thick sample is constant. Collection of samples was carried out from the Finnish research vessel "Aranda" June–July 1993. The selection of the final position of the sampling position was based on topography and structure of the sedimentary cover as documented by a small grid of sediment-echograph profiles (10 Khz and 110 KHz) and occasional side scan records. Two- or three-dimensional topographic pictures of the sampling area considerably improved the quality of the site selection. The sediment surface was inspected with a video camera system and in some cases by a sediment camera. Utmost care was exercised in the precise positioning of the ship for sediment sampling and in accurate position holding, using a Differential Global Positioning System, DGPS. Later analysis showed that R/V "Aranda" can keep the sampling station within 15 m for hours. Samples were taken with the double core (Gemini), internal diameter 80 mm, and sample length ca 30–50 cm. Sediment type, layering, bioturbation structures etc. were described for one core onboard and later by X-ray photos on a special rectangular corer (Axelsson 1983). Several cores were taken from each station and immediately cut into 1 cm thick slices and deep frozen. In most cases they were later freeze-dried and distributed for chemical and other analysis. PH and redox potential were measured on a special set of samples on board the ship.

Quality control and analysis

The objective of the study was to provide a baseline study, which should provide a reliable set of data to serve as reference for further studies. Consequently a comprehensive quality assurance plan for the description of the project including objectives and data quality is needed. This include site selection criteria, sampling procedures for each major measurement including subsampling, storage procedures and a plan for laboratory quality control checks. Each step of each procedure should be duly documented in order to provide the possibility of tracing the results both in time and quality. It was decided that analysis should be carried out by few expert laboratories with formal accreditation and/or quality assurance systems checked by external intercalibrations, among others Quasimeme. It was also decided to determine total metal contents (total digestion), because partial leaching fractions are not well defined.

The following parameters were determined:

- Metals: Al, Li, As, Cd, Cr, Cu, Hg, Ni, Pb, Ti, V, Zn, Fe, Mn and in some cores also Ag and Co
- Organic compounds: PCBs, PAHs, PBDEs, DDTs, EOCl, EPOBr, AOX.
- Supporting parameters: N, P, TC, TOC (S, LOI), water content.
- Dating: Cs137 and Pb210.
- Grain size and mineralogical composition were determined for certain samples.

Selected results

The results of the Baltic Baseline Study will be reported in the near future as an ICES Cooperative Report. Only a few selected results are given here.

The trace element analysis was done by FIMR (Pertillä and Leivouri) and BSH, Hamburg (Albrecht). Looking at the concentrations in the surface samples the outstanding features are as expected (Brügmann & Lange 1990)—high concentrations of Cd, Cu, Zn, Ag, Ni, and Co in the central deep basins, high concentrations of Hg in the Bothnian Bay and in the north eastern Gulf of Finland and very high concentration of As in the Bothnian Bay. For Pb, Cd and Hg apparently anthropogenically influenced distribution patterns were found (Figure 1), with high concentrations in the Western Baltic and Gdansk Bay, in the eastern part of the Gulf of Finland and in the Bothnian Bay, but for lead not in the deep basins.

The baseline study also includes locations previously difficult to access by western research—The Gulf of Riga, off Lithuania and the inner part of the Gulf of Finland. Although these areas are clearly contaminated to some degree, the trace element concentrations are not particular high relative to other areas of the Baltic.
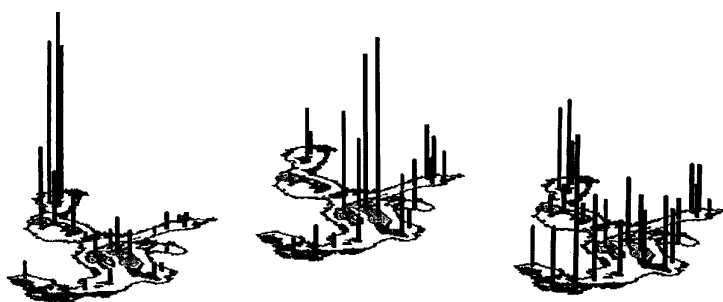
Figure 1 As surface distribution (3.89-221 $\mu g g^{-1}$)
Cd surface distribution (0.085-10.93 $\mu g g^{-1}$)
Pb surface distribution (20.7-200 $\mu g g^{-1}$)

Analysis of organic compounds were mostly the responsibility of SNV. According to Per Jonsson, PCBs and PAHs show an even spatial distribution pattern with somewhat higher concentrations in the south, indicating significant input from the atmosphere. PBDE seem to be spread all over the Baltic while EOCl (extractable organic chlorines) show a similar spatial and downcore distribution pattern in the Gulf of Bothnia and the Baltic proper as in the mid 1980s, with high concentrations off pulp mills. DDTs and PHAs show similar time trends (down core) with peak values in the 1970s. There seems to be a significant difference between the information yielded by the vertical profiles of the chlorinated hydrocarbons in sediments (PCBs), as compared to the long-term development in these compounds in biota. In several cores, the PCB concentration in sediments seems to indicate increasing PCB concentrations upwards, in contrast to the development noted in biota. This is possibly partly explained by the increased deposition of organic matter due to eutrophication and consequently increasing sequestering of PCB to the sediments, reducing their residence time in biota.

Evaluation of stations for monitoring

The content of unsupported Pb210 (that is Pb210 not produced in the sediment) decreases regularly downwards in undisturbed and steadily deposited sediment due to radioactive decay. Departure from this predictable profile permits an assessment of the mixing and/or intermittent erosion as well as the rate of deposition. This is base for an estimate of the sensitivity of the sediment station (Larsen and Jensen 1989). As a supplement, the Csl37 profile and X-ray pictures of the sedimentary structures have been used for an estimate of the expected response of a change of the flux of a persistent contaminant. Of the 25 stations investigated 4 were so disturbed, that no dating or estimate of accumulation rates was possible. Core stations with high accumulation rates (4.5–15 mm yr^{-1}) and/or low mixing by bioturbation are excellent for dating and trend monitoring purposes. Such stations were identified in the Gdansk Basin, off the Lithuanian coast, in the Gulf of Riga, two stations in the Gulf of Finland and 3 in the Bothnian Sea and Gulf. Most of the other stations have accumulation rates around 1.5–2.5 mm yr^{-1} or 250–500 g m^{-2} yr^{-1} and with mixing of the upper 2–4 cm. The sensitivity analysis was based on the following; assuming monitoring by sampling of the uppermost 1 cm every 5 years, a steady state in relation to net accumulation rate and mixing depth and rate, and a 10% relative standard deviation for chemical analysis. Using the results from the individual stations, the sensitivity analysis indicates that we can expect to be able to detect changes in flux of a contaminant in the order of 10-15% (in 5 years) for the best stations, while a 60-200% change in flux is needed to cause a significant change in concentrations at the other stations (See Figure 2). If the standard deviation in the analysis is halved, the needed change is also halved.

In the East Gotland Deep a 7-10 cm layer of fluffy very water-rich material was seen on top of the sea-floor. The fluffy stuff contains relatively high concentrations of Pb210 and high but variable Cs137 contents. Both the Pb210 and the metals distribution with depth suggests that some sediment layers are missing below the fluffy layer. The disturbed Pb210 profiles do not permit an acceptable dating. Niemistö has seen the fluffy stuff at station F81 in 1992—before the inflow (personal communication) and it is speculated that it could be the result of redeposition of nearly recent sediment before the inflow of new bottom water in 1993. In this period the stability of the water column was very low, according to Fonselius. P. Jonsson and V. Axelsson have suggested, based on the faint layers and the distribution of organic pollutants, that in the station in the East Gotland Deep the linear sedimentation rate of the fluffy top layer is very high—about 15 mm in 1990–1992 even if the mass accumulation is only 310 g m^{-2} yr^{-1}. If so, the laminated sediments at the stations in the Gotland deep could be used for monitoring—this has to be verified.

Figure 2 Result of sensitivity analysis based on evaluation of the Pb210 profile

Conclusions

- A reliable set of sediment parameters has been established covering the major basins in the Baltic Sea.

- The sediments provide relevant information on the development of the contaminant status, at least in certain areas, and thus can be included in the pollution monitoring programmes of HELCOM. Monitoring in this sense is to be understood as a programme of repeated sediment studies. The main utility of the sediments, however, is to indicate large scale spacial variability rather than variation over time.

- Sediments respond slowly to input changes so annual trend monitoring is not recommended.

- For selected stations, sediment monitoring is recommended at 5 years intervals.

- Some of the areas sampled in the Sediment Baseline Study should be investigated again for better positions; this is particularly the case for Kattegat, the Bornholm Basin, the Arkona Basin and the northern central Baltic Proper.

- Detailed recommendations for the monitoring program will be given in the final ICES report.

References

Axelsson, V., 1983. The use of X-ray radiographic methods in studying sedimentary properties and rates of sediment accumulation. Hydrobiologica 103,65–69.

Brügmann, L., and Lange, D., 1990. Metal Distribution in Sediment in the Baltic Sea. Limnologica 20, 15–28.

Larsen, B. and Jensen, A., 1989. Evaluation of the Sensitivity of Sediment Stations in Pollution Monitoring. Marine Pollution Bulletin. 320,556–560. (reprinted in ICES Coop.Res. Rep 180).

North Sea Task Force, 1993. North Sea Assessment Report, 1993. Quality Status Report of the North Sea, Subregion 4 (Chapter 3.13).

Pertillä., M., and Brügmann, L., 1992. Review of the sediment studies in the Baltic. ICES Coop.Res.Report 180. Rowlatt, S.M., 1996: NSTF Baseline Survey of Sediments, in Andersen, J., Karup, H.& Nielsen, U.(eds.) 1996: Scientific Symposium on North Sea Quality Status Report 1993. 18–21 April 1994 Ebeltoft Denmark. Proceedings. Danish Environmental Protection Agency.

Oil pollution in the sediments of the Southern Baltic

Edward Kaniewski, Zbigniew Otremba, Adam Stelmaszewski and Teresa Szczepanska

Introduction

Marine oil pollution is one of the most important problems among the environment pollutants. These pollutants are being released into the sea in great quantities. Published estimated data concerning the amount of crude oil and petroleum products released into the sea are very divergent.

There are a lot of sources of hydrocarbons in the sea environment. Live organisms— bacterium, algae, diatoms—are natural sources of these compounds. The amount of oil pollution in the sea is brought about by exploitation by shipping vessels, leakages from underwater oil pipelines, industrial and municipal wastes containing diesel fuel, lubricating oil, fatty acids and other components. Each of these sources introduces characteristic compounds. Close examination (especially using gas chromatography connected with mass spectrometry) allows us to see different compositions of the hydrocarbon mixtures from which we can determinate the source of contamination (Malinski and Szafranek, 1993; Szafranek at all, 1993; Czyz at all, 1993, 1994).

Hydrocarbons in the sea environment was a very popular subject for investigations about ten years ago when introductory investigations were started, but these investigations are rarely continued now. Quite recently Daniel Glód attempted to estimate quantities of hydrocarbons in the Gdansk Bay sediments and determination of policyclic hydrocarbons has been performed by Gesine Witt. It would be interesting to compare the results.

Collection and Storage of Samples

The samples of sediments have been taken up with a Kajak sampler from the bottom of South Baltic and Gdansk Bay, mainly in coastal areas. The sampling locations are shown in Figure 1. The superficial sediments are about 5 cm thick and also cores from some points parted in layers (also 5 cm thick) have been taken for investigation. All samples have been stored below -18°C in glass vessels in the dark.
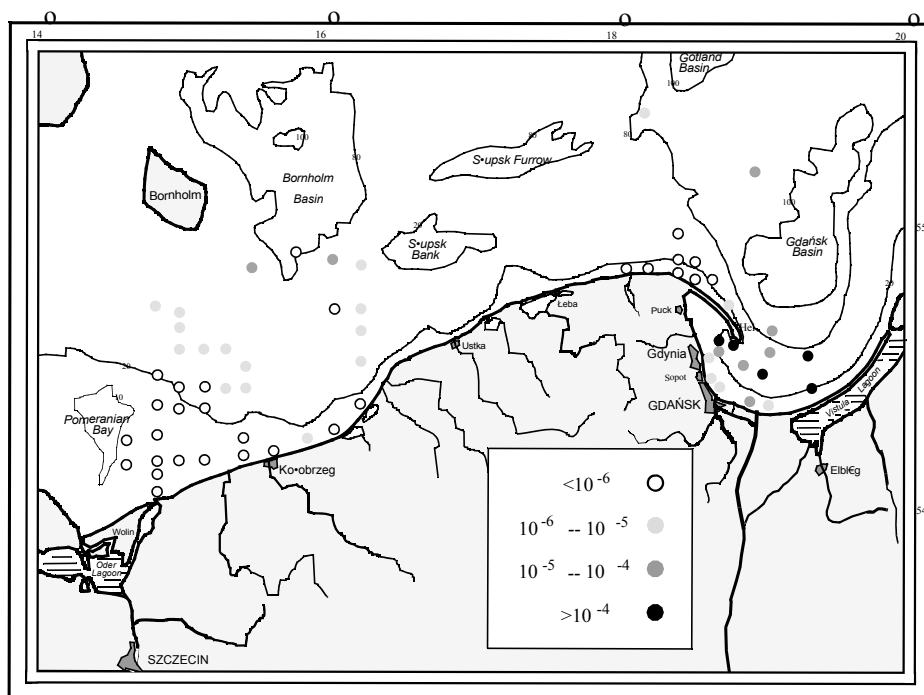

Figure 1 The sampling locations with the ranges of relative hydrocarbon concentration in the surface layer

Determination of Hydrocarbons

First the sediments were lyophilised. Dry samples weighing 30 g were extracted with spectrally pure n-hexane. All work under the duration of the extraction the samples was carried out in darkness—and also the finished extracts were kept in dark conditions.

Determination of hydrocarbon concentrations was conducted using the ultraviolet fluorescence method, which consists of measuring the intensity of the 360 nm wavelength light emitted by the extracts, by excitation with the 313 nm wavelength light. The layout of the measurement set is shown in Figure 2. Crude oil from the North Sea, artificially aged for 2 hours at 120°C, has been used as a pattern.
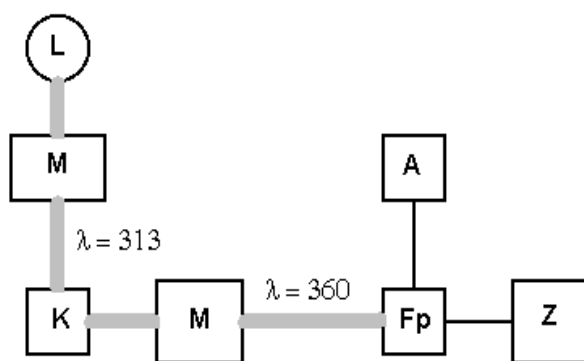
Figure 2 Layout of the measurement equipment (L−lamp; M−monochromator; K−chamber with the sample; Fp−photoelectric multiplier; Z−feeder; A−microamperometer).

Results

The range of the hydrocarbons concentration in the sediments was very wide. The relative concentrations changed from 10^{-8} for cline places up to 10^{-3} for the most polluted areas such as harbour basins. Figure 1 shows the concentration of hydrocarbons in the surface layer of bottom sediments in several places in the South Baltic area. It shows that the Gdansk Gulf is an area with the highest concentration of hydrocarbons, mainly 10^{-4} and 10^{-5}. This corresponds with the higher level of hydrocarbon concentrations in the gulf water compared to the open sea. The hydrocarbon concentrations in the Pomeranian Bay are mainly of the order 10^{-6}. The bottom sediments of the open sea contain more hydrocarbons in the deeper areas (over 20 m deep) than shallow coastal places.

The vertical distribution of the hydrocarbons concentration is an another problem. The sediment cores from some places have been tested. There is no single universal model of these distributions. The concentration in all layers from the surface to 30 cm is higher than at 50 cm and 100 cm depths for each investigated site. The exemplary distributions are shown in Figure 3.
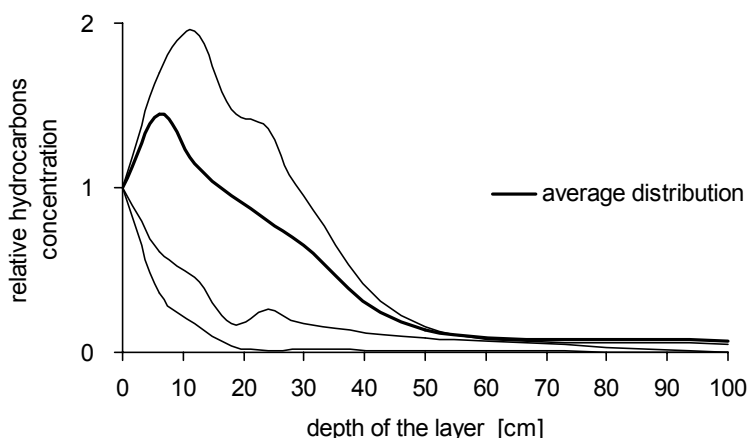
Figure 3 The exemplary distributions (and the average one) of the relative hydrocarbons concentration (determined to the superficial layer) as a function of the layer depth.

Another question is the dependence of the hydrocarbon concentrations on the type of sediment. The organic matter content in some samples of sediment has been measured. The organic matter was determined as a decrement of mass of a dry sample, which has been roasted at 550°C for 1 hour. This test has not shown any correlation between content of organic matter and hydrocarbons concentration (correlation coefficient is 0.48). Figure 4 presents the concentration of hydrocarbons in bottom sediments as a function of their organic matter content.
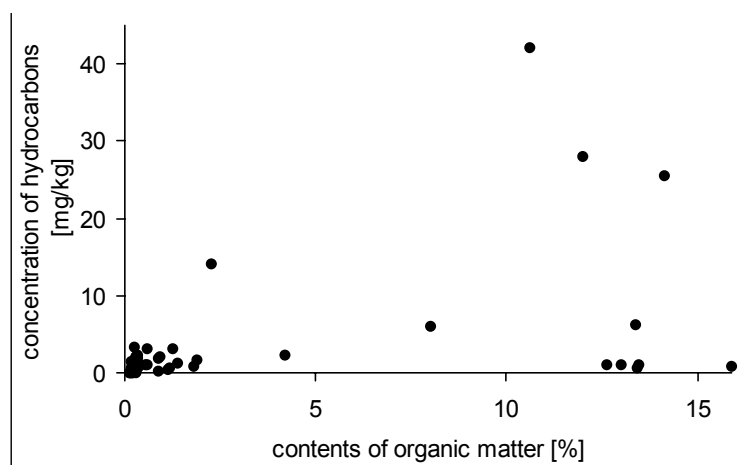
Figure 4 The hydrocarbon concentrations in the South baltic sediments as a function of their organic matter contents.

Conclusion

The relative hydrocarbon concentrations in sediments of the South Baltic bottom is in general at a level of 10^{-7} for the open sea area. This level could be accepted as a level of natural concentration of hydrocarbons. The higher hydrocarbon concentrations in the Pomeranian Bay sediments (10^{-6}) and specially in sediments of the Gdansk Gulf (up to almost 10^{-3}) show that oil pollution is the essential source of hydrocarbons in this environment. The results of determination of the hydrocarbon concentrations in water from open sea, Gulf of Gdansk and river waters [Otremba and Stelmaszewski, 1994] confirm this conclusion.

Measurements of the concentrations of the total hydrocarbons is a first step in the investigation of hydrocarbons in the bottom sediments. The results of these measurements could give a general view of hydrocarbon concentrations in sediments in several areas. This prospect would also allow us to select the most interesting places and investigate them using more precise methods.

References

Czyz B., Otremba Z., Stelmaszewski A., Targowski W., 1993. The total fluorescence spectra and prospects of utilising them to identification of pollution sources. Proc. of the Conference TERB'93, Gdynia, 76−85.

Czyz B., Otremba Z., Stelmaszewski A., Targowski W., 1994. Oil identification by using the total fluorescence spectra. Proc. of the XIX CBO, Sopot, 657−666.

Glód D., 1994. The policyclic aromatic hydrocarbons in the bottom sediments in the Gdansk Bay. Dissertation, Gdynia.

Malinski E., Szafranek J., 1993. Application GC/MS to differentiation and to defining of origin petro- and pirogenic contaminations in the sea environment. Proc. of the Conference TERB'93, Gdynia, 61−74.

Otremba Z., Stelmaszewski A., 1994. Concentration and Origin of the contaminations in the Gdansk Bay coast water. Proc. of the XIX CBO, Sopot, 630−637.

Szafranek J., Zachowicz J., Szczepanska T., Malinski E., 1993. Cycloalcanes as the molecular markers determining origin of contaminations sea with crude oil. Proc. of the Conference TERB'93, Gdynia, 38−52.

Witt G., 1994. Policyclic Aromatic Hydrocarbons in the Baltic Sea. Proc. of the XIX CBO, Sopot, 622−629.

Occurrence and distribution of organic micropollutants in sediments of the western Baltic Sea and the inner coastal waters of Mecklenburg–Vorpommern (Germany)

G. Witt, K. W. Schramm, and B. Henkelmann

Summary

The occurrence and distribution of polycyclic aromatic hydrocarbons, polychlorinated dibenzo-p-dioxins and dibenzo-furans (PCDD/Fs) were investigated in surface sediments (0–2 cm) of the Belt Sea, the Arkona Sea and the internal and external coastal waters of Mecklenburg–Vorpommern. The concentrations of different toxic PAHs and PCDD/Fs congeners were measured.

Sedimentological properties affect the accumulation of organic pollutants. Strong correlations between concentrations of PCDD/Fs and the content of organic carbon (TOC) were established. The results were normalised to TOC.

The sum of PAHs varied between 2.1 μgkg^{-1} TOC and 66.5 μgkg^{-1} TOC for muddy sediments in the Belt Sea and Arkona Sea. Elevated concentrations up to 46 μgkg^{-1} TOC were observed in the surface sediments of the internal coastal waters with highest concentrations in the Warnow estuary and in the Oder Haff. This indicates the significant contribution of river discharge to the contamination of sediments with PAHs. The distribution of the individual PAHs in sediments varies widely depending on their structure and molecular weight. The higher molecular 4 to 6 ring aromatics predominate due to their higher persistence.

The sum of dioxins varied between 2.1 μgkg^{-1} TOC and 66.2 μgkg^{-1} TOC. Higher concentrations were observed in the surface sediments of the internal coastal waters especially in the Warnow estuary and the Oder Haff. This indicates a significant contribution of river discharge to the contamination of sediments with dioxins. Elevated concentrations of dibenzofurans were observed in the Wismar Bight. The most toxic congener, 2,3,7,8-Tetrachlor-p-dibenzodioxin, (Seveso dioxin) was found at only 4 stations.

The fingerprint profiles of the different congener groups are similar in the whole investigated area. The concentration of the dioxins increased with increasing degree of chlorination. Octachlordibenzo-p-dioxin predominates in the whole western Baltic Sea and in the internal coastal waters.

Introduction

The investigations of polycyclic aromatic hydrocarbons, polychlorinated dibenzo-p-dioxins and dibenzofurans have been extensive during the last few years. These compounds are of high environmental concern due to their toxicity and carcinogenic activity.

The distribution of PAHs and PCDD/Fs in different areas of the world ocean have been reported by several authors (Bopp *et al.*, 1991; Broman, 1991; Mosse, 1993, but only very few data are available for the Baltic Sea (Witt, 1995; Broman *et al.*, 1993; Zebühr, 1992; Poutanen, 1981) and there is a lack of information for many regions of the Baltic Sea.

The investigated substances mainly originate from domestic and industrial waste water, river run-off and especially atmospheric deposition of combustion products. Major sources of industrial processes contributing to their production are the combustion of fossil fuels, and especially for the PCDD/Fs metallurgical processes, such as chlorine bleaching of paper pulp and the production of chlorine compounds (PCBs, Pentachlorphenol).

Atmospheric transport should be a major pathway for the input of PAHs and PCDD/Fs into the aquatic environment. In the water column, they become frequently associated with particulate matter due to their hydrophobic nature and may accumulate to high concentrations in sediments (Broman *et al.*, 1989).

Sampling area

The investigated sea area covers parts of the western Baltic Sea and the Baltic Proper. The sampling area also includes a large system of internal coastal waters—Bodden and Haff areas—along the 340 km long southern part of the Baltic

coastline of north-eastern Germany (Mecklenburg–Vorpommern). Boddens and Haffs are lagoons, connected to the sea by shallow or narrow natural sea channels. This coastline is typical for Mecklenburg–Vorpommern. The hydrography of the inner coastal seas is governed mainly by changes in the intensity of water exchange with the Baltic Sea. Freshwater inflow via rivers plays an important role. The main rivers in this area are the Warnow, the Uecker, the Peene and the Oder. The inner coastal waters function as pre-purification areas and are thereby a sink for all types of anthropogenic contaminants.

The investigated surface sediments (0–2 cm) comprise muddy sediments with a high amount of organic carbon. Since sediment structure varies between different sampling sites (grain size effect) a normalisation to TOC was performed to correct this effect. This procedure allows us to compare contamination levels between the different areas.

Sample preparation and analyses

The surface sediment samples were collected with a Van-Veen grab (0–2 cm). The samples were stored in aluminium boxes at –21°C until analysis. The water content, the carbon content and the fraction <63 μm were determined. The carbon content (TC) and inorganic carbon content (TIC) were measured using an ELTRA C/S analyser (METALYT CS 1000S). The difference between TC and TIC yields gives total organic carbon content (TOC).

PAH preparation and analysis are given by Witt (1995). PCDD/F analysis is described by Schramm *et al.* (1995).

Results

Distribution of PAHs in surface sediments

The sum of PAHs varied between $7.5 \mu g g^{-1}$ TOC and $36 \mu g g^{-1}$ TOC in the Belt and Arkona Sea. The highest concentrations were found in the river Warnow. There the concentrations varied between $6.2 \mu g g^{-1}$ and $15.4 \mu g g^{-1}$ TOC (Figure 1).
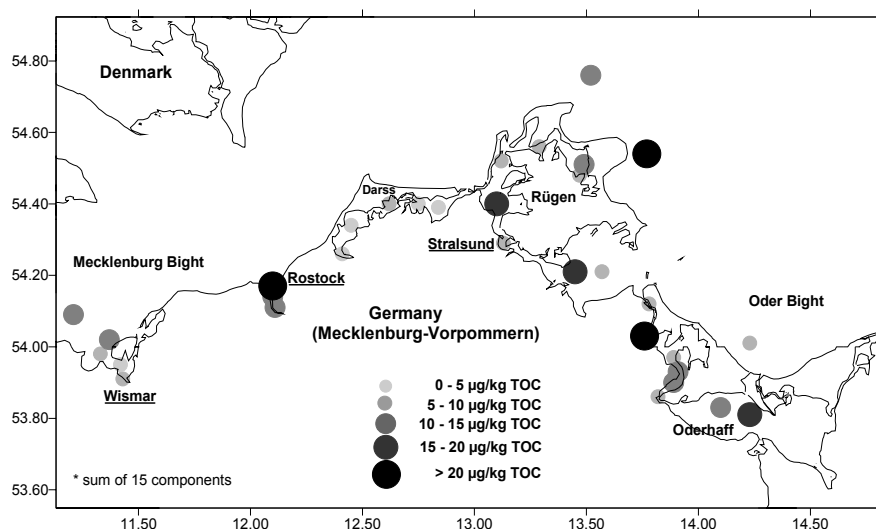
Figure 1 Distribution of PAHs in surface sediments in the investigated area

These high concentrations should be a result of a high anthropogenic input of PAHs in this region. Sources are industrial waste water especially from the shipyards near Rostock, the traffic around Rostock and coke oven emissions.

The PAH content in the muddy sediments of the Oder Haff and the Peenestrom is also relatively high and ranges between 3.45 and $8.14 \mu g g^{-1}$ TOC. The Oder river should be the main source of the significantly higher PAH content in these areas.

The distribution of the individual PAHs varies widely depending on their structure. The higher molecular PAH (e.g. benzo(a)pyrene) predominated due to their higher persistence. A concentration gradient was found with decreasing PAH concentrations from the Oderhaff to the open sea (Figure 2), suggesting that the Oder river could be the major source of significant higher PAH content in this region.

The concentrations of PAHs are more than 1000 times higher than the concentrations of PCDD/Fs.
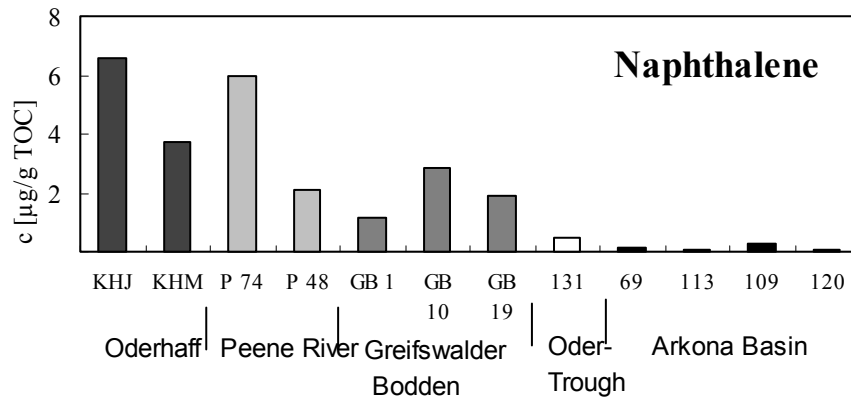
Figure 2 Concentration gradient of naphthalene from the inner coastal water to the open sea

Distribution of PCDD/Fs in surface sediments
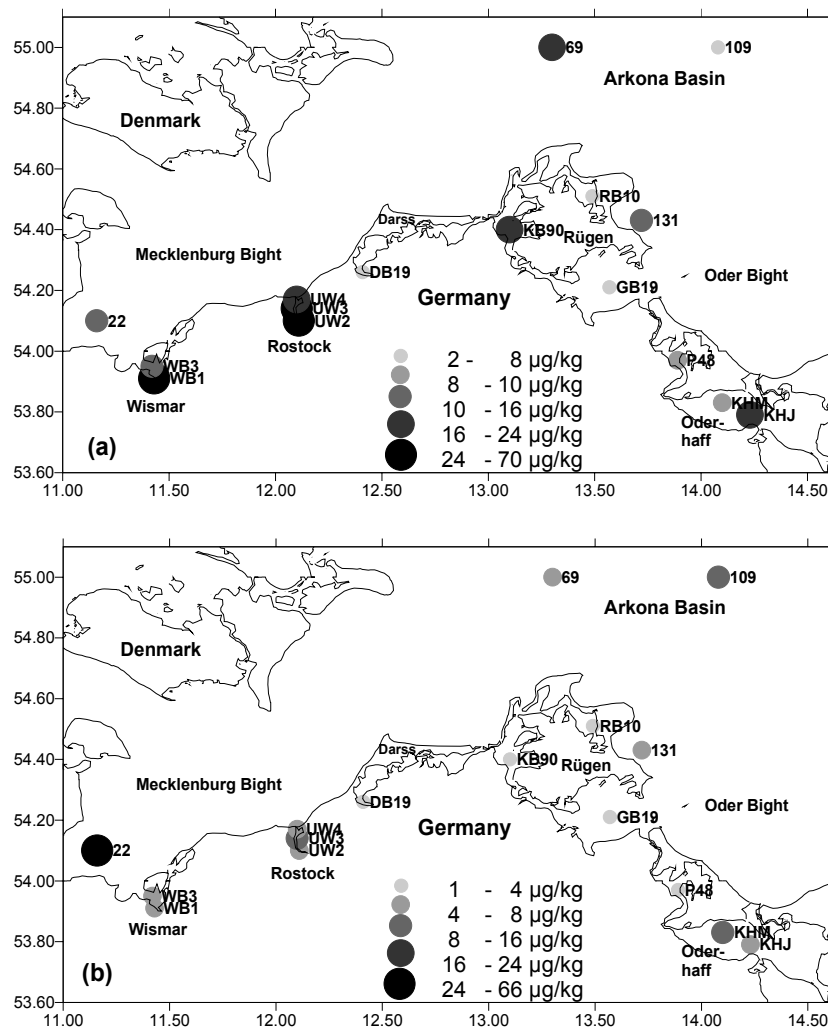
Figure 3 Distribution of PCDDs (a) and PCDFs (b) in the investigated sea area

The concentrations of 15 PCDD/Fs congeners and of the sum of the tetra- (TCDD/F), penta- (PNCDD/F), hexa- (HCDD/F) hepta- (HPCDD/F) and octa- (OCDD/F) dibenzo-p-dioxins and dibenzofurans as well as the total concentration of PCDD/Fs were investigated.

The concentrations in the different sediments show wide variations, depending on the investigated region. The total concentration of the polychlorinated dibenzo-p-dioxins varied between $2.1\,\mu g\,kg^{-1}$ and $66.2\,\mu g\,kg^{-1}$ TOC and the concentrations of the PCDFs ranged between $2.4\,\mu g\,kg^{-1}$ TOC and $65\,\mu g\,kg^{-1}$ TOC (Figure 3) The 2,3,7,8-TCDD, most toxic congener was found at only 4 stations.

The highest concentrations of PCDDs were measured in the river estuaries of the river Warnow and the river Oder (Oderhaff). The concentration of the sum of the investigated dioxins in sediments of the Warnow river ranged between 23 and 66.2 $\mu g kg^{-1}$ TOC. The concentration of the dibenzofurans varied between 5.6 and 9.3 $\mu g kg^{-1}$ TOC. The values of the sediments of the Oderhaff ranged between 9.9 and 21.1 $\mu g kg^{-1}$ TOC for the sum of the investigated dioxins and between 2.4 and 10.4 $\mu g kg^{-1}$ for the sum of dibenzofurans.

The high concentrations in the Warnow estuary may be a result of a high anthropogenic input of PCDD/Fs in this region. Sources are industrial waste water especially from the shipyards near Rostock, the traffic around Rostock and coal combustion emissions. High PCDD/Fs concentrations were also measured near the shipyard of the city of Wismar.

The concentration levels of the PCDD/F in the Boddens are rather low compared to the other parts of the investigated areas. The PCDD concentrations (sum of 6 congeners) ranged between 2.4 $\mu g kg^{-1}$ and 4.5 $\mu g kg^{-1}$ TOC in the sediments of the Bodden area.

The fingerprint profiles of the different congener groups are similar in the whole investigated area (Figure 4). The concentration of the PCDD increased with increasing degree of chlorination (Cl4<Cl5<Cl6<Cl7<Cl8). This trend in conjunction with the presence of Cl4-Cl8 PCDFs strongly suggests the influence of combustion sources. These distribution patterns are also reported as typical profiles in air samples (Reed *et al.*, 1990). The most abundant congener in the whole investigated area was octachlordibenzo-p-dioxin (OCDD). This compound is thought to be a major component of combustion produced PCDDs (Marklund *et al.*, 1986). The highest concentrations, up to 54 $\mu g g^{-1}$ TOC, were analysed in the Warnow river estuary.
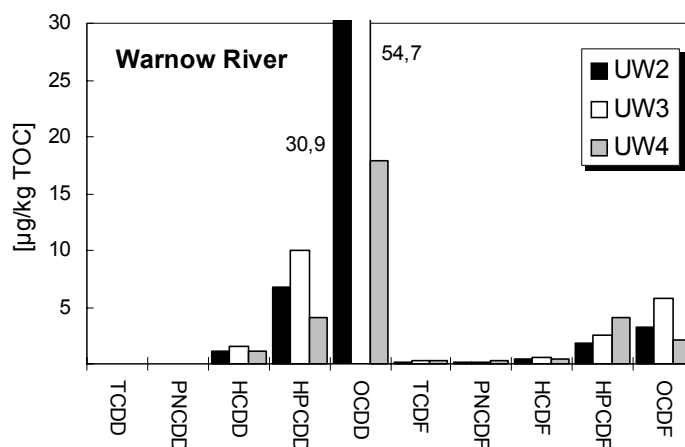
Figure 4 Fingerprint profiles of the different congener groups in the Warnow river estuary

Conclusions

The distribution of polycyclic aromatic hydrocarbons, polychlorinated dibenzo-p-dioxins and dibenzofurans in surface sediments of the Arkona Sea, Belt Sea and the inner coastal area of Germany were investigated.

The highest concentrations of these organic micropollutants were recorded at the rivers and Haff areas. In this case, a great part of the inner coastal waters functions as a trap and a pre-purification basin for organic pollutants which are mainly adsorbed on particulate matter (SPM).

A seaward trend of decreasing PAH concentrations was found especially for the lower molecular weight PAHs. This trend was not observed for the PCDD/F congeners due to their higher persistence.

It is difficult to make an assessment of all potential sources of PCDD/F contamination in the western Baltic Sea. One important source for PAH input to the Oder Haff and the Arkona Basin is the river Oder. Industrial waste water from the shipyards is thought to be the major source for the elevated PAH and PCDD concentrations near Wismar and Rostock. According to the distribution patterns of the individual congener groups of PCDD/Fs another major source might be the atmospheric input of combustion-derived PCDD/F from central Europe.

References

Bopp, R.F., Gross M.L., Tong H., Simpson H.J., Monson S.J., Deck, B.L., and Moser, F.C., 1991. A major incident of dioxin contamination: Sediments of New Jersey Estuaries. Environ. Sci. Technol., Vol. 25, No. 5, 951–956.

Broman, D., Näf, C., Zebühr, Y., Bandh, C., Ishaq, R., and Pettersen, H., 1993. Occurrence, distribution and turnover of some toxic substances un the water mass and sediments in the Baltic Sea. Baltic News, 4, 6–10.

Broman, D., Näf, C., and Zebühr Y., 1991. Long-Term high and low volume air sampling of polychlorinated dibenzo-p-dioxins and dibenzofurans and polycyclic aromatic hydrocarbons along a transect from urban to remote areas on the Swedish Baltic coast. Environ. Sci. Technol., 25, No. 11, 1841–1849.

Broman D., Näf, C., Rolff C., Zebühr Y., Fry B., and Hobbie J., 1992. Using ratios of stable isotopes to estimate bioaccumulation and flux of polychlorinated dibenzo-p-dioxins and dibenzofurans (PCDFs) in two food chains from the northern Baltic. Environmental Technology and Chemistry, 11, 331–345.

Marklund, S., Kjeller, L.-O., Hansson, M., Tysklind, M., Rappe, C.; Ryan, C., Collazo, H., Dougherty, R. (1986). Determination of PCDDs and PCDFs in incineration samples and pyrolytic products. In: Chlorinated dioxins and dibenzofurans in perspective; Rappe, C., Ryan, C., Choudhary, G., Keith, L.H., Eds.; Lewis Publishers: Chelsea, MI, 79–92.

Mosse P.R.L., and Haynes D., 1993. Dioxin and furan concentration in uncontaminated waters, sediments and biota of the Ninety Mile Beach, Base Strait Australia. Mar. Pollut. Bull., 26, 465–468.

Näf, C., 1991. Some biotic and abiotic aspects of the environmental chemistry of PAHs (polycyclic aromatic hydrocarbons) and PCDD/Fs (polychlorinated dibenzodioxins and dibenzofurans). Thesis. Department of Analytical Chemistry, Stockholm University, ISBN 91–87272–24–5, 66 pp.

Poutanen, E.L., 1988. Hydrocarbon concentrations in water and sediments of the Baltic Sea. In: Proceedings of the 16th conference of Baltic Oceanographers, 882–892. Institute of Marine Research of Kiel, Germany.

Schramm, K.W., Henkelmann, B., Kettrup, A., 1995. PCDD/F sources and levels in river Elbe sediments, Wat. Res., 29, 2160–2166.

Wenning, R.J., Paustenbach, D.J., Harris, M.A., Bedbury, H., 1993. Principal component analysis of potential sources of polychlorinated dibenzodioxins and dibenzofuran residues in surficial sediments from Newark Bay, New Jersey. Arch. Environ. Contam. Toxicol., 24, 271–289.

Witt, G., 1995. Polycyclic aromatic hydrocarbons in water and sediment of the Baltic Sea. Mar.Pollut.Bull., 31, 237–248.

Zebühr, Y., 1992. Trace analysis of polychlorinated dibenzo-p-dioxins and dibenzofurans and related compounds in environmental matrices, Department of Analytical Chemistry, Stockholm University, 1992.

Sedimentation rate variabilities in the eastern Gotland Basin

Christian Christiansen, Helmar Kunzerdorf, Kay-Christian Emeis, Rudolf Endler, Ulrich Struck, Dagmar Benesch, Thomas Neumann and Vadim Sivkov

Abstract

This study examines sedimentation rates with a variety of methods. In contrast to previous studies they reveal both spatial and temporal variations in the rates. High resolution seismic recordings and correlation with long sediment cores show increased thickness of strata and higher sedimentation rates ($0.8 \, \text{mm a}^{-1}$) in the SE part of the deep basin than in the NW part ($0.2 \, \text{mm a}^{-1}$) since the Littorina transgression some 7650 years B.P. On shorter time scales, estimates of sedimentation rates based on radiometric dating (^{210}Pb) are in general twice as high as those observed 25 years ago with the same method. This may partly be due to eutrophication, as more carbon is buried in the sediment, and partly due to increased erosion in shallow water areas. However, strong lateral variations are observed. The average rate varies between 119 and $340 \, \text{gm}^{-2} \text{a}^{-1}$ (corresponding to $2.1–2.5 \, \text{mm a}^{-1}$) in the deepest part of the basin. Very high rates of $6100 \, \text{gm}^{-2} \text{a}^{-1}$ ($30 \, \text{mm a}^{-1}$) are observed in an intraslope basin off the coast of Latvia at a water depth of only 70m. The radiometrically determined rates are up to three times higher than rates estimated from average water column concentrations of suspended matter.

Introduction

Sedimentation rates in depositional areas of the Baltic Sea mirror the extent of erosion in the catchment area on land and on the sea floor as well as the state of the chemical and biological environment. They are influenced by riverine discharge, by hydrography, by climatic changes, and by increased biological production as a consequence of an increased supply of nutrients. Oxic or anoxic conditions on the sediment water interface determine whether laminated sediments are deposited at any given time.

A number of methods have been used to evaluate sedimentation rates in the Baltic Sea. By counting varves in postglacial sediments, Ignatius (1958) found that the rate was approximately $1 \, \text{mm a}^{-1}$ over a period of about one thousand years. Ignatius *et al*. (1971) used the depth of dry substance deposited in the Gotland Deep during the last 7000 years to suggest a sedimentation rate of approximately $1 \, \text{mm a}^{-1}$. ^{210}Pb dating of recent upper unconsolidated sediment from the beginning of the 1970s yielded modern sedimentation rates that were $1.0–1.3 \, \text{mm a}^{-1}$ (Niemestö & Voipio, 1974). Similar or slightly higher rates were observed by a number of authors e.g. Suess (1978). Such observations supported the conclusion reached by Ignatius *et al.* (1981) that "the rate of sedimentation has been surprisingly uniform for several thousand years" in the Gotland Basin.

Recent studies have shown greater variabilities in sedimentation rates. Biostratigraphical methods were used by Gelumbauskaite & Grigelis (1995) to infer that 540 mm were deposited at a deep water station in the Gotland Basin during the last millennium, whereas only 25 mm were deposited on the saddle between the Gotland Deep and the Faro Deep in the same period of time. Varve-counting in the upper 5 cm of recent laminated sediments (Jonsson *et al.* 1990) showed sedimentation rates in the range $1.5–4.2 \, \text{mm a}^{-1}$. Many shallow water parts of the Baltic Sea are non-depositional. The depth limit of deposition depends both on the wave base and the position of the permanent pycnocline. Therefore the depth limit is situated at a depth of about >50 m in the western part of the Baltic around the Bornholm Basin (Christiansen & Emelyanov, 1995), and about a depth of >80 m in the Baltic proper (Jonsson *et al.*, 1990).
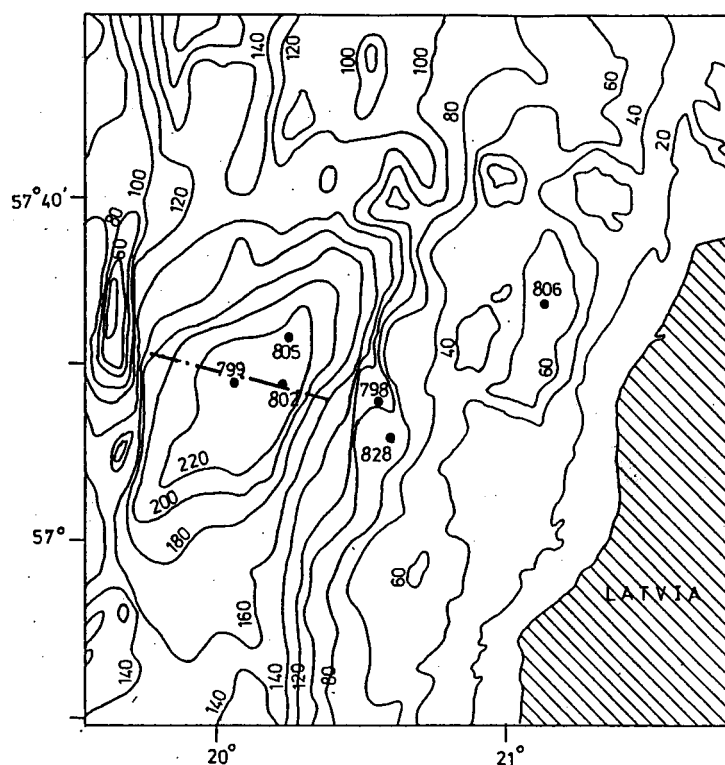
Figure 1 Location map showing seismic line and core sampling positions in the Gotland Basin. Isobaths in m.

The purpose of this paper is to study sedimentation rate variabilities and to reconcile the diverging estimates. For this purpose we have used a number of the above methods in the Gotland Basin (Figure 1).

Methods and Material

A GeoChirp Subbottom Profiler was used for acoustic surveys during the expedition (1994) with R/V "A. v. Humboldt". The Chirp profiler (transmitting signals $2-8\,$kHz or $1.5-11.5\,$kHz, depending on operating mode) consisted of a deck unit and a tow fish. The penetration depth of the unit was up to 40m below the seafloor and typically had high resolution ($0.3-0.5$ m). Based on results of the acoustic surveys, sediment stations were targeted to areas where echograms indicated either high sediment accumulation and a sufficiently resolved recent sediment cover, or where acoustic units were within reach of the gravity coring techniques used. Different tools were used to obtain sediment samples.

1. A multi-corer provided up to eight sediment cores from an area of $1.5\,\mathrm{m}^2$ to a depth of 45cm and recovered bottom water and an intact sediment/water interface. Several of these subcores were sliced in 1cm thick discs on board and either stored frozen for shore-based analyses or were left intact for radiometric dating.

2. For longer cores a gravity corer with an inner plastic liner was used. The corer had a top weight of 1200kg. A maximum length of 10m sediment was recovered with this weight, which was found to be sufficient for penetrating the soft sediment of the Gotland Basin to the icelake stage. The liners were cut into sections of 1m length, capped, and stored for shore-based logging of p-wave velocity, magnetic susceptibility, bulk density with a gamma-ray attenuation porosity evaluator, and structures with a 600 dpi grey-scale scanner in a GEOTEC Multisensor Track.

3. Finally, a Kastenlot of 15x15cm diameter and variable length was used, weighted by $1200-2200\,$kg lead. The longest core recovered with this tool was 970cm. These cores were opened on board, slabs and u-channels were taken over the entire length for x-ray photography and magnetic measurements, and the cores were described after visual examination.

Recent net sedimentation rates were determined from dating of multicores using low-level Gamma-spectrometric measurements. Measurements of ^{210}Pb, ^{137}Cs, and ^{226}Ra activities were carried out using a reverse-electrode coaxial Ge-detector (10 percent rel. efficiency) with energy resolution values of 640eV (at 5.9keV) and 1.7keV (at 1332keV). Subtracting ^{210}Pb supported, i.e. the amount equivalent to the ^{226}Ra activity, the unsupported activity ^{210}Pb$_{\mathrm{unsup}}$ is used to estimate linear sedimentation rates for the cores using the constant initial concentration (CIC) model of interpretation.

Christian Christiansen, Helmar Kunzerdorf, Kay-Christian Emeis, Rudolf Endler, Ulrich Struck, Dagmar Benesch, Thomas Neumann and Vadim Sivkov

127

The historical profiles were constructed using petrophysical core data (density and porosity) and the constant rate of supply (CRS) model for ^{210}Pb.

Under stationary conditions in the sea bottom layer there is a sedimentation-diffusion equilibrium, or a vertical distribution of suspension concentration, at which the gravity flow of sedimentary particles is balanced by the process of vertically oriented diffusion. A concentration gradient is caused by gravity, which results in downward flux of suspensions P_S:

$$P_S = UC \tag{1}$$

where U = settling velocity of suspended particles and C = concentration of particles.

According to Fick's first law, the gradient of concentration gives rise to a diffusive flow P_d, directed upwardly:

$$P_d = -D\frac{dC}{dz} \tag{2}$$

where D = coefficient of turbulent diffusion, C = concentration of suspension, z = depth.

Thus, the sedimentation-diffusion equilibrium can be expressed as follows:

$$UC = -D\frac{dC}{dZ} \tag{3}$$

By integrating equation (3), using separation of variables, we will obtain the exponential (logarithmic) law of vertical distribution of suspension. If suspension concentration in close proximity to the bottom C_0 is considered as a boundary condition, the following expression is available as a result of integration:

$$\ln\left(\frac{C_z}{C_0}\right) = -\alpha z \tag{4}$$

where $\alpha = \dfrac{U}{D}$ and C_z = concentration of suspended matter at a distance z from the bottom.

To calculate α, and further U, we will use expression (4).

Suspension concentrations, found by Stryuk (V.L. Stryuk, personal communication) in the course of expeditions carried out in the central part of Gotland Deep by the Atlantic Branch of the Russian Academy of Science during the last decade, were used as original data for computations. A total of 170 concentration values, obtained by means of nuclear filters (ultra-filtration method), having pore diameter of 0.45 µm have been used to build up an averaged vertical profile of suspension concentration.

Results

Long term sedimentation rates

Examining the high-resolution seismic record of the mud distribution, a clear asymmetry in the thickness of the most recent basinal sediment is discerned (Figure 2). The asymmetry must be a reflection of a deep circulation system in the Gotland Basin, which induces sediment winnowing and accumulation and which results in spatially heterogeneous sediment records at the deep basin floor. Based on the reflector geometry, the asymmetric deposition of sediment in the deep basin began immediately after brackish conditions of the current Littorina stage of Baltic Sea development were established some 7650 years ago. From the reflector geometry, sedimentation rates generally vary from 0.2 mm a^{-1} in the north-western part of the deep basin over 0.4 mm a^{-1} in the central part of the basin to 0.8 mm a^{-1} in the south-eastern part.
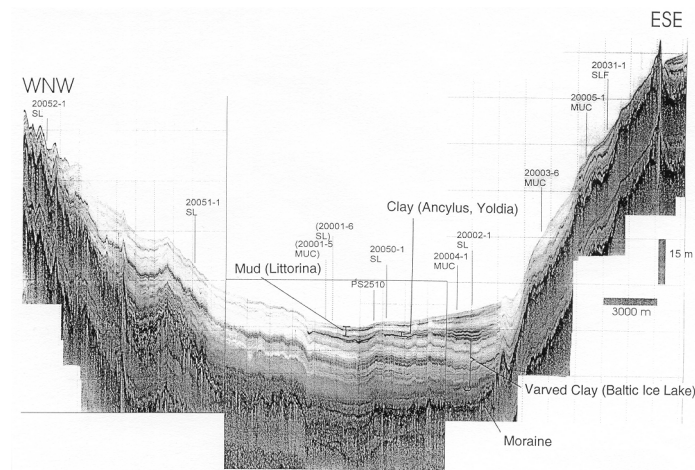
Figure 2 NW-SE seismic profile across the Gotland Basin. The stratigraphy is based on core correlations. For location of the line see Figure 1.

Recent sedimentation rates from concentrations of suspended matter

The vertical concentration profile of suspended matter, in the region with depths ranging from 120 to 220 m, is not exponential (Figure 3). This suggests an occurrence of sedimentation-diffusion inbalance due to action of additional sources of suspension. At these depths two such sources occur:

1. crystallisation of Fe, Mn and other elements from solution at the geochemical barrier $H_2S–O_2$

2. resuspension of bottom deposits by bottom currents, especially over slopes of the basin, where decreased stability of sediments occurs

As the water column in Gotland Deep is strongly stratified, the gravity sedimentation of suspension material, supplied from the above mentioned sources, is hindered, resulting in accumulation of suspension at a depth of the sources. At a depth below the level of 220 m the Gotland Deep bottom flattens, reducing conditions predominate in the water column, while the above mentioned sources are inessential. Thus, the assumption of sedimentation-diffusion balance may generally be valid in the deepest layer of Gotland Deep (220–240 m). Therefore, the computations were carried out using data from this layer only.

Using $C_0 = 1.1\,\text{mg}\,\text{l}^{-1}$, $z = 20\,\text{m}$, $C_z = 0.60\,\text{mg}\,\text{l}^{-1}$, according to means of observations (Figure 3), the following expression is derived:

$$\alpha = 0.03\ (\text{m}^{-1}) = 3 \cdot 10^{-4}\ (\text{cm}^{-1})$$

Taking the coefficient of vertical turbulent diffusion D to be equal to $1\,\text{cm}^2\,\text{s}^{-1}$ (Dyer, 1986), the settling velocity will be as follows:

$$U = \alpha D = 3 \cdot 10^{-4}\ (\text{cm}\,\text{s}^{-1})$$

Since the vertical flow of suspension P_z is determined as $P_z = UC_z$, then for the bottom level (where $C_z = C_0$) it will amount to:

$$P_0 = (3 \cdot 10^{-4}) \cdot (1.1 \cdot 10^{-3}) = 3.3 \cdot 10^{-7}\ (\text{mg}\,\text{cm}^2\,\text{s}^{-1}) = 106\ (\text{g}\,\text{m}^{-2}\text{year}^{-1})$$

This value of P_0 characterises the minimal possible rate of sedimentation, because besides gravitational sedimentation there are other mechanisms of sediment accumulation (saltation, sliding over slope, redeposition, authigenous sedimentation).
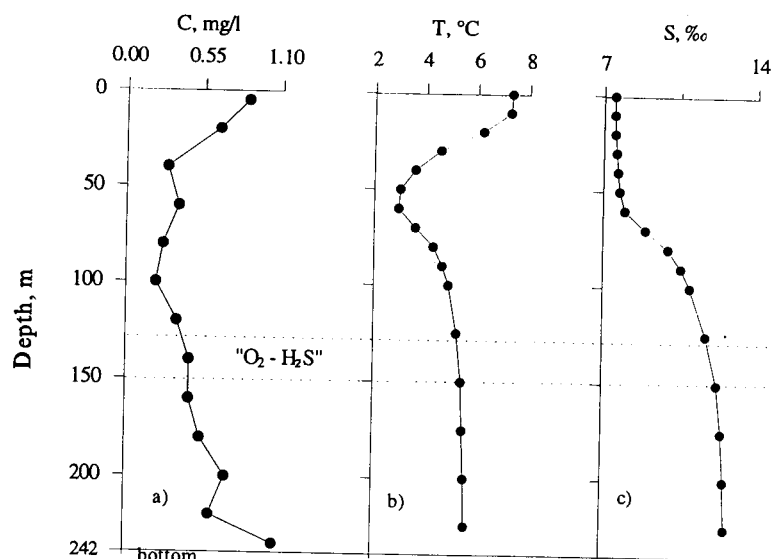
Figure 3 Vertical profile of suspension concentration in the Gotland Deep. Dotted lines show the geochemical "O_2–H_2S" barrier.

Recent sedimentation rates from dating

The accumulation rates calculated from ^{210}Pb profiles and determination of physical properties are highly variable and reflect very different sedimentation rates (Table 1). However, we are confident that they represent true trends and rates, because the ^{137}Cs profiles resulting from the Chernobyl accident corroborate the ^{210}Pb datings in all cores and none had irregular features that indicate hiatuses. In the basinal stations, the accumulation rates range from 119 (upper portion of core 20004) to $322\,gm^{-2}a^{-1}$ at the site of core 20001. The calculated sedimentation rates are between 2.1 and $2.5\,mma^{-1}$, respectively. The slope station 20000 displays a disturbed upper layer of 8 cm thickness; fitting the ^{210}Pb profile below this interval suggests an accumulation rate of $340\,gm^{-2}a^{-1}$ and an average sedimentation rate of $2.5\,mma^{-1}$. The station 20008 in a small intraslope basin (68 m water depth) has uncharacteristically high sedimentation and accumulation rates: The data suggest that the sediment accumulates at a rate of $6100\,gm^{-2}a^{-1}$ and has an average sedimentation rate of $30\,mma^{-1}$. Using wave prediction formula, storm with winds from the west in the area of this intraslope basin may reach the following characteristics: height ~5 m, length ~100 m and period ~8 s. Near-bottom maximum orbital velocities for such waves in areas with a depth of 40–50 m can reach 20–$30\,cms^{-1}$. Such orbital velocities exceed the threshold velocity for grains with sizes of up to $60\,\mu m$ (Christiansen & Emelyanov, 1995). Therefore, the very high sedimentation rate in the basin most probably reflects intensive shallow water erosion along the rim of the basin.

Core	Position	Average sediment rate (mma^{-1})	Average sediment accumul. rate (g m^{-2}a^{-1})	Remarks
20001	57° 18.33 N 20° 03.00 E	2.1 ± 0.1	322 ± 79	
20004	57° 18.28 N 20° 13.66 E	2.5 ± 0.1	279 ± 37	
20007	57° 23.32 N 20° 15.15 E	4.3 ± 0.6	238 ± 19	Disturbed surface
20000	57° 15.17 N 20° 33.64 E	2.5 ± 0.5	340 ± 30	Disturbed surface
20038		3.5 ± 0.3	399 ± 32	Disturbed surface
20008	57° 27.60 N 21° 09.60 E	30 ± 6	6099 ± 1860	Doubtful core

Table 1 Dating results for the cores

Stations on the steep eastern slope of Gotland Basin have disturbances in the depth profiles of both ^{210}Pb and ^{137}Cs activity in the upper centimetres of the sediment (Figure 4). There is no decrease in ^{210}Pb activity, which suggests

sediment mixing and the ^{137}Cs activity increases towards the top which indicate that the mixed layer is settled from suspension. Further, grainsize analysis from station 798 (Figure 5) corroborate such observations in that a general fining-upward sequence in the upper layer is twice abruptly interrupted by sediment coarsening. These observations together indicate that the sediment disturbance is not due to bioturbation. The Chernobyl peak in ^{137}Cs is displaced with depth indicating that the disturbance has taken place in recent years.
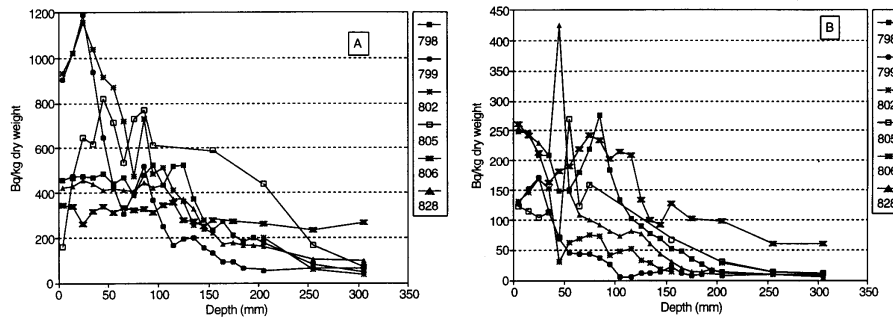
Figure 4 Radiometric profiles of sediment cores from the Gotland Basin. For location of sampling position see Figure 1.
A) Depth profiles of supported ^{210}Pb activities.
B) Depth profiles of ^{137}Cs activities.
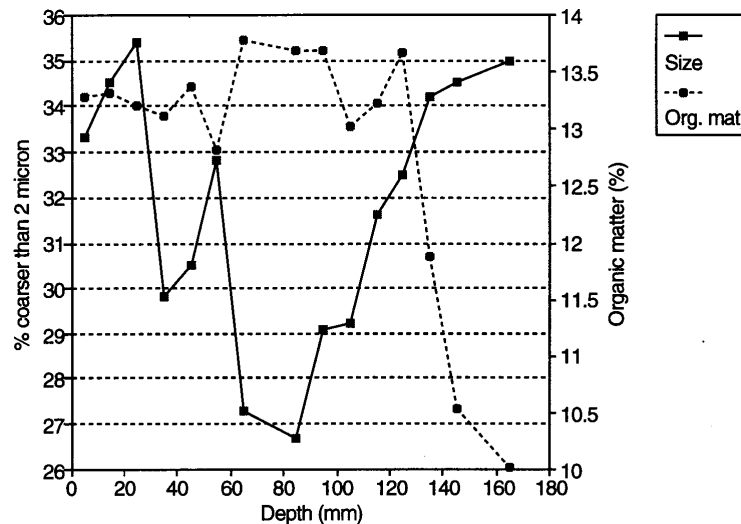
Figure 5 Down-core variations in grain-size and organic matter content of the slope core 20000.

Discussion

The areal asymmetrical distribution of long term sedimentation rates with high rates in the southeastern basinal part may be an indication of winnowing of the steep southeastern slope and lateral transport, as well as for possible contourite deposition in a depth interval characterised by anticlockwise currents around the rim of the Gotland Basin and at deeper levels. Observational data supporting this view of a dynamic deep-basin sedimentary environment have been collected during GOBEX (Mittelstaedt, 1994). Even though detailed measurements of near-bottom currents are scant in the Gotland Basin, initial observations suggest that current speeds at the sediment/water interface are of the order of $1-3 \, \text{cm s}^{-1}$ over periods of days, reaching maxima of up to $20 \, \text{cm s}^{-1}$ during events of hourly duration (E. Hagen, pers. comm. 1995). The image of a stagnant, quiescent and anoxic sedimentary environment in the Gotland Basin thus may be erroneous.

Such a conclusion is corroborated by additional evidence. Estimated sediment accumulation rates from the averaged suspended matter concentration profile were generally 3 times smaller in the central basin than rates from core datings, indicating more sources of sedimentation than primary sedimentation. There is a strong variation in the vertical concentration of suspended matter on Figure 3. However, the estimated sediment accumulation rates $(106 \, \text{g m}^{-2} \text{y}^{-1})$ are in

reasonable agreement with observations from sediment trap studies. Saarso (1995) observed that fluxes in traps ranged from $33-107 \mathrm{g m^{-2} y^{-1}}$. One additional sediment source may be sliding of sediment on slopes. This is evidenced by observations that cores taken on the slope to the central basin had disturbances in their radiometric profiles and their downcore grain-size distributions showed signs of redeposition. Further, geochemical data from the present cores show differences between the deep basin and the slope in enrichment patterns of organic matter (and associated trace elements) and of sulphides (and associated trace elements), suggesting lateral transport (Emeis *et al.*, 1996).

Recent net sedimentation rates from the present study seem to be 1.5–2 times higher than observed from ^{210}Pb datings 20–25 years ago (Ignatius *et al.*, 1971; Niemestö & Voipio, 1974). The present study thereby corroborates the findings by Jonsson *et al.* (1990) estimated from varve counting in recent laminated sediments. A number of factors may explain this apparent increase in sedimentation rate:

1. It may be accidental in that only a few number of datings are involved and the regional variability seems to be high. In a much smaller area in the southwestern Kattegat Christiansen *et al.* (1996a) observed a high variability in that sedimentation rates on accumulation bottoms ranged from 469 to 4290 $\mathrm{g m^{-2} a^{-1}}$.

2. An increase in organic matter is observed in the upper parts of the present cores (Figure 5, see also Neuman *et al.*, 1996). Such observations corroborate the estimations made by Jonsson & Carman (1994) that in general, a more than 1.7-fold increase in sediment organic matter content has taken place in the Baltic proper between the late 1920s and the late 1980s. This may be explained by higher primary production in connection with the present eutrophication.

3. A 16 year long period of bottom water anoxia in recent years (Neumann *et al.*, 1997) may have contributed to better preservation of organic matter and authigenetic mineral production.

4. Erosion of shallow water sediments seems to be the major source of sedimentation in the Gotland Basin. In their nutrient budget for the Baltic proper Jonsson *et al.* (1990) found that as much as 85% of the organic matter and nutrients sequestered in the laminated sediments in the Baltic deeps may have originated from shallow water erosion. Such observations have been corroborated by resuspension studies (Christiansen & Emelyanov, 1995). Shallow water erosion may have been enhanced in recent years. This is apparently the case in the southern Kattegat where a shift in the wind regime has caused increased coastal and shallow water erosion (Christiansen *et al.* 1993) and induced higher sedimentation rates since the beginning of the 1970s (Christiansen *et al.* 1996b). Also, the number of storm surges on the German Baltic coast has increased in the last decades (Baerens & Hupfer, 1995).

Acknowledgements

References

Baerens, C. & Hupfer, P., 1995: On the frequency of storm surges at the German Baltic coast. Proceedings of the 19th Conference of the Baltic Oceanographers, Sopot. Vol. 1, 311–316.

Christiansen, C., Christoffersen, H. & Binderup, M., 1993: Coastal and near shore erosion at Vejrø, Denmark: Combined effects of a changing wind climate and near shore dredging. In: Sterr, J., Hofstede, H.-P. & Plag, P. (eds.): Proceedings of the International Coastal Congress, ICC. Verlag Peter Lang, Frankfurt. 566–575.

Christiansen, C. & Emelyanov, E., 1995: Nutrients and organic matter in southern Kattegat western Baltic Sea sediments: Effects of resuspension. Danish Journal of Geography. 95, 19–27.

Christiansen, C., Gertz, F., Laima, M. J. C., Lund-Hansen, L. C., Vang, T. & Jürgensen, C., 1997: Nutrient dynamics in the southwestern Kattegat, Scandinavia: Sedimentation and resuspension effects. Environment. Geol. 29, 66–77.

Christiansen, C., Kunzendorf, H., Laima, M. J. C., Lund-Hansen, L. C. & Pedersen, A. M., 1996: Recent changes in environmental conditions in the southern Kattegat, Scandinavia. Norges geologiske undersøkelse. Bulletin. 430, 137–144.

Dyer, K. R., 1986. Coastal Estuarine Sediment Dynamics. Chichester, Wiley. 342p.

Emeis, K.-C., Neumann, T., Endler, R., Struck, U., Kunzendorf, H. & Christiansen, C., 1996 Geochemical records of sediments in the Gotland Basin—products of sediment dynamics in a not-so-stagnant anoxic basin? Applied Geochemistry (submitted)

Gelambauskaite, Z. & Grigelis, A., 1995: Contribution to geomorphology of the Gotland depression. GOBEX-Newsletter. 2/5, 4–11.

Ignatius, H., 1958: On the rate of sedimentation in the Baltic Sea. Bulletin de la Commission géologique de Finlande. 180, 135–145.

Ignatius, H., Axberg, S., Niemestö, L. & Winterhalter, B., 1981: Quaternary geology. In: Voipio, A. (Ed.): The Baltic Sea. p. 54–104.

Ignatius, H., Niemestö, L. & Voipio, A., 1971: Variations of redox conditions in the recent sediments of the Gotland Deep. Geologi. 3, 43–46.

Jonsson, P., Carman, R. & Wulff, F., 1990: Laminated sediments in the Baltic—A tool for evaluating nutrient mass balances. Ambio. 19, 152–158.

Mikkelstaedt, B., 1994: Preliminary results of a hydrographic survey in November/December 1993 with R/V Gauss: The subsurface circulation in the Gotland Deep. GOBEX Newsletter. 2/94, 3–5.

Neumann, T., Christiansen, C., Clasen, S., Emeis, K.-C. & Kunzerdorf, H., 1997: Geochemical records of salt-water inflow into the deep basins of the Baltic Sea. Continental Shelf Research. 17, 95–115.

Niemestö, L. & Voipio, A., 1974: Studies on the recent sediments in the Gotland Deep. Havforskningsinstitutets Skrift, Finland. 238, 17–32.

Saarso, M., 1995: Vertical variability of particulate flux in the Baltic Sea. In: Floderus, S., Heiskanen, A.-S., Olesen, M and Wassmann, P. (eds): Sediment trap studies in the Nordic countries. 3. Symposium Proceedings. NurmiPrint, Nurmijarvi. p. 168–183.

Suess, E., 1978: Distribution between natural and anthropogenetic material in sediments. In: Goldberg, E. D. (Ed.) Biogeochemistry of Estuarine Sediments. UNESCO, Paris. p. 224–237.

Acoustic images of Gotland Basin sediments

R. Endler, K.-C. Emeis and T. Förster

Abstract

High resolution acoustic profiling using chirp sonar technology was performed in the Gotland Basin as part of the Gotland Basin Experiment (GOBEX). Digital processing techniques of acoustic data were used to epitomise the acoustic images for general views of the entire postglacial sediment sequence as well as for detailed investigations of the acoustic character of selected layers and structures. Based on the acoustic results, core sampling locations were selected for optimal recovery of sediments representing the depositional environment of the central Baltic Sea.

The acoustic data clearly reflect the character and development of the sedimentation processes (depositional, nondepositional, erosional) in the several regions of the Gotland Basin. Up to nine major acoustic units can be separated in the profiles. They encompass the entire late glacial and postglacial series starting from the glacial till and ending with the recent very soft mud. It is possible to trace them over the entire central basin. Baltic Ice Lake sequences show rather limited lateral variations in thickness and mainly follow the relief of the underlying till. In contrast, the thickness of the Litorina sequence increases from WNW to ESE and has a maximum thickness at the base of the sharp ESE basin slope offshore Latvia. This implies a change in the hydrographic/depositional regime since the end of the Baltic Ice Lake stage.

The first results presented demonstrate the high potential of the acoustic method which may contribute to the better understanding of the structure, of the recent depositional processes, and of the Holocene development of the Gotland basin. Further work in the frame of the GOBEX activity will concentrate on the detailed recognition and geological interpretation of the different reflectors and structural features based on multi-sensor core logging and acoustic modelling.

The Gotland Basin Experiment (GOBEX)

The Gotland Basin (Figure 1) is the largest basin of the Baltic Sea. Because of its size, its location between northern and southern Baltic Sea and its properties it was chosen as a region for integrated studies of the recent oceanographic, biological, chemical and geological environment as well as of the geological history. The water column (with a thickness of about 240 m in the central part) is usually well stratified causing anoxic conditions at the sea bottom. Because of this the sedimentary history is well preserved in the laminated sequences (no bioturbation). The present study focuses on the physical (mainly acoustic) properties of the sediments in order to reconstruct the postglacial history of the basin.
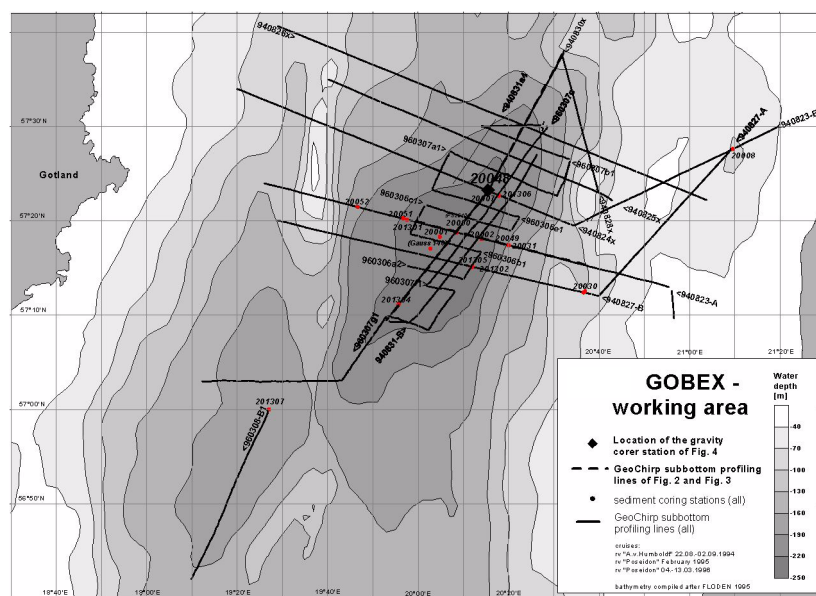

Figure 1 GOBEX working area

Material and Methods

In the frame of the GOBEX activity one expedition with R/V "A. v. Humboldt" (1994) and two cruises with R/V "Poseidon" (1995, 1996) were performed to collect acoustic profiling data and sediment samples (Figure 1). A GeoChirp subbottom profiling system (GeoAcoustics) consisting of the tow fish (transmitter, receiver), the chirp-processor, a Sonar Enhancement System (SES) and a thermo-recorder (Wideline 200/138, Ultra Electronics) were used for acoustic surveys. The bandwidth of the transmitted acoustic pulses was 2–8 kHz with a duration of 32 ms. Reflected acoustic signals were received by a ministreamer (which was attached to the end of the tow fish), amplified and sent to the chirp-processor for matched filtering (signal compression). Further onboard processing, on-line printing and digital storing (SEGY format, 8 mm ExaByte) were performed with the Sonar Enhancement System. Navigation data were collected from a GPS receiver (Sercel NR51, WGS84). During profiling the tow fish was towed at a depth of about 20 m (due to limited cable length) and with a speed of about 5 knots. Two pulses per second were transmitted giving a firing distance of about 1.3 m (at 5 knots). Depending on the sediment type a penetration down to 40 m was achieved with a vertical resolution of about 0.3–0.5 m. Later on, postprocessing using an extended Seismic Unix-package (Cohen & Stockwell, 1994) was performed on an IBM R6000 workstation. The general structure of the postglacial sediments is depicted by two GeoChirp profiles in Figure 2 and Figure 3.
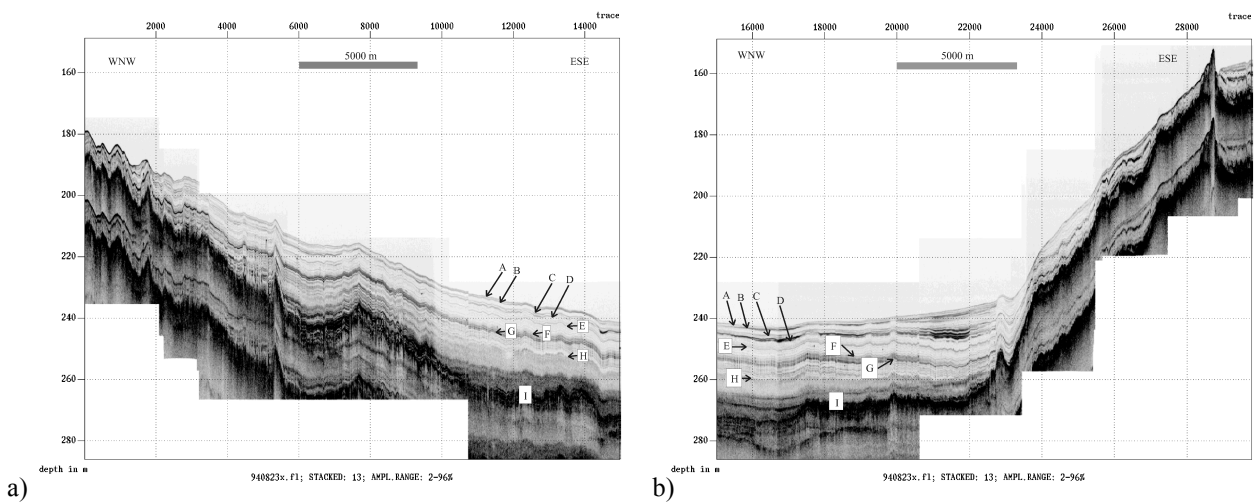
Figure 2 Acoustic image of Gotland Basin sediments—transversal section
a) Geochirp line 940823 western part
b) GeoChirp line 940823 eastern part
Major acoustic reflectors are named by letters (sound velocity for time to depth conversion: 1450 ms^{-1})

Figure 3 Acoustic image of Gotland Basin sediments—longitudinal section
a) GeoChirp line 940830 northern part
b) GeoChirp line 940830 southern part
Major acoustic reflectors are named by letters (sound velocity for time to depth conversion 1450 ms^{-1})

Based on the acoustic records a variety of sediment sampling locations were selected. Gravity corers (6m, 12m) with plastic liners we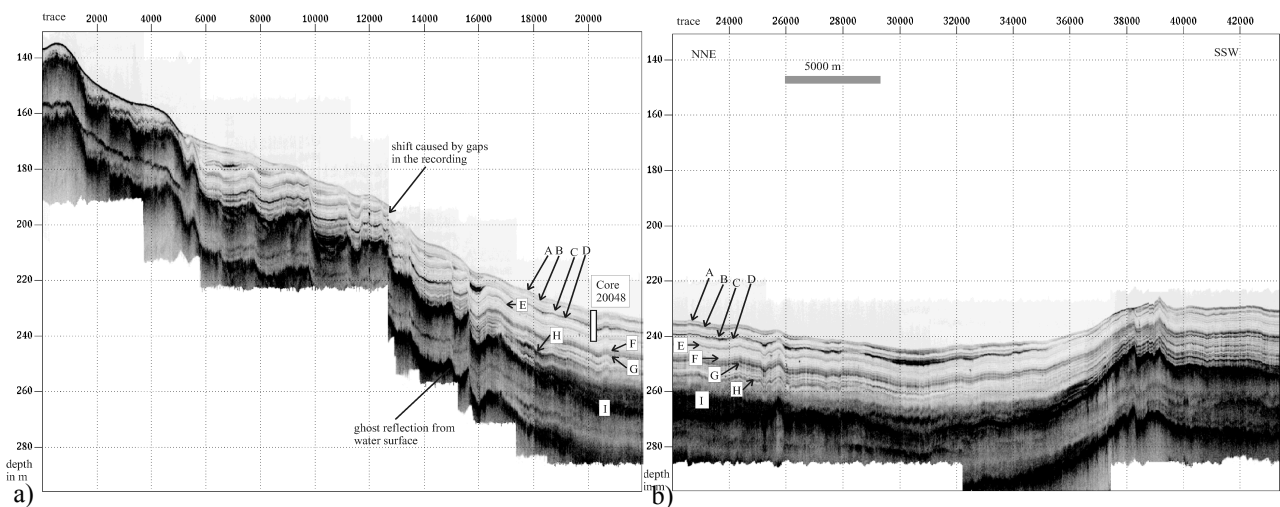re used for sampling the postglacial sediment layers. After recovery the liners were cut into 1m sections, capped and stored (4°C). The physical properties of the split sediment cores were measured with a Multi Sensor Core Logger (MSCL, GEOTEK): optical scan of sediment surface along the core (by gray scale line scanner), wet bulk density (by gamma ray attenuation), sound velocity (by 500kHz pulse transmission) and magnetic susceptibility (Bartington loop and point sensors). Based on the logging data subsamples were taken for further analyses. First results of the measurements on core 20048 are presented in Figure 4.
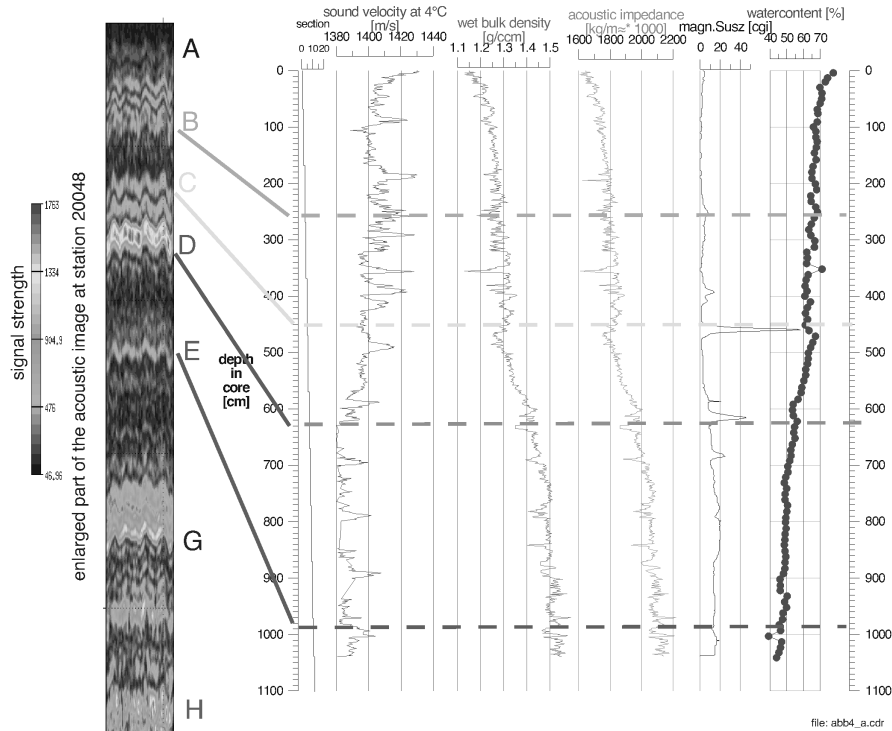
Figure 4 Physical properties of Gotland Basin sediments—results of MSCL logging core 20048 SL

Results and Discussion

In general the central Gotland Basin shows an asymmetric structure. Along the longitudinal basin axis (Figure 3) the water depth slowly increases from about 140m in the north to about 240m in the central part. Further to the south the central basin is bordered by a small elevation with water depth of 230m. The same asymmetric morphology is displayed in the cross section of Figure 2.

The acoustic images of Figure 2 and Figure 3 reflect the structure of the postglacial basin fill which is well penetrated by the acoustic signals. In general the sediments are well layered. Based on the acoustic characteristics a variety of major reflectors were chosen, marked by letters and traced by lines. Because a definitive link from all the acoustic reflectors to the several sedimentological sequences is not yet established, the choice of the reflector names is not based on sedimentological units (e.g. Andren & Sohlenius, 1995).

The lower light line I marks the very rough surface of the glacial deposits (sand, gravel, till). The next sequence up to reflector D contains the varved clays of the Baltic Ice Lake. The thickness of this sequence is approximately 20m and is nearly constant over the entire central basin. During that time sedimentation was rapid without lateral transport (no near bottom currents). From the acoustic image, the varved clays of the Baltic Ice Lake can be subdivided into several units separated by the reflectors H, G and E. This set of reflectors in the varved clays suggests that the sedimentation during the Baltic Ice Lake was not only influenced by seasonal variations (varves) but also by depositional, possibly climatic changes of longer periods. The sediments below reflector H show an acoustically turbulent image in the very central basin whereas a band of reflections appear in the more distal regions. A very prominent reflector is G (from the signal strength) which is the lower boundary of a strong reflection sequence. This reflector can be traced over the entire basin. The reflection band is bounded at the upper end by the reflector F (not indicated in the figures). A rather transparent region follows up to reflector E indicating continuous sedimentation during this period. In the interval between reflectors

G and E, black and irregularly distributed dots appear over the entire basin. It is unclear whether these spots are caused by diagenetic processes or local anomalies during sedimentation.

In Figure 4 an enlarged part of the acoustic record at station 20048 is compared with the core log depth profiles. The subbottom depth of the selected reflectors is calculated with a sound velocity of $1400\,\mathrm{ms}^{-1}$ and marked in the logging profiles. The acoustic reflectors correspond to gradients in the acoustic impedance profile. Most prominent changes in the physical properties occur in the subbottom depth interval between 6 m (reflector D) and 4.5 m (reflector C) indicating the transition from typical Baltic Ice Lake sedimentation (varved clays) to the younger Littorina environment (transition clays of Ancylus and Yoldia stages according to Winterhalter, 1992). The reflector D also marks a change in the sedimentation regime. As a result of strong lateral sediment transport (start of the near bottom circulation) the thickness of the sediments overlying reflector D continuously increases from west towards the steep eastern slope of the basin (Figure 2). A maximum thickness of about 12 m is reached just at the lower edge of the eastern slope. The uppermost band of reflections bounded by reflectors B and A (surface of the recent mud) shows the transition from well laminated gyttja clays of the Litorina stage to the recent very soft, black sulphitic mud. Because of the high water content the uppermost mud is easily transported by lateral currents.

Conclusions

It was demonstrated that the physical properties of the sediment column clearly reflect the variations in the sedimentary environment during the postglacial history of the Baltic Sea. They give important additional information for paleoenvironmental reconstructions which can not be obtained by other methods.

References

Andren, T. & Sohlenius, G. (1995). Late Quaternary development of the north western Baltic Proper—results from the clay-varve investigation. Quaternary International, Vol. 27, pp. 5–10

Cohen, J. K. & Stockwell, J. (1994). Seismic Unix, V. 22 ff. Center for Wave Phenomena, Colorado School of Mines Golden, CO 80401; john@dix.mines.edu

Winterhalter, B. (1992). Late-Quaternary Stratigraphy of Baltic Sea Basins—a Review. Bull. Geol. Soc. Finland 64, Part 2, 189–194

Water exchange, nutrients, hydrography, and database of the Gulf of Riga

Pekka Alenius

Abstract

The Gulf of Riga is a semi-enclosed basin connected by two straits to the Baltic Sea. One of the straits, the Irbe Strait, is broad and the other, Suur Strait, is small. The Gulf of Riga receives large fresh water inputs from rivers. There is continuous water exchange between the Gulf and the Baltic Sea through the straits. The processes governing the water exchange and the water and material balances have been subjects of the physical oceanography sub-project of a joint Nordic Baltic research programme, the Gulf of Riga project, within the Nordic Environmental Programme 1993–1997 financed by the Nordic Council of Ministers. The research programme included a three year field experiment period in 1993–1995 and continues with data analysis and a modelling phase in 1996–1997. This paper gives an introduction to the sub-projects of the physical programme in the Gulf of Riga Project. Extensive measurements in both straits have given qualitative and quantitative pictures of the exchange processes. The observations show that both of the straits are important in the overall water exchange. The processes in the large Irbe Strait are more complicated than in the small Suur Strait. The Suur Strait, however, also contributes significantly into the water exchange because the unidirectional simple exchange can have significant volume fluxes. Both methodologies and databases for reliably estimating the total amounts of nutrients in the Gulf have been further developed within the project. Numerical modelling with several types of models are being continued. The models include both 1D models and 3D models up to a 3D ecosystem model. A common Gulf of Riga database has been established during the project. The project is considered to be a continuation to the valuable research carried out over the last decades by Estonian and Latvian oceanographers in the Gulf of Riga.

Introduction

In 1991 the Nordic Council of Ministers declared a Nordic Environmental Research Programme 1993–1997. The programme has three main fields of interest:

1. Research on climate changes
2. Co-operation on Environmental Research in the Baltic Sea region: The Gulf of Riga Project
3. Research on the socio-economic and political requirements related to the implementation of environmental policies

The projects began by inviting letters of intent of relevant research in these fields. In late 1992, after numerous letters of intent, the expert committee of the Gulf of Riga Project decided to support 18 co-operation projects. They also decided to collect the projects under five coordinated sub-projects:

1. "Drainage basin and the load of the Gulf of Riga"
2. "Pelagic eutrophication"
3. "Sediment and benthos"
4. "Water exchange, nutrients, hydrography and data base"
5. "Toxic substances"

In 1995 a sixth sub-project was established:

6. "Production and transformation of nutrients in the littoral zone"

This paper briefly describes sub-project 4 of the Gulf of Riga Project.

Structure of the water exchange project

The "Water exchange, nutrients, hydrography and data base" project includes three separately funded parts:

- Hydrographic investigations I
- Hydrographic investigations II

- Database

The two first mentioned parts focus on process studies and modelling on hydrography and nutrients. The third part consists of the establishment of a common database for the Gulf of Riga data and its updating and maintenance. The aim of these studies is to estimate the water and material balances of the Gulf of Riga and to model these processes in order to get tools for environmental management. The division to two hydrographic groups has been based in the slightly different focuses. The "Hydrographic investigations I" has focused most of its field experiments into the Suur Strait whereas the "Hydrographic investigations II" has focused mainly on the Irbe Strait. Both of these parts have operated in the open Gulf of Riga and have had intensive modelling efforts. In the modelling work the focus of "Hydrographic investigations I" is more inclined towards 3D ecosystem modelling and the "Hydrographic investigations II" is more focused on physical processes in its 3D modelling.

The Gulf of Riga project is a joint Nordic–Baltic project. The number of participating institutions and countries is different in each sub-project. Our project had participating institutions from Finland, Sweden, Estonia and Latvia. The participating institution from Finland were the Finnish Institute of Marine Research, from Sweden the Swedish Meteorological and Hydrological Institute, University of Gothenburg and University of Stockholm, from Estonia the Estonian Marine Institute, Estonian Meteorological and Hydrological Institute and Tallinn Technical University and from Latvia the Latvian Hydrometeorological Agency, Latvian Fisheries Research Institute and Latvia University (laboratory for mathematical modelling of environmental and technological processes and the Institute of Aquatic Ecology). Over 20 scientists have been active.

The project work is divided into two phases. The first phase was the collection of old data into a database and a field experiment phase in 1993–1995. In 1993 the database was established and preliminary field experiments were organised. The following two years, 1994 and 1995, were so called full scale field experiment years. The second phase 1996–1997 is for data analysis, intensified modelling and synthesis of the results.

The paper gives only an idea of the project. For the results of the project the reader is encouraged to look at the references. The results of the project are described in separate papers in Baltic Marine Science Conference 1996 by the participating scientists. By autumn 1996 five special joint volumes have been published (Toompuu and Elken, 1995, Lips and Lilover, 1995, Kouts and Håkansson, 1995, Suursaar and Astok, 1996 and Tamsalu, 1996). Results are also found in papers in journals and conferences.

The Gulf of Riga as a physical environment

The Gulf of Riga is a semi-enclosed sea area in the Baltic Sea. It is connected to the rest of the Baltic Sea by two straits that are considerably different from each other in character. The area of the Gulf is 16330km^2 and its volume is about 424km^3 (Berzinsh, 1995). The annual fresh water inflow is about 30km^3 mainly entering the Gulf in the south, from the river Daugava. The two straits are almost opposite in character. The Irbe Strait in the west is much wider and deeper than the narrow and shallow Suur Strait in the north. The water exchange characteristics are therefore very different. In the Suur Strait (or Muhu sound or Virtsu sound as it is also called) the water flows practically uni-directionally at times and has rather high velocities up to over 1ms^{-1}. In the Irbe Strait, the flow is variable in both horizontal and vertical directions making the estimation of net water exchange more difficult.

The Gulf of Riga is in some sense like a miniature Baltic Sea. The large freshwater input from one end and exchange of water with the more saline basin on the other end characterises the physics of the Gulf. The Baltic Sea proper waters enter the Gulf through the Irbe Strait and flow along the bottom southwards at the western coast of the Gulf. The fresh water input tends to flow northwards along the eastern side of the Gulf. The saline waters seem to form a quite thin layer near the bottom. There is a clear halocline separating this near bottom layer from the mid layers in summer. The vertical convection reaches the bottom in spring and autumn when the water is generally vertically homogeneous except in the river mouths and strait areas.

Investigations in the Suur Strait

The northern strait of the Gulf of Riga has many names: the Suur Strait, the Virtsu Strait or the Muhu Strait. These names are used variably in different contexts. The experiments and scientific analysis of the data from the Suur Strait have been conducted by a group at the Estonian Marine Institute led by V. Astok. Altogether 10 expeditions were carried out in the area. The length of the experiments varied between one and four weeks. Water exchange data has been collected during

all seasons including mid-winter when the Gulf is ice covered. The measurements include a total of 434 days of current measurements, about 2300 nutrient analyses and wind measurements for 16 months (Suursaar *et al.*, 1996a).

The net water exchange through the Virtsu Strait has been estimated to be of the order of $-25 - -30\,\text{km}^3\text{yr}^{-1}$ (Suursaar *et al.*, 1996b). The contribution of the Virtsu Strait to the total water exchange of the Gulf of Riga is estimated to be about 32% (Suursaar *et al.*, 1996b). These figures show the importance of the narrow strait for the whole system. This is an important aspect for numerical modelling, too. The models should describe the water exchange through the Virtsu Strait in order to describe the Gulf of Riga at all. The water exchange has been modelled by an analytical model (Otsmann *et al.*, 1996). According to the model, the wind is the main driving force for the water exchange in the Gulf. This model can be used for providing boundary conditions for 3D ecosystem model, too.

Investigations in the Irbe Strait

The Irbe Strait investigations have been conducted under the leadership of a group at the Estonian Marine Institute led by J. Elken in international co-operation. The Irbe Strait is the large strait connecting the Gulf of Riga to the Baltic Sea proper. It could a priori be expected that the main water exchange between the Gulf and the Baltic Sea goes through the Irbe Strait. The Strait is a wide area where the more saline Baltic Sea waters and less saline Gulf of Riga waters meet and mix. It is a strong salinity front area where surface salinity change is even 1 ppm (Lips *et al.*, 1995). Because the Strait is wide and has a complicated bottom topography, there is room for complicated frontal processes. A large experiment IRBEX-95 was organised in the Strait (Lips and Lilover 1995) within the framework of our project.

The complexity of the water exchange is seen in the shape of the front in the Irbe Strait. The less saline water generally flows out at the northern coast of the Strait and more saline water goes in at the southern coast of the Strait (Lips *et al.*, 1995, Lilover *et al.*, 1995b). Estimates of the water exchange through the straits show that both of the straits are important in water exchange (Lilover *et al.*, 1995a).

Investigations in the open Gulf of Riga

The open part of the Gulf of Riga has been studies by Estonian and Latvian scientists.

Also the Finnish R/V "Aranda" conducted three cruises to the Gulf of Riga as a part of our project. We tried to have a cruise to the Gulf in each month of 1994 and 1995 in order to get data on the seasonal variability of the hydrographic and nutrient fields. This goal was not fully reached, but the amount of cruises was, however, larger than the number of months both in 1994 and 1995. The only season that we missed is the mid winter, January and February, when no cruises were organised. In addition to the cruises to the open parts of the Gulf of Riga, also near bottom current measurements have been conducted in the middle of the Gulf (Kõuts, 1995).

Modelling studies

Numerical modelling studies have been made in both of the hydrographic groups. The spectrum of models includes several models from one dimensional to fully 3D coupled hydrodynamic-ecosystem model.

One-dimensional models have been applied to the processes of the Gulf by Sennikovs and Bethers (1995) and Vôsumaa *et al.* (1995). The use of one-dimensional models for describing certain processes is one branch of numerical modelling in the project. The other branch is three-dimensional modelling. The GFDL (Princeton) circulation model has been applied to describe the hydrographic problems of the Gulf and the frontal area in the Irbe Strait (Raudsepp and Elken, 1995). The nutrient cycles and ecosystem of the Gulf of Riga have been modelled by a coupled 3D hydrodynamic and ecosystem model FinEst (Tamsalu, 1996).

Summary

The Gulf of Riga Project is a joint system-oriented effort to describe a whole sea area as thoroughly as possible in extensive international co-operation. The Gulf of Riga has already been studied for decades (Ojaveer, 1995). A lot of information already exists, but the Gulf of Riga project has considerably increased the amount of data and understanding of the processes in the Gulf. Within our sub-project this is especially true in the case of water exchange through the Straits. The field experiment phase of the Gulf of Riga Project in 1993–1995 can be considered a success. The modelling

efforts have already given very promising results. We now have a sound basis for the second phase, of the project 1996–1997 that aims at modelling and scientific synthesis of the processes of the Gulf of Riga.

References

Berzinsh, V., 1995. Hydrological regime—in Ojaveer, E. (ed.) Ecosystem of the Gulf of Riga between 1920 and 1990, Academia No.5, Estonian Academy Publishers, pp. 7–31.

Berzinsh, V., Bethers, U. and Sennikovs, J., 1994. Gulf of Riga: bathymetric, hydrological and meteorological databases and calculation of the water exchange—Proc. Of the Latvian Academy of Sciences No.7 /8.

Kõuts, T., 1995. Variability of near-bottom current properties in Gulf of Riga—SMHI RO No. 23, 85–106.

Kõuts, T. and Håkansson, B., (eds.), 1995. Observations of water exchange, currents, cO sea levels and nutrients in the Gulf of Riga.—SMHI RO No. 23.; 141 pp.

Lilover, M.-J., Raudsepp, U. and Kõuts, T., 1995a. Velocity fields in the Gulf of Riga—EMI Report Series, No.1, 35–81.

Lilover, M.-J., Vôsumaa, Ü., Liljebladh, B. and Eilola, K., 1995b. Hydrographic measurements by R/V Skagerrak—in Lips and Lilover (eds.) IRBEX-95 Data Report, EMI Report Series No.2., 30–50.

Lips, U., Laanearu, J. and Mägi, L., 1995. Hydrographic measurements by R/V Kiir—in Lips and Lilover (eds.) IRBEX-95 Data Report, EMI Report Series No.2., 12–29.

Lips, U. and Lilover, M.-J., (eds.), 1995. IRBEX-95 Data Report—EMI Report Series, No.2., 112 pp.

Ojaveer, E., (ed.) 1995. Ecosystem of the Gulf of Riga between 1920 and 1990—Academia No.5, Estonian Academy of Sciences., 277 pp.

Otsmann, M., Astok, V., Suursaar, Ü. and Kullas, T., 1996. Water exchange model for the Gulf of Riga—EMI Report series No.3, 81–94.

Sennikovs, J. and Bethers, U., 1995. Modelling of the vertical temperature and salinity structure of the Gulf of Riga—Latvian Journal of Physics and Technical Sciences, No.1, 19–41.

Suursaar, Ü. And Astok, Y., (eds.), 1996. Studies on measuring and modelling the water and nutrient exchange of the Gulf of Riga—EMI Report Series, No.3., 109 pp.

Suursaar, Ü, Astok, V., Kullas, T., Otsmann, M. and Alenius, P., 1996. Thermohaline regime and currents in the Suur Strait in 1993–1995—EMI Report Series, No.3, 7–58.

Suursaar, Ü., Astok, V., Kullas, T. and Otsmann, M., 1996. New estimation of the water and nutrient exchange between the Gulf of Riga and the Baltic Proper—EMI Report series No.3., 95–108.

Tamsalu, R., (ed.), 1996. Coupled 3D hydrodynamic and ecosystem model FinEst—RMI Report Series, No.5., 113 pp.

Toompuu, A. and Elken, J., (eds.), 1995. Hydrographic studies within the Gulf of Riga Project, 1993–1994—EMI Report Series, No.1, 176 pp.

Vosumaa, Ü., Eilola, K. and Stigebrandt, A., 1995. Application of an enhanced one-dimensional model to the Gulf of Riga—EMI Report Series, No.1, 121–141.

BASYS: Baltic Sea System Study

EU project contract: MAS3-CT96-0058
EU programme: MAST—Marine Science and Technology
European Commission—Directorate General 12: Science, Research and Development
Participating countries: Denmark, Germany, Estonia, Finland, Lithuania, Latvia, Netherlands, Norway, Poland, Russia, Sweden, United Kingdom
Number of partner institutes: 50
Duration:1996-08-01—1999-97-30

Objectives and methodology

Recent evaluations have described the lack of capability to predict unequivocally future developments as the most serious gap in environmental research in the coastal oceans. It was identified that this is mainly due to insufficient quantification of fluxes of key elements and the inability to differentiate between the effects of climate variability and human interventions. Albeit the Baltic Sea is one of the best investigated marine areas in the world, this, in general holds also true for this semi-enclosed marginal sea.

Therefore, to improve this situation, two overall objectives were chosen for BASYS:

- to further the understanding of the susceptibility of the Baltic Sea to external forces
- to improve the quantification of past and present fluxes
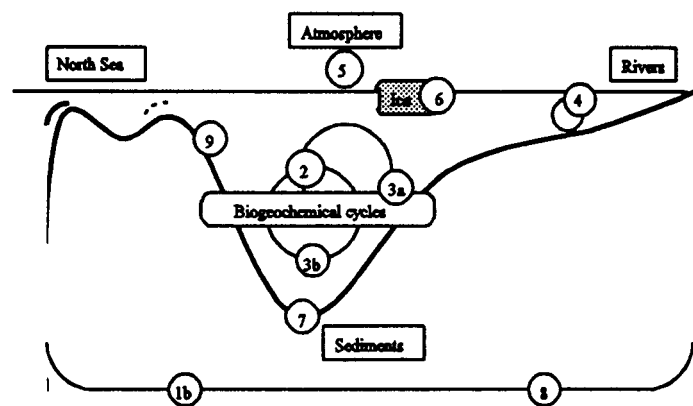
Figure 1 Fluxes through the Baltic Sea. Major external forcing is manifested through the fluxes to the North Sea, atmospheric load, coastal and riverine discharge and position of matter in the sediments. Biogeochemical cycles are involved at each stage of description. The subproject activities are indicated by their numbers.

To achieve a significant progress towards these objectives a system approach was chosen which requires a multitude of scientific activities, handling of large amounts of data and close international cooperation. This is reflected by the large number of participants from EU-member countries and all riparian countries as well as by the according subdivision of BASYS into a Coordination-Data management subproject and 10 scientific subprojects.

The methodologies chosen in BASYS cover the application of a selected range of modem analyses of variables sampled in the field, data processing and model tools which are described in detail in the individual subprojects. Generally, the approach of BASYS to meet the objectives covers time scales from seasons, years, decades and centuries including the postglacial development of the ecosystem to which all subprojects will contribute individually as well as collectively:

- Present day fluxes on biogenic and non-biogenic matter into and within the system are investigated on seasonal and annual scales in the pelagial and the benthal from the coast-line to the deep basins.

- Natural variability in the ecosystem on the decadal scale is analysed by evaluation of historical data on climatology, hydrography, chemistry and biology including anecdotal information which will reach into the pre-industrial period.

- Results will be integrated by model simulation, model experiments and data assimilation including hindcasting of 20 to 100 years.

- Time scales from 5 000 years BP to present are followed by the use of a variety of proxies for ecosystem variables in laminated sediments with high resolution particularly for the last 500 years.
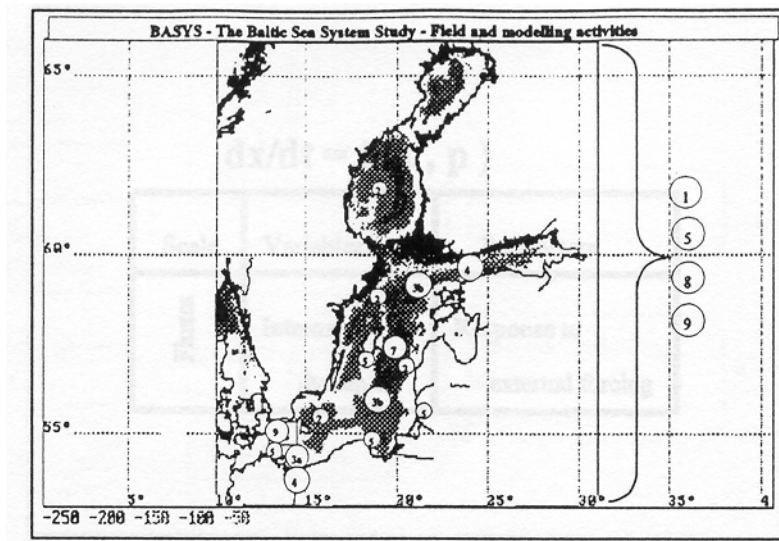
Figure 2 Target regions for BASYS subprojects.

$$dx/dt=j(x,p)$$

Scale	Variables	Parameters
Fluxes	Internal dynamics	Response to external forcing

Figure 3 Schematic graph of the system study approach of BASYS: fluxes dependent on the actual state of the environment (internal biogeochemical fluxes) and on external forcing (past fluxes and response in the ecosystem)

The various subsystems in the Baltic Sea differ considerably in their biogeochemical behaviour. The field work on vertical and lateral fluxes in the pelagial and benthal, therefore, covers the major basins in the Baltic Proper and Bothnian Sea. Lateral fluxes will be studied from the Odra mouth into the Arkona and Bornholm Basin and from the Gulf of Finland into the Gotland Basin. Results from the field work are upscaled by historical data sets and model efforts. The atmospheric load scenario will encompass the entire Baltic Sea embedded in a Europe wide model. The studies on Basin circulation and diapycnal processes will be focused on the Arkona, Bornholm and Gotland basin. The effects of variations in sea ice formation in the northern Baltic will be investigated for the entire Baltic Sea circulation. The sample for the reconstruction of the paleoenvironment will be obtained from the central basins.
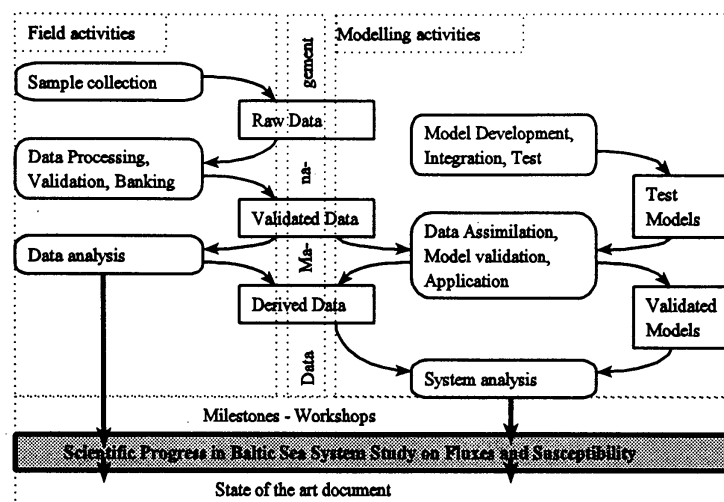
Figure 4 Methodological approaches utilised in BASYS

The combination between process oriented work, assembling of historic data, geological record and modelling will allow for robust testing for the predictive capability of modelling and for the development of generic strategies for ecosystem research in coastal oceans.

Task structure of the project

To meet the objectives we organised the work into analytical and synthetic parts:

Subproject tasks—analytical work

Each subproject has tasks and subtasks according to the specific scientific questions (Table 1).

SP1b:	Processing of historical data
SP2:	Pelagic fluxes
SP3a:	Coastal-basin fluxes
SP3b:	Basin-basin fluxes
SP4:	Nearshore and coastline processes
SP5:	Atmospheric load
SP6:	Baltic sea Ice
SP7:	Paleo-environment
SP8:	System analysis and models
SP9:	Circulation and diapycnal exchange

Table 1 BASYS subprojects

Cross-project research foci—synthetic work

However, to enforce scientific, functional and operational links throughout the BASYS project beyond the commitment to the project's objectives, a conceptual frame is established. This is illustrated by the multiple contributions of the tasks of the respective subprojects to the major research foci of BASYS. The research foci are identified in Table 2.

Focus A:	External and internal biogeochemical fluxes, matter balances and accumulation in the system
Focus B:	Assessment of spatial and temporal scales of significant changes
Focus C:	Differentiation between natural and anthropogenically induced climate variability
Focus D:	Upscaling of model hierarchies, nesting and data assimilation

Table 2 BASYS research foci

The sea aerosol emission from the coastal zone

Maria Chomka and Tomasz Petelski

Abstract

The problem of modelling of the aerosol emission from the coastal zone is presented in this paper. The model has been based on the equation describing wind wave energy dissipation within the coastal zone of the sea.

The model enables calculation of the emission of the aerosol from any coastal zone when the parameters of undulating at deep sea and bathymetry are known.

The calculations of the aerosol emission for the real bottom profile (the coastal station in Lubiatowo, south Baltic Sea) are shown.

The effect of the sea bottom profile on the aerosol emission has been discussed on the grounds of numerous implementation of the model. The logarithmic relation between the total flux of aerosol emission from the coastal zone and the tangent of the slope of the bottom as well as the increased total aerosol emission from the coastal zone from over the smooth-profile sea bottom in comparison to the emission from over the rough bottom have been realised. The aerosol emission flux does not depend on the wave size of the deep water for smaller distances from the shore.

Introduction

The problem of physical parametrisation and obtaining models that describe the flux of the sea aerosol emission under the influence of the dynamics of its interaction with the atmosphere is the subject of profound research. A lot of models describing the aerosol emission from open sea areas have already been developed. However, as far as the most energoactive area—i.e. the coastal zone—is concerned, no models, in which the complex conditions characteristic of only this zone are taken into account, have been known yet. So far the following parameters have been taken to describe aerosol emission flux from the coastal zone: the sea surface covered by whitecaps (Monahan, 1971, Monahan & MacNicall, 1986), Reynolds roughness (Garbalewski, 1983), as well as humidity and latent heat transfer (Ling i Leo, 1976). The above examples concerning transfer of the sea aerosol do not comprise the effect of the sea bottom, which is particularly important for the emission within the coastal zone. The effect of dissipation of wind wave energy on mass emission and the model of aerosol emission within the coastal zone are presented in this paper. The model is based on the equation of wave energy where bathymetry was taken into consideration.

Measurements

The data were collected in the coastal zone of the southern Baltic sea at the Lubiatowo station and onboard r/v "Oceania". The aerosol formation was measured with six-stage impactors located at different heights. According to the survey made using impactors the concentration of the sea salt in the unit of volume at various altitudes on the beach as well as at open sea was calculated.

Interesting results were obtained, among others through the comparison of the mass concentration of sea salt for the open sea and the beach (Figure 1). In this picture the concentration of the aerosol on the beach is considerably higher at open sea, whereas the differences of concentrations are small when the wind is weak and they are significant when the wind reaches the velocity of $7.0\,\mathrm{ms}^{-1}$. It should be stressed that the reverse tendency in concentrations was observed at points 10 and 19—an increase in concentration despite a decrease in wind velocity. This is the result of continuous undulation within the coastal zone. At the sea, aerosol concentrations respond quicker to the change of the wind velocity.
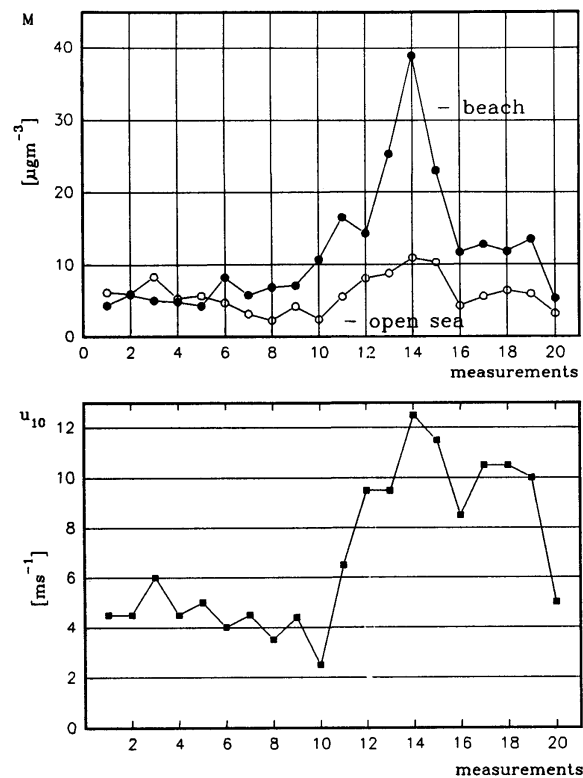
Figure 1 The comparison of the mass concentration of sea salt for the open sea and the beach as a function of wind speed.

The findings presented in Figure 1 were a prerequisite for the statement that the aerosol emission within the coastal zone should be related to the undulation parameters rather than to the changes of wind velocity. The values of aerosol flux were calculated and correlated with various dynamic quantities in order to check whether or not it was worth searching for such a parametrisation. The maximum correlation coefficient of 0.87 was obtained for the energy loss to the 3/4 power. This means the idea that the wind wave energy as the key factor of parametrisation of aerosol emission flux within the coastal zone was right. This concept was applied to create the model.

Assumption of model

The aerosol emission model within the coastal zone was based on the following assumptions:

- coordinate system:
  - x: horizontal axis perpendicular to the shoreline
  - y: horizontal axis parallel to the shoreline
  - z: vertical axis (upwards)
- stationariness
- horizontal homogeneity along the shoreline
- breaking waves is the only mechanism of the aerosol emission
- the number of bursting air bubbles is proportional to the size of the water thrown by the wave
- the volume of water thrown by the wave is proportional to the change of the wave height to the third power

Model

Having taken into consideration the above assumptions and according to analysis carried out by Thorton and Guzy (1982, 1983) we obtain the following model equations:

The sea aerosol emission from the coastal zone

$$F_E = A_P(\langle dE \rangle)^{\frac{3}{4}}$$

$$\frac{\partial}{\partial x}EC_{gx} = \langle dE \rangle$$

$$C_{gx} = \frac{C}{2}\left(1 + \frac{2kh}{\sinh 2kh}\right)\cos\theta \tag{1}$$

$$\langle dE \rangle = \frac{3\sqrt{\pi}}{16}\rho_w \cdot g \cdot B^3 \cdot f\frac{H^5_{rms}}{\gamma_f \cdot h^3}\left[1 - \frac{1}{\left[1 + \left(\frac{H_{rms}}{\gamma_f \cdot h}\right)^2\right]^{\frac{5}{2}}}\right]$$

where:

C_{gx} is the group wave velocity component,

E is the wave energy,

H_{rms} is the wave height quadratic mean,

C is the phase velocity of the wave,

θ is the angle between the wave radius and the line perpendicular to the shoreline,

k is the index of wave refraction,

f is the undulation frequency,

γ_f is the parameter representing the slope of the sea bottom i the value of the wave curvature.

Constants in the model

Parameters B and γ_f regarding wave breaking and the wave slope were adopted from the Szmytkiewicz and Skaja (1993) model for the experiment conditions, that is B=0.88 and γ_f=0.41. In case there is not enough experimental data concerning undulation, it is possible, according to the Thornton model, to assume that B=1.54, γ_f=0.42. In this model it is crucial to determine the parameter A_p connecting aerosol emission and wave energy dissipation. Average values of emission flux which was calculated from balance of aerosol emission flux over coastal zone (Petelski and Chomka, 1996) and dissipation of undulating energy for all the coastal zone were used to calculate the parameter A_p. The average wave energy related to the sea area unit was calculated assuming that the energy is lost evenly along all the breaking zone:

$$\langle dE \rangle = \frac{E_p}{D_p} \tag{2}$$

where:

E_p is the total undulating energy loss within the breaker zone,

D_p is the width of the breaker zone.

The values of E_p and D_p parameters were obtained using the Thornton model, where the sum of all values of E_p was taken as E_p and the maximum distance where dissipation of wave energy was more than 0.001 (that is dE>0.001) was taken as D_p. Figure 2 shows the relation between the aerosol emission flux and the above stated average undulating energy dissipation to the power of 3/4. The regression line in this picture is described by the equation FE=99.4(dE)+3.5. For these values the correlation coefficient is 0.86. The broken curves on both sides of the straight line represent a 95% confidence interval. Consequently the A_p factor can be taken as 99.4.
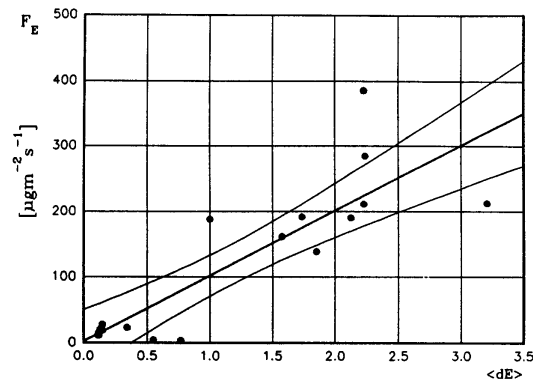
Figure 2 the emission flux of aerosol as a function of dissipation of wave energy to the power of 3/4

Calculations of model

The presented model enables calculating the aerosol emission along the profile perpendicular to the shoreline when we know the following quantities:

- quadratic mean of wave height
- direction of wave propagation
- bathymetry
- frequency

Calculations should be carried out from the deep water to the shore throughout the point network with a 0.5 m step. The ground is the following equation written in the form of finite differences and solved numerically.

On the basis of further equations the average loss of energy, the component (along the x-axis) of the waves' group velocity for each point and the quadratic mean of the wave height for each point were calculated, which made it possible to determine the aerosol emission flux according to the formula.

Result and discussion

The values of aerosol emission flux in Lubiatowo were numerically obtained from the model. The sea ground profile in Lubiatowo is shown in Figure 4.

The values of aerosol emission flux shown in Figure 3 were calculated on the basis of the model for three variations of boundary conditions characteristic of that area, that is gentle and moderate wind as well as stormy. The top line shows the values calculated with the assumption that the wave coming into the modelled zone has the average height of 3.6 m and its period is 8 s whereas the middle line assumed 1.6 m and 5.5 s accordingly. In Figure 3 the emission does not depend on the wave size at the deep water for the actual sea bottom as well as for the bottom of constant slope and also for small distances from the shore. The maximum values of aerosol emission occur in such places where there are shoals accompanied by considerably sloping bottom. The more local sloping of the bottom, at limited depths, the bigger values of the maximum emission flux. Not only is this conclusion true for local values of maximum but also for the sloping bottom throughout the coastal zone.
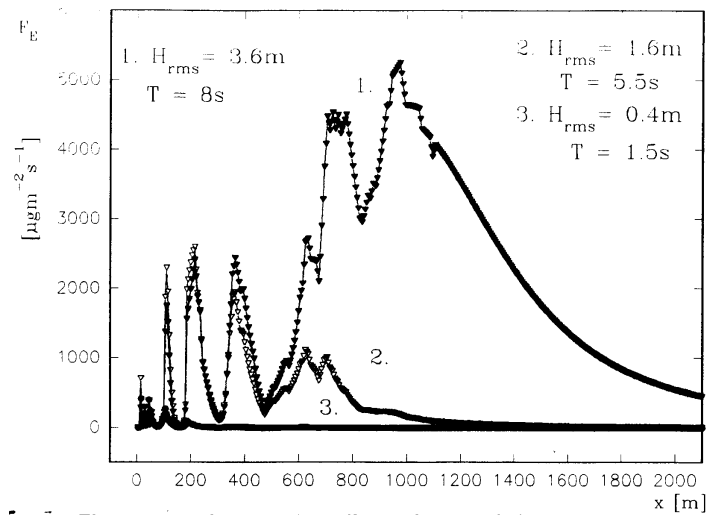
Figure 3 The aerosol emission flux obtained from model for three boundary conditions for the sea bottom profile in Lubiatowo
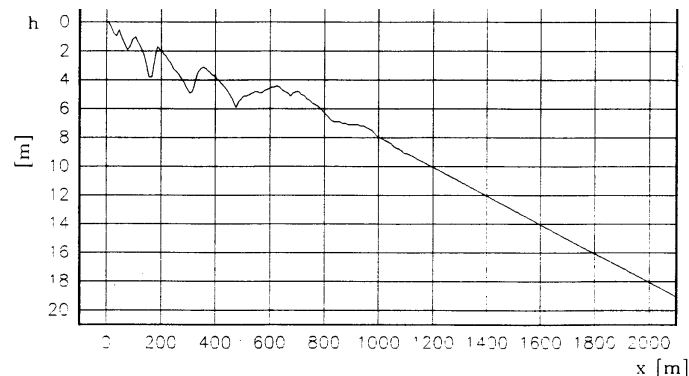
Figure 4 The sea bottom profile in Lubiatowo (BAEX I. II)

Conclusions

The presented model enables us to obtain the horizontal profile of the value of the emission flux within the coastal zone if the undulating beyond the zone and the bottom profile are known.

To sum up there can be some interesting conclusions drawn from numerical experiments run using this model:

- the slope of the sea bottom within the coastal zone has a decisive effect on aerosol emission; the steeper the slope of the sea bottom the smaller values of the emission from the coastal zone

- the total emission from the coastal zone is higher over the bottom of a smooth profile than from a rough bottom. The bigger the amplitude of the sea bottom the smaller is the total emission and the average value of the emission from the coastal zone

- local values of the aerosol emission flux behave reversely to the total emission; the maximum values of the emission flux occur where there is maximum shoal. The steeper the local slope of the sea bottom, the bigger the values of the maximum emission flux

- the emission flux does not depend on boundary conditions for deep water and is entirely determined by the depth in the shallower, active part of the zone

- for each wave size outside the coastal zone there is such an area, within the zone, from which the emission will not increase despite the general increase in the undulating. This means that the width of the breaker zone is a parameter which accurately describes the quantity of aerosol emission from the coastal zone

References

Garbalewski, C., 1983. Aerosol exchange between atmosphere and sea. Stud. i Mater. Oceanol., 50,10–18.

Ling, S. C., and Leo, T. W., 1976. Parametrisation of Moisture and Heat Transfer Process over the Ocean under Whitecap Sea States. J. Phys. Oceanogr. 6,306–315. Monahan E.C, 1971, Oceanic whitecaps. J. Phys. Oceanogr. 1, 139–144.

Monahan, E. C., and MacNicall, G., 1986. Oceanic whitecaps and their role in air-sea exchange processes. D. Reidel Pub. Co., Dortrecht, Holland, 1–129.

Petelski, T., and Chomka, M., 1996. Marine aerosol fluxes in the coastal zone—BAEX experimental data. Oceanologia, 4.

Szmytkiewicz, M., and Skaja, M., 1993. Model pradow wzdluzbrzegowych dla rewowego profilu dna i wielokrotnego zalamywania fali. Rozp. Hydrotech., PAS mw, 56, 86–110 (in Polish).

Thornton, E. B., and Guza, R. T., 1982. Energy saturation and phase speeds measured on a natural beach. J. Geophys. Res. 87, 3564–3579.

Thornton, E. B., and Guza, R. T., 1983. Transformation of wave height distribution. J. Geophys. Res. 88, 5925–5938.

The transport of Baltic water along the deep channel in the Gulf of Kaliningrad and its influence on fields of salinity and suspended solids

Boris V. Chubarenko and Irina P. Chubarenko

Introduction

The deep (8–10 m) Kaliningrad Navigable Channel (Figure 1, points 11–21) passes along the northern coast of the shallow (up to 5 m depth) Gulf of Kaliningrad (Russian part of the Vistula lagoon), and is a continuation of the Pregel river, whose mouth is located in the eastern corner of the Gulf of Kaliningrad (marked in Figure 1 by points 22–26). The channel goes directly to the Baltic coast and is separated from the proper Gulf by a set of dams (artificial islands) with narrow (10–30 m) and shallow (0.5–1.5 m) straits between them.

These features determine the specific regime of water exchange in this lagoon-river system. The main water exchange between the Navigable Channel and the Gulf is realised in two ways, the first is through a strait of 5 m depth between islands near the Pregel mouth (between points 21 and 22), and the second one through the part of the Channel (point 13) with a depth of 4 m which is not closed by islands.
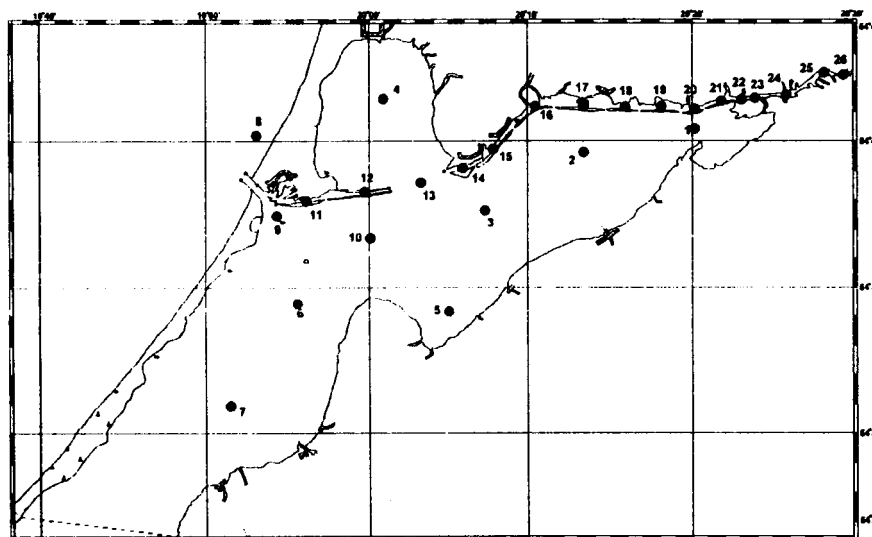
Figure 1 Chart of monitoring stations in the Gulf of Kaliningrad and Kaliningrad Marine Channel

The Channel, together with both the downstream area of the Pregel river and the Gulf of Kaliningrad, forms the estuarine-lagoon system, characterised by seasonal and short-term variations in vertical and horizontal structure. The results of the combination and inter-influence of these systems are considered here in terms of salinity and suspended matter fields.

Methods

The field data on salinity and suspended matter were collected on the net of monitoring stations (Figure 1). Seven of them are in the central and eastern parts of the Vistula lagoon. The rest of the stations are located in the aquatory of the Kaliningrad Navigable Channel and downstream of the Pregel river (Chubarenko, *et al.*, 1998). The data for the lagoon area were collected during 1994–1995, whereas the monitoring program in the Channel was held only in 1995. The frequency of measurements was about once per month. A period of a week was used only for station 1, situated near the river Pregel mouth.

The CTD profiler "Seacat profiler" (production "Sea-bird Electronics") 0.7 m long and 0.1 m in diameter was used for salinity measurements. It was observed that relative deviation in salinity between instantly repeated measurements is close to 3.5% at station 1 and 1.7% at station 6, while the equipment accuracy is 0.1%. Permanent occurrence of this

difference speaks for the existence of natural patchiness of salinity fields. This natural microscale variability is a major source of measurement result variations and defines the accuracy of monitoring data. It is reasonable to consider, that natural patchiness of water does not permit the measuring of any parameter with accuracy greater than 3.3% and 1.7% in the vicinity of river Pregel mouth and lagoon entrance respectively.

Drifter current measurements in the Kaliningrad Marine Channel were performed during autumn of 1994. Upper (1 m) and bottom (6 m) layers drifters with a sail area of $0.3\,m^2$ were used. It was theoretically evaluated (for the construction of drifter used) that wind forcing does not exceed 7% of current driving force.

Analyses on suspended solids were obtained by filtration of 250–400 ml of water through the GF/C Whatman Production filters (England) with a general diameter 4.7 cm, and also nuclear filters of Incorporated Institute of Nuclear Researches (Dubna, Russia) with a general diameter 4.7 cm and diameter of holes of 0.5 microns. The average error for suspended solids concentration was within the limits of 1.0–1.1 mg per litre (Chubarenko *et al.*, 1998).

Results

Three typical situations of salinity distribution along the Kaliningrad Navigable Channel are represented in Figure 2 and clearly visualise that the studied area has a typical estuarine hydrological behaviour.
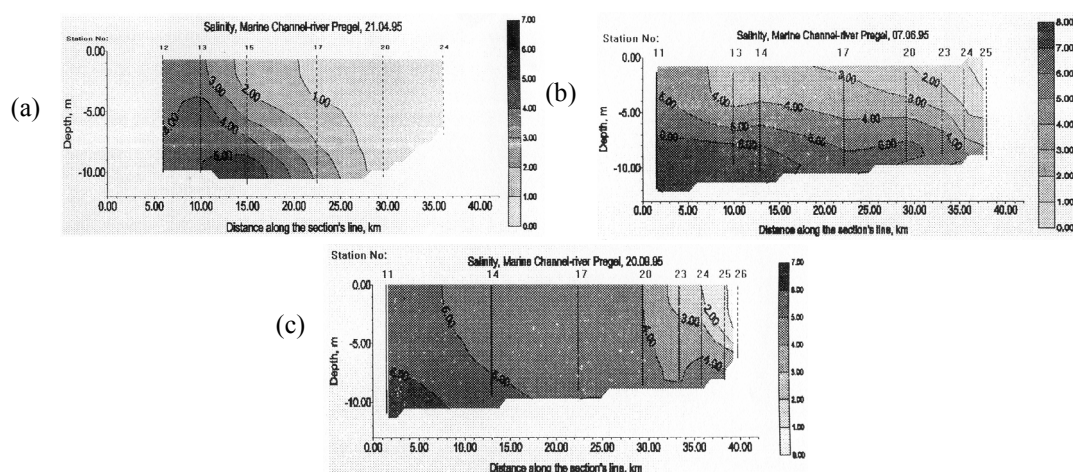
Figure 2 Salinity distributions along the Kaliningrad Marine Channel in Spring (a), Summer (b) and Autumn (c)

Salinity distribution after the spring maximum of river discharge (Figure 2a, 21 April 1995) is characterised by the spreading of river water (isohaline 1 ppm) up to the middle of the Channel. The other half of the Channel area is occupied by water with intermediate salinity (1–3.5 ppm). The water with salinity greater than 5 ppm was found in the bottom layer of the deepest Channel area. The mixing zone is characterised by a horizontal gradient of 0.2 ppm per km in the upper and intermediate layers, and 0.4 ppm per km in the bottom layer. The vertical gradient ranges up to 0.6 ppm per m.

The salinity distribution on 7th June (Figure 2b) represents a typical summer situation, when river water (salinity less than 1 ppm) was observed only in the upper layer far above the geographical mouth of the Pregel river (point 22). The central Channel area (points 13–20) is covered by vertically stratified water with salinity from 2–3 ppm in the upper layer to 6 ppm at the bottom. All isohalines have an inclination caused by opposite movement of water in the upper and bottom layers. The horizontal gradient varies from 0.08 ppm per km in the upper layer to 0.2 ppm per km in the bottom layer. The vertical gradient is 0.5 ppm per m on average.

The weak river drain during summer causes penetration of saline water far upstream along the Pregel river in the autumn (Figure 2c, 20 September 1996). The water with boundary salinity (1 ppm) shifts to the centre of the Kaliningrad city (point 25) in the upper layer, meanwhile, bottom salinity here already reaches 4 ppm. The transition zone is narrow and it is shifted far upstream along the Pregel river. It is characterised by a horizontal salinity gradient of 1 ppm per km in the bottom layer and 0.25 ppm per km in upper one. The vertical gradient exceeds 1.2 ppm per m. The Channel area is occupied by well-mixed water this time.

Horizontal variations and the temporal course are the dominant characteristics of salinity distribution in the Vistula lagoon. Vertical gradients were observed only near the Pregel river mouth and lagoon entrance (Baltyisk strait) during

the spring time or during the strong sea water inflow in the lagoon. The spatial-temporal diagram of the upper layer salinity variations in the Gulf of Kaliningrad (points 1–7) is represented in Figure 3.
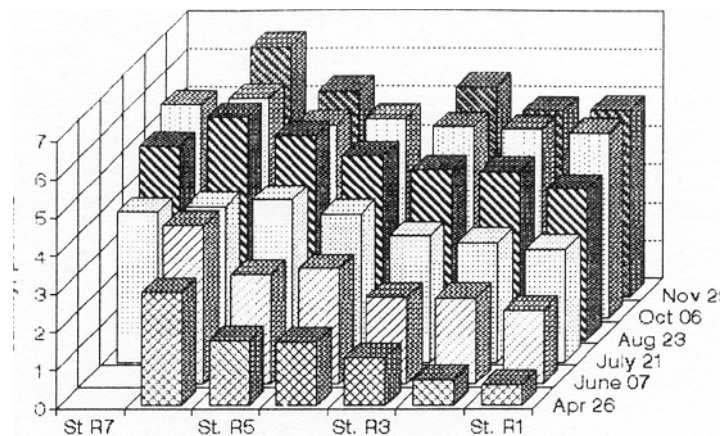
Figure 3 Spatial and temporal variability of upper layer salinity in the Gulf of Kaliningrad

Minimum salinity in the Gulf was observed after the spring high rivers drain. Then the salinity of lagoon waters increases during summer and autumn till ice coverage. It is stipulated by the periodic penetration of salty water in the lagoon basin caused by variations in the wind and sea level. In the autumn period of 1994 and 1995 the salinity increased up to 4.9 and 4.5 ppm nearest to the Pregel river mouth (Station 1) and up to 6.5 and 6 ppm for the central part of the lagoon (Station 6).

The salinity averaged over a year has a maximum in the region adjacent to the lagoon entrance and minimum in the eastern part of the lagoon, where the influence of the Pregel river (the main fresh waters source for the Vistula lagoon) is maximal. The strongest spatial variations in the salinity field are observed in the spring, when the horizontal gradient exceeds 0.11 ppm per km. The spatial gradient of salinity decreases from spring to autumn. Maximal annual salinity variations take place in the part of the lagoon closed to the Pregel river (0.5−4.9 ppm), and minimal variation is found in its southern part (2.7−4.3 ppm).

Current measurements in the Kaliningrad Navigable Channel were made on 27, 28 September and 7, 11, 14, 18, 21, 28, October 1994 at 5 points of the Channel at two levels (1 and 6 m depth). The arrows on Figure 4 simultaneously represent the data for two layers in the Channel bottom currents in the lagoon (measured by current meters) and wind. The occurrence of currents in the opposite direction of the wind in the central part of the Channel is usual for winds of more than $5 \, \mathrm{m \, s^{-1}}$ lengthwise along the lagoon axis. During gentle wind conditions the Channel is the natural continuation of the Pregel river and has a current structure like in the river.

Discussion

The central part of the Channel plays a specific role in the water dynamics of the Vistula lagoon eastern part. For wind directions along the lagoon axis it plays a specific compensating role in water dynamics providing water flux backward into the wind. This mode appears under strong winds (more than $5 \, \mathrm{m \, s^{-1}}$) from the south-eastern or north-western directions, which drives the big mass of water along the central the line of the lagoon main aquatory.

Pushed by the south-western wind the upper layer lagoon water comes to the Pregel river mouth, and both goes in part upstream the Pregel river and forms the compensating current (opposite to the wind direction) in the Channel and in the deep along the lagoon axis (Figure 4b). The compensating current along the channel also appears for north-eastern winds and directs to the Pregel river mouth (Figure 4a), but this process is usually not so distinct as for south-western winds.

The main driving force for this feature of the Channel is the barotropic pressure difference between its ends which is bigger than the wind stress. The barotropic pressure gradient is caused by surge water level differences, and, at the same time, the wind stress is reduced by islands with the trees on them. The influence of the wind on the currents in the channel is also restricted because of the high ratio between the Channel depth and its width.
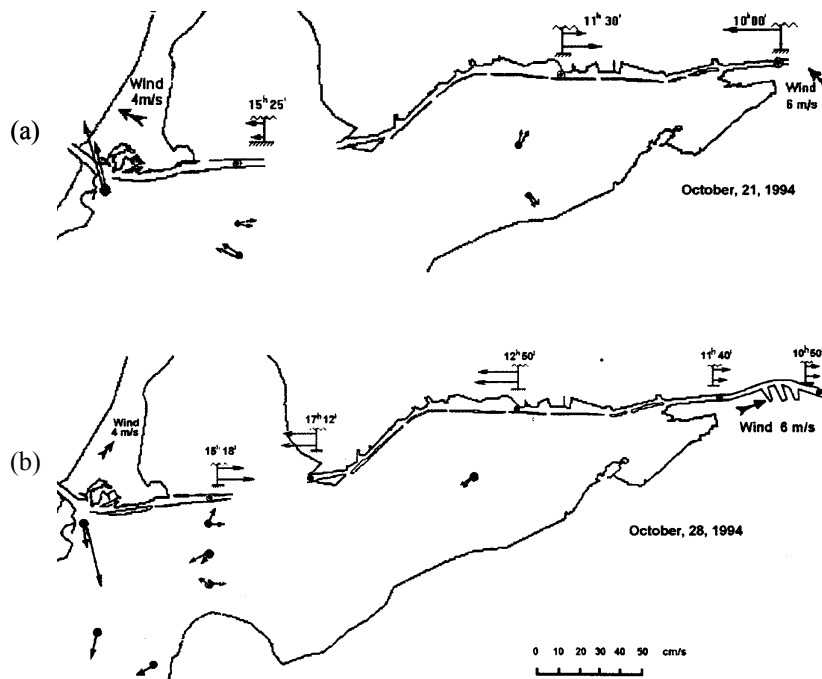
Figure 4 Currents in Kaliningrad Marine Channel and the Gulf of Kaliningrad with winds from the south-east and south-west

The existence of this large natural mixing system in the eastern part of the Vistula lagoon results in the formation of homogenous salinity and suspended matter fields here. The hydrological surveys along the Channel at the end of summer and the beginning of autumn show the low spatial salinity gradients between stations 13 and 20. Analogously, small spatial variations in salinity (Figure 3) or suspended matters (Figure 5) are observed between stations 1, 2 and 3 in the second half of the year.
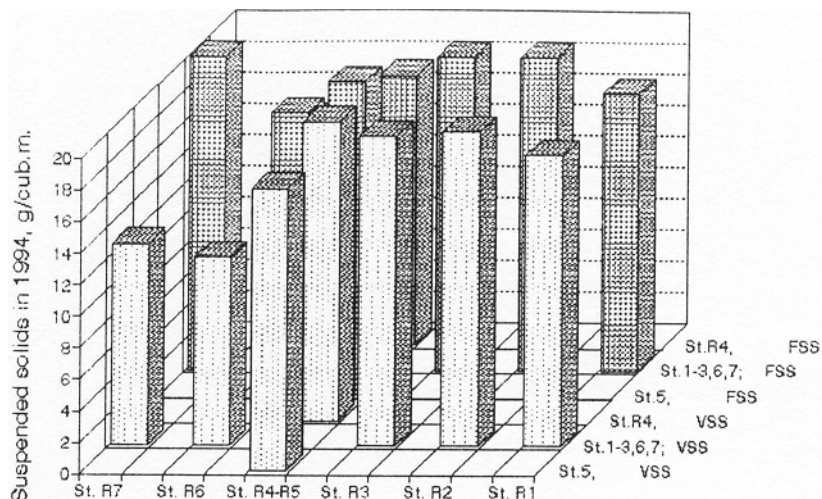
Figure 5 Spatial variability of annual mean values of fixed and volatile suspended solids for the Gulf of Kaliningrad

The next effect of the deep Channel influence on the lagoon hydrodynamics is the transport of salty water in the deep layers of the Channel toward the Pregel river mouth (station 22). Weekly hydrological measurements sometimes indicate intrusions of salt water into the eastern part of the Vistula lagoon from the Channel. Such salt water transport is a typical estuarine feature in the behaviour of the joined system of the Channel and the Pregel river (Figure 2).

Thus, there are three points of salty water penetration into the Vistula lagoon aquatory:

1. the lagoon entrance
2. an open area of the Channel that is not closed by the dam's islands (around station 13, Figure 1)
3. strange though it may seem, the region near the Pregel river mouth

Both of these effects result in a more intensive process of salinity increase than can be proposed without taking into consideration the existing of the Channel. For example, the results of annual salinity course simulation fulfilled by the MIKE21 numerical model (Prioritising Hot Spot Remediations ..., 1998) in comparison with real monitoring data are represented on Figure 6. These simulations were performed on the course grid without taking into account the real Channel bathymetry, and results show:

1. the general salinity level is less than in reality
2. the difference in salinity between the stations 1, 2 and 3 is higher than in monitoring data.
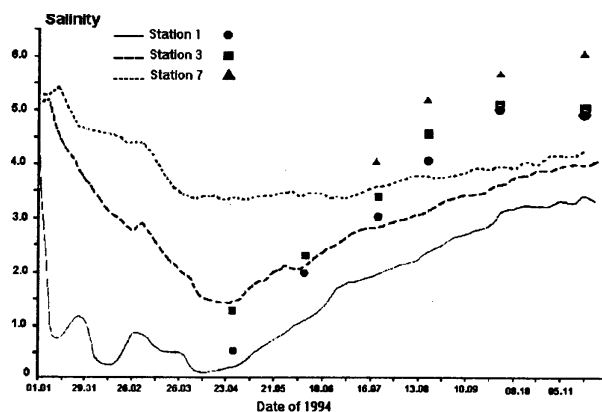
Figure 6 Annual course of salinity for stations 1, 3 and 7; simulation results and the monitoring data

Conclusions

The deep Kaliningrad Navigable Channel forms a part of the Pregel river estuary together with the down stream area of the Pregel and plays a specific role in water dynamics of eastern part of the Vistula lagoon. Its influence becomes especially significant after the spring maximum river drain. The transport of salty water along the Channel toward the Pregel river mouth supplies the income of salty water to the eastern part of the Vistula lagoon, which is the reason for more intensive salting of the lagoon water up to the end of autumn. This process depends on seasonal and short-term water level and local wind variations.

The Channel is the pass for intensive compensating flows (opposite to wind direction) occurring during western and eastern winds. This effect of intensive large scale water mixing between the Channel and the eastern part of the lagoon makes possibility for more homogeneous conditions in salinity and suspended matter fields in the lagoon than it would be without existence of the Channel.

It is necessary to develop special sink-source techniques for two-dimensional numerical simulations with the aim of taking into consideration the effect of additional salty water inflow in the point of the Pregel river mouth.

Acknowledgements

References

Chubarenko, Boris V., Chubarenko, Irina P., and Kuleshov, Alexey F. (1998). The results of 1994–1997 investigations of hydrological structure and transparency of water in the Russian part of the Vistula lagoon—Proceedings of Symposium "Freshwater fish and the herring population in the coastal lagoons: environment and fisheries", May 6–7, 1998, Gdynia, Poland—Sea Fishery Institute, Gdynia, 1998, Pp. 45–59.(in English).

Chubarenko, B. V., Kuleshov, A. F., and Chechko, V. A. (1998). Field study of spatial-temporal variability of suspended substances and water transparency in Russian part of Vistula lagoon. In Monographs in System Ecology (Eds.

Tilickis, B., Razinkovas, A., Stankevicius, A., Lapinskas, E., Gaziunaite, Z.) Vol.2. Klaipeda, 1998, pp.12–17. (in English).

Prioritising Hot Spot Remediations in Vistula Lagoon Catchment: Environmental Assessment and Planning for the Polish and Kaliningrad parts of the lagoon (1994–1997). Report on the international project. Erik K. Rasmussen (Ed.). Water Quality Institute, Danish Hydraulic Institute, GEOMOR, Atlantic Branch of P.P. Shirshov Oceanology Institute. Hoersholm, Denmark, 1998.

Baltic research in a wider perspective

Stig Fonselius

Introduction

Some twenty years ago the R/V "Atlantis II" from Woods Hole Oceanographic Institution visited the Baltic Sea. The ship spent some days in Kiel. The chief scientist explained in a presentation speech that the Americans had come to the Baltic sea in order to fill up this white spot on the oceanographic world map. Everybody who knew Klaus Grasshoff, can imagine his reaction on this statement.

Modern oceanography was actually born in the Baltic sea area. Names such as Fritjof Nansen (Norway), Martin Knudsen (Denmark), Otto Pettersson and Vagn Walfrid Ekman (Sweden), Kurt Buch (Finland), Karl Möbius, Otto Krümmel, Victor Hensen and Hermann Wattenberg (Germany) may be mentioned as examples of world famous pioneers in oceanographic research from the Baltic sea area.

In this connection I would like to mention A. E. Nordenskjöld, who was the first to sail through the North east passage. On this voyage, oceanographic observations were made. I was born in Finland and I learned at school that Nordenskjöld was a very famous Finnish scientist. When I moved to Sweden in 1951, I found out that Nordenskjöld was considered to be a very famous Swedish scientist. In 1966 I visited the Arctic Institute in Leningrad. On the wall there was a large painting showing Nordenskjöld. I was told by the Russian scientists that Nordenskjöld was a very famous Russian scientist. Well, Nordenskjöld was born in Finland and studied at the University of Helsinki. That means he was a Finn. But Finland was at that time a part of Russia and therefore the Russians considered him to be a Russian. But because of some political activities Nordenskjöld was forced to move to Sweden and from Sweden he started his famous voyage with the VEGA. Thus he was a Swede. This may serve as an example of a real Baltic scientist (Figure 1).

Figure 1 A. E. Nordenskjöld (1832–1901)

Many other Baltic scientists will be mentioned in connection with the different problems mentioned here. The International Council for Exploration of the Sea, the ICES, was founded by scientists from the Baltic sea area. The Baltic sea is probably the most investigated sea in the world. Observation series of salinity, temperature and oxygen exist from the 1890s for several deep stations.

General

Here I will mainly limit myself to internationally important work in oceanography in the Baltic sea area from the time before WW II. I will not include the work on water level, waves, sediments, etc. The first salt and water exchange calculations for the water exchange between the Baltic sea and the Kattegat were carried out by Martin Knudsen in 1901 and the well known Knudsen's formula was established (Knudsen, 1900a). At that time most general facts of the Baltic sea were already known, the halo- and thermoclines, the low oxygen content of the deep water, etc. Pettersson and G. Ekman had in 1897 come to the conclusion that the state and variations of the Baltic sea could be kept track of by measuring hydrographic data from only a few deep stations. It should therefore be easy to follow these variations from season to season and year to year by measuring the main hydrographic parameters regularly at the main stations (Pettersson and Ekman, 1897).

Another important theoretical contribution by V. W. Ekman in 1902–1905 was the well-known "Ekman spiral" (Ekman 1906).

Major components of seawater

The Swedish scientist T. O. Bergman analysed seawater in 1788. He reported the following components: Common salt, salinited magnesia (magnesium chloride) and loose gypsum. He also observed that sea water was slightly alkaline (Bergman, 1788).

The Danish scientist J. G. Forchhammer analysed several hundred samples of seawater in 1865 for calcium, magnesium, chloride and sulphate and a few samples for potassium. He determined the sodium by difference, assuming that the cations were equivalent to the chloride plus sulphate and ignoring the presence of carbonate and bicarbonate. Salinity was calculated as the sum of these components (Forchhammer, 1865) (Figure 2). Forchhammer's work confirmed Marcet's conclusion that sea water over the whole world contained the same ingredients and nearly in the same proportions. Forchhammer also established that the amount of the total dissolved salts could be obtained by multiplying the chloride content with the factor 1.812, not very far from the value used today, 1.80655.

Composition of sea salts according to Forchhammer (1865), Schmelck (1882) and Dittmar (1884) (g./100g. Cl + Br)

	Forchhammer	Schmelck	Dittmar Ave.	Dittmar Ave.*
Cl + Br	100·000	100·000	100·000	100·000†
SO_3	11·88	11·46	11·575	11·558
CO_2	—	—	0·274	0·275
CaO	2·93	2·99	3·027	3·025
MgO	11·03	11·40	11·212	11·269
K_2O	1·93	—	2·405	2·445
Na_2O	—	—	74·462	74·486

*Recalculated Lyman and Fleming's (1940) data. These data were themselves recalculated from the original figures using 1939 atomic weights.
†Br = 0·340.

Figure 2 Composition of sea water by different scientists in the 1800s

Temperature

The difficulty in temperature measurements was of course, that the temperature changed on the way up to the surface. On the Pommerania expedition in 1871 a well isolated thermometer was used (Figure 3). The thermometer had to be held for one hour at the desired depth and had to be transported up to the deck within 10 minutes, not a very practical arrangement (Meyer *et al.*, 1873). In the Swedish investigations during the 1870s–1880s Ekman's insulated water sampler was used. Around 1900 Richter, in collaboration with Nansen, developed the reversing thermometer. In this connection the reversing Nansen series water sampler was constructed (Dietrich, 1967). The principle of the reversing thermometer has been used all over the whole world. J. P. Jacobsen already used an electric conductivity thermometer in 1931 (Jacobsen, 1935). In the Baltic sea we have temperature observation series beginning from the 1890s (Figure 4).
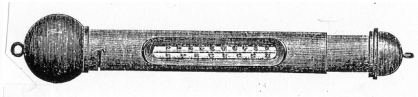
Figure 3 Deep sea thermometer used on board the "Pommerania" in 1871
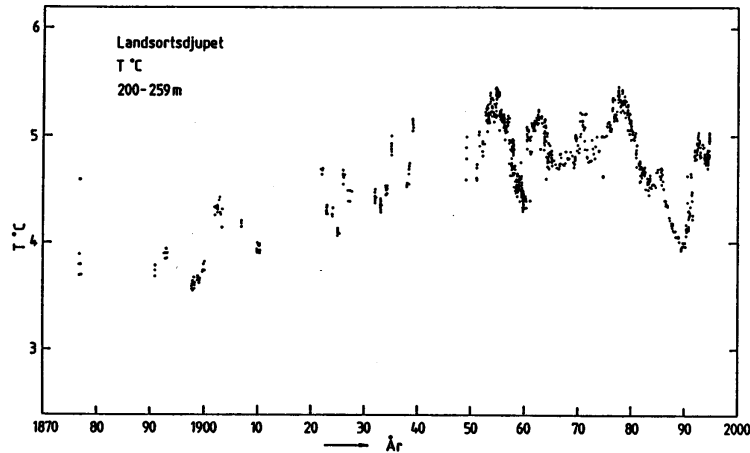
Figure 4 Temperature variations in the Landsort Deep at 200–259 m from 1877 to 1994.

Salinity

The interrelationship between chlorinity, salinity and density of seawater was investigated by Forch, Knudsen and Sörensen and definitions of chlorinity and salinity were worked out in 1902 (Forch *et al.*, 1902). In 1899 Knudsen published an elegant routine method for determination of chlorinity and salinity by titrating with silver nitrate (Knudsen, 1899). He also introduced the "Normal water" as a standard for the silver nitrate solution. The chlorinity titration method is still used in some laboratories, but has in most cases been replaced by conductivity methods. In 1901 Knudsen together with S. P. I. Sørensen and Nils Bjerrum prepared the world famous Knudsen Tables for calculation of salinity, density and other physical parameters of sea water. These tables were used all over the whole world until the 1960s, when the measurement of salinity by the electrical conductivity method made it possible to replace them with more accurate tables worked out by UNESCO. The technique had however been known since the beginning of the century (Knudsen, 1900) (Figure 5).

Figure 5 Martin Knudsen (1871–1949)

In earlier times the density of seawater was used for salinity determinations using different kinds of hydrometers. At the Bornö field station of the Swedish Board of Fisheries a gold chain hydrometer was used for routine salinity determina-

tions until the 1970s. In the Baltic sea we have salinity observations at the major deep stations from around 1890 (Figure 6).
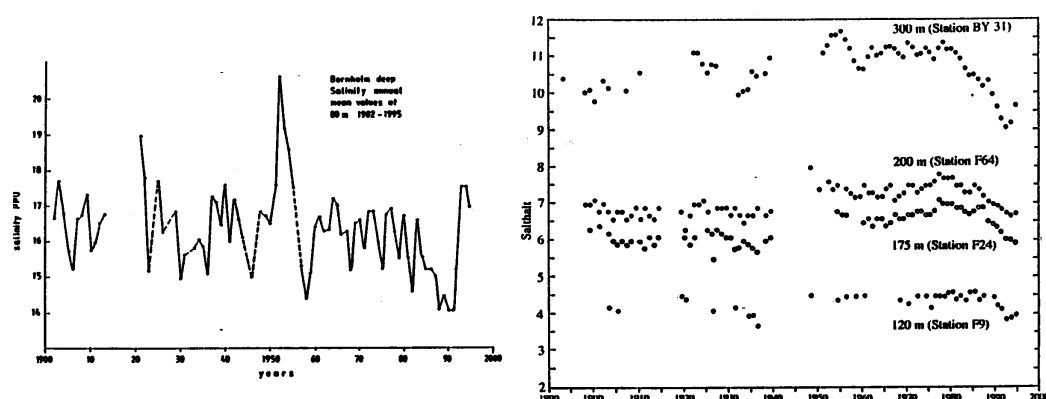
Figure 6 Salinity variations in the deep water in different parts of the Baltic sea from 1890 to 1994. Left: Bornholm Deep. Right: Landsort Deep (BY31), Åland Deep (F64), Ulvö Deep (F24), Bjurö Deep (F9)

Oxygen

O. Jacobsen in 1873 used a method by Bunsen for removal of gases from sea water for determination of dissolved oxygen on board the "Pommerania" (Jacobsen, 1873). The Winkler titration method (Winkler, 1888) is still, in slightly modified form, the standard method for oxygen analysis in sea water. Also for oxygen we have observation series at the deep stations from the beginning of the century (Figure 7).
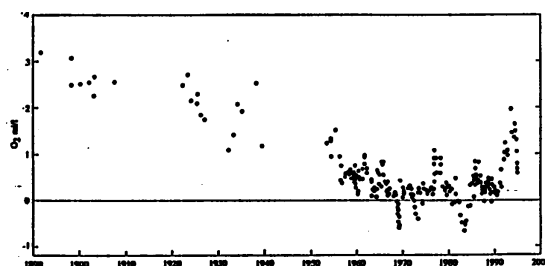
Figure 7 The oxygen and hydrogen sulphide variations in the Landsort Deep at approximately 400 m from 1891 to 1994 in mll^{-1}. Hydrogen sulphide is expressed as negative oxygen.

J. P. Jacobsen in 1912 used the Winkler method for investigating the diurnal variations of the oxygen content, caused by the photosynthesis and respiration of plants (Jacobsen, 1912).

Carbon dioxide, alkalinity and pH

Bergman (1788) was the first to observe the alkalinity of seawater in 1788. Lichtenberg (1811), Hamberg from Finland (1885) and Krogh from Denmark (1904) contributed to determination of carbon dioxide in seawater.

No satisfactory method for pH determinations existed until the pioneer work of Sørensen and Palitzsch in 1910 on the colorimetric determination of pH (Sørensen *et al.*, 1910).

In 1917 the Finnish scientist K. Buch started his monumental work on the carbonic acid equilibrium in sea water by investigating the quantitative relationship between the total concentration and partial pressure of carbon dioxide, the alkalinity and the hydrogen ion concentration (Buch, 1917). Together with Harvey, Wattenberg and Gripenberg, in 1932 Buch made very careful measurements of the first and second apparent dissociation constants of carbonic acid at various salinities and temperatures and published tables for calculation of the different carbonic acid parameters (Buch *et al.*, 1932). Buch found that the relation Salinity/Alkalinity increases with decreasing salinity in the Baltic sea (Figure 8).

Baltic research in a wider perspective
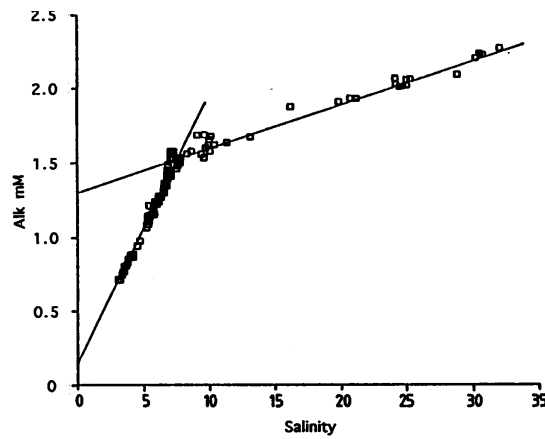
Figure 8 The relation Salinity/Alkalinity in the Baltic sea

The carbon dioxide cycle now has renewed worldwide interest in connection with the discussion of the "Greenhouse effect".

Hydrogen sulphide

Forchhammer was the first scientist to observe the existence of hydrogen sulphide in seawater, rich in organic matter, in 1865. He observed that the ratio of sulphate to chloride was apparently lower in such water and explained that, I quote, "in this kind of decomposition where sulphuretted hydrogen is formed, the organic matter is changed into carbonic acid and water while the oxygen which this change requires, is taken from the sulphates" (Forchhammer, 1865). It is interesting to note that the formation of hydrogen sulphide from sulphate ions in the sea was known 130 years ago. In the Baltic sea hydrogen sulphide was observed for the first time in 1931–32, but the concentration was not measured. In the Baltic sea there is a clear relation between high density and low hydrogen sulphide concentration, which demonstrates the effects of salt water inflows (Figure 9).
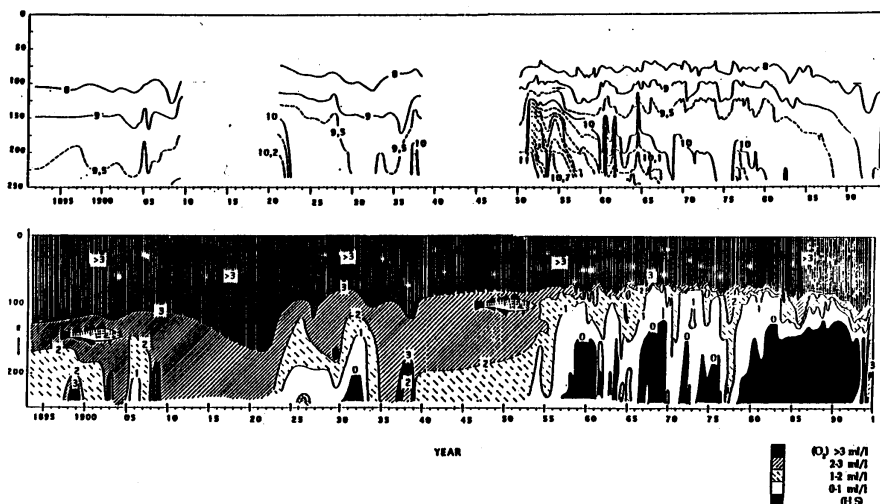
Figure 9 Measurements in the Gotland Deep from 1893–1994 showing density distribution (above) and oxygen conditions (below)

Trace elements

In 1825 Pfaff from Germany detected iodine in Baltic water. Until that time no trace elements had been definitely detected in seawater (Pfaff, 1825). In 1865 Forchhammer detected ammonia, phosphate, silica, manganese, iron, aluminium and barium in addition to the major components strontium and fluorine (Forchhammer, 1865). Winkler showed in 1916 that both iodide and iodate were present in the water (Winkler 1916).

The German scientist Karl Brandt (Brandt, 1899, 1902) investigated the cycles of nitrogen and phosphorus in the sea during 1899 to 1902 and was able to show that marine plants assimilated ammonia, nitrite and nitrate from the sea and

built them into organic compounds, needed for their metabolism. He also found that dissolved inorganic nitrogen compounds were not formed in the sea by bacterial nitrification of dissolved nitrogen. He concluded that ionic nitrogen was supplied to the sea by rivers or rainwater. He and also Feitel (1903) found seasonal variations of the nutrient salts and discussed the possible production limiting effect of phosphate (Brandt, 1916–1920) (Figure 10). Also here we can see that the limiting effect of nutrients in seawater was known at the beginning of the century.
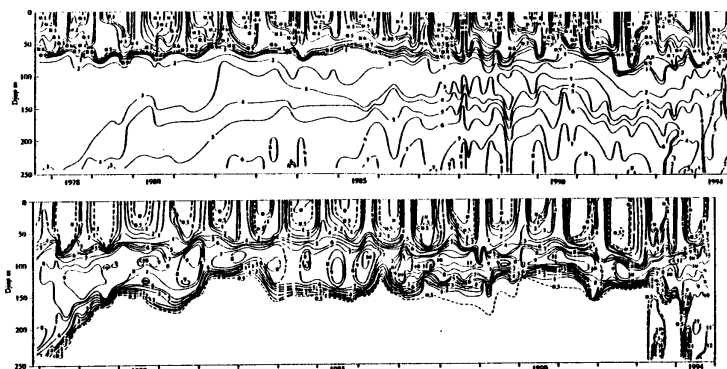
Figure 10 The phosphate (above) and nitrate (below) distribution at the Gotland Deep station from 1878 to 1994 in $\mu mol\,l^{-1}$

In 1925 Hermann Wattenberg developed photometric methods for the routine determination of micronutrients. He designed and set up a chemical laboratory on the "Meteor" in which analyses were carried out for salinity, dissolved oxygen, pH, phosphate, alkalinity and partial pressure of carbon dioxide, demonstrating that useful chemical routine work was possible at sea (Dietrich 1967).

Optics and organic matter

In 1922 Martin Knudsen studied the penetration of light in seawater (Knudsen, 1922). Hans Pettersson constructed a transparency meter in 1934 and studied transparency in seawater. Kurt Kalle worked with organic matter in 1933 and introduced the expression "Yellow substance" which is related to the humus concentration (Kalle, 1933). In the Baltic sea the humus concentration increases with lower salinities (Figure 11).
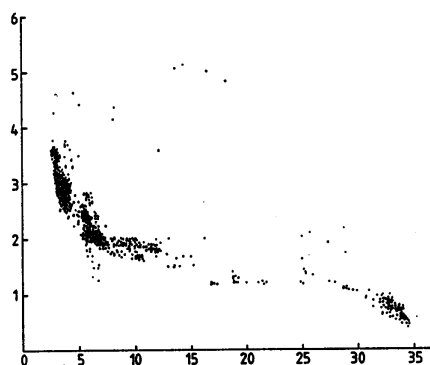
Figure 11 Example of the relation between salinity and humus in the Baltic sea, the Kattegat and the Skagerrak

Primary production

The Danish scientist Steeman-Nielsen developed a new method in 1952 for measurement of the primary plankton production using the well known carbon-14 method. This production measurement method is used all over the world (Steeman-Nielsen, 1952) (Figure 12).
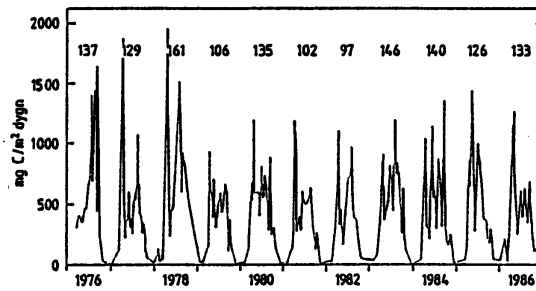
Figure 12 Results of primary production measurements at Askö in 1976–1986. The numbers above the peaks show the yearly production as gCm^{-2} for every year.

Radioactivity

Hans Pettersson and his co-workers developed methods for radium analysis in sediments (Pettersson, 1930). Føyn, Karlik, Pettersson and Rona analysed the radioactivity of seawater (Føyn *et al.*, 1939).

Oceanographic instruments

Otto Pettersson constructed a photographically registering current meter in 1911, which worked excellently. The working time was 2 weeks (Svansson, 1996) (Figure 13). The American Richardson current meter from around 1960 was constructed on the same principle. Another well-known current meter was constructed by V. W. Ekman in 1905.
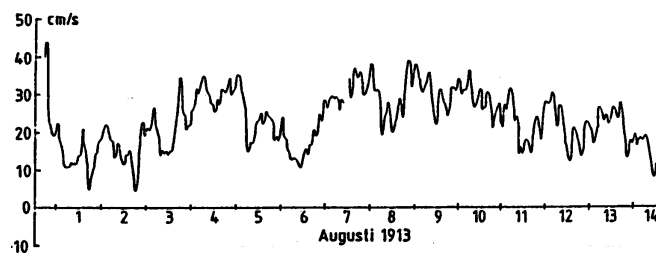
Figure 13 Current measurements with the Pettersson current meter in the Jutland current in August 1913 at 80 m depth. Component towards ENE.

Another world famous instrument is the deep sea piston corer, which was constructed by B. Kullenberg in 1946. As an anecdote I can mention that from the beginning it was thought that the long sediment core could be forced out from the metal tube by help of compressed air. The result was that when the pressure increased, the core started slowly to move out, but suddenly it flew over the ship rail far out in the sea splashing sediment over the whole deck.

These are some examples of the influence of scientists from the Baltic sea area on the development of oceanographic research.

Earlier monitoring work

If we look closer at the oceanographic work carried out in the Baltic sea, we find that real routine work was started in the 1890s. Observations on light ships had already started in the 1870s. Temperature, salinity and currents were measured.

The International Council for Exploration of the Sea, the ICES, was founded by scientists from the Baltic sea area. The founding of the ICES in 1902 signified the start of regular reporting and publication of oceanographic observations (Figure 14). Data were collected at fixed stations, including the most important deep stations, e.g. the Gotland Deep, the Landsort Deep, the Åland Deep, the Ulvö Deep, the Bornholm Deep, etc. The Baltic sea was divided into different areas and these areas were worked by Finland, Sweden, Denmark and Germany.
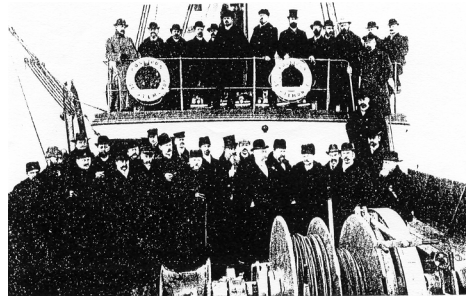
Figure 14 ICES participants on board S/S. "Poseidon" during the Hamburg meeting in 1904

I believe that few young scientists today realise the enormous work behind the data from the beginning of the century. All data for salinity, oxygen and alkalinity had to be titrated, pH had to be determined colorimetrically by comparing the colour of the sample with standards. The work on board was often carried out by the leading scientists themselves. The drawing of maps and diagrams had to be done by hand, mean values had to be computed without help of calculators. Reports and scientific papers had to be written. Few scientists had the help of competent assistants. Before WW I, only temperature, salinity and dissolved oxygen were reported on a routine basis. All years were not covered and for most years only one series of results exists for the main deep stations. After WW I we find in addition alkalinity and pH in the data reports. A few nutrient values were published. The work still had to be carried out by hand. Due to the slow work and few available research ships, we mostly find only one observation series per year. A large gap in the observations in the open sea exists for the war years from 1914 to 1921. Also WW II caused a long gap in observations from 1939 to 1950. Due to the scarce series of observations it was difficult to draw conclusions on the secular changes of salinity and oxygen and obviously nobody really tried to do that (Figure 15).
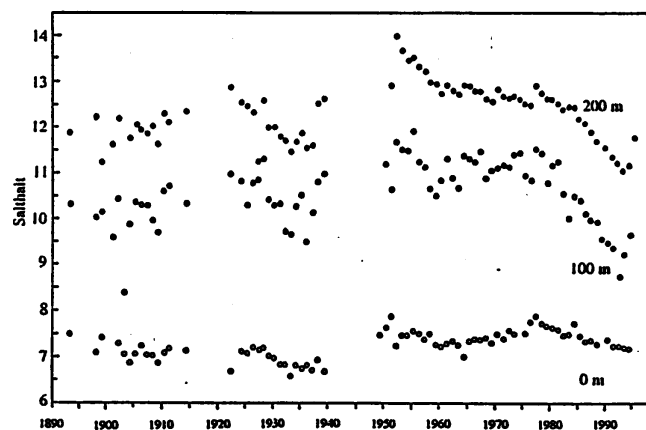
Figure 15 Salinity variations at different levels in the Gotland Deep from 1890 to 1994

What I really miss is results from Russian observations. The routine observations before WW I were carried out by Finland, which at that time was in union with Russia. After WW I the Soviet Union was not very eager to report their results. In Soviet publications from the first decades after WW II, we find some long time series from the Gotland Deep, but the data until WW II obviously mostly originate from the Finnish annual expeditions (Soskin, 1963). When the hydrographic work again started after WW II around 1950, the difficulties were enormous. Few research ships remained, many scientists had died in the war or had disappeared, oceanographic laboratories had been destroyed, equipment was missing. Anyhow the work was slowly started and after 1960 routine analysis of phosphate was introduced and some years later routine analysis of nitrite and nitrate. Later also analysis of silicate and ammonia were added.

I still remember the conditions in the Göteborg laboratory in 1960. Artur Svansson was head of the laboratory and I was his assistant. For the routine work, which consisted of salinity and oxygen titrations, we had two laboratory technicians. We had very few beakers, flasks and pipettes, but we had got a spectrophotometer. For work at sea we sometimes had help from the Navy hydrographic office. Our research ship, the "Skagerrak", was in bad condition and had been used during the war as an auxiliary cruiser, actually the only Swedish man of war which managed to shoot down an intruding aeroplane.

During the 1920s and 30s conferences of Baltic hydrologists had been held for example in Tallinn (1928), Warsaw (1930), Leningrad (1933), Finland (1936) and Germany (1938). These traditions were renewed in 1957 as Conferences of Baltic oceanographers.

In 1943 Kalle described the large water exchange in 1932 in the Gotland Deep (Kalle 1943). A new much larger inflow of salt water occurred in 1951. This caused a stagnation period in the Gotland Deep, which lasted until 1961. This was something new in the Baltic research and that started an intensive study of the chemical changes in the deep water. Cooperative programmes were introduced. The amount of routine hydrographic data increased enormously due to new faster standard methods. Long-term results for salinity, temperature, oxygen and later nutrients could be worked out covering the time from around 1900 to present time. A whole new era began in which the secular variations could be studied.

Modelling of water, salt, and nutrient balances could now be carried out. The introduction of electronic equipment for sampling, calculations and, later, computers sped up the scientific work both on board ships and in the shore laboratories. Autoanalysers for determination of nutrients and several other parameters were introduced.

Before WW II there were very few cooperative ships expeditions. One was carried out in the central Baltic sea in 1938 with participants from Finland, Sweden and Germany. When the Conferences of Baltic Oceanographers were organised, the first cooperative program was carried out in 1964 with participants from Helsinki, Leningrad, Riga, Gdynia, Warnemünde, Kiel and Göteborg. The cooperation was very good and a new cooperation, called the International Baltic Year was carried out in 1969–1970. According to the programme, expeditions by different ships were carried out almost every month, according to a schema which included the important deep stations. Several intercalibrations of methods were performed, for example in Leningrad (1966) and Copenhagen (1968). The cooperation was very successful and important results were achieved. After that followed the BOSEX 77, the PEX 86 and the SKAGEX 90–91.

These large cooperative expeditions, the SKAGEX with 16 participating ships, have shown that scientific cooperation can successfully be carried out with scientists from very different countries with different political systems. Basic science is of course the same regardless of political systems.

The future

Now it is no longer necessary for the scientists to go out with the research ships for sampling data, most of the work is done automatically and the equipment on board is operated by skilled technicians. The scientists can sit at home in the laboratory, working on modelling with the help of computers. All calculations are carried out with the help of computers and diagrams are also drawn by the computer. Much more time is available for scientific thinking. Data may be corrected by the computer by introducing error limits. There are, however, some dangers in this development. The scientist may lose contact with reality. He may accept all data delivered by the computer as correct. He has poor or no knowledge of how well the sampling is carried out, the contamination danger on board a ship and even the condition of the assistant carrying out the work on board. Seasickness is a reality on board ship and may reduce the accuracy of the work. A machine may be able to draw figures with isolines but the intelligent guess of an experienced scientist cannot be replaced by a computer and unrealistic isolines may be introduced.

The enormous capability and possibilities of the modern computers have given us a new tool for working out mathematical models for different sea areas, which can predict hydrographical and ecological changes.

Remote sensing is the newest tool in oceanography. The sea surface is studied with the help of satellites (Figure 16). Already the first results from satellite images have shown that the sea surface is much more complicated than what was believed earlier. By help of infrared cameras we can see the distribution of colder and warmer water, we can see upwelling areas, borders between water masses, gyros, etc. Earlier we had the view that the sea surface was quite homogenous and that only few measurements of temperature, salinity or some other parameter were enough for describing the conditions. Drifting buoys can now be followed by help of satellites.
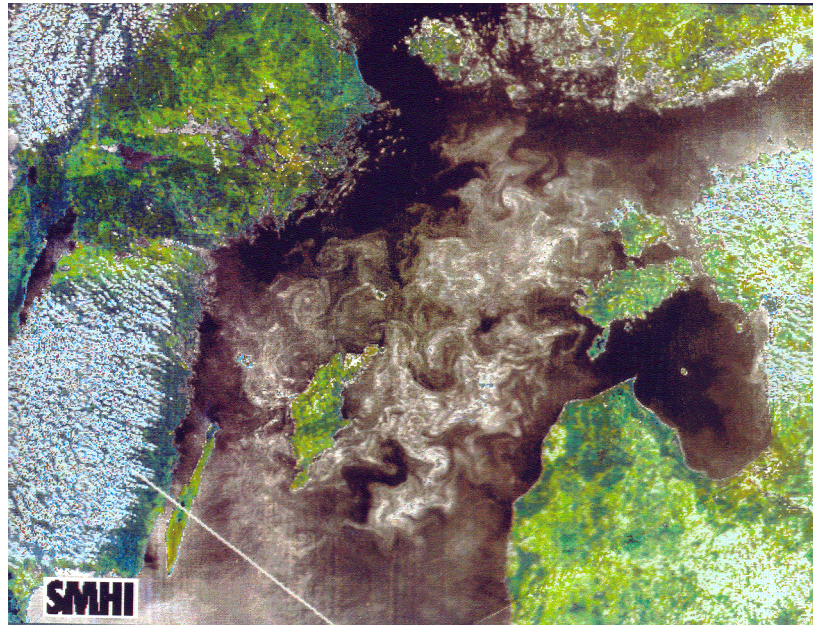
Figure 16 Bloom of blue-green algae in the Baltic sea in July 1991

During the last decade the Baltic sea scientists have been involved in international scientific work on a much wider scale. Baltic sea scientists have a lot of experience on ice conditions and winter work and have therefore been invited to Arctic and Antarctic expeditions. Even ships from the Baltic sea countries have participated in such work, for example the "Aranda" from Finland, the "Ymer" and the "Oden" from Sweden and the "Polarstern" from Germany.

I will finish my talk with the following remark. We have worked in the Baltic sea for more than hundred years, but still we do not know enough to be able to tell our governments and the general public in a convincing way exactly what effects discharge of nutrients, especially nitrogen compounds, from the atmosphere the and in the rivers and the construction of the bridges and tunnels between Sweden, Denmark and Germany will have on the hydrography and ecology of the Baltic sea itself. Our governments are spending enormous amounts of research money on oceanographic work, for example in the Antarctic sea. I saw some weeks ago in a newspaper that the costs for the Swedish "Oden" expedition to the Arctic last summer amounted to over 20 million Swedish Kronor. For Baltic research it is very difficult to get enough money. It would be good if some of these millions could be spared for enforcing research on physical and ecological effects of human activities in the Baltic sea itself. Such studies would perhaps be possible with the modelling technique and computer capability we have today if enough money is available.

References

Bergman, T. O. (1788). Physical and chemical Essays, Vol. III. J. Murray, London.

Brandt, K. (1899). Wissensch.Meeresunters. Abt. Kiel, N. F. 4, 213

Brandt, K. (1902). Ibid. 6, 24

Brandt, K. (1916–1920). Ibid. 18, 185.

Buch, K. (1917). Finn. Hydrol, biol. Untersuch. Nr. 14.

Buch, K., Harvey, H. W., Wattenberg, H., and Gripenberg, S. (1933). Rapp. Cons. Explor. Mer, 79, 1.

Ekman, V. W. (1906). Ann. d Hydrographie u Marit. Meteorologie 34 pp 423–430.

Dietrich, G. (1967). General Oceanography. John Wiley et Sons Inc., p 126

Forch, C., Jacobsen, J. P., Knudsen, M., and Sørensen, S. P. L. (1902). Kongl. Danske Vidensk. Selsk. 12.1

Forchhammer, G. (1865). Phil. Trans. 155, p 203.

Føyn, E., Karlik, B., Pettersson, H., and Rona, E. (1939). Göteborgs Kungl. Vetensk. o. Vitterh. Samh. Handl. (Medd. Oceanogr. Inst Göteborg) Följd 5, Ser. B, band 6, Nr. 12.

Hamberg, A. (1885). Bihang Sv. Vetensk. Akad. Handl. 10, p 31

Jacobsen, J. P. (1912). Rep. Dan. Ocean. Exp Medit. (1908–1910), 1. p 207

Jacobsen, J. P. (1935). Medd. fra Komm. for Danmarks Fiskeri- og Havunsers. Ser. Hydrogr. Bd. 3 Nr. 1, 1935

Jacobsen, O. (1873). Liebigs Ann. 167, 1.

Kalle, K. (1933). Ber. Dtsch. Komm. Meeresforsch. 6, p 273.

Kalle, K. (1943). Ann. Hydrogr. 71, pp 4–6.

Knudsen, M. (1899). The Danish Ingolf exp. Vol. 1, part 2, pp 22–161. Copenhagen 1899.

Knudsen, M. (1900a). Ann. der Hydrogr. u. Marit. Meteorologie, Juli 1900.

Knudsen, M. (1900b). Beretn. Komm. for Vidensk. Undersøg. Danske Farvende 2. 15 pp København.

Knudsen, M. (1901). Hydrogr. Tables. G. E. C. Gadd, Copenhagen.

Knudsen, M. (1922). Bull. de Circonstance No 76.

Krogh, A. (1904). Medd. Grönland, 26 p 331.

Lichtenberg, F. D. (1811). J. f. Chemie u. Physik 2, p 252.

Meyer, H. A., Möbius, K., Karsten, G., and Hensen, V. (1873). Jahresb. der Komm. zur wissensch. Untersuch. Der Deutschen Meere in Kiel f.das Jahr1871.

Pettersson, H. (1930). Imp.de Monaco, Fasc. 81, 1.

Pettersson, O. (1883). Vegaexpeditionens vetenskapliga iakttagelser Bd 2, pp 247–380. Utg. av A. E. Nordensjöld.

Pettersson, O., and Ekman, G. (1897). Kungl. Sv. Vetensk. Akad. Handl. 29 (5) pp 1–125.

Pfaff, C. (1825). J. Chem. u. Physik 15, p 378.

Soskin, I. M. (1963). Hydrometeorological Press, Leningrad (in Russian).

Steeman Nielsen, E. (1952). J. Cons. Int. l´Éxplor. Mer 18:2.

Svansson, A. (1996). Vikarvets årsberättelse 1994–1995, pp 106–114.

Sørensen, S. P. L., and Palitzsch, S. (1910). C. R. Lab. Carlsberg 9, 8.

Winkler, L. W. (1888). Ber. Dtsch. chem. Ges. 21, 2843.

Winkler, L. W. (1916). J. angew. Chemie 29, p 205.

Seasonal and spatial variability of major organic contaminants in solution and suspension of the Pomeranian Bight

M. Graeve and D. Wodarg

Abstract

Studies of hexachlorocyclohexane-isomers (HCHs) and selected triazine herbicides in solution and suspension were carried out in the Pomeranian Bight in 1995. The concentrations of HCHs and triazines were determined by gas-liquid chromatography (GC) or by GC in connection with quadrupole mass spectrometry (GC/MS). Particulate and dissolved material were separated by means of an in-situ filtration/extraction system.

The seasonal variability and regional distribution of the various components were investigated in January, April, July and September 1995. Their distribution in the western Pomeranian Bight is described. The concentrations of individual hexachlorocyclohexane-isomers were in the range of $100–1000\,\mathrm{pg}\,\mathrm{l}^{-1}$ in solution and 20 to $60\,\mathrm{pg}\,\mathrm{l}^{-1}$ in suspension. The levels of the triazines in solution showed pronounced differences between the individual components (atrazine ($2–20\,\mathrm{ng}\,\mathrm{l}^{-1}$), simazine ($5–30\,\mathrm{ng}\,\mathrm{l}^{-1}$), terbuthylazine ($<5\,\mathrm{ng}\,\mathrm{l}^{-1}$)), but they were one order of magnitude higher compared with the hexachlorocyclohexane-isomers. The concentration of triazines in suspension was low, often below the limit of detection ($25\,\mathrm{pg}\,\mathrm{l}^{-1}$).

Introduction

The triazine herbicides (e.g. atrazine, simazine) are the most used pesticides in the world. They amount to about 50% of the world market of pesticides. The greatest quantity is used in U.S.A., France, Japan and Germany. In 1992 Germany produced about 40 000 tons of herbicides (Hock *et al.*, 1995). They are mainly applied to corn, sugar cane and wheat.

The major derivatives of the s-triazines used in Germany are atrazine, simazine and terbuthylazine, they are usually applied pre-emergence as a water dispersed spray or in liquid fertiliser, although preplant and post emergent applications are occasionally used. Triazines enter the Baltic and North Sea via riverine runoffs and atmospheric transport. In Germany atrazine and simazine have been prohibited since 1991 and 1992 respectively.

Triazines are inhibitors of the photosystem II, effecting the electron transport within the chloroplasts. Due to this property, triazines are able to effect phytoplankton, macrophytes, zooplankton benthic invertebrates and fish (Peichel *et al.*, 1985, Stay *et al.*, 1989, Solomon *et al.*, 1996).

Recent investigations of atrazine, simazine and terbuthylazine were carried out in the western Baltic Sea and the Arcona basin by Bester and Hühnerfuβ (1993). They reported on triazine concentrations of $1–13\,\mathrm{ng}\,\mathrm{l}^{-1}$. However, there is a lack of information about the concentration of triazines in the Pomeranian Bight and the coastal areas off Rügen and Usedom. Our investigation gives an overview of the distribution and concentration of major triazines in the pelagial of the Pomeranian Bight.

Lindane or gamma-hexachlorocyclohexane (γ-HCH) is an organochlorine insecticide which had been used worldwide on a wide range of insects. Commercial lindane contains up to 99% percent γ-hexachlorocyclohexane. Technical-grade hexachlorocyclohexane is a mixture of isomers containing 64% α-, 10% β-, 13% γ-, 9% δ- and 1% ε-HCH. These values may vary with the manufacturer. Lindane is highly toxic and persistent. There is sufficient evidence for the cancerogenity of technical-grade hexachlorocyclohexane and α- hexachlorocyclohexane and limited evidence to establish the carcinogenicity to the beta and gamma isomers.

Materials and Methods

Samples were taken during a cruise of R/V "A. v. Humboldt" to the Pomeranian Bight in different seasons in 1995. Applying an in-situ filtration and extraction system (Petrick *et al.*, 1996) at a 5 m depth, samples were separated into dissolved and suspended material. By means of our sampling system the seston was separated by a GF/C-glass filter (Ø=140 mm), precombusted at 500°C. The filtrate (60–160 l) was pumped through an adsorption column, which had been filled with 90 g precleaned XAD-2 adsorption resin. This set-up allowed for extraction of non polar and less polar

substances. The whole sampling procedure lasted for 4–6 hours. The columns were stoppered with glass seals and kept at 4°C. The GF/C-filters were tightly wrapped in aluminium foil and kept deep-frozen.

In the laboratory water samples were processed according to the method of Schulz *et al.* (1995) using a soxlett-extractor modified after Ehrhardt (1987). The XAD-2 were extracted with 150 ml acetonitrile:water (85:15, v:v) for 3 hours. Subsequently the extract was concentrated with a rotary evaporator to 50 ml. To obtain the HCH-isomers the extract was shaken three times with 10 ml hexane for 15 minutes. The combined hexane phases were dried over sodium sulphate and concentrated to a volume of about 100 µl. Thereafter the samples were extracted again three times with 10 ml dichloromethane (DCM) to get the triazines followed by the drying procedure as described for the hexane phase.

The filter samples were shaken for 1 hour with acetonitrile. Thereafter the extract was concentrated to 10–15 ml by a rotary evaporator, 30 ml bidistilled water was added and the solvent was concentrated down to 10 ml to remove acetonitrile. Subsequently the solution was extracted as described before. Lipids were removed by applying an aluminia column. HCH-isomers were estimated by GC, whereas the measurement of the herbicides was performed by using a GC-MS method.

Results and Discussion

Regional distribution

Our study is focused on three triazine derivatives (atrazine, simazine, terbuthylazine) and the α-, β- and γ-isomers of hexachlorocyclohexane. The samples were taken at various seasons and stations along different transects in 1995 (Figure 1). The summer cruise (July 1995) was selected in order to show the regional distribution of pesticides. A strong easterly wind during this cruise was responsible for an Odra outflow, which was directed north-westwards along the coast of Usedom. Due to this reason, strong increasing levels of simazine from North-East-Rügen ($8 \, \text{ng} \, \text{l}^{-1}$) to the Swina mouth ($22 \, \text{ng} \, \text{l}^{-1}$) were observed (transect A, Figure 2). From the total quantity of pesticides used in Poland during 1989, simazine amounted for only 0.5% and atrazine for 3.1% (Zeleckowska 1992). This circumstance implies higher levels of atrazine than those of simazine.
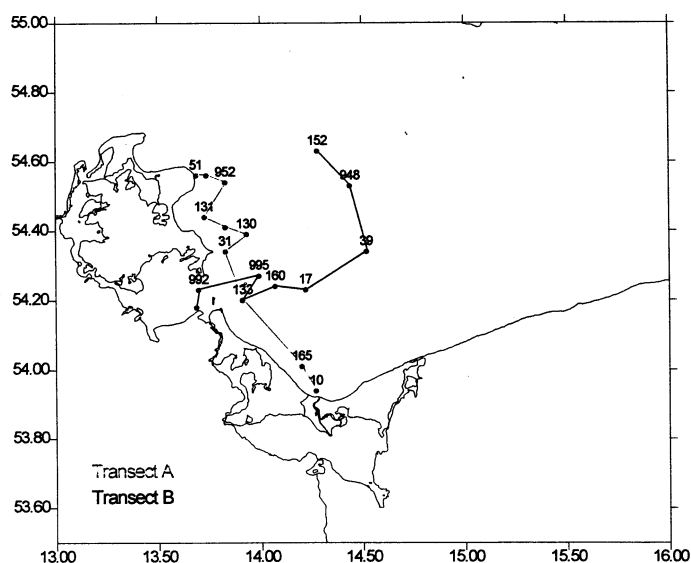
Figure 1 Location of stations during the "A. v. Humboldt" cruise to the Pomeranian Bight in 1995

Along transect B (Figure 2) from the Greifswalder Bodden (station 992) via the Odra Bank to the 25 m depth line (#152) of the outer Pomeranian Bight a strong gradient occurred between station #133 and #160. From the Greifswalder Bodden (#992) to the station #160 and #17 the concentration of simazine decreased from about $15–27 \, \text{ng} \, \text{l}^{-1}$ to less than $5 \, \text{ng} \, \text{l}^{-1}$. At the Odra Bank (#39) slightly higher levels were found. Atrazine followed this trend, but at all stations, it was only half of the levels of simazine. One reason could be the limitations of using atrazine (since 1991) and simazine (since 1992) by the German government. However, on the territory of the former GDR old inventories of both triazines are probably still in use.
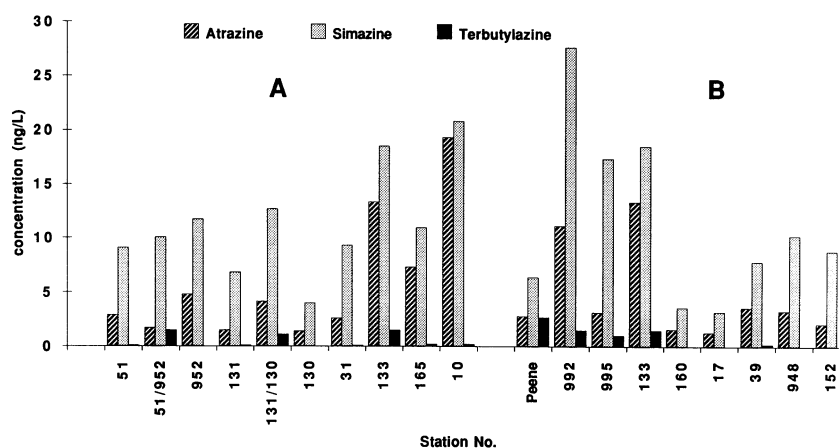
Figure 2 Concentrations of selected triazine components in the Pomeranian Bight in July 1995

Beside the main triazines, terbuthylazine was detected in the area of the Greifswalder Bodden. Concentrations of about $2\,ngl^{-1}$ were analysed, however, with increasing distance to the Bodden their levels reached the limit of detection. The slightly higher levels of terbuthylazine in vicinity to the Greifswalder Bodden in comparison to other areas investigated, may be explained by the intensive agriculture in this region especially the cultivation of sugar cane.

The regional distribution of dissolved lindane and α-HCH, β-HCH at both transects in July 1995 was more homogenous as compared to trazines. On transect A the concentrations of HCH-isomers were in the range of about $100\,pgl^{-1}$ to $300\,pgl^{-1}$ except at station #51, #952 and #133 (Figure 3). At these spots the concentration of the HCH-isomers were relatively high ($400–1050\,pgl^{-1}$). The HCH-concentrations on transect B also showed a homogenous distribution with highest levels at station #133 and lowest at station #152. This finding could be explained by mixing processes by water from the outer Baltic Sea. For this area Gaul (1991) reported on HCH-concentrations of about $4400\,pgl^{-1}$ (α-HCH) and $2200\,pgl^{-1}$ (γ-HCH). Later investigations showed concentrations between $500–1000\,pgl^{-1}$ for α-HCH and $1500–1800\,pgl^{-1}$ for the γ-HCH (Dannenberger 1995). As reported by the latter author we could not detect spatial differences between the alpha- and gamma-isomers of HCH.
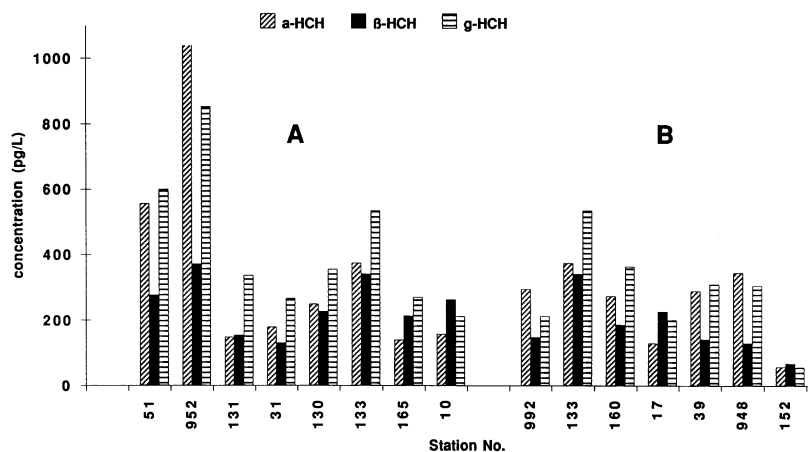
Figure 3 Concentrations of dissolved hexachlorocyclohexane-isomers in the Pomeranian Bight in July 1995

In contrast to the HCH-isomers in solution, a clear spatial distribution was found for HCH-isomers in suspension (Figure 4). From station #51 to #10 their values increased from $10\,pgl^{-1}$ to $70\,pgl^{-1}$. The high amounts of HCH-isomers at station #39 are remarkable, situated on the Odra Bank. Due to the low water depth (8m), it is possible that HCH-isomers bound to sediment particles influenced the distribution of HCH-isomers in the suspended material of the upper water layer. The specific load of SPM by HCH-isomers follows the trend of the absolute concentration of HCHs (Figure 5).
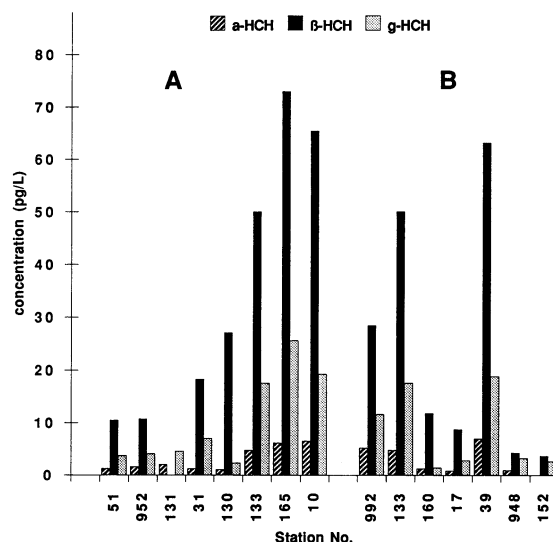
Figure 4 Concentration of suspended hexachlorocyclohexane-isomers in the Pomeranian Bight in July 1995
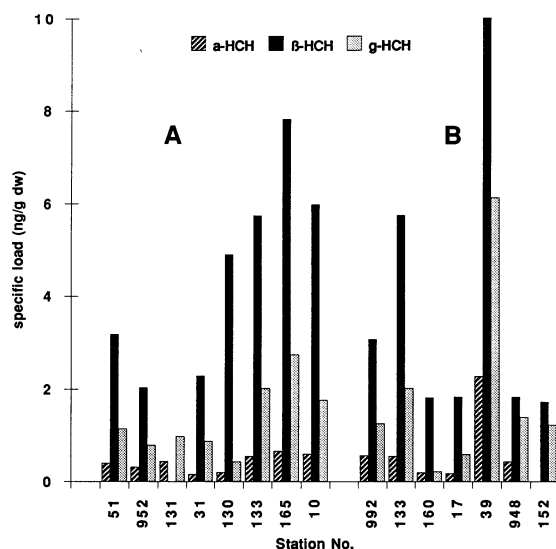
Figure 5 Specific load of HCH-isomers (ngg^{-1} SPM)

Seasonality

The seasonal distribution of trazines and hexachlorocyclohexane-isomers at station #10, #992, #133 and #39 is shown on Figure 6, Figure 7 and Figure 8 respectively.

A pronounced seasonality existed for atrazine and simazine at the Greifswalder Bodden (#992) with highest concentrations in July and April. This is in accordance with the application period for those herbicides, which is mainly in the spring. Lowest levels were found in October when the ground was cultivated. A more or less pronounced seasonality was found for stations #10 and #133.

The comparison of the seasonal distribution of HCH-isomers of the water phase at selected stations indicates a decrease of HCH-levels from January to October (Figure 7). For γ-HCH highest levels were found in January except at station #39 (Odra Bank) The average levels of α- and γ-HCH were slightly higher than those of the beta-isomer (Figure 8). The gamma/alpha-isomer ratio showed only in January at station #10 an enhanced level (γ/α-HCH 3.7), all other values were in the range 1.0–2.0. Investigations by Knauth *et al.* (1993) corroborate our data. These findings indicated an input of "fresh" γ-HCH in winter 1995 from the Swina-mouth. Hühnerfuβ *et al.* (1990) suggests that the relations of concentrations of γ-HCH/α-HCH can be utilised for characterising ages of water body. Water masses stemming directly from river inflows exhibits γ-HCH/α-HCH of 3–4 and older inventories showed values of γ-HCH/α-HCH of about 1.

Less pronounced seasonal variations could be observed for HCH-isomers in suspended material. The beta-isomer was the dominating component of the SPM with values of about 10–65 pg l^{-1}. The HCH-isomers investigated, revealed highest average data in July (α-HCH: 6 pg l^{-1}; β-HCH: 52 pg l^{-1}; γ-HCH: 17 pg l^{-1}) and lowest values in October with 0.5 pg l^{-1} α-, 10 pg l^{-1} β- and 3 pg l^{-1} γ- HCH (Figure 8). The concentration of HCH-isomers in suspension was about 2 orders of magnitude lower than those of the water phase. The specific load of SPM in the Pomeranian Bight compared to the Elbe estuary showed a maximum in late winter as well.

Differences in biological activities and main agricultural application in spring are the major reason of the variabilities of HCH-isomers.
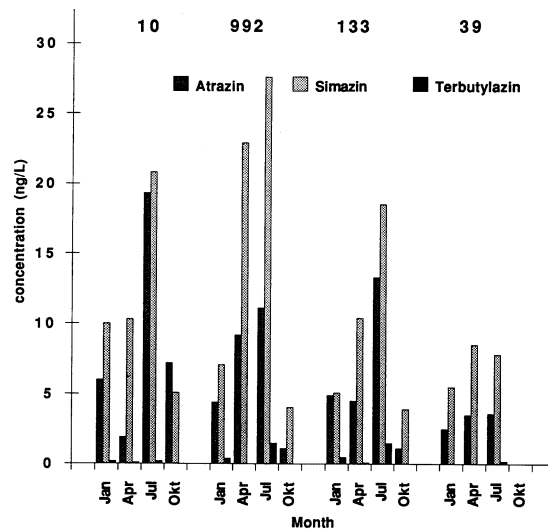
Figure 6 Seasonality of triazines in the Pomeranian Bight in 1995
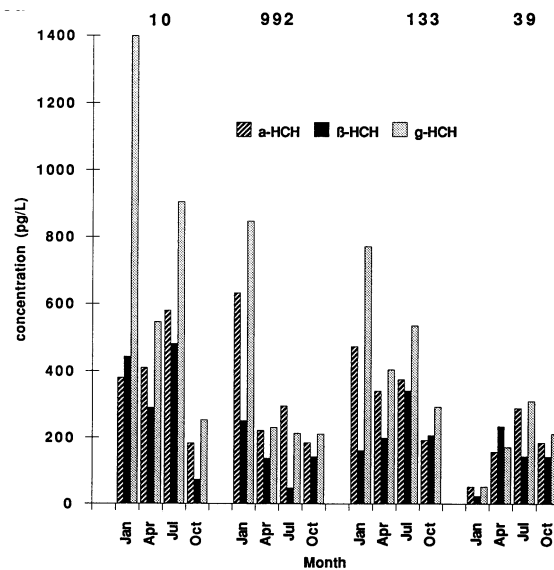
Figure 7 Seasonality of HCH-isomers in solution in the Pomeranian Bight in 1995
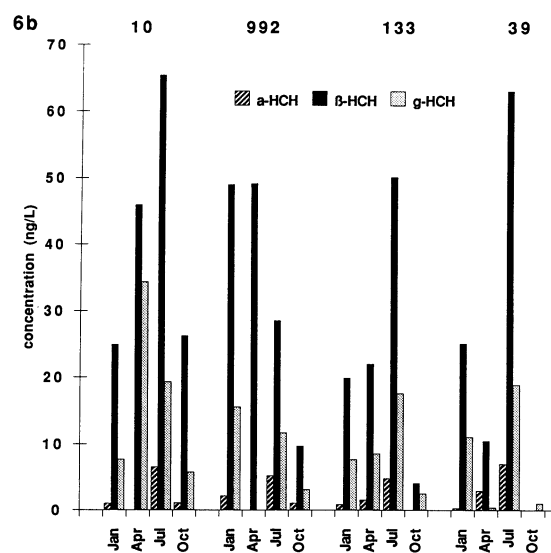
Figure 8 Seasonality of HCH-isomers in suspension in the Pomeranian Bight in 1995

References

Bester, K., and Huhnerfuss, H. (1993). Triazines in the Baltic and North Sea. Mar. Pollut. Bull. 26: 301–312.

Dannenberger, D., and Lerz, A. (1995). The Distribution of Selected Chlorinated Microcontaminants in Baltic Waters, 1992 to 1994. Dt. hydrogr. Z. 47 H5 253–272

Ehrhardt, M. (1987). Lipophilic organic material: An apparatus for extracting solids for their concentration from sea water. ICES, Techniques in the marine environmental science, No.4

Gaul, H. (1991). Temporal and spatial trends of organic micropollutants in sea water of the Baltic Sea, North Sea and NE-Atlantic. In: ICES, Variability Symp. No. 8, Session 1

Hock, B., Fedtke, C., and Schmidt, R.R. (eds.) (1995). Herbizide-Entwicklungen, Anwendungen, Wirkungen, Neben-wirkungen. Thieme Verlag Stuttgart, pp 358.

Huhnerfuβ, H., Dannhauer, H., Faller, J., and Ludwig, P. (1990). Dt. hydrogr. Z. 43 H5 253–272

Knauth, H.-D., Sturm, R., and Gandraβ, J. (1993). Vorkommen und Verhalten organischer und anorganischer Mikroverunreinigungen in der mittleren und unteren Elbe. Forschungsbericht 102 04 363. Umweltbundesamt Berlin (ed), Erich Schmidt Verlag Berlin, pp 1–351.

Peichel, L., Lay, J.P., and Korte, F. (1985). Effects of atrazine and 2,4-dichloro- phenoxyacetic acid to the population density of phyto- and zooplankton in an aquatic outdoor system. J. Water-Wastewater-Res. 18: 217–222.

Petrick, G., Schulz, D.E., and Duinker, J.C. (1988). Clean-up of environmental samples by high-performance liquid chromatography for analysis of organochlorine compounds by gas chromatography with electron-capture detection. J. Chromatogr. 435: 241–248.

Petrick, G., Schulz, D.E., Martens, V., and Duinker, J.C. (1996). An in-situ filtration/extraction system for the determi-nation of trace organics in sea water solution and suspension down to 6000 m depth. Mar. Chern. (in press).

Schulz-Bull, D.E., Petrick, G., Kannan, N., and Duinker, J.C. (1995). Distribution of individual chlorobiphenyls (PCB) in solution and suspension in the Baltic Sea. Mar. Chem., 48: 245–270.

Solomon, K.R., Baker, D.B., Richards, R.P., Dixon, K.R., Klaine, S.J., La Point, T.W., Kendall, R.J., Weisskopf, C.P, Giddings, J.M., Giesy, J.P., Hall, L.W., and Williams, W.M. (1996). Ecological risk assessment of atrazine in North American surface waters. Environ. Toxicol. Chem., 15: 31–76.

Stay, F.S., Katho, A., Rohm, C.M., Fix, M.A., and Larsen, D.L. (1989). The effects of atrazine on microcosms developed from natural ponds. Arch. Environ. Contam. Toxicol. 18: 866–875.

Zeleckowska, A. (1992). Pesticides in the surface waters of Poland and agricultural pollution. Proceedings of the HELCOM workshop on from diffuse sources, Nov. 1992, Gdansk, Presentation No 13.

GOBEX: Gotland Basin Experiment—a European research initiative

E. Hagen, K.-Ch. Emeis, and Ch. Zülicke

Objective and Methodology

The Gotland Basin Experiment (GOBEX) was an international multidisciplinary study of all riparian countries of the Baltic Sea during 1994–1995. Its planning was funded by the European Committee on Ocean and Polar Sciences (ECOPS) which is partly sponsored by the European Science Foundation (ESF). The GOBEX activities were considered as preparation for the start of investigations, which should be carried out by the EU funded project BASYS (Baltic Sea System Study) during the MAST-III period (1996–1999).
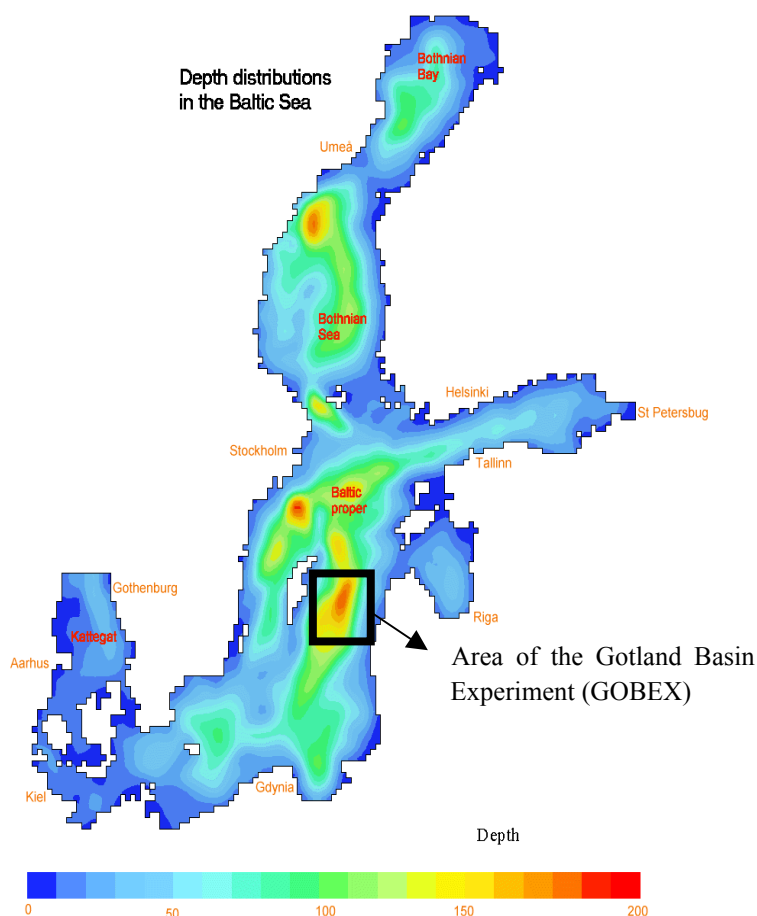
Figure 1 The main area of investigation for GOBEX

Several workshops elucidated the main objectives for joint efforts. The principal aim of the project was a better understanding of the water exchange processes between coastal areas and central parts of the Eastern Gotland Basin and their consequences for the ecosystem of the 'Baltic Proper'. The area under consideration is shown in Figure 1 while identified research topics are compiled in Figure 2.

GOBEX

Air-Sea Exchange
Baltic Sea—North Sea Water Exchange and General Circulation
Inshore and Coastline Processes
Coastal—Basin Interactions

Data Management and Ecosystem Analysis

Food Web Dynamics and Berthic-Pelagic Coupling
Processes of Anthropogenic Influence
Paleoenvironment
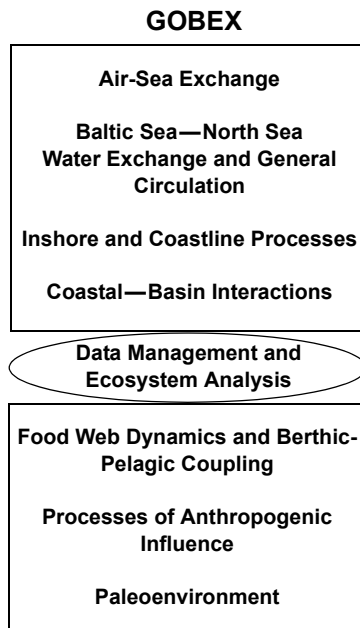
Figure 2 GOBEX research topics

Scheduled field campaigns should be concentrated in the Eastern Gotland Basin. It was recommended that most of the hydrographic station positions coincide with those of the Baltic Year (BY) programme, which was carried out in 1969–1970. These efforts included, inter alia, the quantification of various past and present fluxes between different inorganic and organic compartments, different ecological zonations and food webs. In a first approximation step there were the setup of four working groups:

- Meso-scale dynamics
- Benthic processes
- Data management—hydrography/geology
- History of the Baltic Proper

Such an approach involves all marine disciplines working on different temporal and spatial scales. For example, sedimentation processes of the basin scale should be influenced by the deep water circulation, associated water-mass transformation, and related mixing and exchange processes, which are based on different physical mechanisms. Their better understanding is needed for the development of an integrated model describing these relationship in a proper way.
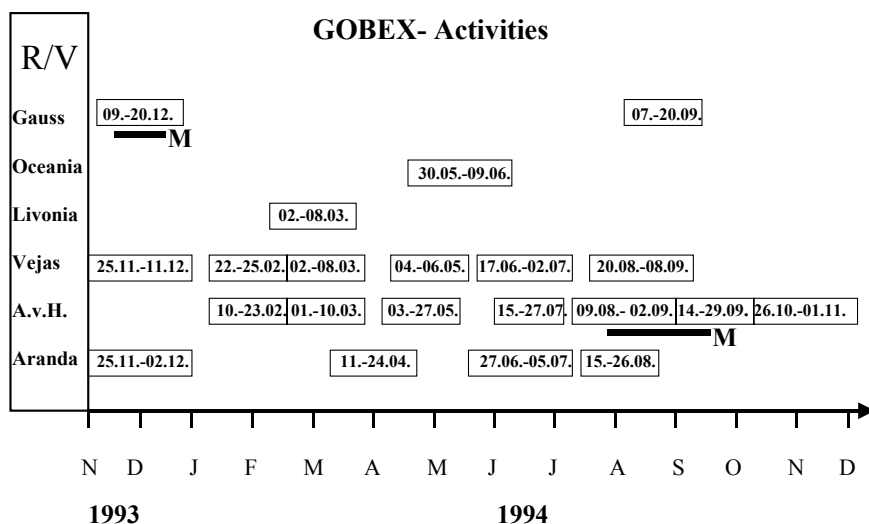
Figure 3 Time table summarising all cruise activities of participating research vessels (R/V: A.v.H. = "Alexander von Humboldt") and moored current measurements (M) in the area shown in Figure 1

The GOBEX programme only provided the first step in that direction. The success of marine investigations strictly depends on planned cruise logistics as well as on the ease of data access. The management of the national hydrographic data was, for instance, supported by the ICES in Copenhagen/Denmark. In summary, Figure 3 depicts the timetable of all cruise activities. Time windows of moored current measurements are also indicated. Their logistics were coordinated by the Institute for Baltic Sea Research Warnemünde (IOW)/Germany. Relevant news was distributed monthly/bimonthly via e-mail as the GOBEX-Newsletter, which served for a fast presentation of preliminary results as well as for logistics, data exchange, device calibration procedures, guest researchers, etc.

Selected Research Topics

The interdisciplinary research was conducted mainly in hydrography and geology. For instance, the GOBEX hydrographic data set of the IOW was represented by Zülicke and Hagen (1997) while the corresponding status report of geological efforts was provided by Emeis and Struck (1998). With respect to further details we refer to Neumann *et al.* (1997), Emeis *et al.* (1998), and Kunzendorf *et al.* (1998). From the hydrographic point of view, first scientific results were published in the GOBEX Summary Report (Baltic Marine Science Reports, Vol.19, Baltic Sea Research Institute Warnemünde, 1996). Here, we briefly introduce the major research topics and quote a selection of results from the report. Central topics of hydrographic investigation were:

- Parametrisation of exchange processes between atmosphere and ocean acting on different temporal and spatial scales
- How do the sporadically appearing salt water inflows affect the water masses below the halocline in different Baltic basins?
- For which time scales does water exchange between the basins take place and what are the basic trigger mechanisms that start sill overflow?
- How does the basin ecosystem at different trophic levels react on a salt water inflow?

Joint experimental and theoretical studies are necessary for a sufficient description of dynamics within the turbulent surface mixed layer. Released mixing controls all fluxes between atmosphere and ocean. It is usually parametrised by exchange coefficients describing the vertical momentum transfer. Acceptable values can be estimated at the base of 1-hour means of meteorological standard parameters and radiometer measurements, Zülicke *et al.* 1996. Microstructure measurements in coastal zones and central parts of deep Baltic basins indicate the magnitude of $10^{-6}\,\mathrm{W\,kg^{-1}}$ for the associated dissipation rate of kinetic energy, Stips (1996). In open Baltic areas, most of the dissipation results from a local production via the Reynolds-stress. Within coastal zones, however, patches of enhanced dissipation rates are frequently not balanced locally. Coastal jets sporadically advect intensified dissipation patches, cf. Zülicke and Henning (1996), Zülicke *et al.* (1996), and Zülicke *et al.* (1998). Resulting eddy diffusivities fluctuate in the relatively large range between 10^{-2}–$10^{-4}\,\mathrm{m^2\,s^{-1}}$.

Following Elken *et al.* (1988) with respect to the existence of eddy-like water lenses in deep layers of the Eastern Gotland Basin, the IOW carried out an expedition with R/V "Alexander von Humboldt" during 14–29 September, 1994. Its main objective was the study of the exchange of deep water from the Bornholm Basin through the Stolpe Furrow into the Gotland Basin. Inter alia, time series measurements for over three days (22.09.95-06:00–25.09.95-03:00 UTC) were done at the Baltic Year station BY15A, just above the Gotland Deep. The series was sampled once per hour to resolve short-term fluctuations. The temporal behaviour of isopycnals is plotted in Figure 4. The intrusion of denser water ($PD>9.7\,\mathrm{kg\,m^{-3}}$) occurs in layers deeper than 200 m for about 40 h. This has to interpreted as a hint for the existence of temporal/spatial changes in the baroclinic mass field with a time scale of a few days.

Their origin and associated trigger mechanisms are still unclear. Such events could be caused by single baroclinic eddies travelling with the deep background circulation or it could be ingredients of topographically trapped low-frequency waves. Nevertheless, there is some observational evidence that such eddy-like phenomena start in the transition area between the Stolpe Furrow and the entrance of the Eastern Gotland Basin, Zhurbas and Paka (1996). It is expected that associated fluctuations in the motion field rhythmically modify the deep circulation in the central part of the Eastern Gotland Basin. Current measurements, which were carried at three positions along the 220 m depth contour during two weeks in November 1993, suggest a cyclonic deep water circulation with velocities between $2\,\mathrm{cm\,s^{-1}}$ and $6\,\mathrm{cm\,s^{-1}}$, Mittelstaedt (1996).
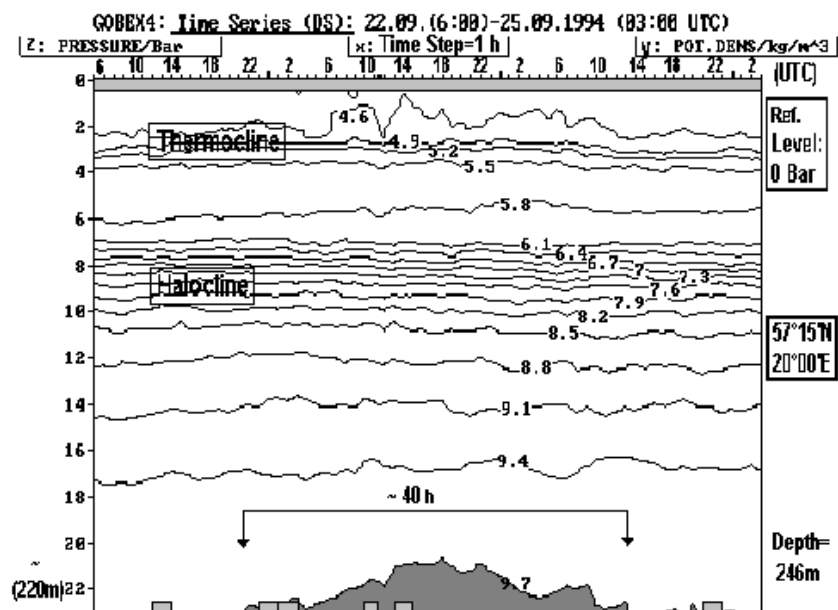
Figure 4 Plotted time series of the potential density (PD) sampled with a time step of 1 h at the position of station BY15A above the Gotland Deep according to Hagen and Feistel (1996); PD > 9.7 kg m^{-3} is black

Sporadically occurring intrusions of dense deep water into the deepest parts of the basin elucidate not only their impact on changed hydrochemical conditions, cf. Nausch and Matthäus (1996), but also on sedimentation and deposition. Relevant research topics of geological efforts were:

- Which accumulation rates have to be expected for inorganic/organic material in different Baltic basins during the seasonal cycle?
- At which spatio-temporal scales does the sedimentation in the basins proceed under distinct hydrographic conditions?
- Is it possible to reconstruct the ecosystem state from sediments and to explain its temporal response on hydrographically determined changes in the past?

The analysis of porewater, which is based on three sediment cores sampled at 68 m, 112 m, and 236 m water depth, revealed that each of them indicates a different amount of organic matter as well as different redox-conditions, Matthiesen (1996). During August 1994 two cruises with R/V "Alexander von Humboldt" were carried out to the GOBEX area. In particular, signals of inflows to the Gotland Basin in the sedimentary record were studied by Christiansen and Kunzendorf (1996). The analysis of a multicore probe near the station BY15A showed the following results: Significant peaks in the Fe and Mn concentrations were also found in the 70 and 100 mm level. These can be attributed to the 1971 and 1951 salt water inflow with the 210Pb dating method. This finding suggests that inflows not only may be observed in concentrations of imported elements. Hence, it seems to be possible to recognise such events from sediments from ancient times and to increase knowledge on the cyclic behaviour of their appearance.

References

Christiansen Ch., and Kunzendorf, H. (1996). Signals of inflows to the Gotland Basin in the sedimentary record. In: E. Hagen (Editor), GOBEX—Summary Report. Meereswissenschaftliche Berichte, No.19. Institut für Ostseeforschung Warnemünde, 10–13.

Elken, J., Pajuste, M., and Kouts, T. (1988). On intrusive lenses their role in mixing in the Baltic deep layers. Proceedings of the 16th Conference of the Baltic Oceanographers, Institute of Marine Research Kiel, Kiel, 367–376.

Emeis, K.C., Neumann, T., Endler, R., Struck, U., Kunzendorf, H., and Christiansen, Ch. (1998). Geochemical records of sediments in the Gotland Basin—products of sediment dynamics in a not-so-stagnant anoxic basin? Applied Geochemistry, 13, 349–358.

Emeis, K.-C., and Struck, U. (Editors) (1998). Gotland Basin Experiment (GOBEX): Status report on investigations concerning benthic processes, sediment formation and accumulation. Meereswissenschaftliche Berichte, No. 34., Institut für Ostseeforschung Warnemünde, 1–122.

Hagen, E., and Feistel, R. (1996). Lenses of relative saline deep water in the Eastern Gotland Basin. In: E. Hagen (Editor), GOBEX—Summary Report. Meereswissenschaftliche Berichte, No.19. Institut für Ostseeforschung Warnemünde, 34–37.

Kunzendorf, H., Emeis, K. C., and Christiansen, Ch. (1998). Sedimentation in the Central Baltic Sea as viewed by non-destructive Pb-210 dating. Danish Journal of Geography, 98, 1–9.

Matthiesen, H. (1996). Fe and S in sediment from 3 stations from the GOBEX area. In: E. Hagen (Editor), GOBEX—Summary Report. Meereswissenschaftliche Berichte, No.19. Institut für Ostseeforschung Warnemünde, 15–19.

Mittelstaedt, E. (1996). The subsurface circulation in the Gotland Deep. In: E. Hagen (Editor), GOBEX—Summary Report. Meereswissenschaftliche Berichte, No.19. Institut für Ostseeforschung Warnemünde, 20–23.

Nausch, G., and Matthäus, W. (1996). Present changes of the hydrographical and hydrochemical situation in the Gotland Deep. In: E. Hagen (Editor), GOBEX—Summary Report. Meereswissenschaftliche Berichte, No.19. Institut für Ostseeforschung Warnemünde, 30–33.

Neumann, T., Christiansen, Ch., Clasen, S., Emeis, K. C., and Kunzendorf, H. (1997). Geochemical records of salt-water inflows into the deep basins of the Baltic Sea. Cont. Shelf Res., 17(1), 95–115.

Stips, A. (1996). First investigations of the near surface turbulence structure and energy dissipation caused by wind mixing in the Baltic Sea. In: E. Hagen (Editor), GOBEX—Summary Report. Meereswissenschaftliche Berichte, No.19. Institut für Ostseeforschung Warnemünde, 64–75.

Zhurbas V. M. and Paka, V.T. (1996). Observations of meso-scale eddy-like structures and thermohaline intrusions in the Gotland Basin after the 1993 Major Baltic Inflow. In: E. Hagen (Editor), GOBEX—Summary Report. Meereswissenschaftliche Berichte, No.19. Institut für Ostseeforschung Warnemünde, 38–63.

Zülicke, Ch., Schuffenhauer, I., and Stips, A. (1996). Baltic measurements of turbulence in the surface mixed layer. In: E. Hagen (Editor), GOBEX—Summary Report. Meereswissenschaftliche Berichte, No.19. Institut für Ostseeforschung Warnemünde, 76–91.

Zülicke, Ch., and Hagen, E. (1997). GOBEX Report: hydrographic data at IOW. Meereswissenschaftliche Berichte, No.21. Institut für Ostseeforschung Warnemünde, 1–72.

Zülicke, Ch., Hagen, E., and Stips, A. (1998). Dissipation and mixing in a coastal jet: a Baltic Sea case study. Aquatic Sciences, 60 (3), 220–235.

Zülicke, Ch. and Henning, O.(1996). Surface energy fluxes and mixed layer depth. In: E. Hagen (Editor), GOBEX—Summary Report. Meereswissenschaftliche Berichte, No.19. Institut für Ostseeforschung Warnemünde, 92–104.

Hydrographic investigations in the Fehmarn Belt in connection with the planning of the Fehmarn Belt link

Flemming Jakobsen, Niels H. Petersen, Helmer M. Petersen, Jacob S. Møller, Thomas Schmidt, and Torsten Seifert

Abstract

The hydrographic investigations in connection with a Fehmarn Belt link connecting Denmark and Germany are being carried out by the Fehmarn Belt Environmental Consultants as subconsultant to COWI-Lahmeyer Joint Venture. The clients are Trafikministeriet (Denmark) and Bundesministerium für Verkehr (Germany). The planning of the Fehmarn belt link will involve environmental design criteria, but these are not finally decided yet. Phase I of the preliminary investigation was carried out from December 1, 1995 to June 1, 1996 and included collection and analysis of hydrographic data, as well as 3-dimensional simulations of the flow in the Fehmarn Belt by two independent oceanographic models. Some results from the investigations are outlined, e.g. the flow distribution in the Fehmarn Belt and the size and importance of the blocking of the planned link solutions. During phase II a permanent monitoring programme outlined for 3-dimensional simulations was installed. The first measurements from the programme are presented.

Introduction

The hydrographic investigations in connection with a Fehmarn Belt link connecting Denmark and Germany are being carried out by the Fehmarn Belt Environmental Consultants (FEC). FEC consists of the Danish Hydraulic Institute, Water Quality Institute, Institut für Ostseeforschung Warnemünde and LIC engineering. FEC act as a subconsultant to the COWI-Lahmeyer Joint Venture. The clients are Trafikministeriet (Denmark) and Bundesministerium fur Verkehr (Germany). The sole responsibility for the contents of the present paper lies on the authors.

The planning of the Fehmarn Belt link will involve environmental design criteria. The Great Belt and the Øresund link involve the environmental design criteria, that the links should not alter the transport of water and salt (zero blocking solutions), thereby ensuring that no change in the physical and biological conditions should occur in the Baltic Sea due to the links. The zero blocking solutions are achieved by compensating the increased flow resistance induced by bridge piers and causeways by means of dredging close to the link (Møller & Ottesen Hansen, 1990). The design criteria for the Fehmarn Belt link are not yet finally decided.

Phase I of the environmental investigation by FEC was carried out from December 1, 1995 to June 1, 1996 and included collection and analysis of hydrographic data (Trafikministeriet, 1996; COWI-Lahmeyer, 1996A + B), as well as 3-dimensional simulations of the flow in the Fehmarn Belt by two independent oceanographic models (COWI-Lahmeyer, 1996C). The 3-dimensional simulations were used to investigate the influence of 7 different link solutions. Also oxygen conditions, sediment transport and coastal morphology are investigated by FEC, but are not treated further in the present paper.

During phase II, amongst other things, a permanent monitoring programme outlined for 3-dimensional simulations has been installed. The monitoring programme was measuring on October 15, 1996 and is planned to be stopped on October 15, 1997. As part of the monitoring programme two surveys of two weeks each, are planned to take place as follows: one in January 1997 and one in August 1997.

The paper is divided as follows. Firstly, the important features regarding the overall and local hydrography are outlined. Secondly, the velocity distribution in the Fehmarn Belt is discussed. Thirdly, the investigated link solutions are outlined and the blocking of the link solutions is related to other influences. Finally, the most important conclusions are summarised.

Hydrographical introduction

The drainage basin of the Baltic Sea is $1\,721\,200\,\mathrm{km}^2$ and the mean (1921–75) river inflow is determined to be $14\,895\,\mathrm{m}^3\mathrm{s}^{-1}$, see HELCOM (1986). This inflow of fresh water combined with the inflow of high saline water from the

North Sea creates a stratified system in the Baltic Sea. During periods with decreasing river inflow the salinity at the surface at Anholt will increase and vice versa, see Figure 1. The close and strong correlation between the river inflow and the hydrography of the Baltic demonstrates the sensitivity of the Baltic to changes within the boundary conditions (including the bathymetry of the transition area). The influence of a link can crudely be imagined as a very small but systematic increase in the river inflow.
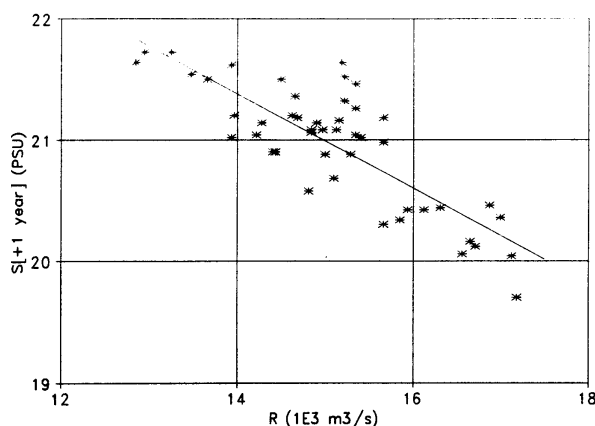
Figure 1 The relation between the five-year moving average surface salinity at Anholt and the five-year moving average river inflow into the Baltic Sea, where the salinity is compared to the river inflow one year earlier. Based on river inflow data in HELCOM (1986) and salinity data in Svansson (1975), though the yearly mean salinity in 1914 was corrected to be 20.7 PSU.

The Baltic Sea has changed considerably on several time scales, see e.g. Møller & Hansen (1994). Such changes are important when considering a zero-solution of a bridge construction in the transition:

• how large and rapid are the natural changes compared to the influence of the construction?

• is it possible to observe and/or measure a change caused by a fixed link?

Seen on the geological time scale, bathymetrical changes are the main reasons for the changing conditions of the Baltic Sea. Today we still experience a land elevation of up to 1 cm per year in the northern part of the Baltic Sea, while there is no elevation in the Danish Straits (Binderup & Frich, 1993). Measurements of the hydrographic conditions in the Baltic Sea have existed through the last 120 years. The time series show a fluctuating pattern for the parameters measured: e.g. salinity, temperature and oxygen; and also for some parameters, a general trend (Matthäus, 1979). In the future, the green house effect will inevitably affect the hydrography of the Baltic, see later.

Local hydrography

The Fehmarn Belt, the Kiel Bight and the Mecklenburg Bight are part of the Belt Sea (Figure 2), which hydrographically forms part of the transition area between the Baltic Proper and the North Sea. It is important to note the shallow Darss Sill (~18 m depth) between the Fehmarn Belt and the Arkona Sea, which acts as a salt water trap, and the 90 degrees turning from the Langelands Belt to the Fehmarn Belt.

The water masses in the Belt Sea and the Kattegat consist of low saline water from the Baltic Proper, which, close to the surface, flows through the Belt Sea and the Kattegat, and high saline water from the North Sea, which forms a lower layer. In June, the wind conditions are weak, and the two-layer exchange flow between the North Sea and the Baltic Proper is clearly identified to provide a strongly stratified water column in the Belt Sea, see Figure 3 and Figure 4. In December, the wind conditions are strong whereby the stratification is destroyed by mixing of the water masses, see also Matthäus & Franck (1992) and Jakobsen (1995) on major inflows during this season.
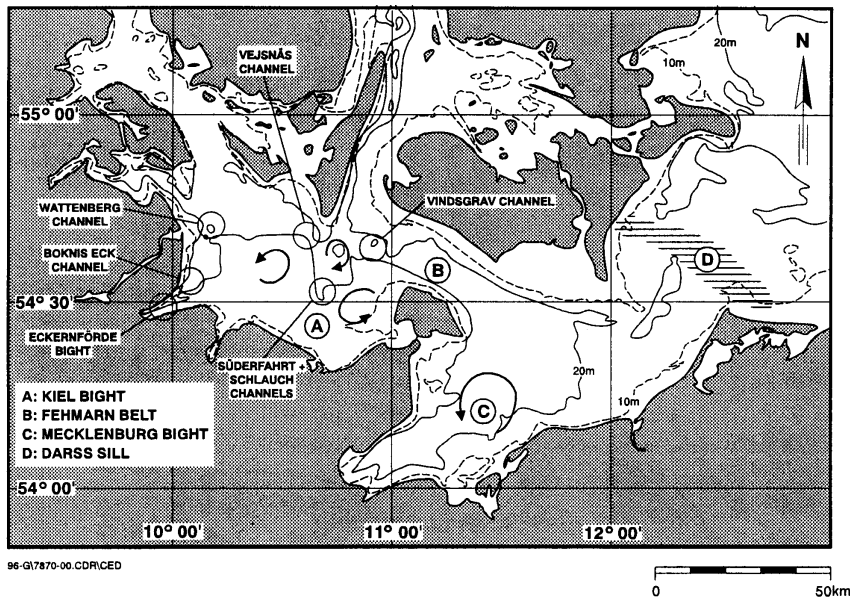
Figure 2 Detailed map of the near Fehmarn Belt area. In the Kiel Bight three topographic fixed eddies are shown, and in the Mecklenburg Bight one quasi-stationary eddy is shown.
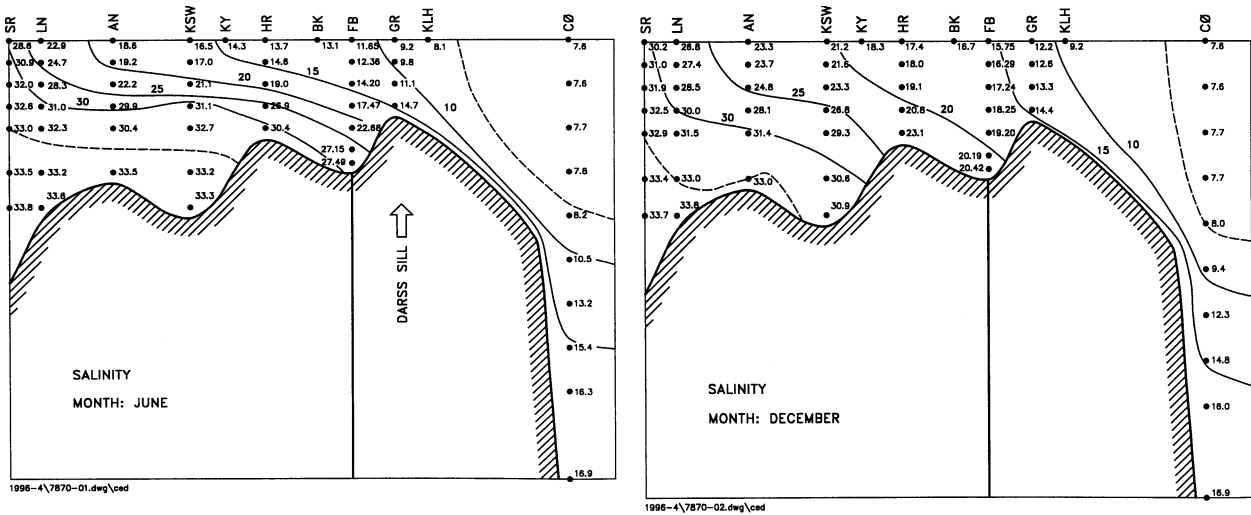
Figure 3 Cross-section showing the longitudinal salinity distribution as monthly means from Skagerrak through Fehmarn Belt and into the Baltic Proper (the vertical link shows the position of the planned link). Drawn by data given in Sparre (1984A), Lange *et al.* (1991) and Jakobsen (1991).
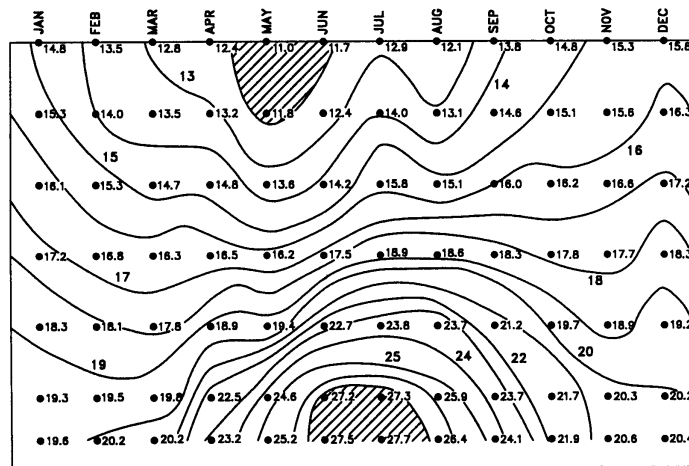
Figure 4 The yearly salinity variation at Fehmarn Belt lightship based on monthly average conditions presented in Lange *et al.* (1991). The hatching shows the minimum and maximum salinity.

The short-term variation of the hydrography is mainly determined by the meteorological variations: westerly winds force inflow while easterly winds force outflow. The winds are controlled by high and low pressures passing Scandinavia at a time scale of about one week, see Stigebrandt (1980) and Lass *et al.* (1987).

A typical situation changing between in- and outflow can be described as follows. During an inflow to the Baltic Proper the salinity of the inflowing water is higher than the Baltic Proper surface water, which causes the inflowing water to plunge south of the Darss sill, see COWI-Lahmeyer (1996B). The plunging position is also referred to as the Belt front. When the current changes from in- to outflowing most of the water with a salinity higher than 10–15 PSU, which passed the sill during the inflow, continues to flow into the Baltic Proper along the bottom. One may consider the sill as a salt water trap. At the beginning of an outflowing current situation, water with a salinity of 10–15 PSU from the Baltic Proper flows as a plume into the Belt Sea across the Darss sill, pushing and entraining Kattegat surface water with a salinity of approximately 20 PSU down and out. The flushing time scale of the sill area is less than 2 days. A front between the Baltic Proper and Kattegat surface water masses is present, it moves outwards and out of the Belt Sea within one week. If the strong wind and current conditions cease, the system will rapidly develop into a two-layer system even at the Darss sill. Thus, moderate, high saline Kattegat surface water is baroclinically transported into the Baltic Proper.

Statistically, the surface current in the Fehmarn Belt shows inflow during 47% of time and outflow during 54% of time, while the current near the bottom shows inflow during 67% of time and outflow during 33% of time, see Lange *et al.* (1991). The inflow is thus more frequent in the lower layer. Most inflow situations at the surface have a duration less than 3 to 5 days, while outflow situations tend to last 1 or 2 days longer. The longest inflow situation lasted 14 days, and the longest outflow 17 days. Near the bottom, the inflow has a typical duration of 3 to 5 days, with the longest situation observed lasting 21 days. Outflow is very rare but has occurred with durations up to 5 to 7 days.

The velocity distribution

The velocity distribution along the alignment is very important when designing the link. On the basis of historical measurements some information can be obtained, see Figure 5.
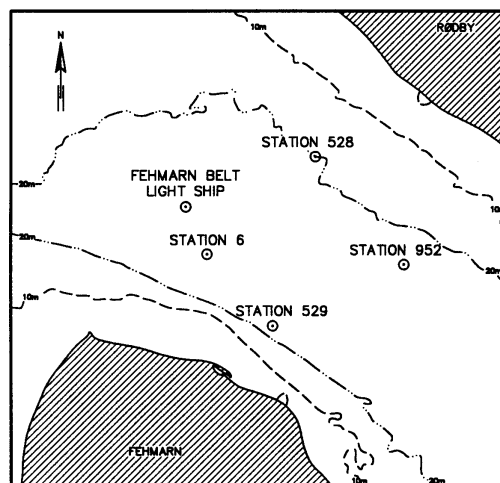
Figure 5 The position of the stations in the Fehmarn Belt area.

The surface current roses in Figure 6 show two main current directions in the upper layer: A) towards WNW or NW, which is out of the Baltic Proper; and B) towards ESE or SE, which is into the Baltic Proper. The main directions are not as clearly defined at a 20 m depth.
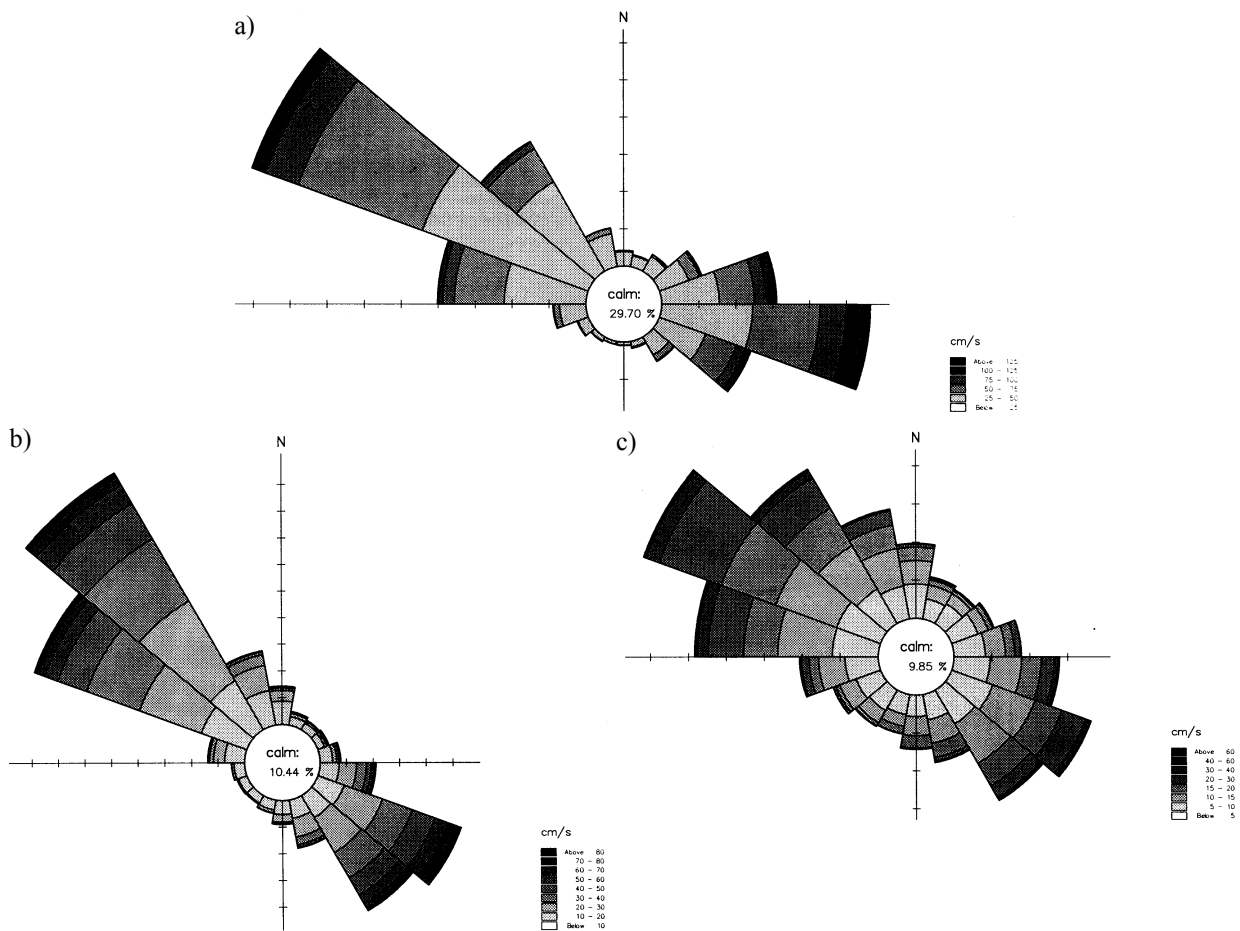
Figure 6 Current roses: a) at Fehmarn Belt lightship during the period 1970 to 1984
b) station 528 during the Belt Project at 7 m depth
c) station 528 during the Belt Project at 20 m depth.

Comparison of the current at Fehmarn Belt lightship and at 7 m depth at station 528 shows, in Figure 7, that the current magnitudes and direction are highly correlated (secondary flow seems not too important).

On this basis: current roses and comparison; we may assume that the current in the Fehmarn Belt is strongly related to the bathymetry and the water exchange, and only weakly related to secondary flows (eddies)—it behaves in many respects as a channel. This will be further elucidated through the ongoing field measurement programme.

Three DYNOCS field campaigns have been carried out with R/V "Prof. A. Penck" in the Fehmarn Belt area. Unfortunately, the survey lines did not cover the area close to the Danish coast. Still, based on the surveys, the following conclusions were made. In the quasi-stationary situation in the upper layer by far the most water exchange takes place as a unidirected current, while in the lower layer only a weak counter-current takes place. During transient situations, the current features might be much more complicated, but this is not considered important, because these situations are characterised by short duration and weak currents.
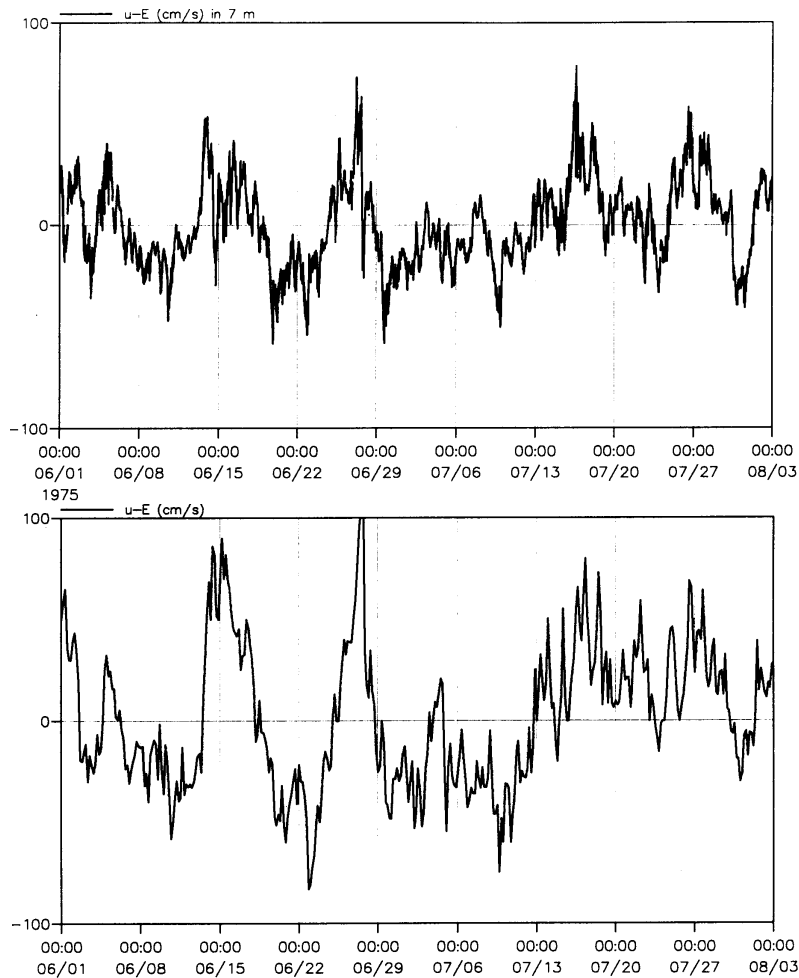
Figure 7 Current development at station 528 at 7 m depth (above) and at the Fehmarn Belt lightship (below).

Hardtke (1978) presented the velocity distribution in the Fehmarn Belt during inflow to the Baltic based on ship measurements, see Figure 8. The distribution shows an outflow near Lolland. In Pedersen (1996) it is argued that the outflow near Lolland is a typical feature during inflow to the Baltic.
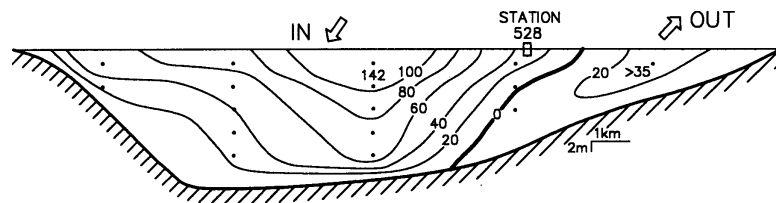
Figure 8 The velocity distribution in the Fehmarn Belt during inflow to the Baltic based on ship measurements from 15.00 to 16.30 on 27 June, 1977.

The current speed towards N at station 532 at 10 m depth in Langelands Belt, towards E at station 528 at 12 m depth and at Fehmarn Belt lightship is shown in Figure 9. The measurements in Langelands Belt show a constant inflow to the Baltic during the period, while a redistribution is seen in the Fehmarn Belt with a current change near Lolland. Investigating the salinity variations revealed that the current change near Lolland is caused by up-welling of dense bottom water, which only very rarely takes place, see COWI-Lahmeyer (1997).
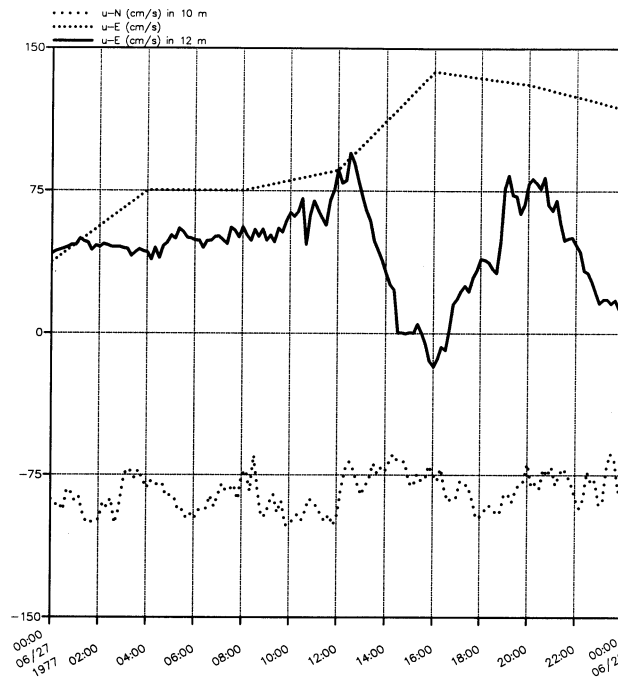
Figure 9 Current speed towards N at station 532 at 10 m depth in Langelands Belt, and towards E at station 528 at 12 m depth and at Fehmarn Belt lightship.

The seven link solutions and the blocking

Seven link solutions were investigated during phase I. Some of these solutions were divided into sub-solutions with minor variations. A description of the link solutions and the resistance of the link calculated by hand are given in Table 1. 3-dimensional simulations were also used to rank the solutions (COWI-Lahmeyer, 1996C). The model area only covered the Kiel Bight, Fehmarn Belt and Mecklenburg Bight: the model boundaries were not placed in infinite un-influenced basins and thus do not show the actual resistance of the links. On basis of the hand calculations and the 3-dimensional simulations the solution model 6.0 was ranked as the most blocking solution.

		Variant	Tunnel roof above s. b.	K_U $(10^{-13}s^2m^{-5})$	K_L $(10^{-13}s^2m^{-5})$
TUNNEL	Bored railway tunnel with/without shuttle service	1.0	-	0.06	1.0
	Immersed railway tunnel with/without shuttle service	2.0	0 m	-	-
		2.1	4–6 m	0.06	2.4
	Bored tunnel for road and rail	4.0	-	0.06	1.0
	Immersed tunnel for road and rail	5.0	0 m	-	-
		5.1	4–6 m	0.06	2.4
COMBI	Bridge and immersed tunnel, transition island for road and rail	6.0	0 m	2.0	23.1
BRIDGE	Cable-stayed bridge for rail and road. Coast–coast	3.0	-	1.0	9.2
		3.1	-		
	Suspension bridge for road and bore tunnel for rail	7.0	-	1.0	9.2

Table 1 A description of the link solutions and the resistance of the link calculated by hand in COWI-Lahmeyer (1996A)

Comparison with other influences

The blocking of the link solution should, if possible, be related to other impacts on the hydrographic system as will be done in the following section.

The immediate transport through the straits can be related to the water level difference between the Baltic Proper and the Kattegat by the following transport-equation:

$$\overline{\Delta\eta} \approx K_{B\varnothing}abs(\overline{Q})\overline{Q} \tag{1}$$

where $\Delta\eta$ (m) is the water level difference from the Baltic Proper to the Kattegat,
$K_{B\varnothing}[s^2m^{-3}]$ is the 'resistance' and
$Q[m^3s^{-1}]$ is the discharge.

The resistance through the Great Belt and the Fehmarn Belt (K_{GB}) is determined to be

$38\cdot10^{-12}[s^2m^{-5}]$ (Jacobsen, 1980),

through the Little Belt and the Fehmarn Belt (K_{LB}) to be

$3439\cdot10^{-12}[s^2m^{-5}]$ (recalculated according to equation (1), see Jakobsen & Ottavi, 1996),

and through the Øresund ($K_{\varnothing}$) to be approximately

$239\cdot10^{-12}[s^2m^{-5}]$ (Jakobsen $et\ al.$, 1996).

The resistance through the Great and Little Belt Sea can be calculated to be:

$$K_B = \frac{K_{GB}K_{LB}}{(\sqrt{K_{GB}}+\sqrt{K_{LB}})^2} = 31.1\cdot10^{-12}[s^2m^{-5}] \tag{2}$$

and through the Belt Sea to be:

$$K_{B\varnothing} = \frac{K_BK_{\varnothing}}{(\sqrt{K_B}+\sqrt{K_{\varnothing}})^2} = 16.4\cdot10^{-12}[s^2m^{-5}] \tag{3}$$

The Great Belt link **without** compensation dredging increases the resistance in the Great Belt (K_{GB}) by

0.38–$0.77\cdot10^{-12}[s^2m^{-5}]$

corresponding to a blocking of the gross flow through the Belt Sea of 0.33–0.66%, while the Øresund link **without** compensation dredging increases the resistance in Øresund ($K_{\varnothing}$) by

$2.41\cdot10^{-12}[s^2m^{-5}]$

corresponding to a blocking of the gross flow through the Belt Sea of 0.13%, see also Stigebrandt (1992). The Little Belt links increase the resistance in Little Belt ($K_{\varnothing}$) by

$48.2\cdot10^{-12}[s^2m^{-5}]$

(recalculated according to equation (1), see Jakobsen & Møller, 1996) corresponding to a blocking of the gross flow through the Belt Sea of 0.05%. Disregarding solution model 6.0 the Fehmarn Belt link **without** compensation dredging increases the resistance in the Fehmarn Belt (K_B) by a maximum of

$0.06\cdot10^{-12}[s^2m^{-5}]$ (bridge solution assuming the upper and lower layer to be parallelly connected)

corresponding to a blocking of the gross flow through the Belt Sea and Øresund of 0.07%. The maximum blocking is thus approximately equal to the blocking of the Little Belt links.

To evaluate the greenhouse effect on the Baltic Sea we shall at this point only consider the water rise of 0.4–0.6 m (DMI, 1992). The decrease in the resistance may be evaluated on the basis of the following equation, see DHI/LIC (1995):

$$Blocking = -3\frac{\Delta\eta}{H} \approx -3\frac{0.5m}{25m} = -6.0\% \tag{4}$$

where H is a typical water depth in the Belt Sea. This shows that the changes due to the expected green house effects are two order of magnitude larger than the influence of the Fehmarn Belt Link.

The phase II monitoring programme

The monitoring stations during phase II are shown in Figure 10. Two ADCPs are placed on the bottom in the investigated alignment. During the surveys, effort will be made to investigate the flow distribution along the alignment.
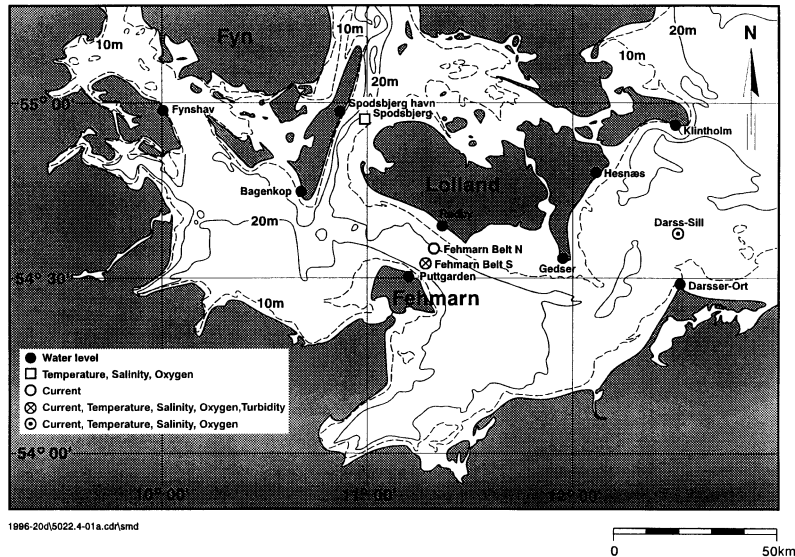
Figure 10 The monitoring stations during phase II

Figure 11 shows some of the first measurements from the monitoring station. The measurements only cover a very short period and are not analysed yet.
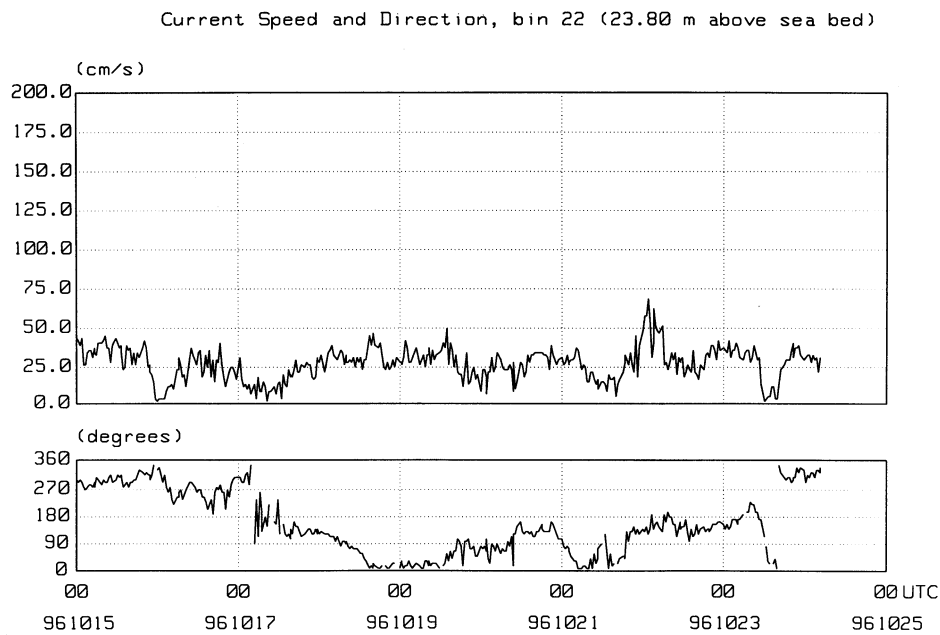
Figure 11 Examples of first measurements coming from the monitoring stations during phase II.

Conclusion

The changes of the Baltic Sea on all time scales are important, when considering the environmental impact of a bridge construction in the transition:

- how large and rapid are the natural changes compared to the influence of the construction?
- is it possible to observe and/or measure a change caused by a fixed link?

The answers to the questions are, that we expect the natural changes to be larger than the influence of the construction, and that it is not possible to measure the change caused by the fixed link, especially if the environmental design criteria are set as restrictively as in the Great Belt and Øresund link cases.

The velocity distribution along the alignment is very important, when designing the details of the link between Denmark and Germany. On the basis of historical measurements, we may assume that the current in the Fehmarn Belt is strongly

related to the bathymetry and the water exchange, and only weakly related to secondary flows. It should, however, be noted that during inflow to the Baltic an outflow near Lolland may be a typical feature, which needs to be further explored during phase II.

Seven link solutions were investigated during phase I. On the basis of the hand calculations and the 3-dimensional simulations, the solution model 6.0—the combi solution—was ranked as the most blocking solution and will not be considered in phase II. Disregarding solution 6.0, the maximum blocking of the Fehmarn Belt link solutions is approximately equal to the blocking of the Little Belt link, and much smaller than the estimated influence of the expected greenhouse effect.

References

Binderup M., and Frich, P. (1993). Sea-level variations, trends and cycles, Denmark 1890–1990: Proposal for a reinterpretation. Ann. Geophysicae, 11, pp. 753–760.

DHI/LIC (1995). Hydrographic investigations, Campaign I–VI. Report for Øresundskonsortiet by DHI/LIC and SMHI. 7209/FU.

DMI (1965). Oceanographical observations from Danish light-vessels and coastal stations. Yearbook from the Danish Meteorological Institute.

DMI (1992). Drivhuseffekt og klimarendringer. Særtryk Danmarks Meteorologiske Institut, 103 pp.

COWI-Lahmeyer (1996A). Initial Environmental Design Evaluation Fehmarn Belt Feasibility Study, Phase 1, Technical note by FEC.

COWI-Lahmeyer (1996B). Hydrographic data collection and review Fehmarn Belt Feasibility Study, Phase 1, Technical note by FEC.

COWI-Lahmeyer (1996C). Hydraulic modelling Fehmarn Belt Feasibility Study, Phase 1, Technical note by FEC.

COWI-Lahmeyer (1997). Determination of cross sectional velocity Fehmarn Belt Feasibility Study, Phase 2, Technical note by Prof. Fl. Bo Pedersen & FEC.

Hardtke, G. (1978). About the velocity field in the Kiel Bay. Proceedings, Conference of Baltic Oceanographers (Rostock, Germany, pp. 756–779).

HELCOM (1986). Water Balance of the Baltic Sea" Helsinki Commission, Baltic Marine Environment Protection Commission, Baltic Sea Environment Proceedings, 16.

Jacobsen, T.S. (1980). Sea Water Exchange of the Baltic, Measurements and methods. The Belt Project, 106 pp.

Jakobsen, Fl. (1991). The Bornholm Basin—Estuarine Dynamics. Technical University of Denmark, Institute of Hydrodynamics and Hydraulic Engineering, Series Paper, 52, 199 pp.

Jakobsen, Fl. (1995). The Major Inflow to the Baltic Sea during January 1993. Journal of Marine Systems, Vol. 6, No.3, pp. 227–240.

Jakobsen, Fl., Lintrup, M.J., and Møller, J.S. (1996). Observations of the Specific Resistance in Øresund. Submitted.

Jakobsen, Fl., and Møller, J.S. (1996). Transporten gennem Lillebælt. Submitted.

Jakobsen, Fl., and Ottavi, J. (1996). The transport through the contraction area in the Little Belt. Submitted.

Lange, W., Mittelstaedt, E. and Klein, H. (1991).Strömungsdaten aus der Westlichen Ostsee. Deutsche Hydrographische Zeitschrift, Ergänzungsheft Reihe B, 24.

Lass, H.-U., Matthäus, W., Francke, E., and Schwabe, R. (1987). On the dynamics of water exchange between Baltic and North Sea. Beiträge zur Meereskunde, 56, pp. 27–49.

Matthäus, W. (1979). Long term Variations in the primary Halocline in the Gotland Basin. ICES, C.M. 1979/C:22, mimeo.

Matthäus, W., and Franck, H. (1992). Characteristics of major Baltic inflows—a statistical analysis. Continental Shelf Research, 36, pp. 1375–1400.

Møller, J.S., and Hansen, I.S. (1994). Hydrographic processes and changes in the Baltic Sea. Dana, 10, pp. 87–104.

Møller, J.S., & Ottesen Hansen, N.-E. (1990). The Great Belt Link, How to achieve zero environmental impact on the Baltic Sea. Twenty-Second Coastal Engineering Conference. Coastal Eng. Res. Council/ASCE, July 2–6 1990, Delft.

Pedersen, FI.B. (1996). Hydrografiske forhold i Kiel Bugt–Femer Bælt–Darss Tærsklen. Unpublished manuscript, 60 pp.

Sparre, A. (1984A). Salinity A; means, extremes and frequency. The climate of Denmark, Summaries of observations from light vessels IV, No. 11.

Stigebrandt, A. (1980). Barotropic and baroclinic response of a semi-enclosed basin to barotropic forcing from the sea. In: Fjord Oceanography, Eds. H.J. Freeland, D.M. Farmer & C.D. Levings, Plenum, pp. 151–164.

Stigebrandt, A. (1992). Bridge-induced Flow Reduction in Sea Straits with Reference to Effects of a Planned Bridge Across Öresund. Ambio, 21, 2, pp. 130–134.

Svansson, A. (1975). Physical and Chemical Oceanography of the Skagerrak and Kattegat. Fishery Board of Sweden, Institute of Marine Research, Report No.1, 88 pp.

Trafikministeriet (1996). Undersegelser vedrerende Femer Bælt-forbindelsen. Fase 1 af kyst til kyst-undersøgelserne, 128 pp.

Nested 3D model of the North Sea and the Baltic Sea

H. René Jensen and Jacob S. Møller

Abstract

A two-way interactive nested three dimensional model of the North Sea, the Baltic Sea and the Danish waters has been established under the MAST II research project DYNOCS. The objective of the modelling is to hindcast a period of one year and investigate the dynamics of the complicated flow in the Danish waters between the North Sea and the Baltic Sea.

Introduction

As part of the CEC-sponsored MAST II research project DYNOCS (DYNamics Of Connected Seas), a three dimensional numerical model of the North Sea, the Baltic Sea and the Danish waters has been established. The model is based on Danish Hydraulic Institute's (DHI) general 3D modelling system, MIKE 3, which is a non-hydrostatic baroclinic model. To resolve the narrow Danish straits a special version of MIKE 3 which includes an interactive two-way nesting facility has been applied. The objective of the project is to hindcast a one year period of the complicated flow in the Danish waters which to a high degree is governed by the dynamics of the North Sea and the Baltic Sea. This paper describes the model set-up and some preliminary results.

The numerical model

The MIKE 3 model is a general non-hydrostatic numerical modelling system developed by DHI (Rasmussen *et al.*, 1990) for a wide range of applications in areas such as oceanography, coastal regions, estuaries and lakes. It simulates unsteady three-dimensional flows, taking into account density variations, bathymetry and external forcing such as meteorology, tidal elevations, currents and other hydrographical conditions.

The mathematical foundation in MIKE 3 is the mass conservation equation;

$$\frac{1}{\rho c_s^2}\frac{\partial P}{\partial t} + \frac{\partial u_i}{\partial x_i} = S_{SS}$$

the Reynolds-averaged Navier-Stokes equations, including the effects of turbulence and variable density (the momentum equations);

$$\frac{Du_i}{Dt} + 2\Omega_{ji}u_j = \frac{1}{\rho}\frac{\partial P}{\partial x_i} - g_i + \frac{\partial}{\partial x_j}\left(\nu_t\left\{\frac{\partial u_j}{\partial x_i} + \frac{\partial u_i}{\partial x_j}\right\}\right) + F_{ext} + u_i S_{SS}$$

and the conservation equations for salinity and temperature in three dimensions;

$$\frac{1}{\rho}\frac{D(\rho S)}{Dt} = \frac{\partial}{\partial x_j}\left(D_S\frac{\partial S}{\partial x_j}\right) + S_{SS}$$

$$\frac{1}{\rho}\frac{D(\rho T)}{Dt} = \frac{\partial}{\partial x_j}\left(D_T\frac{\partial T}{\partial x_j}\right) + \frac{1}{\rho}Q_H + S_{SS}$$

together with the equation of state relating the local density to salinity, temperature and pressure.

There are several types of equations of state for the density of sea water. In MIKE 3, the definitions given by UNESCO (1981) have been adopted.

In the equations, ρ is the local density of the fluid,
u_i the velocity in the x_i-direction,
Ω_{ij} the Coriolis tensor,
P the fluid pressure,
g_j the gravitational vector,

v_T the turbulent eddy viscosity,

δ the Kronecker's delta,

k the turbulent kinetic energy,

c_S is the speed of sound in sea water,

S is the salinity,

T is temperature,

D_S and D_T are the dispersion coefficients for salinity and temperature, respectively,

Q_H is the heat exchange with the atmosphere and

t denotes the time.

S_{SS} refers to the respective source-sink terms and differs from equation to equation.

In most three-dimensional models the fluid is assumed incompressible. However, using the divergence-free (incompressible) mass equation, the set of equations will inevitably form a mathematically ill-conditioned problem. In most models this is solved through the hydrostatic pressure assumption whereby the pressure is replaced by information about the surface elevation. In order to retain the full vertical momentum equation (i.e. non-hydrostatic conditions) an alternative approach has been adopted in MIKE 3. This approach is known as the artificial compressibility method (Chorin, 1967, and Rasmussen, 1993) in which an artificial compressibility term is introduced whereby the set of equations mathematically speaking becomes hyperbolically dominated.

The decomposition of the prognostic variables into a mean quantity and a turbulent fluctuation leads to Reynolds stress and turbulent flux terms in the governing equations to account for the non-resolved processes both in time and space. By the adoption of the eddy viscosity concept these effects are expressed through the eddy viscosity and the gradient of the mean quantity. The problem of determining the eddy viscosity is solved in MIKE 3 by using closure models such as the Smagorinsky sub-grid (zero equation) model, the k- (one equation) model, the k-epsilon (two-equation) model, see Rodi (1980) or a mixed Smagorinsky-k-epsilon model. In the present case the sub-grid model proposed by Smagorinsky (1963) is applied, in which the eddy viscosity is linked to the filter size (grid spacing) and the eddy strain rate, i. e. gradients of the resolved flow field. Buoyancy effects are accounted for via a damping function depending on the Richardson number, see for example Munk and Anderson (1948).

The equations are spatially discretised on a rectangular Arakawa C staggered grid. Scalar quantities such as pressure, salinity, temperature, etc. are defined in the grid nodes, whereas the velocity components are defined halfway between adjacent nodes in the respective directions. The adopted staggered grid allows for the spatial discretisation of the governing partial differential equations into a finite-difference scheme.

The mass equation and the three momentum equations thus form a (huge) set of differential equations in time, which is solved by an Alternating Direction Implicit (ADI) algorithm. Usually, iterative methods are required for the inversion of the system matrices due to the non-linear terms in the momentum equations. However, a non-iterative ADI algorithm is applied in MIKE 3 through the use of the "fractional-step" technique (basically a time-staggering of the prognostic variables) and "side-feeding" (a semi-linearisation of the non-linear terms).

For the advection-diffusion of salinity and temperature the QUICKEST scheme (Quadratic Upwind Interpolation for Conservative Kinematics with Estimated Streaming Terms) is applied, see Leonard (1979) and Vested et al. (1992). This method is based on a control volume formulation. Upstream interpolation is used to determine higher order derivatives. This procedure limits the stability problems of central differencing while remaining free of the inaccuracies of numerical diffusion associated with usual upstream differencing. The resolution of fronts is further improved by the implementation of an exponential interpolation at steep fronts (SHARP), see Leonard (1988).

Bottom-fitted co-ordinates have been introduced in MIKE 3. The model equations at the bottom grid cells have been adjusted to take into account the exact water depths. Thus, the position of the sea bed is not just truncated to fit the applied constant vertical grid size.

MIKE 3 also includes a "flood and dry" facility, making it possible to include the effects of flooding and drying of shallow areas when the water surface moves up and down due to e. g. tidal variations or wind set-up.

Heat exchange with the atmosphere is implemented based on the four physical processes: sensible heat flux (convection), latent heat flux (vaporisation), net short wave radiation and net long wave radiation.

An interactive two-way nesting grid facility has been developed for MIKE 3 which allows for nesting from coarser to finer grids by a factor of three.

Model set-up

The model consists of three levels of nesting: A 9 nm grid covering the North Sea and the Baltic Sea, a 3 nm grid covering the Danish waters and a 1 nm grid of the Danish Straits and the western Baltic Sea, see Figure 1.
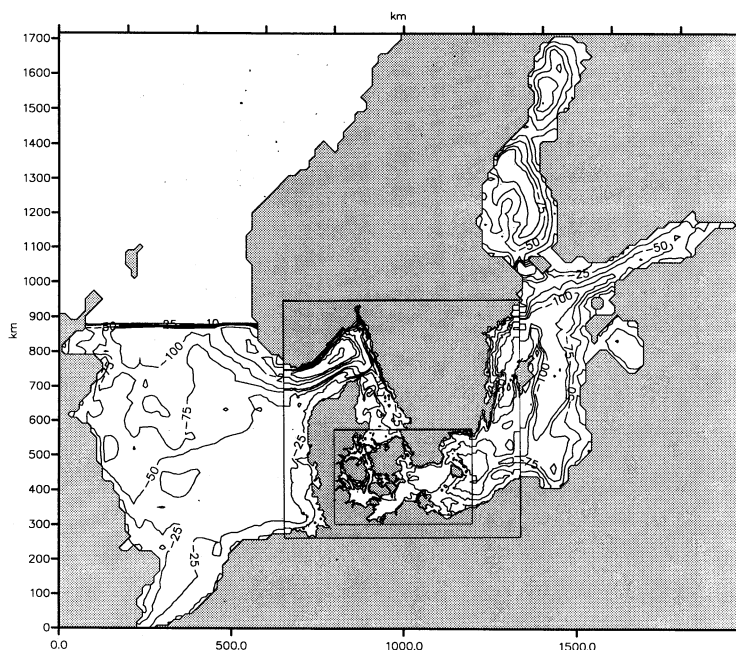
Figure 1 The DYNOCS model set-up with 3 levels of two-way interactive nesting; 9 nm, 3 nm and 1 nm grid resolution

The vertical resolution is 2 m with up to 40 layers. So-called bottom-fitted co-ordinates are applied within the lower layer to account for the actual depths and depths larger than approximately 80 m. The surface layer thickness is initially 5 m but varies with the movements of the free surface. The thickness of the surface layer is limited by the maximum and minimum surface elevation as this layer must not be dry during simulation (only in shallow areas, where the seabed is just below!). In the DYNOCS model this is most critical along the East coast of England due to the high tides.

The barotropic forcing of the model consists of tidal forcing and meteorological forcing:

At the two open boundaries in the North Sea; in the British Channel (between Dungeness (UK) and Wissant (France)) and between Wick (Scotland) and Stavanger (Norway), the tidal water levels are prescribed by tidal predictions based on the 10 largest tidal constituents (M_2, S_2, N_2, K_2, μ_2, K_1, O_1, P_1, M_4, MS_4) along the boundaries.
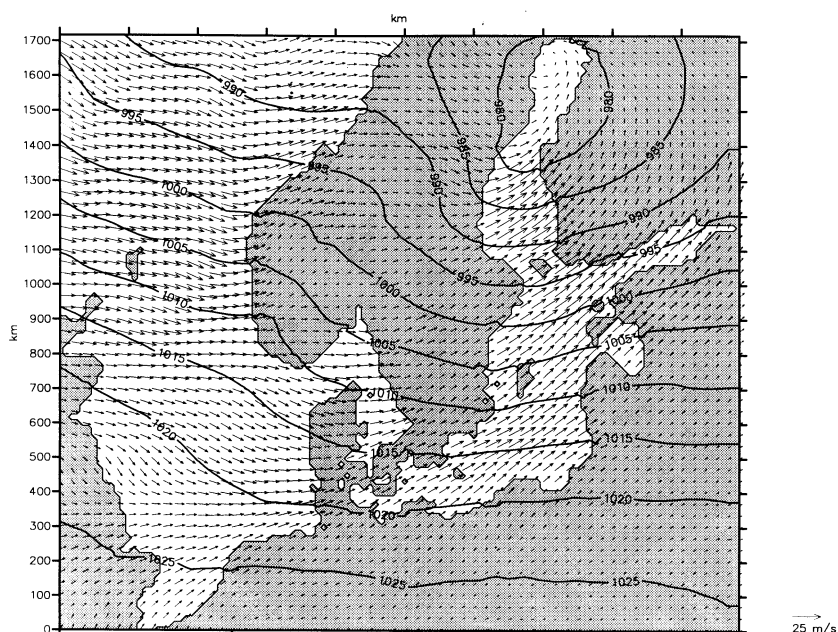
Figure 2 Applied Meteorological Forcing (Example from 24 November 1994, 00 GMT, every second vector is shown)

Nested 3D model of the North Sea and the Baltic Sea

The meteorological forcing consists of analysed wind (10m) and surface air pressure fields covering the full so-called DYNOCS Year (starting 15 September 1994). The meteorological data taken from the operational meteorological model, HIRLAM (Danish Meteorological Institute (DMI)) has a temporal resolution of 6 hours and a spatial resolution of 0.21 degrees. In Figure 2, the model wind and air pressure for the 24 November 1994, after spatial interpolation from the meteorological grid to the DYNOCS 9nm grid, is shown. The meteorological fields are further (automatically) interpolated to the 3nm and the 10nm grids during simulation.

The reduced wind over land is due to the higher friction.

The baroclinic forcing at the two open boundaries in the North Sea consists of monthly climatological salinities and temperatures in each grid point which have been established based on data provided by ICES.

The model has been initialised by climatological (10 year September average values) 3D fields of salinity and temperature. In Figure 3 and Figure 4, the initial surface salinities and temperatures, respectively, are shown for the fine grid (1nm resolution) where the largest gradients exist. The 3D fields have been established by application of Akima (Akima, 1970) and Kriging (Cressie, 1991) interpolation methods in data provided by ICES.
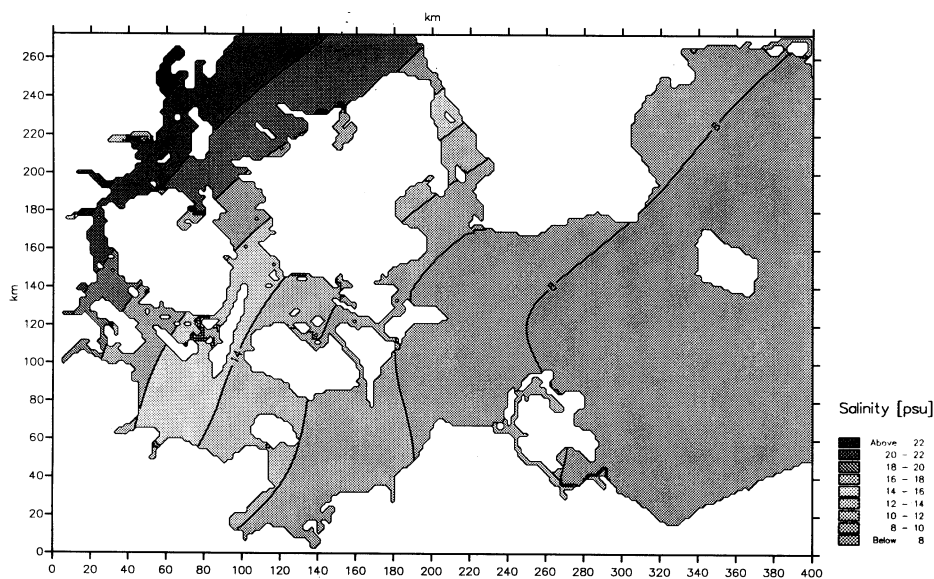
Figure 3 Initial surface layer salinity (1nm grid)
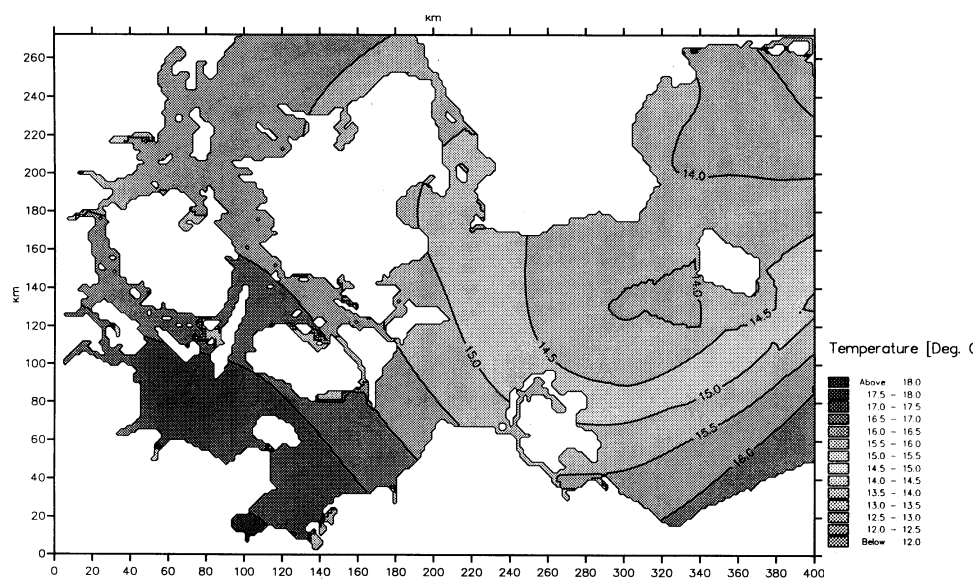
Figure 4 Initial surface layer temperature (1nm grid)

To simulate the long term physical processes of an almost enclosed basin such as the Baltic Sea, it is important to include all elements of the water balance in the model. Accordingly, the fresh water inflow (20 year average, Mikulski, 1986, and

Bergström, 1993) to the Baltic Sea has been employed by a relative distribution of monthly discharge to the main rivers. Also, main rivers of the North Sea have been included bringing the total numbers of rivers up to 17.

Model fields of precipitation and evaporation have been established on a monthly basis using climatological mean values for 7 sub-basins of Kattegat and the Baltic Sea (Dahlström, 1986). For the North Sea an annual mean value of precipitation and evaporation was used (Grindley, 1972) with an added monthly variability deduced from the Baltic Sea climatology.

For the heat balance calculations the model needs input in the form of air temperatures 2 m above sea level which have been provided by DMI on a 6 hourly basis over the whole model (9 nm horizontal resolution, as for the wind and air pressure). An example of the temperature fields is shown in Figure 5.
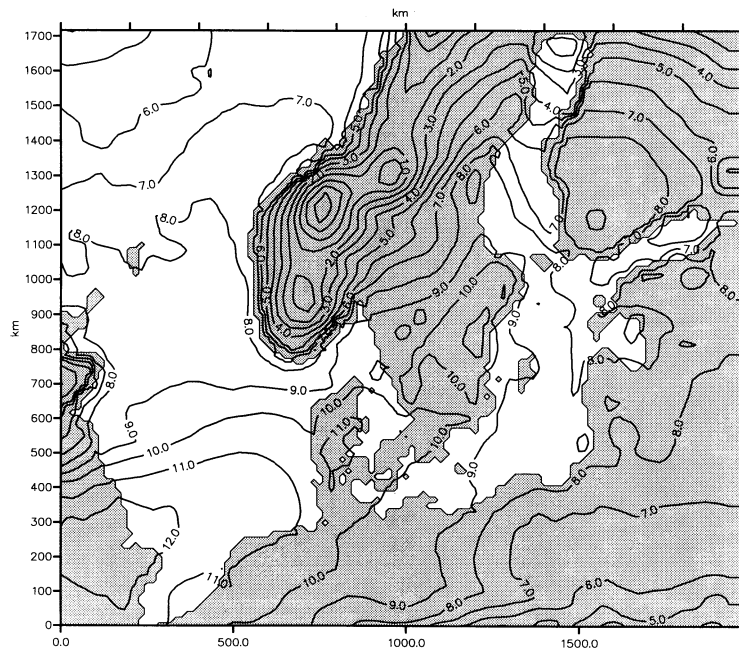
Figure 5 Example of air temperature distribution used in the heat exchange calculations (24 November 1994 00 GMT)

Results

Within the defined DYNOCS Year, three field campaigns have been carried out to establish a data base, together with a large number of permanent stations in the area, for calibration and validation of the numerical model. The model will be used for hindcasting the DYNOCS year and for providing boundary data, within selected periods, to local models of the western Baltic Sea established by Institut für Ostseeforschung (IOW), Sveriges Meteorologiska och Hydrologiska Institut (SMHI) and DMI/DHI, respectively. As the DYNOCS project is still ongoing (November 1996) only preliminary results from part of the year to be simulated will be presented here.
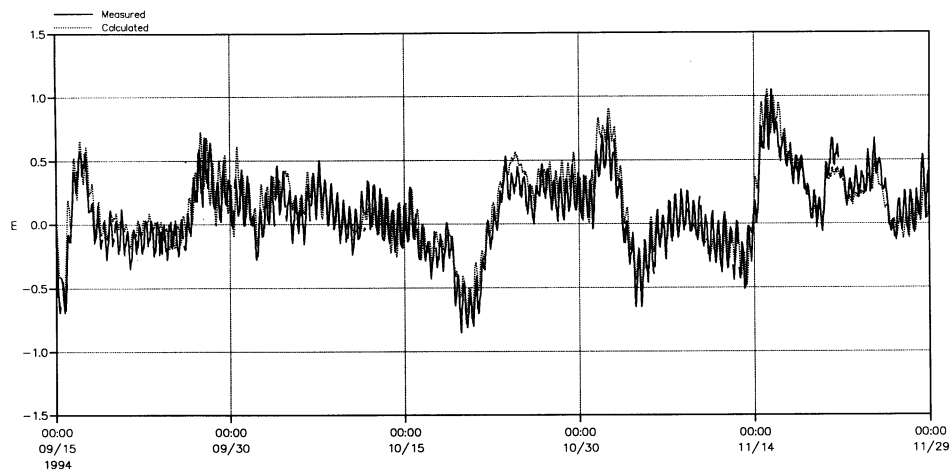
Figure 6 Comparison of calculated and measured water levels at Hanstholm

Nested 3D model of the North Sea and the Baltic Sea

As an example of the barotropic behaviour a time-series of the calculated and measured water levels at the entrance to the Danish waters in Skagerrak (Hanstholm) for a period of 2.5 months is shown in Figure 6. This signal contains both the tidal and the meteorological effects.

In Figure 7, the surface current and salinity distribution in the fine grid (1 nm resolution) are shown for a strong inflow situation the 24 November 1994. The figure clearly shows the position of the Drogden Sill and the Darss Sill fronts.
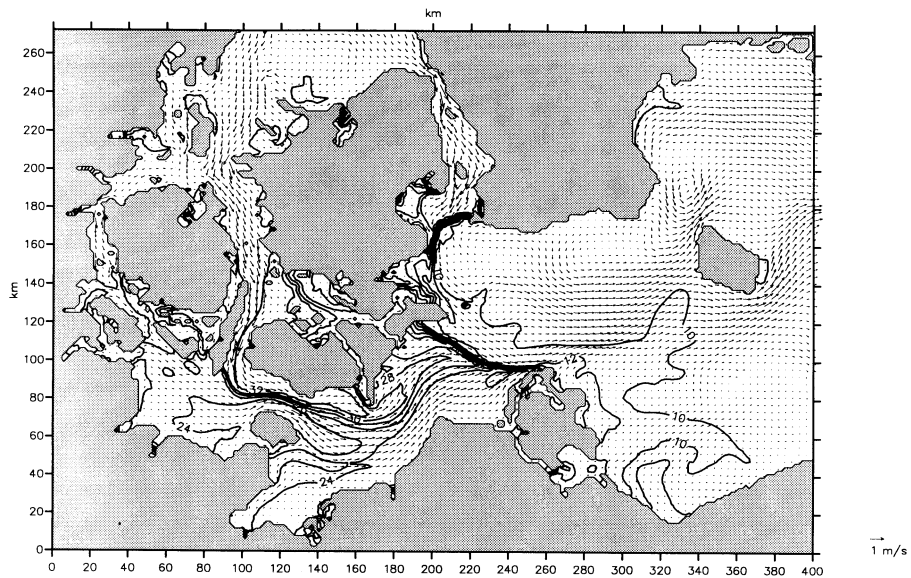
Figure 7 Calculated surface currents and salinities in 1 nm grid (24 November 1994, every second vector is shown)

Figure 8 and Figure 9 show the vertical distribution of salinity and temperature along a line from the Kattegat through the Great Belt, the Fehmarn Belt, the Darss Sill, the Arkona Basin to the Bornholm Basin for the same inflow situation.
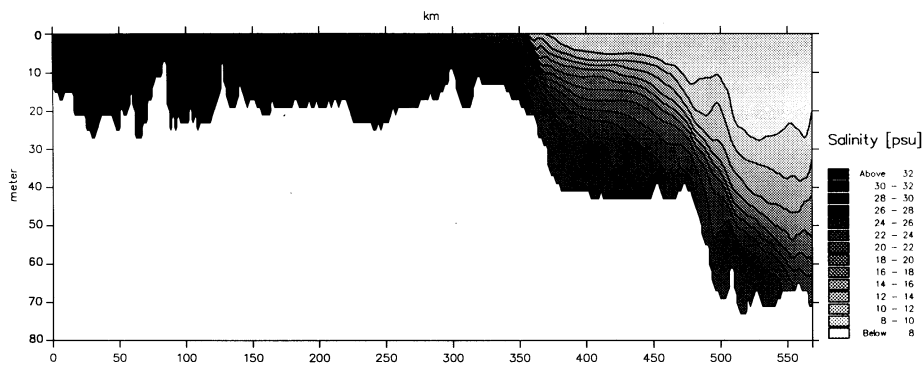
Figure 8 Vertical distribution of salinity along a line from Kattegat to Bornholm Basin (24 November 1994)
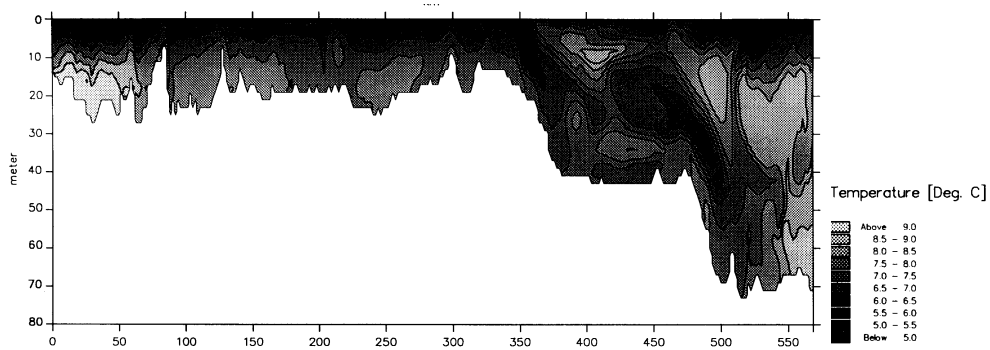
Figure 9 Vertical distribution of temperature along a line from Kattegat to Bornholm Basin (24 November 1994)

Again, the Darss Sill front is easy to identify. Notice also the cooling of the surface layer and the pull-down of cold water at the Darss Sill front into the Arkona Basin (Figure 9).

The calculated discharge through Øresund is compared to measured (actually estimated based on current measurements, see Jacobsen (1995) and Jacobsen (1996)) discharges in Figure 10.
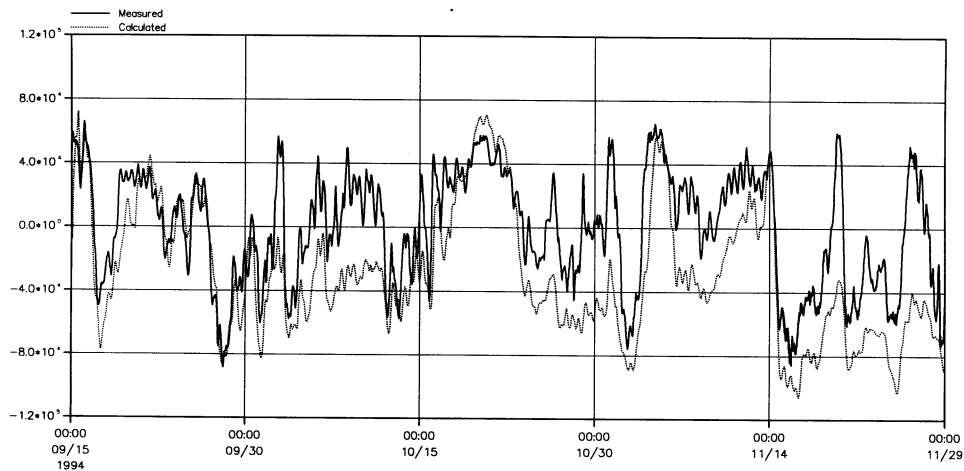
Figure 10 Calculated and measured discharge through Øresund (positive is outflow from Baltic Sea)

From the figure, it is seen that the transports to the Baltic Sea are overestimated in the model for the inflow situation of 24 November, but the magnitude is still realistic.

A time-series of calculated salinities is shown in Figure 11 where calculated and measured salinities at station Nordre Røse in Øresund are compared.
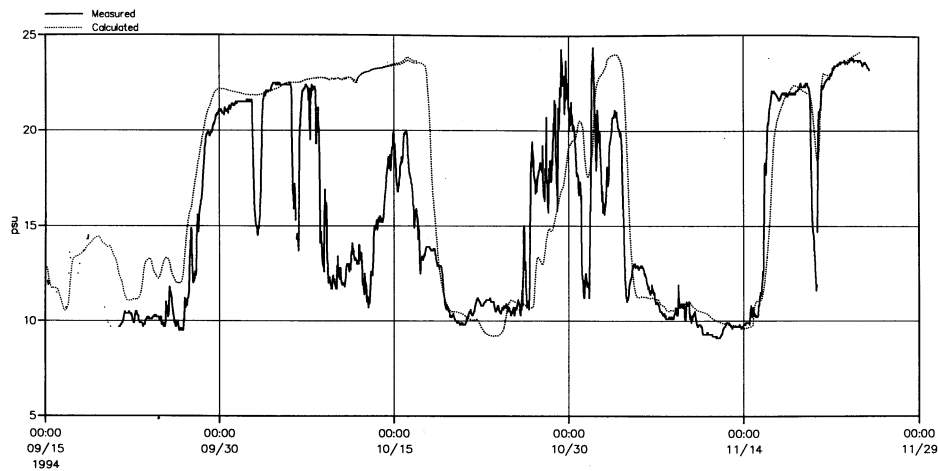
Figure 11 Calculated and measured salinity at Nordre Røse in Øresund (5.4 m below surface).

The DYNOCS project will be finalised by mid 1997.

Acknowledgements

References

Akima, A. (1970). A new method of interpolation and smooth curve fitting based on local procedures, Journal of Applied Computational Mathematics, J J 7, 589–602.

Bergström, S., and Carlsson, B. (1993). Hydrology of the Baltic Basin. Inflow of fresh water from rivers and land for the period 1950–1990, Report No.7. SMHI, Sweden.

Chorin, A. J. (1967). A numerical method for solving incompressible viscous flow problems, J. Comput. Phys., 2, J 2–26.

Cressie, N. (1991). Statistics for spatial data, John Wiley and Sons Inc., 900 pp.

Dahlström, B. (1986). Determination of areal precipitation for the Baltic Sea, Report No. RMK 54. SMHI, Sweden.

Grindley, J. (1972). Hydrology of the North Sea: Run-off and precipitation, Meteorological Magazine, 101.

Jacobsen, Fl., and Castejon, S. (1995). Calculation of the discharge through Øresund at the Drogden Sill by two fixed station measurements, Nordic Hydrology, Vol. 26, No. 3, pp. 237–258.

Jacobsen, Fl., and Lintrup, M. J. (1996). The exchange of water and salt across the Drogden Sill in Øresund during the period from September 1993 to November 1994, Nordic Hydrology, in press.

Leonard, B.P. (1979). A Stable and Accurate Convective Modelling Procedure Based on Upstream Interpolation. Computational Methods in Applied Mechanical Engineering, 19,59–98.

Leonard, B.P. (1988). Simple High Accuracy Resolution Program for Convective Modelling of Discontinuities, International Journal for Numerical Methods in Fluids, 8, 1291–1318.

Mikulski, Z. (1986). Inflow from drainage basin, Baltic Sea Environment, Proceedings, No. 16. Baltic Marine Environment Protection Commission, Helsinki Commission

Munk, W. H., and E. R. Anderson (1948). Notes on a theory of the thermocline, J. Mar. Res. 7, 276–295.

Rasmussen, E.B., H.J. Vested, P. Justesen and L.C. Ekebjærg, (1990), SYSTEM3: A Three Dimensional Hydrodynamical Model, Danish Hydraulic Institute.

Rasmussen, E.B. (1993). Three-dimensional Hydrodynamic Models, in Abbott, MB. and N.A. Price (eds.): Coastal, Estuarial and Harbour Engineers' Reference Book, Chapman & Hall, London.

Rodi, W. (1980). Turbulence Models and their Application in Hydraulics, A State of the Art Review, SFB 80/T/127. Inc, London.

Smagorinsky, J. (1963). General Circulation Experiments with the Primitive Equations, 1. The Basic Experiment, Mon. Wea.Rev., 91, 99–164.

UNESCO (1981). The practical salinity scale 1978 and the international equation of state of seawater 1980, UNESCO technical papers on marine science.

Vested, H.J., Justesen, P. and Ekebjærg, L.C. (1992), Advection-dispersion modelling in three dimensions, Appl. Math. Modelling, 16, 506–519.

Baltic Stations Darss Sill and Oder Bank

Siegfried Krueger, Wolfgang Roeder, and Klaus-Peter Wlost

The Baltic Sea Research Institute in Warnemünde carries out the German Baltic Sea Monitoring by contract with the Federal Maritime Agency (BSH) in Hamburg. In addition to the ship-borne monitoring the IOW got the task to construct and to operate four new automatic Baltic Fixed Monitoring Stations in front of the Mecklenburg coast. With these four new stations the BSH extends the German Coastal Monitoring Network to the western Baltic. The new stations will be located on the "Darss Sill", in the "Pomeranian Bay", the "Arkona Sea" and in the "Mecklenburg Bay".
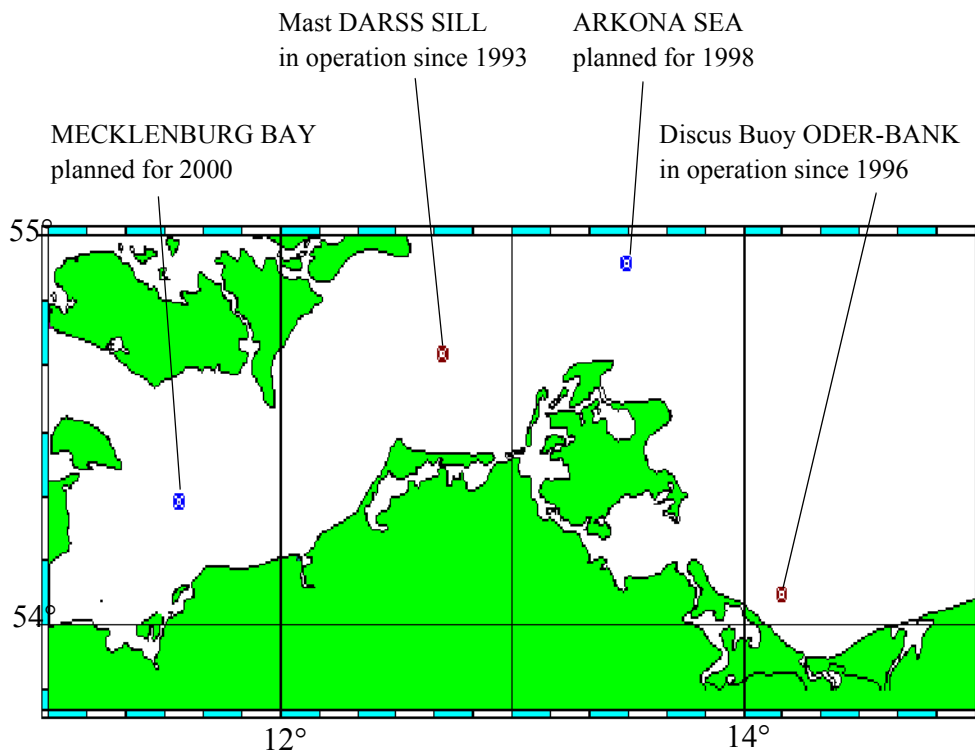
Figure 1 Locations of the new stations

The Fixed Monitoring Stations will continuously measure physical, chemical, biological water parameters and meteorological data.

Every hour each station sends a message via METEOSAT to the BSH in Hamburg. There the data are stored in a database and can be accessed by different users via the German science Network (WINET, FTP). These four new stations will play an important role in the German contribution to GOOS.

The first new IOW-station has been in operation on the "Darss Sill" since 1993. The Darss Sill is an important barrier limiting the water exchange between the North Sea and the Baltic Sea. Near bottom inflowing salt-rich North Sea water is normally impeded by the shallow Darss Sill from flowing into the deeper Basins except a small permanent undercurrent. Only at specific meteorological conditions larger salt water inflows can pass the Darss Sill.

The monitoring and observation of this processes is the main task of the automatic station DARSS SILL. The actual design is based on the so called IOW-Articulated Mast. The basic idea of this construction is a cigar-like mast of different air-filled aluminium tube modules. This "cigar" is fixed on the bottom in a flexible way by a heavy bottom weight and a universal joint. In the water the mast is erected by the buoyancy force, so that the top comes out of the water and can carry a platform. The buoyancy force carries the mast like a reversed pendulum in the water. For a water depth on the Darss Sill of 21 m, a 25 m long "cigar" was designed. The diameter of the biggest tube module is 75 cm. Because the Baltic Sea has practically no tides the platform is always about 4m above the surface. The buoyancy force is so enormous

that the platform can carry more than 500 kg of equipment. The mean inclination is about ±3°, in very heavy weather seldom more than ±10°. The roll period is about 15 sec, higher wave frequencies have practically no energy.

For the Mast station the IOW-group developed a new instrumentation concept with split intelligence and split resources, which is supplied by environmental energy only (wind, solar). This concept gave a very high reliability of the station since the start in 1993. The station currently records 30 meteorological, hydrological and housekeeping parameters. In four main levels the water temperature, the conductivity, oxygen and current are measured. In some extra levels the system measures additional temperatures. The complete instrumentation is modular and expandible. All instruments have their own battery, which can be "overridden" by the main power supply. They are equipped with their own intelligence, their own time base and with long term storage facilities. All instruments and communication units are connected via RS232-lines with the platform-host (multitasking handheld). Every hour a complete data set is transmitted via a METEOSAT-satellite to the data base in Hamburg. An additional bidirectional online connection via GSM-radiotelephone is available for service, extra data transmission and event handling.
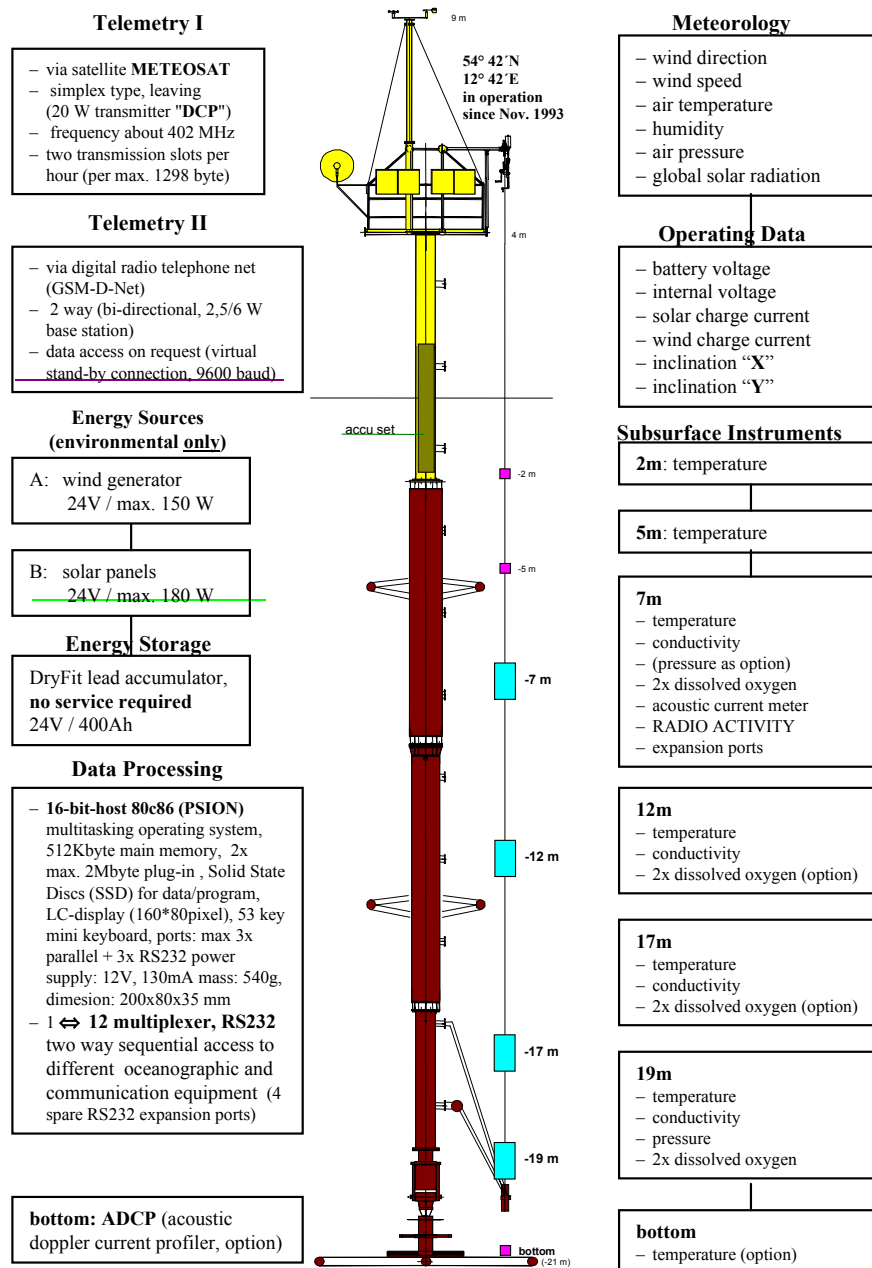
Figure 2 Baltic Station—DARSS SILL Mast

The main power supply system is a balanced combination of a wind generator, 4 solar panels and a 400 Ah dryfit lead battery package. This system can supply about 1.5 A at 24 V permanently. The instrumentation needs about 0.5 A. With fully charged batteries all systems can operate about 50 days without any wind or solar energy input. An extraordinary

advantage of the IOW-Mast is the possibility to fill some sections with water, to put down the complete carrier on to the sea bed in the case of sea ice, as it was necessary from February to April 1996.

General recording frequency
(database at BSH, Hamburg; transmission via METEOSAT) (2nd connection to IOW via GSM-D-Net radio telephone, bidirectional) — **1 complete scan per hour**

	operating data:			sensor/system	recorded data
*	battery voltage				
***	internal voltage			IOW/@	1 MV^3 per hour
***	solar charge current				
***	wind charge current				
*	inclination 1				
*	inclination 2				

	meteorological parameters:				
	parameter	**range**	**precision**	**sensor/system**	**recorded data**
***	wind speed	0.3–40 ms^{-1}	±0.2 ms^{-1}	@	1 MV^1 per hour
***	wind direction	0–360°	2°	@	1 MV^2 per hour
***	air temperature	–30–+80°C	±0.3 K	@	1 MV^1 per hour
***	air pressure	800–1060 hPa	±0.5 hPa	@	1 MV^3 per hour
***	humidity	0–100%	±3%	@	1 MV^3 per hour
***	solar radiation	0–1400 Wm^{-2}	±0.5%	@	1 MV^1 per hour

		hydrological parameters:				
		parameter	**range**	**precision**	**sensor/system**	**recorded data**
*****	2m	temperature	–10–+30°C	±10 mK	Pt1000/IOW/$	1 MV^3 per hour
*****	5m	temperature	–10–+30°C	±10 mK	Pt1000/IOW/$	1 MV^3 per hour
***	7m	radioactivity			#/@	1 MV^4 per hour
*		temperature	–5–+35°C	± 10 mK		1 MV^3 per hour
*		conductivity	0–70 mScm^{-1}	±10 µScm^{-1}	$	1 MV^3 per hour
*		pressure	0–680 kPa	±1 kPa	$	1 MV^3 per hour
****		oxygen 1	0–15 mll^{-1}	±0.2 mll^{-1}	§	1 MV^3 per hour
****		oxygen 2	0–15 mll^{-1}	±0.2 mll^{-1}	§	1 MV^3 per hour
****		current	± 2 ms^{-1}	1 cms^{-1}	ACCM-§/@	1 MV^5 per hour
***	12m	temperature	–5–+35°C	±10 mK	$	1 MV^3 per hour
***		conductivity	0–70 mScm^{-1}	±10 µScm^{-1}	$	1 MV^3 per hour
***	17m	temperature	–5–+35°C	±10 mK	$	1 MV^3 per hour
***		conductivity	0–70 mScm^{-1}	±10 µScm^{-1}	$	1 MV^3 per hour
**	19m	temperature	–5–+35°C	±10 mK	$	1 MV^3 per hour
**		conductivity	0–70 mScm^{-1}	±10 µScm^{-1}	$	1 MV^3 per hour
*****		oxygen 1	0–15 mll^{-1}	±0.2 mll^{-1}	$	1 MV^3 per hour
*****		oxygen 2	0–15 mll^{-1}	±0.2 mll^{-1}	$	1 MV^3 per hour
**		pressure	0–680 kPa	±1 kPa	$	1 MV^3 per hour

Table 1 Parameters measured on the IOW "DARSS SILL" mast station

The second new station near the "ODER-BANK" (Pomeranian Bay) started in May 1996. The station helps to monitor the complicated water exchange between the Pomeranian Bay and the Arkona Sea.

The platform of this station is a heavy discus buoy (ø 10 m) with an instrumentation container (ø 4 m × 4 m), developed by BSH. This concept was chosen as a more robust design for a shallower region with ice every year. The container gives more room for special instrumentation in the future.

The IOW-group designed and constructed the basic instrumentation concept. It is similar to the system on the Mast "Darss Sill". 25 parameters are measured here for the time being, under water parameters in two main levels.

The environmental energy supply has twice the capacity for extensions and an extra diesel generator and heating are available. The sampling concept is a little bit different according to the effects of the faster moving buoy on the measurements.

The station works with the same reliability as DARSS SILL since May 1996.

The plans for at least four IOW stations will be continued. The carrier for the third new station (ARKONA SEA) is already under development.

meteorological sensors and antenna assemby

wind generator

ODAS-light

Instrumentation container
– data acquisition systems
– special instruments
– radio equipment
– batteries
– Diesel generator

solar panels

discus buoy with moon pool

UW-level 1

sensor chain

UW-level 2

10m

6,4m

3.9m

0,92m

0m

–3m

–12m

–15m

Meteorology
– Wind direction
– wind speed
– air temperature
– humidity
– air pressure
– global radiation

Data transmission
– **METEOSAT** (> BSH 1 per hour)
– **GSM-D-telephone** (<> on request)

Data processing
– **16-bit host computer 80c86**, multitasking system, 2x max. 4Mb chipcards display (160*80 pix), ports: max. 3x parallel + 3x serial power consumption: 12V, 130 mA
– **1 ⇔ 12 multiplexer, RS232**

Housekeeping parameters
– Supply voltages
– solar charge current
– wind charge current
– inclination
– earth magnetic field components
– GPS-position (opt.)

Power supply
– **wind generator max. 200 W**
– **solar panels max. 360 W**
– **dryfit lead batteries 24V/960 Ah**
– Diesel generator max. 2400 W
– Diesel heating max. 4500 W

In situ parameters
3m, 12m
– **temperature**
– **conductivity**
– **oxygen**
– acoust. currentmeter
– spare inputs

Figure 3 Discus Buoy at ODER BANK for monitoring of the exchange processes between the Pomeranian Bay and the Arkona Basin

General recording frequency
(database at BSH, Hamburg; transmission via METEOSAT) (2nd   **1 complete scan per hour**
connection to IOW via GSM-D-Net radio telephone, bidirectional)

operating data:
*   battery voltage
*   internal voltage
*   diesel starter voltage
*   solar charge current
*   wind charge current
*   (consumed) supply current
*   earth magnetic field components (HDG)
**   inclination 1
**   inclination 2
(see also meteo. parameters)

meteorological parameters:

	parameter	range	precision	sensor/system	recorded data
*	wind speed	$0.3–40\,ms^{-1}$	$\pm0.2\ ms^{-1}$	@	1 MV[1] per hour
*	wind direction	$0–360\ °$	$2°$	@	1 MV[2] per hour
*	air temperature	$-30–+80°C$	$\pm0.3\ K$	@	1 MV[1] per hour
*	air pressure	$800–1060\ hPa$	$\pm0.5\ hPa$	@	1 MV[3] per hour
*	humidity	$0–100\%$	$\pm3\%$	@	1 MV[3] per hour
*	solar radiation	$0–1400\ Wm^{-2}$	$\pm0.5\%$	@	1 MV[1] per hour

hydrological parameters:

		parameter	range	precision	sensor / system	recorded data
*	3m	temperature	$-5–+35°C$	$\pm10\,mK$	$	1 MV[5] per hour
*		conductivity	$0–70\,mScm^{-1}$	$\pm10\,\mu Scm^{-1}$	$	1 MV[5] per hour
*		oxygen	$0–15\,mll^{-1}$	$\pm0.2\,mll^{-1}$	$	1 MV[5] per hour
*		current	$\pm2\,ms^{-1}$	$1\,cms^{-1}$	ACCM-§	1 MV[5] per hour
*		spare volt. inp.	$0–+5V$	$\pm1\,mV$	$	1 MV[5] per hour
*		spare volt. inp.	$0–+5V$	$\pm1\,mV$	$	1 MV[5] per hour
**		extra temp.	$-10–+30°C$	$\pm10\,mK$	$	1 MV[5] per hour
**		extra temp.	$-10–+39°C$	$\pm10\,mK$	$	1 MV[5] per hour
*	12m	temperature	$-5–+35°C$	$\pm10\,mK$	$	1 MV[3] per hour
*		conductivity	$0–70\,mScm^{-1}$	$\pm10\,\mu Scm^{-1}$	$	1 MV[3] per hour
*		pressure	$0–680\,kPa$	$\pm1\,kPa$	$	1 MV[3] per hour
*		oxygen	$0–15\,mll^{-1}$	$\pm0.2\,mll^{-1}$	$	1 MV[3] per hour
*		current	$\pm2\,ms^{-1}$	$1\,cms^{-1}$	ACCM-§	1 MV[5] per hour
*		spare volt. inp.	$0–+5V$	$\pm1\,mV$	$	1 MV[5] per hour
*		spare volt. inp.	$0–+5V$	$\pm1\,mV$	$	1 MV[5] per hour
**		extra temp.	$-10–+30°C$	$\pm10\,mK$	$	1 MV[5] per hour

Table 2 Parameters measured on the IOW Discus Buoy station "Oder Bank"

@	Integrated measuring system—© Ammonit, Germany	MV	Mean value, general measuring frequency 0.1 Hz
#	Radioactivity-logger—© BSH, Germany	MV[1]	MV of continuous measurement bursts over one hour
$	SeaCat—© Seabird, USA	MV[2]	Special procedure; speed and direction calculated from the MVs of 6 component measurement bursts (10 min long)
§	Oxygen sensors, ACCM—© ME, Germany	MV[3]	MV of 6 single measurements (every 10 minutes)
*	In operation since 16/11/93	MV[4]	MV of a 1000 s continuous measurement burst (once per hour)
**	In operation since 15/12/93	MV[5]	MV of a 10 min continuous measurement burst (once per hour)
***	In operation since 8/06/94		
****	In operation since 17/10/94		
*****	In operation since 20/05/96		

Table 3 Explanation for Table 1 and Table 2
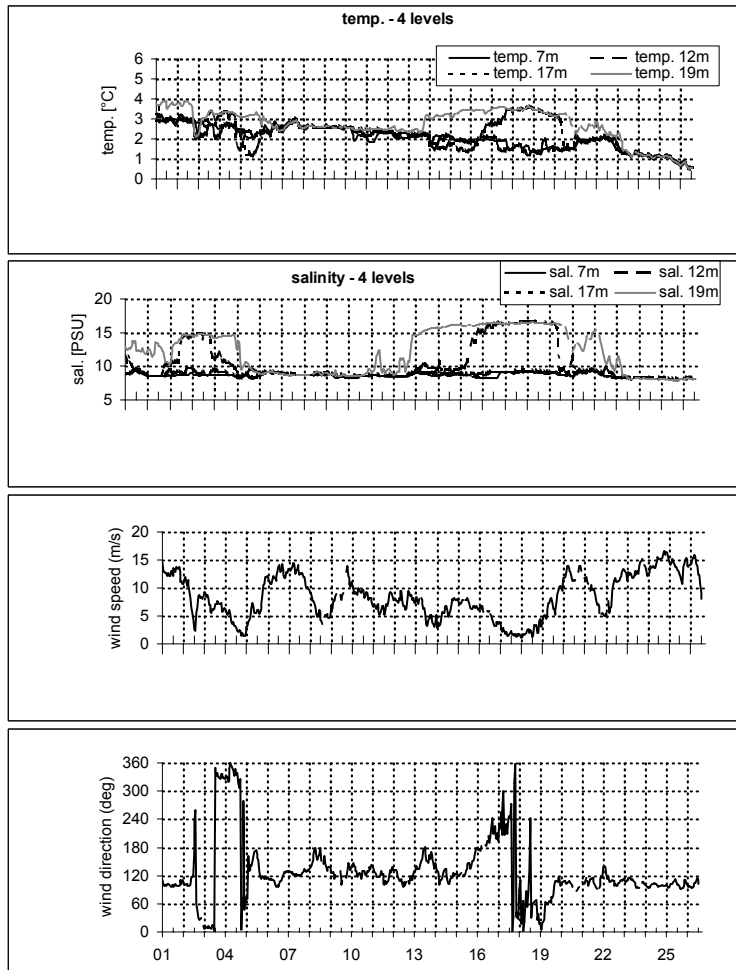
Figure 4 Measurements from mast station "DARSS SILL" for January 1996
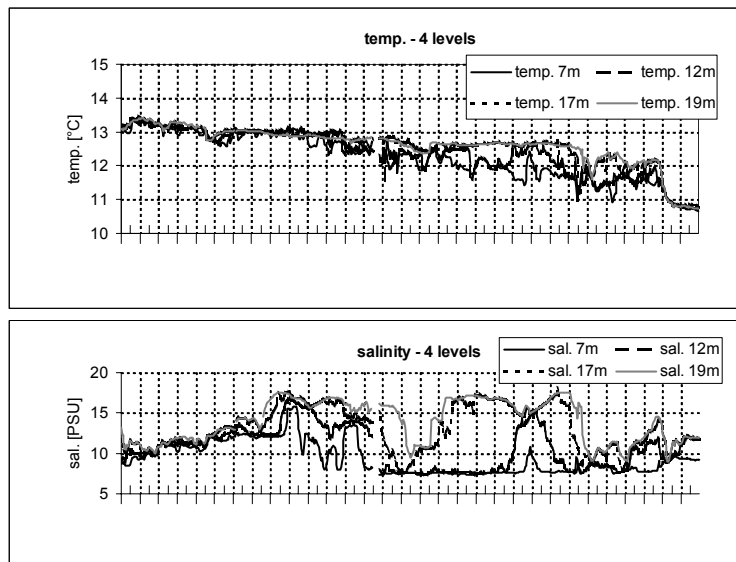
Figure 5 Measurements from mast station "DARSS SILL" for October 1996

Hiddensee upwelling field measurements and modelling results

H.-V. Lass, T. Schmidt and T. Seifert

Abstract

Characteristics of an upwelling filament, stretching from the west coast of Hiddensee island in north-westerly direction onto Mön, are outlined by an analysis of 26 events mainly based on NOAA-AVHRR satellite data (SST). For the first time field measurements of this dynamic feature have been carried out in July 1995, presented here together with a time series of SST-images. The vertical structure and water mass characteristics can now be considered, in addition to time and horizontal spatial scales, as well as currents measured by towed ADCP. By this means the origin of the upwelling water was revealed.

Model experiments, with the high resolution Warnemünde Ostsee Modell (WOM), a) for a barotropically driven outflow out of the Baltic Sea and b) for the same with additional local east wind forcing, have been carried out in order to understand the full dynamic background of this upwelling phenomenon. We argue that it is linked to the dynamics of general outflow situations at the Darss Sill and local Ekman off-shore transport at the north coast of Rugia.

Results

An upwelling filament, stretching from the west coast of the Hiddensee island in a northwesterly direction to Mön (see Figure 1), is well documented by some ten events, mainly based on NOAA-AVHRR satellite data (SST), see Horstmann (1983), Lass *et al.* (1994) or Siegel *et al.* (1994). Figure 1 displays the general bottom topography of the western Baltic Sea and the Belt Sea area. The area of investigation is zoomed at the right-hand side, with depth contour interval of 2 metres between 10 and 30m demonstrating the complex coastline geometry and bottom topography especially at the Darss Sill. The saddle depth of 17m at the Darss Sill is the shallowest obstacle for the water exchange between the North Sea and the Baltic Sea, see Fennel and Sturm (1992).
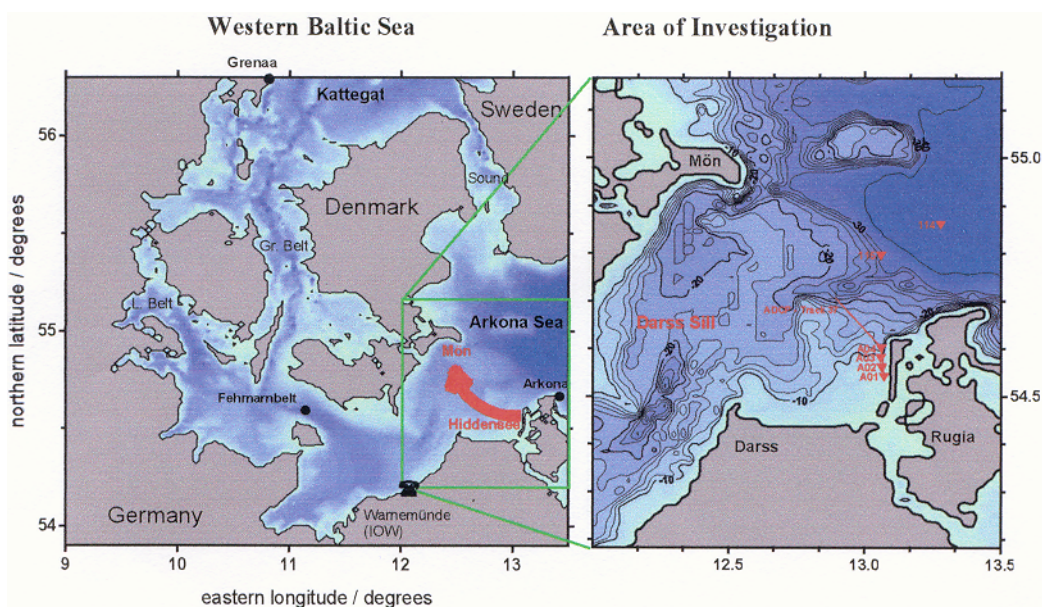
Figure 1 Topography of the transition area between the North Sea and the Baltic Sea with schematic Hiddensee upwelling filament (left) and area of investigation with hydrographic stations (right)

Characteristic scales of the mesoscale upwelling feature considered in the following starting at the west coast off Hiddensee island are a) 20 km basis at shore, b) 60 km offshore length, c) duration of 5 days and d) temperature deviation of –4 K.

For the first time field measurements of this dynamic feature have been carried out on 30th July 1995, presented in this paper (see Figure 2). The sea surface temperature distribution is shown Figure 2 measured by means of a thermosalino-

graph unit, mounted within the cooling water inlet of r/v "Professor Albrecht Penck", placed 1.2 metres below the sea surface. Dots represent every tenth value of the continuous temperature recording along the ships track, white cm-stations and ADCP-tracks have been performed. 10 and 20m depth contours are included as dashed lines for better orientation. The survey was performed within approx. 30 hours under a steady outflow and calm east wind regime. The lowest sea surface temperature observed was approximately 11°C within the upwelling illament, white the ambient surface water temperature was up to 21°C.
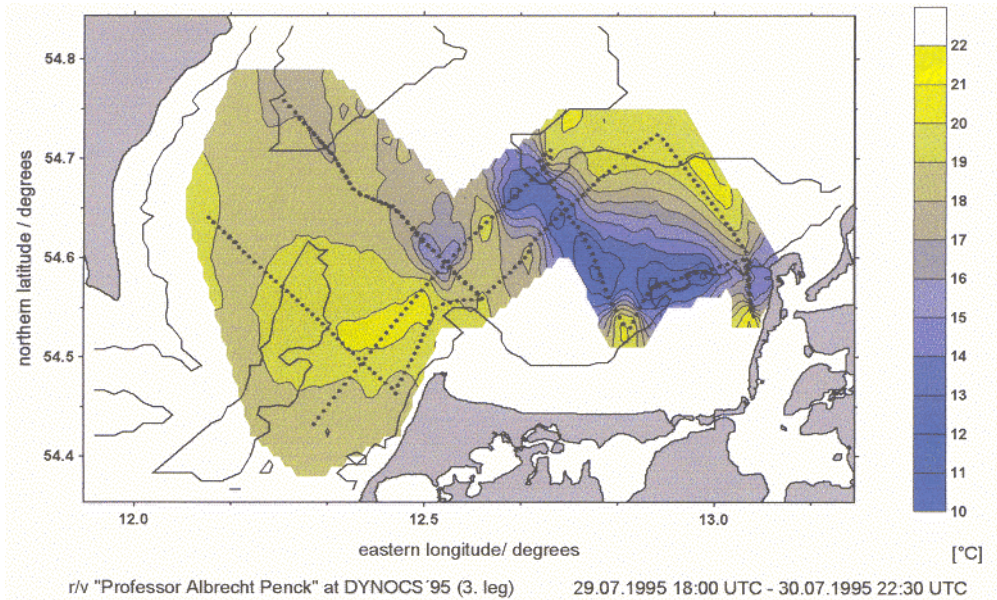
Figure 2 Distribution of sea surface temperature measured by the thermosalinograph of r/v "Professor Albrecht Penck". The dotted lines mark the ship's tracks.
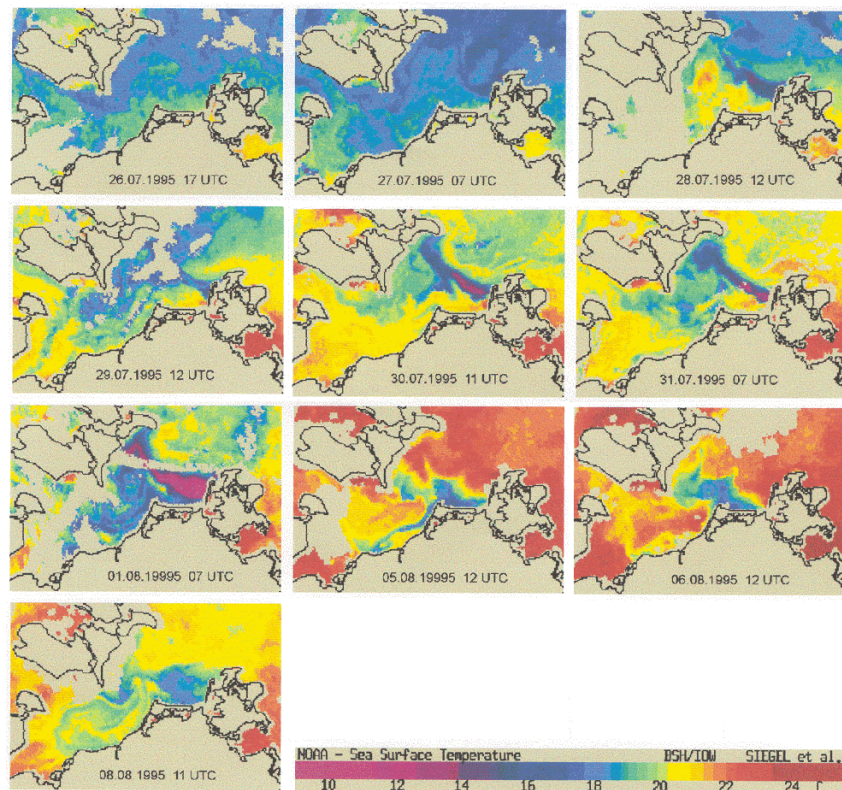
Figure 3 Distribution of sea surface temperature derived from NOAA-AVHRR data

A time series of NOAA-A VHRR satellite sea surface temperature (SST) scenes (provided by courtesy of BSH Hamburg and Dr. Siegel of IOW) shown in Figure 3 covers the whole event. This series reveals that the upwelling water appeared at the sea surface after 26th July, clearly seen at 27th July 07 UTC as darker shaded filament-like structure. The cloud

coverage is blanked e.g. on 29th July. The coincidence of ship and satellite based surface temperature measurements at 30th July is remarkable, even in details as e.g. the warm water intrusion at Darss Sill.

Vertical CTD-sections of water temperature (Figure 6) and salinity (not shown here) reveal that cold intermediate winter water of the Arkona Basin welled up at the northern coast of Hiddensee island. In Figure 6 CTD-casts along stations A01–A04, measured at 30th July 1995 have been supplemented by CTD profiles taken on stations 114 and 115 during the seasonal cruise of r/v "Alexander von Humboldt" on 5th August 1995, for position see Figure 1. The temperature section to station 115 located at the eastern slope of Darss Sill doesn't show intermediate winter water of the Arkona basin in contrast to the section ending in the central Arkona Basin at station 114. Obviously, the cold water tongue at the Darss Sill as seen in Figure 2 and Figure 3 is not due to local upwelling.

The upwelled water is advected westward from the north coast of Rügen and Hiddensee islands within the filament by a strong surface jet with velocities up to $75\,\mathrm{cm\,s^{-1}}$ as shown in Figure 4. The observed velocities in this jet are comparable to current observations north of Rügen Island reported by Lass and Schmidt, 1992. Velocity was measured by a catamaran towed along the track, shown in Figure 1, carrying a downward looking 300 kHz broad band ADCP. The projected current component is regarded as perpendicular to the track pointing into the Baltic. The jet is trapped at the bottom slope just northward of Hiddensee island between approx. the 20m and 10m depth contours. Its width is about 20km. The jet deepens at its southern edge, reaching down to the bottom within a band with a width of about 4km.

r/v PAP, DYNOCS´95, 3rd leg, towed BB-ADCP, track 37
Begin: 54° 43.39' N, 012° 54.45' E - End: 54° 32.65' N, 013° 03.79' E
Time : 30.07.95, 07:51 UTC   30.07.95, 10:23 UTC
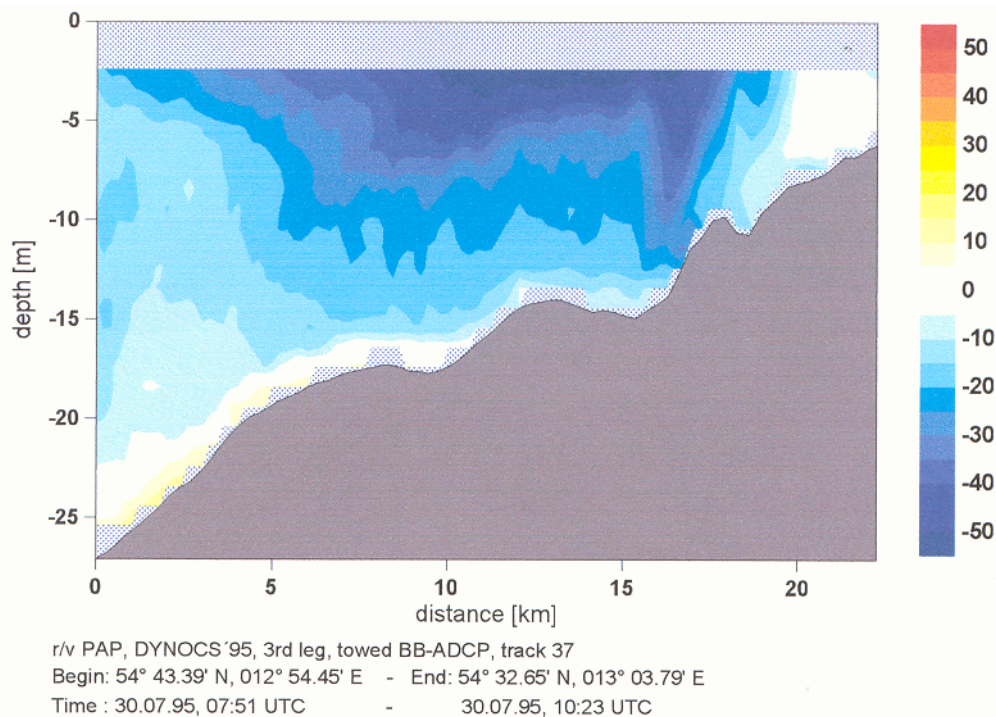
Figure 4 Projected component of current measured by a towed 600kHz ADCP of RDI. Positive values are towards 63°. The bottom contour is shaded grey.

A comparison between Figure 3 and Figure 5 reveals that the upwelling filament appeared on 27th July 1995 simultaneously with the onset of outflow marked by the change of current direction in Fehmarn belt to 300°. Moreover Figure 5 displays the turn of the wind direction from west to east (see negative east component of wind at Arkona; data of weather station Arkona by courtesy of German Weather Service). The easterly wind caused the observed lowering of sea level in the Kattegat at Grenaa and subsequently the decrease of the mean sea level of the Baltic (tide gauge at Landsort). After the decline of this outflow event the upwelling filament also disappeared (satellite picture for 5th August).
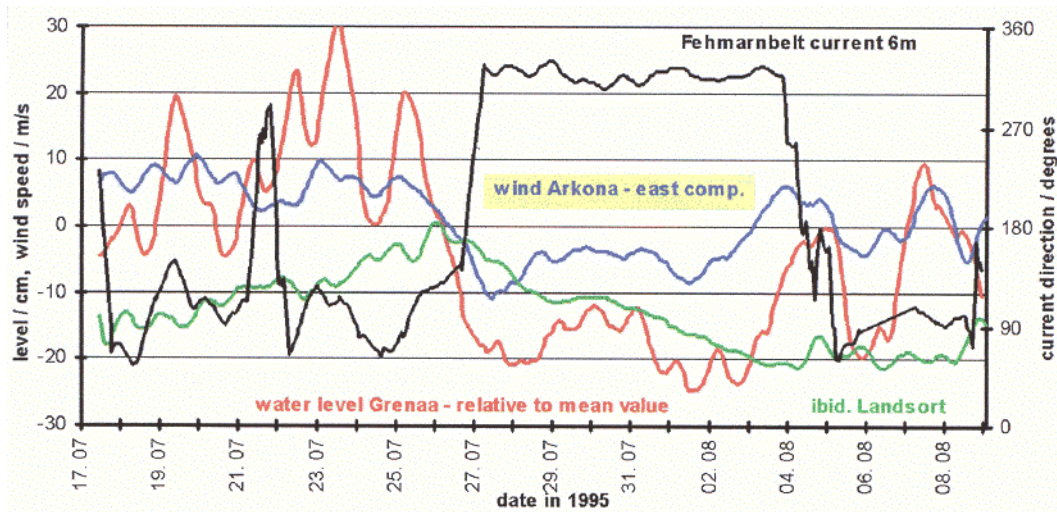
Figure 5 Time series of east component of wind velocity measured at the meteorological station Arkona (blue), sea level at Grenaa in the Kattegat (red) and Landsort in the Baltic proper (green), and direction of current measured in the Fehmarn Belt at a depth of 6 m (black). Outflow from the Baltic Sea toward the Kattegat is about 310° in the Fehmarn Belt.
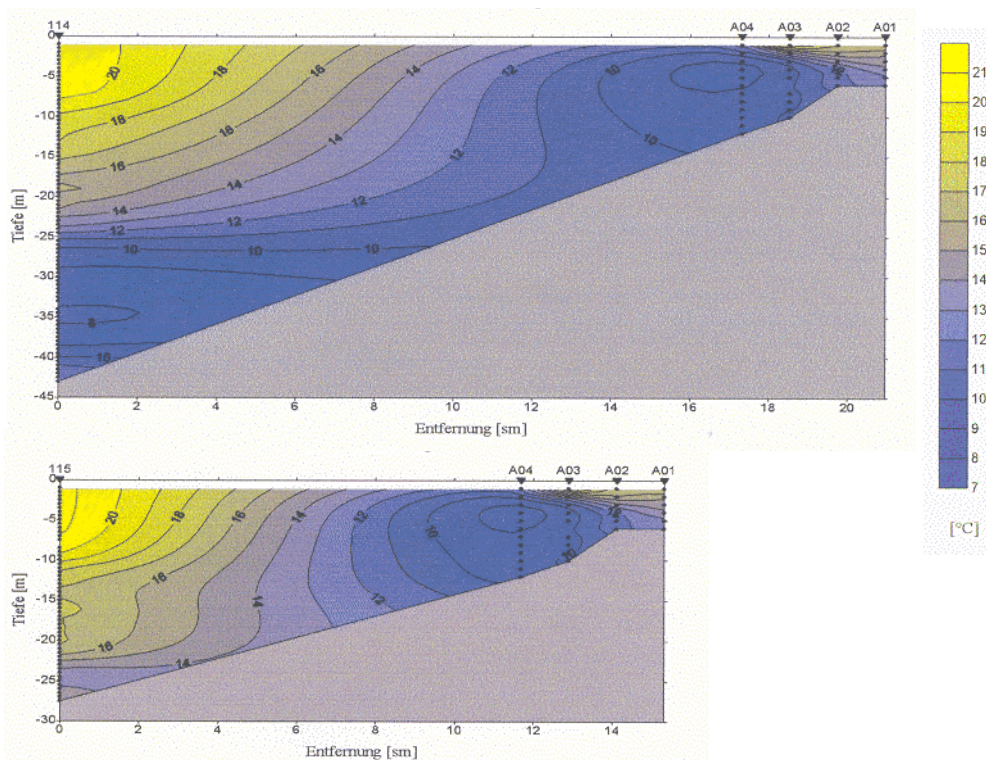
Figure 6 Vertical temperature distribution from the central Arkona Basin towards Hiddensee (above) and from the eastern rim of the Darss Sill towards Hiddensee (below). The locations of the stations are shown in Figure 1.

Simulations of the described observations with a high resolution circulation model of the Baltic Sea (WOM, see Fennel *et al.* (1994)) reveal that a westward directed jet establishes a response to the lowering of sea level in the Kattegat (see Figure 7). The jet stretches from the Darss Sill to the west coast of Hiddensee island continuing along the northern coast of Rügen island. Local Ekman upwelling at the northern coasts of Rügen and Hiddensee islands driven by easterly winds feeds this jet with cold intermediate water from the Arkona Sea.
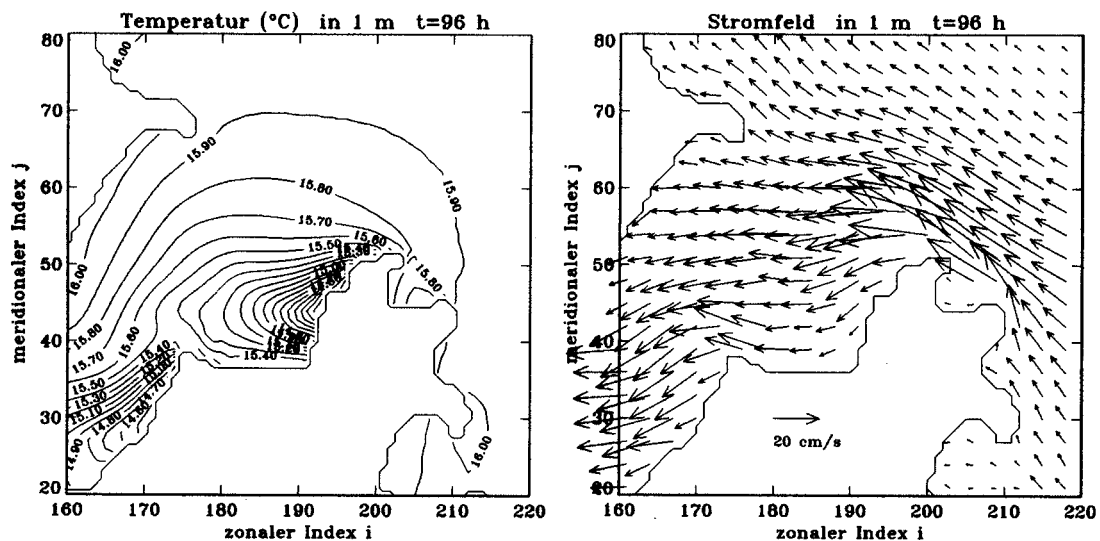
Figure 7 Modelled sea surface temperature (left) and current (right), 96 h after a step-like lowering of the sea level of the North Sea by 30 cm and the onset of a localised east wind in the Western Baltic

Summary

The Hiddensee upwelling filament fed by local upwelling with cold intermediate water from the Arkona Sea is generated by an adjustment process between the Darss Sill and the southern Arkona basin to a lowering of the sea level in the Kattegat. This is in contrast to upwelling filaments commonly observed at straight coasts which are mainly driven by advection of long lasting Ekman offshore transport.

Comparisons between observations and modelling reveal that both modelled currents and temperature fronts are too weak. This may be due to large horizontal exchange coefficients used in the model.

References

Fennel, W., and Sturm, M. (1992). Dynamics of the western Baltic, Journal of Marine Systems, Vol. 3, p. 183–205

Fennel, W., Schmidt, M., and Siefert, T. (1994). Hochauflösendes Zirkulationsmodell der westlichen Ostsee, (High resolution circulation modell of the western Baltic Sea) Abschlußbericht (Report) BMFT, BEO/7l 03F0057A

Horstman, U. (1983). Distribution patterns of temperature and water colour in the Baltic Sea as recorded in satellite images: Indicators for Phytoplankton Growth, Berichte aus dem Institut für Meereskunde Kiel, Nr. 106, Vol. 1

Lass, H.U., and Schmidt, Th. (1992). Observations of coastal jets in the Arkona Basin, Proceedings of 18th Conference of Baltic Oceanographers, St. Petersburg, 1993 and International Council for Exploration of the Sea, Rostock, Paper C.M. 1992/C:32, pp 11

Lass, H.U., Schmidt, Th., and Siefert, T. (1994). On the dynamics of upwelling observed at the Darss Sill, Proceedings of 19th Conference of Baltic Oceanographers, Sopot, p. 247–261

Siegel, H., Gerth, M., Rudloff, R., and Tschersich, G. (1994). Dynamical features in the western Baltic Sea investigated using NOAA-AVHRR data, Deutsche Hydrographische Zeitschrift, Vol. 46, No.3, p. 191–209

Geostrophic flow resistance in the Öresund

Johan Mattson
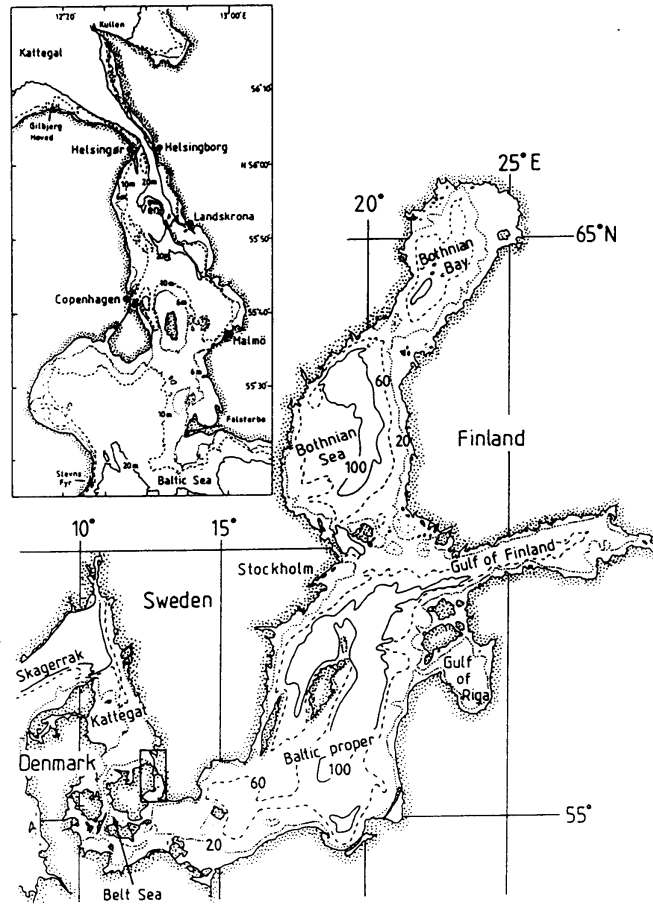
Figure 1 Map of the area

The idea of a geostrophic flow resistance was probably first presented by Garrett and Toulany in a pair of papers from the beginning of the eighties (Garrett and Toulany, 1982, and Toulany and Garrett, 1984). It appeared in a model of the flow through a strait driven by the sea level difference between two basins connected by the strait.
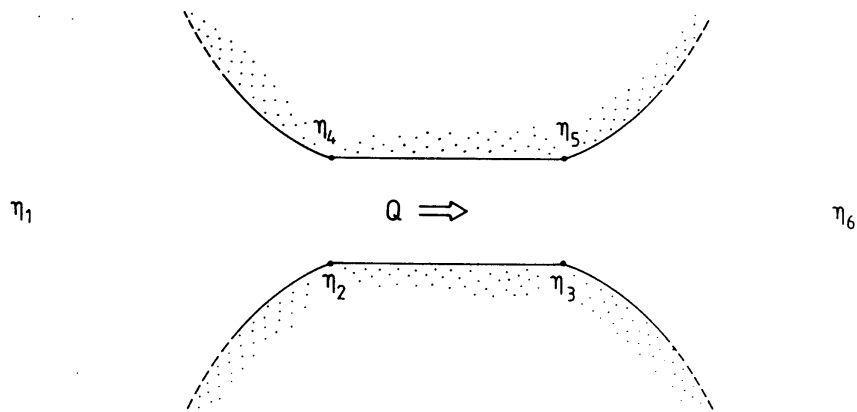
Figure 2 The sea level (η) at various positions in and outside a strait with flow rate $Q=VHW$

The model (Figure 2) is based on an assumption of cross-strait geostrophy

$$\eta_2 - \eta_4 = \eta_3 - \eta_5 = \frac{fW}{g}V \tag{1}$$

and an along-strait balance between the pressure gradient due to sea surface slope, acceleration and friction

$$\eta_2 - \eta_3 \;=\; \eta_4 - \eta_5 \;=\; \frac{L}{g}(\text{acc} + \text{fric})\,V \qquad\qquad (2)$$

L is the length of the strait and g the gravitational acceleration
V is the mean velocity,
W is the width of the strait and
f is the Coriolis parameter.

The problem is closed by a coupling between the basin and the strait sea levels. The assumptions that the highest level in the strait equals the upstream level ($\eta_2=\eta_1$) and the lowest level in the strait equals the downstream sea level ($\eta_6=\eta_5$), give together with (1) and (2) a relationship between the flow rate and the sea level difference between the basins

$$VWH \;=\; Q \;=\; gH\Delta\eta\left[f + (\text{acc} + \text{fric})\frac{L}{W}\right]^{-1} \qquad\qquad (3)$$

where $\Delta\eta=(\eta_1-\eta_6)$ is the forcing sea level difference between the two basins. The flow rate for given forcing is determined by the flow resistance. Thus, the effect of rotation is a contribution to the flow resistance, according to this model.

A feature of this model which was given special attention by its originators, is its form in the limit of steady state and no friction. In this case the sea level difference across the strait equals the sea level difference between the two basins. By arguing that it cannot be more, this state is referred to as a state of geostrophic control. In conclusion, we have

$$Q \leq \frac{gH}{f}\Delta\eta \qquad\qquad (4)$$

The idea of geostrophic resistance, which, quoting Chris Garrett, "seemed good at the time", has had some trouble being accepted. This is obviously due to the matching conditions between the basins and the strait, which completely govern the solution but are somewhat arbitrarily determined. In the major part of the treatments discussing the geostrophic control, the proposed flow situation is realised by propagating Kelvin waves (Pratt, 1991). While the basin–strait matching is consistent with Kelvin wave propagation in two infinite basins with equal depth in the basins and the strait, problems arise with unequal depths in the basins and the strait, or with basins having finite area. Further objections can be raised when long time scales are considered. Linear solutions to the Rossby adjustment problem in a strait give Kelvin waves propagating away from the initial discontinuity, leaving a steady flow equal to that given by the geostrophic control. The non-linear solutions show that this realisation is slowly advected, however, leaving a symmetric flow behind. This solution is identical to the subcritical solution given by inviscid hydraulic theory. For hydraulically subcritical flows the solution is symmetric and the sea level difference between the upstream and the downstream basin is zero.

An assumption of downstream dissipation is often used in models of non-rotating strait flow (Stigebrandt, 1980). Potential energy is spent to accelerate the flow through the narrow strait, but it is assumed that, as the flow expands, it cannot climb the pressure hill. This means that the lowest level in the strait equals the downstream basin sea level. In effect, downstream dissipation causes energy losses, i.e. flow resistance. This is in contrast with inviscid hydraulic theory, by which the only possible energy losses are through hydraulic jumps.

Thus, it appears that downstream dissipation is a prerequisite for geostrophic resistance in steady state. There is no way, however, to find an analytical solution involving downstream dissipation based on the equations of motion. The existence of a geostrophic resistance has to be shown empirically.

A modification of the above theory will be presented. In what follows a steady state is described and the along-strait balance is frictional, given by

$$\eta_2 - \eta_3 \;=\; \eta_4 - \eta_5 \;=\; \frac{c_D L}{gH}V^2 \qquad\qquad (5)$$

The frictional resistance is modelled using a quadratic friction law, where c_D is a drag coefficient. The model of Toulany and Garrett was originally designed to analyse time series of sea level data in the frequency domain, and so is linear by necessity. The advective terms are neglected and the frictional effects are modelled with a linear friction law. Due to the rather unrealistic linear friction law the model cannot explain the flow resistance in a shallow strait like the Öresund, where frictional effects dominate.

As suggested by the concept of downstream dissipation, the lowest level in the strait will still be assumed equal to the downstream basin sea level, i.e. ($\eta_6=\eta_5$). The coupling between the upstream basin and the strait is the sum of a non-rotating and a rotating part $\eta_1-\eta_4=(\eta_1-\eta_{RT})+(\eta_{RT}-\eta_4)$ (cf. Whitehead, 1986), where the non-rotating part is

$$\eta_1 - \eta_{RT} = \frac{1}{2g}V^2 \tag{6}$$

and the rotating part is:

$$(\eta_{RT} - \eta_4) = \frac{1}{2}\frac{fW}{g}V \tag{7}$$

The non-rotating part is the Bernoulli setdown, caused by the acceleration towards the strait. The rotating part is based on cross-strait geostrophy, and the factor 1/2 corresponds to a geostrophic tilt that is distributed such that the sea level is depressed over half the width of the strait compared to the non-rotating solution. These basin-strait couplings result in the expression

$$\Delta\eta = \frac{1}{2}\frac{fW}{g}V + \left(\frac{1}{2g} + \frac{c_D L}{gH}\right)V^2 \tag{8}$$

However, for $V<fW$, the sea level at the right hand side of the strait may formally become higher than the upstream sea level ($\eta_2>\eta_1$). This is not possible for streamlines originating in a motionless upstream basin. By simply requiring that $\eta_2=\eta_1$ for $V<fW$ we have

$$\Delta\eta = \frac{1}{2}\frac{fW}{g}V + \left(\frac{1}{2g} + \frac{c_D L}{gH}\right)V^2 ; V \geq fW$$

$$\Delta\eta = \frac{fW}{g}V + \frac{c_D L}{gH}V^2 ; V < fW \tag{9}$$

This is the model that should be tested against observations, and which accurately describes the low frequency flow through the Öresund. The model gives the flow resistance as a combination of the linear contribution from the geostrophic resistance and two quadratic contributions, one related to the Bernoulli setdown and the other due to frictional drag. The physical explanation for the geostrophic resistance is then clear. A pressure drop is required to accelerate the water towards the strait, and this pressure drop is not recovered downstream. This may be seen as a kind of form drag. In rotating systems an additional pressure drop is needed to geostrophically balance the flow, and this effects adds to the form drag.

Expression (9) can be written

$$\Delta\eta = K_t Q + K_q Q^2 \tag{10}$$

where K_t and K_q are flow resistance coefficients to be determined from observations. In a paper by the present author (Mattsson, 1995), where 1802 simultaneous observations of sea level difference and flow rate from the Öresund were used (Figure 3), a least-squares fit gave $K_q=1.29\cdot10^{-10}\,\text{s}^2\text{m}^{-5}$ and $K_t=0.32\cdot10^{-5}\,\text{sm}^{-2}$.
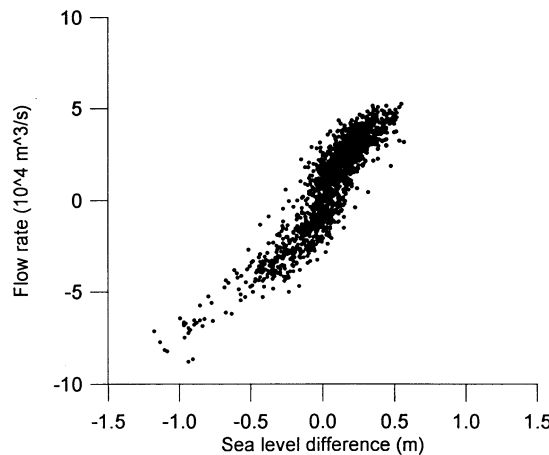
Figure 3 1802 simultaneous estimates of flow rate and sea level difference

Returning to expression (9), which can be written

$$\Delta\eta = \frac{1}{2}\frac{f}{gH}Q + \left(\frac{1}{2gH^2W^2} + \frac{c_DL}{gH^3W^2}\right)Q^2; Q \geq fHW^2$$

$$\Delta\eta = \frac{f}{gH}Q + \frac{c_DL}{gH^3W^2}Q^2; Q < fHW^2 \qquad (11)$$

it follows that

$$K_t = \frac{f}{2gH}; Q \geq fHW^2$$

$$K_t = \frac{f}{gH}; Q < fHW^2 \qquad (12)$$

Inserting appropriate values (cf. Mattsson, 1996) and using an amplitude distribution based on the observations, K_t should during 40 percent of the time correspond to $0.37 \cdot 10^{-5}$ and to $0.31 \cdot 10^{-5}$ during 60 percent of the time. The weighted sum is $0.33 \cdot 10^{-5}$, which is very close to what was empirically found. Thus, the data strongly supports the existence of a geostrophic resistance as defined by the model.

Traditionally, the flow resistance in the Öresund has been modelled using a quadratic relation only (e.g. Jacobsen, 1980, Omstedt, 1987 and Stigebrandt, 1992). The skill of such a model appears to be very good, measured by an explained variance of over 80 percent. The reason for its success is obviously the strong frictional influence on the flow resistance. When the geostrophic resistance is included the explained variance only increases by about 2 percent. This appears insignificant, and has put the combined model (the model combining a quadratic and a linear term) in doubt. However, the increase by 2 percent is exactly what can be expected. In a hypothetical case, trying to fit a quadratic function to a linear relation, the explained variance would differ by only 6.25 percent, and any combined model having both a quadratic and a linear term would have a smaller difference.

Instead, the main effect of using a quadratic model without the geostrophic term is an incorrect amplitude frequency distribution. A closer inspection shows that flow rates for weak forcing are systematically overestimated and vice versa. This becomes clear in a plot of the amplitude probability density function for the flow rate, based on observations, the quadratic model and the combined model (Figure 4). The least-squares fit using the quadratic model, in its attempt to minimise the deviation (i.e., maximise the explained variance), apparently shifts the distribution towards higher flow rates. The combined model is much more successful in explaining the correct distribution. Again measuring the skill with the explained variance, the geostrophic term increases the explained variance by 30 percent, from 67 to 97 percent. The linear term, i.e., the geostrophic resistance, is obviously necessary to model the flow resistance and hence reproduce the flow through the Öresund.
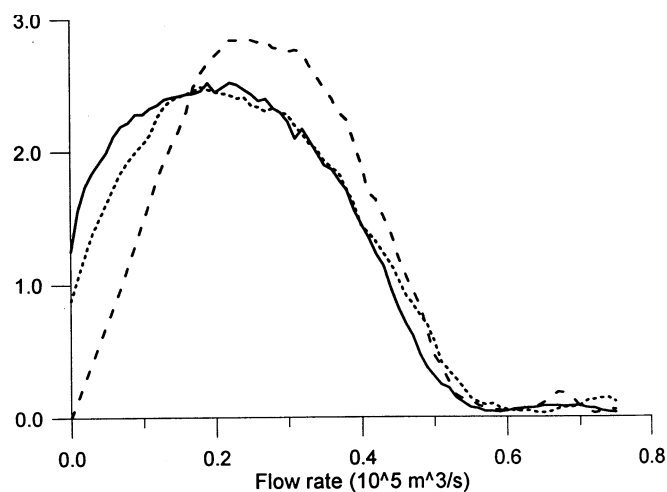
Figure 4 The probability density function of the absolute flow rate, $p(|Q|)$, for the observed flow rate (solid line), the flow rate according to the quadratic model (dashed line) and according to the combined model (dotted line)

In the general case, guidance can be provided by the non-dimensional version of expression (11). Introducing the primed dimensionless variables $\Delta\eta = H\Delta\eta'$ and $Q = (g^{1/2}H^{3/2}W)Q'$ gives

$$\Delta\eta' = \frac{1}{2}\frac{W}{a}Q' + \left(\frac{1}{2} + c_D\frac{L}{H}\right)Q'^2 ; Q' \geq \frac{W}{a}$$

$$\Delta\eta' = \frac{W}{a}Q' + c_D\frac{L}{H}Q'^2 ; Q' < \frac{W}{a} \tag{13}$$

where a is the Rossby radius of deformation. The geostrophic control limit refers to cases where the strait is of order of the deformation radius, small length to depth ratios and for small flow rates $Q' \to 0$.

References

Garrett, C. and Toulany, B., 1982. Sea level variability due to meteorological forcing in the northeast Gulf of St. Lawrence, J. Geophys. Res., 87, 1969–1978.

Jacobsen, T. S., 1980. Sea Water Exchange of the Baltic. Measurements and Methods, The Belt Project. 107 pp. The National Agency for Environmental Protection. Denmark.

Mattsson. J., 1995. Observed linear flow resistance in the Öresund due to rotation, J. Geophys. Res. 100, C10. 20779–20791.

Mattsson, J., 1996. Some comments on the barotropic flow through the Danish straits and the division of the flow between the Belt Sea and the Öresund. Tellus, 48A. 456–464.

Omstedt. A., 1987. Water cooling in the entrance of the Baltic Sea. Tellus. 39A, 254–265.

Pratt. L. J., 1991. Geostrophic versus critical control in straits. J. Phys. Oceanogr. 21. 728–732.

Stigebrandt, A., 1980. Barotropic and baroclinic response of a semi-enclosed basin to barotropic forcing from the sea. in Fjord Oceanography. pp. 151–164. Plenum Press. New York.

Stigebrandt. A., 1992. Bridge-induced flow reduction in sea straits with reference to effects of a planned bridge across Öresund, Ambio. 21. 130–134.

Toulany, B. and Garrett, C., 1984. Geostrophic control of fluctuating barotropic flow through straits. J. Phys. Oceanogr. 14. 649–655.

Whitehead, J. A., 1986. Flow of homogeneous rotating fluid through straits. Geophys. Astrophys. Fluid Dyn. 6. 101–125.

Distribution patterns of nutrients discharged by the river Odra into the Pomeranian Bight

Klaus Nagel

Summary

With a focus on chemical parameters, several types of distribution patterns for the matter discharged by the river Odra into the Pomeranian Bight can be classified. Two types of hydrographically controlled distribution patterns are discussed, the 'west wind situation' and the 'east wind situation'. Both types are characterised by the directions in which the riverine material is transported. The amount of discharged material that reaches the offshore regions of the Baltic Sea does not only depend on water supply, but also on transformation and modification processes taking place in the plume. The influence of these processes on the distribution patterns is dominated by seasonal effects, mainly controlled by the biological activity in the water.

Introduction

The TRUMP project (Transport and Turnover Processes in the Pomeranian Bight) was established to describe the transport and transformation of material discharged by the river Odra and some smaller freshwater inflows into the Pomeranian Bight and the influence of these processes upon the marine ecosystem in the offshore regions of the Baltic Sea. In an interdisciplinary approach, complex datasets of meteorological, hydrographic, chemical and biological parameters were analysed in cooperation with Polish and German institutions.

Objectives of the project are the characterisation of the transport mechanisms and distribution patterns of the discharged material and the description of processes responsible for the transformation and modification of this material.

Experimental strategies

Between September 1993 and January 1996, seven cruises were performed within the TRUMP project as multiship surveys. At least two ships were operating simultaneously for 2–3 weeks in the area under investigation. Experiments on one ship focused on transport processes while the second ship concentrated on the analysis of transformation processes.

For the characterisation of transport processes and distribution patterns, samples were taken within 60–80 hours by one of the ships on a station grid covering the whole bight (Figure 1). Besides standard meteorological, hydrographic and chemical parameters, which were analysed at all stations, additional measurements were performed at selected stations: dissolved and particulate organic carbon and nitrogen, some naturally occurring organic compounds (e. g. urea, carbohydrates, amino acids, etc.), contaminants, biological variables, sediment analysis, etc. 2–4 samples were taken at the grid stations in time intervals of 48–96 hours during each cruise.

During the experiments, additional measurements were performed by other Polish and German ships and institutions in the river mouth, the lagoons and at inshore stations.

This paper focuses on the classification of distribution patterns of nutrients depending on meteorological and seasonal conditions. An illustration of other aspects of the TRUMP project is given elsewhere (e.g. Bulletin of Sea Fisheries Institute 3 (136), 1995; TRUMP, 1996).
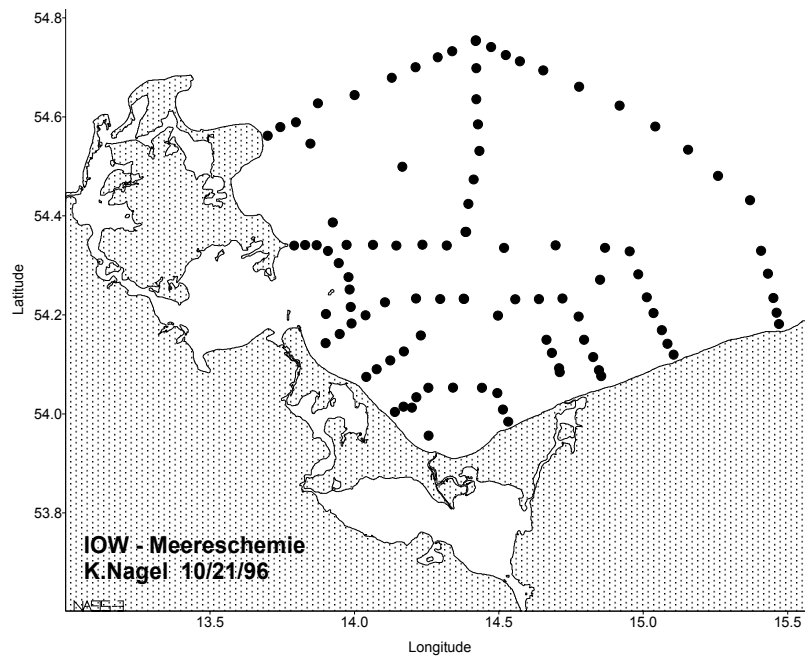
Figure 1 TRUMP: Station grid in the Pomeranian Bight

Results

During the TRUMP cruises in 1993–1996 concentrations of nutrient salts were measured in the plumes of the river Odra (via the rivers Swina and Dziwna) or the river Peene (via Greifswalder Bodden). Concentrations of all nutrient salts are highly variable showing great fluctuations within one or two days. As an example, variations of nitrate concentrations very close to the Swina mouth are shown in Figure 2. Factors responsible for these high variations are:

- 'Preconditioning' of the riverine discharge in the lagoons, mainly due to the modification and transformation processes caused by high biological activity found in the lagoons in late spring and in summer. This preconditioning effect is strengthened by the fact that freshwater discharge from the river Odra is lower in the period with high biological activity (May–November) and higher in the period of low biological activity (December–April).

- 'Pulsating' of the riverine outflow showing distinct 'outflow events' (Figure 3). Outflow events are mainly controlled by differences of the water levels between the Baltic Sea and the lagoons (Lass, 1994; Lass *et al.*, 1995a). The riverine water with low salinity spreads in the surface layer during an outflow event, while mixing with subsurface water occurs in a second step which is controlled by meteorological and hydrographic factors (e.g. wind directed circulation of water masses).
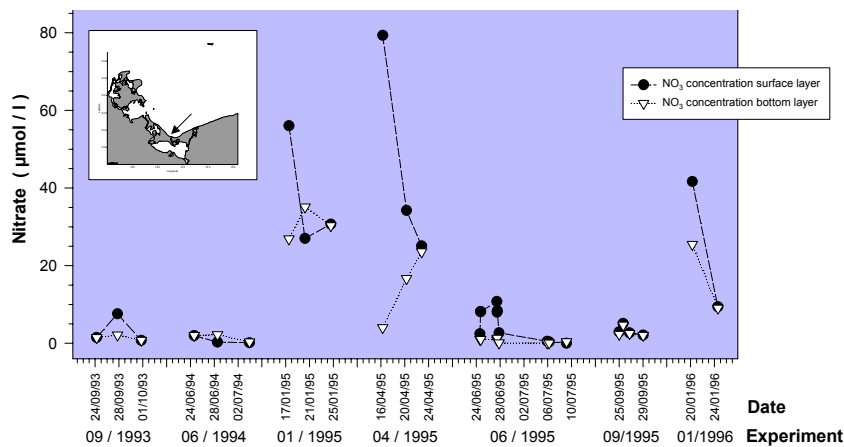
Figure 2 Concentrations of nitrate in the surface and bottom layer at station 10 situated very close to the Swina mouth. Results obtained during each experiment are linked by a line.
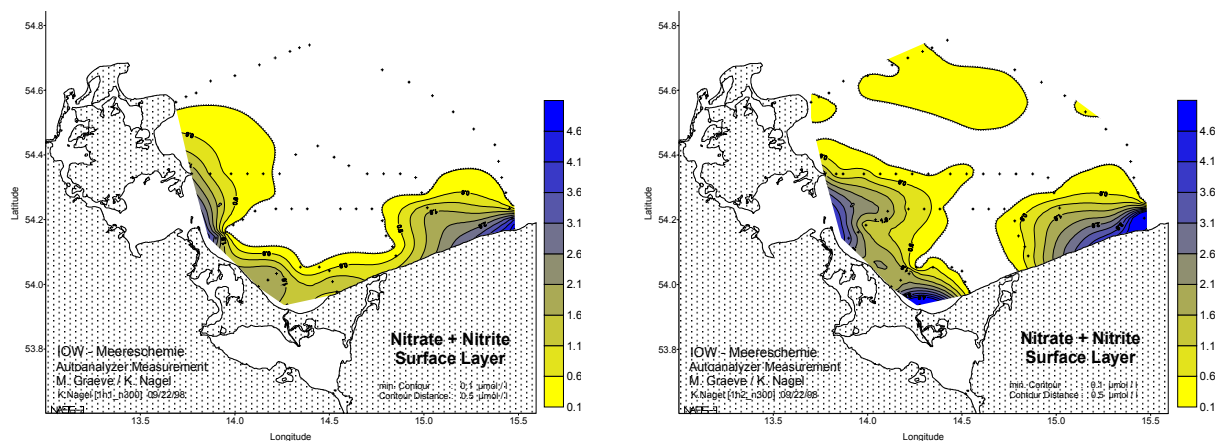
Figure 3 Distribution patterns of nitrate in the surface layer before (left) and during (right) and outflow event in September 1993. Sampling positions are marked on the map with a plus (+))

Generally, concentrations of all nutrients in the outflowing riverine water are higher during winter and early springtime. While amounts of N-containing nutrients are significantly lower during the summer, phosphate is depleted in the discharges in late springtime and summer. In autumn an increase of phosphate is observed some weeks before the increase of nitrate concentrations starts again. This difference in seasonal minima of N- and P-containing nutrient salts is caused by the tie-lag between the start of plankton bloom in the lagoons and the inner parts of the Pomeranian Bight in springtime and the beginning of remineralisation processes in both areas in late summer. As a result of the phosphate depletion in the discharged water biological activity in the inner parts of the bight can be limited by phosphate in late springtime.

Characterisation of standard and special situations

'West wind situation' and 'Summer conditions' (TRUMP experiment in June/July 1994)

Material of the river plume is transported in a small strip along the coast towards the eastern parts of the Baltic if westerly winds (including directions from north to southwest) predominate for several days (Figure 4). Such transport bands can sometimes be followed from the Pomeranian Bight to the Gulf of Gdansk in satellite images (Lass *et al.*, 1995a). The riverine water with lower salinity is mixed down to the bottom layer in this shallow area. In summer, similar 'transport bands' shown for nitrate in Figure 4 are also found for salinity and chlorophyll.
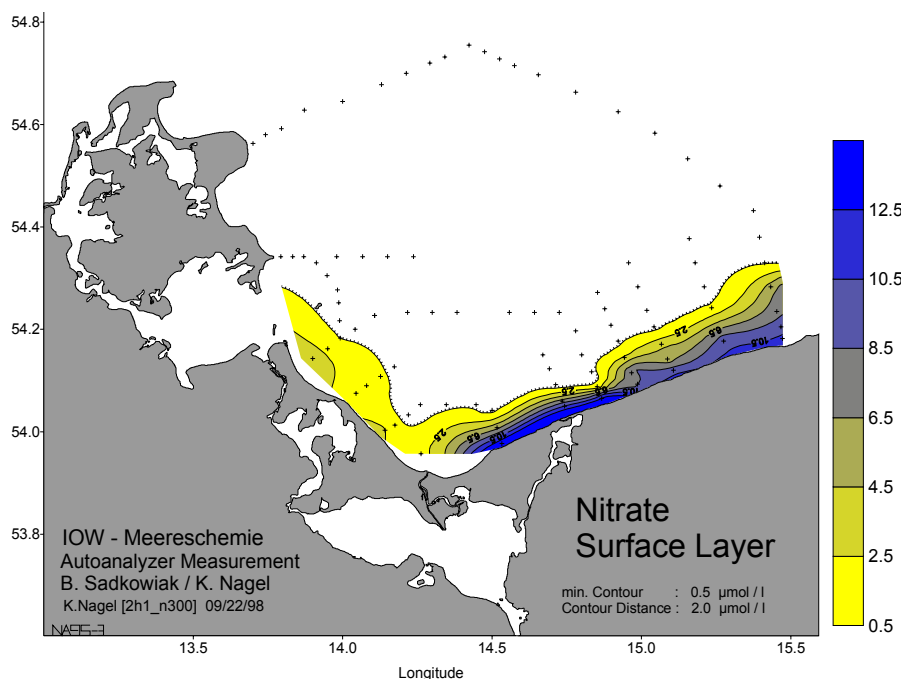
Figure 4 Distribution pattern of nitrate in June 1994. Samples have been taken from the surface layer at the first sampling from the grid stations.

Nutrient salts are nearly depleted in the whole bight due to the high biological activities in summer. While phosphate and nitrate are near or below the detection limit in the central parts of the bight, low concentrations are found for ammonia and silicate ($0.1-3\,\mu\text{moles}\cdot\text{dm}^{-3}$ and $5-15\,\mu\text{moles}\cdot\text{dm}^{-3}$, respectively).

Distribution patterns differ significantly for the individual nutrient salts in the plume since transformation processes and modification of material take place in the lagoons as well. Highest concentrations of ammonia were found in the Dziwna estuary (far more than $3\,\mu\text{moles}\cdot\text{dm}^{-3}$), while the main source of nitrate was the Swina during this cruise. Phosphate was below the detection limit at all stations in this region. Silicate concentrations were higher in the coastal zone, but no pronounced effect of the plume was observed (Nausch *et al.*, 1995).

As the fate of the riverine matter in the bight is mainly controlled by transformation and modification of material under summer conditions, these processes superimpose the effects caused by the transport of the freshwater discharge.

'East wind situation' and 'Winter conditions' (TRUMP experiment in January 1996)

'East wind situations' become established if the dominating wind directions are between northeast and south for several days. Under this regime, riverine water is spread northwards along the coast of Usedom and Rügen within an area covering the whole western part of the bight (Figure 5). Distribution of material is more homogenous than during 'west wind situations' and no steep horizontal and vertical concentration gradients are found.
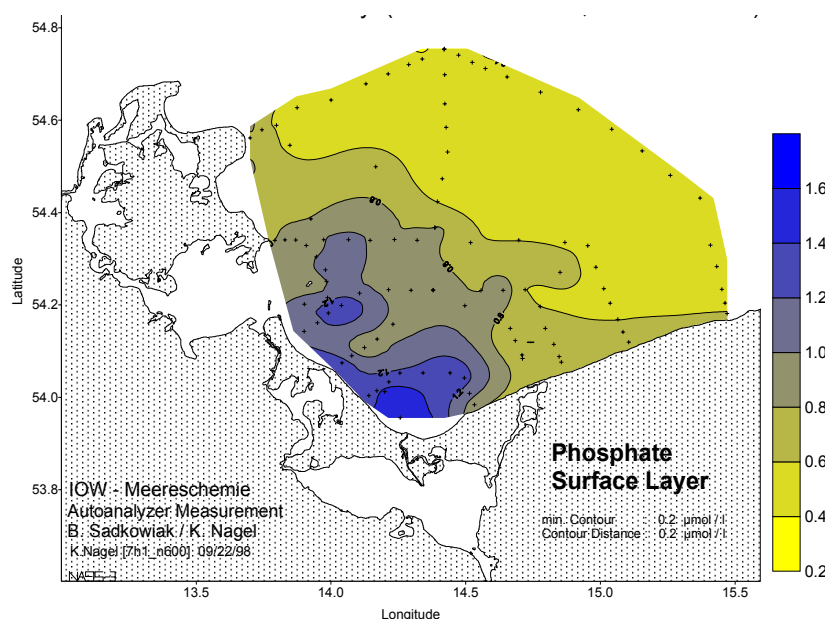
Figure 5 Distribution pattern of phosphate in January 1996. Samples have been taken from the surface layer at the first sampling from the grid stations.

The distribution patterns for salinity and the individual nutrient salts were found to be very similar in the experiments performed in winter. Due to low biological activity at this time of the year, transformation processes seem to be negligible. Variations in the distribution patterns are primarily based on the transport of material by advective processes and mixing of riverine water with the seawater in the bight. This effect is expressed by significant correlations between the individual nutrients and between nutrients and salinity (Figure 6).
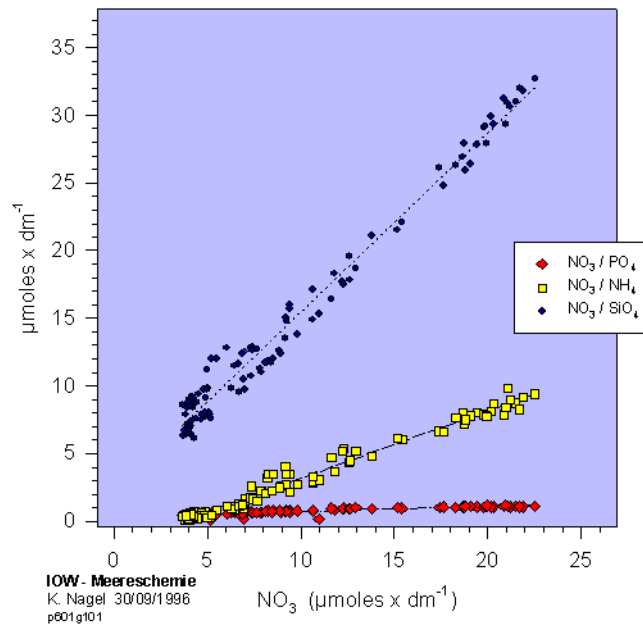
Figure 6 Correlations between the concentrations of individual nutrient salts in January 1996. Samples have been taken from the surface layer at the first sampling from the grid stations.

Distribution patterns caused by special situations (e.g. TRUMP experiments in September 1993 and September/October 1995)

During some cruises, distinct areas were found which differ significantly from the surroundings with respect to hydrographic conditions, nutrient concentrations or the biological activity. Examples for such patterns were observed during the cruises in September 1993 (for details see Pastuszak *et al.*, 1996) and in September/October 1995 (Figure 7). North of Usedom a water body was identified which is characterised by low salinity and nutrient concentrations but high biological activity. It had been observed for several days in the same area. This 'enclosure' developed after the reversal of water circulation in the bight caused by the change of the wind direction from south to west shortly after an outflow event occurred. As verified by ADCP measurements, this water mass is stabilised by two currents: one is moving directly near the coastal line to northwest, the other one is going southwest several miles in front of the coast (Lass *et al.*, 1995b). Physicals aspects of this phenomenon are discussed elsewhere (Mohrholz 1998).
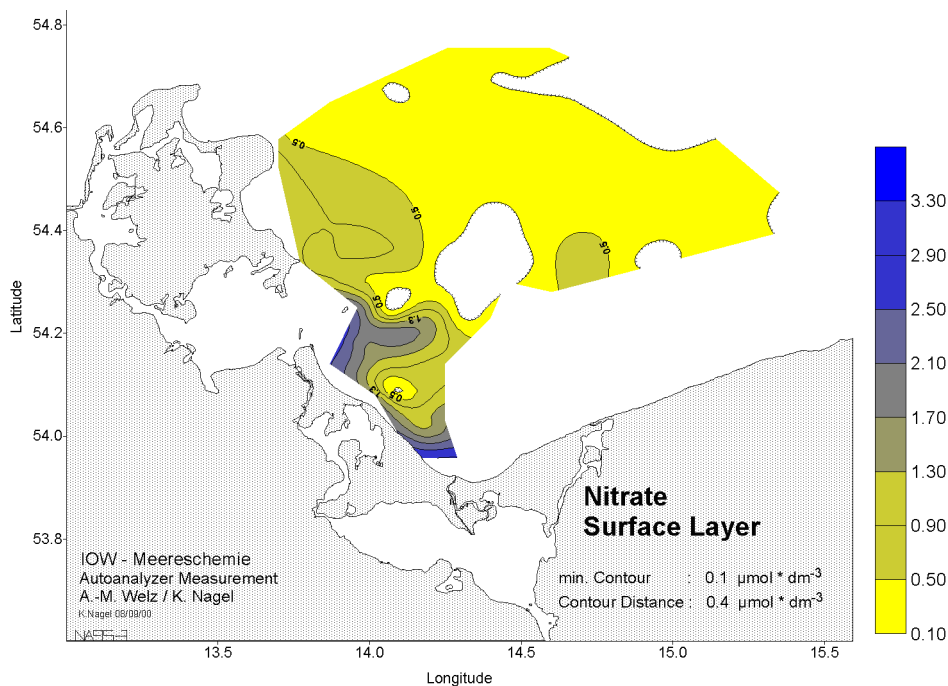
Figure 7 Distribution pattern of nitrate in September 1995. Samples have been taken from the surface layer at the first sampling from the grid stations.

Distribution patterns of nutrients discharged by the river Odra into the Pomeranian Bight

A separated and stable water body like that observed in September 1995 offers an excellent opportunity to study in detail the transformation and modification processes in an 'enclosure' under natural conditions.

Conclusions

Distribution patterns of nutrients identified during the TRUMP experiments can be classified according to the predominance of transport or transformation processes. Transport mechanisms are dominated by meteorological factors (west wind−east wind situations), while the comparison of seasonal patterns (summer−winter conditions) reveal the influence of transformation and modification processes mainly controlled by the biological activity. Data sets produced during each of those standard situations are a good tool for the test and verification of numeric models, which are necessary to describe the influence of riverine inputs on the marine ecosystem in offshore regions of the Baltic Sea. Water masses separated and stabilised by hydrodynamic mechanisms are of special interest for the estimation and validation of transformation rates needed for the forcing of models taking into account biological processes.

References

Lass, H. U. (1994). Preliminary Studies of a Pilot Study of TRUMP. Proc. 5th German-Polish Seminar on Coastal and Estuary Dynamics, October 26-30, 1993, Geesthacht, 5: 261−279

Lass, H. U., Fennel, W., Siegel, H., Sattler, K., Gerth, M., and Rüβ, D. (1995a). Zirkulations- und Transportprozesse in der Pommerschen Bucht. TRUMP, 1. Zwischenbericht 1994, pp 17−38

Lass, H. U., Mohrholz, V., and Nagel, K. (1995). Beobachtungen in einer isolierten Fluβwasserfahne vor der Küste Usedoms. (Poster zum 2. Statusseminar des GOAP-Projekts in Greifswald (13 & 14/12/1995)

Mohrholz, V. (1998). Transport- und Vermischungsprozesse in der Pommerschen Bucht. Meereswissenschaftliche Berichte 33: 1−106.

Nausch, G., Nagel, K., Nehring, D., Kerstan, E., Sadkowiak, B., and Welz, A.-M. (1995). Verteilungsgradienten chemischer Ökosystemparameter in der Pommerschen Bucht. TRUMP, 1. Zwischenbericht 1994, pp 39−68

Pastuszak, M., Nagel, K., and Nausch, G. (1996). Variability in nutrient distribution in the Pomeranian Bay in September 1993. Oceanologica 38: 195−225

TRUMP, 2. Zwischenbericht 1995 (1996)

Petroleum hydrocarbons in the onshore zone

Zbigniew Otremba, Adam Stelmaszewski, Krystyna Kruczalak, and Roman Marks

Introduction

Petroleum hydrocarbons in the onshore zone have different origins; the main source is discharge by rivers (over 50%), storm water from municipalities and municipal sewage (20%), operational and accidental discharges from shipping (1–20%) and the remainder come from atmospheric deposition, oil terminals, etc. (Enckell, 1986). Recent investigations conducted at the Maritime Academy in Gdynia also confirmed significantly higher petroleum hydrocarbons contamination of river waters compare to that recorded in the Baltic Sea coastal waters (Otremba and Stelmaszewski, 1996).

General data on the distribution of oil pollution concentrations in water as recorded within the $1\,\mu\mathrm{g\,dm^{-3}}$ range are plotted in Figure 1. The predominant occurrence of petroleum hydrocarbons in the sea water ranged within $1-2\,\mu\mathrm{g\,dm^{-3}}$, while in the river water the recorded concentrations ranged from 10 to $50\,\mu\mathrm{g\,dm^{-3}}$. The results again confirmed that rivers and streams are the main source of oil pollution in Baltic Sea onshore regions.
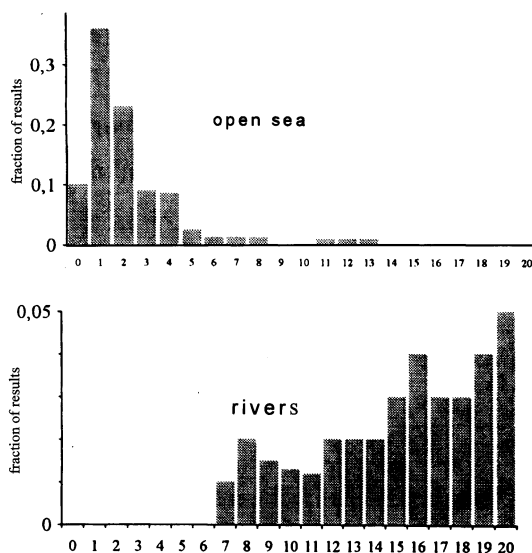
Figure 1 Oil content in the sea water and water from rivers entering the Baltic Sea on the Polish coast

Part of the petroleum hydrocarbons entering the coastal waters are transferred into sediments. Within the Polish coastal waters very high concentrations in sediments were recorded in the Gulf of Gdansk and the Pomeranian Bay. The highest values were recorded in the Gulf of Gdansk, eastward from the Vistula river mouth (Figure 2). This might be caused by continuous transport of oil pollution by river water and their sedimentation at the bottom.

Petroleum hydrocarbons in the sea water are subject to continuous transformation. After entering into the sea water the oil is degraded by bacteria and sunlight. The decay intensity depends on environmental conditions like temperature or coastal dynamics. In the coast zone the wave/sediments interaction may in particular control both dispersion and further horizontal and vertical transport. In addition however the sea to air transport of oil pollution can be expected. This particular research has been undertaken by our group. Until now however only preliminary data have been collected.

In order to trace the fate of the petroleum hydrocarbons in the coastal environment, complex measurements of the petroleum hydrocarbon concentration in water, sand, sediments and sea foam were performed.
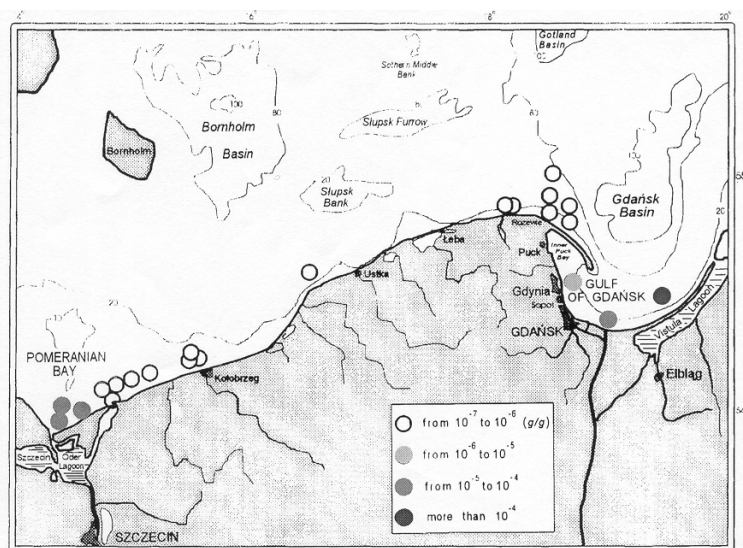
Figure 2 Concentration of hydrocarbons in the sediments near the Polish coast (Kaniewski *et al.*, 1995)

Method

Data presented in this work were collected within the Baltic Aerosol Experiment (BAEX). Measurements were conducted at Lubiatowo Research Station located over Southern Baltic Sea Coast. Data were collected during two field experiments in the autumn of 1994 and 1995 (Schulz *et al.*, 1996). During the BAEX experiment 53 subsurface water samples, 34 aerosol samples and 8 sand samples were collected. Water samples were taken from surface layer, subsurface and at 1m depth. The thicknesses of the collect surface layers were 90μm and 250μm depending on method. The foam samples were collected along the shore. Oil pollution content in the sea water, foam, aerosol and sand were analysed by the spectrofluorymetry method at the Gdynia Maritime Academy. All samples were extracted with hexane and the extracts were excited by 313nm light. The fluorescence intensity (wavelength 360nm) was a measured of amount of oil concentration. The quantity of oil was determined base on a calibration curve obtained for a standard which was the crude oil from the North Sea aged at 120°C for 2 hours.

Results

As a first approach all data on oil content in the sea water as related to offshore distance are plotted in Figure 3, Figure 4 and Figure 5. As shown in Figure 3 the recorded concentrations of oil in subsurface decreases with increasing distance from the water line. The same tendency was observed for surface water samples, see Figure 4. In this case however the recorded concentrations were about four times higher than that for subsurface water. At the same time oil in the micro-layer (250μm), see Figure 5, appears to have about ten times lower concentrations than in the surface layer (90μm). This result suggests than oil might be concentrated at the surface and near the bottom. Probably oil pollution accumulates in suspended matter which can sediment at the bottom or can be resuspended and fractionated by the breaking waves and bubbles.
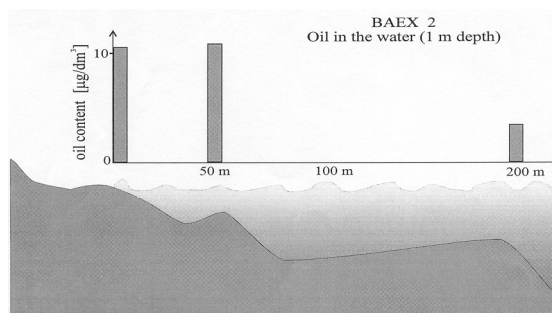
Figure 3 Concentration of hydrocarbons in subsurface layer as related to offshore distance
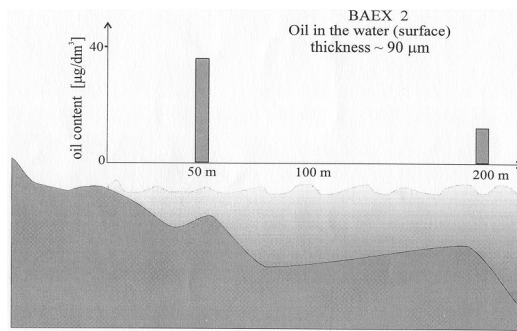
Figure 4 Concentration of hydrocarbons in the surface layer as related to offshore distance
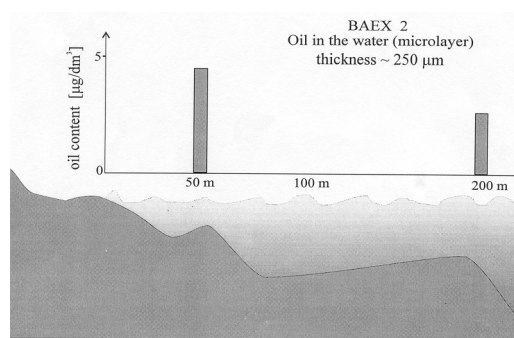
Figure 5 Concentration of hydrocarbons in the microlayer as related to offshore distance

As part of the experiment, the oil concentrations in aerosol were also investigated. Aerosol samples were collected on Whatman filters and were analysed using the same method as for the water. The data obtained are plotted in Figure 6 and Figure 7. In general the data recorded demonstrate a significant scatter (Figure 6). Further study however confirmed that distribution of data points strongly depends on the wind direction sector (Figure 7).
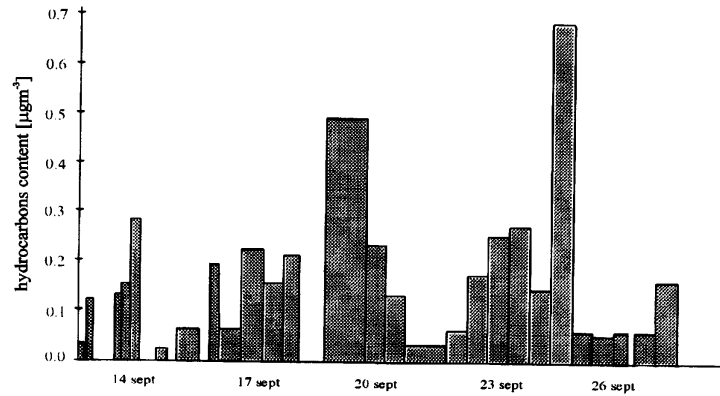
Figure 6 Concentrations of hydrocarbons in the air. Width of rectangles represents time of collection
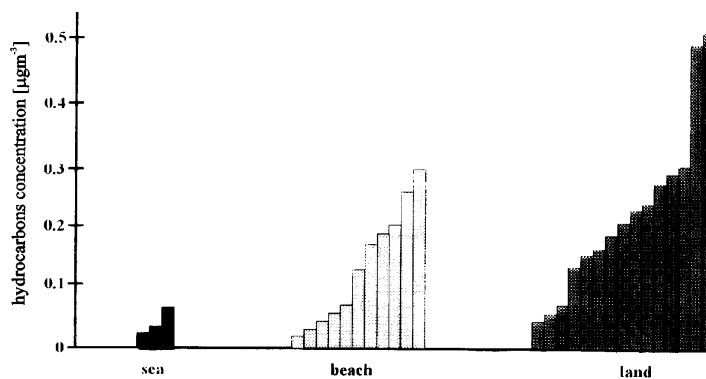
Figure 7 Concentrations of hydrocarbons in air as related to air advections from sea, beach and land

For comparison in Figure 8 the data on oil concentration in water as measured in various offshore distances is plotted for different wind direction sectors. Interpretation of these results is difficult, although data distribution suggest possible interpretation.
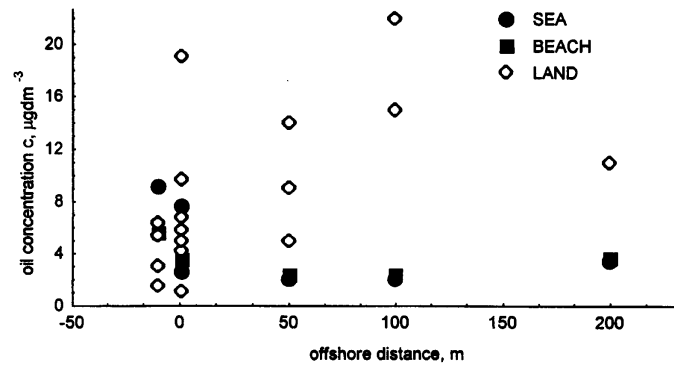
Figure 8 Concentration of hydrocarbons in seawater for different wind sectors: from sea, from land or along the coast.

In Figure 9 the concentration of oil in the onshore water is plotted against wind speed. The results obtained suggest that the amount of oil in the onshore water strongly depends on wind speed and breaking wave action, which may possibly control both dispersion and transport of oil contaminated sediments.
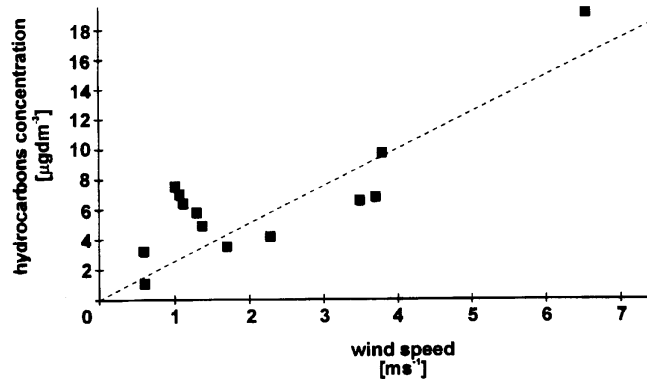
Figure 9 Hydrocarbon concentrations in subsurface water as a function of wind speed. Data collected in the breaking wave zone (Lubiatowo, September 1995)

To complete the experimental measurements the oil concentration in sand were also investigated. The vertical profile of the oil content in sand samples is plotted in Figure 10. Recorded lower concentrations of oil in surface sand can be an effect of intense degradation due to microbe and sun radiation. Next to the surface the amount of oil showed highest values and than decreased with distance from the surface. The lower oil concentrations in sand at 1 m or below suggest significant degradation by bacteria.
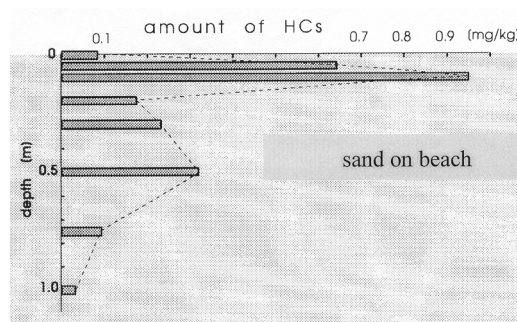
Figure 10 Concentration of hydrocarbons in beach sand for different depths

Extremely high oil concentrations were found in foam. Measured concentrations were 1000 times higher than in the water sampled at the same place.

Conclusions

Oil pollution is spread over the Southern Baltic Sea environment and is present in air, water, sand, sediments and in particular in foam.

The concentrations of oil pollution in the coastal waters were found to increase with increasing wind speed and wave action.

Significant amounts of petroleum hydrocarbons can be advected with land originated air pollution.

The petroleum hydrocarbons are concentrated at the water surface, therefore sea to air oil pollution transport can be expected.

Complex modelling of the fate of petroleum hydrocarbons in water/air/sediments system over the Southern Baltic environment is currently underway.

Acknowledgments

References

Otremba Z., and Stelmaszewski A., 1996. Amount and origin of petroleum hydrocarbons at the Polish east coast. Under preparation.

Enkell E., 1986. Oil pollution load to the Baltic Sea; A compilation of measured and estimated load. Baltic Sea Environment Proceedings No. 22.

Schulz M., Marks R., and Spirkauskaite N., 1996. BAEX—Baltic Aerosol Experiment, Joint research project. Progress report No. 4, EU—Contract NO. CIPA-CT93-0086.

Two-channel model for water exchange (the Gulf of Riga case)

Mikk Otsmann, Villu Astok, Tiit Kullas, and Ülo Suursaar

Introduction

The Gulf of Riga is connected to the Baltic Proper by two straits and therefore its water exchange is rather complicated. The Irben Strait has a width of 27 km, the sill depth is 21 m and the area of the cross-section 0.37 km^2. Another outlet is actually a system of straits, called Väinameri ("the sea of straits", in Estonian). The Suur Strait is the southernmost, the narrowest (5 km) and the deepest (21 m) area in this system. The flow in the Suur Strait is nearly unidirectional over the cross-section and our direct current measurements cover about 45% of the period 1993–95. The measurements in the Irben Strait are not equally representative since the strait is wider, the velocities smaller and the two-layer or two-directional water exchange scheme is frequent. The existence of two channels in the Gulf of Riga does not enable the application of the models known for water exchange description. Though the area of the cross section of the Suur Strait is 9 times smaller than that of the Irben Strait, we are going to prove that the role of the Suur Strait is far more important. The major task of the present study is to present a new water exchange model and investigate the water exchange processes in a system where a large and a small water body are connected by two channels. The further aim of modelling is to cover the gaps in our field data sets for the Suur Strait and to estimate the resultant flows in the Irben Strait.

Model description

The reaction of the basin connected to open sea by one strait (channel) to the changes of the sea levels outside the basin has been discussed by for example LeBlond & Mysak (1978). Astok & Otsmann (1981) applied the one-channel model for the Baltic Sea. For the Gulf of Riga the two-channel version should be used. The new model was first outlined in Otsmann *et al.* (1996a, b).

The configuration of the Gulf and the positions of the straits and model parameters are presented in Figure 1. The model input (forcing functions) are the sea level outside the gulf (H), wind stress (τ) in the channels and river inflow into the gulf (Q_J). The differences in water density (salinity) inside and outside the Gulf are remarkable ($\Delta S = 1-2$ PSU), but their influence on the water exchange can be estimated as being insignificant. The influence of air pressure differences (Δp_a) is negligible due to the small area of the Gulf. For that reason $\Delta \rho_w$ and Δp_a have not been taken into account in this model. The model outputs include the flow volumes (Q_1, Q_2) in the straits and the average water level in the Gulf (h).

Figure 1 Plan of the Gulf of Riga and the model parameters

The model is based on the motion equations in straits integrated along the coordinates z, y, z, and the water balance equation for the Gulf:

$$\frac{dQ_i(t)}{dt} + RQ_i(t) + \frac{gF_i}{L_i}h(t) = f_i(t) \tag{1}$$

$$F\frac{dh(t)}{dt} = Q_i(t) + Q_k(t) + Q_J(t) \tag{2}$$

where:

$$f_i(t) = F_i\left(\frac{g}{L_i}H_i(t) + \frac{\tau_i(t)}{d_i}\right), \, i, k = 1, 2; i \neq k \tag{3}$$

$i=1$ in the Suur Strait; $i=2$ in the Irben Strait

$t-$ time

$F-$area of the Gulf of Riga (the value used was $1.63\cdot10^{10}\,\text{m}^2$)

F_i-cross-section of the channel ($F_1=4\cdot10^4$; $F_2=3.7\cdot10^5\,\text{m}^2$)

L_i-length of the channel ($L_1=7.5\cdot10^4$; $L_2=2\cdot10^4\,\text{m}$)

d_i-channel depth ($d_1=10.5$; $d_2=19\,\text{m}$)

$g-$acceleration of gravity

$R-$friction coefficient ($3.5\cdot10^{-5}\,\text{s}^{-1}$)

Q_i-volume flow in the channel; $u_i=Q_i/F_i$

Q_J-river inflow ($1\cdot10^3\,\text{m}^3\text{s}^{-1}$)

H_i-water level in the Baltic Proper

$h-$water level in the Gulf

τ_i-wind stress projection on direction of channels; $\beta_1=155^\text{o}$; $\beta_2=65^\text{o}$;

$$\tau_i = |\vec{\tau}|(-1)\cos(\beta_i - \varphi), |\vec{\tau}| = c\left(\frac{\rho_a}{\rho_w}\right)|\vec{u}_a|^2 \tag{4}$$

ρ_a-air density, ρ_w-water density, u_a-wind velocity, $\varphi-$wind direction

$c-$nondimensional coefficient ($c=1.2\cdot10^{-3}$)

$RQ_i(t)$ in the left side of equation (1) describes the influence of the bottom friction on the motion in the linear approximation. This approximation could be used in small motion velocities (determined as $|\vec{\tau}| \leq 1\,\text{cm}^2\text{s}^{-2}$) since the description of the motion with nonlinear friction in the analytical case is more complicated but essentially of the same nature. In the numerical solution the nonlinear friction was used in the realistic forcings. Combining (1) with (2) we obtain the equations for $Q_i(t)$, $h(t)$ and $Q(t)=Q_1(t)+Q_2(t)$:

$$\left(\frac{d^2}{dt^2} + R\frac{\text{d}}{\text{d}t} + \omega_0^2\right)h(t) = \frac{f_1(t) + f_2(t)}{F} + \frac{1}{F}\left(\frac{\text{d}}{\text{d}t} + R\right)Q_J(t) \tag{5}$$

$$\left(\frac{d^2}{dt^2} + R\frac{\text{d}}{\text{d}t} + \omega_0^2\right)Q(t) = \frac{\text{d}}{\text{d}t}(f_1(t) + f_2(t)) - \omega_0^2 Q_J(t) \tag{6}$$

$$\left(\frac{d^2}{dt^2} + R\frac{\text{d}}{\text{d}t} + \omega_0^2\right)Q(t) = \frac{\text{d}}{\text{d}t}f_1(t) - \omega_{0i}^2(Q_k(t) + Q_J(t)) \tag{7}$$

where: $\omega_0^2 = \omega_{01}^2 + \omega_{02}^2$; $\omega_{0i}^2 = \frac{gF_i}{L_iF}$; i,k=1,2; $i \neq k$ (8)

Equations (5) to (7) are known in mechanics as the forced oscillation equations. The right sides of the equations represent the sum of external forces evoking the oscillations. Parameters ω_0 and ω_{0i} are the eigenoscillation frequencies of the system in the absence of frictional forces. The given model parameter values (including friction) yield the period of the eigenoscillations:

$$T_{01} = \frac{2\pi}{\omega_{01}} \approx 90\text{h}; \; T_{02} = \frac{2\pi}{\omega_{02}} \approx 24\text{h}$$

The oscillations with a period of 24h are common in the current velocity records obtained for the Irben Strait (Петров, 1979). The oscillations with a period of 3−4 days could be also found in the spectra calculated from the velocities of the Suur Strait (Suursaar *et al.*, 1995), but the influence of atmospheric synoptical activities should also be considered in that case.

The model shows that the reaction of the straits to the change of the external forcings is very different. Note also that the eigenoscillation frequency of the system of the Gulf with two channels is higher than the frequencies of individual channels:

$\omega_0 > \max(\omega_{01}, \omega_{02})$ and $T_0 < \min(T_{01}, T_{02})$. If $Q_k(t) \equiv 0$ in (7), we get the equation describing the one-channel basin water exchange.

Model behaviour: response to quasistationary and changing conditions

Although stationary conditions could be rarely observed in the Gulf of Riga, the analysis of the stationary case is justified, since it takes longer than one day for the flow to pass through the strait and the role of oscillations with periods of less than one day is considerably smaller than the motions induced by atmospheric synoptical activities (3−4 days) (Suursaar *et al.*, 1995). For the model the water exchange could be considered quasistationary in the frequencies $\omega^2 \ll \omega_0^2$. For that frequency band the derivative (by time) could be omitted in equation (1).
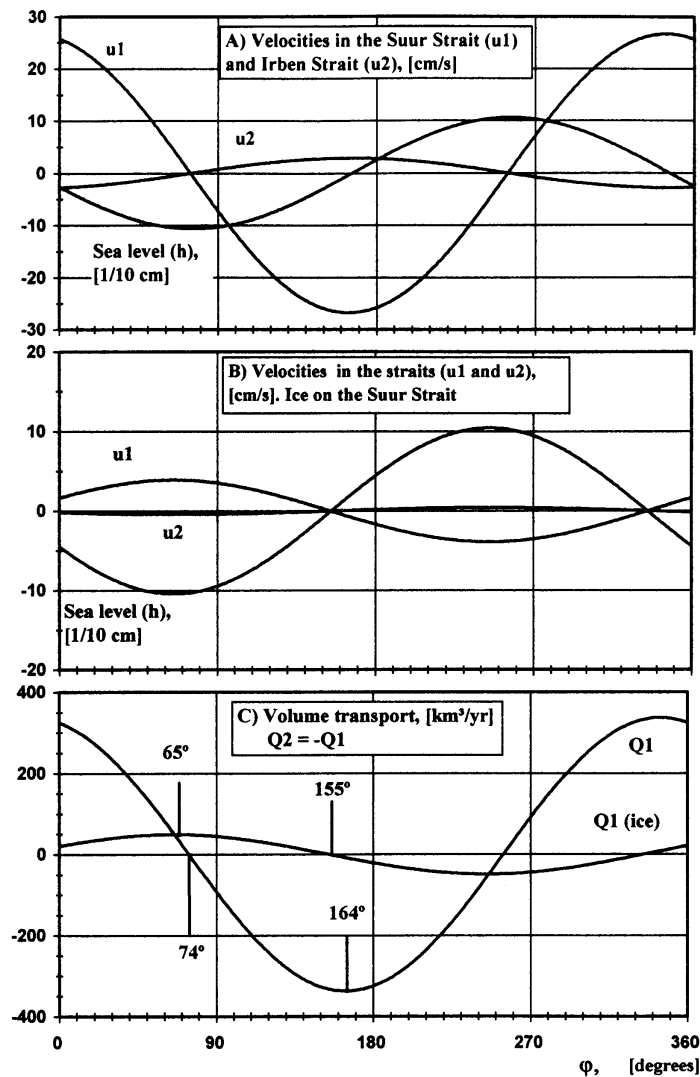
Figure 2 Dependence of velocities and volume transports in the Suur Strait and the Irben Strait on the wind direction (φ, module=7ms^{-1}) and on existence of ice in the Suur Strait area. $Q_j = H_1 = H_2 = 0$.

The maximum flows (and the difference in the sea levels $|h(t)–H(t)|=0$) in case the wind directions are $\varphi=164°$ and $164°+180°$ (Figure 2 and Figure 3A): the forces of the wind stress are in balance with the frictional forces. In case of one channel such an intensive wash-through does not exist, since the difference in the sea levels balances with wind stress and therefore $Q=0$. For wind directions $\varphi=74°$ and $254°$ the flow does not exist in the straits, but the sea level deviations inside the Gulf are maximal (Figure 3B). When one of the straits (Suur Strait) is covered by ice, the volume flows are smaller and the "optimal" wind directions for the exchange are $65°$ and $245°$ (Figure 2B, C and Figure 3C), but respective inflows−outflows appear in different straits in reversed order. It is interesting to note that the flow does not exist both in $155°$ and $335°$, and the sea level (h) is then 0. On the contrary, the level $h=0$ is coupled with the maximal velocities in the absence of ice (Figure 3A vs. Figure 3D).

The response of the Gulf to the alternating external conditions is reflected in the model outputs. But the form of the frequency-relationship $k(\omega)$, and hence the displacement and the form of the resonance peak depend only on the ω_0 and R, i.e., on the measures of the channels and the Gulf and frictional forces.
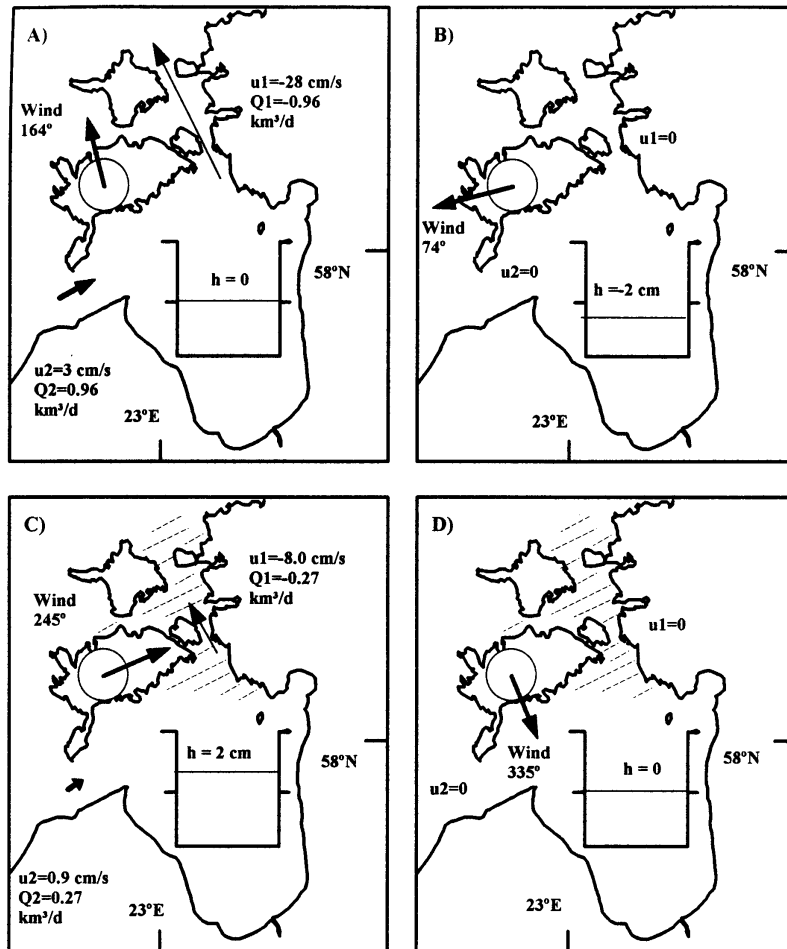
Figure 3 Water exchange and mean sea level in the Gulf of Riga for some special wind directions ($\tau=1\,\text{cm}^2\text{s}^{-2}$, $Q_2=-Q_1$, see also Figure 2). A and B show the situation without ice while C and D show ice on the Väinameri area (typical winter situation). The situation with the wind from $344°$ is similar to A but with opposite flows in the straits; $254°$ is similar to B but with the sea level $h=2\,\text{cm}$; $65°$ is similar to C but with the sea level $h=−2\,\text{cm}$ and $155°$ is identical to D.

The response to the rise of the sea level outside the Gulf (Figure 4B) and reaction to the rapid increase in the wind velocity are different (Figure 4A). Should the open sea level increase close to one channel, the response on that channel would be maximal. (Figure 4B). Should both the H_1 and H_2 have an equal increase, the flows Q_1 and Q_2 would be very weak, and the level h equal to the levels $H_1=H_2$. The directions $74°$ (Figure 4A), $164°$, $65°$ and $155°$ are the exceptional directions which also appear prominently in Figure 2 and Figure 3. The direction $119°$ is the average of $74°$ and $164°$.
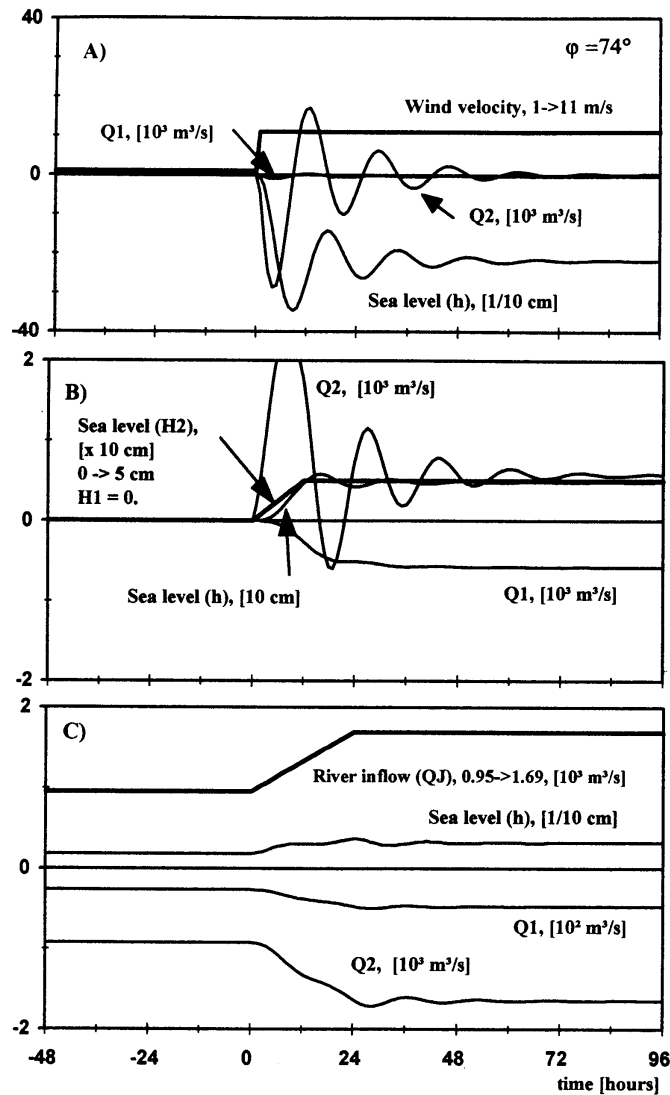
Figure 4 Some examples of model behaviour. Response of volume flows (Q_i) and sea level (h) to A) the increase in the wind velocity, B) open sea level H_2 (5 cm for 12 h) and C) river inflow.

The increase in inflows through the rivers (similar to the spring flood) occurs mainly in the Irben Strait, due to of the smaller cross-section and higher resistance of the Suur Strait (Figure 4C).Note that the magnitude of Q_1 is at least 10 times smaller than Q_2 in that case. However, it is not correct to draw the simple conclusion that also in the realistic conditions "the Daugava River flows out through the Irben Strait".

Verification and application

The model was verified against the field data gained in October–November 1993 (Figure 5). Generally, the model inputs are the measured wind stresses above the straits averaged over the area of these straits, and the sea levels measured at the entrance to the strait (closest to the open sea). In our case the wind measured at one point (by Aanderaa automatic weather station located at the height of about 10 m in Viirelaid Isle, Suur Strait) was used. The wind stresses for both straits ($\tau_1(t)$, $\tau_2(t)$, Figure 5A) were calculated from the same wind data, but representing the different projections. The wind data measured with 10 minutes time interval were averaged on 1 hour intervals. The water level data were not used, since their quality was low (one-day average data interpolated into 1 h interval).

The model parameters ω_1 and ω_2 were found by the average measures of the straits. The frictional forces were taken $\sim r u_i^3(t)$. The coefficient r was found from the cut of measurements (3–4 days) where both the wind and the flow velocities in the Suur Strait were quasistationary. For verification the currents measured in the Suur Strait ($u_1(t)$) by Aanderaa current meter were used. The mooring station was deployed at 12 m (the depth in that part of the strait is 19 m) and the data measured every 10 minutes were averaged over one hour period similarly to the wind data. According to estimations

based on velocity profilings (Suursaar *et al.*, 1996) the values obtained at the depth of 10–12 m could be taken as average velocities over the whole cross-section of the Suur Strait.

The measured and calculated velocities in the Suur Strait were in good accordance and other calculated results were also reasonable. It should be noted, that quite a good correlation coefficient (0.95) between the u_1 and u_1* (Figure 5) was obtained without using the sea level data and the actual data of the wind stress above the other strait. It shows, once again, the leading role of the wind stress in the water exchange processes of the Gulf of Riga. However, we hope to get even better results using the whole complex of inputs. This could also provide adjusted values for ω_{01}, ω_{02} and r.

In future we intend to apply this model for water and nutrient exchange calculations in tIe Gulf of Riga using the wind, sea level and nutrient data.
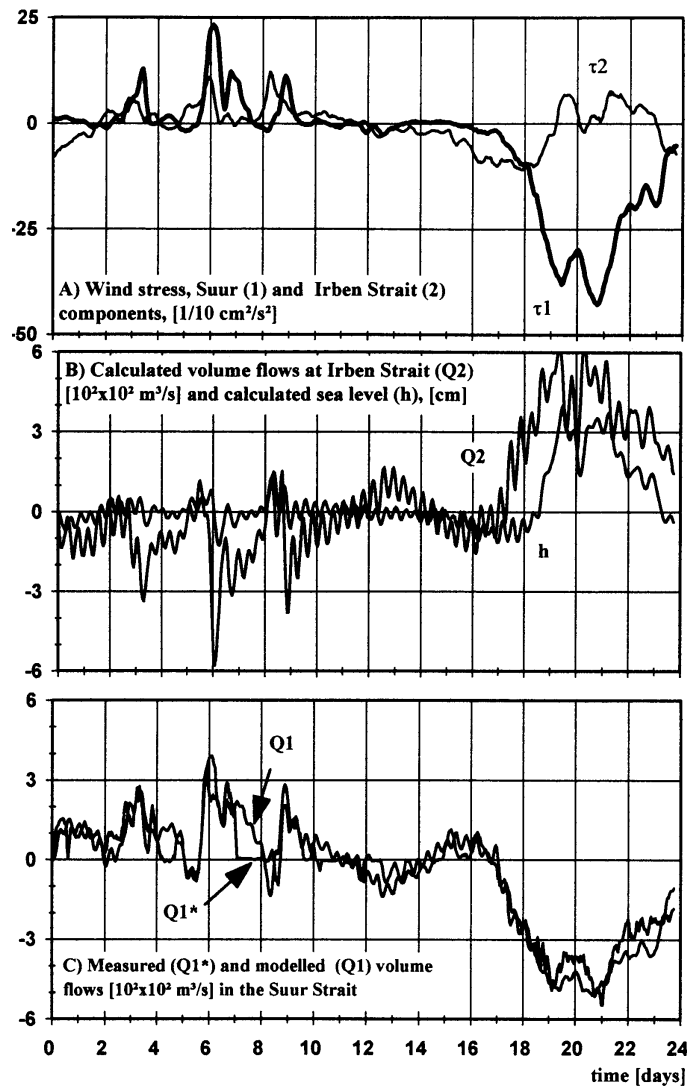
Figure 5 Comparison of the modelled and measured velocities in the Suur Strait (C) and some other modelled values (B) in the realistic external forcings (A). Note the malfunction (entangling) of the measuring equipment on the 8th day (Q_1* in C).

Conclusions

- Due to the existence of two channels the water exchange is more intensive than in the case of one channel. The water exchange depends considerably on the direction and configuration of the channels.
- The system of the Gulf of Riga amplifies oscillations with a period of about 24 hours, which can be noted significantly in the velocities in the Irben Strait.
- The main factor for the water exchange in the Gulf of Riga is wind. The sea-level differences and salinity gradients are secondary factors. The water exchange is the most intensive with SSE and NNW winds. In winters with ice-cover

the water exchange scheme is different: the velocities are $3-4$ times smaller and the water exchange is the most intensive with WSW and ENE winds.

- The described model can be used for water and nutrient exchange calculations and for providing boundary conditions for the ecological models of the Gulf of Riga.

Acknowledgements

References

Astok, V., and Otsmann, M., 1981. A model tor calculating water exchange between the North and Baltic Seas. Investigations and modelling of processes in the Baltic Sea, Part II, Tallinn, $5-10$.

LeBlond, P.H., and Mysak, L.A., 1978. Waves in the Ocean. Elsevier Oceanographic Series 20, Amsterdam. 602 pp.

Otsmann, M., Astok, V., and Suursaar, Ü., 1996a. A model for water exchange between a large and a small water body: the case of the Baltic Sea and the Gulf of Riga. Nordic Hydrological Conf. 1996, Akureyri, Iceland. NHP-Report No. 40, Vol. 2, $496-505$.

Otsmann, M., Astok, V., Suursaar, Ü., and Kullas, T., 1996b. Water exchange model for the Gulf of Riga. Studies on measuring and modelling the water and nutrient exchange of the Gulf of Riga. EMI Report Series, No.3, $81-94$.

Suursaar, Ü., Astok, V., Kullas, T., and Otsmann, M., 1996. New estimation of the water and nutrient exchange between the Gulf of Riga and the Baltic Proper. EMI Report Series, 3, $95-108$.

Suursaar, Ü., Astok, V., Kullas, T., Nõmm, A., and Otsmann, M., 1995. Currents in the Suur Strait and their role in the water and nutrient exchange between the Gulf of Riga and the Baltic Proper. Proc. Estonian Acad. Sci. Ecol., 1995, 5, 3/4, $103-123$.

Петров, В. С. 1979. Водный баланс и водообмен Рижского залива с Балтийск им морем. In: Сб. Работ Рижской гидрометеорологической обсерватор ий, 18, 20-40.

Investigation on mesoscale dynamics of the Baltic Sea

V.T. Paka, N.N. Golenko, and V.M. Zhurbas

Introduction

Since 1991, the Shirshov Institute of Oceanology, Moscow, and especially its Atlantic Branch, Kaliningrad, has fulfilled a wide program of field measurements in the Baltic Sea to learn mesoscale motions and structures and their role in deep water ventilation.

These measurements consisted of closely spaced CTD profiling and current velocity recording at moorings. All the CTD data were obtained with a Mark III NBIS CTD profiler. To achieve high horizontal resolution, the CTD profiling was carried out from a winch-driven towed undulating vehicle. The vehicle was equipped with a heavy chain under it to prevent the vehicle touching the ground (Figure 1). Such a method made it possible to attain the horizontal resolution on CTD transects of about a few hundred metres and take measurements as close as 2 m to the sea bottom.

1. winch
2. ⊓-frame
3. armoured electric cable
4. CDT probe,
5. heavy chain
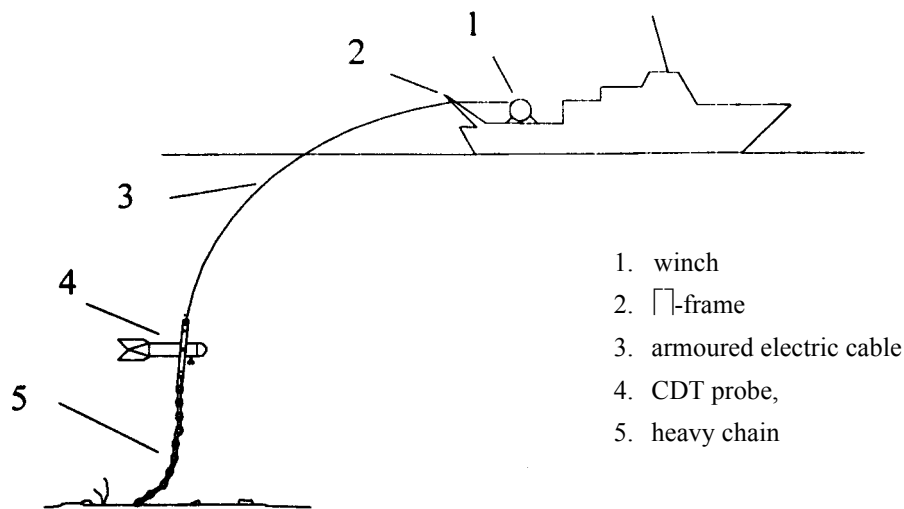
Figure 1 Technique for closely-spaced CDT profiling

Our measurements were located in the Stolpe Furrow, the Eastern Gotland Basin, and the Gdansk Bay.

In this contribution, the most interesting findings (in our opinion) of the CTD measurements in the Stolpe Furrow and the Gotland basin are briefly outlined. However the measurements in the Gdansk Bay, especially flow velocity, cannot be presented because they were still being processed and analysed at the time of writing.
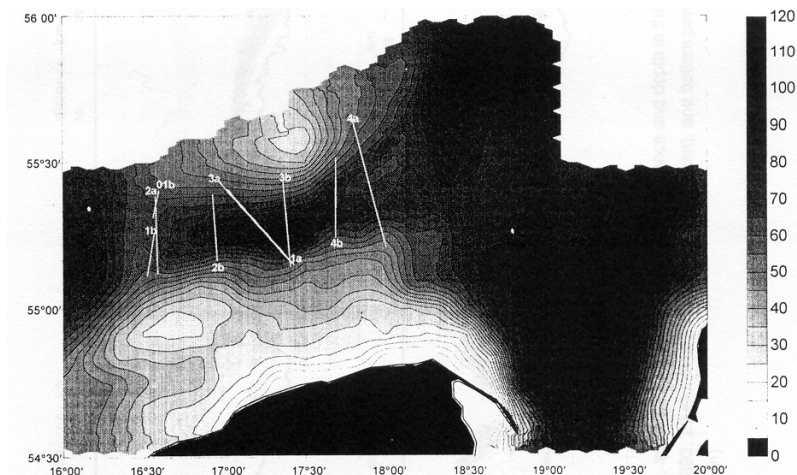
Figure 2 Detailed bathymetry of the Stolpe Furrow. 1a−4a are the PS-29 CDT transects (06−14.04.93) and 01b/1b−4b are the PS-33 transects (22−23.09.94)

Mesoscale thermohaline structure of the Stolpe Furrow and its dynamics

The Stolpe (Slupsk) Channel (Furrow) is an area of special interest for Baltic oceanographers. Being the only pass for the salty water from the Bornholm Basin to enter the Gotland Deep and Gdansk Bay, this elongated basin is extremely important to deep water ventilation in the Central and Northern Baltic.

Here, we closely analyse the spaced CTD surveys from two cruises: the 29th cruise of r/v "Professor Shtockman" (PS-29, 6-14 April, 1993) and the 33rd cruise of the same vessel (PS-33, 22-23 September, 1994). A map of PS-29 and PS-33 CTD surveys in the Stolpe Channel is shown in Figure 2. The PS-29 measurements were carried out two and a half months after the January 1993 Baltic inflow event, just in time to catch the inflowing waters finishing their way to the Gotland Deep (Matthäus, 1993). To distinguish the data of two cruises, the four CTD transects of PS-29 are referred as #la−#4a, while the four transects of PS-33 are referred as #lb−#4b. Temperature T, salinity S and potential density anomaly σ_t versus distance and depth for all the transects are presented in Figure 3−Figure 6 using standard orientation: North is to the right. The transects 2a and 1b/01b are located in the vicinity of the Stolpe Sill (about 60 m deep) which separates the Stolpe Channel from the Bornholm Basin, the transects la, 3a, 2b, 3b are from the central part of the channel where the maximum sea depth is about 90 m, and the transects 4a, 4b are from the marginal zone between the Stolpe Channel and the Gdansk/Gotland Basin where the drainage depth is about 80 m.

The weather conditions during the field measurements were as follows: On 6 April, 1993 (transect la), the Baltic Sea was under the cast periphery of a cyclone centred over Scotland and moving in a south-east direction with a wind speed of 3−8 ms^{-1}. On 12−14 April, 1993 (transects 2a−4a), the weather was determined by an anticyclone with its centre over Northern Scandinavia, and the north-east wind speed was 4−9 ms^{-1}. On 22−23 September, 1994 (transects lb−4b) over the Stolpe Channel the prevailing west wind velocity was from 2−8 ms^{-1}.

Western part of the Stolpe Channel

In April 1993, the thermohaline structure of the western part of the Stolpe Channel was characterised by a two layer system: the upper mixed layer with salinity of about 7.5 PSU and temperature 3.2 °C, and the lower, halocline layer of higher temperature and salinity (Figure 3). In September 1994, there was an intermediate cold layer over the halocline, separated from the upper warm mixed layer by a sharp seasonal thermocline at a depth varying from 22 to 42 m. For the intermediate layer, the core of cold water, where T<3 °C, is shifted to south and located at the southern edge of the #1b/01b transect. The upper boundary of intermediate layer is not flat, being subjected to internal wave deformation with a long wave length of about 25−30 km, and a short one of about 2−3 km.
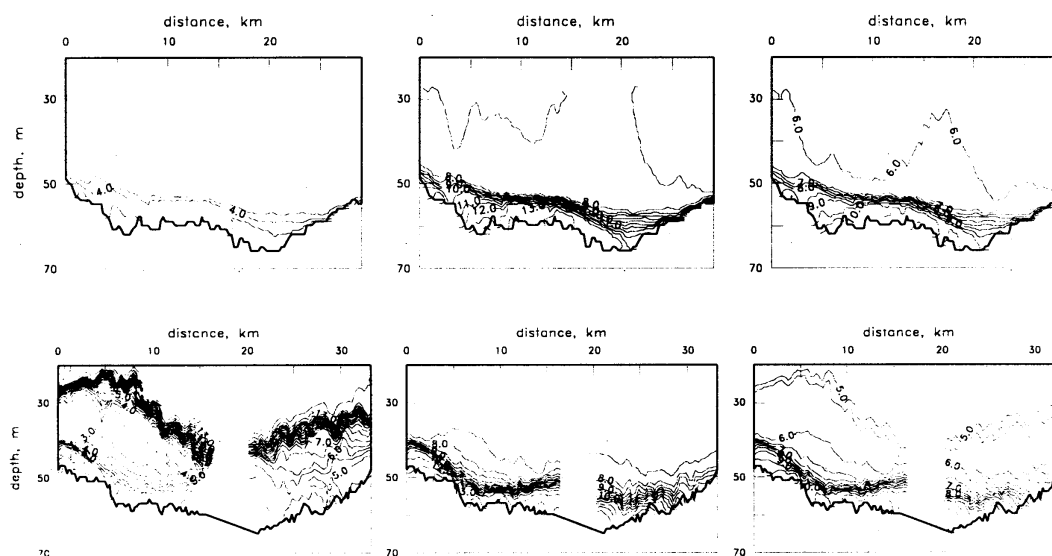
Figure 3 Temperature, salinity, and potential density anomaly vs. distance and depth in the western part of the Stolpe Furrow (over the sill). Top panels are from transect 2a (April 1993, 29th cruise of r/v "Professor Shtockman"), and bottom panels are from transect 1b/01b (September 1994, 33rd cruise of r/v "Professor Shtockman")

The upper boundary of the permanent halocline is characterised by an isohaline of 8.5 PSU. Both in April 1993 and September 1994, it was inclined with respect to the horizon being deepened when advancing north. The line of the sea

bed at the central part of the transects 2a and 1b/01b has the same slope, so the thickness of halocline layer is nearly constant at about 8−10 meters. The maximum salinity was 13.93 PSU for transect 2a and 14.26 PSU for transect #1b/0lb.

Resemblance of the upper boundary of the halocline and the sea bed shape suggests that the halocline tilt could be of no wave-induced origin implying an eastward flow of salty underlying water over the Stolpe Sill both in April 1993 and September 1994. Geostrophic estimate of the velocity of this flow can be obtained using the two layer model. The velocity difference $\Delta u = u_2 - u_1$ across inclined, geostrophically balanced front is expressed by a formula

$$\Delta u = -\frac{g \tan \alpha}{f} \frac{\Delta \rho}{\rho_0} \tag{1}$$

where

$\Delta \rho = \rho_2 - \rho_1$ is the tilt of the front in yz-plane with respect to y-axis,
ρ_2, ρ_1, u_2, u_1 are density and x-component of current velocity for the lower (subscript 2) and the upper (subscript 1) layers,
g is gravity acceleration,
$f = 2\Omega \sin \varphi$ is the Coriolis parameter,
Ω is the angular velocity of the Earth rotation,
φ is latitude,
ρ_0 is reference density,
x, y, z -axes are directed east, north, and upward respectively.

This expression is known from literature on atmospheric dynamics as the Margules formula.

Assuming from Figure 3 that $\alpha = -5 \cdot 10^{-4} 1°C^{-1}$, $\Delta \rho / \rho_0 = 0.005$, and taking $g = 9.8\,ms^{-2}$, $f = 1.2 \cdot 10^{-4} s^{-1}$ ($\varphi = 55.3°$), we get $\Delta u \approx 20\,cm\,s^{-1}$.

Hence, if the velocity of the overlying layer is taken to be zero, the salty water in the halocline is estimated to move eastward over the Stolpe Sill at a speed of about 20 $cm\,s^{-1}$, whether it is April 1993 or September 1994. In the case of transects 2a and 1b, the cross-section area of the halocline over the sill is about $8\,m \times 25\,km = 0.2\,km^2$, and if the value of $2\,cm\,s^{-1}$ is taken, the mean volume rate of salty water inflow through the channel to deep basins will be estimated as $4 \cdot 10^4 m^3 s^{-1} = 3.5\,km^3$ per day $= 1260\,km^3$ per year. The last value is unexpectedly high and more measurements are required to examine whether the situation we have observed is typical, and also the role of internal waves in salty water transport across the Stolpe Sill.

Central part of the Stolpe Channel

In April 1993 the mean depth of the upper boundary of the halocline (8.5 PSU isohaline) was 52 and 54 metres for transects #la and #3a respectively, which is a bit less than that of the western part of the channel (56m for the #2a transect).

The shape of the maximum gradient layer in the halocline has changed from bending down on 6 April to bending up on 13 April which is most likely to be caused by internal waves (Figure 4). The bending down shape of the halocline in section #la is accompanied by a sharp breaking of isolines as soon as they reach the northern slope of the channel. This looks like the internal surf, but more data are needed to confirm this suggestion and to examine the conditions when it happens.

The maximum salinity in the bottom layer in April 1993 was rather high, namely 15.20 PSU for transect #la and 15.06 PSU for transect #3a. This seems to be about the only direct remnant of the recent January 1993 inflow event, because by September 1994 maximum salinity in the central part of the channel had lowered to 14.03 PSU and 13.86 PSU for #2b and #3b transects respectively (Figure 5). For the same period, the mean depth of 8.5 PSU isohaline had increased to 60m for #2b transect and to 63m for #3b transect, implying a substantial decrease of the cross-section area for the salty water layer.
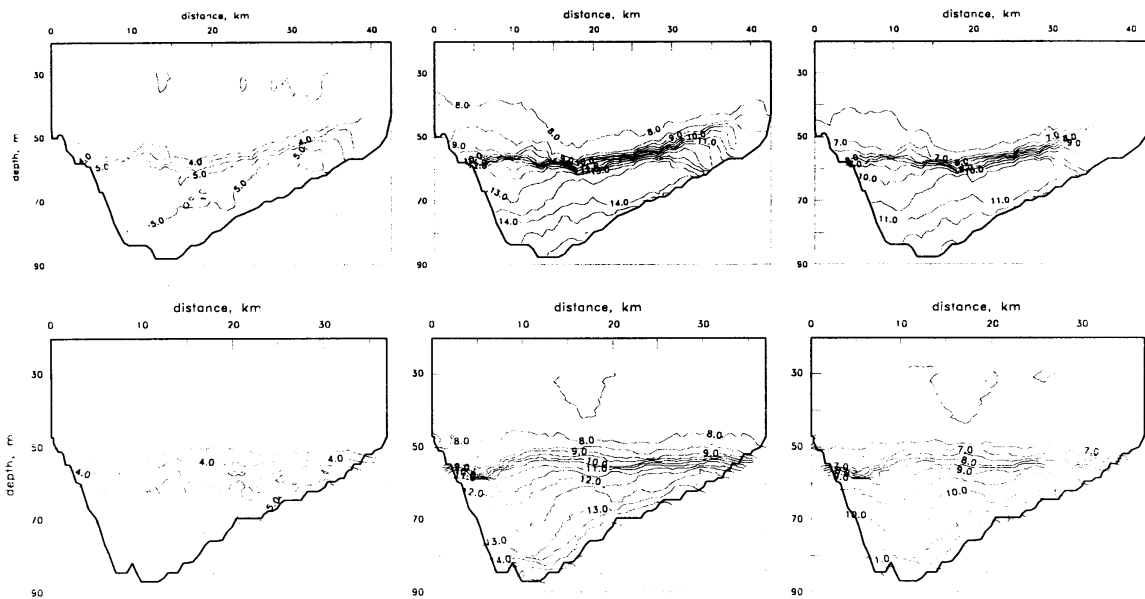
Figure 4 Temperature, salinity, and potential density anomaly vs. distance and depth for transects across the Stolpe Furrow (April 1923, 29th cruise of r/v "Professor Shtockman"). Top panels are from transect 1a and bottom panels are from transect 3a.
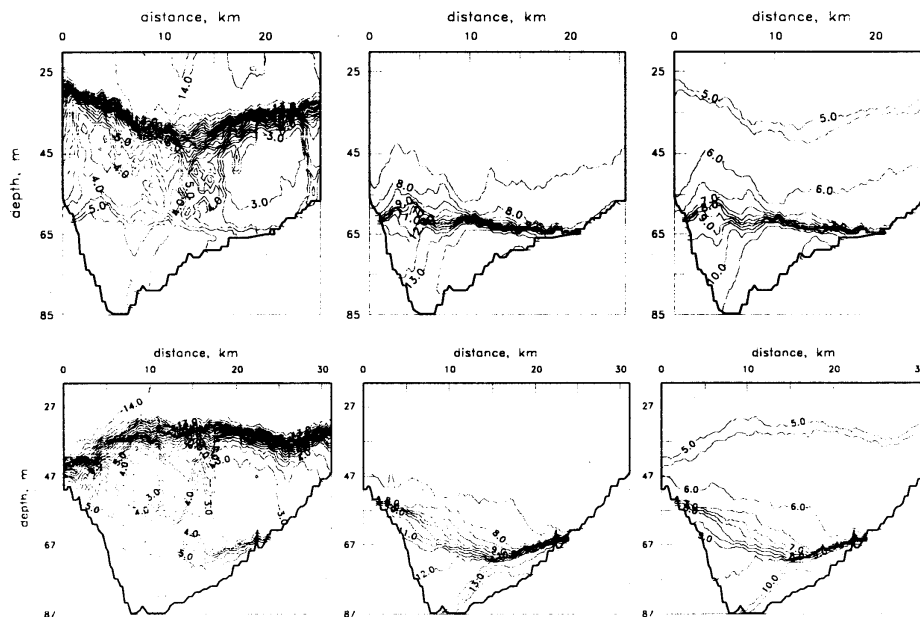
Figure 5 Temperature, salinity, and potential density anomaly vs. distance and depth for transects across the Stolpe furrow (September 1994, 33rd cruise of r/v "Professor Shtockman"). Top panels are from transect 2b, and bottom panels are from transect 3b.

In contrast to the western part of the channel, the seasonal cold intermediate layer in the central part has two core structures. The first, more pronounced cold core is located above the northern slope of the channel, while the second one is located close to its longitudinal axis. Like the upper boundary of the halocline in April 1993, in September 1994 the shape of upper boundaries for both intermediate and halocline layers varies in a manner indicating internal waves with amplitudes of the order 10 m.

The most remarkable feature concerning thermohaline structure in the central part of the Stolpe Channel, especially for September 1994 (#2b and #3b transects), is its prominent asymmetry observed in the halocline. That is, the interface between halocline and overlying intermediate (or upper mixed) layers being sharp over the northern slope of the channel widens to the south, and a fan-like divergence of isohalines/isopycnals takes place. This "fan-like" effect is accompanied

with northward displacement of the saltiest and densest water pool from the deepest connection line of the channel. The fan-like effect and the northward displacement of densest water took place not only in September 1994, but to some extent in April 1993 (see #1a and #3a transects).

Eastern part of the Stolpe Channel

For the eastern part of the channel, the fan-like effect and the northward displacement of densest water were clearly revealed both in April 1993 and September 1994 (see Figure 6, transects #4a and #4b).
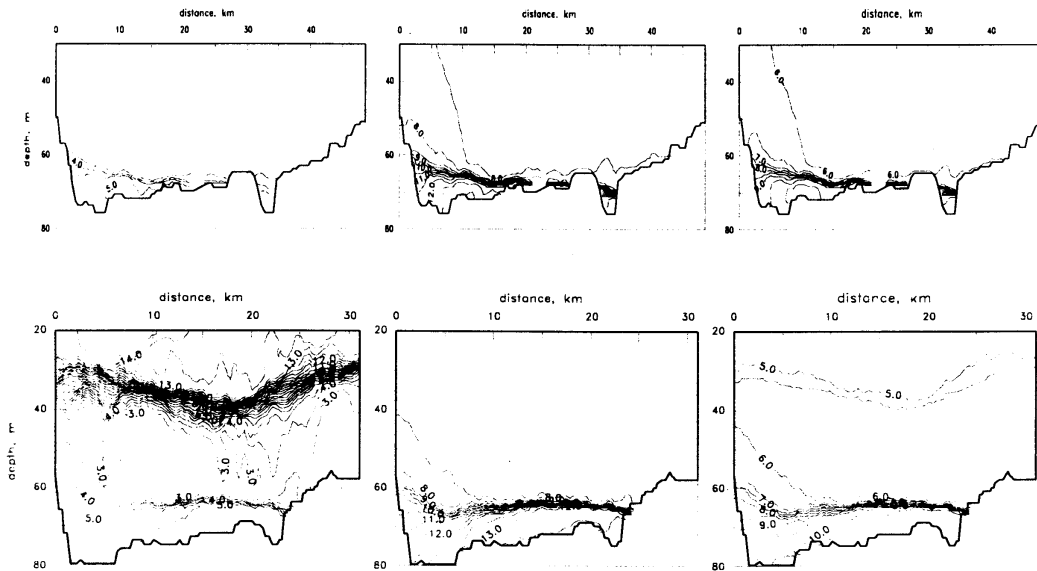
Figure 6 Temperature, salinity, and potential density anomaly vs. distance and depth for transects across the eastern part of the Stolpe Furrow. Top panels are from transect 4a (April 1923, 29th cruise of r/v "Professor Shtockman"), and bottom panels are from transect 4b (September 1994, 33rd cruise of r/v "Professor Shtockman")

The sea bottom in the eastern part of the Stolpe Channel is also elevated relative to its central part, but less than in the western one. This is evidenced by Figure 2, plotted according to the data being taken from the Polish geological map (Pikies, 1990). The bottom topography is illustrated there with an isobath offset of 5 m. As the sea bottom is lower down further to the east and the north-east, this elevation must also be considered as a sill for the near-bottom currents, directed into the Gdansk/Gotland Basin. The eastern sill is 20 km wider than the western one, and its profile is more complicated. In its middle part there is a spacious elevation of the bottom up to 67−70 m. Both to the north and south of this elevation, there are two valleys of nearly the same depth (about 80 m) open to the east which may be considered as preferable passages for salty water from the Stolpe Channel to get the Gdansk/Gotland basin. When the depth of the upper boundary of halocline is greater or close to that of the bottom elevation, as it took place in the case of #4a transect, the near bottom flow of high salinity water separates into two parts: the wide southern and the narrow northern ones.

Due to the fan-like effect and the northward displacement of densest water, both in April 1993 and September 1994 salinity of near bottom water for the northern valley was more than 1 PSU greater than that for the southern one. It means that the northern passage, despite being narrower (only 3−4 km wide), is more important for the deep water ventilation in the Central and Northern Baltic than the southern one which is several times wider at the same depth.

Discussion

First of all we shall try to examine what features of thermohaline structure are common for both of the periods of observation in the Stolpe Channel. The weather conditions have changed from moderate south-east winds on April 12−14, 1993 to moderate westerly winds on September 22−24, 1994, and the common features should be considered as independent from the wind direction, at least for weak and moderate winds.

The first common feature is the deepening of the upper boundary of halocline at the sill in the western part of the channel when advancing north. It implies eastern transport of underlying salty water from the Bornholm Basin to the Stolpe Channel for both of the periods of observation. This results is not consistent with the numerical modelling of circulation in the Baltic (Krauss and Brügge, 1991). The model predicted westward transport through the Stolpe Channel in its lower layers only for northerly and easterly winds, while southerly and westerly winds developed the opposite, eastward

transport. A possible reason for discrepancy between the model results and our observations is the usage of horizontally uniform density distribution as the initial condition for the model runs, which avoided density-driven near-bottom current. Another reason for this discrepancy could be internal waves which might be responsible, at least partially, for the observed slopes of the halocline.

The second common feature is a coupled effect of southward fan-like divergence of isohalines/isopycnals and the northward displacement of saltiest/densest water from the deepest connection line of the channel. The coupled effect was observed in the whole length of the Stolpe Channel except its western part, both in April 1993 and September 1994. The most likely cause of this effect is the transport in the bottom Ekman layer, as it is illustrated schematically in Figure 7.
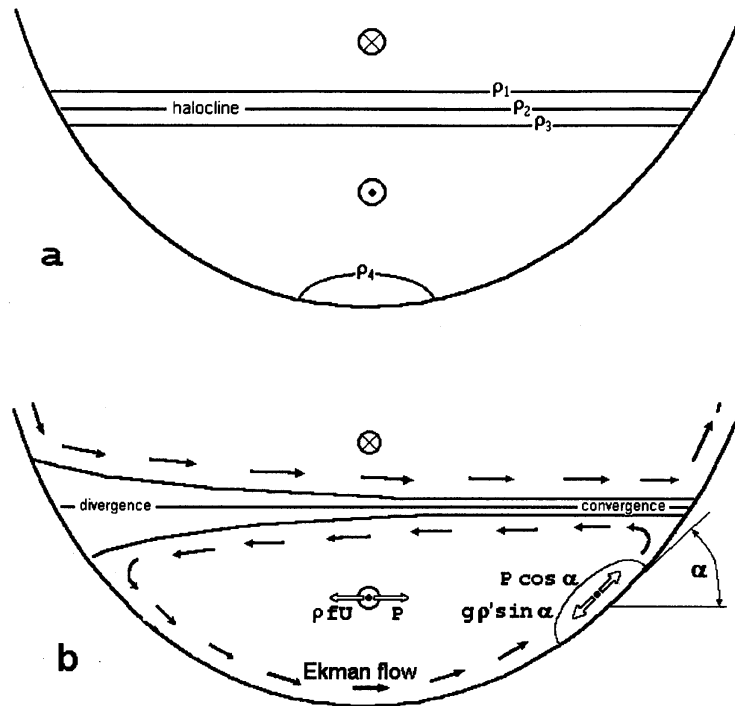
Figure 7 An explanation of the fan-like shape of isopycnals and northward displacement of the densest water pool from the deepest connection observed on transects across the Stolpe Furrow.

Figure 7a is a sketch of a cross-section of the Stolpe Channel in which three isopycnals represent the halocline, the top layer is supposed to be moving westward (into the picture) while the flow in the lower layer is directed east (from the picture) with the velocity u.

Figure 7b represents the same cross-section, but for the case when the bottom friction and the Earth rotation are taken into consideration. It causes northward/southward Ekman transport in the lower/top layer, providing two-cell circulation with divergence/convergence of the flow over northern/southern slope of the channel. This circulation explains both the fan-like picture of isopycnals/isohalines and the northward displacement of denser water. In fact, the circulation exists only for a finite period of time, because it produces a disturbance of density which works against the Ekman transport. Finally, in the layer near the sloping bottom where the flow velocity reduces to zero, an equilibrium is attained between the horizontal pressure gradient and the buoyancy forces, instead of the Coriolis one, and the Ekman transport arrests itself. This effect is known as the arrested Ekman layer (Garrett *et al.*, 1993).

Using the arrested Ekman layer theory, some estimates can be made concerning the northern displacement of the densest water from the deepest connection of the Stolpe Channel. In accordance with Figure 7b, in the main body of the halocline the geostrophic balance takes place:

$$ fu = -\frac{1}{\rho_0}\frac{\partial p}{\partial y} \tag{2} $$

where p is pressure.

In accordance with Figure 7b, the condition for the equilibrium for the pool of the densest water on sloping bottom is:

$$-\frac{\partial p}{\partial y}\cos\alpha_b \;=\; g(\Delta\rho)_b\sin\alpha_b \qquad\qquad (3)$$

where $(\Delta\rho)_b$ is the density anomaly for the pool (the difference between water density of the pool and that of the deepest connection),

α_b is the bottom slope for a place where the pool is located.

Using (2) and (3), an expression for u, the flow velocity in the halocline interior required to equilibrate the pool at the sloping bottom, is obtained:

$$u \;=\; \frac{g}{f}\tan\alpha_b\,\frac{(\Delta\rho)_b}{\rho_0} \qquad\qquad (4)$$

According to the transects #2b−3b (see Figure 5), $\alpha_b \approx 1.8{\cdot}10^{-3}$ $\dfrac{(\Delta\rho)_b}{\rho_0} = (0.2{-}0.5){\cdot}10^{-3}$. This yields the estimate: $u=3{-}7.5\,\mathrm{cms}^{-1}$.

Another, simpler kinematic explanation of the fan-like effect even without the direct application of the Ekman layer dynamics can be made using only the Margules formula (1). The density structure in the halocline and its upper vicinity may be considered as a number of homogeneous layers of different density, and formula (1) is applicable to every pair of these layers. If we suppose that in the central layers of such a halocline there is an eastward flow which reduces to zero in the top and bottom layers, formula (1) will predict upward sloping interfaces (i.e. isopycnals) between the top layers and downward sloping for the bottom layers when advancing south—just the fan-like behaviour of isopycnals that was observed in the central and eastern part of the Stolpe Channel.

An important result following from this last explanation is the possibility to use the fan-like distribution of isopycnals as evidence of eastward flowing salty water through the Stolpe Channel for the both periods of observation.

It is worth noting that the fan-like effect implies non-instant, time-averaged eastward flow, and the period of averaging can be estimated as equal to the "shut down time" for the Ekman layer to be arrested. In our case the shut-down time t_* is estimated as $t_* = l/u_E$, where l is the distance between the deepest connection and the place where the maximum density pool is located, and u_E is the velocity of the Ekman layer transport.

Assuming that $u_E \approx u$ (Garrett *et al.*,1993),

and, in accordance with our data, taking $u=3\,\mathrm{cms}^{-1}$, $l=1$ km, we obtain

$t_* = 3.3{\cdot}10^5\,\mathrm{s}=3.9$ days.

We expect that our estimate of t_* is still on the low side because in fact u_E should be much less than u.

At least two important consequences follow from the above estimate of t_*.:

1. Quite a long period of time is required to develop the fan-like structure, and it explains why this structure was not observed in the western part of the Stolpe Channel: the salty water in that place is too "young" since it just came from the relatively deep Bornholm Basin.

2. Our obtained value for t_* is a bit larger than the typical synoptic period (3 days), and it explains why our observations of thermohaline structure predict eastward flow in the halocline regardless of the direction of the wind blowing over the area. This is likely to be the main reason for discrepancy in our results with the predictions of numerical modelling of Baltic circulation (Krauss and Brügge, 1991).

The above statement is strong evidence for the fan-like effect to be a permanent feature of thermohaline structure in the central and especially eastern part of the Stolpe Channel. It makes the narrow northern valley in the eastern part of the channel exclusively important for the salty water to pass from the Bornholm Basin to deep central and northern basins.

Underwater mesoscale cyclonic eddy in the Gotland Basin after the 1993 inflow event

In the PS-29, a 157km long closely spaced CTD transect, A−B, was carried out in the Eastern Gotland Basin on 17−18 April 1993. The location of the transect is shown in Figure 8.
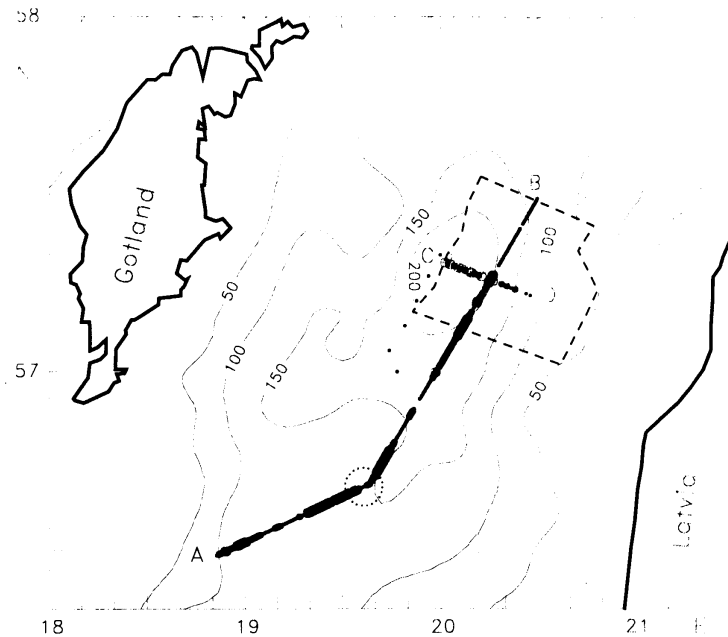
Figure 8 A map of the experiment in the Eastern Gotland Basin, March−April, 1993. Filled circles of different sizes, mainly coupled by bold lines, are CTD stations of the second stage of the experiment (16−18 April). The large dotted circle close to the breakpoint of the A−B transect denotes the location of the cyclone.

Figure 9 displays the potential density anomaly, σ_θ, versus pressure and distance for the halocline layer of the AB transect. The most outstanding feature in Figure 9 is a convergence of isopycnals inside the halocline at a distance of 48−55 km, which may be interpreted as a mesoscale cyclonic eddy covering the whole halocline layer. In addition, there are a few cases of local divergence of isopycnals, namely at distances of 116−129 km and 138−150 km, which may be considered as anticyclonic eddies covering only some parts of the halocline layer.
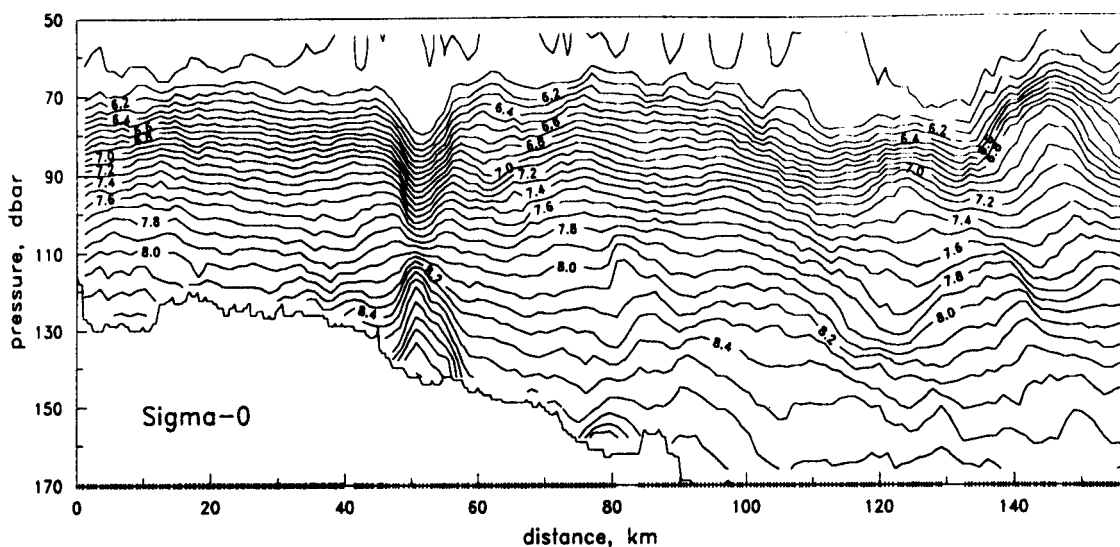
Figure 9 Potential density vs. pressure and distance from the A−B transect

To be sure that the feature of 48−55 km is really a mesoscale cyclone rather than, for example, a topographically steered tongue of intrusion, we have to have at least a few differently directed transects across it. Unfortunately, we had no possibility to make any additional transects, and the following should be considered as an "eddy hypothesis", which provides a likely, self-consistent description of the data and will stimulate field studies in this area in the near future.

We shall consider dynamic properties of the hypothetical cyclone in more detail. It is worth doing, because such eddies can contribute to the salt water transfer and deep water ventilation in the Baltic Sea.

Using density versus hydrostatic pressure and distance, $\rho(p,x)$, the empirical geostrophic flow function $F_g(p,x)$ has been computed:

$$F_g(p, x) = \frac{1}{f} \int_p^{p_0} \left[\frac{1}{\rho(p,x)} - \frac{1}{\rho(p,\infty)} \right] dp \tag{5}$$

where $\rho(p,\infty)$ is the background density versus pressure away from the cyclone,
p_0 is some reference pressure level of no geostrophic current. The value of p_0 was taken to be equal to 140 decibars, the pressure just above the sea bed at the cyclone location.

The cross-transect component of geostrophic velocity, u_g, is written as the x-derivative of the flow function $u_g \equiv \dfrac{\partial F_g}{\partial x}$.

Figure 10 shows the geostrophic flow function computed for a fragment of the A−B transect, which includes the central part of the cyclone and its northern periphery, where the pressure at the sea bed is no less than 140 decibars. This function is a minimum at $p \approx 107$ decibars, indicating a horizon of the cyclone's core, and increases to a close-to-zero noise level over the halocline and away from the cyclone. Thus, we can conclude that the cyclone is located in the halocline, being dynamically undetectable on the sea surface.
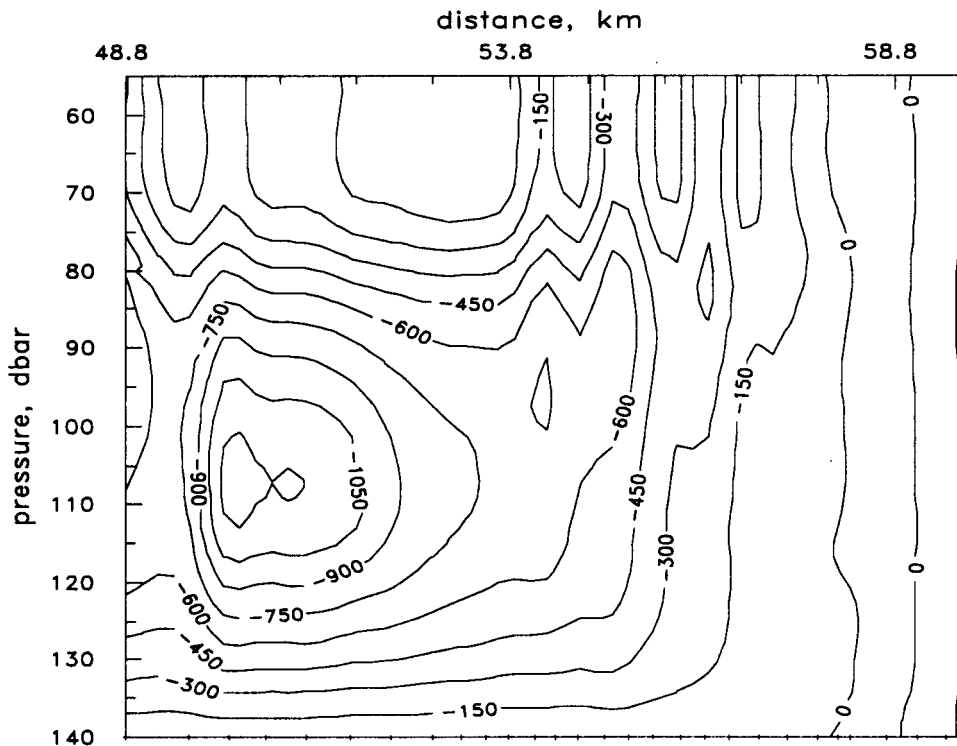
Figure 10 Geostrophic flow function vs. pressure and distance for a fragment of the A−B transect including the cyclone and its northern periphery

To estimate characteristics of the cyclone (its size and velocity of rotation), according to Zhurbas *et al.* (1992), the empirical geostrophic flow function at the level of p=107 decibars has been approximated by an analytical function, namely the Gauss curve:

$$F_g(x) \equiv F_g(p, x)|_{p = 107 \text{ dbar}} = A\exp - \frac{(x - x_0)^2}{2R^2} \tag{6}$$

where A, x_0, R are parameters to be determined.

Using the least square technique (non-linear regression), the following values were obtained:

A=−1116 m²s⁻¹, x_0=51.15 km and R=2.94 km.

Since only a single transect across the cyclone is available, the distance between the transect and the cyclone's centre is unknown. One should estimate what kind of errors are introduced into parameters of the cyclone by this uncertainty. If the cyclone is axisymmetric and its flow function is described by the two-dimensional Gauss curve:

Investigation on mesoscale dynamics of the Baltic Sea

$$F_g(x, y) = A'\exp - \frac{(x - x_0')^2 + (y - y_0)^2}{2R'^2} \qquad (7)$$

where x_0', y_0, R', A' are "real" parameters of the flow function. Making the transect along the x-axis at the distance of $y_1 - y_0$ from the eddy's centre, we will come to (6) instead of (7) with the following relationships between "real" and "measured" parameters: $x_0 = x_0'$, $R = R'$, $A = A'\exp[-(y_1 - y_0)^2/2R'^2] < A'$. Thus, having a single transect, the right value of the eddy's size R and underestimated values of the eddy's intensity A will be obtained. Otherwise, if the flow function is equal to a non-zero constant inside an axisymmetric eddy, turning into zero outside it, a single transect will give the right value of the eddy's intensity and underestimated values of its size. The first case, with Gauss-like flow function, seems to correspond more closely to reality. That is why we expect that we have got the right value of the cyclone's size, while the cyclone's intensity and, as a consequence, its frequency of rotation could be underestimated.

According to (6), geostrophic estimates of azimuthal velocity and frequency of the cyclone's rotation are:

$$u_g(r) \equiv \frac{\partial F_g}{\partial r} = -\frac{Ar}{R^2}\exp - \frac{r^2}{2R^2}, \ \omega_g \equiv \left. \frac{\partial u_g}{\partial r} \right|_{r=0} = -\frac{A}{R^2} \qquad (8)$$

where $r = x - x_0$ is the radius of that feature. With the above values of A and R, the second of formulae (8) yields

$\omega_g = 1.29 \cdot 10^{-4}\text{s}^{-1}$ which is comparable with the value of the Coriolis parameter $f = 2\Omega\sin\varphi = 1.22 \cdot 10^{-4}\text{s}^{-1}$.

Here Ω is the frequency of Earth rotation, φ is the latitude; $\Omega = 0.727 \cdot 10^{-4}\text{s}^{-1}$, $\varphi = 56.7°$. Since ω_g and f are of the same order of magnitude, a centripetal acceleration u^2/r (u is azimuthal velocity) must be taken into account. Thus, instead of geostrophic balance, the cyclone has to be described by the balance of Coriolis acceleration, horizontal pressure gradient, and non-linear term of equation of motion, namely the centripetal acceleration:

$$-\frac{u^2}{r} = -fu_g + fu \qquad (9)$$

By solving quadratic equation (9) for u, we obtain:

$$u(r) = -\frac{fr}{2}\left[1 - \left(1 + \frac{4u_g}{fr}\right)^{\frac{1}{2}}\right] \qquad (10)$$

(10) gives the following expression for the frequency of eddy rotation:

$$\omega \equiv \left. \frac{\partial u}{\partial r} \right|_{r=0} = -\frac{f}{2}\left[1 - \left(1 + \frac{4\omega_g}{f}\right)^{\frac{1}{2}}\right] \qquad (11)$$

By substituting the above values of ω_g and f into (11), we calculate $\omega = 0.785 \cdot 10^{-4}\text{s}^{-1} = 1.29(f/2)$. Thus, with regard to centripetal acceleration, the estimate of frequency of the cyclone rotation is decreased by factor 1.64 with respect to that of geostrophic balance. Nevertheless, it remains greater than 1/2, the upper limit for frequency of anticyclone rotation, confirming the well-known statement that cyclones are more energetic than anticyclones in both the atmosphere and the ocean. As for the maximum azimuthal velocity in our cyclone, u_{max}, the geostrophic estimate, $u_{gmax} = 23\,\text{cm}\,\text{s}^{-1}$ at $r = 2.94\,\text{m}$, decreases to the value of $u_{max} = 16\,\text{cm}\,\text{s}^{-1}$ at $r = 3.33\,\text{km}$ when centripetal acceleration is taken into account. It should be noted that, having been calculated from single transect data, the above values of ω and u_{max} are probably on the low side.

The thermohaline structure of the cyclone is shown in Figure 11, where isolines of temperature in the distance−potential density plane are presented. In the upper layer of halocline, at $O_\theta < 6.4\,\text{kg}\,\text{m}^{-3}$, the cyclone is purely baroclinic: despite a strong deformation of isopycnals (see Figure 3), the temperature on isopycnals is nearly constant. On the contrary, in the middle layer of halocline, at $6.4\,\text{kg}\,\text{m}^{-3} < \sigma_\theta < 8.4\,\text{kg}\,\text{m}^{-3}$, the temperature of isopycnals inside the cyclone is 0.2−0.3° C below its value outside the cyclone. At last, in the lower layer, adjusted to the sea bed, density and salinity inside the cyclone are greater then their respective maximum values in the surroundings. Thus, the cyclone is shown to transport heterogeneous water in the middle and lower layers of the halocline, while in the upper layer it reduces to a solitone-wave-like bend of isopycnals of no thermohaline anomaly.
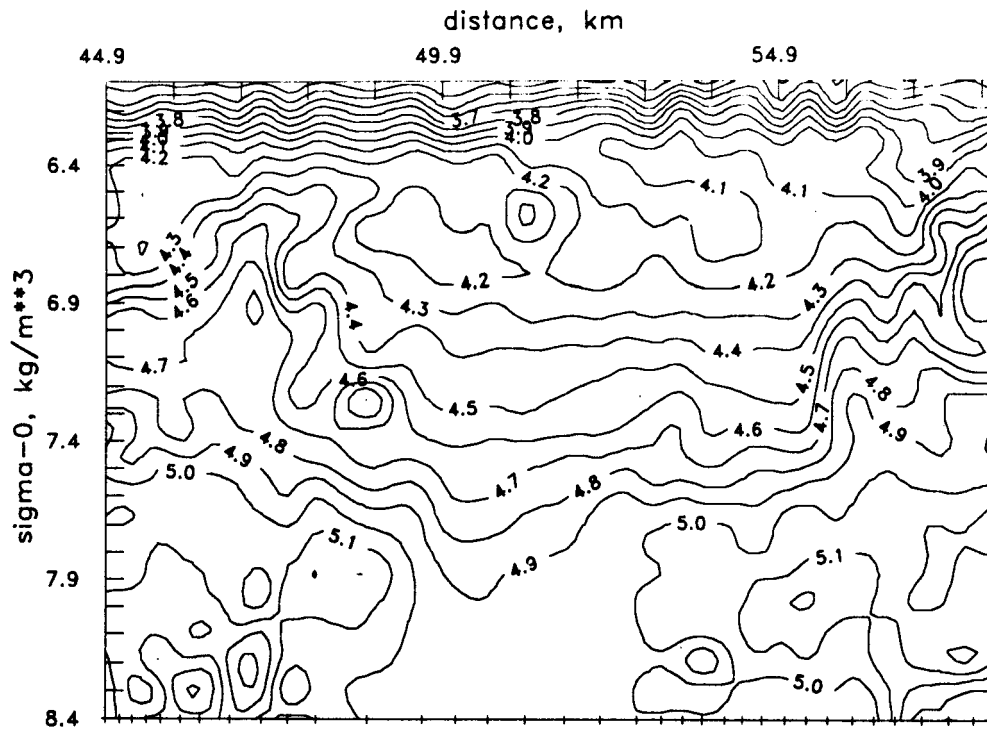
Figure 11 Temperature vs. potential density and distance in the cyclone

To illustrate the transfer of salty water by the cyclone, Figure 12 displays the same fragment of A–B transect in salinity. The maximum salinity in the cyclone is greater than 11.5 PSU. It is worth remembering that the maximum salinity in the bottom layer of the Gotland Deep was 11.0 PSU in the middle of March, 1993, and increased to 11.7 PSU by June due to the major Baltic inflow in January 1993 (Dahlin *et al.*, 1993). Thus, the cyclone is proved to transfer salty water originated from the 1993 inflow event, contributing to the deep water renewal in the Eastern Gotland basin.
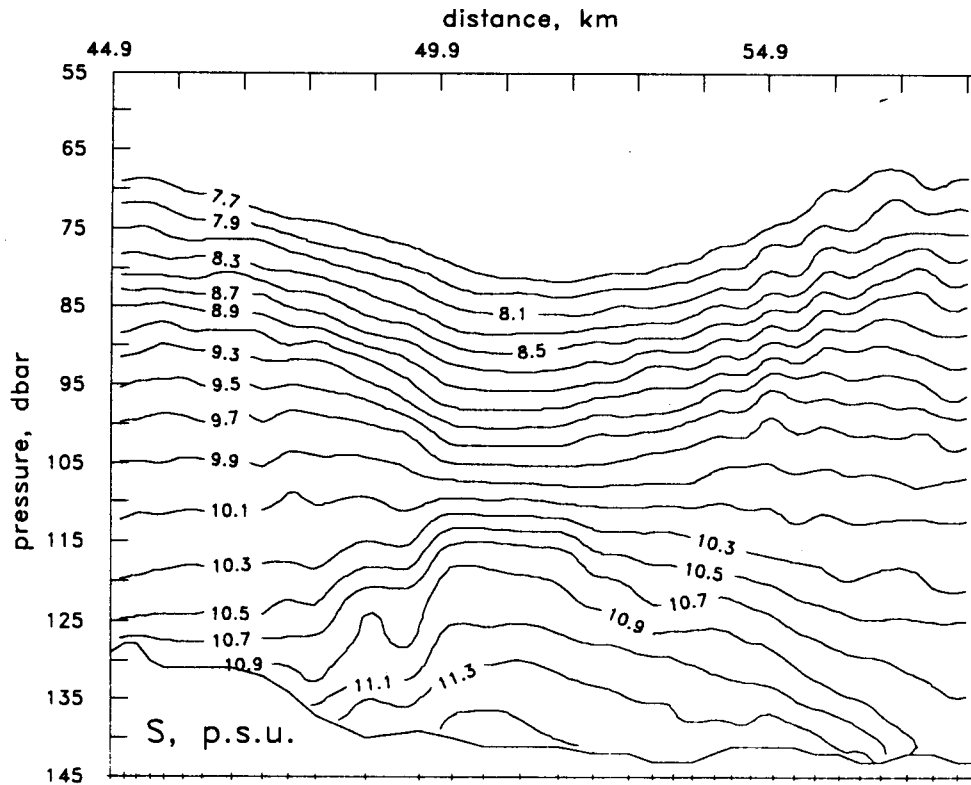
Figure 12 Salinity vs. pressure and distance in the cyclone

Conclusions and Perspectives

Closely spaced CTD profiling in the Stolpe Channel and the Eastern Gotland Basin made it possible to reveal and investigate two interesting mesoscale dynamic features associated with salty water motion toward deep basins of Central and Northern Baltic.

The first is the northward displacement of denser water from the deepest connection of the Stolpe Channel which is accompanied by a fan-like divergence of isopycnals when advancing south. This effect has been explained taking into account the Ekman transport by sloping boundary of the channel.

The second is the underwater cyclonic eddy which was revealed south the Gotland Deep in April 1993. The cyclone was carrying salty water after the 1993 inflow event. Such eddies should be considered as a possible way of ventilating deep waters in the Baltic Sea.

In the near future we will carry out specialised field experiments to answer the following questions:

- What is the role of internal waves in salty water transfer over the Stolpe Sill and how can it be quantified?
- What drives thermohaline intrusions in the Baltic halocline and what is the role of inertial oscillations in this?

References

Dahlin, H., Fonselius, S., and Sjöberg, B., 1993. The changes of the hydrographic conditions in the Baltic Proper due to inflow to the Baltic sea. ICES Statutory Meeting 1993, C.M.1993/C:58, Session V.

Garrett, C., MacCready, P., and Rhines, P., 1993. Boundary mixing and arrested Ekman layers: rotating stratified flof near a sloping boundary. Annu. Rev. Fluid Mech., v.25, p.291−323

Krauss, W., and Brügge, B., 1991. Wind-produced water exchange between the deep basins of the Baltic Sea. J. Phys. Oceanogr. v.21. #3 p.373−384.

Matthäus, W., Lass, H.-V., and Tiesel, R., 1993. The major Baltic inflow in January 1993. ICES Statutary Meeting 1993, C.M.1993/C:51, Sess. V.

Paka, V.T., 1996. Thermohaline structure of the water on cross-sections in the Slupsk Channel of the Baltic Sea in spring of 1993. Oceanology, v.36−2, pp. 207−217.

Pikies, R. 1990. Geological map of the Baltic Sea. Ed. Mojski E. Sheets 15, 16. Slupsk Channel. Warsaw.

Zhurbas, V.M., Kouts, T., Laanemets, J.J., Lips, V.K., Sagdiev, A.M., and Elken, J., 1992. Spatial distribution of finestructure intensity in a Mediterranean salt lens. Oceanology (Engl. Ed.), 32(3). 273−278.

Oil content in Baltic Sea water and possibilities for detection and identification by the Lidar method

Jacek Piskozub, Violetta Drozdowska, Tadeusz Krol, Zbigniew Otremba, and Adam Stelmaszewski

Introduction

Oil contamination measurements in sea water are carried out by intensively employing many physical and chemical methods. In recent years remote measurements of the marine environment for detection of oils and other substances which occur in the sea water has started to play an important role.

In our experiment we applied the lidar method which enables remote detection of fluorescent substances in the sea water (Wehry *et al.*, 1981), (Bristow *et al.*, 1981) and the laboratory system for fluorescence measurements of oil substances (Otremba and Stelmaszewski, 1994).

So far, laser-induced fluorescence spectroscopy for quantitative classification of aromatic hydrocarbons and for measuring of water contamination with oil components has been used (Bublitz and Schade, 1995), (Moise *et al.*, 1995). In recent years scientists have used the lidar because of the many possibilities of application of lidar methods for the detection of oil distribution (Goncharov *et al.*, 1995).

This experiment attempts to measure oil contamination in the surface layer of water by the lidar method in the southern Baltic Sea. The measurements carried out in the Institute of Oceanology PAN used the lidar system FLS-12. This lidar allows for registration of fluorescence in the range of 425 nm to 800 nm which is sufficient for the measurements of the real distribution of oil components and other fluorescent substances in the sea water.

To confirm and verify the correctness of this method we simultaneously took up the water probes from the same sites to use for standard fluorescent laboratory method measurements. Figure 1 shows a map of the southern Baltic Sea with the sites of the remote measurements and observations carried out during expeditions of the research vessel "Oceania". Figure 2 shows a distribution curve for all results obtained in the open sea and in the Gdansk Bay.
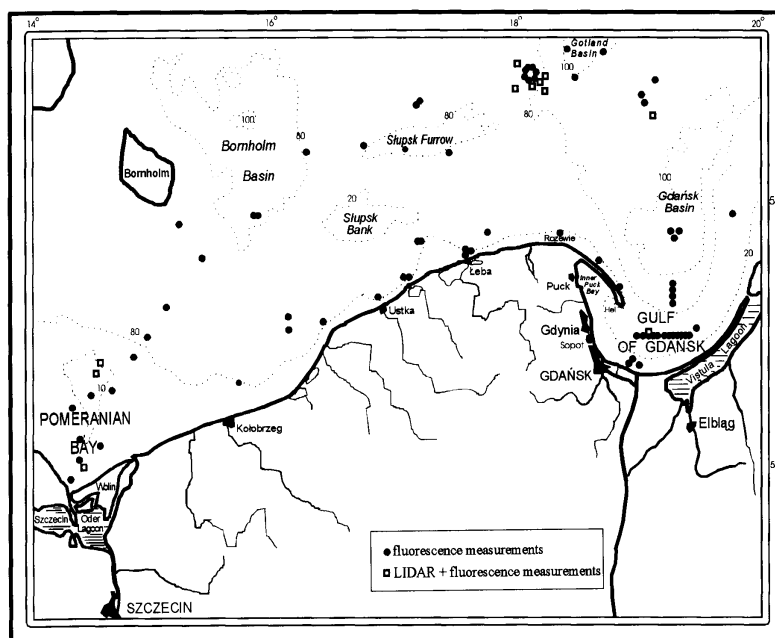
Figure 1 Map showing sites of measurements and observations visited by r/v "Oceania"
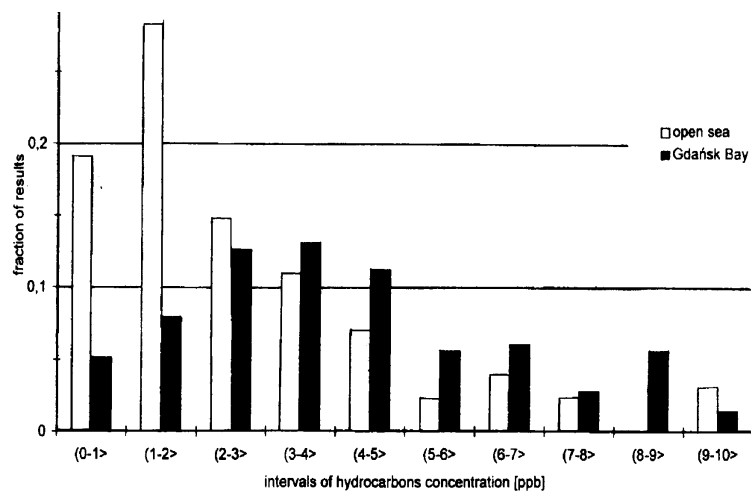
Figure 2 Distribution of the results contained in several concentration intervals for open sea and bay water

Methods

The FLS-12 lidar system used for the measurements is a tuneable laser system designed for remote sensing of the aquatic environment in the visible spectrum (Piskozub *et al.*, 1994). It consists of two lasers: the excimer laser (308 nm) which is the UV pumping source and the dye laser. We used the dye "coumarine 120" with maximum fluorescence at 440 nm.

The backscatter signal is collected by the telescope and registered by CCD camera. The measurements are controlled by special software. The lidar-emitted light excites all sea water components possessing fluorescence properties. The backscattered signal is made up of the lidar and the water Raman backscattered light and fluorescence comes from all fluorescent components. The fluorescent maxima for the basic Baltic water components are as follows (Babichenko *et al.*, 1992): phycoerythrin (575 nm), phycocyanin (645 nm), chlorophyll 'a' (685 nm), humus substances (600 nm) and oil substances (250 nm–500 nm). Figure 3 presents backscattered laser signal (440 nm), backscattered water Raman signal (521 nm), oil fluorescence (470 nm), fluorescence of pigments and humus substances (635 nm) and fluorescent band of chlorophyll 'a' (685 nm). Assuming that we know maxima and halfwidths of all fluorescent bands we can approximate the experimental curve to the theoretical gauss curve and then to reduce it to component gauss curves (Figure 4).
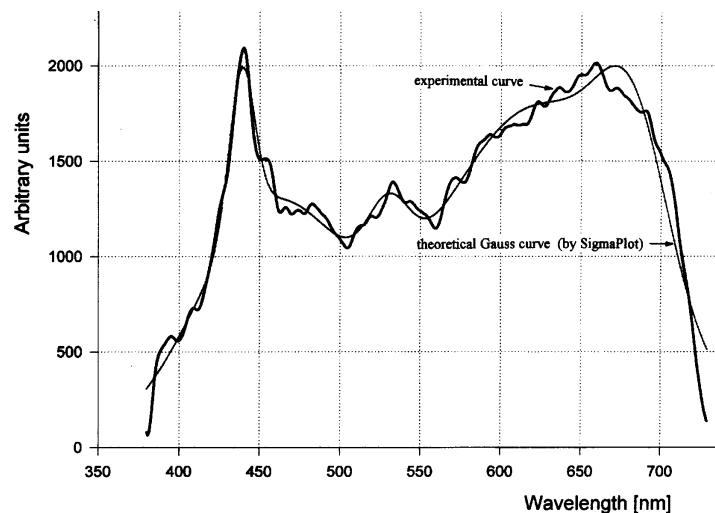
Figure 3 Experimental and calculated fluorescent spectrum
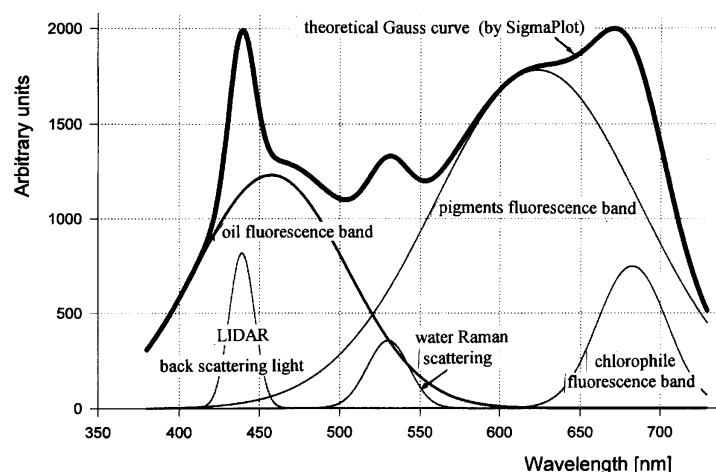
Figure 4 Calculated LIDAR fluorescent spectrum and theoretical fluorescent bands

The fluorescent band intensity is proportional to the fluorescent substance concentration. But this spectrum is subject to errors connected with light attenuation and water density changes in the sea water. The solution to this problem is the concurrent laser-induced Raman emission of liquid water, which is used as an indicator for changes in optical attenuation. Dividing bands of the fluorescent substance and backscattered water Raman we obtain the fluorescent coefficient of the fluorescent substance. This expression mainly depends on the fluorescent substance concentration and is independent of many parameters such as laser power, distance from the object and sensor efficiency coefficients which are the same for both bands. In this way we can determine the fluorescent coefficient of the oil which is the measurement of the oil concentration.

The theory of the fluorescent substance concentration measurements by the lidar method is given by Bristow (1981).

Simultaneously in the sites where the lidar measurements of water contamination with oil component were carried out the water probes were taken for the laboratory measurements in Physics Department of Gdynia Maritime University (Otremba and Stelmaszewski, 1994).

Results

No.	Oil fluorescence coefficient	Hydrocarbon concentration [μgkg^{-1}]
25	10.3	1.9
26	4.5	1.6
28	21.2	4.9
29	7.2	1.6
31	5.4	0.4
32	4.6	0.5
33	9.5	1.4
34	6.6	1.6
36	4.1	3
38	8	0.7

Table 1 Results of measurements made by two different methods
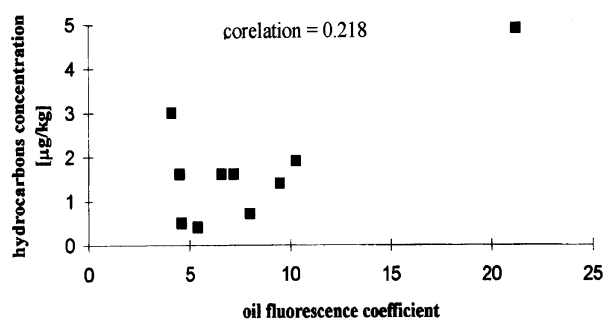
Figure 5 Correlation of the fluorescence coefficient and real concentration of hydrocarbons in water

Oil content in Baltic Sea water and possibilities for detection and identification by the Lidar method

Table 1 shows results of the measurements made by both of methods. Generally a good correlation does not occur between them (Figure 5).

The small correlation which is shown in Table 1 can be caused by the fact that backscattered light, which is registered by the lidar, originates from the surface of water but water probes are collected partially from under surface of water. This way measurements can give different results.

Secondly if there was oil emulsion on the surface of water the backscattered lidar signal would indicate a large oil concentration as opposed to the laboratory fluorescent method.

Moreover the light which radiates in sea water is absorbed and reduced in many ways so the backscattered lidar signal can be attenuated and change the real information about the oil concentration.

Conclusion

Results show that oil investigations in the sea water should use the UV-source of the excitation, because using 440 nm wavelength lidar excitation gives two overlapping bands. It also can lead to incorrect results obtaining by the lidar method.

References

Wehry, E. (ed.), 1981. Modern Fluorescence Spectroscopy. Plenum Press, New York and London (Chap.5 and 7).

Bristow M. *et al.*, 1981. Laser Fluorosensor Use of Water Raman Emission to Correct Airborn Data for Effect of Water Optical Attenuation. Appl.Opt.Vol.20 pp.2889–2906.

Babichenko S. *et al.*, 1992. Laser Remote Sensing of Phytoplankton. Remote Sensing of Environment.

Bublitz J., and Schade W., 1995. Multiwavelength laser-induced fluorescence spectroscopy for quantitative classification of aromatic hydrocarbons, Proc.SPIE, Vol.2504, p.265–276, Environmental Monitoring and Hazardous Waste Site Remediation.

Moise N. *et al.*, 1995. Measuring of water and soil contamination with oil components using laser-induced fluorescence transmitted through optical filters, Proc.SPIE, Vol.2461, p.636–643.

Goncharov V. *et al.*, 1995. Possibilities of application of lidar methods for the discovery of oil discharge from under-water sources on the sea shelf, Proc. SPIE, Vol. 2380, p.344–348.

Klimkin V. *et al.*, 1993. Spectrofluorimeter for remote analysis of oils on the surface of water. Proc SPIE Vol. 2107, p.18–231

Vinas M. *et al.*, 1992. Fluorescent sensor as an engine oil quality indicator, Proc. of the meeting, Los Angeles, CA, p.238–247.

Zhu Y., and Junfu M., 1992. Study on determination of micro amount oil in water by laser time-resolution fluorescence spectroscopic technique, Proc. SPIE Vol. 1637, p.285–290.

Gillispie G., and Germain R., 1992. In-situ tunable laser fluorescence analysis of hydrocarbons, Proc. SPIE Vol. 1637, p.151–162.

Piskozub J. *et al.*, 1994. Oil content in the Baltic Sea Water and Possibilities of Detection and Identification by the Lidar Method, Proc.19th CBO, p.166–171.

Otremba Z., and Stelmaszewski A., 1994. Concentration and Origin of Oil Contaminations in the Gdansk Bay Coast Water, Proc. CBO, p.593–603.

Hydrographic and hydrochemical structure of waters in the Luga-Koporye region during the summer period

Pyotr P. Provotorov, Vladimir P. Korovin, Yuri I. Lyakhin, Alexei V. Nekrasov, and Valery Y. Chantsev

The hydrographic and hydrochemical structure of waters in the Luga-Koporye region (south-east part of the Gulf of Finland) is studied on evidence derived from the four (1993–1996) summer surveys of the oceanographic "polygon" 20×50 sea miles (Figure 1) performed within the framework of the UNESCO/IOC/HELCOM "Baltic Floating University" programme. STD measurements of water samples at about 45 stations in the polygon carried out during the cruises of research vessels "Professor Sergei Doirofeev" (1993), "Persey" (1994) and "Nikolai Matusevich" (1995 and 1996) have been used together with a few hundred sounding measurements with 2 m vertical spacing at anchored stations with duration up to 6 days. The near-shore shallow stations of each survey were measured by the sailing catamaran "Orients".
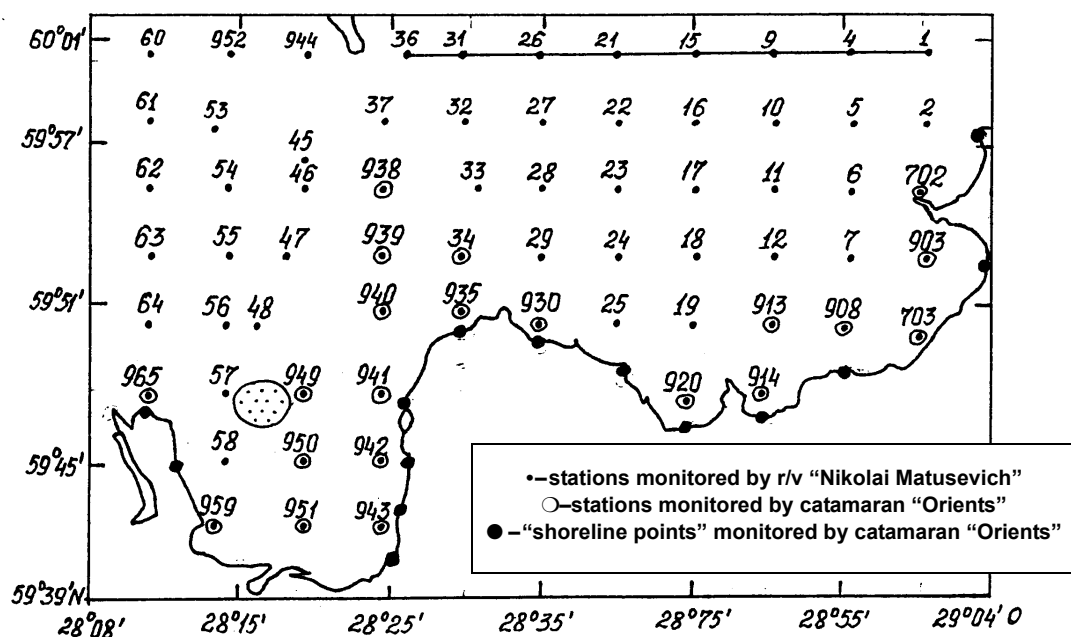
Figure 1 Positions of stations at the Luga-Koporye polygon (survey of July 24–29, 1995, r/v "Nikolai Matusevich" and "Orients")

The temperature (T), salinity (S) and density (ρ) patterns reproduced from the measurements are typical for the stage of summer heating, being composed of: (a) upper mixed layer 10–15 m thick; (b) transient layer with pronounced gradients of characteristics and (c) near-bottom thermohalocline resulting from transformed waters penetrating from the open part of the Gulf using the irregularities of bottom topography. Given the obvious stratification of waters, the T, S-curves (Figure 2), even for the mostly offshore stations, have the form of straight "mixing lines" indicating that the quasistationary diffusion seems to suggest the formation of the vertical thermohaline structure in the Eastern Gulf of Finland.
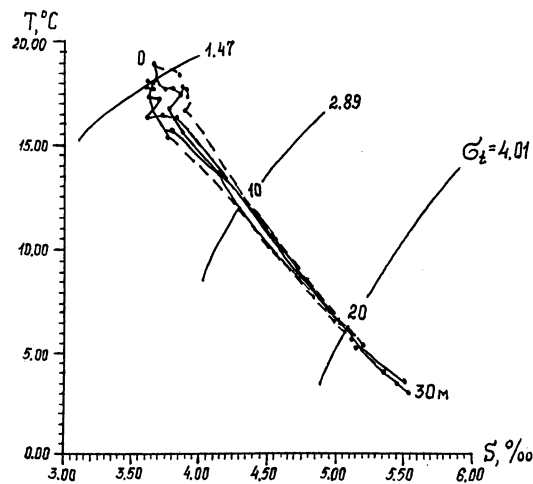
Figure 2 *T, S*-curves for stations of the Luga-Koporye polygon obtained from STD-sounding with vertical spacing $z = 2$ cm
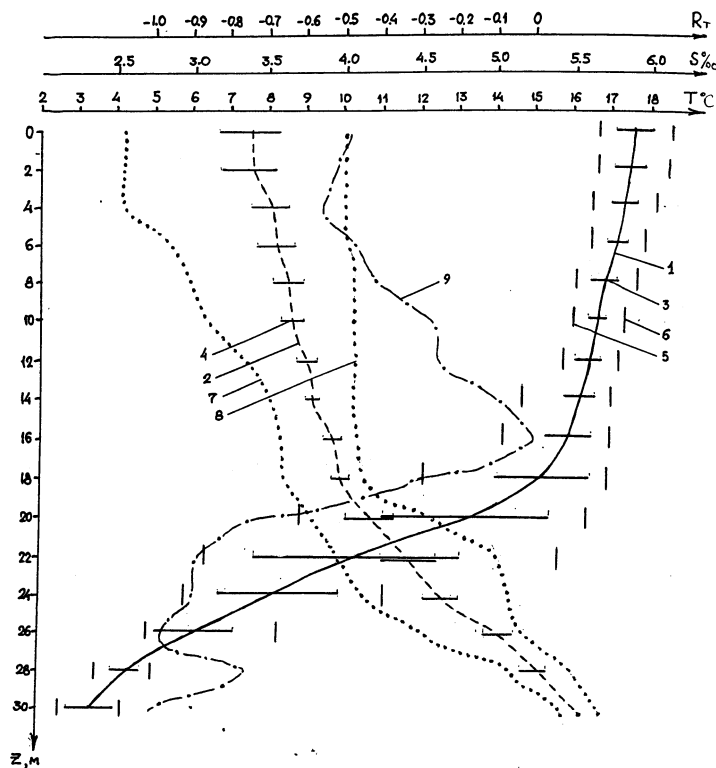
Figure 3 Vertical profiles of temperature (1) and salinity (2) as well as m.r.s. deviations (3) and (4). Extreme values T_{min} (5) and T_{max} (6), S_{min} (7) and S_{max} (8) are shown together with the correlation coefficient between T and S (9)

Figure 3 demonstrates the vertical T and S profiles (averaged over all the stations of the polygon) with their r.m.s. and extreme values at different depths. The most spatial variability is inherent in the near-bottom layer where the deviations of T and S reach, correspondingly, 5°C and 0.5%. The coefficients of correlation R between the fields of T and S, calculated for different levels from the observational data and considered as random samples, are negative across the whole depth (curve 9 in Figure 3). The elevated (in magnitude) values of R for the undersurface and near-bottom layers are circumstantial evidence that the corresponding horizontal surfaces are isopycnic. For intermediate layers, the diapycnicity is more characteristic, resulting in a rather weak interrelation between the temperature and salinity fields.

It is known that the density background of the vertical stratification in the Baltic Sea is formed mainly after the type of "complete stability" with an inherent drop in T and increase in S with depth. A fragment of a stratification diagram developed with the use of the temperature (E_T) and salinity (E_S) stability components for the Luga-Koporye stations is given in Figure 4. Such a background stratification is not favourable for a fine structure development and, consequently, mixing is caused by the differential-diffusive (thermoconcentration) convection. The mixing and exchange of substances

in the Eastern Baltic summer pycnocline is effected by the internal wave break-up, some edge effects and turbulent diffusion in coastal waters [1,2].
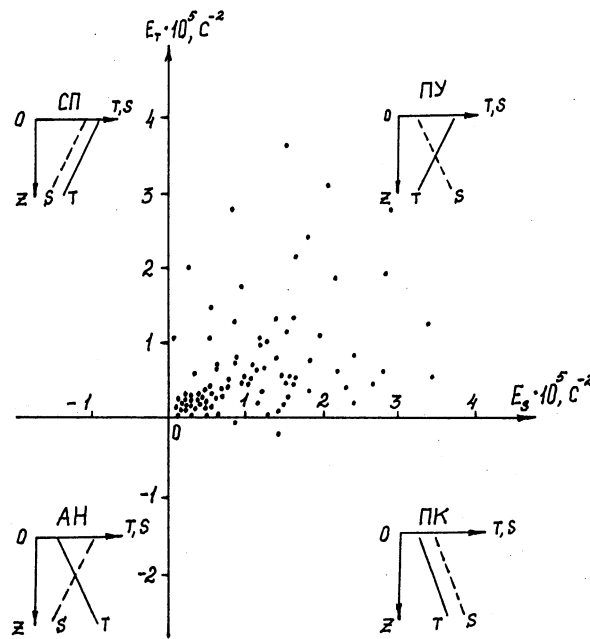
Figure 4 Types of thermohaline conditions characterising stratification (K. Ferorov's diagram) obtained from the measurements at stations of the polygon. C−solt fingers-like, Y−complete stability, K−layer-to-layer convection, AH− complete non-stability. E_T and E_S are temperature and salinity stability components.

Judging from the density relation:

$$R_\rho = \frac{\alpha \Delta T}{\beta \Delta S} = -\frac{E_T}{E_S} \tag{1}$$

(α, β being coefficients of thermal expansion and salinity compaction of water and ΔT, ΔS differences in T and S across the layer) both the factors are contributive in the density stratification. However, the salinity contribution prevails in the upper layer while the temperature effects dominate near the bottom (Figure 5).
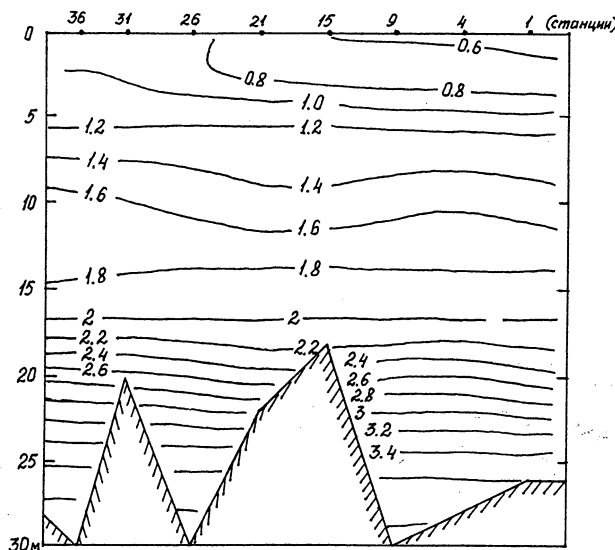
Figure 5 Distribution of density relation $R_\rho = -E_T/E_S$ at the transect along the parallel of latitude 60° N (stations 36-31-26-21-15-9-4-1)

Spatial patterns of T and S distribution are caused by local differences in heating by radiation, freshwater runoff and wind/wave mixing. The inflow of relatively cold and saline water from the open part of the Gulf is mostly in evidence at

the western polygon boundary whence it propagates to the east by mixing progressively with the shallow waters. The local spots of advective origin are fixed between the Luga and Koporye bights.

The course of T, S and ρ isolines at the meridianal and latitudinal transects implies a weak baroclinity (isopycnic lines and isobars are parallel) and absence of distinct frontal separations. Only in the vicinity of the mouth of the Luga River is it possible to perceive salinity frontal zones due to local freshwater discharge.

The peculiarities of stratification and probability of fronts formation between stratified and mixed waters can be characterised by the potential energy anomaly [3]

$$\varphi = \frac{1}{H} \int_{-H}^{0} (\bar{\rho} - \rho_i) g z \, dz \qquad (2)$$

where $\bar{\rho} = \dfrac{1}{H} \displaystyle\int_{-H}^{0} \rho \, dz$ is a vertically mean density in a water column.

φ is the anomaly of potential energy if a stratified water column to that of a totally mixed one. Formation of frontal zones is probable where the elevated values of horizontal gradients of φ take place. Estimation of this criterion for the Luga-Koporye stations shows that the probability of frontal separation does not seem to be very high. The existing weak frontal zones belong to a thermoclinic type. Unlike baroclinic fronts, these can be manifested in T and S fields but the contributions of T and S compensate each other in a density field.

The arrow of STD data obtained from the 6-day (one hour timely spaced measurements) anchored station (59°50'N, 28°10'E) provides the basis for revealing the features of thermohaline variability. During the period of measurements (28.07–03.08.1995), the weather was sunny, anticyclonic, with a weak wind of variable direction—favourable for intensive heating of water. The temperature variations in the upper layer lie in the range 16.98–19.79 °C with the mean temperature equal to 18.53 °C and r.m.s.= 0.65 °C. The corresponding characteristics for salinity are 2.56–3.57%, mean salinity equal to 3.06 and r.m.s.=0.20%. In the transient layer the variability of T and S decreases but in the near-bottom thermocline it sharply increases again. The evolution of thermocline structure can be demonstrated by plotting T and S as a function of z (depth) and t (time). It can be seen that intensive oscillations (increasing as the bottom is approached) are manifested against the background of diurnal variations and intensive surface heating.

To be able to judge the type and possible mechanism of local thermocline structure violations, the so-called δ-parameter was calculated:

$$\delta = \frac{\tilde{R}_\rho - 1}{|\bar{R}_\rho| - 1} \qquad (3)$$

where $R_\rho = \dfrac{\alpha \rho_t}{\beta \rho_s}$ is a combination akin to the density relation constructed of m.r.s. amplitudes of temporal T and S series for fixed depths;

$\tilde{R}_\rho = \dfrac{\alpha \Delta \bar{T}_z}{\beta \Delta \bar{S}_z}$ is the mean density relation for the layer considered;

$\Delta \bar{T}_z$, $\Delta \bar{S}_z$ are the T and S vertical gradients in this layer averaged over the period of measurements.

It is evident that in case of purely isopycnic (advective) intrusion the conditions

$$\frac{\rho_t}{\sigma_s} \approx \frac{\beta}{\alpha}; \delta \to 0 \qquad (4)$$

are fulfilled, whereas in the case when the vertical processes dominate in forming the structure, the following condition holds.

$$\frac{\rho_t}{\sigma_s} \approx \frac{\Delta \bar{T}_z}{\Delta \bar{S}_z}; \delta \to 1 \qquad (5)$$

Estimation of δ-criterion showed that it tends to zero in the near-bottom layer and grows to $0.6-0.8$ above. This means that on average the T and S variations were caused by horizontal (near the bottom) and vertical (in the remainder of water column) processes.

The hydrochemical investigations were related appreciably with the study of nutrients concentration and eutrophication state of the areas under consideration. The Eastern Gulf of Finland is subjected to a strong influence of runoff of many rivers (Neva, Luga and others) providing the discharge of great amount of nutrients and organic matters (both natural and anthropogenic). During $1960-1990$ the anthropogenic load grew, resulting in trends of many hydrochemical characteristics and producing an eutrophication hazard in this basin. The variability of hydrochemical conditions in the Luga-Koporye region can be followed basing on the data obtained.

The hydrochemical structure of this region follows the hydrographic one and also consists of three layers: the upper quasi homogeneous layer, the transient layer and the near-bottom layer. In the upper $6-8$ m the intensive blooming of plankton takes place by which the nutrients are extracted from the water as the oxygen content as well as pH increase. In transient and deep layers the organic detritus is subjected to a biochemical decomposition, the pH and oxygen content reduces and nutrients regenerate. However, as it was shown by investigations during last four years, the qualitative characteristics of these processes do not remain unchanged.

According to observations of 1993 the area considered was entirely encompassed by a powerful blooming of phytoplankton with the blue-green algae dominating in the layer from the surface to a depth of $6-8$ m. Very high values of pH (up to 8.7) and oxygen concentration ($110-125\%$) were measured here with extraordinary (for summer) concentrations of phosphates ($9-15\,\mu g\,l^{-1}$) and nitrates ($20-40\,\mu g\,l^{-1}$) and with nitrites universally present (up to $3\,\mu g\,l^{-1}$). Below the thermocline and close to the bottom the pH values decreased down to $7.50-7.70$ with oxygen content being about $70-80\%$, while the concentration of phosphates increased up to $25-40\,\mu g\,l^{-1}$ and that of nitrates—up to $160-250\,\mu g\,l^{-1}$. The data led to the noting of a deep eutrophication in the Luga-Koporye region. The runoff of nutrients from the land (especially that provided by the Luga River) was so large that the phytoplankton, even though enormously developed, could not completely utilise the phosphates and nitrates from the upper layer waters.

The data from August 1994 show that the end of the summer in the Luga-Koporye region was characterised by a appreciable decay in the photosynthesis activity since the pH values and oxygen content reduced to $8.1-8.3$ and $100-110\%$ correspondingly while the nutrients concentration diminished to $0-4\,\mu g\,l^{-1}$ (phosphates) and $10-20\,\mu g\,l^{-1}$ (nitrates). However, in the near-bottom layers the value of pH reduced to $7.1-7.2$ with the oxygen content being $20-30\%$ and phosphates and nitrates concentrations increasing up to $40-50$ and $200-260\,\mu g\,l^{-1}$, correspondingly. The situation originated in relation to the nutrient discharge provided by rivers. Hence, while the phytoplankton was able to cope at the end of the summer with most of nutrient load, the destruction of the abundance of detritus provokes a critical state of intensive eutrophication in the near-bottom layer.

Results obtained in 1995 revealed a radical alteration in the state of the Luga-Koporye region in comparison with preceding years.

The amount of phytoplankton reduced considerably while the proportion of diatoms noticeably increased. Hydrochemical gradients between upper and bottom layers were smoothed. In the upper layer the pH values were $8.4-8.6$ with oxygen content being $105-110\%$, phosphates—$0-2.5\,\mu g\,l^{-1}$, nitrates—$0-3\,\mu g\,l^{-1}$. In the bottom layer the pH values were $7.9-8.2$ with oxygen content being $80-90\%$, phosphates—$3-6\,\mu g\,l^{-1}$ nitrates—$2.5-16\,\mu g\,l^{-1}$. This is indicative of a reduction of nutrient load, the values of hydrochemical parameters approaching normal long-standing means with no evidence of eutrophication.

In July 1996 the distribution pattern of nutrients was obtained for the whole area of the Eastern Gulf of Finland. Maximum concentrations of phosphates (more than $30\,\mu g\,l^{-1}$) and nitrates (up to $70\,\mu g\,l^{-1}$) were observed at the surface in the head of the Gulf (29°20' E), which can be explained by the discharges from the northern and southern St. Petersburg purification systems in the Neva Bight. In spite of diluting and consumption by phytoplankton, the nutrients seem to be transported up to and including the Luga-Koporye region and even further to the west. Additional coastal sources of nutrients were noticeable in the Luga and Koporye Bights. As a result, the concentrations of phosphates and nitrates have relatively high levels ($7-20\,\mu g\,l^{-1}$ and $0-10\,\mu g\,l^{-1}$, correspondingly) in the upper layer of the area considered. The oxygen content in the bottom layer of the Luga-Koporye region is somewhat below the level of 1995, but much higher than that in 1994 (the latter can be considered as an eutrophic year). The amount of nutrients in the water was much less than in 1993, but rather more than in oligotrophic 1995. It is believed that the nutrient runoff from land had been increased in 1996 and hence a further development of eutrophication should be expected.

References

1. Озмидов Р.В. Особенности процессов перемешивания в Балтийском море. (29 рейс НИС "Профессор Штокман"). Океанология. 1993. т.33 № 5.

2. Озмидов Р.В. Роль краевых эффектов в перемешивании глубинных вод Балтийского моря. Океанология. 1994. т.34 № 4. с. 490-495.

3. Боуден К. Физическая океанография прибрежных вод. М., Мир. 1988. с.250-267.

4. Федоров К.Н. О термохалинных характеристиках фронтов в океане. Докл. АН СССР. 1988. т. 302, № 1. с. 206-210.

5. Журбас В.М. и др. К вопросу о возможности классификации тонкой термохалинной структуры по результатам расчета ее статистических характеристик. Сб. Структура гидрофизических полей Норвежского и Гренландского морей. М., ИОАН СССР. 1987. с. 43-48.

An assessment of the functional linkages between Baltic marine research and the development of resource management policies

Arno Rosemarin

Abstract

There is a large gap between the scientific/technical knowledge base surrounding natural systems making up the Baltic Sea and the governance/policy systems that attempt to manage these resources. This paper analyses the organisation of marine research in the Baltic area (the major scientific disciplines) including nodes of government and university expertise. It also assesses the development of priorities for research based on the "needs-to-know" of the various sectors of society (e.g. transportation, defence, recreation, fisheries, marine information, minerals, oil/gas, etc.). It takes a critical view of monitoring programmes that tend to collect "non-targeted" data. It then reviews the major modes of publication and outreach in Baltic marine science, where the material is being published and how accessible it is, including citation frequencies. The plague of specialist science in today's world that needs systems solutions, is a major theme here. The paper then reviews the available functional linkages between scientific knowledge and policy development at international, national and local levels (including the role of HELCOM, ICES, the high-level ministerial meetings in recent years and the media). How marine science fits into the other sciences of the Baltic drainage basin especially in the coastal zone where human and natural systems intimately interact, is a key to discovery here. A few case examples are given including pulp and paper industry, transportation sector, oil spills and eutrophication, where engineering assessments seem to dominate and natural ecosystem aspects appear misunderstood or neglected. Science organisations such as BMB, MGB and CBO need to rethink and reorganise somewhat in order to participate better in the on-going full-scale development of management policy in the Baltic arena.

Introduction

That the Baltic Sea has received much attention in the area of environmental research in an attempt to aid the process of policy development to improve environmental protection is common knowledge. Just how effective this process works and to what extent the existing bottlenecks in the system slow things down is the subject of this paper. What always amazes is the contrast between the impressive amount of knowledge that exists surrounding natural and man-made processes within the Baltic drainage basin and the rather crude, highly politicised governance systems that have managed to persist in, for example, the carrying out of environmental impact assessment—may it be a planned bridge over Öresund, the building of a sewage treatment plant in St. Petersburg, expansion of oil terminal in Klaipéda or pulp mill in Mönsterås. The theme is recurring—technology assessment takes priority and licensing occurs on a piecemeal basis—comprehensive ecosystem evaluation is given very little central attention. As a result, environmental issues are still treated as they were 20 years ago—in the form of confrontation. The voice for natural science is usually split up and bureaucratised with specialists dealing with disconnected issues. The holistic aspects are taken on by NGOs such as WWF and Greenpeace and some university research groups. Thus the confrontational approach continues.

Marine scientists could play a much stronger role in policy development if they were better represented through their professional organisations, through systems analysis groups and proper national and international assessments that examine trends on an independent basis. The natural scientists are usually only token contributors to important debates and not central in the process of building public opinion. Swedish marine science has traditionally been a rather silent component in Swedish society. Not until 1988 when there occurred massive mortalities of fish, invertebrates and algae due to toxic blooms of *Chrysochromulina polylepis* (Rosenberg *et al.*, 1988) and also death of seals due to an aphocine distemper virus epidemic (Helander, 1990), was there some public interest in marine biological science in Sweden. The gradually polluted Baltic with dead bottom zones that came and went along with saltwater influxes received much international attention during the 1970s but never really hit home politically like the acute mortalities along the west coast. The vulnerability of natural ecosystems was finally addressed by politicians and more money than ever before became available for research. But the gap between science and policy is still large.

The Natural Step (DNS), an organisation that makes its living by exploiting the gap between science and policy in the eyes of big industry, claims that we researchers are only noisy apes on the tree of research science spitting out conflicting pieces of evidence and only confusing the policy makers, public and industry. This message we should take more seriously because it is an indication of failure on the part of the scientists to communicate their work to society—the people paying the bills. There IS more than one way to examine a problem involving natural systems and there ARE more than one or two possible explanations for natural phenomena. We have to make this clear. Simplification is not the goal, explanation is.

The percolation rate of critical scientific material from the research desk to the international policy arena is extremely slow. Much of the fine tuning available from research is lost in the rather awkward political process of international negotiation. Such decisions as the 50% reduction target for all effluents (point and diffuse) to the Baltic Sea (1985) within 10 years reflect just how gross the political machinery is in its attempt to create policy. This goal was mainly political and impossible to achieve in reality. Whose fault is this? Where were the marine scientists in determining policy for the 1990 Prime Ministerial meeting in Ronneby and where were they again in 1996 in Visby?

HELCOM

One could argue that there is a well-developed system in HELCOM for dissemination of technical knowledge about the Baltic Sea and appropriate policy development. HELCOM is primarily involved with the environmental protection of the marine environment. It does not take on a systems approach in suggesting policies to prevent land-based resource-use activities such as forestry, agriculture practice, energy use, transportation, etc.

HELCOM was, however, put in the limelight following the Ronneby meeting in 1990. This meeting resulted in the Joint Comprehensive Environmental Action Programme (JCP) which identified some 132 pollution hot-spots for cleanup. The Programme is very ambitious and encompasses a 20 billion ECU investment over 20 years. There has been success in the financing of sewage treatment plants but much work is required to reduce diffuse sources of nitrogen (agriculture and traffic) and certain industrial effluents. A personal observation however (Rosemarin, 1996) is that the natural scientists have had very little to do with this gigantic programme. It has primarily been a question of engineering companies and banks. The question is what scientific ecosystem criteria have gone into the norms used to assess the degree of pollution and how will the politicians and financial institutions know that the investments have succeeded in environmental improvements. There is a need for rapid appraisal methods, something very few marine scientists are prepared to develop. The gap between marine ecosystem science and marine engineering science is enormous. What can be done?

Bringing Agenda 21 into the Baltic Sea Region—the need for a systems approach towards sustainable development

As follow up to the Heads of State meeting in Visby, May 1996, an informal meeting of Baltic environment ministers on October 20–21 1996, in Sweden, was set up to discuss a possible regional Agenda 21. A declaration was drafted and agreed upon. Linking the work arising from the Earth Summit (1992) in Rio to the Baltic Sea Region is in fact unique for the world. No regional Agenda 21 plan of this scale has been suggested before. A background document for the October meeting describes in broad terms what sort of challenge an Agenda 21 for the Baltic Region will be (SEI, 1996). Agenda 21 is really nothing more than a policy platform encompassing many aspects of natural and human systems. Its success will only be as good as the technical/scientific information fed into it and the degree of understanding and participation among all stakeholders (sectors of society). Thus it is of interest for Baltic marine scientists to become more aware of and contribute to the Baltic 21 activities.

Giving HELCOM a broader mandate

The CBSS (Council of the Baltic Sea States) meeting in Kalmar in July 1996 has led to certain planned improvements for HELCOM. In particular the following has been highlighted:

- the up-dating and strengthening of the JCP and the instrumental role of HELCOM and the JCP in the development of an Agenda 21 for the Baltic Sea Region
- the establishment of the long-term goal for hazardous substances, meaning the reduction of discharges, emissions and losses of hazardous substances thereby moving towards the target of their cessation within one generation (25 years)
- the speedy implementation of the HELCOM Strategy for Port Reception Facilities and the international assessment of future environmental risks of increased handling and transportation of oil in the Baltic Sea Region

- the strengthening of actions to further limit leaking of nutrients from agriculture consistent with the goal to restore the ecological balance of the Baltic Sea, and the development of an annex to the Helsinki Convention on agriculture

- the development of a coherent policy for sustainable fishing in the Baltic Sea by the Baltic Sea Fisheries Commission

- the protection of biodiversity and nature conservation, including the further development of integrated coastal zone management.

So between an enhanced HELCOM and an Agenda 21 for the Baltic Region, there is ample opportunity for policy development in the whole area of sustainability.

Research

How then is marine research organised around the Baltic? Where is the expertise and what mechanisms exist to broadcast critical results? The attempt here is not to deliver an all-encompassing assessment of Baltic marine research, but to analyse some of the functions connecting research with policy. Research can be divided into various categories mainly depending on purpose and funding source.

Generation of needs and priorities in a sectored society

This is essentially a sector-driven system whereby information priorities arise on a need-to-know basis. A systems approach for this has not yet evolved. The two latest developments, VASAB (Vision 2010 for spatial planning and development) (VASAB, 1994) and Baltic 21 (an Agenda 21 for the Baltic Region) (SEI, 1996) discussed by the ministers as late as Oct 20–21, 1996 have potential. Five spheres of interest can be identified:

- government or intergovernmental orientation (part of a legal instrument)
- industrial applications
- financial institutions
- research foundations — government or private (applied or basic)
- NGOs

It is necessary that the research community give policy makers clear objectives and timetables as well as criteria that can be used to measure progress. The best example I have seen of this is something produced by the Swedish Environmental Protection Agency (SEPA, 1996). It is a list of some 18 environmental quality objectives for the marine coastal zone. They are sufficiently detailed and sophisticated to design a research program as well as a policy programme around. At the same time they are sufficiently simple enough for non-specialists and the general public to be able to appreciate. They are not based on engineering or technology criteria, but biological and chemical criteria connected to an ecosystem subsystem.

Expertise in marine science — a multitude of sector disciplines

Expertise is found sectored within:

- governmental bodies (national, regional, local) and intergovernmental organisations
- universities
- industry
- financial institutions
- NGOs
- media

Research and policy expertise is distributed throughout these sectors. Marine science research is dominated by government and university institutions with geographic and scientific specialisation. Regional projects occasionally bring together the research, especially in the co-ordination of large monitoring projects e.g. Baltic Basin Drainage Project, Gulf of Riga Project, BASYS, Baltic Basin Case Study Towards Sustainability (EU-MAST), Gulf of Bothnia Year, Gulf of Finland Year, BALTEX, etc. There are the professional organisations (e.g. BMB, CBO, MGB, etc.) as well.

Marine science is highly sectored as a multitude of applied sciences, e.g. hydrology, meteorology, geology, oceanography, ecology, engineering, biology, chemistry plus all the sub-categories associated with each discipline. Most universities are split up into a large array of institutions each specialising in a narrow scientific niche.

Organisation of policy—overlapping sectors

Policy development in the Baltic Sea Region is also highly sectored. Many of the different organisations deal with the same questions and the sectors tend to converge somewhat. The following is a partial list of actors involved:

- National parliaments and governments (environment, foreign affairs, trade, industry and energy, transportation and communication, agricultural and fisheries, health and welfare, etc.)
- HELCOM
- ICES
- IMO
- EU
- OECD
- UNDP
- UNEP
- Nordic Council of Ministers
- CBSS—Council of the Baltic Sea States
- BCCA—Baltic Chambers of Commerce
- Financial Institutions e.g. NEFCO, EBRD, IBRD, EIB, IMF, NIB, Associations of commercial banks, national banks,
- Associations of Cities, Municipalities and Regions
    - UBC—Union of Baltic Cities
- Federations of Industry and Employers Associations,
- Farmer's Associations and Chambers of Agriculture
- Trade Unions
- Academies of Science and University and College Associations
    - Baltic University
- Youth and Sports Organisations
- Equality Affairs
- Environmental and Nature Conservation NGOs
    - CCB—Coalition Clean Baltic
    - WWF
    - Greenpeace

The red tape of monitoring programmes

A lot of the research competence available to policy makers has been given the task of performing monitoring. This form of applied research in many cases has dominated the activities of entire university institutions. Creative researchers have been able to introduce innovation into these programmes, in order to test new hypotheses. Routine monitoring, however, is not something that helps the science develop and can in fact hamper creativity. It also can end up alienating the expert from the policy arena, where he/she is needed the most by society.

Monitoring programmes try to provide a basis for trends, that is, certain parameters are on the way up or on the way down. Large-scale changes do not usually occur overnight or in one season unless there they are driven mainly by major shifts in weather (i.e. high precipitation, extreme temperatures, extremes in meteorological phenomena). Trends in ecosystem response are usually slow and can only be observed accurately over long observation periods. Policy systems are not at all equipped to work along such time restrictions. People want to see immediate effects. Monitoring can therefore become a misunderstood activity—a sort of "Catch 22". There is general criticism of "blind" institutionalised, non-adaptive monitoring—that appears to be collecting data for no obvious purpose. It is important that monitoring programmes be creative and as systems-oriented as possible. Especially important, however, is the annual or biannual reporting of trend data. This has to be done in a sufficiently attractive and useful manner that environmental statistics turn out to be an "added value" product that can interest various sectors of society—much like the stock market is for the economic world. Software that examines the trends is usually difficult to translate into simple terms and political decision makers have really no clue as to what is being measured or what the trends really look like. Satellite imagery is

expensive and doesn't answer all the questions at hand. So monitoring can turn out to be self-defeating if we the marine scientists do not develop interesting methods to communicate these results.

GIS and black box computer models

Researchers can make beautiful things like maps and diagrams that attempt to simplify complex data series and aid the reader. These are becoming more and more available. At the same time, a generation of "visual graphics"-oriented scientists has evolved, where information technology and environmental accounting has evolved almost completely empty of the rudiments of natural science. The ISO 14001 standard for environmental accounting within industry has yet to incorporate ecosystem-based targets or quality objectives. For that matter the entire Baltic Sea Action Plan for clean up is essentially free of ecosystem science and is steered entirely by technological criteria. There is much to be done by marine scientists in the area of bringing critical information central into the technological sphere.

Publication process

Publication is the prime method used by scientists to communicate their work. Launching of new concepts through conferences and workshops can, of course, add to this process, but publication is the definitive platform combined with peer review. Publication strategies for a specialist researcher may not at all include policy formulation as a priority. Publishing therefore Baltic science in a refereed international journal in Australia or North America can have its merits. As a result, databases have to be rigorous in order to be able to search and find particular results. The tragedy of professional publication is that because there is so much being produced, there is little time to read and the use the material effectively. Most scientific publications receive only a few citations. What is worse, however, is that very little effort is made to write reviews that take on general themes. It might be useful for Baltic scientists to consider initiating a new review journal dealing with Baltic marine science.

Journalists and politicians are the least informed groups with the most influence. Scientists are the most informed (at least when it comes to specific technical issues) but have little or no political influence. The vehicles available to systematically inform society are many but most scientists are not normally involved in using them. For example outreach can be accomplished by targeting publications and summaries of research results to policy makers. In the case of the Baltic Sea Region, HELCOM and ICES are the most obvious fora to use. HELCOM's committee system with representatives from each country should be able to funnel critical findings to the surface. But there is still an enormous wealth of information and knowledge within the scientific community that has not seeped down into the public-policy arena.

Where is Baltic Science being published today?

Dialog

Dialog is an on-line search system that connects to all major abstract databases that covers published papers in scientific journals. Using the search profile 1980 to 1996 and Baltic Sea, 3323 papers were uncovered from 30 different databases including Aquatic Science Abstracts, BIOSIS, Oceanic Abst, SciSearch, GEOBASE, Toxline, Geoarchive, CAB Abstracts, Pollution Abstracts, Environline, Meteor. & Geoastro. Abs.

LIBRIS

LIBRIS is probably the most common database used by policy-makers, at least in Sweden. A search for the period 1970 to present and the key words Baltic and marine gave only 130 hits in LIBRIS which contains some 5.2 million reports, books and conference proceedings. Changing the search words to Baltic Sea gave 376 hits but these included all aspects of the Baltic including transportation, trade, co-operation, politics, security, health, energy, naval policy, Baltic Europe, economy, technology transfer and education. Of the marine publications listed, they include material from HELCOM (Proceedings series, workshops, etc.), University of Stockholm, BMB (symposium proceedings and special publications), SMHI, ICES, Marine Geological Conferences, Nordic Council of Ministers, Linköping University, Öresund Consortium, SNV, Finnish Department of Environment, Kiel university, Latvia Academy of Sciences, Finnish Institute of Marine Research, Geological Survey of Finland, Karlskrona Conferences, University of Helsinki, French Hydrographic and Oceanographic Service, Gothenburg County, University of Gothenburg, Finnish Geological Service, Tallinn Technical University, OECD, Åbo Academy, University of Sczcecin, SCB, Estonian Geological Institute, Stockholm Contributions in Geology (series), IVL, MFG, Beijer Institute, SLU (Uppsala), Warnemünde, Association of Finnish Local Authorities, Lund University, Tallinn Technical University, Societas Scientarium Fennica. This may be an impressive list but it only covers a very small percentage of the publications available and institutions involved.

This shows that the marine literature on the Baltic Sea is not easily accessible using LIBRIS. Almost all the eastern Baltic publications are not listed and only sporadic or uneven entries are found. There are occasional PhD theses but only a few, conference proceedings, the odd book produced by an independent publisher, a special BMB publication (only some of them are listed, and so on). The literature that the experts are aware of is not accessible. LIBRIS is the most accessible of databases and cheapest to use but does not, unfortunately, serve our purposes at present.

BALTIC marine database

HELCOM's literature database specialising in the Baltic Sea area marine environment is available online via the Swedish EPA library, and includes some 10000 entries going back to 1970. It is also available on the Internet on a commercial server in Finland (http://otatrip.hut.fi/vtt/baltic/intro.html). For the entire database the rate of growth of entries has been impressive with about 360 entries per year on average (Figure 1).
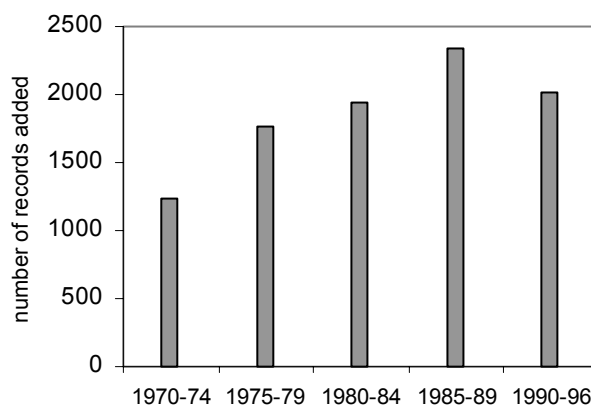
Figure 1 Number of literature entries added to the Baltic Marine Database (http://otatrip.hut.fi/vtt/baltic/intro.html) at 5-year intervals between 1970 and 1996.

Searching for the term Baltic finds 4,173 entries. There are of course entries that are specific to areas such as the Bothnian Sea, Gulf of Finland or Gulf of Riga, etc.

Growth in the Baltic Database with the term Baltic in the text is as follows:

1970−74	320
1975−79	483
1980−84	808
1985−89	1340
1990−96	1055

Sweden and Finland have together produced some 5600 titles. Germany follows with some 1500 titles, followed by Russia and Poland (about 1000 each) and the finally the Baltic States (around 200 in total) (Figure 2). The language of publication has been predominately English but there are high percentages of the published materials only available in one of the Baltic Sea region languages, which restricts international communication (Figure 3).

The HELCOM marine database tends to provide fairly good coverage of the grey literature generated within the region and many of the institutionally generated reports. In the early period (1970−85) not all journals around the world were monitored. The database seems to cover the eastern and western Baltic literature very well including the commercial and academic refereed journals.
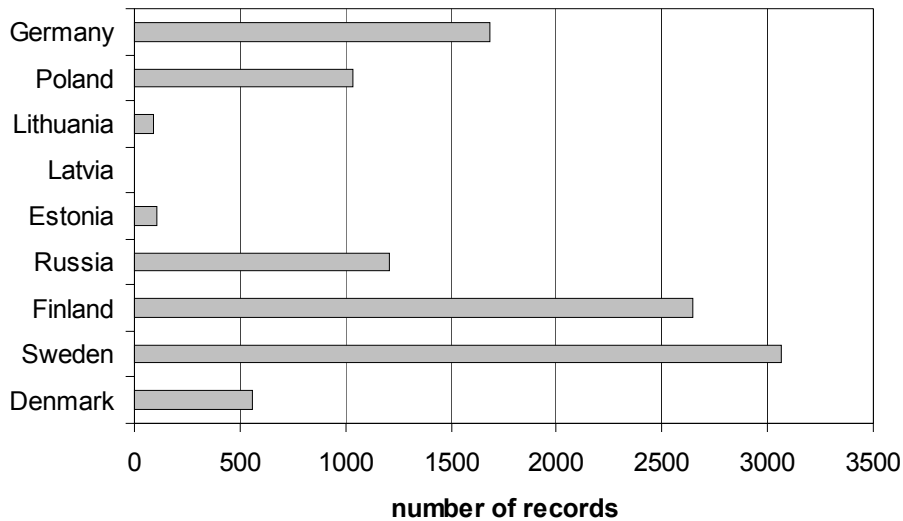
Figure 2 Distribution of records in the Baltic Marine Database by country.between 1980 and 1996

Language and Origin of Records
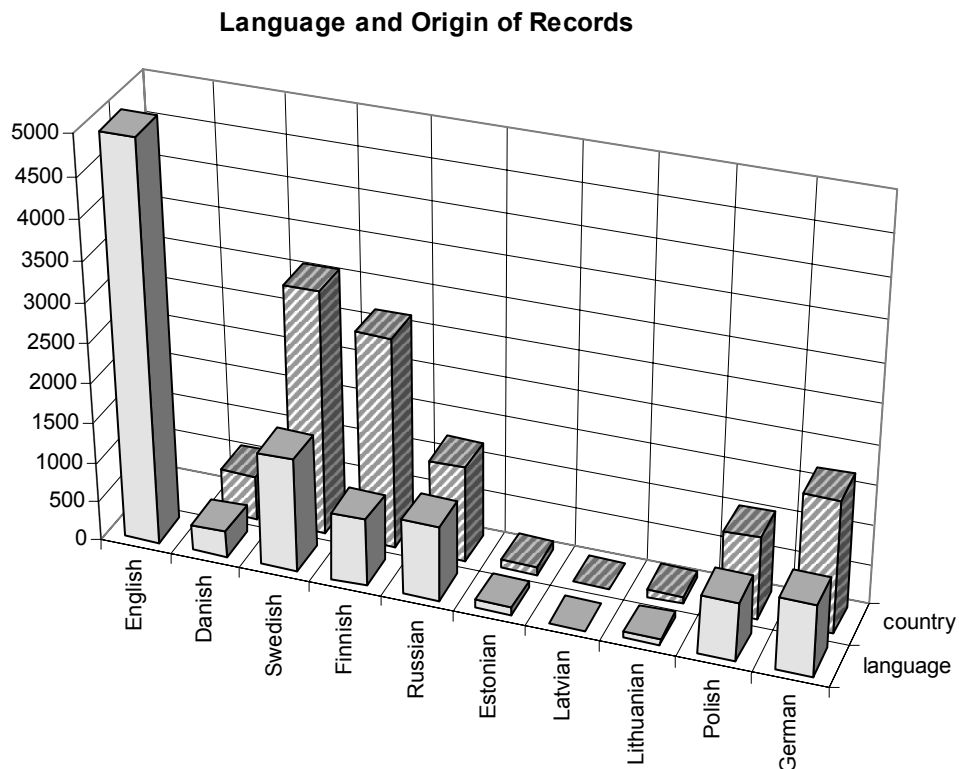
Figure 3 Distribution of language and country origin of records in the Baltic Marine Database. The difference in height of the bars is the number of records written in English by that country

Carl Corporation Database

This commercial database covers some 17,000 scientific journals. The search profile used was: 1990–1996 and the term Baltic Sea. 360 papers were found, in 135 journals; 112 of which deal with marine biology, chemistry, geology, oceanography, etc.

These journals break down as follows:

- **Biology** 51 journals; dominated by AMBIO, Marine Ecology Progress Series, Hydrobiologia, Int Revue der Gesam. Hydrobiologia.
- **Chemistry** 5 journals dominated by Chemosphere and Marine Chemistry
- **Geology** 27 journals dominated by Estuarine, Coastal and Shelf Science and Quarternary International

- **Oceanography** 13 journals dominated by Oceanology and Beitrage zer Meereskunde and Limnology and Oceanography
- **Policy** 16 journals
- **General environmental** 18 journals dominated by Marine Pollution Bulletin and Science of the Total Environment
- **General interest** 6 journals

Role of Media

Media's role in communicating to the public the problems at hand has been plagued with incompetence and a lack of interest to invest in comprehensive journalism. "The Baltic is dying" is all that was heard in the 1980s. It is no longer fashionable to describe the Baltic in these terms since it hasn't died yet and does not appear to be approaching death in any way. Now we hear messages like nothing is being done or very little about the steady improvements actually being made. All in all marine scientists are not properly heard through the media. Some speciality science programmes and science pages cover Baltic marine questions, but the policy assessment linkages are seldom made. Science is considered as a separate media product quite disconnected from the mainstream political news. Such phenomena as blue-green algal blooms, increases in pollution, extremes in ice conditions or mass mortalities of fish due to anoxic conditions can occasionally make headlines only because of the drastic nature of these occurrences.

The problems of being blinded by the Baltic Sea Proper, ignoring the more site-specific coastal zone issues

In an attempt to make generalisations about the Baltic as a whole, or some of the larger gulfs, the coastal zones have been very much ignored and poorly assessed by HELCOM and its designated scientists. Even the national programmes have similar handicaps. The sheer size of the water mass is a distracting phenomenon. As a result, when policy makers, media and the general public say Baltic Sea we don't really know what they mean. Is it the coastal zone areas, where pollution is most obvious? Or is it the pelagic zones, deep holes, etc. Coastal zone management is site-specific in nature and monitoring and research programmes need to be tailor-made. This requires a different approach to problem diagnosis and solution than when dealing with large pelagic areas. Coastal zone management is receiving much attention around the world. Surprisingly, the Baltic Sea is slow in getting the attention it needs in this area.

The controversy of nitrogen limitation arises in this regard. Pelagic oceanographers think it unnecessary to build sewage plants that remove nitrate. Coastal zone biologists beg to differ since nitrate in the coastal zones during the spring causes benthic algal overgrowth (filamentous forms) and planktonic algal blooms. Both groups of scientists are actually correct in their arguments. It is just a matter of temporal and spatial perspective that causes the split in opinion. Policy makers will become very confused if such matters are not clearly explained by such organisations as BMB and CBO.

Conclusions

- there is a large gap between the scientific/technical knowledge base surrounding natural systems making up the Baltic Sea and the governance/policy systems that attempt to manage these resources
- environmental issues are still treated as they were 20 years ago—highly sectored, piecemeal and in the form of confrontation between interest groups
- marine scientists could play a much stronger role in policy development if they were better represented through professional organisations, through systems analysis groups and proper national and international assessments that examine trends on an independent basis
- HELCOM's function is not all-encompassing since it focuses on the marine environment and many of the sources of the environmental and natural resource problems have their origin higher up in the drainage basins
- Future sustainable development within the Baltic Sea Region will depend on how well HELCOM can adapt and enhance its role, to what extent a Baltic 21 can be developed for the Region and to what extent the VASAB 2010 vision initiative can make use of these two capabilities
- Research activities and policy work are highly sectored making it difficult to extract a systems view
- The publication process is somewhat fragmented and there is sometimes difficulty in finding the results of work carried out. The HELCOM Marine Database, however, is a dependable source of literature and is now on the Internet.

- There is a need for comprehensive scientific reviews of published materials generated within the Baltic Region; a suggestion is that Baltic marine scientists initiate a new journal specialising in reviews only

References

AMBIO, 1996. The Gulf of Bothnia Year 1991. Special Report No. 8. 35 p.

Helander, B., 1990. Inventeringar av gråsäl och knubbsäl vid svenska Östersjökusten. Rapport till PMK för verksamhet-såret 1989. Swedish Museum of Natural History.

HELCOM, 1993. The Baltic Sea Joint Comprehensive Environmental Action Programme.

Ministry for Foreign Affairs, Sweden, 1996. Actors Around the Baltic Sea: An Inventory of Infrastructures, Initiatives, Agreements and Actors. Compiled by Carl-Einar Stålvant.

Rosemarin, A., 1996. Development of a Rapid Appraisal System for the Shallow Coastal Zone of the Baltic Sea: Criteria to Set Clean-up Targets and to Evaluate Incremental Environmental Improvements. Proc BMB 14. Pärnu, Estonia.

Rosenberg, R., Lindahl, O., and Blank, H., 1988. Silent Spring in the Sea. Ambio 17: 289–290.

SEI, 1996. Baltic 21: Creating an Agenda 21 for the Baltic Sea Region. Background Report for the Environment Ministers Meeting on Oct 21–22, 1996 in Saltsjöbaden, Sweden.

Swedish Environmental Protection Agency. 1996. The Baltic—A European Sea. Enviro No. 20.

VASAB, 1994. Visions and Strategies around the Baltic Sea 2010. Report to the Third Conference of Ministers for Spatial Planning and Development. Tallinn, Dec 7–8, 1994. 96 p.

Effects of Baltic Sea coastal zone atmospheric peculiarities (during BAEX) on the ^{7}Be concentration in the air

Narciza Spirkauskaite, Klemensas Stelingis, Viktoras Lujanas, Galina Lujaniene, and Tomasz Petelski

Abstract

This paper documents the analysis of the ^{7}Be atmospheric concentrations, measured in the Baltic Sea coastal zone, when studying their time variations depending on weather conditions. It was unexpectedly found that an increase in ^{7}Be concentrations was related to air masses transported from the Atlantic Ocean or over the Baltic Sea, in spite of the washout processes taking place near the water surface.

Introduction

In the frame of Baltic Aerosol Experiment (BAEX), cosmogenic ^{7}Be was used as a tracer in the study of the processes of atmospheric pollutants' transfer through the air-sea interface in the southern part of the Baltic Sea coastal zone. This involved an analysis of the ^{7}Be atmospheric concentrations, measured in the Baltic Sea coastal zone, when studying their time variations depending on weather conditions. In spite of the presence of large number of investigations studying ^{7}Be concentration variations depending on the latitude, seasons, weather conditions, sun activity, etc. (Lujanas, 1979; Young and Sieker, 1974; Wallbrink and Murray, 1994; Bettoli *et al.*, 1995), the question on the ^{7}Be concentration over the sea is still open.

Following one of the main BAEX aims—to answer the question of whether processes of atmospheric self-cleaning from the pollutants taking place in the coastal zone may be compared with the open sea ones, it had to be cleared up whether the factors affecting the concentration variations of ^{7}Be (as a tracer of constant rate of production in the atmosphere over the Baltic sea latitude) in the coastal zone are the same as those on the continent. It is known (Lujanas, 1979) that ^{7}Be concentrations at the same latitudes are higher in air masses of continental origin due to the existence of the secondary ^{7}Be component (resuspension of the nuclide from the earth's surface with dust). ^{7}Be concentrations in the air decrease during precipitation owing to the washout of the carriers of this nuclide (Lujanas *et al.*, 1993). A significant increase in the ^{7}Be concentration in the air takes place in the stratospheric air having entered the troposphere through the tropopauze breaks (Lujanas, 1979). During BAEX-3 in the Baltic Sea southern region (12–29 September, 1995) baric situations promoting such tropopauze penetrations were not observed.

The coastal zone is distinguished for specific peculiarity—the transfer of pollutants, including radionuclides from sea to land in sea sprays (McKay *et al.*, 1994). Investigations of these processes have showed that increased concentrations of some artificial radionuclides were observed in vegetation within 1000 m of the seashore zone (Nelis *et al.*, 1994).

Experiment

Daily ^{7}Be concentrations were measured during BAEX-3 (12–29 September, 1995) in Lubiatowo (seashore, Poland), in Preila station (seashore, Lithuania) and in Vilnius (continent, Lithuania, –350 km from the Baltic Sea).

Atmospheric aerosol samples were collected on Petrianow type filters FPP-15-1.7. The productivity of air-pumps was equal to 700 m^3·h^{-1} (in Lubiatowo and in Preila). In Vilnius equipment with 2000 m^3·h^{-1} productivity was used. The measurements of the ^{7}Be carrier sizes were made using a 6-stage SIERRA 230 impactor.

To determine the air mass origin (continental or marine), short-lived radon daughter products were used as tracers. For the evaluation of the concentration of the short-lived radon daughter products in the air, a small air pump (flow rate – 2.83 m^3·h^{-1}) with the Petrianow filters of RSP type (diameter 2.4 cm) and an alpha-radiometer RV-4 were used. ^{7}Be concentrations of the aerosol samples were measured by a gamma-spectrometer with the Ge(Li) semiconductor detector.

Results and discussion

Measurement results show that ^{7}Be concentrations in the air during the experiment changed in the same manner and ranged from $0.86 \cdot 10^{-3}$ to $7.2 \cdot 10^{-3}$ Bq·m^{-3} in Lubiatowo, from $0.76 \cdot 10^{-3}$ to $6.43 \cdot 10^{-3}$ Bq·m^{-3} in Preila and from $2.1 \cdot 10^{-3}$ to $6.02 \cdot 10^{-3}$ Bq·m^{-3} at the continental site (Vilnius) (Table 1). The mean ^{7}Be concentrations were found to be 4.07 mBq·m^{-3}, 4.06 mBq·m^{-3} and 4.08 mBq·m^{-3}, respectively.

Minimum ^{7}Be concentrations were measured when it rained (^{7}Be carriers were washed out from the ground atmospheric layer) (15, 23, 28, 29 September, Table 1).

Lubiatowo				Preila			Vilnius		
Date, Sept 1995	Weather	Wind dir.	mBq.m^{-3}	Weather	Wind dir.	mBq.m^{-3}	Date, Sept 1995	Wind dir.	mBq.m^{-3}
11	-	-	-	rain	SW	2.23	8–11	W	3.11
12	calm sea	S	1.92	rain	W	2.38	12–13	NE	3.15
13	calm sea	SE	2.69	rain	NE	1.79			
14	calm sea	SE	3.69	fog	E	2.71	14–15	E	2.74
15	rain	NW	1.16	rain	E	0.76			
16	rain	E	0.86	rain	E	3.81	16–18	E	6.02
17	white caps on sea	E	5.08	white caps on sea	E	4.00			
18	calm sea	SE	2.94	white caps on sea	E	5.88			
19	calm sea	SE	5.25	small waves	E	6.28	19–20	W	4.12
20	calm sea	E	6.80	calm sea	W	4.88			
21	white caps on sea	NE	7.20	white caps on sea	NE	5.01	21–22	N	4.05
22	white caps on sea	NW	5.70	white caps on sea	N	6.43			
23	small waves	W	3.63	rain	W	3.22	23–25	S	4.67
24	calm sea	SW	3.60	small waves	SW	3.24			
25	calm sea	SW	3.91	small waves	S	4.21			
26	white caps on sea	W	5.93	rain	SW	5.41	26–27	SW	3.82
27	white caps on sea	W	4.74	rain	SW	4.95			
28	storm, rain	NW	1.75	storm, rain	SW	1.76	29–29	SW	2.10
29	rain, storm	NW	1.75	rain, storm	SW	2.62			

Table 1 Concentrations of ^{7}Be in air samples during BAEX-3

Analysis of the ^{7}Be air concentration course during BAEX-3 shows that contrary to Vilnius data a significant increase in ^{7}Be concentration in the air was measured on 19–22 and 26–27 September in Lubiatowo as well as in Preila (Figure 1). These values of ^{7}Be concentrations during BAEX-3 (7.2; 6.43; 5.93; 5.41 mBq·m^{-3}) were the largest (Table 1) when the whole sea surface was covered with white caps producing intensive flux of spray droplets to the atmosphere.
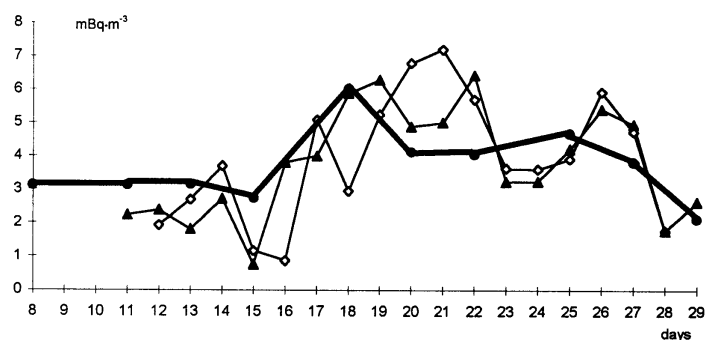
Figure 1 Distribution of the ^{7}Be concentration in the air in Lubiatowo (◊), in Preila (Δ) and in Vilnius (●) during BAEX-3 (September 1995)

Measurements of the ^{7}Be carriers' activity size distribution, carried out with a 6-stage Sierra impactor in Lubiatowo during 15–21 September on the beach, show that a large percent of coarse particles in this period in the air was measured. ^{7}Be carriers in air masses of stratospheric origin over the continent are as a rule <0.4 μm in size.

^{7}Be enrichment factors of sea foam samples, collected during 17–24 September, reached a value of $-1.2 \cdot 10^{-3}$. It is known that with increased wind velocity, the surf zone foam is blown out to the beach, and may also be resuspended.

A decrease in the α-activity of short-lived radon daughter products in Lubiatowo on 21 and 26 September, when [7]Be concentrations in the air reached a maximum, showed that marine air advection had taken place in this region (Figure 2). This is also confirmed by the air masses transport trajectories to Lubiatowo during BAEX-3 (Figure 3).
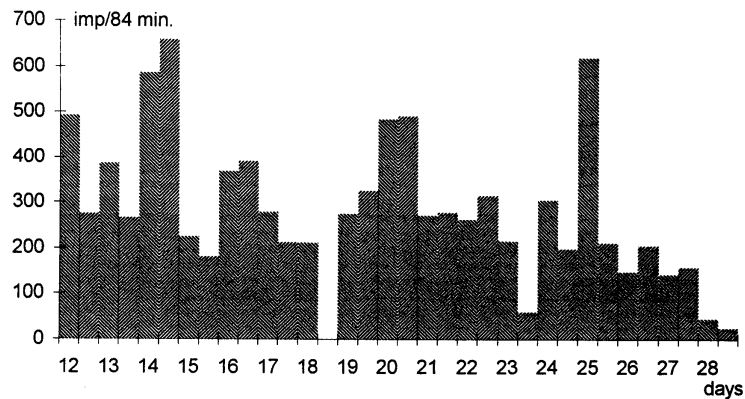
Figure 2 Distribution of the α-activity of short-lived radon daughter products in the air in Lubiatowo during BAEX-3 (September 1995)
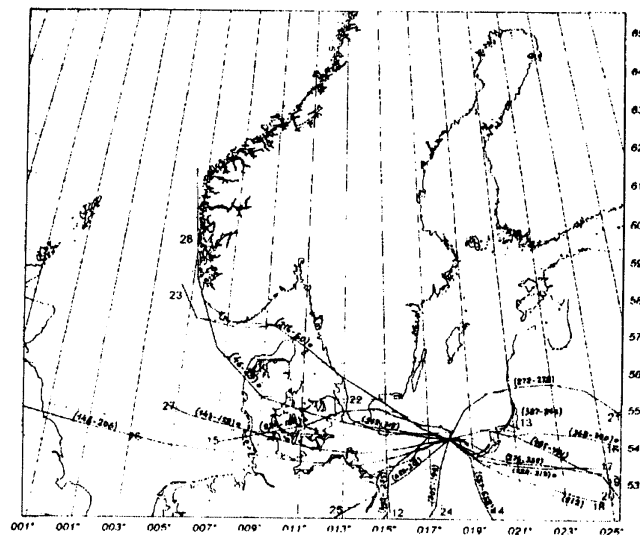
Figure 3 Diagram showing air mass transfer trajectories during BAEX-3 (12–28 September, 1995). Numbers on the curves show the date of air mass arrival at Lubiatowo along the track covered in 24 hours. Numbers in brackets show the α-activity of the short-lived radon daughter products (imp/84 min)

Analysis of the synoptic charts of 21 and 26 September showed that weather conditions in the southern Baltic Sea region were caused by cyclonic circulation (Figure 4). However, any [7]Be concentration increase during the air masses' transport in the same low pressure field systems was not observed in Vilnius. At that time [7]Be concentrations in the air in the coastal zone in Lubiatowo as well as in Preila at comparatively strong onshore or along-shore winds (5–7 m·s^{-1}) were twice as high as those in Vilnius (continent) (Table 1).
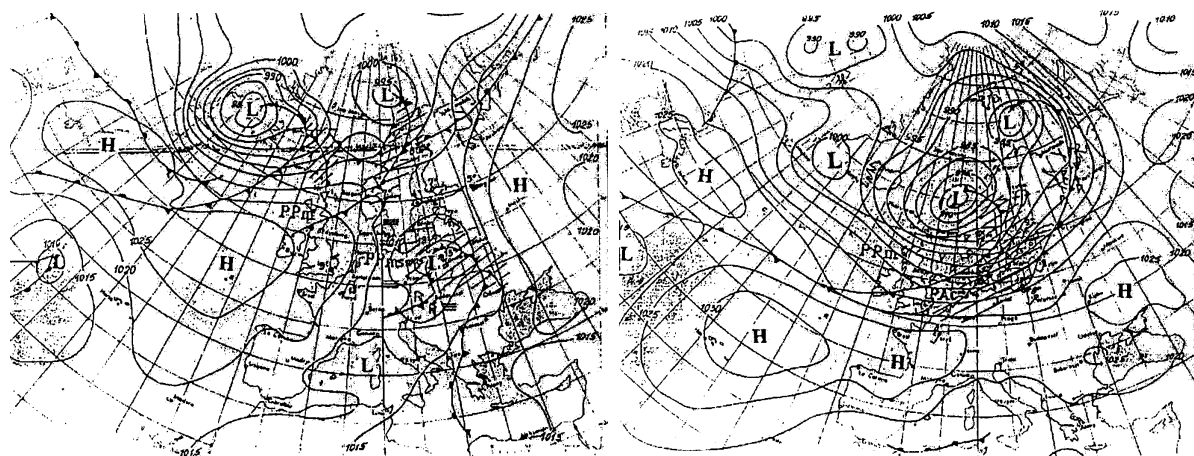
Figure 4 Synoptic charts from 00h 21.09.95 (left) and 00h 26.09.95 (right)

Conclusions

An increase in [7]Be concentrations in the air in the Baltic Sea coastal zone in some cases during BAEX-3, in spite of the dominating along seashore and offshore wind directions, shows that, when studying processes at the air-sea interface in the coastal zone, [7]Be secondary atmospheric component must be taken into account.

Acknowledgements

References

Bettoli, M.G., Cantelli, L., Degetto, S., Tositti, L., Tubertini, O. and Walcher, S., 1995. Preliminary investigations of [7]Be as a tracer in the study of environmental processes. J. of Radioanalytical and Nuclear Chemistry, 190, 1, 137−147.

Lujanas, V., 1979. Cosmogenic radionuclides in the atmosphere. Mokslas Publishers, Vilnius, 192.

Lujaniene, G., Lujanas, V., Spirkauskaite, N., Tarasiuk, N. and Grenda, S., 1993. Physico-chemical properties of artificial and cosmogenic radionuclides in the environment. J. Ecol. Chern., 2−3, 139−144.

McKay, W.A., Garland, J.A., Livesley, D., Halliwell, C.M. and Walker, M.I., 1994. The characteristics of the shore-line sea spray aerosol and the landward transfer of radionuclides discharged to coastal sea water. Atmospheric Environment, 28, 20, 3299−3309.

Nelis, P.M., Branford, D. and Unsworth, M.H., 1994. A model of the transfer of radioactivity from sea to land in sea spray. Atmospheric Environment, 28, 20, 1213−1223.

Wallbrink, P.J. and Murray, A.S., 1994. Fallout of [7]Be in South Eastern Australia. J. Environ. Radioactivity, 25, 213−228.

Young, J.A. and Silken, W.B., 1974. The determination of air-sea exchange and oceanic mixing rates using [7]Be during the Bomex Experiment. J. of Geophysical Research, 79, 30, 4481−4489.

Water and nutrient exchange through the Suur Strait (Väinameri) in 1993−1995

Ülo Suursaar, Villu Astok, Tiit Kullas, and Mikk Ostmann

Introduction and the study area

This paper is mainly focused on the role of the Suur Strait in the water and nutrient exchange between the Gulf of Riga and the Baltic Proper. In addition, the Gulf of Riga with its two outlets is an interesting and quite complex system for studying the interaction processes between the open sea and coastal areas. The Gulf of Riga has an area of $16\,395\,km^2$, and a volume of $424\,km^3$. Ecologically the Gulf of Riga is under the influence of heavily loaded river water inflow averaging $31\,km^3$ a year. Its nutrient conditions therefore differ substantially from those of the Baltic Proper and feature especially high nitrogen content and hypothetical phosphorus-limiting conditions for phytoplankton. The influence of the heavily polluted Gulf of Riga on the water quality of the Baltic Proper depends on the efficiency of nutrient sedimentation within the Gulf and on the intensity of the water exchange processes via the straits.

The Irben Strait is one of the two straits connecting the Gulf of Riga to the Baltic Proper. It has a width of $27\,km$, a sill depth of about $21\,m$ and a cross-sectional area of $0.37\,km^2$. For a long time this strait has been considered to be the main and the only connection. Another outlet, the Väinameri (Figure 1) first proceeds through the Suur Strait, which is the narrowest ($4−5\,km$) area in this system. The area of the cross-section is $0.04\,km^2$. The maximum depth of the strait is $20\,m$, but northwards the strait becomes wider and shallower. The minimum sill depth of the whole system is only $5\,m$ on the southern side of the Väinameri basin. The next strait on the northern border of the Väinameri is the Hari Kurk Strait, having a width of $8−10\,km$ and a sill depth of about $10\,m$. The Väinameri has an area of $2243\,km^2$ and a volume of $10.6\,km^3$. It could really be treated as a separate sub-basin of the Baltic (analogous to the Archipelago Sea). If not, it should rather be regarded more as a part of the Gulf of Riga than of the Baltic Proper.
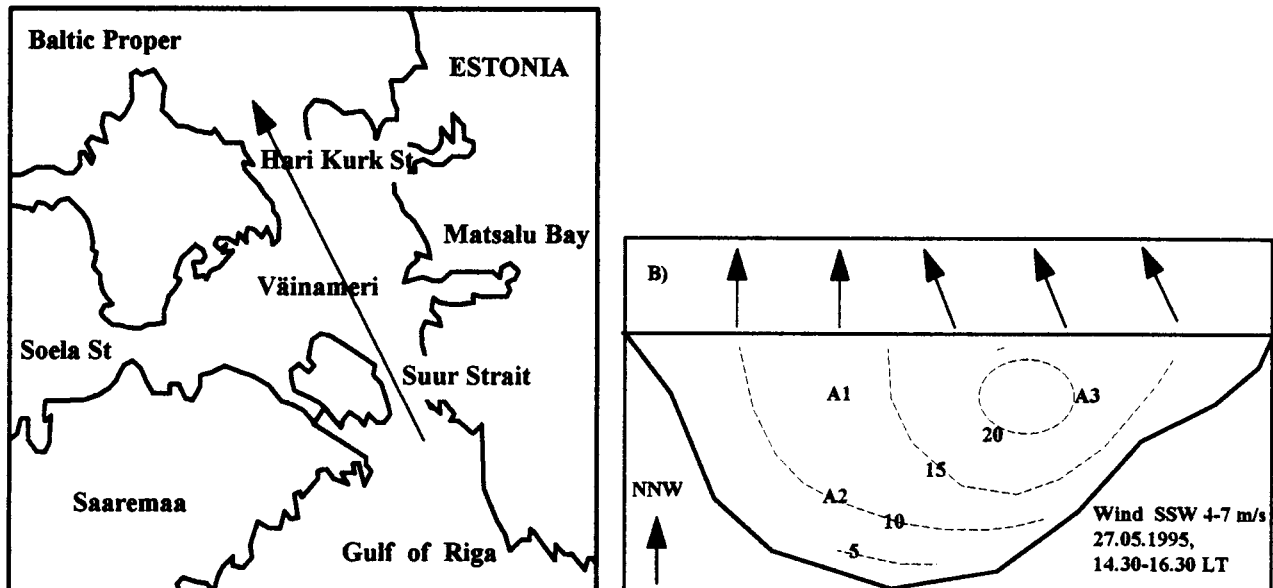
Figure 1 The Väinameri area and the cross-section of the Suur Strait; current velocities in $cm\,s^{-1}$. AI, A2 and A3 mark the positions of the mooring stations.

Measurements

Extensive investigations were carried out within the Gulf of Riga Project in $1993−96$. The field-work in the Väinameri area was done during ten expeditions lasting from one to four weeks each. Two recording current meters (Aanderaa RCM-7 and RCM-4) were used, providing data on the directions and velocities of currents as well as water temperatures and salinities. Additional current measurements were carried out between the expeditions as well. The upper instrument

was moored at a depth of 3–6 m in the Suur Strait and the lower at 10–13 m. The direct current measurements cover altogether about 470 days. The spatial structure of the currents was investigated by salinity and temperature (CTD) and velocity (ACM) profiles carried out in spring and autumn of 1993, and by measurements with Hammer's pendulum current meters (HPCM) carried out in the Hari Kurk Strait and the Suur Strait in 1995 and 1996 (e.g. Figure 1B).

We have tried to measure currents, water temperatures and salinities simultaneously with nutrient measurements. The water samples for analysing nutrient concentrations (P_{tot} and N_{tot}) were collected on board R/V "Junga" (expeditions I, II, IV), "Lest" (V), "Kiir" (VII, VIII), from ice (III, IX) and by boat (VI). The samples were usually taken at two layers (0–1 m and 15–16 m), mostly three times a day during expeditions or along certain spatial sections. Components of nutrients (P-PO$_4$, N-NO$_2$, N-NO$_3$, N-NH$_4$) were measured less frequently. Chemical analyses were performed mostly by the laboratory of the Environmental Engineering Institute, Tallinn Technical University. Altogether about 2300 analyses of nutrients were made in 1993–96. In addition, regular vertical soundings of O_2 and temperature using a Marvet Fluid analyser and Secchi measurements of water transparency were carried out. A more comprehensive overview of measurements can be found in the reports (e.g. Suursaar and Astok, 1996).

Results and discussion

Variability of currents. thermohaline regime and nutrients

Currents seem to be the crucial factor for the state of the Väinameri since the front dividing the quite different water masses (the Gulf of Riga estuarine-type and the Baltic Sea marine-type) happens to be located somewhere in the Väinameri and pulsating north- or southwards depending on prevailing winds and currents. For example, though seasonality is the main factor influencing water temperatures, also advective variations up to 6–8°C within less than 24 hours were found, especially in early summer when the shallow Väinameri becomes warmer than the larger and deeper neighbouring basins. Also the salinity regime in the Suur Strait is very variable since it is affected by two water masses alternating from time to time. The salinity differences through the front are usually 1–1.5 PSU. The average gradients were estimated as 0.02–0.05 PSU km^{-1}. Also, because of its shallowness and clearly defined morphometry, the Väinameri acts as a certain buffer-zone, where mixing processes of the different water masses take place. Therefore the frontal zone may appear somewhat diffused in some cases.

Spatially the currents have a relatively simple and mostly unidirectional structure in the Suur Strait. It was therefore possible to find simple empirical relationships between the flow volume and the mean current velocity for different positions of the mooring stations. Two directions of currents clearly dominated (130–160° and 340–350°), determined by the bottom topography of this relatively narrow strait. The variance of the axial (NNW–SSE) component of the velocity vector fluctuations comprises about 92–97% of the total variance, leaving only a small share for the perpendicular component. Temporal variations are far more interesting. The dominant feature of the temporal variability of currents in the Suur Strait is the prevalence of motions induced by atmospheric synoptic activities over the diurnal, semi-diurnal and other short-term components. The relatively significant peak above the background spectra at 12.5 (± 0.1–0.3) h, which could be the M_2 (lunar semi-diurnal) tide, still has, in absolute terms, a smaller amplitude than the motions with the periods of 24–30 h and 3–4 days. The periodicity of 24 h is the most prominent feature in the Irben Strait (e.g. Петров, 1979) and it seems to be also the period of the eigenoscillations of the Gulf of Riga in the system with two straits (see also Otsmann *et al.*, 1996).

The seasonal and interannual variability could also be substantial, depending on the variability of large-scale atmospheric circulation types above the North Atlantic and ice conditions in the Gulf. According to our investigations the mean velocity module in the Suur Strait was about 25 cm s^{-1} in 1993–95. According to Petrov (Петров, 1979) the mean velocity in the Irben Strait is about 6 cm s^{-1}. Thus, the smallness of the Suur Strait compared to the Irben Strait is compensated by higher velocities. The maximum velocities measured up to now for the Suur Strait (103 cm s^{-1} in the upper layer) were presented by Mey (1922). The maximum values measured by us were 100 cm s^{-1} for both the inflowing (at 12 m on 1 October 1995) and outflowing currents (at 12 m on January, 23, 1995; Wind velocities were up to 27 m s^{-1} at Viirelaid). As these values were obtained in a relatively deep part of the strait, the real maximum values in the surface could be estimated as 1.3 to 1.5 m s^{-1}.

The differences in chemical properties of the above mentioned water masses acting in the Väinameri are even more evident. It is a well known fact that the trophic status in the Gulf of Riga is considerably higher compared to the Baltic Proper and even in the Väinameri. While the long-term average concentrations of phosphates in the Gulf of Riga are about 0.4–0.8 μM in early winters and the typical values for nitrates are about 10–20 μM, the corresponding values in the Baltic Proper and in the entrance section of the Gulf of Finland are about 0.3–0.6 μM PO$_4$ and only 4–10 μM NO$_3$. The

corresponding P_{tot} content is roughly 1–1.5 vs 0.7–1µM and 30–50 vs 15–30µM for N_{tot} (e.g. Suursaar, 1995). Average values obtained during our expeditions can be seen in Figure 2.
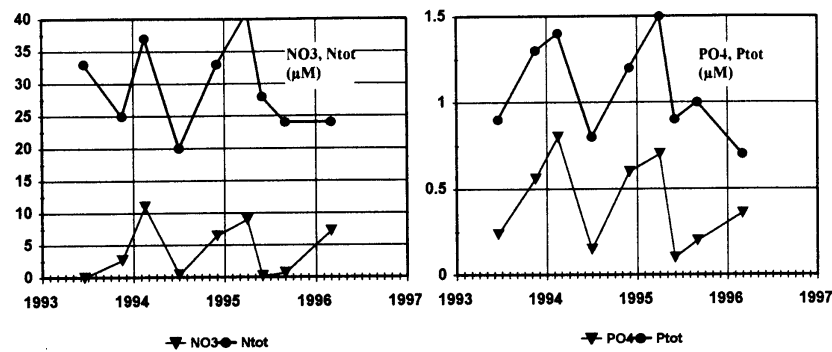
Figure 2 Long-term variations in average values of N_{tot}, NO_3, PO_4 and P_{tot} content during the expeditions in 1993–1996.

It was found that a connection between the nitrogen content and the currents can often be followed in the Suur Strait area, especially when the flow has been long-standing (Figure 3A, B). However, the dependence of the phosphorus content on the currents is rather weak. The explanation could be that the gradients in the phosphorus values between the Gulf of Riga and the Baltic Proper are not as strong as those in nitrogen. Moreover, some local effects tend to overshadow such variations. For example, a strong release of phosphorus compounds with the suspended material occurs in the Suur Strait area during storms (e.g. Figure 3C, D). A simultaneous decrease in water transparency after each storm event could be noticed. A strong relationship ($R=-0.81$) between the measured transparency and corresponding phosphorus values was found.
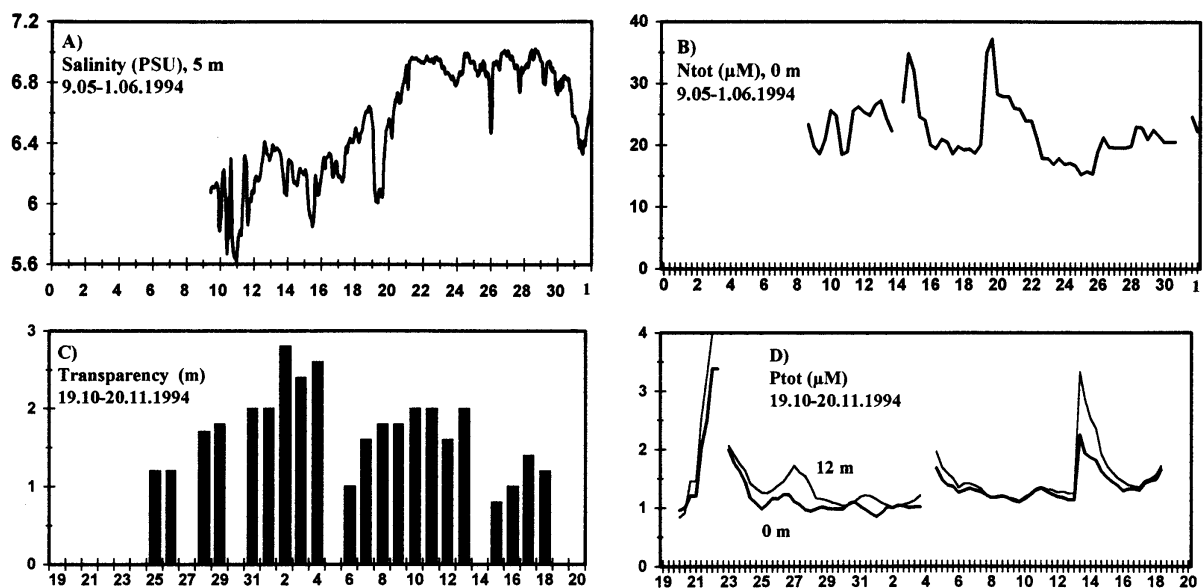
Figure 3 Temporal variations in salinity (A) and total nitrogen content (B) on 09.05–01.06.1994. Temporal variations in water transparency (C) and total phosphorus content (D) on 19.10–20.11.1994.

The role of the Suur Strait in the water and nutrient exchange between the Gulf of Riga and the Baltic Proper

It was quite easy to convert the velocities in the Suur Strait into volume flows. However, problems arise in the case of the second strait and also at a conceptual level. It is easy to see that the different methods for obtaining the water exchange estimates—direct measurements of currents, flow estimations by the volume changes inside the basin and by retaining the volume and salt balances, density gradients, frontal positions, etc.—and the different time-scales for averaging represent somewhat different aspects of the water exchange processes and produce quite different estimates. Thus for the Irben Strait it has been found several times in the past that the direct measurements could not be applicable, because the

strait is relatively wide and two-layer-two-directional flow regime is quite frequent. Therefore, it was decided that the salt-budget (also Knudsen) method or the volume-difference methods could be the best choices.

Unfortunately the other outlet, the narrow-seeming Suur Strait, was neglected. However it is now evident that these flows in the Suur Strait are too remarkable to be neglected. Moreover, it was found that the water exchange processes of the whole Gulf take place due to the existence of two straits: the straits "work together" (Otsmann *et al.*, 1996).

We start with the Suur Strait, not because the strait is "better", just because our information on that Strait is more extensive. Summing up the measured individual flows may lead to almost correct averages provided the number of direct measurements is very high. Such calculations in our case yield in total 165km^3 of inflows and 189km^3 for outflows (Q_{out}) per year, and the annual net exchange (Q_{net}) will be -20km^3. Mardiste (Мардисте, 1975) had about 100, -150 and -50 kmyr^{-1}, respectively. Figure 4 presents the evolution of the estimates according to the length of the measured series. The total extension of measurements is quite big to stabilise (convergement) results in the vicinity of certain "true" values.
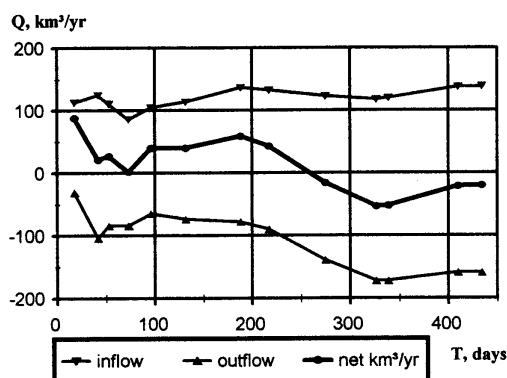
Figure 4 Evolution of the estimates of total in- and outflows and net exchanges depending on the lengthening of the direct measurements series in 1993–95

Evidently these Q_{in} and Q_{out} values describe all the volumes participating in the water exchange, and therefore also a large extent of the to-and-fro movements of the same water, which actually may not be exchanged. While Q_{net} describes the lower boundary of the water exchange, Q_{in} and Q_{out} represent the upper boundary for water exchange estimates, in all aspects and whatever method applied. The "real", or let us say, "effective" flows should be something between Q_{net} and Q_{in} or Q_{out}. They could be calculated simply as the integral (or cumulative) water transport. Such cumulative transport curves are presented in Figure 5. We need to decide which kind of change in directions to consider as relevant. Fortunately it can be seen that even quite typical periods of oscillations around 3–4 days and below (which usually produce flows less than 5km^3) are smoothed down. Figure 5 indicates that the flows in different months tend to group on a seasonal basis. Summer (Figure 5A) mostly displays the inflows (ranging from -2 to $+13 \text{km}^3$ in a month), winter (Figure 5B) displays strong outflows (from $+2$ to -26km^3 per month) and spring and autumn are certain transition periods when both the inflows and outflows may occur ($\pm 8 \text{km}^3$). In winter the water exchange depends strongly on the existence if the ice-cover in the northern part of the Gulf of Riga. We have experiences with both mild winters (such as 1994/95) and with severe winters (1993/94 and 1995/96).
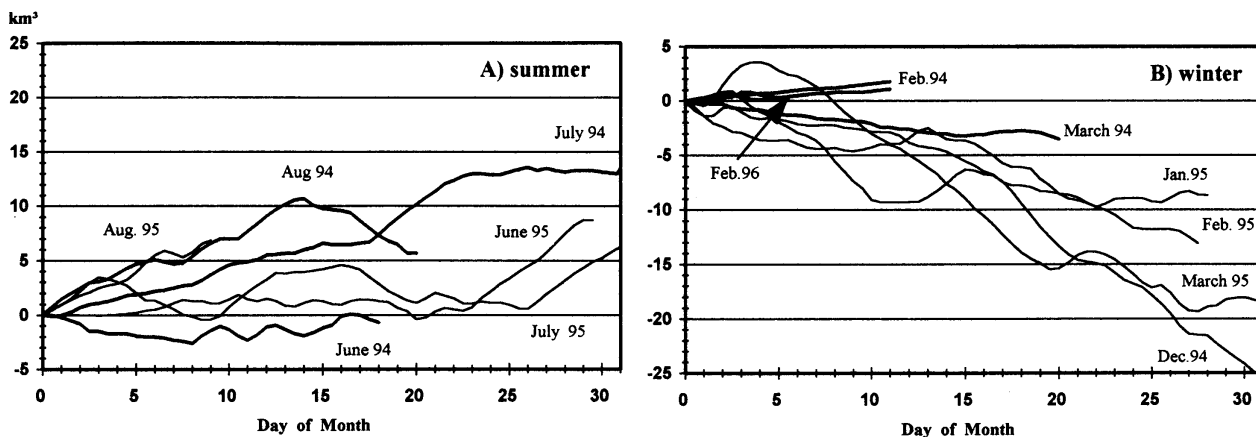
Figure 5 Integral volume transports grouped by seasons and months.

When we arrange all the curves (some of them depicted in Figure 5) in consecutive order with the actual gaps between the measurements, we obtain one of the curves ("measured") presented in Figure 6. (Again, the dominant seasonal pattern is very clear). By filling the gaps from Oct. 1993 to Oct. 1995 we get an estimation of a continuous two-year period (the other curve, "measured/estimated") representing the years with both cold and mild winters. The fill-up was made based on the wind-coefficient (if the wind data were available) or on the similarity of the curves presented in Figure 5. In future the gaps will be covered using the water exchange model (Otsmann *et al.*, 1996).
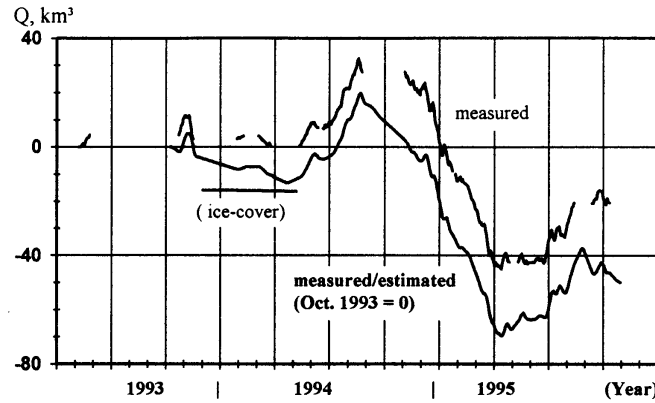
Figure 6 Cumulative volume transport in the Suur Strait in 1993–95. The gaps in measurements are filled to obtain a continuous measured/estimated curve.

We got the "effective" flows in the Suur Strait for two "seasons" or "half-years". Now, from also knowing the river inflows, we can easily find the resultant flows in the Irben Strait. The problem is dividing these resultant flows between simultaneous in- and outflowing components. From the work by Berzhins *et al.* (1994) we obtained the water exchange estimates in the "cold" and "warm" half-years for the whole Gulf of Riga (attributed to one anonymous strait). They were calculated by the modified Knudsen method on the basis of salinity and water level data obtained in Latvia. Adding the data we just got for the Suur Strait we obtain: The inflow in the cold half-year averaged 53 km^3 (all through the Irben Strait) and for outflow –80 km^3 (–45 km^3 via the Suur Strait and –35 km^3 via the Irben Strait). The average river inflow during the cold half-year was 22 km^3 and the volume change –5 km^3. The average inflows during the warm half-years were 59 km^3 (32 km^3 for the Suur strait and 27 km^3 for the Irben Strait) and outflows –68 km^3 (–15 and –53 km^3 respectively). In summer river inflow is 14 km^3 and the volume changes about +5 km^3 (Figure 7).
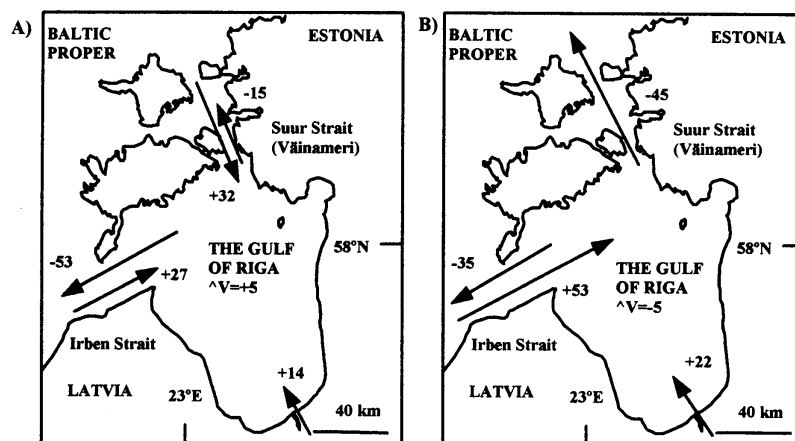
Figure 7 Sketch of the water exchange in "summer" (A: May–October) and in "winter" (B: November–April). The flows and the volume differences ($^\wedge$V) in km^3 for the corresponding half-years.

Discussing these results we would like to stress that they are really sketches in a quantitative meaning, but as a principle they should be quite representative. Comparing our results with the findings by Petrov (Петров, 1979) and Pastors (Пасторс, 1963) we notice that the estimates by Petrov are about twice as large (about 320 km^3 both for inflows and outflows in the Irben Strait). Pastors (Пасторс 1963) gave 183 km^3 for inflow and 215 km^3 for outflow (not shared between the straits). The study by Petrov has usually been taken as a prestigious source for other studies. We explain the overestimation of volume flows presented by Petrov by his choices of typical salinities in filling the salt-budget

equations. Namely, filling in the balance-equations he used the typical salinities of inflows and outflows (having considerably smaller differences due to mixing processes in the transition-areas of the straits) against the average salinity of the Gulf. Since the difference in salinities he used was only about 0.5 PSU, we realise that in order to keep the salt balance, such water masses must be exchanged in 2 times larger volumes than in the case where the difference is 1 PSU, for example. The water exchange estimates by Petrov also represent the backflows in addition to "pure" exchange in the transition zones of straits.

In our case, the share of the Suur Strait in "effective" flows could be quantified at about 32%, the share of the Irben Strait about 57%, leaving about 11% for the rivers. (neglecting precipitation and evaporation, which are equally around $9 \mathrm{km}^3$ a year). Assuming that the inflowing currents carry waters with concentrations of $0.8 \mu\mathrm{M}$ P_{tot} and $20 \mu\mathrm{M}$ N_{tot}, and outflowing $1.2 \mu\mathrm{M}$ P_{tot} and $40 \mu\mathrm{M}$ N_{tot} we obtain the nutrient fluxes through the straits as follows: The annual loss of phosphorus is $2500-2800 \mathrm{t}$, and $49000-54000 \mathrm{t}$ for nitrogen. The estimates of annual outflowing fluxes of P_{tot} ($2700 \mathrm{t}$) by Yurkovskis *et al.* (1993) are surprisingly close to our results. Unfortunately Yurkovskis *et al.* (1993) has no estimates for N_{tot}, but fluxes of inorganic nitrogen are presented at about $-22000 \mathrm{t}$. The estimates close to ours could be obtained if the proportion of inorganic nitrogen from the total nitrogen were taken as 30%. Yurkovskis *et al.* (1993) argue that the major proportion of the (inorganic) nitrogen load entering the Gulf of Riga (about $100000 \mathrm{t}$ per year) is deposited in the bottom sediments and only 25% is exported via the straits, while the phosphorus load ($2800 \mathrm{t}$ per year) is exported almost entirely. However, it could also be argued that both N and P are exported proportionally (about $15-20\%$) to their pools in the Gulf. Still, nitrogen appears in excess (the N:P molar ratio in the Gulf is well over the Redfield's 16:1 ratio) and the gradients between the open Baltic and the Gulf are much stronger in nitrogen contents than in the case of phosphorus. Therefore, the water exchange processes in the straits ventilate the Gulf of Riga especially in relation to excessive nitrogen amounts.

We can speculate about one more effect: The absence of ice in winters 1988/89, 1989/90, 1991/92, 1992/93 and 1994/95 could be a remarkable cause for the negative nutrient trends reported for the Gulf of Riga in the last $5-10$ years. (Measurements made by us for only $3-4$ years display these negative trends as well—see Figure 7). The outflows during autumn and ice-free winter could be about twice as strong as in cold winters, roughly $-50...-80$ vs $-30...-40 \mathrm{km}^3$, which makes some $1000-1500$ extra outflowing tons of phosphorus and $10000-20000$ tons of nitrogen. That is doubtlessly a remarkable proportion compared to the total annual load to the Gulf (about $100000 \mathrm{t}$ of nitrogen and $3000 \mathrm{t}$ of phosphorus according to Andrushaitis *et al.*, 1995). It is also evident now, that the above mentioned nutrient amounts driven by currents are considerably bigger than the local pollution load entering the Haapsalu and Matsalu Bay (in total roughly about $70-100 \mathrm{t}$ of P_{tot} and $2000-3000 \mathrm{t}$ of N_{tot} annually). The amounts entering the Väinameri from these bays are even smaller due to nutrient sedimentation processes within these bays. Thus, local pollution from these much discussed bays has only a very limited effect on the state of the Väinameri.

Conclusions

1. The mechanisms controlling the hydrophysical and nutrient regime in the Väinameri could be listed as: normal seasonality; pulsations of the frontal zone and alternating of the water masses of different types; storm events causing strong turbulent mixing and catching up the suspended material from bottom sediments in the shallow waters; the negative trend caused by increased water exchange and decreased pollution load; the local pollution load from the Matsalu and Haapsalu Bays. Due to strong variability of currents and hydrochemical situation, the Väinameri is not suitable for (low-frequency) water quality monitoring.

2. The present study gives the estimates of the water exchange in the Suur Strait as follows: total inflows to the Gulf of Riga $120-140 \mathrm{km}^3$ per year; total outflows $150-170 \mathrm{km}^3$ per year, the net exchange about $-20-30 \mathrm{km}^3$ per year and $80-100 \mathrm{km}^3$ per year for integral ("effective") flows. Inflows of saline water usually take place in warm seasons and outflows in cold seasons. Maximum velocities in the Suur Strait could be estimated as $1-1.5 \mathrm{ms}^{-1}$, the average values being about $0.25 \mathrm{ms}^{-1}$.

3. The share of the Suur Strait in the water budget of the Gulf of Riga is about 32%, the Irben Strait has about 57% and the rivers about 11% (neglecting precipitation and evaporation). The different results by different authors exploit the different aspects of the water exchange. Our estimates for the water exchange in the Irben Strait are about two times lower than those presented by Petrov. We think that the results by Petrov include in addition to "pure" exchange also the backflows in the transition zones of straits. It might have been the result of the fact that the salt-budget method is very sensitive to choosing the "right" salinities, and to averagings.

4. The annual nutrient loss due to the water exchange through the straits is about $2500-2800\,t$ of P_{tot} and $49000-54000\,t$ of N_{tot}, which are $1.2-2$ times lower than the loads entering the Gulf. The improvement in the ecological state of the Gulf of Riga during the last $5-6$ years could partly be explained by successive ice-free winters (1988/89, 1989/90, 1991/92, 1992/93, 1994/95) enabling a strong ventilation of the Gulf through the straits.

Acknowledgements

References

Andrushaitis, A., Seisuma, Z., Legzdina, M., and Lenshs, E., 1995. River load of eutrophying substances and heavy metals into the Gulf of Riga. In: Ecosystem of the Gulf of Riga Between 1920 and 1990. (Ed. by E. Ojaveer), Academia, 5, 32–40. Estonian Academy Publishers, Tallinn.

Berzhins, V., Bethers, U., and Sennikovs, J., 1994. Gulf of Riga: bathymetric, hydrological and meteorological databases, and calculation of the water exchange. Proc. Latvian A cad. Sci. Section B, No. 7/8, 107–117.

Mey, J., 1922. Baltimere hüdrograafia ill. Laevandus, 7, 179–182.

Suursaar, Ü., 1995. Nutrients in the Gulf of Riga. In: Ecosystem of the Gulf of Riga Between 1920 and 1990. (Ed. by E. Ojaveer), Academia, 5, 41–50. Estonian Academy Publishers, Tallinn.

Suursaar, Ü., and Astok, V. (ed.), 1996. Studies on measuring and modelling the water and nutrient exchange of the Gulf of Riga. EMI Report Series, 3, 109 p.

Otsmann, M., Astok, V., and Suursaar, Ü., 1996. A model for water exchange between a large and a small water body: the case of the Baltic Sea and the Gulf of Riga. Nordic Hydrological Conference, Akureyri, Iceland 13–15 August 1996. NHP Report No 40, Vol. 2,496–505.

Yurkovskis, A., Wulff, F., Rahm, L., Andruzaitis, A., and Rodriguez-Medina, M., 1993. A nutrient budget of the Gulf of Riga; Baltic Sea. Estuarine, Coastal and Shelf Science, 37, 113–137.

Мардисте, Х. Х., 1975. О расходах воды в проливах Мухі (Вяйиамери). In: Динамика вод Блтийского моря. Талинн, Изд, АН ЭССР, 88–94

Пасторс, А. А., 1963. Водный баланс Рижского залива. – Труды ГОИН, 73, 96–105.

Петров, В. С., 1979. Водный баланс и водообмен Рижского залива с Балтийск им морем. In: Сб. Работ Рижской гидрометеорологической обсерватор ий, 18, 20–40.

Investigation of the atmospheric impurity washout in the Baltic Sea coastal wave breaking zone during BAEX using radio-active tracers

Nikolaj Tarasiuk, Narciza Spirkauskaité, Klemensas Stelingis, Galina Lujaniené, Michael Schultz, and Roman Marks

Abstract

[7]Be and ^{137}Cs as radionuclides of different origin were used as tracers to study the influence of the surf zone upon the dry deposition of atmospheric pollutants and to study effects of sea self cleaning in the coastal zone during BAEX (Baltic Aerosol Experiment, 1994–1995) in Lubiatowo (northern Poland) and Preila (western Lithuania) stations. [7]Be dry deposition velocities were measured depending on the distance from the shoreline. A considerable growth of this velocity (up to 30 mm·s^{−1}) was fixed in stormy weather near the surf zone. Estimations show that [7]Be secondary atmospheric component (resuspended from the sea surface with spray droplets and salt particles) is responsible for 38% of this value.

Activity size distributions of [7]Be carriers in the air show that the main part of [7]Be during experiments was associated with submicron aerosols of geometric mean aerodynamic diameters of $0.52-0.72\,\mu m$.

Temporary sediments of the coastal zone are actively participating in the sea coastal zone self-cleaning onshore flux existing as onshore pollutant secondary atmospheric and foam fluxes.

Evaluating the ^{137}Cs load of the unstable part of the sea beach (changeable by storms), sand may be treated as sea sediments and characterised by the ^{137}Cs partition coefficient K_d.

Introduction

The sea coastal zone where wave energy dissipates is an area of the most intensive interaction between the sea and the atmosphere. Wave breaking and spray generation, arising in shallow waters at comparatively weak winds, enhance the dry deposition of particles by shunting high transfer resistance to a smooth water surface (Williams, 1981). Calculations show that in this case the dry deposition velocity of submicron aerosols may be of the same order as the velocity of the momentum transfer. This effect may be very strong for the Baltic Sea where shallow water areas are very extensive and atmospheric loadings of the coastal zone must be taken into account in the balance of the total atmospheric load.

Possible effects of enhancement of the dry deposition flux of atmospheric pollutants in the Baltic Sea coastal zone were studied in the frame of Baltic Aerosol Experiment (BAEX) using cosmogenic [7]Be as a tracer. Among a number of advantages of this nuclide (Lujanas *et al.*, 1994; Bettoli *et al.*, 1995), the most important ones are those that [7]Be is of atmospheric origin and activity size distribution of its carriers is typical of aerosol particles of industrial pollutants of long-term transport (Papastefanou and Joannidou, 1995). [137]Cs and [7]Be were used as tracers in the study of associated problems with sea self cleaning in the coastal zone.

Experiment

The experiment aimed to measure the enhanced dry deposition flux of [7]Be to the beach close to the surf zone, where spray droplets were blown to the beach by onshore wind, deposited owing to large gravitational settling velocities to the beach surface on their pathways capturing submicron aerosols marked by [7]Be. The method was thought to be a comparative one, when [7]Be dry deposition velocity, calculated for collectors deployed near the surf zone, is compared with the data measured for collectors exposed on the land under the same weather conditions. Since exposure times lasted for several days (up to a week), [7]Be dry deposition velocities were averaged over all meteorological situations (except rain, when collectors were closed). The experiment was carried out in Lubiatowo (northern Poland) and Preila (western Lithuania) in 1994 (BAEX-2) and 1995 (BAEX-3). During BAEX-2 dry depositions of [7]Be were collected on horizontal Petrianow filters $0.85\times1.5\,m^2$ deployed on the beach and at two different distances from the shoreline (40 m and 150 m). Filters exposed on the beach near the surf zone were mounted on 80 cm high platforms; the others on a solid background

5 cm thick. During BAEX-3 near the surf zone two filters were exposed simultaneously on platforms of different height—60 and 120 cm—and for comparison one filter on the top of the dune. Filters were placed facing the atmosphere on a gauze surface and mounted on book-type holders which were closed manually before rain and taken away.

Two air pumps in Lubiatowo and Preila with a flow-rate of 700 $m^3 \cdot h^{-1}$ were used for daily sampling of the atmospheric aerosols on Petrianow filters.

An optical counter LAS-X (PMS), providing 46 size classes for aerosols from 0.1 to 7.5 μm, was used to measure horizontal profiles of sea droplets and particles near the surf zone over the beach during BAEX-2 in Lubiatowo. The counter was mounted on a mobile platform.

A high pressure slotted impactor (Sierra instruments, series 230) of 5 stages and with a back up filter was used in Lubiatowo during BAEX-3 to evaluate activity size distribution of ^{7}Be carriers in the air over the beach (at about 15 m from the surf zone). Calculated aerodynamic cut-off diameters for used flow rate (68 $m^3 \cdot h^{-1}$) were as follows for stages from 1 to 5: 7.0, 3.0, 1.7, 0.86, 0.47 μm (Steiger *et al.,* 1989). Aerosol deposits on the impactor stages were collected on Whatman-41 filters.

To study the effects of sea self-cleaning from radionuclides in the coastal zone during BAEX, beach sand cores 12×12 cm^2 and sea foam samples were taken. ^{137}Cs vertical profiles were measured in beach sand cores up to the depth of 60−90 cm to evaluate the radionuclide load of the beach. Sea foam samples (volume up to 1.5 L) were filtered through Filtrak type filters for separate definition of radionuclide content in filtrate and suspended matter form.

A γ-spectrometer with the Ge(Li) semiconductor detector was used for ^{7}Be and ^{137}Cs nuclides analysis of the samples. Calibration was carried out using radioactive sources of different density and mixed radionuclide content prepared by the Russian Scientific Research Institute of Physico-Technical and Radiometric Measurements (Moscow). Measurement errors of radionuclide content values for aerosol samples of the pumps, beach sand and sea foam samples as well as impactor back up and high number stages filters and high activity filter of dry depositions were equal to about 30%. These errors for reasonable measurement time (about a day) amounted to 50% for collector filters of long-term exposition and deposits on middle stages of the impactor. Deposits on low number stages of the impactor as well as dry deposition filters exposed for a short time during BAEX-3 were measured with errors of about 100%.

Results and discussion

The course of the ^{7}Be concentration in the air over the beach in Lubiatowo during BAEX-3 is depicted in Figure 1. Gaps in the ^{7}Be concentration course are related to precipitations.
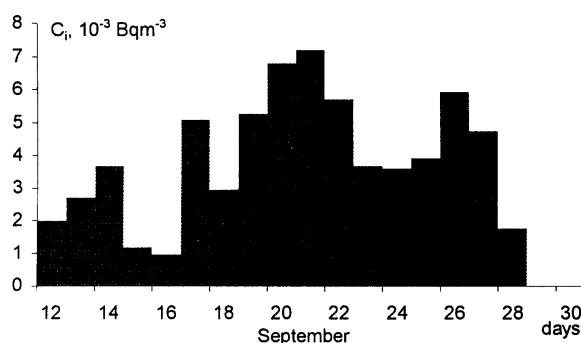
Figure 1 Course of the ^{7}Be concentration in the air over the beach in Lubiatowo during BAEX-3 (1995)

The velocity of ^{7}Be dry deposition was evaluated using the following expression:

$$V = \frac{A}{S_F \sum_i C_i \Delta t_i}$$

where

A is the ^{7}Be dry deposition activity of the filter
S_F is the surface area of the filter
C_i is the ^{7}Be concentration in air in accordance with the course of variations during collector filter exposition (Figure 1)
Δt_i is the time interval of constant C_i value.

Data of ^{7}Be dry deposition velocity evaluation experiments in Lubiatowo during BAEX program realisation are shown in Table 1 and Table 2. Meteorological data were used from Leba Station—one of the nearest to Lubiatowo Polish stations on the Baltic Sea coast. Table 1 and Table 2 inform about time intervals of dry deposition filters exposition and impactor measurements, periods of the use of the optical particle counter as well as present visual observation data of the waving and wind direction during light time in Lubiatowo and calculated values of ^{7}Be dry deposition velocities.

Date	20	21	22	23	24	25	26	27	28	29
Leba station, GMT=0 wind direction	E	NE	NNE	SSE	WSW		WSW	SW	WNW	SW
Leba station, GMT=0 Max wind velocity ms^{-1}	1.5	7.9	5.4	1.5	1.5	0.2	7.9	7.9	20.7	13.8
Lubiatowo, waves: — calm sea, * small, ** white caps, *** stormy	—	**	**	*	*	—	*	*	***	***
Lubiatowo, direction of air advection: offshore−off (S, SE, SW) onshore−on (N, MW, NE) along shore−al. (E, W)	al. (E)	al. (E)	al. (W)	al. (W)	—	off (SW)	off (SW)	on (NW)	on (NW)	al. (W)

Optical particle counter

dry deposition filter exposure (——) showing dry deposition velocity of ^{7}Be

F_1−open square in the forest $F_1(155.3)$ 1.1 mm·s^{-1}

F_2−on top of dune $F_2(154.7)$ 1.0 mm·s^{-1}

F_3−on platform near surf zone $F_3(74)$ 1.4 mm·s^{-1}

$F_i(t)$−net time of exposure (h) $F_3(24)$ 30.2 mm·s^{-1}

Table 1 Data of ^{7}Be dry deposition experiment in Lubiatowo during 20–29 September, 1994 (BAEX-2)

Date	12	13	14	15	16	17	18	19	20	21	22	23	24	25	26	27	28	29
Leba station, GMT=0 wind direction	S		E	W	E	E	ESE	SE	ESE	NE	SSW	WSW	SSW	S	SW	SSW	W	W
Leba station, GMT=0 Max wind velocity ms^{-1}	3.3	0.2	10.7	3.3	5.4	7.9	3.3	3.3	7.9	7.9	1.5	10.7	3.3	5.4	10.7	3.3	20.7	10.7
Lubiatowo, waves: — calm sea, * small, ** white caps, *** stormy	—	—	—	**	*	**	—	—	—	**	**	*	—	—	*	**	***	***
Lubiatowo, direction of air advection: offshore−off (S, SE, SW) onshore−on (N, MW, NE) along shore−al. (E, W)	off (S)	—	off (SW)	on (NW)	al. (E)	al. (E)	off (SE)	off (SE)	al. (E)	on (NE)	on (NW)	al. (W)	off (SW)	off (SW)	al. (W)	al. (W)	on (NW)	al. (W)

Impactor measurements

dry deposition filter expo-sure (——) showing dry deposition velocity of ^{7}Be

F_2−on top of dune

F_3'−at 60 cm in surf zone

F_3''−at 120 cm in surf zone

$F_i(t)$−net time of exposure

$F_2(121)$ 0.7 mm·s^{-1}
$F_2(141.3)$ 0.4 mm·s^{-1}
$F_2(75.7)$ 0.5 mm·s^{-1}
$F_3'(30.3)$ 1.2 mm·s^{-1}
$F_3'(39.3)$ 0.8 mm·s^{-1}
$F_3'(31.3)$ 2.0 mm·s^{-1}
$F_3''(26)$ 0.7 mm·s^{-1}
$F_3''(39.3)$ 1.0 mm·s^{-1}
$F_3''(31.3)$ 0.8 mm·s^{-1}

Table 2 Data of ^{7}Be dry deposition experiment in Lubiatowo during 12–29 September, 1995 (BAEX-3)

As may be seen from Table 1 and Table 2, weather conditions were not convenient for the experiment—offshore winds and winds along the seashore direction dominated. ^{7}Be dry deposition velocities in good weather for the filter on the top of the dune (and in the forest—for BAEX-2 only) in Lubiatowo were: 1–1.1 mm·s^{-1} (2.2 mm·s^{-1} in Preila at the same time) during BAEX-2 and in the range of 0.4–0.7 mm·s^{-1} (0.4–0.5 mm·s^{-1} in Preila) during BAEX-3. Somewhat higher values were measured for filters near the surf zone—1.4 mm·s^{-1} in Lubiatowo (2.7 mm·s^{-1} in Preila) during BAEX-2 and in the range of 0.7–2.0 mm·s^{-1} for filters deployed in the surf zone (small waves) during BAEX-3 (0.5–1.0 mm·s^{-1} in Preila). It has to be noted that with the exception of one case (including Preila's data) filters mounted on the lower platform in the surf zone were somewhat more activated than those on the higher platform.

Data of the measurements of horizontal profiles of sea aerosol concentrations in the air across the beach carried out in Lubiatowo during BAEX-2 for wind of WNW direction helped to analyse the situation during filter activation near the surf zone (Table 3). A large decrease in the concentration of coarse particles in the size range $2.55-7.5\,\mu m$ with the increasing distance from the shoreline showed that filter activation might be mainly efficient only directly near or inside the surf zone.

Distance from shoreline (m)	Time of measurement	Particle concentration (cm^{-3})				
		Size range (μm)				
		0.1−7.5	0.1−0.2	0.2−0.75	0.75−2.55	2.55−7.5
0	16h 26' 17"	1395	911.4	475.2	8.06	0.264
5	16h 32' 20"	1340	889.1	447.0	4.21	0.062
10	16h 38' 19"	1340	891.3	445.3	3.71	0.044
15	16h 44' 13"	error	error	435.2	3.30	0.034
20	16h 51' 44"	1302	863.4	435.6	3.37	0.072
30	16h 57' 39"	1283	849.6	430.2	3.35	0.058
40	17h 3' 46"	1295	848.2	443.8	3.46	0.062

Table 3 Horizontal profile of aerosol particle concentration on the beach of Lubiatowo on 23 September, 1994 (wind WNW, 3-5 ms^{-1})

Activity size distributions of ^{7}Be carriers were measured for two aerosol samples taken with the high pressure impactor during BAEX-3 (Table 2, Figure 2). They are both almost log-normal, but activity size distribution of the first sample (13−15.09.95) is shifted to the left to larger aerodynamic diameters of ^{7}Be carriers, apparently owing to the transport of the activated sea aerosols from the surf zone. A geometric mean aerodynamic diameter (GMAD) of this distribution is $0.72\,\mu m$. It seems that air masses of off-shore wind direction dominated during the second long-term aerosol sampling (15−21 September, 1995). So ^{7}Be was mainly associated in this sample with the particles of smaller aerodynamic diameters (GMAD was equal to $0.52\,\mu m$). Nevertheless in good weather these differences had a small influence on the ^{7}Be dry deposition velocity value (Table 2) and may testify to the existence of the ^{7}Be secondary atmospheric component in the coastal zone (Figure 2a), resuspended from the sea surface with droplets and salt particles.
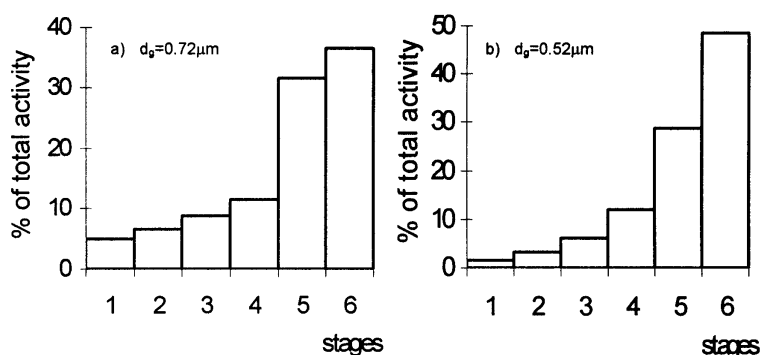
Figure 2 ^{7}Be carrier size g-activity distribution in the air over the beach in Lubiatowo during BAEX-3:
a) air sample volume 3400 m^{3} (13−15.09.1995)
b) air sample volume 7980 m^{3} (15−21.09.1995)
Cut-off diameters of stages (μg): 1—7.0, 2—3.0, 3—1.7, 4—0.86, 5—0.47, 6—backup filter. d_g is the geometric mean aerodynamic diameter (DMAD) of ^{7}Be carriers.

We succeeded in exposing one filter in stormy weather with an onshore NW wind (Table 1). An extraordinarily large value of ^{7}Be dry deposition velocity (30.2 mm·s^{-1}) was calculated, larger than it was predicted in theory (Williams, 1982), and corrected for possible collector filter pollution by ^{7}Be secondary (resuspension) component. Data of radionuclide content in a foam sample taken during the filter exposition (Table 4) and measured total amount of main ions (Na^{+}, Mg^{+}, K^{+}, Cl^{-}) in the filter (130 mg, Flame Photometer) were used for the evaluation of this correction. Calculation showed that filter pollution by ^{7}Be secondary component was responsible for 38% of the measured value of the ^{7}Be dry deposition velocity (Table 1). So a residual part of this value (about 18 mm·s^{-1}) may be treated as evidence of the existence of large dry deposition fluxes of atmospheric pollutants to the sea surface in stormy weather. At the same time it is evident that dry deposition velocity data, presented in Table 1 and Table 2 were only the upper limit of these values, and also must be corrected for the ^{7}Be secondary atmospheric component.

Samples, date	^{137}Cs, β(γ)-activity, Bq·m^{-3}		EF*	^{7}Be, γ-activity, Bq·m^{-3}		EF*
	Filtrate	Suspended matter		Filtrate	Suspended matter	
Lubiatowo, BAEX-2 28.09.1994	$3.16 \cdot 10^3$	$2.42 \cdot 10^4$	320	$4.37 \cdot 10^3$	$9.11 \cdot 10^4$	$6.4 \cdot 10^4$
Lubiatowo, BAEX-3 17–24.09.1995	170	860	12	430	1300	1200
Lubiatowo, BAEX-3 29.09.1995	930	1500	28	5000	4700	6500
Preila, BAEX-3 28.09.1995	93	420	6	200	510	470
* Enrichment factors were evaluated for ^{137}Cs and ^{7}Be concentrations in sea water equal to 87 and 1.5 Bq·m^{-3} respectively						

Table 4 Concentrations of ^{137}Cs and ^{7}Be in sea foam samples (filtrate and suspended matter) and enrichment factors (EF) during BAEX

Data of the foam radionuclide content (Table 4) show that temporary sediments of the shallow waters owing to the flotation actively participate in the self-cleaning processes of the coastal zone—the main part of ^{137}Cs is associated with the suspended matter (^{7}Be depositing to the sea surface is not in time to be dissolved and also is associated in foam with the suspended particles). It is known that onshore radionuclide flux related with foam is followed by other sea self-cleaning fluxes related to spray droplets and salt particles, where dissolved substances (with enriched concentrations) and sediment particles also take part (Belot *et al.*, 1982; McKay *et al.*, 1994). It is obvious because sea foam and spray droplets originate from the sea surface microlayer. Therefore radionuclide content of ^{7}Be secondary atmospheric component owing to the sea aerosol onshore flux may be compared to that of sea foam. Large enrichment factors (EF) of ^{137}Cs and ^{7}Be in sea foam in stormy weather show that secondary atmospheric components of these nuclides under these stormy conditions may be very significant. Evaluating EF values for ^{7}Be (Table 4), concentration of this nuclide in sea water was taken from publications (Olsen *et al.*, 1989).

Data of the investigations of possible additional radioactive pollution of the beach (compared with soil) owing to the existence of the onshore radionuclide flux in the sea coastal zone are depicted in Figure 3.
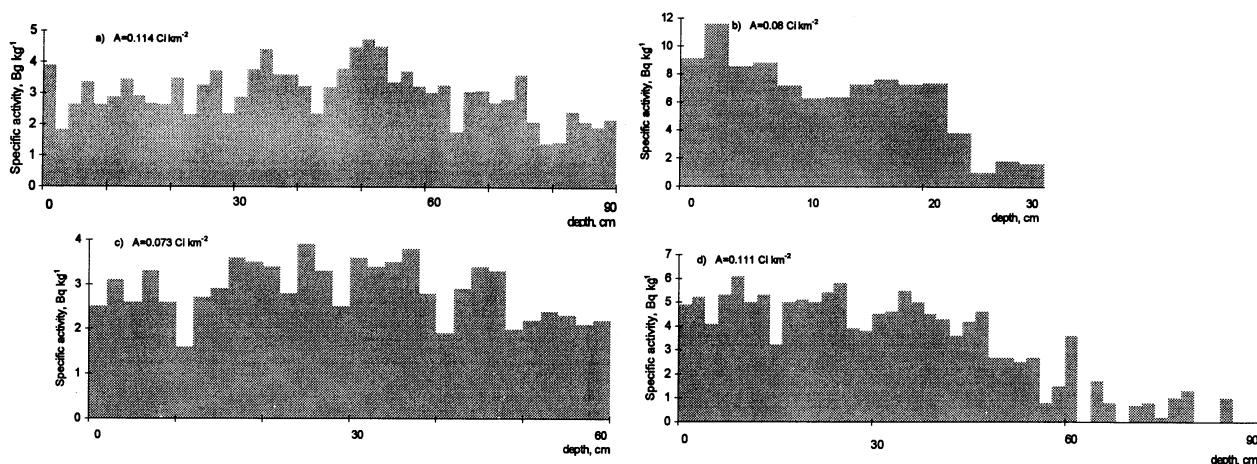
Figure 3 Vertical profiles of ^{137}Cs specific activity in soil and beach sand:
a) Lubiatowo, beach sand, 16 m from surf zone
b) Lubiatowo, soil sample from the meadow
c) Lubiatowo, beach sand, 11 m from surf zone
d) Preila, beach sand, 32 m from surf zone
A is the ^{137}Cs load of sand core

The analysis shows that the sea beach area may be divided into a stable part with a typical ^{137}Cs vertical profile in sand cores (Figure 3d) and an unstable part (changeable by storms)—^{137}Cs vertical profiles in Figure 3a and c (also typical). All sand cores ^{137}Cs vertical profiles (Figure 3) are more extended than the soil profile owing apparently to the higher rate of nuclides vertical migration and are irregularly peaked due to possible fixation of ^{137}Cs in sand layers by organic substances and alternate impulses of radioactive foam during storms. ^{137}Cs vertical profile in the Preila sand core

decreases up to ^{137}Cs zero concentrations in sand layers and underlaying fresh water. The ^{137}Cs load of this sample is about the same as environment soil ones ($0.11-0.12$ $C_i \cdot$km^{-2}). Sand in the unstable part of the beach (as a rule—a narrow strip of about $15-20$ m width—in Preila) may be treated as sea sediments with the characteristic ^{137}Cs partition coefficient K_d (of about $3.4 \cdot 10^{-2}$ m$^3 \cdot$kg^{-1} for Lubiatowo sand), when beach sand and underlaying sea water are really joint vessels. Apparently the ^{137}Cs surplus on the beach surface is quickly removed to the sea water by fast horizontal and vertical migration. Therefore the ^{137}Cs load of the beach over the sea water level (in the unstable part) grows with the increase in distance from the shoreline proportionally to the thickness of a sand layer over the level of underlaying sea water. So the ^{137}Cs load of the beach reaches its maximum values at the upper limit of the beach unstable zone.

Conclusions

- Dry deposition flux of the atmospheric pollutants to the sea surface in the coastal zone owing only to the washout of submicron aerosols by spray droplets in stormy weather may rise ten-fold. Investigations of the dry deposition fluxes in the coastal zone are essential for the evaluation of the total atmospheric load to the Baltic Sea.

- Owing to the existence of the onshore flux of spray droplets and salt particles, the secondary atmospheric component—onshore atmospheric flux of radionuclides (^{137}Cs, ^{7}Be) and other pollutants (heavy metals, organic compounds, etc.)—exists. This component must be taken into account when evaluating dry deposition fluxes of the atmospheric pollutants to the beach and coastal zone, especially in stormy weather.

- Due to the flotation processes, temporary sediments of the sea coastal zone take part in the formation of the onshore flux of pollutants in the form of secondary atmospheric component and foam.

- When evaluating the ^{137}Cs load in the unstable part of the beach, sand may be treated as sea sediments and characterised by the ^{137}Cs partition coefficient K_d.

Acknowledgements

References

Belot, Y., Caput, C., and Gauthier, D., 1982. Transfer of americium from sea water to atmosphere by bubble bursting. Atmospheric Environment, 16, 1463–1466.

Bettoli, M.G., Cantelli, L., Degetto, S., Tositti, L., Tubertini, O., and Valcher, S., 1995. Preliminary investigations on ^{7}Be as a tracer in the study of environmental processes. J. of Radioanal. and Nucl. Chemistry, Articles, 190, 137–147.

Lujanas, V., Lujaniene, G., Tarasiuk, N., Stelingis, K., and Spirkauskaite, N., 1994. Possibilities of application of radioactive tracers in the aerosol washout studies in the wave breaking zone on the seashore. Proceedings of the 19th Conference of the Baltic Oceanographers, Sopot, Poland, 29 August–1 September, 1994, p.p. 47–51.

McKay, W.A., Garland, J. A., Livesley, D., Halliwell, C. M., and Walker, M.I., 1994. The characteristics of the shoreline sea spray aerosol and the landward transfer of radionuclides discharged to the coastal sea water. Atmospheric Environment, 28, 3299–3309.

Olsen, C.R., Ihein, M., Larsen, I.L., Lowry, P.D., Mulholland, J., Cutshall, N. H., Byrd, J.T., and Windom, H.L., 1989. Plutonium, lead-210 and carbon isotopes in the Savannah estuary: Riverborne versus marine sources. Environ. Sci. Technol., 23, 1475–1481.

Papastefanou, C., and Ioannidou, A., 1995). Aerodynamic size association of ^{7}Be in ambient aerosols. J. Environ. Radioactivity, 26, 273–282.

Steiger, M., Schulz, M., Schwikowski, M., Naumann, K., and Dannecker, W., 1989. Variability of aerosol size and its implication to dry deposition estimates. J. Aerosol Sci., 20, 1229–1232.

Williams, R.M., 1982. A model for the dry deposition of particles to natural water surfaces. Atmospheric Environment, 16, 1933–1938.

Seasonal variability of the solar radiation flux and its utilisation in the Southern Baltic

B. Wozniak, A. Rozwadowska, S. Kaczmarek, S. B. Wozniak, and M. Ostrowska

Abstract

The results of theoretical analysis and experimental studies of the solar radiation transfer through the atmosphere to the South Baltic waters as well as its utilisation for different processes in the sea, especially for heating and primary production, are presented. The following results were achieved:

- typical values of the optical parameters of the Baltic atmosphere were determined and a initial spectral model of the solar radiation transfer through the atmosphere was developed

- analytical approximation of the relationships between both solar radiation transmittance and reflectance by the wave-roughened sea surface, and hydro-meteorological factors was determined

- the model of the bio-optical states of the Baltic was developed. It relates the main characteristics of the spectral underwater light field to the chlorophyll field and primary production in the sea. It also allows determination of the solar energy absorbed at different depths. Based on the statistical models and generalisations, seasonal variability of the selected elements of the solar radiation balance for three exemplary areas of a different trophic types in the South Baltic was determined.

Introduction

Ecosystem productivity and climate are the main natural determinants in mankind's existence. Incoming solar radiation is the critical factor influencing both climate and biosphere on Earth. What is meant here is first of all the energy budget of this radiation (i.e. alternative possibilities of energy utilisation for various processes) and heat balance of an area in the traditional meaning (Pomeranec, 1966 and Dera, 1992). In this paper they both are referred to as energy balance (see Figure 1).
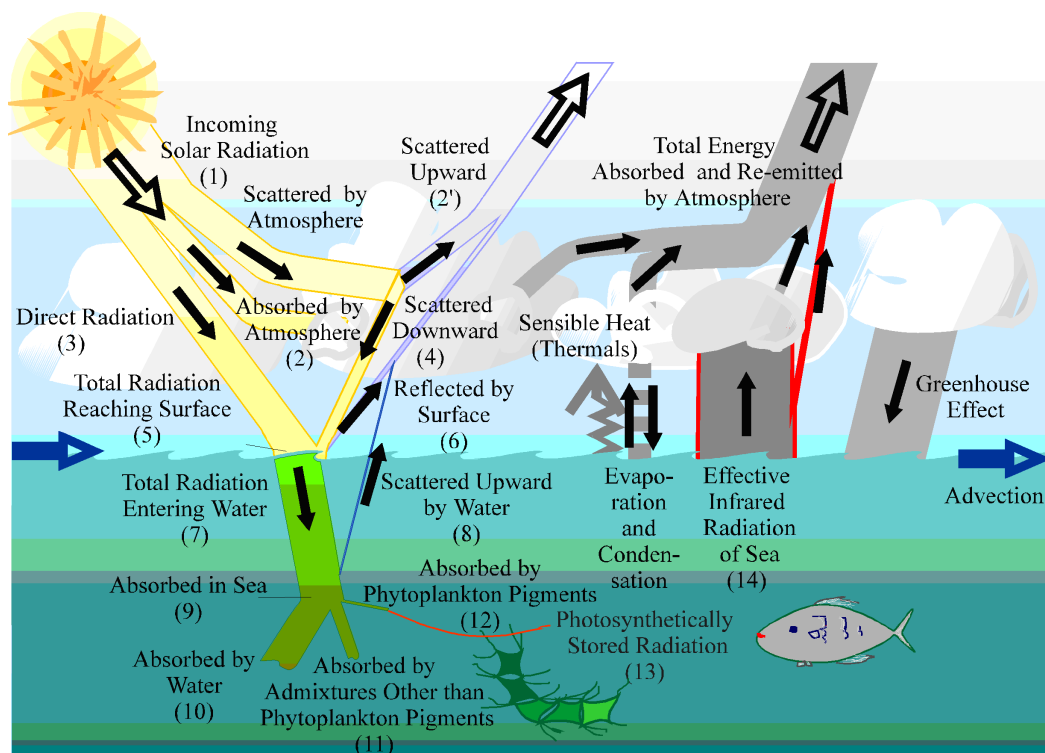
Figure 1 The main elements of energy balance in the atmosphere-sea system

Utilisation of solar radiation energy for various processes (backward scattering and absorption by the atmosphere, reflectance by the sea or land surface, backward scattering in the oceans, global absorption, absorption by phytopigments, photosynthetically used (stored) radiation, etc. (see fluxes (1)–(13) in Figure 1) indirectly determines the amount of vegetation biomass, which, in turn, is food for the all links of the trophic chain at the end of which is a human being (Lieth and Whittaker, 1975).

This outgoing solar energy along with both reverse and feedback processes forced by energy circulation (infrared radiation, latent heat flux connected with water evaporation and condensation and ice melting and water freezing, and sensible heat flux connected with conductivity and turbulent energy exchange) completes the heat balance of earth or its regions as well as determine thermal regimes and global or local circulations determining the climate (Trenberth, 1992).

Therefore precise quantitative estimation of elements of solar radiation energy balance and global scale processes stimulated by this radiation is indispensable for both climate and biosphere modelling on earth. It can only be achieved by means of precise local investigations carried out in various seas and land areas. Our research, confined to the Baltic, has two aspects:

1. energetic feeding of ecosystems (bioproduction) by solar radiation inflow
2. stimulation of climate-shaping processes by solar radiation absorption.

The choice of the Baltic as an area to be investigated is very important because of its great impact on the European environment.

In spite of some significant achievements in Baltic research, the problem of precise determination of its energy balance is still open.

Pomeranec (1966) elaborated the complex model of heat budget in the Baltic Sea. He used about 70000 hydro-meteorological measurements, carried out from 1867 to 1955 together with available actinometric data. Pomeranec approximately described all elements of the energy budget (which are necessary for climate modelling). However, in the case of radiative fluxes he gave non-spectral characteristics. Later, many methodical works, useful for the budget component's analysis, were published (see monographic reviews: Iwanoff, 1972, Timofeyev, 1985, Dera, 1992, Omstedt, 1995, etc.). Also some complex models of Baltic region climate were elaborated (BM—BALTEX Modell, EM—Europa Modell), but the complete model of the energy budget for the Baltic was still not performed. The repetition of Pomeranec's procedure, including new data sets and spectral characteristics of radiative fluxes, will be very profitable.

The theoretic goal of this paper is to develop the complex modelling of the energy budget in the Baltic, which enables analysis of transfer and utilisation of solar radiation in various processes in the sea–atmosphere system. The second, practical goal, is the application of the model to the estimation of seasonal variability of the solar radiation flux and its utilisation in the South Baltic, for different South Baltic areas. The paper contains the initial version of the model, which was applied for description of seasonal variability of main energy fluxes in three various Baltic Sea regions.

Modelling

The following semi-empirical and theoretical mathematical models for solar radiation–environment interaction were developed by our team:

- Spectral model for solar radiation transmittance through the atmosphere over the South Baltic (Wozniak and Rozwadowska, 1995),
- Model for solar radiation transmittance and reflectance by wind-ruffled sea surface (Wozniak, 1996a, b, 1997),
- Bio-optical model for solar radiation transmittance, backscattering, absorption and utilisation for photosynthesis in the Baltic (Wozniak *et al.*, 1992, 1995a, b, Kaczmarek and Wozniak, 1995).

These models with necessary supplements constitute the core of the complex model for solar radiation fluxes and its utilisation for various processes in the sea, presented in this paper. In Figure 2 the simplified block diagram of this complex model is shown. The mathematical apparatus of the model (with necessary parameters) is given in the appendices. The mathematical formulae enable computation of various parameters influencing the transmittance and utilisation of solar energy in the atmosphere–sea system as well as, in further stages of the model, 12 elementary energy fluxes (fluxes 1 to 7 and 9 to 13 in Figure 1).
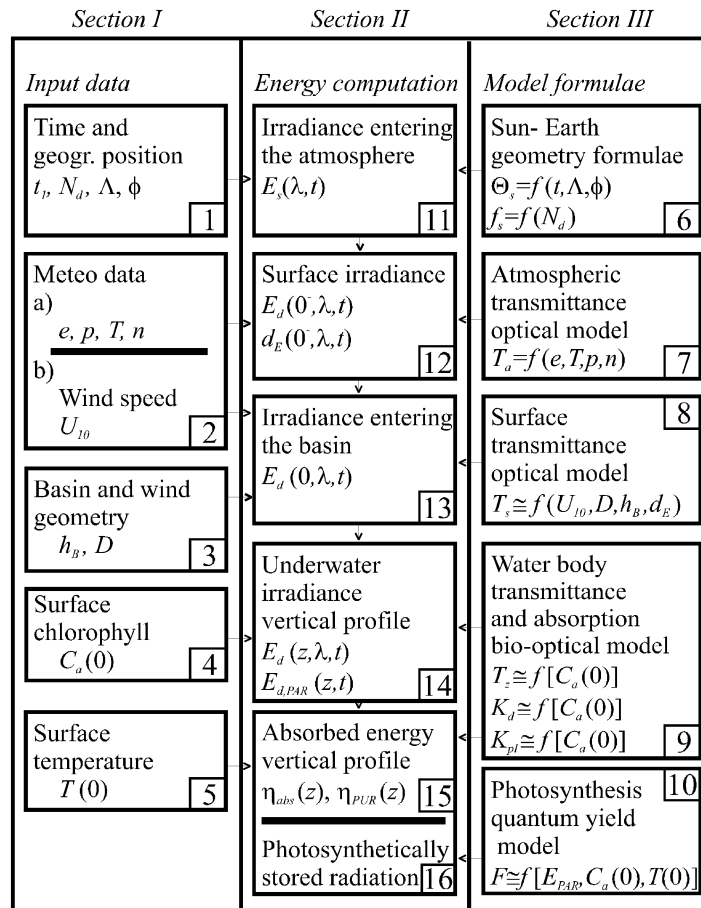
Figure 2 Block diagram of the algorithm (Dera *et al.*, 1995)

Section I	Section II	Section III
Input data	*Energy computation*	*Model formulae*
Time and geogr. position t_l, N_d, Λ, ϕ — 1	Irradiance entering the atmosphere $E_s(\lambda,t)$ — 11	Sun- Earth geometry formulae $\Theta_s=f(t,\Lambda,\phi)$ $f_s=f(N_d)$ — 6
Meteo data a) e, p, T, n b) Wind speed U_{10} — 2	Surface irradiance $E_d(0^-,\lambda,t)$ $d_E(0^-,\lambda,t)$ — 12	Atmospheric transmittance optical model $T_a=f(e,T,p,n)$ — 7
Basin and wind geometry h_B, D — 3	Irradiance entering the basin $E_d(0,\lambda,t)$ — 13	Surface transmittance optical model — 8 $T_s\cong f(U_{10},D,h_B,d_E)$
Surface chlorophyll $C_a(0)$ — 4	Underwater irradiance vertical profile $E_d(z,\lambda,t)$ $E_{d,PAR}(z,t)$ — 14	Water body transmittance and absorption bio-optical model $T_z\cong f[C_a(0)]$ $K_d\cong f[C_a(0)]$ $K_{pi}\cong f[C_a(0)]$ — 9
Surface temperature $T(0)$ — 5	Absorbed energy vertical profile $\eta_{abs}(z), \eta_{PUR}(z)$ — 15 Photosynthetically stored radiation — 16	Photosynthesis quantum yield model — 10 $F\cong f[E_{PAR},C_a(0),T(0)]$

Moreover, we include the formulae for approximate values of effective infrared radiation of sea (flux 14 in Figure 1) and radiation scattered upward by water (flux 8 in Figure 1) used here, which are not included in the algorithm presented in Figure 2.

The energy flux scattered upward by sea to atmosphere was calculated from modelled values of radiation entering the sea $E_d(0^+,\lambda)$ according to the dependencies:

$$E_u(0^-,\lambda)=E_d(0^+,\lambda)\cdot R'(\lambda)$$

and

$$\eta_7 = \int\limits_{t_r}^{t_s} \int\limits_{\lambda=300nm}^{4000nm} E_d(0^-,\lambda,\tau)\cdot R'(\lambda,\tau)d\lambda dt$$

where $R'(\lambda)$ gives the spectral values of the irradiance reflectance coefficients. The seasonal changes of these coefficients, typical for investigated areas (see section 4, Figure 4), were calculated by Darecki from empirical data (Figure 3—unpublished materials).

Seasonal variability of the solar radiation flux and its utilisation in the Southern Baltic
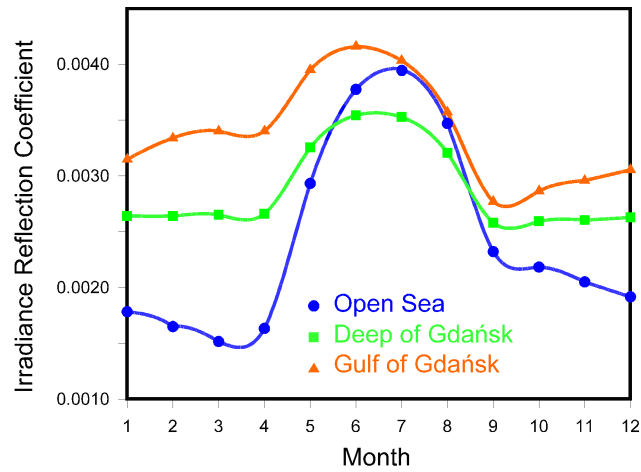
Figure 3 Seasonal and spatial variability of irradiance reflectance coefficient
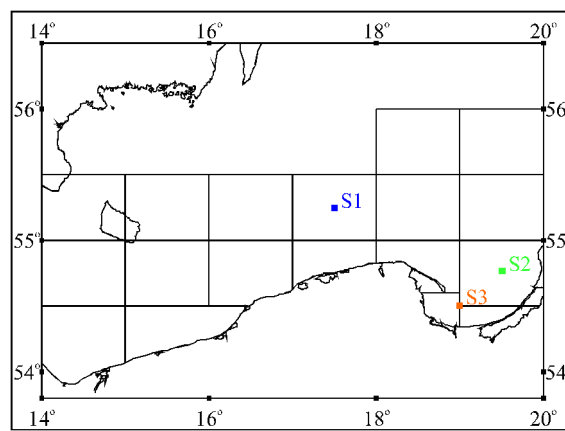
Figure 4 Location of sites for which radiative energy budget components are modelled

The flux of effective infrared radiation of sea (flux 14) was estimated approximately, using hydro-meteorological data (surface air temperature T_1 [K], water temperature T [K], surface humidity of air e_1 [mb], total cloud cover n):

$$\eta_{14} = s\sigma T_1^4(0.39 - 0.0077e_1)(1 - 0.75n^2) + 4\sigma T_1^3(T - T_1)$$

where:

s=0.95,

σ is the Stefan-Boltzmann constant for a time period of twenty four hours ($\sigma = 4.899\cdot10^{-3}\mathrm{J\,day^{-1}m^{-2}K^{-4}}$)

A similar algorithm was proposed by Efimova (see Timofeyev, 1983). It was modified using information and numerical data from Pomeranec (1966), Dera (1992), and Ivanoff (1972). More accurate estimation of this energy flux needs further investigation.

The experimental verification of the models

To check the accuracy of the energy fluxes estimated by the algorithm, some estimated values, X_{model} were compared with measured ones, X_{measur} the sets of relative errors, $\{\varepsilon_i\}$ were calculated using formula:

$$\varepsilon_i = \frac{(X_{\mathrm{model},i} - X_{\mathrm{measur},i})}{X_{\mathrm{measur},i}}$$

The arithmetic and logarithmic statistics of these errors sets were elaborated. A mean error ε means the systematic error of the model, whereas the standard deviation σ means statistical error. The examples of such verification are presented in Table 8. It can be seen that both types of error are relatively small, especially concerning daily doses of energy.

Results of model application

Seasonal variability of some radiative budget components were analysed for the following South Baltic areas, different in both location and water trophic type:

- site 1, representative of the open sea conditions (surface chlorophyll concentration: mean $1.7\,\mathrm{mgm^{-3}}$, variability range $0.5-3.0\,\mathrm{mgm^{-3}}$)

- site 2, near Deep of Gdansk (surface chlorophyll concentration: mean $2.2\,\mathrm{mgm^{-3}}$, variability range $0.35-5.4\,\mathrm{mgm^{-3}}$)

- site 3, Bay of Gdansk (surface chlorophyll concentration: mean $3.4\,\mathrm{mgm^{-3}}$, variability range $1-9\,\mathrm{mgm^{-3}}$).

Locations of these sites are shown in Figure 4.

The following data sets were adopted as model input data (see Table 9):

- average values of meteorological data from $1956-1980$ (Augustyn, 1985)

- average values of surface chlorophyll concentration from $1973-1995$ (our data).

Radiative energy fluxes (1)–(14) (see Figure 1) were estimated using the models and the principles briefly described above.

The results obtained are presented in Table 10 and Table 11 as well as in Figure 5 and Figure 6.
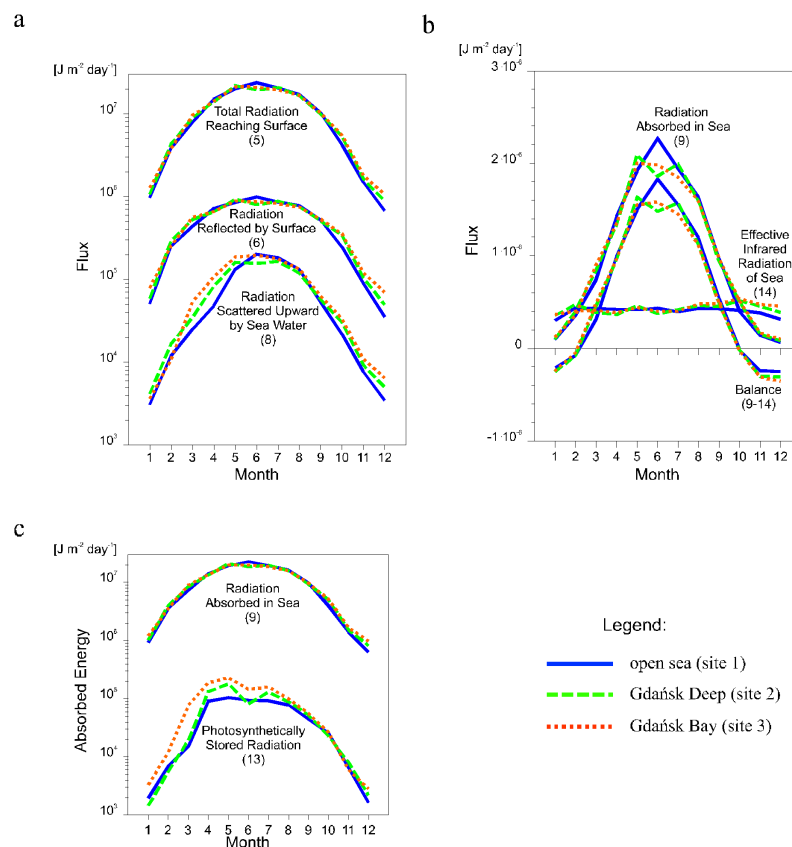
Figure 5 Seasonal variability of: a) radiation fluxes at the sea surface, b) radiative balance and its components, and c) radiation absorbed in the sea (9) and photosynthetically stored radiation (13)
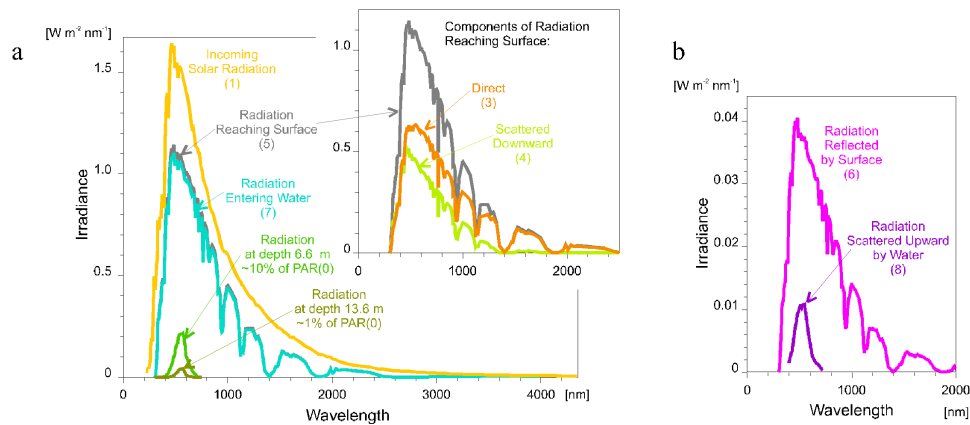
Figure 6 Spectra of a) downward and b) upward radiation fluxes (example values for May 15, solar noon, site 1).

Conclusions

The modelling results presented, which were made for three various regions of the Baltic show that our complex model (even in its initial form) enables estimation of the values of energy fluxes in the atmosphere−sea system. The next step of this modelling is elaboration of the similar yearly characteristics of the energy fluxes for the Polish coastal zone (rectangles in Figure 4). To improve the model the following work is needed:

- development of parametrisation of the other radiation fluxes in the sea and the atmosphere,
- development of parametrisation of the radiative fluxes in the atmosphere on the basis of a layered model of the atmosphere and more realistic approach to clouds,
- take into account seasonal and spatial variability of aerosol optical thickness,
- application of more realistic albedo of sea foam,
- improvement of mathematical description of relationships between characteristics of underwater irradiance fields and sea water components,
- improvement of dependency of quantum yield of photosynthesis on solar radiation and other abiotic factors,
- continuation of field work to improve empirical dependencies.

The above tasks need numerous sets of empirical data to precise mathematical formulae and its verification.

References

Augustyn M., 1985. Characteristics of Southern Baltic Climate, IMGW, Gdynia, 61.

Bird, E. R., and Riodan, C., 1986. Simple solar spectral model for direct and diffuse irradiance on horizontal and titled planes at the Earth surface for cloudless atmospheres. Solar Energy, 25, 87−97.

Dera, J., 1992. Marine physics, Elsevier, Amsterdam etc., 515.

Dera, J., Wozniak, B., Rozwadowska, and A., Kaczmarek, S., 1995. Solar Radiation Energy Absorbed by Baltic Waters; the Example of the Gdansk Basins, [in:] Omstedt [ed.], 1995, (op. cit.), 63.

Dziewulska−Losiowa, A., 1991. Ozone in atmosphere, (in Polish), PWN, Warszawa, 396.

Hale, G. M., and Querry, M. R., 1973. Optical constants of water in the 200−nm to 200−microm wavelength region, Appl. Opt.12 (3) 555−563.

Ivanoff, A., 1972. Introducion a L'Oceanographie, Paris Libraire Vuibert, Paris, (authors used Russian translation, 1978), 574.

Kaczmarek, S., and Wozniak, B., 1995. The application of the optical classification of waters in the Baltic Sea investigation (Case 2 waters), Oceanologia 37 (2), 285−297.

Krylov, J. M., Striekalov, S. S., and Cyplukhin, V. F., 1976. Wind waves and its effect on marine constructions, Gidrometeoizdat, Leningrad, 256.

Lieth, H., and Whittaker, R. H., 1975. Primary productivity of the Biosphere, Springer−Verlag, Berlin etc., 339.

Omstedt, A., [ed.], 1995. First Study Conference on BALTEX, Visby, Sweden, August 28−September 1, 1995, Conference Proceedings, SMHI−Norrköping, Sweden, 190.

Pomeranec, K. S., 1966. Baltic Sea heat budget, (in Polish), Report PIHM, 1, 19−48.

Timofeyev, N. A., 1983. Radiation Regime of the Oceans, (in Russian), Nauk. Dumka, Kiyev, 247.

Trenberth, K. E. [ed.], 1992. Climate System Modelling, Cambridge University Press, 788.

Wozniak, B., Dera, J., and Koblentz−Mishke, O. J., 1992. Bio-optical relationships for estimating primary production in the Ocean, Oceanologia, 33, 5−38.

Wozniak, B., Dera, J., Semovski, S., Hapter, R., Ostrowska, M., and Kaczmarek, S., 1995a. Algorithm for estimating primary production in the Baltic by remote sensing, SiMO, 68−Marine Physics 8, 91−123.

Wozniak, B., Smekot−Wensierski, W., and Darecki, M., 1995b. Semi-empirical modelling of backscattering and light reflection coefficients in WC1 seas, SiMO 68−Marine Physics 8, 61−90.

Wozniak, B., and Rozwadowska, A., 1995. Mathematical semi-empirical model for solar radiation transmittance through the atmosphere over the South Baltic, Internal report IO PAN, Sopot, 15.

Wozniak, S. B., 1996a. Sea surface slope distribution and foam coverage as functions of the mean height of wind waves, Oceanologia, 38 (3), 317−332.

Wozniak, S. B., 1996b. Mathematical preliminary spectral model of solar irradiance reflectance and transmittance by the wind ruffled sea surface. Part 1: Physical problem and mathematical apparatus, Oceanologia, 38 (4), 447−467.

Wozniak, S. B., 1997. Mathematical preliminary spectral model of solar irradiance reflectance and transmittance by the wind ruffled sea surface. Part 2: Modelling results and application, Oceanologia, 39 (1), 17−34.

Appendix 1: Sun-Earth geometry formulae determining incoming solar radiation

Input parameters of the model are the number of the day in the year - N_d , local solar time - t_l [h] and latitude Φ of the observation point.

Model formulae are:

1) A formula for spectral downward irradiance at the top of the atmosphere $E_S(\lambda, t)$ [W m^{-2}nm^{-1}] is:

$$E_S(\lambda, t) = S_{\oplus,\lambda} f_S \cos\theta_S \tag{A1.1}$$

where:

$$\cos\theta_S = \sin\phi\sin\delta + \cos\phi\cos\delta\cos LHA , \tag{A1.2}$$

$$LHA = 15t_l - 180° , \tag{A1.3}$$

$$\delta = (0.006918 - 0.399912\cos\psi + 0.070257\sin\psi - 0.006758\cos 2\psi + \\ + 0.000907\sin 2\psi - 0.002697 \cdot \cos 3\psi + 0.001480\sin 3\psi) \cdot 180°/\pi \tag{A1.4}$$

$$f_S = 1.00011 + 0.034221\cos\psi + 0.00128\sin\psi + 0.000719\cos 2\psi + 0.000077\sin 2\psi \tag{A1.5}$$

$$\psi = 360(N_d - 1)/365 \tag{A1.6}$$

2) The daily values doses of incoming solar radiation η_1 (flux (1)) are calculated using the formula:

$$\eta_1 = \int\limits_{t_r}^{t_s} \int\limits_{300nm}^{4000nm} S_{\oplus,\lambda} f_S \cos\theta_S \, d\lambda \, dt = \\ = 480 \cdot S_\oplus f_S \left\{ \left[arc\cos(-\text{tg}\,\phi\,\text{tg}\,\delta)\sin\phi\sin\delta \right] + \frac{180°}{\Pi}\sin\left[arc\cos(-\text{tg}\,\phi\,\text{tg}\,\delta)\cos\phi\cos\delta \right] \right\} \tag{A1.7}$$

where: $S_\oplus = \int\limits_{300nm}^{4000nm} S_{\oplus,\lambda}(\lambda) d\lambda$ and t_r, t_s are sunrise and sunset times respectively; the angles are expressed in degrees.

Appendix 2: Mathematical apparatus of atmospheric transmittance optical model (Wozniak and Rozwadowska, 1995)

Input parameters of the model are: meteorological data, such as: atmospheric pressure - p [hPa], surface air temperature - T [K], surface relative humidity - e [range 0 -1], total cloud cover n - (range 0 - 1), atmospheric aerosol amount and contents – (aer), atmospheric ozone amount - (O_3) [atm-cm].

Model formulae are:

1) Inherent spectral optical properties of the atmosphere, such as: total optical thicknesses $\tau(\lambda)$, single scattering albedos $\omega_0(\lambda)$ and the parameters x_1 , as well as their constituents (for Rayleigh scattering R , gas absorption g, ozone absorption OZ , water vapour absorption H_2O , aerosol absorption and scattering (aer) can be computed on the basis of meteorological parameters and light propagation directions $\mu = \cos\theta$ using following formulae:

$$\tau(\lambda) = \tau_R(\lambda) + \tau_g(\lambda) + \tau_{OZ}(\lambda) + \tau_{H_2O}(\lambda) + \tau_{aer}(\lambda) \tag{A2.1}$$

$$\omega_0(\lambda) = \frac{\tau_R(\lambda) + \tau_{aer}^{scat}(\lambda)}{\tau(\lambda)} \tag{A2.2}$$

$$x_1(\lambda) = \frac{\tau_{aer}^{scat}(\lambda) \cdot x_{1,aer}(\lambda)}{\tau_R(\lambda) + \tau_{aer}^{scat}(\lambda)} \tag{A2.3}$$

$$\tau_R(\lambda) = 0.1380 \frac{p}{1013} \left(\frac{500}{\lambda}\right)^{-4} \exp\left[0.05022\left(\frac{500}{\lambda}\right)^2\right]$$

(A2.4)

$$\tau_g(\lambda) = 1.41 a_g(\lambda)\frac{p}{p_0}\left[1 + 118.3 a_g(\lambda)m(\mu)\frac{p}{p_0}\right]^{-0.45}$$

(A2.5)

$$m(\mu) = \frac{1.002432\mu^2 + 0.148386\mu + 0.0096467}{\mu^3 + 0.149864\mu^2 + 0.0102963\mu + 0.000303978}$$

(A2.6)

$$\tau_{OZ}(\lambda) = a_{OZ}(\lambda)O_3$$

(A2.7)

where: $a_{OZ}(\lambda)$ is the ozone absorption coefficient (see table 1),

the O_3 values used to the model are shown in table 2

$$\tau_{H_2O}(\lambda) = 0.3 a^*_{H_2O} w[1 + 25.25 a^*_{H_2O} w \cdot m(\mu)]^{-0.45}$$

(A2.8)

where: $w = \int\limits_0^\infty \rho_{H_2O}(h)\exp(-0.1134h)dh$

(A2.9)

$$\rho_{H_2O}(h) = \frac{\rho_0(1 + 0.012n \cdot h)}{10^{(0.214h+0.0024h^2)(1.14-0.008\rho_0)}}$$

(A2.10)

$$\rho_0 = 1000 \cdot \frac{e \cdot \exp\left(-\frac{-5416}{T} + 26.23\right)}{461.51 \cdot T}$$

(A2.11)

$$\tau^{abs}_{aer}(\lambda) = [1 - \omega_{0,aer}(\lambda)]\tau_{aer}(\lambda)$$

(A2.12)

$$\tau^{scat}_{aer}(\lambda) = \omega_{0,aer}(\lambda)\tau_{aer}(\lambda)$$

(A2.13)

For mean values of $\tau_{aer}(\lambda)$, $\omega_{0,aer}(\lambda)$ and $x_{1,aer}(\lambda)$ for the South Baltic as well as absorption coefficients $a_g(\lambda)$, $a_{OZ}(\lambda)$, $a^*_{H_2O}$ and ozone amount (O_3), see tables 1, 2 and 3, respectively.

2) Dependencies of the total $T^0(\mu_S,\lambda)$, direct $T^{0,S}(\mu_S,\lambda)$, and diffuse $T^{0,D}(\mu_S,\lambda)$ irradiance transmittances for the clear parts of the sky on the solar zenith angle θ_S ($\mu_S = \cos\theta_S$) and the real properties of the atmosphere are as follows:

$$T^0(\mu_S,\lambda) = \begin{cases} \frac{\omega_0^*(\lambda)}{2}\left\{\left[m(\mu_S)^{-1}\ln\left(\frac{1}{m(\mu_S)-1}\right) - 1\right]\exp(-\tau^*(\lambda)m(\mu_S)) - C\right\} + \exp(-\tau^*(\lambda)m(\mu_S)) \\ \qquad\qquad\qquad\qquad\qquad \text{for} \qquad\qquad \mu_S \neq 0 \\ \frac{\omega_0^*(\lambda)}{2}\left[(\gamma + \ln(\tau^*(\lambda)))\exp(-\tau^*(\lambda)) + (\tau^*(\lambda) - 1)E_i(-\tau^*(\lambda))\right] + \exp(-\tau^*(\lambda)) \\ \qquad\qquad\qquad\qquad\qquad \text{for} \qquad\qquad \mu_S = 0 \end{cases}$$

(A2.14)

$$C = m(\mu_S)^{-1}\exp(-\tau^*(\lambda)m(\mu_S))E_i^*(\tau^*(\lambda)m(\mu_S) - \tau^*(\lambda)) - $$
$$+ (m(\mu_S)^{-1} - \tau^*(\lambda))E_i(-\tau^*(\lambda)) + \exp(-\tau^*(\lambda))$$

(A2.14a)

$$T^{0,S}(\mu_S,\lambda) = \exp(-\tau(\lambda)m(\mu_S))$$

(A2.15)

$$T^{0,D}(\mu_S,\lambda) = T^0(\mu_S,\lambda) - T^{0,S}(\mu_S,\lambda)$$

(A2.16)

$$\omega_0^*(\lambda) = \frac{[3 - x_1(\lambda)]\omega_0(\lambda)}{3 - x_1(\lambda)\omega_0(\lambda)}$$

(A2.17)

$$\tau^*(\lambda) = \left[1 - \frac{x_1(\lambda)}{3}\omega_0(\lambda)\right]\tau(\lambda) \tag{A2.18}$$

The symbols γ, $E_i^*(x)$, $E_i(x)$ denotes Euler constant, integral-differential function for positive and negative arguments respectively.

3) The average for the South Baltic empirical relationships between irradiance transmittance for the clouds $T_C(\lambda)$ and the total cloud cover n and cloud type are:

$$T_C(\lambda) = T_{C,SEL}(\lambda)T_{C,N}(\lambda) \tag{A2.19}$$

$$T_{C,N}(\lambda) = \begin{cases} 1 - 0.787n + 0.487n^2 - 0.421n^3 & for & n < 1 \\ 0.453 & for & n = 1, type = transparent \\ 0.204 & for & n = 1, type = opaque \end{cases} \tag{A2.20}$$

$$T_{C,SEL}(\lambda) = \exp\left(-w_C a_w(\lambda)\right) \tag{A2.21}$$

where: $a_w(\lambda)$ - absorption coefficient for liquid water (see Table 4),

$$w_C = \begin{cases} 0.61 & for & n < 1 & and & n = 1, type = opaque \\ 0.26 & for & n = 1, type = transparent \end{cases} \tag{A2.22}$$

4) Total E_d, direct E_d^S, and diffuse E_d^D spectral downward irradiances at the sea surface under the real atmosphere as well as the diffuseness d_E can be calculated on the basis of $T^0(\lambda)$, $T^{0,S}(\lambda)$, $T_C(\lambda)$, E_S and n using formulae:

$$E_d(0^-,\lambda,t) = \left[(1 - n_\theta(\theta_S))E_d^0(0^-,\lambda,t) + n_\theta(\theta_S)E_d^{C,D}(0^-,\lambda,t)\right] \tag{A2.23}$$

$$n_\theta(\theta) = 1 - \left[1 - n_\theta(0)\right]\exp\left[0.5n_\theta(0)(1 - \sec\theta)\right] \tag{A2.24}$$

$$n_\theta(0) = 0.3236n^{3.04} + 0.6764n^{1.27} \tag{A2.25}$$

$$E_d^0(0^-,\lambda,t) = E_S T^0 \tag{A2.26}$$

$$E_d^{C,D}(0^-,\lambda,t) = E_d^0(0^-,\lambda,t)T_C(\lambda,n) \tag{A2.27}$$

$$E_d^S(0^-,\lambda,t) = \left[1 - n_\theta(\theta_S)\right]E_d^{0,S}(0^-,\lambda,t) \tag{A2.28}$$

$$E_d^{0,S}(0^-,\lambda,t) = E_S T^{0,S} \tag{A2.29}$$

$$E_d^D(0^-,\lambda,t) = E_d(0^-,\lambda,t) - E_d^S(0^-,\lambda,t) \tag{A2.30}$$

$$d_E(0^-,\lambda,t) = \frac{E_d^D(0^-,\lambda,t)}{E_d(0^-,\lambda,t)} \tag{A2.31}$$

5) Total fluxes of daily solar energy doses: absorbed and scattered upward by the atmosphere η_2 (fluxes (2+2')), direct η_3 (flux (3)), diffuse η_4 (flux (4)) and total η_5 (flux (5)) radiation reaching the sea surface, are calculated on the basis of known irradiances (see stage 4) and known η_1 using formulae:

$$\eta_4 = \int_{t_r}^{t_s}\int_{300nm}^{4000nm} E_d^D(0^-,\lambda,t)d\lambda dt, \tag{A2.32}$$

$$\eta_3 = \int_{t_r}^{t_s}\int_{300nm}^{4000nm} E_d^S(0^-,\lambda,t)d\lambda dt, \tag{A2.33}$$

$$\eta_5 = \int_{t_r}^{t_s}\int_{300nm}^{4000nm} E_d(0^-,\lambda,t)d\lambda dt, \tag{A2.34}$$

$$\eta_2 = \eta_1 - \eta_5 \tag{A2.35}$$

Appendix 3: Mathematical apparatus of the model of energy transfer through sea surface (Woźniak, 1996c).

Input data: sun zenithal angle Θ, diffuseness of irradiance d_E, cardioidal distribution parametr B of diffuse irradiance, the mean height of wind waves $\overline{H}$ (or hydrometeorological and geometrical factors: the wind speed v, the wind fetch D, the sea depth h, the shape of the coastal region, etc., which are functionally connected with $\overline{H}$, using e.g. Krylov's method (see Krylov et al.,1976))

(an example of Krylov's formula for a straight coast line):

$$\frac{g\overline{H}}{v^2} = 0.16\left[1 - \left[\frac{1}{1 + 6.0 \cdot 10^{-3}\left(\frac{gD}{v^2}\right)^{1/2}}\right]^2\right] \times th\left[0.625\frac{\left(\frac{gh}{v^2}\right)^{0.8}}{1 - \left[1 + 6.0 \cdot 10^{-3}\left(\frac{gD}{v^2}\right)^{1/2}\right]^{-2}}\right] \tag{A3.0}$$

g- acceleration due to gravity.

Approximate equations for:

- real surface solar irradiance reflectance

$$R(\lambda) = (1-s)[(1-d_E)R_S(\lambda) + d_E R_D(\lambda)] + s \cdot A_f(\lambda) \tag{A3.1}$$

- real surface solar irradiance transmittance

$$T(\lambda) = (1-s)[(1-d_E)T_S(\lambda) + d_E T_D(\lambda)] + s \cdot T_f(\lambda) \tag{A3.2}$$

where elements are given by equations:

- surface reflectance and transmittance of solar irradiance with direct light

$$R_S(\lambda) = \exp\left\{\sum_{j=0}^{3}\left(\sum_{i=0}^{3} a_{\lambda,i,j}(\cos\Theta)^i\right)\overline{H}^j\right\} \tag{A3.3}$$

$$T_S(\lambda) = 1 - R_S(\lambda) \tag{A3.4}$$

- surface reflectance and transmittance of solar irradiance with diffuse light

$$R_D(\lambda) = \sum_{j=0}^{2}\left(\sum_{i=0}^{2} b_{\lambda,i,j}B^i\right)\overline{H}^j \tag{A3.5}$$

$$T_D(\lambda) = 1 - R_D(\lambda) \tag{A3.6}$$

- surface foam coverage

$$s = 1,2 \cdot 10^{-5} \cdot \left(\sqrt{55,46\overline{H}}\right)^{3,3} \text{ (for } \overline{H} \le 1.46m)$$
$$s = 1,2 \cdot 10^{-5} \cdot \left(\sqrt{55,46\overline{H}}\right)^{3,3}\left(0,225\sqrt{55,46\overline{H}} - 0.99\right)\text{(for } \overline{H} \ge 1.46m) \tag{A3.7}$$

-spectral albedo and transmittance of the foam, in this work for a simplification one assumed constant value

$$A_f(\lambda) = 0.8 \tag{A3.8}$$

$$T_f(\lambda) = 0.2 \tag{A3.9}$$

Appendix 4: Mathematical apparatus of the model of marine primary production (Woźniak et al. 1992, 1995a).

Input parameters of the model are the chlorophyll concentration vertical profile $C_a(0)$ [mg m^{-2}], available solar irradiance at the surface $E_d(\lambda,t,0)$ [quanta m^{-2} nm^{-1} s^{-2}] and sea surface temperature T [°C]

Model formulae are:

1) Dependences between vertical profiles of chlorophyll $C_a(z)$, surface concentration $C_a(0)$ and number of the day in the year N_d are as follows:

$$C_a(z) = C_a(0) \frac{C_{const} + C_m \exp\left\{-\left[(z - z_{max})\sigma_z\right]^2\right\}}{C_{const} + C_m \exp\left\{-\left[(z_{max})\sigma_z\right]^2\right\}} \qquad (A4.1)$$

where:

$$C_{const} = \left[0.77 - 0.13\cos\left(2\Pi \frac{N_d - 74}{365}\right)\right]^{C_a(0)}$$

$$C_m = \frac{1}{2M}\left[(0.36)^{C_a(0)} + 1\right]\left[M + 1 + (M - 1)\cos\left(2\Pi \frac{N_d - 120}{365}\right)\right]$$

$$M = 2.25(0.765)^{C_a(0)} + 1$$

$$z_{max} = 9.18 - 2.43\log C_a(0) + 0.213(\log C_a(0))^2 - 1.18(\log C_a(0))^3$$

$$\sigma_z = 0.118 + 0.113\log C_a(0) + 0.0139(\log C_a(0))^2 + 0.112(\log C_a(0))^3$$

2) Dependences of downwelling irradiance attenuation coefficient $K_d(\lambda)$ [m^{-1}] and its phytoplankton $K_{pl}(\lambda)$ [m^{-1}] and allochtonic substances $\Delta K(\lambda)$ [m^{-1}] on chlorophyll concentration C_a are given by:

$$K_d(\lambda) = K_w(\lambda) + C_a\left\{A_1(\lambda)\exp\left[-a_1(\lambda)C_a\right] + k_{d,i}(\lambda)\right\} + \Delta K(\lambda) \qquad (A4.2)$$

$$K_{pl}(\lambda) = C_a\left\{A_2(\lambda)\exp\left[-a_2(\lambda)C_a\right] + k_{c,j}(\lambda)\right\} \qquad (A4.3)$$

$$\Delta K(\lambda) = 0.0716\exp\left[-0.0117(\lambda - 550)\right] \qquad (A4.4)$$

where λ - [nm]

For the values of constant $A_1(\lambda)$, $a_1(\lambda)$ $k_{d,i}(\lambda)$, $A_2(\lambda)$, $a_2(\lambda)$, $k_{c,j}(\lambda)$ and the attenuation of pure water $K_w(\lambda)$, seeTable 7.

3) Dependences of the photosynthesis quantum yield $\Phi(z)$ [quanta (atom C)$^{-1}$] on underwater irradiance $E_{d,PAR}(z)$ in PAR (photosynthetic active radiance 400-700 nm) range, sea surface chlorophyll concentration $C_a(0)$ and euphotic zone temperature T_e, are given by:

$$\Phi(z) = \Phi_{max}\left(C_a(0)\right) \frac{E_{d,PAR,1/2}(T_e)}{E_{d,PAR,1/2}(T_e) + E_{d,PAR}(z)} I(E_{d,PAR}) \qquad (A4.5)$$

$$\Phi_{max}\left(C_a(0)\right) = 0.051 \frac{C_a(0)^{0.66}}{0.44 + C_a(0)^{0.66}}$$

$$I(E_{d,PAR}) = \exp\left\{\left[-4.9 \cdot 10^{-21} m^2 s \cdot quanta^{-1}\right]E_{d,PAR}\right\}$$

$$E_{d,PAR,1/2}(T_e) = 3.16 \cdot 10^{19}\left[quanta \cdot m^{-2} s^{-1}\right] \cdot 2^{T_e/10}$$

(let T_e be approximately equal to sea surface temperature T).

Principles of computations of some environmental characteristics of primary production in the sea:

1) Vertical profiles of spectral optical properties $K_d(\lambda, z)$ and $K_{pl}(\lambda, z)$ can be calculated on the basis of $C_a(z)$ using eqs (A4.1),(A4.2) and (A4.3);

2) Vertical profiles of the downward spectral irradiance $E_d(\lambda, t, z)$ [quanta·m^{-2}·s^{-1}·nm^{-1}], the daily irradiance dose in the PAR $\eta_{PAR}(z)$ and total $\eta(z)$ spectral range [quanta·m^{-2}], the average downward irradiance in the PAR range $E_{PAR}(z)$ [quanta·m^{-2}·s^{-1}] and daily energy absorbed by phytoplankton $\eta_{PUR}(z)$ [quanta·m$^-$

^{3}], admixture other than phytoplankton pigments $\eta_\Delta(z)$ [quanta·m^{-3}], and water $\eta_w(z)$ [quanta·m^{-3}], can be calculated on the basis of $K_d(\lambda,z)$, $K_{pl}(\lambda,z)$, $K_w(\lambda,z)$ and the input data of surface irradiance $E_d(\lambda,t,0)$ using the formulae:

$$E_d(\lambda,t,z) = E_d(\lambda,t,0)\left\{\exp\left[-\int_0^z K_d(\lambda,z)dz\right]\right\} \tag{A4.6}$$

$$\eta_{PAR}(z) = \int_{t_r}^{t_s}\int_{400nm}^{700nm} E_d(\lambda,\ t,z)d\lambda dt \tag{A4.7}$$

$$\eta(z) = \int_{t_r}^{t_s}\int_{\lambda_1}^{\lambda_2} E_d(\lambda,\ t,z)d\lambda dt \tag{A4.8}$$

where t_r and t_s are the sunrise and sunset times respectively;

$$E_{PAR}(z) = \eta_{PAR}(z)/(t_s - t_r) \tag{A4.9}$$

$$\eta_{PUR}(z) \approx 1.2\int_{t_r}^{t_s}\int_{400nm}^{700nm} E_d(\lambda,t,z)K_{pl}(\lambda,z)d\lambda dt \tag{A4.10}$$

$$\eta_\Delta(z) \approx 1.2\int_{t_r}^{t_s}\int_{400nm}^{700nm} E_d(\lambda,t,z)\left(K_d(\lambda,z) - K_w(\lambda,z) - K_{pl}(\lambda,z)\right)d\lambda dt \tag{A4.11}$$

$$\eta_w(z) \approx 1.2\int_{t_r}^{t_s}\int_{400nm}^{700nm} E_d(\lambda,t,z)K_w(\lambda,z)d\lambda dt \tag{A4.12}$$

4) Daily values of vertical distributions of primary production $P(z)$ [atoms C·m^{-3}] are calculated on the basis of known $\eta_{PUR}(z)$, $E_{PAR}(z)$, $C_a(0)$ and the formulae:

$$P(z) = \Phi(z)\eta_{PUR}(z); \quad P_{tot} = \int_0^{z(P=0)} P(z)dz \tag{A4.13}$$

5) Total fluxes of energy in water column [quanta m^{-2} day^{-1}]: absorbed in the sea η_9 (flux (9) in Figure 1), absorbed by water η_{10} (flux (10)), absorbed by phytoplankton $\eta_{12} \equiv$ PUR (flux (12)), total primary production $\eta_{13} \equiv$ PSR (flux (13)), are calculated from known $\eta(z)$, $\eta_\Delta(z)$, $\eta_{PUR}(z)$, $P(z)$, using formulae:

$$\eta_{10} = \int_0^{z_{min}}\eta_w(z)dz; \quad \eta_{11} = \int_0^{z_{min}}\eta_\Delta(z)dz; \quad \eta_{12} = \int_0^{z_{min}}\eta_{PUR}(z)dz; \quad \eta_{13} = 1.1\cdot10^{23}\int_0^{z_{min}}P(z)dz \tag{A4.14}$$

where z_{min} is the depth at which irradiance or primary production decreases to a level so small that it does not affect the overall production $P_{tot} = \eta_{13}$.

Wave-length [nm]	Solar constant [Wm^{-2}nm^{-1}]	[cm^{2}g^{-1}]	[atm-cm^{-1}]	[km^{-1}]	Wave-length [nm]	Solar constant [Wm^{-2}nm^{-1}]	[cm^{2}g^{-1}]	[atm-cm^{-1}]	[km^{-1}]
300.0	0.5359	0.0	10.0	0.0	980.0	0.7670	1.48	0.0	0.0
305.0	0.5583	0.0	4.8	0.0	993.5	0.7576	0.1	0.0	0.0
310.0	0.6220	0.0	2.7	0.0	1040.0	0.6881	0.00001	0.0	0.0
315.0	0.6927	0.0	1.35	0.0	1070.0	0.6407	0.001	0.0	0.0
320.0	0.7151	0.0	0.8	0.0	1100.0	0.6062	3.2	0.0	0.0
325.0	0.8329	0.0	0.38	0.0	1120.0	0.5859	115.0	0.0	0.0
330.0	0.9619	0.0	0.16	0.0	1130.0	0.5702	70.0	0.0	0.0
335.0	0.9319	0.0	0.075	0.0	1145.0	0.5641	75.0	0.0	0.0
340.0	0.9006	0.0	0.04	0.0	1161.0	0.5442	10	0.0	0.0
345.0	0.9113	0.0	0.019	0.0	1170.0	0.5334	5.0	0.0	0.0
350.0	0.9755	0.0	0.007	0.0	1200.0	0.5016	2.0	0.0	0.0
360.0	0.9759	0.0	0.0	0.0	1240.0	0.4775	0.002	0.0	0.05
370.0	1.1199	0.0	0.0	0.0	1270.0	0.4427	0.002	0.0	0.30
380.0	1.1038	0.0	0.0	0.0	1290.0	0.4400	0.1	0.0	0.02
390.0	1.0338	0.0	0.0	0.0	1320.0	0.4168	4.0	0.0	0.0002
400.0	1.4791	0.0	0.0	0.0	1350.0	0.3914	200.0	0.0	0.00011
410.0	1.7013	0.0	0.0	0.0	1395.0	0.3589	1000.0	0.0	0.00001
420.0	1.7404	0.0	0.0	0.0	1442.5	0.3275	185.0	0.0	0.05
430.0	1.5872	0.0	0.0	0.0	1462.5	0.3175	80.0	0.0	0.011
440.0	1.8370	0.0	0.0	0.0	1477.0	0.3073	80.0	0.0	0.005
450.0	2.0050	0.0	0.003	0.0	1497.0	0.3004	12.0	0.0	0.0006
460.0	2.0430	0.0	0.006	0.0	1520.0	0.2928	0.16	0.0	0.0
470.0	1.9870	0.0	0.009	0.0	1539.0	0.2755	0.002	0.0	0.005
480.0	2.0270	0.0	0.014	0.0	1558.0	0.2721	0.0005	0.0	0.13
490.0	1.8960	0.0	0.021	0.0	1578.0	0.2593	0.0001	0.0	0.04
500.0	1.9090	0.0	0.030	0.0	1592.0	0.2469	0.00001	0.0	0.06
510.0	1.9270	0.0	0.040	0.0	1610.0	0.2440	0.0001	0.0	0.13
520.0	1.8310	0.0	0.048	0.0	1630.0	0.2435	0.001	0.0	0.001
530.0	1.8910	0.0	0.063	0.0	1646.0	0.2348	0.01	0.0	0.0014
540.0	1.8980	0.0	0.075	0.0	1678.0	0.2205	0.036	0.0	0.0001
550.0	1.8920	0.0	0.085	0.0	1740.0	0.1908	1.1	0.0	0.00001
570.0	1.8400	0.0	0.120	0.0	1800.0	0.1711	130.0	0.0	0.00001
593.0	1.7680	0.075	0.119	0.0	1860.0	0.1445	1000.0	0.0	0.0001
610.0	1.7280	0.0	0.120	0.0	1920.0	0.1357	500.0	0.0	0.001
630.0	1.6580	0.0	0.09	0.0	1960.0	0.1230	100.0	0.0	4.3
656.0	1.5240	0.0	0.065	0.0	1985.0	0.1238	4.0	0.0	0.20
667.6	1.5310	0.0	0.051	0.0	2005.0	0.1130	2.9	0.0	21.0
690.0	1.4200	0.016	0.028	0.15	2035.0	0.1085	1.0	0.0	0.13
710.0	1.3990	0.0125	0.018	0.0	2065.0	0.0975	0.4	0.0	1.0
718.0	1.3740	1.8	0.015	0.0	2100.0	0.0924	0.22	0.0	0.08
724.4	1.3730	2.5	0.012	0.0	2148.0	0.0824	0.25	0.0	0.001
740.0	1.2980	0.061	0.01	0.0	2198.0	0.0746	0.33	0.0	0.00038
752.5	1.2690	0.0008	0.008	0.0	2270.0	0.0683	0.50	0.0	0.001
757.5	1.2450	0.0001	0.007	0.0	2360.0	0.0638	4.0	0.0	0.0005
762.5	1.2230	0.00001	0.006	4.0	2450.0	0.0495	80.0	0.0	0.00015
767.5	1.2050	0.00001	0.005	0.35	2500.0	0.0485	310.0	0.0	0.00014
780.0	1.1830	0.0006	0.0	0.0	2600.0	0.0386	15000.0	0.0	0.00066
800.0	1.1480	0.035	0.0	0.0	2700.0	0.0366	22000.0	0.0	100.0
816.0	1.0910	1.6	0.0	0.0	2800.0	0.0320	8000.0	0.0	150.0
823.7	1.0620	2.5	0.0	0.0	2900.0	0.0281	650.0	0.0	0.13
831.5	1.0380	0.5	0.0	0.0	3000.0	0.0248	240.0	0.0	0.0095
840.0	1.0220	0.155	0.0	0.0	3100.0	0.0221	230.0	0.0	0.001
860.0	0.9987	0.00001	0.0	0.0	3200.0	0.0196	100.0	0.0	0.8
880.0	0.9472	0.0026	0.0	0.0	3300.0	0.0175	120.0	0.0	1.9
905.0	0.8932	7.0	0.0	0.0	3400.0	0.0157	19.5	0.0	1.3
915.0	0.8682	5.0	0.0	0.0	3500.0	0.0141	3.6	0.0	0.075
925.0	0.8297	5.0	0.0	0.0	3600.0	0.0127	3.1	0.0	0.01
930.0	0.8303	27.0	0.0	0.0	3700.0	0.0115	2.5	0.0	0.00195
937.0	0.8140	55.0	0.0	0.0	3800.0	0.0104	1.4	0.0	0.004
948.0	0.7869	45.0	0.0	0.0	3900.0	0.0095	0.17	0.0	0.29
965.0	0.7683	4.0	0.0	0.0	4000.0	0.0086	0.0045	0.0	0.025

Table 1 Spectral distribution of the solar constant and absorption coefficient for the atmospheric gases (after Bird and Riordan, 1986)

Month	I	II	III	IV	V	VI	VII	VIII	IX	X	XI	XII
O$_3$ [atm-cm^{-1}]	0.360	0.390	0.399	0.405	0.386	0.372	0.310	0.331	0.310	0.298	0.296	0.326

Table 2 Monthly means of the ozone content O$_3$ in the atmosphere in Belsk, after Dziewulska-Losiowa, 1991

Wavelength [nm]	$\tau_{aer}(\lambda)$	$\omega_{0,aer}(\lambda)$	$\chi_{1,aer}(\lambda)$	Wavelength [nm]	$\tau_{aer}(\lambda)$	$\omega_{0,aer}(\lambda)$	$\chi_{1,aer}(\lambda)$
300	0.2022	0.9410	2.1551	1536	0.1005	0.9574	2.2803
330	0.1914	0.9531	2.1469	1800	0.0928	0.9655	2.3153
400	0.1753	0.9620	2.1553	2000	0.0874	0.9658	2.3379
488	0.1597	0.9640	2.1641	2250	0.0820	0.9683	2.3657
515	0.1550	0.9621	2.1648	2500	0.0750	0.9500	2.4211
550	0.1507	0.9624	2.1607	2700	0.0647	0.7996	2.5638
633	0.1407	0.9656	2.1756	3000	0.0778	0.5036	2.4467
694	0.1353	0.9649	2.1837	3200	0.0798	0.6758	2.3132
860	0.1237	0.9600	2.2059	3392	0.0760	0.8652	2.2348
1060	0.1147	0.9576	2.2311	3500	0.0736	0.9205	2.2249
1300	0.1064	0.9582	2.2531	3750	0.0684	0.9557	2.2436
				4000	0.0646	0.9497	2.2594

Table 3 The optical properties of the Baltic aerosol

Wavelength [nm]	$a_w(\lambda)$ [m^{-1}]	Wavelength [nm]	$a_w(\lambda)$ [m^{-1}]	Wavelength [nm]	$a_w(\lambda)$ [m^{-1}]
300	0.6702	800	1.9635	2800	516118.7931
325	0.4176	825	2.7722	2850	815711.7767
350	0.2334	850	4.3317	2900	1161305.9740
355	0.1239	875	5.6154	2950	843437.7565
400	0.0584	900	6.7858	3000	1139350.9357
425	0.0384	925	14.4004	3050	988829.1631
450	0.0285	950	38.7573	3100	778304.2445
475	0.0247	975	44.8523	3150	538558.7406
500	0.0251	1000	36.3168	3200	362853.9515
525	0.0316	1200	103.5678	3250	235861.1100
550	0.0448	1400	1238.6851	3300	140134.0723
575	0.0787	1600	671.5154	3350	97905.1561
600	0.2283	1800	802.8515	3400	72071.8315
625	0.2795	2000	6911.5038	3450	48080.0267
650	0.3171	2200	1650.7641	3500	33749.6811
675	0.4152	2400	5005.6043	3600	17976.8913
700	0.6014	2600	15321.3057	3700	12226.7390
725	1.5860	2650	28926.3625	3800	11243.5948
750	2.6138	2700	88430.0154	3900	12244.1560
775	2.3998	2750	269605.7695	4000	14451.3262

Table 4 Absorbtion coefficients for liquid water, after Hale and Querry (1973)

wavelength [nm]	j\i	$a_{\lambda,i,j}$				$b_{\lambda,i,j}$		
		0	1	2	3	0	1	2
350	0	-0.422144	-4.11179	-2.81417	3.48857	0.062803	-0.00513406	0.000328398
	1	-0.313709	-0.664235	3.66746	-2.7454	-0.0134884	0.000431751	0
	2	0.153736	0.00921289	-0.965797	0.799547	0.00435328	0	0
	3	-0.0227758	0.0113698	0.109506	-0.0969769			
480	0	-0.423154	-4.11331	-2.84072	3.50759	0.062479	-0.00511804	0.000326918
	1	-0.31501	-0.659662	3.66509	-2.74634	-0.0133878	0.000428375	0
	2	0.154337	0.006869	-0.964053	0.799565	0.00431201	0	0
	3	-0.0228619	0.0117175	0.109222	-0.0969571			
680	0	-0.427284	-4.11999	-2.94761	3.58434	0.061228	-0.00508236	0.000324659
	1	-0.320352	-0.640599	3.65458	-2.74974	-0.0133197	0.000430917	0
	2	0.156806	-0.00290944	-0.956486	0.798391	0.00430214	0	0
	3	-0.0232161	0.013169	0.107996	-0.0968376			
2600	0	-0.441766	-4.14907	-3.30258	3.84156	0.057095	-0.00495214	0.00031631
	1	-0.339206	-0.570636	3.61049	-2.75739	-0.0130499	0.00042926	0
	2	0.165523	-0.0385433	-0.926851	0.796917	0.00425764	0	0
	3	-0.0244664	0.0184469	0.103261	-0.0961647			
2740	0	-0.533176	-4.51611	-4.9941	5.14654	0.0378804	-0.00400513	0.000254665
	1	-0.464031	-0.027848	3.11038	-2.67879	-0.0109745	0.00037837	0
	2	0.223327	-0.308517	-0.641764	0.725397	0.00371896	0	0
	3	-0.0327639	0.0581536	0.0595172	-0.0840167			
3070	0	-0.356327	-4.08803	-0.656739	1.97162	0.0917298	-0.00562398	0.000361017
	1	-0.226101	-0.917913	3.6931	-2.60154	-0.0151908	0.000440104	0
	2	0.113329	0.144452	-1.02752	0.765038	0.00471862	0	0
	3	-0.0169861	-0.00891757	0.120924	-0.0937082			
10000	0	-0.501932	-4.2762	-4.66126	4.82568	0.0437964	-0.00438208	0.000279217
	1	-0.414819	-0.268795	3.39228	-2.76796	-0.0116649	0.000401383	0
	2	0.20055	-0.191008	-0.789481	0.778009	0.00386879	0	0
	3	-0.0244951	0.0409813	0.0816163	-0.0921739			
18000	0	-0.334154	-3.47745	-0.685479	1.70815	0.119294	-0.0064136	0.000412255
	1	-0.107732	-1.3199	4.03758	-2.65854	-0.0172609	0.000467475	0
	2	0.0550908	0.316047	-1.13213	0.749172	0.00519396	0	0
	3	-0.00841382	-0.0305541	0.127307	-0.0853786			

Table 5 Constants of the model $a_{\lambda,i,j}$ and $b_{\lambda,i,j}$ (see appendix 2)

wavelength [nm]	estimated reflectance R_S		estimated reflectance R_D	
	systematic errors $\langle \varepsilon_{R_S} \rangle$	statistical errors $\sigma_{\varepsilon, R_S}$	systematic errors $\langle \varepsilon_{R_D} \rangle$	statistical errors $\sigma_{\varepsilon, R_D}$
350	0.000338	0.0264	0.00101	0.0391
480	0.000338	0.0268	0.00102	0.0393
680	0.000337	0.0264	0.00106	0.0403
2600	0.000356	0.0274	0.00119	0.043
2740	0.0005	0.0324	0.0024	0.0628
3070	0.000249	0.0226	0.00051	0.0264
10000	0.00134	0.0515	0.00189	0.0555
18000	0.000203	0.0205	0.000361	0.0218
total	0.000458	0.0301	0.00118	0.042

Table 6 Systematic and statistical errors of estimated reflectances R_S and R_D where $\langle \varepsilon_{R_S} \rangle$ is the mean value of

$$\varepsilon_{R_S} = \frac{(\varepsilon_{R_S,\text{ estimated}} - \varepsilon_{R_S,\text{ model}})}{\varepsilon_{R_S,\text{ model}}, \sigma_{\varepsilon, R_A}}, \; \sigma_{\varepsilon, R_S} \text{ is the standard deviation of } \varepsilon_{R_S} \text{ and likewise for} \varepsilon_{R_{DS}}$$

wavelength [nm]	a_1 [m^{3}mg^{-1}]	a_2 [m^{3}mg^{-1}]	A_1 [m^{2}mg^{-1}]	A_2 [m^{2}mg^{-1}]	$k_{d,i}$ [m^{2}mg^{-1}]	$k_{c,j}$ [m^{2}mg^{-1}]	K_w* [m^{-1}]
400	0.441	1.94	0.141	0.0531	0.0675	0.0251	0.0209
410	0.495	1.83	0.137	0.0720	0.0643	0.0273	0.0197
420	0.531	1.80	0.131	0.0730	0.0626	0.0284	0.0187
430	0.580	1.70	0.119	0.0730	0.0610	0.0309	0.0177
440	0.619	1.70	0.111	0.0733	0.0609	0.0317	0.0176
450	0.550	1.68	0.107	0.0690	0.0569	0.0308	0.0181
460	0.487	1.60	0.0950	0.0685	0.0536	0.0285	0.0189
470	0.500	1.59	0.0970	0.0660	0.0479	0.0265	0.0198
480	0.500	1.47	0.0780	0.0645	0.0462	0.0242	0.0205
490	0.509	1.53	0.0774	0.0610	0.0427	0.0221	0.0230
500	0.610	1.63	0.0672	0.0570	0.0389	0.0197	0.0276
510	0.594	1.85	0.0598	0.0480	0.0363	0.0182	0.0371
520	0.590	2.03	0.0610	0.0390	0.0319	0.0169	0.0473
530	0.693	2.02	0.0573	0.0337	0.0288	0.0144	0.0513
540	0.606	1.93	0.0506	0.0289	0.0285	0.0118	0.0567
550	0.514	1.91	0.0432	0.0217	0.0274	0.0106	0.0640
560	0.465	1.61	0.0425	0.0143	0.0248	0.0100	0.0720
570	0.384	2.57	0.0288	0.0114	0.0240	0.00988	0.0810
580	0.399	3.49	0.0230	0.00820	0.0231	0.00987	0.107
590	0.365	3.60	0.0180	0.00619	0.0231	0.00970	0.143
600	0.333	3.90	0.0171	0.00478	0.0225	0.00944	0.212
610	0.304	3.95	0.0159	0.00337	0.0216	0.00918	0.236
620	0.316	4.03	0.0150	0.00173	0.0225	0.00936	0.264
630	0.421	4.10	0.0183	0.00135	0.0225	0.00944	0.295
640	0.420	5.08	0.0216	0.00058	0.0226	0.0105	0.325
650	0.346	5.40	0.0164	0.00045	0.0236	0.0133	0.343
660	0.348	5.4	0.0141	0	0.0260	0.0190	0.393
670	0.173		0.00939	0	0.0267	0.0230	0.437
675	0.173		0.00436	0	0.0270	0.0255	0.455
680	0.173		0	0	0.0258	0.0246	0.478
690			0	0	0.0190	0.0180	0.535
700			0	0	0.0125	0.0115	0.626
710			0	0	0.0050	0.0044	0.830
720			0	0	0.0016	0.0014	1.178
730			0	0	0.0005	0.0004	1.807
740			0	0	0.00007	0.00007	2.430
750			0	0	0.00001	0.00001	2.510

* for infrared range $K_w(\lambda)$ were calculated based on the $a_w(\lambda)$ taken after Hale and Querry, 1973 (see Table 4))

Table 7 Parameters in the bio-optical classification of seas

estimated properties	systematic error [%]	statistical error [%]	Data number
hourly means of irradiances reaching sea surface: (arithmetic statistics)			
total	- 4.9	±43.2	375
UV+VIS	- 3.7	±43.0	375
IR	- 4.8	±48.2	375
Daily fluxes of solar irradiation reaching sea surface: (arithmetic statistics)			
total	- 5.9	±14.1	22
UV+VIS	- 6.6	±14.1	22
IR	- 5.1	±14.6	22
Irradiance attenuation coefficients in the sea (logarithmic statistics)	+4.37	-19 +34.4	ca 4700
total daily primary production in water column	+2.0	-44 +77	177

Table 8 Errors of the models

| Site 1 | | | | | | | | | |
Month	n	t_1 [°C]	p [hPa]	e	v [ms⁻¹]	WD	$\bar{H}$ [m]	t_0 [°C]	C_a [mgm⁻³]
January	0.92	2.3	1015.3	0.852	7	W	0.5	3.9	0.60
February	0.75	0.0	1014.5	0.846	6	W	0.5	2.3	0.53
March	0.72	0.6	1014.3	0.818	7	E	0.6	2.3	0.54
April	0.59	4.5	1013.2	0.820	5	W	0.4	3.7	3.02
May	0.55	7.7	1015.6	0.799	5	SW	0.4	6.4	2.54
June	0.49	14.3	1014.7	0.798	5	NE	0.6	12.7	1.72
July	0.62	15.6	1013.6	0.826	6	W	0.5	15.3	2.04
August	0.59	17.1	1014.4	0.834	5	W	0.4	17.1	2.11
September	0.66	12.7	1015.2	0.830	8	E	0.6	13.2	2.02
October	0.78	10.5	1016.1	0.852	6	W	0.5	12.1	2.99
November	0.84	5.8	1011.8	0.857	10	SW	0.8	7.8	1.99
December	0.91	4.6	1013.0	0.860	5	W	0.4	6.2	0.86
Site 2									
Month	n	t_1 [°C]	p [hPa]	e	v [ms⁻¹]	WD	$\bar{H}$ [m]	t_0 [°C]	C_a [mgm⁻³]
January	0.91	0.3	1015.3	0.872	6	SW	0.3	3.3	0.35
February	0.71	-0.1	1015.4	0.868	7	W	0.5	2.1	0.34
March	0.66	2.9	1015.6	0.836	6	E	0.3	2.4	0.65
April	0.66	5.0	1013.9	0.837	5	NE	0.4	3.9	5.36
May	0.45	9.4	1016.1	0.821	5	NE	0.4	8.2	4.51
June	0.68	14.0	1015.0	0.800	6	W	0.4	13.5	1.79
July	0.60	16.3	1013.3	0.822	5	N	0.7	16.4	3.11
August	0.61	16.9	1014.2	0.828	6	NE	0.4	17.7	2.57
September	0.68	14.2	1015.7	0.831	7	S	0.3	15.4	2.56
October	0.65	10.5	1016.4	0.857	5	E	0.3	12.8	1.99
November	0.81	6.0	1013.7	0.873	8	S	0.3	9.4	2.35
December	0.84	3.8	1013.2	0.879	10	SW	0.6	6.2	0.90
Site 3									
Month	n	t_1 [°C]	p [hPa]	e	v [ms⁻¹]	WD	$\bar{H}$ [m]	t_0 [°C]	C_a [mgm⁻³]
January	0.86	0.3	1015.3	0.872	6	SE	0.2	2.7	0.92
February	0.78	-0.1	1015.4	0.868	6	S	0.2	1.9	1.24
March	0.62	2.9	1015.6	0.836	6	E	0.4	2.4	4.25
April	0.65	5.7	1013.9	0.837	5	NE	0.4	4.7	9.00
May	0.51	10.6	1016.1	0.821	5	NE	0.4	9.3	6.74
June	0.63	14.8	1015.0	0.800	5	W	0.3	14.1	3.52
July	0.66	16.1	1013.3	0.822	5	N	0.6	16.3	4.30
August	0.61	16.9	1014.2	0.828	6	NE	0.4	18.1	2.93
September	0.66	14.1	1015.7	0.831	7	SW	0.2	15.4	2.70
October	0.64	9.8	1016.4	0.857	5	SE	0.2	12.5	2.33
November	0.78	4.9	1013.7	0.873	8	S	0.2	8.4	1.45
December	0.77	2.5	1013.2	0.879	9	SW	0.3	5.5	1.02

Table 9 The set of model input data: n−cloud cover (range 0–1), t_1−air temperature over sea surface, p−atmospheric pressure, e−relative humidity over sea surface (range 0–1), v−wind speed, WD−wind direction, $\bar{H}$−mean height of wind waves, t_0−surface water temperature, C_a−surface chlorophyll "a" concentration.

Open Sea Station (Site 1)

Month	1	2+2'	3	4	5	6	7	8	9	10	11	12	13	14	Balance 9-14
1	5.79E+6	4.82E+6	4.37E+4	9.25E+5	9.68E+5	5.10E+4	9.17E+5	3.07E+3	9.14E+5	6.49E+5	2.35E+5	2.99E+4	1.94E+3	2.99E+6	-2.08E+6
2	1.15E+7	7.61E+6	9.87E+5	2.86E+6	3.85E+6	2.52E+5	3.60E+6	1.20E+4	3.58E+6	2.54E+6	9.32E+5	1.13E+5	7.06E+3	4.37E+6	-7.87E+5
3	1.96E+7	1.17E+7	2.97E+6	4.96E+6	7.92E+6	4.41E+5	7.48E+6	2.50E+4	7.45E+6	5.23E+6	1.99E+6	2.41E+5	1.51E+4	4.30E+6	3.15E+6
4	2.96E+7	1.46E+7	7.85E+6	7.16E+6	1.50E+7	7.20E+5	1.43E+7	4.79E+4	1.43E+7	9.45E+6	3.78E+6	1.02E+6	9.06E+4	4.22E+6	1.00E+7
5	3.75E+7	1.73E+7	1.16E+7	8.60E+6	2.02E+7	8.50E+5	1.93E+7	1.33E+5	1.92E+7	1.28E+7	5.19E+6	1.22E+6	1.06E+5	4.15E+6	1.50E+7
6	4.15E+7	1.76E+7	1.47E+7	9.17E+6	2.39E+7	9.90E+5	2.29E+7	2.03E+5	2.27E+7	1.53E+7	6.26E+6	1.15E+6	9.37E+4	4.36E+6	1.83E+7
7	3.99E+7	1.94E+7	1.10E+7	9.43E+6	2.05E+7	8.60E+5	1.96E+7	1.82E+5	1.94E+7	1.28E+7	5.49E+6	1.09E+6	9.21E+4	3.97E+6	1.55E+7
8	3.33E+7	1.62E+7	9.23E+6	7.95E+6	1.72E+7	7.80E+5	1.64E+7	1.33E+5	1.63E+7	1.08E+7	4.56E+6	9.22E+5	7.80E+4	4.33E+6	1.19E+7
9	2.41E+7	1.38E+7	4.56E+6	5.72E+6	1.03E+7	5.22E+5	9.76E+6	5.31E+4	9.70E+6	6.47E+6	2.70E+6	5.34E+5	4.50E+4	4.27E+6	5.43E+6
10	1.48E+7	1.06E+7	1.14E+6	3.10E+6	4.24E+6	2.46E+5	4.00E+6	2.18E+4	3.98E+6	2.61E+6	1.08E+6	2.86E+5	2.56E+4	4.13E+6	-1.55E+5
11	7.64E+6	6.15E+6	1.73E+5	1.32E+6	1.49E+6	8.80E+4	1.40E+6	7.65E+3	1.40E+6	9.48E+5	3.72E+5	7.63E+4	6.47E+3	3.82E+6	-2.42E+6
12	4.61E+6	3.94E+6	2.15E+4	6.49E+5	6.71E+5	3.50E+4	6.36E+5	3.46E+3	6.32E+5	4.48E+5	1.62E+5	2.30E+4	1.65E+3	3.13E+6	-2.50E+6
Year	8.23E+9	4.38E+9	1.96E+9	1.89E+9	3.85E+9	1.78E+8	3.67E+9	2.52E+7	3.65E+9	2.44E+9	9.99E+8	2.05E+8	1.72E+7	1.46E+9	2.18E+9

Deep of Gdansk (Site 2)

Month	1	2+2'	3	4	5	6	7	8	9	10	11	12	13	14	Balance 9-14
1	6.08E+6	5.01E+6	5.87E+4	1.01E+6	1.07E+6	5.90E+4	1.01E+6	4.17E+3	1.01E+6	7.24E+5	2.56E+5	2.57E+4	1.45E+3	3.55E+6	2.54E+6
2	1.18E+7	7.46E+6	1.25E+6	3.06E+6	4.31E+6	2.91E+5	4.02E+6	1.66E+4	4.00E+6	2.87E+6	1.03E+6	1.02E+5	5.68E+3	4.76E+6	7.60E+5
3	1.99E+7	1.09E+7	3.81E+6	5.22E+6	9.03E+6	5.28E+5	8.50E+6	3.51E+4	8.47E+6	5.92E+6	2.25E+6	2.91E+5	1.92E+4	3.90E+6	4.57E+6
4	2.98E+7	1.58E+7	6.74E+6	7.26E+6	1.40E+7	6.60E+5	1.33E+7	8.32E+4	1.33E+7	8.44E+6	3.41E+6	1.40E+6	1.33E+5	3.67E+6	9.59E+6
5	3.76E+7	1.56E+7	1.39E+7	8.19E+6	2.20E+7	9.30E+5	2.11E+7	1.61E+5	2.09E+7	1.36E+7	5.39E+6	1.93E+6	1.80E+5	4.61E+6	1.63E+7
6	4.15E+7	2.20E+7	9.86E+6	9.69E+6	1.95E+7	8.00E+5	1.87E+7	1.56E+5	1.86E+7	1.23E+7	5.29E+6	9.88E+5	8.14E+4	3.74E+6	1.48E+7
7	4.00E+7	1.90E+7	1.16E+7	9.36E+6	2.09E+7	8.80E+5	2.00E+7	1.66E+5	1.99E+7	1.29E+7	5.50E+6	1.46E+6	1.30E+5	4.20E+6	1.57E+7
8	3.35E+7	1.68E+7	8.80E+6	7.94E+6	1.67E+7	7.60E+5	1.60E+7	1.20E+5	1.59E+7	1.04E+7	4.43E+6	1.02E+6	8.90E+4	4.62E+6	1.12E+7
9	2.43E+7	1.44E+7	4.28E+6	5.66E+6	9.94E+6	5.08E+5	9.43E+6	5.71E+4	9.37E+6	6.17E+6	2.61E+6	6.02E+5	5.26E+4	4.54E+6	4.83E+6
10	1.51E+7	9.77E+6	1.95E+6	3.43E+6	5.37E+6	3.40E+5	5.03E+6	3.05E+4	5.00E+6	3.38E+6	1.35E+6	2.69E+5	2.27E+4	5.17E+6	1.68E+5
11	7.93E+6	6.29E+6	2.26E+5	1.42E+6	1.64E+6	1.05E+5	1.54E+6	9.31E+3	1.53E+6	1.03E+6	4.06E+5	9.27E+4	8.07E+3	4.55E+6	-3.02E+6
12	4.88E+6	4.01E+6	5.56E+4	8.16E+5	8.71E+5	4.94E+4	8.22E+5	4.97E+3	8.17E+5	5.78E+5	2.09E+5	3.02E+4	2.18E+3	3.90E+6	3.08E+6
Year	8.31E+9	4.48E+9	1.91E+9	1.92E+9	3.83E+9	1.80E+8	3.65E+9	2.58E+7	3.63E+9	2.39E+9	9.81E+8	2.51E+8	2.22E+7	1.56E+9	2.07E+9

Gdansk Bay (Site 3)

Month	1	2+2'	3	4	5	6	7	8	9	10	11	12	13	14	Balance 9-14
1	6.22E+6	4.94E+6	1.09E+5	1.17E+6	1.28E+6	7.90E+4	1.20E+6	3.65E+3	1.20E+6	8.40E+5	3.10E+5	4.58E+4	3.32E+3	3.68E+6	-2.48E+6
2	1.19E+7	8.11E+6	9.27E+5	2.88E+6	3.81E+6	2.53E+5	3.56E+6	1.08E+4	3.55E+6	2.44E+6	9.50E+5	1.56E+5	1.21E+4	4.03E+6	-4.84E+5
3	2.01E+7	1.04E+7	4.33E+6	5.30E+6	9.63E+6	5.62E+5	9.07E+6	5.35E+4	9.01E+6	5.89E+6	2.31E+6	8.12E+5	7.54E+4	4.12E+6	4.89E+6
4	2.99E+7	1.57E+7	6.97E+6	7.28E+6	1.42E+7	6.60E+5	1.36E+7	1.08E+5	1.35E+7	8.22E+6	3.35E+6	1.90E+6	1.88E+5	3.84E+6	9.63E+6
5	3.77E+7	1.66E+7	1.26E+7	8.47E+6	2.11E+7	8.90E+5	2.02E+7	1.87E+5	2.00E+7	1.26E+7	5.03E+6	2.39E+6	2.31E+5	4.45E+6	1.55E+7
6	4.16E+7	2.07E+7	1.12E+7	9.64E+6	2.09E+7	8.60E+5	2.00E+7	1.95E+5	1.98E+7	1.28E+7	5.43E+6	1.60E+6	1.45E+5	3.98E+6	1.58E+7
7	4.00E+7	2.05E+7	1.01E+7	9.45E+6	1.95E+7	8.20E+5	1.87E+7	1.77E+5	1.85E+7	1.17E+7	5.04E+6	1.71E+6	1.59E+5	4.03E+6	1.45E+7
8	3.36E+7	1.68E+7	8.85E+6	7.95E+6	1.68E+7	7.50E+5	1.61E+7	1.34E+5	1.59E+7	1.04E+7	4.42E+6	1.12E+6	9.92E+4	4.81E+6	1.11E+7
9	2.44E+7	1.41E+7	4.59E+6	5.72E+6	1.03E+7	5.31E+5	9.78E+6	6.35E+4	9.72E+6	6.39E+6	2.68E+6	6.44E+5	5.66E+4	4.80E+6	4.92E+6
10	1.53E+7	9.75E+6	2.06E+6	3.48E+6	5.54E+6	3.56E+5	5.18E+6	3.36E+4	5.15E+6	3.46E+6	1.38E+6	3.05E+5	2.63E+4	5.40E+6	-2.54E+5
11	8.08E+6	6.27E+6	2.90E+5	1.52E+6	1.81E+6	1.22E+5	1.69E+6	1.10E+4	1.68E+6	1.16E+6	4.45E+5	7.65E+4	6.13E+3	4.77E+6	-3.09E+6
12	5.02E+6	3.96E+6	1.04E+5	9.58E+5	1.06E+6	7.00E+4	9.92E+5	6.44E+3	9.86E+5	6.97E+5	2.51E+5	3.79E+4	2.82E+3	4.57E+6	-3.58E+6
Year	8.35E+9	4.50E+9	1.90E+9	1.95E+9	3.85E+9	1.82E+8	3.67E+9	3.01E+7	3.63E+9	2.34E+9	9.65E+8	3.30E+8	3.07E+7	1.60E+9	2.03E+9

Table 10 Radiation budget and its elements. Monthly means of daily totals $[Jm^{-2}day^{-1}]$ and annual sums $[Jm^{-2}year^{-1}]$. Numbers in the header correspond to the fluxes' numbers given in Figure 1

Month:	1	2	3	4	5	6	7	8	9	10	11	12	year
S1	0.423	0.407	0.423	1.362	1.179	0.877	0.978	0.989	0.947	1.280	0.916	0.520	0.986
S2	0.288	0.296	0.477	2.110	1.854	0.902	1.354	1.154	1.140	0.925	1.045	0.534	1.274
S3	0.559	0.700	1.771	2.933	2.464	1.515	1.760	1.281	1.188	1.044	0.728	0.579	1.755

Table 11 Values of photosynthetic index, ε_{TOT} [%], e.g. ratio of Photosynthetically Stored Radiation to Photosynthetically Available Radiation

Numerical study on the reducing influence of ice on water pile–up in Bothnian Bay

Zhanhai Zhang and Matti Lepparanta

Introduction

The aim of this work is to examine the dynamic behaviour of the ice-ocean response on wind force and especially the reducing influence of ice on water pile-up in the Baltic Sea. Also, a goal is to test the possibility to use a coupled ice–ocean dynamic model for predicting sea level changes in wintertime.

In the Baltic Sea, the wind stress is the principal force for the circulation and piling up of water. In winter when large parts of the sea are ice-covered, the motion of the sea is highly affected by the extent and strength of the ice pack. The air stress acting on the moving ice cover transmits energy into the ice–ocean system. A portion of the energy is dissipated through internal ice friction and ridging processes and the remainder is transmitted into the sea. The momentum energy input to the sea is then changed. At conditions of high ice concentration and strength, the mobility of the ice cover rapidly decreases and the energy transferred to the sea from air is therefore strongly prevented.

The reducing influence of ice on the wind-driven water pile-up in the Baltic Sea winter was first reported by Lisitzin (1957). She examined the Kemi–Vaasa water level difference in the Gulf of Bothnia and found that this difference was damped down to 1/3 from ice-free cases in severe ice seasons. This damping is due to internal friction which uses much of the wind energy input in the ice deformation (Lepparanta, 1981). Omstedt and Nyberg (1991) further examined sea level statistics and obtained a maximum ice damping factor of 1/2 for the water level slope.

The role of sea ice in winter time circulation and water pile-up is examined in this work using a coupled ice–ocean dynamics model. The area of study is the Bothnian Bay, the northern basin of the Gulf of Bothnia (Figure 1). In section 2 we describe the ice–ocean model and cases studied in this work. In section 3 simulated results are shown and are compared with the observed data. In addition, the energy budget in the ice–ocean system is discussed.
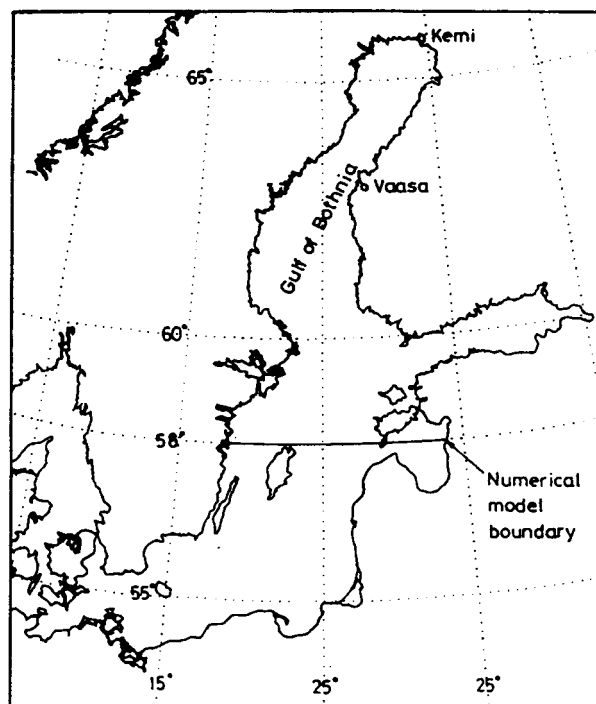
Figure 1 The Gulf of Bothnia, divided (at about the Vaasa level) into the Bay of Bothnia and the Sea of Bothnia

Numerical Model

Model equations

A dynamically coupled ice–ocean model (Zhang and Lepparanta, 1995) is applied to investigate the dynamic behaviour of the ice–ocean system. The ice model is a modified version of Hibler (1979), in which the momentum equation is in the steady state form and a three level description is used for the ice thickness. The ice model equations are

$$\nabla\sigma + A(\overrightarrow{\tau_{ai}} + \overrightarrow{\tau_{wi}}) - \sigma_i hf\overrightarrow{k} \times \overrightarrow{V}_i = 0 \tag{1}$$

$$\frac{\partial}{\partial t}(A, h_u, h_d) = -V_i \cdot \nabla(A, h_u h_d) + (\Psi_A, \Psi_u, \Psi_d), 0 \le A \le 1 \tag{2}$$

where $\overrightarrow{V}_i$ indicates the ice velocity,
f is the Coriolis parameter,
$\overrightarrow{k}$ is the unit vector vertically upward,
ρ_i is the ice density,
h the ice thickness,
A the ice compactness,
h_u, h_d are the thicknesses of undeformed and deformed ice, respectively
$A(h_u+h_d)=h$, and
(Ψ_A, Ψ_u, Ψ_d) is the mechanical thickness redistributor

$\nabla\sigma$ is internal ice force (Hibler, 1979), and
$\overrightarrow{\tau_{ai}}, \overrightarrow{\tau_{wi}}$ are stresses of wind and water on ice, usually expressed by the quadratic dependencies on velocities (Zhang and Lepparanta, 1995).

The ocean part is a two-dimensional vertically integrated hydrodynamic model and the governing equations are

$$\frac{d\overrightarrow{V}_w}{dt} + f\overrightarrow{k} \times \overrightarrow{V}_w = -g\nabla\zeta + \frac{1}{\rho_w(H+\zeta)}[(1-A)\overrightarrow{\tau_{aw}} - A\overrightarrow{\tau_{wi}} - \overrightarrow{\tau_b}] \tag{3}$$

$$\frac{\partial\zeta}{\partial t} + \nabla[(H+\zeta)\overrightarrow{V}_w] = 0 \tag{4}$$

where $\overrightarrow{V}_w$ is vertically integrated current velocity of the ocean,
ζ is the elevation of free surface,
H is the water depth,
$\overrightarrow{\tau_{aw}}$ is the wind stress on the water (Garratt, 1977) and
$\overrightarrow{\tau_b}$ is the bottom friction stress.
Note that $\overrightarrow{V}_w$ is now the vertically integrated average current velocity.

The coupling between ice and ocean is described by the tangential stress on the ice/water interface which in the two-dimensional case is

$$\overrightarrow{\tau_{wi}} = \rho_w C_{wi} |\overrightarrow{V_w} - \overrightarrow{V_i}| [\cos\theta(\overrightarrow{V_w} - \overrightarrow{V_i}) + \sin\theta\overrightarrow{k}(\overrightarrow{V_w} - \overrightarrow{V_i})] \tag{5}$$

where C_{wi} is the ice–water drag coefficient, and
θ is the turning angle in the water (Lepparanta and Omstedt, 1990).

Note that $\overrightarrow{\tau_{wi}}$ drives the ice while $-\overrightarrow{\tau_{wi}}$ drives the sea.

The open sea boundary is fixed along the 58°N latitude (see Figure 1). In the ice model, at the land boundary the ice velocity and mass are zero, and the velocity of fast ice is taken as zero and its concentration is one. In the ocean model, on the coast the normal velocity is zero.

The spatial discretisation of the model is made in Arakawa's 'B' and 'C' grid configurations for the ice and ocean models, respectively. The grid size is 10 nautical miles, and the time-steps are 6 hours and half hour, respectively. The initial velocities and the sea level elevation are zero. The numerical solution of the model is obtained using a finite-

difference technique. When integrating the oceanic part, the ice variables are kept fixed and vice versa. The details of numerical methods are found in Hibler (1979) and Zhang and Lepparanta (1995).

Cases

Studied cases with strong wind were simulated during the periods of 25 February to l March 1982 and 1 to 5 March 1986. The initial ice data consisted of compactness and thickness (see Figure 2) obtained from the ice maps of the Finnish Institute of Marine Research (FIMR, 1982, 1986). The ice almost covered the Bothnian Bay and Sea and the fast ice covered the skerries along the coasts. The wind fields were based on estimates of regional surface wind (10 regions in the Northern Baltic Sea) given by the Finnish Meteorological Institute (FMI). In case 1, strong southerly winds were dominant and northerly and southerly winds prevailed alternately in case 2. The averaged wind speed and direction of both cases in the Bothnian Bay is showed in Figure 3. The sea level data are hourly values from the FIMR stations at Kemi and Vaasa.
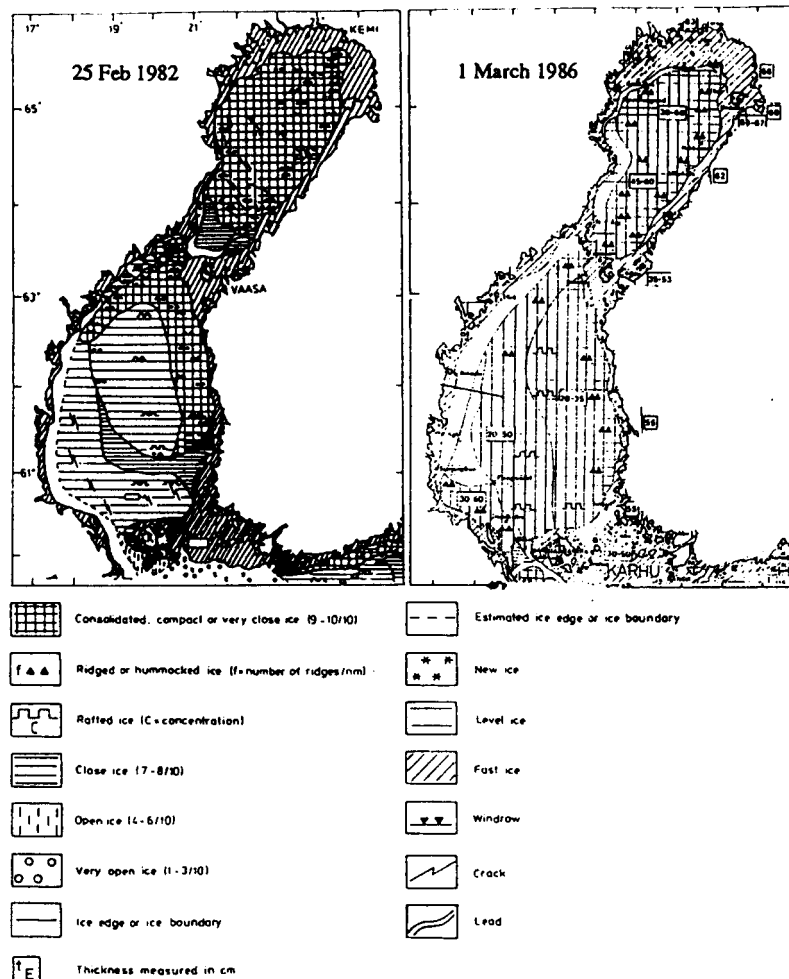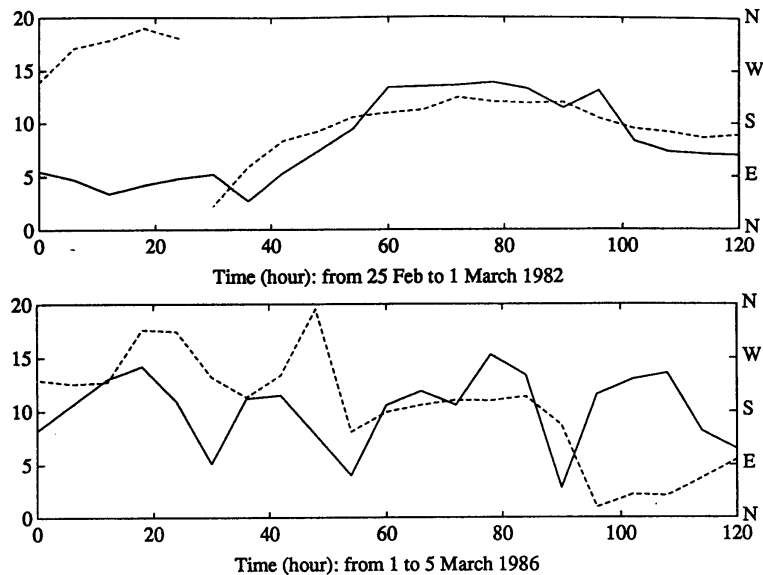

Figure 2 The initial ice situations in the Gulf of Bothnia for the two study cases

Figure 3 Wind speed (solid line) and direction (dashed line) for the two study cases

Model runs were performed with the full coupled ice−ocean model and, for comparisons, with an "ice-free" model where the ice cover was totally ignored. The difference between these two kind of model runs gives information about modifications due to the ice on circulation and sea level changes.

Results and discussion

The calculations for the water pile-up between Kemi and Vaasa (Figure 4) agrees quite well with the observations while the ice-free model shows considerably different output. The reducing influence of the ice on water pile-up is thus seen clearly. The influence is remarkable for strong wind s but not noticeable for weak winds. The ice-caused slope reduction factor (ζ_i/ζ, ζ_i is the elevation in an ice-covered situation) was 0.28 in case 1 and was 0.24 in case 2, a bit stronger than the Lisitzin's factor of 1/3 (averaged value for February and March). Also, the results illustrate that the coupled model is suitable for the winter sea level calculation.

The influence of sea ice on current fields was pronounced. The model velocity fields from case 1, averaged for the strong wind period (24 hours), are given in Figure 5. It is seen that the speed is decreased by a factor of five when the ice cover is included. Also the current direction is modified by the ice. The maximum damping in the current is found in the fast ice areas.
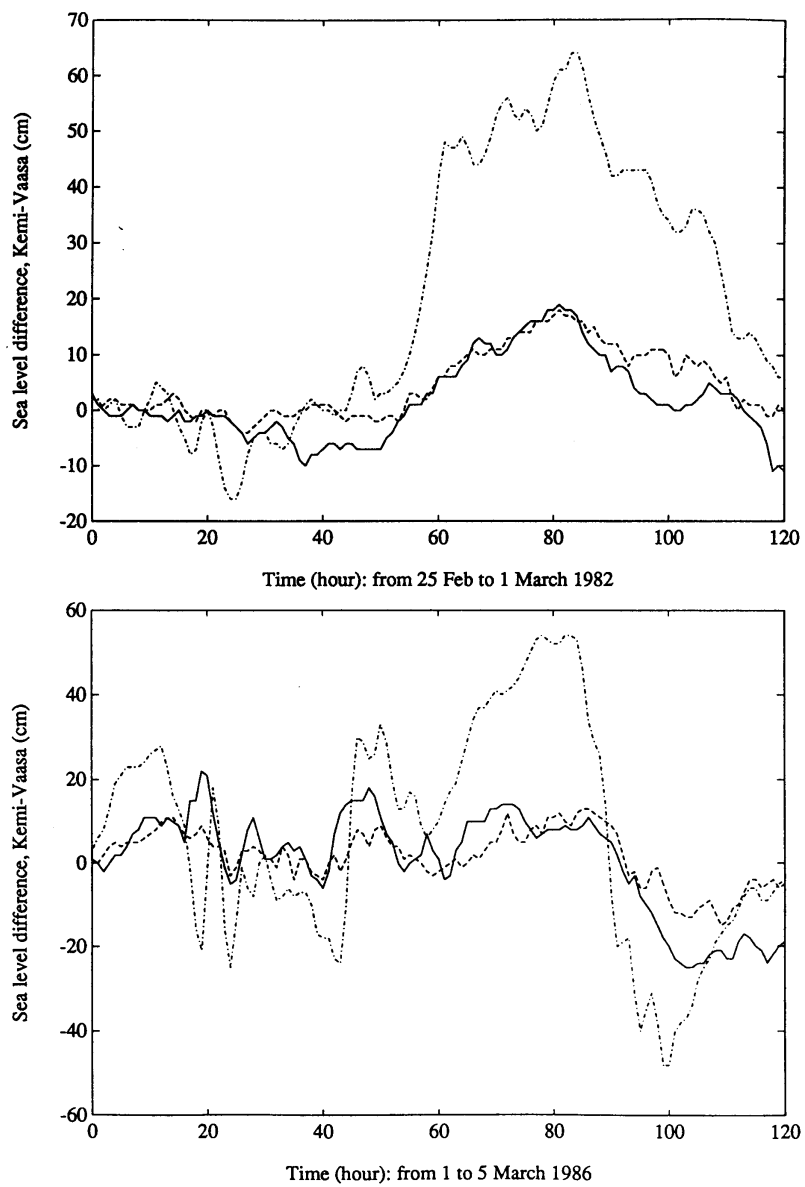
Figure 4 Time series of the water pile-up between Kemi and Vaasa. The solid line indicates observed data, the dashed line is from the coupled model and the dash-dot line is from the ice-free model.
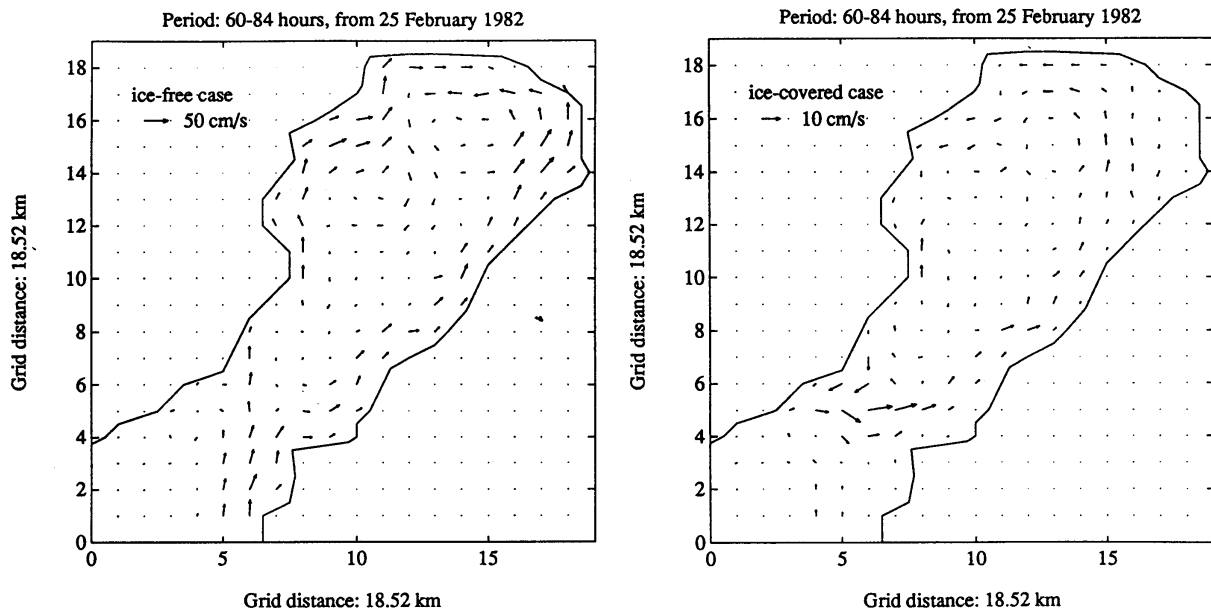
**Figure 5** The depth-averaged current velocity in the Bay of Bothnia in case 1. The velocities are means over the strongest winds period (24 hours)

The spectra of time series of the water pile-up were calculated, and the result for case 1 is shown in Figure 6. The spectral density peaks at low frequencies; over 95% of the total variance is at less than 0.04 cycles per hour (cph) ≈ 1 cycle per day. It can be seen that the agreement between the coupled model and the observed data is quite good. The spectral level decreases substantially due to the presence of the ice.
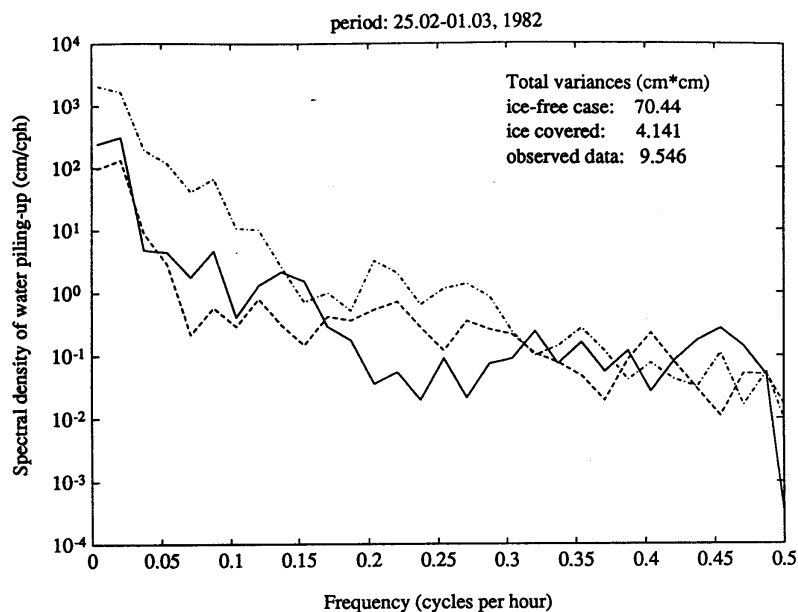
Figure 6 The spectra of the water pile-up between Kemi and Vaasa (case 1). The solid line indicates observed data, the dashed line is from the coupled model and the dash-dot line is from the ice-free model.

To illustrate how the energy from wind stress can be dissipated into the ice–ocean coupled system, attention is turned to examine energy balance. Firstly, let us linearise the ocean model, then multiply the equations (3) and (4) scalarly with $\rho_w H \vec{V}_w$ and $\rho_w g \zeta$, respectively. Furthermore, averaging over a finite area, the equation of the energy balance for the ocean part is obtained

$$\frac{\partial}{\partial t}(E_p + E_k) = E_{\underset{w}{a}} + E_{obp} - E_{\underset{w}{i}} - E_{bot} \tag{6}$$

where the left-hand side indicates the rate of change of mechanical energy averaged over the area, on the right-hand side, the first terms denote the power input from wind into the ocean, the second indicates the horizontal flux of the power via open sea boundary, the third represents the power done on the ocean by ice/ocean interface stress, and the fourth is the power dissipated by ocean bottom friction.

An equation expressing the energy balance for the ice cover has been derived by Coon and Pritchard (1979) in a general form

$$E_{\underset{i}{a}} - E_{\underset{i}{w}} + E_f - E_d = 0 \tag{7}$$

where each term indicates an average of power over the finite area, the first term represents the power input from wind, the second gives the rate of work done on the ice by ice/ocean stress, the third is the rate at which work is done on the boundary and the fourth indicates the energy that is dissipated or stored in the ice cover. The signs in equation (6) and (7) have been chosen so that the terms are positive.

We select the Bothnian Bay as the finite area and the open boundary locates at 65° N. Integrating equations (6) and (7) over the strong wind period (24 hours) in case 1, we gain the quantitative calculations of the energies. Table 1 and Table 2 show the results of ice-free and ice-covered situation, respectively. It is seen that about half of total input energy was dissipated by the bottom friction, and 23% and 12% were transferred to change of the potential and kinetic energies in the ice-free situation. The change of potential energy was large than that of kinetic energy. The deviation (13%) of the energy between input and output may be due to omitting the nonlinear term in the ocean model.

Energy input		Change of mechanical energy		Energy dissi-pation
$E_{a/w}$	E_{obd}	E_p	E_k	E_{bot}
2473	335	653	327	1585
E_{inp}		divided by E_{inp}		
2808		23%	12%	56%

Table 1 Calculated energy budget for ice-free situation in case 1 (unit: Jm^{-2})

Energy input into water		Change of mechanical energy		Energy dissipation		Energy input into ice	
$E_{a/w}$	E_{obd}	E_p	E_k	E_{bot}	$E_{i/w}$	$E_{a/i}$	$E_{w/i}$
65	43	56	10	17	21	3300	1512
E_{inp}		divided by E_{inp}				$E_{w/i}/E_{a/i}$	
108		52%	9%	16%	19%	46%	

Table 2 Calculated energy budget for ice-covered situation in case 1 (unit: Jm^{-2})

The energy budget in the ice-covered situation (Table 2) reveals that much less energy (4% of ice-free value) was directly input into the region from the air and the open boundary. It should be noted that the change of the mechanical (potential and kinetic) energy of the ocean was substantially decreased compared with the ice-free situation. On the other hand, it is seen that 46% of the energy transmitted from the atmosphere to the ice cover was lost due to the ocean drag. In present cases, because no work is done on the land boundary and the horizontal flux of the ice at the open boundary was almost negligible (because of the presence of fast ice there, the open area of the sea is quite narrow), the term E_f then can be omitted. Thus the difference $E_d = E_{\underset{i}{a}} - E_{\underset{i}{w}}$ indicates the energy dissipated by the ice deformation.

In other words, all the energy in the ice was dissipated since it cannot be transmitted across the boundaries.

Conclusions

The influence of sea ice on wind-driven sea level variations has been examined. A coupled ice−ocean model was used to simulate the evolution of the sea level in various ice and wind forcing situations.

The results show that variations in the water pile-up in the Bay of Bothnia are strongly suppressed in winter due to the presence of ice. The results agree with observations fairly well. It has been clear that the ice cover reduces the water pile-up variations particularly at low frequencies (less than 0.04 cph). This reducing influence is related to the strength of the ice cover, i.e. ice compactness and thickness. In the present cases the sea surface slope may drop to less than 1/3 of the ice-free value in similar wind conditions. Besides reducing the sea level changes the ice cover also affects the current field. In the severe ice cage the modelled current speeds were only 20 percent of the ice free values. Maximum decrease in current velocity was found in the fast ice areas.

The analysis on the energy budget indicates that the change of the mechanical energy of the ocean was substantially decreased when the ice cover was presence. The energy transmitted from the atmosphere to the ice was dissipated in two ways, a portion of it (a little bit more than half) was lost in the ice deformation and the remainder was transmitted into the ocean.

Acknowledgements

References

Coon, M.D. and Pritchard, R.S., 1979. Mechanical energy considerations in sea−ice dynamics, J. Glacio., 24(9), 377−389.

FIMR, 1982, 1986. Ice charts over the Baltic Sea. Published twice a week, Finnish Institute of Marine Research, Helsinki.

Garratt, J.R., 1977. Review of drag coefficients over oceans and continents. Mon. Wea. Rev., 105,915−929.

Hibler, W.D. III, 1979. A dynamic thermodynamic sea ice model. J. Phys. Oceanogr., 9(4),815−846.

Lepparanta, M., 1981. On the structure and mechanics of pack ice in the Bothnian Bay. Finnish Marine Research, 248, p. 3−86.

Lepparanta, M. and Hibler, W.D. III, 1985. The role of plastic ice interaction in marginal ice zone dynamics. J. Geophys. Res. 90(C6), 11899−11909.

Lepparanta, M. and Omstedt, A., 1990. Dynamic coupling of sea ice and water for an ice field with free boundaries. Tellus, 42A, 482−495.

Lisitzin, E., 1957. On the reducing influence of sea ice on the pile-up of water due to wind stress. Commentat. Physico-Math. Soc. Sci. Fenn., 20(7), 1−12.

Omstedt, A. and Nyberg, L., 1991. Sea level variations during ice-covered periods in the Baltic Sea. Geophysica, 27(1−2): 41−61.

Zhang, Zh.-h. and Lepparanta, M., 1995: Modeling the influence of ice on sea level variations in the Baltic Sea, Geophysica, 31(2), 31−45.

Zhang, Zh.-h. and Wu, H.-D., 1990: Numerical simulation for storm surges in the China Sea. Marine Forecasts, Vol. 7, No. 2, 10−19 (in Chinese).

Surface mixed-layer dynamics

Christoph Zülicke, Eberhard Hagen, Adolf Stips, Ingo Schuffenhauer and Olaf Hennig

Introduction

Exchange processes between air and sea are essential parameters, which influence both atmospheric and oceanic dynamics. Unfortunately, many numerical approaches use coarse-grained grids, which can not sufficiently resolve the involved spatial temporal scale of contributing processes. Coupled circulation models need their parametrisation for a proper description of associated fluxes on different spatial and temporal scales. To measure associated fluxes, field campaigns were carried out sporadically by research vessels, ships of opportunity, moored and drifting buoys, aircraft, and satellites in different regions during different environmental conditions. In shallow water areas of semi-enclosed basins, like that of the Baltic Sea, we have a wind-driven hydrographic regime, which mainly determines all circulation dynamics and associated fluxes on different spatial and temporal scales.

From the experimental point of view time series of meteorological and hydrological parameters should allow for the adequate description of the mean boundary conditions near the air-sea interface. Friction at this density jump causes turbulent fluctuations in conjunction with increased dissipation. Hence, it is necessary to directly measure such turbulent parameters, which appear to be highly variable at the micro-scale ($\mathrm{cm\,s}^{-1}$) and intermittent at the meso-scale ($\mathrm{m\,hour}^{-1}$).

The turbulent quantities are guided by the turbulent kinetic energy (TKE):

$$E_{\text{turb}} = \frac{\rho}{2}(\langle u'^2 \rangle + \langle v'^2 \rangle + \langle w'^2 \rangle) \tag{1}$$

Here, primes denote fluctuations from the mean value and brackets indicate mean values. The dynamics of the TKE can be expressed for the statistically stationary and horizontally homogeneous model case (Landolt & Boernstein, 1986, NSV/3b page 169 eq. 48a; Monin and Ozmidov, 1982, eq. 2.16; Kraus, 1972, corrected eq. 1.52') using a right-hand coordinate system (x, y, z) respectively velocities (u, v, w), pointing to the East, North and upwards.

$$\frac{\partial E_{\text{turb}}}{\partial t} = -g\langle \rho' w' \rangle - \rho\langle u' w' \rangle \frac{\partial u}{\partial z} - \rho\varepsilon - \frac{\partial j_{E_{turb}}}{\partial z} \tag{2}$$

Here, as usual, *t* denotes the time, *g* the acceleration due to gravity, ρ the density, ν the kinematic viscosity and the dissipation ε is

$$\varepsilon = \nu \left\langle \left(\frac{\partial u'}{\partial z}\right)^2 + \left(\frac{\partial v'}{\partial z}\right)^2 + \left(\frac{\partial w'}{\partial z}\right)^2 \right\rangle$$

According to equation (2), turbulence is changed by buoyancy (first term) and shear (second term) and it is lost through dissipation (third term). Non-local effects are described with the flux term (last item).

Fluctuations lead to mean transports through cross-correlation with the velocity components. In particular we find this for the vertical turbulent transport of density $\langle \rho' w' \rangle$. This quantity corresponds to an transport of buoyancy, i.e. potential energy (cf. first term of eq. (2)). Another aspect is that the vertical flux of density realises diapycnic mixing, which alters the thermodynamic properties of water masses. Turbulent transports can be approximated by diffusion-like ansatzes relating the mean flux to the driving force in the form of the mean gradient:

$$\langle \rho' w' \rangle = -K_\rho \frac{\partial p}{\partial z} \tag{3}$$

Here, the eddy coefficient for density is denoted by K_ρ—for which ansatzes have to be made. On the other hand this quantity can easily be introduced into numerical models.

Considering the net energy balance of the Surface Mixed Layer (SML), bulk formulations of this kinetically mixed slab are useful for a coarse-grained description. The central quantity is the Surface Mixed Layer Depth (SMLD) h_1 which is the distance between the surface and the pycnocline. It is defined as

$$h_1 = \int \frac{E_{\text{turb}}}{E_{\text{turb},1}} dz \tag{4}$$

where $E_{\text{turb},1}$ is the average turbulent kinetic energy in the layer between $z=0$ and $z=-h_1$. In general, such bulk models give information on the time evolution of energy, density, temperature and salt in the SML and the effective coupling with the waters below the pycnocline.

In the following sections we briefly summarise field observations gathered during some cruises, where we attempted to characterise turbulent exchange processes. We give the relevant theoretical background, design the instrumental setup and sampling strategy and derive conclusions for future campaigns.

Turbulent Transport Coefficient

A frequently used approach for the eddy coefficient K_ρ based on the dissipation method is recommended by Peters *et al.*, (1978):

$$K_\rho = \gamma_{\text{mix}} \varepsilon N^{-2} \tag{5}$$

with the empirically introduced mixing intensity $\gamma_{\text{mix}}=0.2$. Further, the variations in the transport coefficient K_ρ are related to the non-dimensional Richardson number:

$$Ri = N^2 \left(\frac{\partial \rho}{\partial z} \right) \tag{6}$$

as a measure of the strength of shear in relation to shear. This way, the turbulent fluctuations are parametrised through mean values only:

$$\langle \rho' w' \rangle = -K_\rho(Ri) \frac{\partial \rho}{\partial z} \tag{7}$$

The database was acquired during the GOBEX expedition "GX950307.AVH" (07.03–17.03.95) of the Institute for Baltic Sea Research Warnemünde in cooperation with the Institute for Remote Sensing Applications (Ispra). Several dissipation profiles were obtained offboard the R/V "Professor Albrecht Penck" accompanied by meteorological and hydrographic measurements including a shallow water mooring system (for more details see Zülicke *et al.*, 1996). In Table 1 we indicate the coordinates of the selected time series.

Station	Position (Deg)	Time (UTC)	Time (DOY)	Depth (m)
R6B	54.3980 N 13.09867 E	16.03.95–05:45 16.03.95–16:10	75.239583– 75.673608	18

Table 1 R6B station parameters of the cruise GX950307.AVH

This station was located at the North-West of the Rügen island. During most of the time the wind was blowing from North-North-East between 4 and 10 ms^{-1} and the ship was anchored in the wind shadow of the island.

The vertical profiles of dissipation and CTD were first projected onto a 1 metre/1 hour grid. Based on this, at each grid point the transport coefficient was calculated according to equation (5). The time series is shown in Figure 1.

In Table 2, 10-hour average values over the bulk of the surface near layer ($z=-4.5 - -10.5$ m) are represented. The notation for this bulk average is:

$$\langle K_\rho \rangle = \langle \gamma_{\text{mix}} \varepsilon N^{-2} \rangle_{\text{bulk}} \tag{8}$$
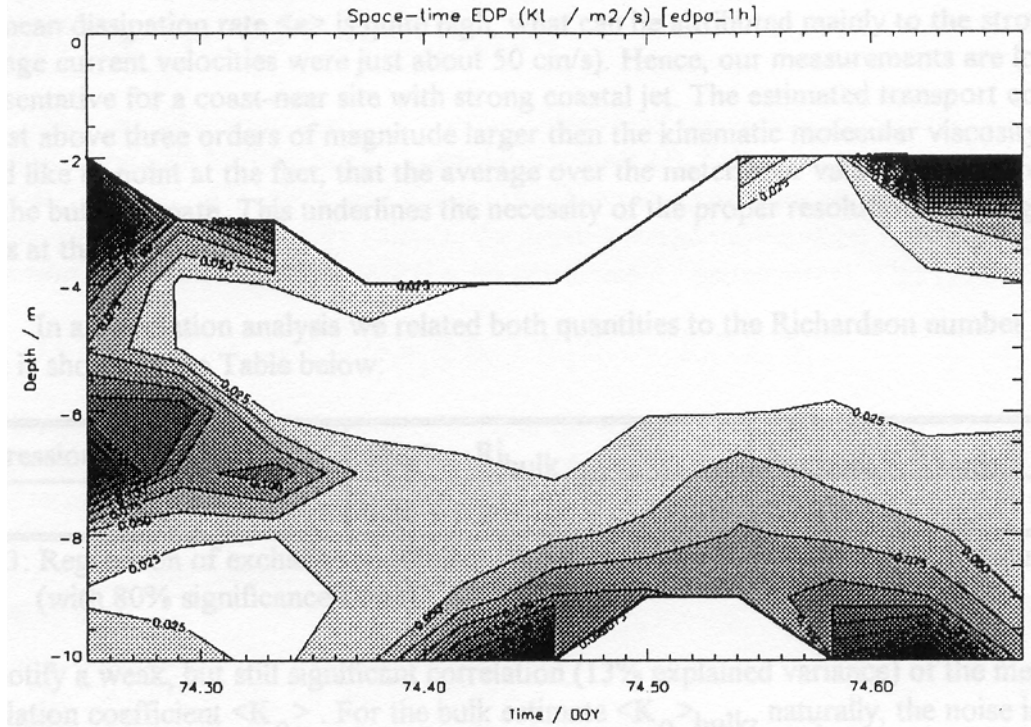
in contrast to the bulk estimate:

$$\langle K_\rho \rangle_{\text{bulk}} = \gamma_{\text{mix}} \langle \varepsilon \rangle_{\text{bulk}} \langle N^{-2} \rangle_{\text{bulk}} \tag{9}$$

which is based on depth averages or differences.

$\left(\dfrac{\partial u}{\partial z}\right)^2_{\text{bulk}}$ $10^{-3}\,\text{s}^{-2}$	N^{-2}_{bulk} $10^{+3}\,\text{s}^2$	$\dfrac{1}{Ri_{\text{bulk}}}$	$<\varepsilon>$ $10^{-6}\,\text{Wkg}^{-1}$	$<K_\rho>$ $10^{-3}\,\text{m}^2\text{s}^{-1}$	$<K_\rho>_{\text{bulk}}$ $10^{-3}\,\text{m}^2\text{s}^{-1}$
0.90 ± 0.42	1.16 ± 0.14	1.03 ± 0.48	121 ± 26	50.0 ± 15.9	27.4 ± 38.0

Table 2 10-hourly mean values and standard deviations over the depth interval 4.5–10.5 m

Figure 1 Space-time contour plot of exchange coefficient K_ρ: the parameter shown over depth (m) and time (days) is the eddy coefficient for the density K_ρ in contours of $0.025\,\text{m}^2\text{s}^{-1}$. Quite high values (larger than $0.1\,\text{m}^2\text{s}^{-1}$) are characteristic at the beginning; there is an increase again with higher values above 4 and below 6 m in time. The white region at the top corresponds to extremely low density gradients.

The mean dissipation rate $<\varepsilon>$ is quite high, what can be attributed mainly to the strong shear (average current velocities were just about $50\,\text{cm}\,\text{s}^{-1}$). Hence, our measurements are locally representative for a coast-near site with strong coastal jet. The estimated transport coefficients are just above three orders of magnitude larger then the kinematic molecular viscosity. We would like to point out the fact that the average over the metre/hour values is two times larger then the bulk estimate. This underlines the necessity of the proper resolution of energy-rich events at this scale.

In a correlation analysis we related both quantities to the Richardson number Ri. The result is shown in Table 3:

Regression coefficient	$<K_\rho> \sim Ri_{\text{bulk}}$	$K_{\rho,\text{bulk}} \sim Ri_{\text{bulk}}$
r	0.36 ± 0.29	0.68 ± 0.23

Table 3 Regression of exchange coefficient with Richardson number based on 10 hour samples (with 80% significance t-test)

We noticed a weak, but still significant correlation (13% explained variance) of the mean correlation coefficient $<K_\rho>$. For the bulk estimate $<K_\rho>_{\text{bulk}}$, naturally, the noise is suppressed and the correlation is larger (46% explained variance). However, this observation must be interpreted as a hint for energy rich fluctuations, which must be averaged out properly. This requires a time series long enough to cover a number of these events. If we imagine these as connected with baroclinic processes, this translates into some inertia periods (14h), i.e. at least one day.

Surface Mixed Layer Depth

Here, we attempt to discuss the energy balance of the surface mixed layer in conjunction with the Surface Mixed Layer Depth (SMLD). Following the general ideas of Krauss & Turner (1967) (Niiler and Kraus, 1977) we imagine a moving homogeneous slab of the thickness h_1. For the energy balance, we depth-average the equation for the turbulent kinetic energy for the stationary case (i.e. no entrainment/detrainment). This results in:

$$0 \ = \ m_1 u_{*0}^3 + \frac{C_{D1} u_1^3}{3} + \frac{h_1 B_0}{2} + \left(\frac{h_1}{2} - \frac{1}{\gamma}\right) R_0 - \varepsilon_1 h_1 \tag{10}$$

Here, the first term is the production of TKE at the surface by wind and waves (the maximal available mechanic energy flux is given with $m_1=1$; u_{*0} is the surface friction velocity). The second terms produces TKE as well, namely through friction at the pycnocline at the bottom of the SML (in this context a parametrisation of the momentum flux with a drag coefficient CDI$=1.0 \cdot 10^{-3}$ was made). The third term models destabilisation by surface cooling (buoyancy flux):

$$B_0 \ = \ g\left(\frac{\alpha}{c_p \rho} Q_0 - \beta S_0 (E_0 - P_0)\right) \tag{11}$$

The effects of solar radiation are described with the next term:

$$R_0 \ = \ g \frac{\alpha}{c_p \rho} R_{SW0} \tag{12}$$

First we have a destabilising contribution due to the absorption of solar radiation in the bulk of the water leading to a heating there (equivalent to a cooling at the surface) and then the stabilising contribution due to heating over the absorption length l/γ (set to l/γ=10.0 m for later calculations). The last, but not least, item is the energy dissipation with the average rate of ε_1.

The data were acquired by two cruises of the R/V "Alexander von Humboldt" during running GOBEX activities in the Arkona, Bornholm, and Eastern Gotland Basin in March and September, 1994 (cf. Zülicke and Hennig, 1996). Our measurements were carried out in the framework of the sub-project "Baltic Radiation Budget (BARB)", which was jointly organised by the Institute for Baltic Sea Research Warnemünde (IOW) and the Institute for Remote Sensing Applications (IRSA) of the European Research Centre in Spar, Italy, to provide new calibration procedures for remotely sensed data in the Baltic Sea. The acronyms used are tabulated in Table 4 together with timetables and target areas. Obtained data cover standard meteorological parameters in combination with measurements of solar and thermal radiation.

Acronym	GX940301.AVH	GX940913.AVH
Time	01.03.94 – 10.03.94	013.09.94 – 29.09.94
Target region	Arkona Basin Bornholm Basin	Bornholm Basin Gotland Basin

Table 4 Data acronyms, time table, and target areas of the GOBEX sub-project BARB

The surface energy fluxes were estimated from the atmospheric side using standard bulk formulae for meteorological measurements (Landolt and Boernstein). The mean values over the cruises are listed in Table 5.

Parameter / Mean and Standard Deviation	GX940301.AVH	GX940913.AVH
Surface friction velocity u_{*0} (ms^{-1})	0.0139 ± 0.0113	0.0117 ± 0.0118
Surface heat flux Q_0 (Wm^{-2}) (upwards positive; latent and sensible heat and thermal radiation)	30.9 ± 59.2	120.2 ± 71.8
Surface solar radiation flux R_{SW0} (Wm^{-2}) (downwards positive)	50.2 ± 97.7	71.1 ± 116.9

Table 5 Mean values of surface flux quantities

Now we estimate the SMLD from equation (10):

$$h_1 = \frac{\left(m_1 u_{*0}^3 + \frac{C_{D1} u_1^3}{3} - \frac{1}{\gamma} R_0 \right)}{\varepsilon_1 - \frac{1}{2} B_0 - \frac{1}{2} R_0} \tag{13}$$

For this purpose we must make some assumptions on quantities which we have not measured at the mentioned campaigns.

1. We do not have available precipitation measurements P_0. This would have been quite cumbersome to measure and has, on the other hand, small impact in the surface buoyance flux (the temperature contributions are mostly larger then the salt component).

2. The dissipation rate ε_1 was not measured. As a check value we adopt $\varepsilon_1 = 1.0 \cdot 10^{-6} \mathrm{Wkg}^{-1}$.

3. The current velocity u_1 was not measured. We adopt as a largest value the Stokes drift $u_{1,S}$ from the wind speed u_a ($u_{1,S} = 0.03\, u_a$) (Kraus, 1972).

The material constants are listed in the appendix—the result of calculations in Table 6.

Parameter	GX940301.AVH	GX9409I3.AVH
Surface shear production $m_1 u_{*0}^3$ (Wmkg^{-1})	$2.24 \cdot 10^{-6}$	$1.64 \cdot 10^{-6}$
Surface buoyancy B_0 (Wkg^{-1})	$1.24 \cdot 10^{-8}$	$4.83 \cdot 10^{-8}$
Surface solar radiation flux R_0 (Wkg^{-1})	$2.02 \cdot 10^{-8}$	$2.86 \cdot 10^{-8}$
Bulk Shear Production $\frac{C_{D1}}{3} u_{1,S}^3$ (Wmkg^{-1}) ($u_{1,S} = 0.03\, u_a$)	$1.07 \cdot 10^{-5}$	$7.95 \cdot 10^{-6}$
Surface Wind-Mixed Layer Depth h_1' (m) ($u_1 = 0$)	2.1	1.4
Surface Mixed Layer Depth h_1 (m)	10.7	7.9

Table 6 Energy balance of the SML and its depth

According to the stronger winds during the March cruise we have a larger input of surface shear than in September. The thermal properties in both seasons differ as well: the heat losses as well as the solar insulation are larger in September, but the net heat balance (solar heating minus thermal losses) is positive in March (heating) and negative (cooling) in September.

In a first approximation the depth of the wind mixed layer h_1' is calculated (bulk shear neglected due to a resting slab SML model, $u_1 = 0$ in eq. (13)): we find some metres for the depth, a little higher values in March. For a first approximation wind-energy input and dissipation would be sufficient. The second, more complete approximation, includes the current shear in the bulk of the water (ul $<>$ 0 in eq. (13)). As can be seen, the bulk shear contribution is absolutely dominating. We find values for the SMLD, which are experienced in the field. Unfortunately, we can not conduct a direct comparison with directly measured depth of the kinetically mixed layer due to lack of data. However, we point out that the movement of the SML slab is energetically important, the bulk shear may be even dominating. In conclusion, for wind-dominated situations (as we have experienced it in March and September), the SMLD hopefully could be approximated by

$$h_1 \approx \frac{\left(m_1 u_{*0}^3 + \frac{C_{D1}}{3} u_1^3 \right)}{\varepsilon_1} \tag{14}$$

Summary and outlook

We reported on some experimental components, which are jointly necessary to approach the problem of a kinetically active Surface Mixed Layer (SML). The newly introduced component is the directly measured dissipation rate. It is important on the one hand for the estimation of transport coefficients with the dissipation method. On the other hand it is a necessary ingredient for bulk models.

The dissipation measurements were made in near coastal zones. The regime in the bulk of the water was mainly determined by the current shear. However, the background field of stratification influenced the transports as well. Especially in the Baltic vertical gradients both the current as well as in the density field are quite large. This is based on the wind-induced mixing from above and the strong stratification due to riverine input of fresh water and the subduction of salty water from the North Sea. Hence, the Baltic seems to be a good candidate for the test of different flux parametrisations under extreme conditions. Measurements of dissipation, current and density profiles combined with direct measurements of vertical fluxes of density $<w'\rho'>$ at fixed depths should be performed jointly with the observation of the atmospheric parameters.

We may conclude that, with enough data in time, there is a good possibility to estimate turbulent quantities. However, to attribute more distinct short-term and long-term effects to the turbulence and transport variability and to obtain more accurate numeric relations, it is necessary to extend the length of time series to some days (at least some inertia periods). The sampling rate of 15 minutes was appropriate.

References

Kraus, E. B., 1972. Atmosphere-Ocean Interaction. (Clarendon, Oxford).

Kraus, E.B., and Turner. A one-dimensional model of the seasonal thermocline. II: The general theory and its consequences. Tellus 19 (1967) 98−106.

Landolt & Boernstein. Numerical Data and Functional Relationships in Science and Technology (Springer, Berlin).

Monin, A.S., and Ozmidov, R.Y., 1982. Turbulence in the Ocean. (Reidel, Dordrecht).

Niiler, P.P. and Kraus, E.B. One-dimensional models of the upper ocean. in: Modelling and Prediction of the Upper Layers of the Ocean. Proc. NATO Advanced Study Inst. (E.B.Kraus Ed.) (pergamon, Oxford, 1977) 143−172;

Peters, H., Gregg, M.C., and Toole, J.M., 1988. On the parametrisation of equatorial turbulence. J. Geophys. Res. 93, C2, 1199−1218

Zülicke, Ch. and Hennig, O. Surface Energy Fluxes and Mixed Layer Depth. in E. Hagen (Editor): GOBEX Summary Report. Marine Science Reports. Volume 19 (Baltic Sea Research Institute, Warnemünde, 1996) page 92 ff.

Zülicke, Ch., Schuifenhauer, I., and Stips, A. Exchange coefficients and dissipation measurements. in E. Hagen (Editor): GOBEX Summary Report. Marine Science Reports. Volume 19 (Baltic Sea Research Institute, Warnemünde, 1996) page 76 ff.

Appendix

Material constants (Landolt & Boernstein)

Parameter (Landolt & Boernstein)	Baltic Sea (Rheinheimer) (p=0; T=15; S=20)
Isobaric thermal expansion coefficient α (K^{-1})	$1.69 \cdot 10^{-4}$
Isobaric heat capacity c_p (Jkg^{-1}K^{-1})	4069
Density ρ (kgm^{-3})	1014

Towards operational regional satellite oceanography for the Baltic Sea

Serge V. Victorov

Abstract

This paper supports the EuroGOOS objective for space-based information on operational oceanography. The paper provides discussion of the two branches of modern Satellite Oceanography (SO), namely Regional SO and Global SO. Requirements for satellite data for problems of Regional SO are presented. State-of-the-art of Regional SO in the Baltic states is discussed with an emphasis on its operationalisation. Technological and managerial aspects of future development of Operational Regional SO in the Baltic area are briefly discussed. Relevant recommendations on two-level international cooperation are made.

Introduction

In recent years satellite oceanography has obviously shown a tendency to split into two branches, namely Global Satellite Oceanography and Regional Satellite Oceanography. **Regional Satellite Oceanography** is an interdisciplinary (oceanography/remote sensing) science which is based on satellite imagery analysis and deals with processes and phenomena mainly in the seas, coastal zones and separate parts of the ocean, while Global Satellite Oceanography deals mainly with processes and phenomena in the World Ocean as a whole.

There are many differences between the Regional SO and the Global SO. The two differ in:

- Objects and objectives of studies
- Requirements for satellite data (temporal, spatial and spectral), which may lead to different modes of payload operation
- Availability and quality of sea-true in situ data, which may lead to different levels of accuracy of information retrieval in Regional and Global SO
- Algorithms for data processing
- Users
- Formats of output information products, etc.

For comprehensive analysis of the two branches of SO see (Victorov, 1996). Nowadays the **Regional Satellite Oceanography** is focused on:

- Operational marine forecasting
- Monitoring of the marine environment
- Study of water masses dynamics within the water body
- Study of spread of river discharge
- Monitoring of water quality and transfer of pollutants
- Study of biological productivity in local areas
- Complex monitoring of coastal zone
- Study of the interaction between coastal zone and off-shore waters
- Study of ice cover morphology, etc.

Further we will focus on the problems of Regional Satellite Oceanography and its operationalisation.

Regional satellite oceanography: State-of-the-art

It is believed that Regional Satellite Oceanography is capable of providing operational/non-operational information in the following three areas (the concept of these areas is taken from (ESA, 1995):

Mapping and monitoring

- Sea surface wave patterns
- Surface slicks
- Sea-ice extent, type, concentration and thickness
- Sea-ice movement
- Sea surface temperature
- Sea water colour anomalies ('water quality')
- Shallow water bathymetry

Process understanding

- Ocean features (eddies, upwellings, jets, frontal boundaries)
- Sea-ice related processes

Modelling for forecasting

- Regional circulation
- Estuarine processes
- Coastal sediment transport and erosion
- Climate-change-related predictions

A detailed review of the achievements of Regional Satellite Oceanography, including the case study of the Baltic Sea, is given in (Victorov, 1996).

The Steering Committee of the Baltic Marine Science Conference has developed a concept of presentation of papers dealing with the use of satellite data. According to this concept the original contributions with satellite images and relevant charts and schemes were to be presented as posters. This was aimed at providing sufficient time for viewing the imagery and discussion of patterns and features recorded in the imagery between the authors and other participants rather than just a quick look at the images projected on overheads. As a member of the Steering Committee I would like to thank the authors of very interesting posters giving a strong impression of real development of the Baltic Regional Satellite Oceanography in recent years.

Requirements for satellite data

Generalised requirements for satellite data in problems of regional satellite oceanography are presented in Table 1 (Victorov, 1996).

Parameter	Problems	
	General	Local
Dimension of studied area, km	50–1000	1–50
Ground resolution, m	100–1000	20–100
Temporal resolution, h	3–24	3–6

Table 1 Requirements for satellite data

In recent years the issue of "Requirements" has attracted the attention of many science and technology communities, international organisations and their committees and panels.

The right balance between the desired requirements, the real needs—sometimes the dreams —on the one hand, and the realistic capabilities of technology, engineering and informational sciences, on the other hand, was the goal of numerous discussions.

Among others, I would like to mention two sources of information on this subject.

Source 1

Polar Orbiting Satellites and Applications to Marine Meteorology and Oceanography (1996). Report of the CMM-IGOOS-IODE Sub-group on Ocean Satellites and Remote Sensing (OSRS) set up by the Intergovernmental Oceanographic Commission (of UNESCO) and the World Meteorological Organisation.

Along with the overview of requirements for satellite data relevant to some of the GOOS modules, this document contains assessments of the ability of a certain satellite sensor to deliver the data with the characteristics required. Each oceanographic/geophysical parameter is assessed for each instrument type capable of making that measure and the degree to which parameter can address the requirement. These assessments were made for global and **regional** scales. The assessments provide quantitative answers to the question 'how many sensors/satellites do we need to match the requirements sanctioned by WMO and IOC?' and thus clearly show the distance between the real operational satellite oceanography of the 2020s and that of the 1990s.

Source 2

Use of Satellite Data for Environmental Purposes in Europe (1994) Final Report. Scot Conseil and Smith System Engineering Ltd. in conjunction with DGXII-D-4 of the European Commission.

This document presents the requirements for satellite data with an emphasis on environmental issues. It gives qualitative assessments of the sensors capabilities to provide data according to the requirements in the European context.

Detailed analysis of both sources and the comparison of the requirements presented in them, is given in (Victorov, 1996).

What kind of operational satellite oceanography exists in the Baltic area nowadays?

Operational marine applications require rapid processing, interpretation and dissemination of information to regional users. It is recognised that demonstration of the potential to extract information from satellite data is not enough. Relevant infrastructure, technical facilities and services should be and are currently being established in some regional seas. Operational sea-state forecasts are being made available to marine users community. Shipping companies (optimal routing) and oil/gas companies (logistics of seismic surveys, mooring strategies for the connection of oil tankers to riser pipes, large-scale engineering works for offshore operations etc.) are notable here.

Nowadays many research groups and teams are working in the area of the Baltic Regional Satellite Oceanography. In many cases they do not exchange their ideas, approaches and results (or do it with a great delay). The Baltic Marine Science Conferences should provide a platform for these contacts in future. Nevertheless among many other regional seas the Baltic Sea should be considered as an area with advanced operational oceanographic applications of satellite data.

Satellite information is being incorporated into operational **Sea-ice** monitoring and forecasting services and routinely used by ice centres in Sweden, Finland and Russia. ERS SAR-based **Oil-slick** services which are operational in Norway since 1994 (Pedersen *et al.*, 1996) are being developed and integrated with existing services in other countries. Space-based **Algal bloom** monitoring and forecasting services are being developed in the Baltic countries.

In the above mentioned activities the following sensors/satellites are being used in (quasi-) operational mode:

- A VHRR/NOAA—4–6 and more orbits daily
- SAR/ERS-1, -2—depends on cycle

Still gaps exist and will continue to exist in the future for cloudiness and technological reasons. The ways out are:

1. To use models to interpolate between two consequent satellite observations
2. To use operational technologies with satellite data assimilation into models

Strictly speaking, both mean: **Quasi-operational Regional Satellite Oceanography** at best. According to Johannessen *et al.* (1996), "There has, over the last decade, been a rapid development of various data assimilation methods which can be used with ocean and ecosystem models. At present, none of these methods are used operationally". This was a general statement. As for the Baltic Sea the HIROMB (High Resolution Operational Model of the Baltic Sea) (Kleine, 1996) which, according to Funkquist (1996), "has been in a so called preoperational mode since autumn 1995", is probably the most promising one. At least, sea-surface temperature simulation results obtained with this eddy-resolving model will be compared with relevant satellite patterns (Funkquist, 1996).

Future satellites and sensors

What are the prospects for operationalisation of Regional Satellite Oceanography from the satellite/sensors side? Future civilian satellites and sensors (with contribution to operational regional oceanography) are:

ERS-2 1995–2000 with altimeter, scatterometer, SAR (Synthetic Aperture Radar), ATSR (Along-Track Scanning Radiometer)

ENVISAT 1999–2004 with the same advanced instruments: Sltimeter, SAR, ATSR and a new instrument: MERIS (Medium Resolution Imaging Spectrometer)

METOP 2002–2017 with advanced scatterometer

NOAA series with modified scanning radiometers AVHRR/3 (1994–1999) and VIRSR (1997–2000)

RADARSAT (since 1995) is currently providing data on sea state and ice

SeaStar satellite with Sea WiFS colour scanner is expected to be launched in 1997; if not, a similar instrument EOS COLOUR will be launched on EOS satellite in the late 1990s.

Meanwhile ADEOS with another ocean colour instrument OCTS was launched on 18 August 1996.

OKEAN-O missions with real aperture radar RAR and MSU-SK scanner as well as RESURS-O missions with MSU-SK, MSU-E scanners will be continued in the late 1990s.

Though the above list is not complete (for a comprehensive information see Polar ..., 1996), it is obvious that there will be no drastic improvements in terms of operational satellite oceanographic SYSTEM in the next decade. Various pilot operational and quasi-operational single satellites and series of satellites will still complement each other, and it will probably be a difficult task to harmonise data from various sources. Data handling (acquisition, storage, processing, fusion, interpretation, assimilation, dissemination of output informational products) will definitely become a crucial point in the Baltic Regional Satellite Oceanography in the nearest future.

Future: Institutional / Managerial aspects

From the technological point of view, one Centre can provide satellite data acquisition, processing and dissemination of output informational products for the whole Baltic Sea region. It is possible for this Centre to run the sophisticated ocean models (now and in the nearest future) and ecological models (in the distant future) in operational mode. And it probably could be the best option in terms of costs and benefits.

Do we need one or more centres? Will we need one or more centres for the Baltic area in the future united Europe?

Here is an attempt to answer the questions basing on the technical reasons only.

On the regional level

For the open Baltic Sea a single Joint Centre of Operational Oceanography could well provide marine forecasts and other centralised services within the area. The use of standard codes, measuring devices, data processing schemes and standardised output informational products for most oceanographic parameters by the Centre could save both financial and human resources in the Baltic states. Presumably a single Unit of Regional Satellite Oceanography could fit the needs of the Joint Centre of Operational Oceanography. Needless to say that this approach goes in line with the EuroGOOS concept.

On the local level

Broadly speaking, it is up to the local authorities and local users communities to decide whether they should run local operational oceanographic services in the existence of the Joint Centre of Operational Oceanography. It is probably worthwhile to run them if they needs detailed information for some specific purposes, when local in situ data bases and knowledge bases are required, and if tailor-made oceanographic informational products are actually needed.

Examples: ice conditions and water quality in local bays

Interplay between the Regional and the Local levels

Local level operational oceanographic units could provide the Joint Centre of Operational Oceanography with a selected informational products which could be used in the Centre to tune their models and algorithms for the relevant local areas. In its turn the Centre could supply the local operational units with high resolution satellite data for local areas, thus providing integration of local level in situ data with regional level remotely sensed data complemented with local knowledge bases.

Concluding remarks and suggestions

- Current achievements of Joint Centre of Operational Oceanography in the Baltic Sea are encouraging
- **Baltic Operational Satellite Oceanography** exists, though, mainly, in quasi-operational mode
- The level of operationalisation of Joint Centre of Operational Oceanography in the Baltic Sea varies considerably for different oceanographic parameters
- Further progress in satellite sensors and space-based ocean observing systems is needed to meet the requirements of **Regional Operational Satellite Oceanography**
- There is high scientific potential for cooperation in the **Baltic Operational Satellite Oceanography** which is as yet unclaimed.

The Baltic Marine Science community is kindly invited to start discussions aimed at:

- Working out a concept of the Joint Centre of Operational Oceanography in the Baltic Sea
- Working out a concept of joint regional satellite monitoring in the (open) Baltic Sea
- Finding mechanisms for cooperation in the development of methods of satellite monitoring of the Baltic coastal zone (with an emphasis on coastal erosion, sedimentation, shallow water bathymetry, 'water quality')

Acknowledgements

References

ESA, 1995. New Views of the Earth. Scientific Achievements of ERS-1.SP-1176/1, p.152. Funkquist, L., 1996. Modelling of Physical Processes in the Baltic. In: Abstracts of the Baltic Marine Science Conference, (22–26 October, Rønne, Denmark), p.31.

Johannessen, O.M., Bjorgo, E., Petterson, L.H., *et al.*, 1996. Proposed strategy for the use of satellite remote sensing in EuroGOOS. In: Conference Preprints of the First International Conference on EuroGOOS, (7–11 October 1996, The Hague), pp.93–114.

Kleine, E., 1996. HIROMB—a High Resolution Operational Model of the Baltic. In: Abstracts of the Baltic Marine Science Conference, (22–26 October, Rønne, Denmark), pp. 30–31.

Pedersen, J.P., Seljelv, L.G., Bauna, T., *et al.*, 1996. Towards an operational oil spill detection service in the Mediterranean? The Norwegian experience: A pre-operational early warning detection service using ERS SAR data. In: Proc. ERS Thematic Workshop on Oil Pollution Monitoring in the Mediterranean, Frascati, Italy, ESA.

Polar Orbiting Satellites and Applications to Marine Meteorology and Oceanography, 1996. Report of the CMM-IGOOS-IODE Sub-group on Ocean Satellites and Remote Sensing. Marine Meteorology and Related Oceanographic Activities. Report No.34. WMO/TD No.763.

Victorov, S. V., 1996. Regional Satellite Oceanography. Taylor and Francis, London, 312 pp.

Vistula Lagoon water level oscillations: numerical modelling and field data analysis

Irina P. Chubarenko

Introduction

The response of complicated geophysical systems on external actions depends essentially on its own features. The Vistula Lagoon (Baltic Sea) can be considered as a hydrodynamic system, where the level and current oscillations are under external forcing of local wind, Baltic level variations and river drain. Aiming to estimate the influence of external parameters oscillations on the lagoon water body requires determination of its own oscillation characteristics.

The level oscillations in various parts of the aquatory, which appear after the disturbance of the level from the horizontal equilibrium by wind action, were analysed. The comparison between the temporal periodicity of external forcing and the time periods of response in the lagoon level oscillations gave rise to the conclusions both for hierarchy of external forcing factors for different time scales and their energetic significance for hydrodynamic processes in the lagoon.

Methods

The main point of the work presented was to study (with help of numerical modelling) the features of level oscillation processes in Vistula lagoon after instant switch off of the wind action. Numerical model MIKE21 of Danish Hydraulic Institute was used for simulations. The hydrodynamic module of MIKE21 is based on the two-dimensional "shallow water" hydrodynamic equations (MIKE21, 1993). The model was preliminary saturated by real data (bathymetry, river discharges and its positions) and calibrated on the results of a special autumn 1994 field study during the Danish-Russian-Polish project "Vistula lagoon" (Prioritising..., 1998). The results of calibration were as follows: wind friction coefficient—0.0017, bed resistance coefficient—32 $m^{1/3}s^{-1}$, eddy viscosity coefficient—20 m^2s^{-1}. It was concluded after verification of the model that it quite satisfactorily represents not only the current structure and relative level oscillations, but also the absolute values of level variations (Calibration..., 1996).

The bathymetry field was determined in the nodes of a grid with 1 km steps. Water level temporal variations were calculated in six points located at the lagoon coast (Kaliningrad, Baltiysk, Krasnoflotskoe, Nowa Paslenka, Tolkmicko, Nowo Batorowe; see Figure 1). External conditions were as follows: the rectangle wind impulse ($10 ms^{-1}$) for each of 8 directions: N, NE, E, SE, S, SW, W and NW. Some simulations for $5 ms^{-1}$ and $35 ms^{-1}$ were also done for testing. The time duration of constant wind action was not less than 3–5 periods of steady currents establishment for the whole lagoon aquatory. The non-disturbed level and zero currents were used as initial conditions. The rivers' discharges and Baltic level variations were not included in the consideration, because precisely the own inertial oscillations in the lagoon were under investigation.

Figure 1 Vistula Lagoon

Results and discussions

The simulation results were obtained in the form of

1. temporal level courses for six points
2. steady currents charts for each wind direction (Chubarenko, 1996).

The main results are presented in Table 1.

Stations	Winds along the length-wise axes				Cross-wise winds			
	NE		SW		NW		SE	
	t_{rel}, h	T, h	t_{rel}, h	T, h	t_{rel}, h	T, h	t_{rel}, h	T, h
Kaliningrad	14.3	10	15	9.5	6.8	10, 9	6.8	10
Baltiysk	8.8	9.5	9	9.5	1.6	10	1	10
Krasnoflotskoe	6	9.5	6	9.5	2.6	9	1.5	10.5
Nova Paslenka	4	9.5	4	9.5	2	10	2.5	10
Tolkmicko	18.5	9.5	19	9.5	8	9	8	9
Nova Batorove	19.3	9	19.5	9.5	8.3	10	8.5	8

t_{rel} relaxation time; after this time lapse the water level variations become less than 1 cm

T   period of the main oscillation.

Table 1 Water level variations characteristics. Numerical model MIKE21. Wind speed $10\,\mathrm{m\,s^{-1}}$.

Wind was changed during the simulations as follows: momentarily started up to $10\,\mathrm{m\,s^{-1}}$ and simultaneously switched off after two weeks of modelling time. Under this condition the times intervals of the establishment of steady solution in level (level variations not exceed 1 cm) and current were 12 hours and 3 days correspondingly for any point along the lagoon coast. Under lengthways wind of $5\,\mathrm{m\,s^{-1}}$ and $10\,\mathrm{m\,s^{-1}}$ the simulated level diversities between north-east and south-west ends of lagoon (Kaliningrad and Nowo Batorowe) were 13.5 cm and 52 cm respectively. This is in good agreement with field measurements.

As a whole, the general behaviour of level variation curves allow the conclusion that the classical inertial damping oscillations are excited in the lagoon after the impulsive wind influence. While the oscillations at different points around the lagoon have different characteristics, and the most complicated oscillations occur in the northeastern part of the lagoon under transverse winds (SE and NW), the amplitude everywhere of the first oscillation is an order of magnitude greater than the other ones. Therefore, it may be concluded that the lagoon behaves as a single oscillating system in summation. As for processes of level relaxation after both lengthways and cross-wise winds, the own oscillating period is about 9.5 hours for all points in the aquatory (see Table 1). The relaxation times, i.e. the times after which a lapse of which water level variations become smaller than 1 cm, are also presented in Table 1.

The axis of lengthwise oscillations of the Vistula lagoon is easily indicated from the simulation: it is located between Nowa Paslenka and Krasnoflotskoe, slightly north of the Russian–Polish border. The axis direction is 315 degrees (SE–NW). The axis of transverse oscillations has a direction of 50 degrees (SW–NE).

The water level variations have an interesting feature during the process of level establishment after wind switch-off: level deviation aspires to zero (non-disturbed position), but, at first, passes an equilibrium position and then deviates from it in the opposite direction with an amplitude of little more then before switching of the wind. This peak deviation is characterised by the following values: its maximum (or minimum) value does not exceed the stationary level (before switching off the wind) more then 4 cm (for $10\,\mathrm{m\,s^{-1}}$ wind), the relaxation time (from peak to zero level) is no more than 5 hours. It is necessary to take this feature into consideration when forecasting the storm surge or high level events, especially at the ends of the lagoon (Kaliningrad and Nowo Batorowe).

The following hierarchy of the significance of external factors influenced on water level variations in the lagoon can be deduced from the analysis of natural data and numerical solutions:

• both river discharge and long-term Baltic water level variations determine the annual and seasonal mean volume of water in the lagoon reservoir;

• the Baltic water level near the lagoon entrance determines the present-day level of equilibrium of lagoon water body;

- the wind action gives the main input in short-period dynamics of level oscillation. Extremely high or low water level events (in south-western and north-eastern corners of the lagoon) are almost entirely stipulated by local wind.

The lagoon's own oscillations of periods 2–15 hours are presented also both in the Baltic level and wind variations. According to the statistical analysis performed by Dr.V.F. Dubravin (Institute of Oceanology of Russian Academy of Sciences, Atlantic Branch), the oscillations with a 9-hour period, for example, are contained both in level variations in Baltic and wind over the lagoon with a certainty of not less than 0.8. So, they should pump a considerable part of energy into lagoon water body dynamics. It is quite probable, that exactly this agreement between external influence and internal lagoon response was the main reason of the forming of the current lagoon geomorphological shape, characterised by the main period of its own inertial oscillation of the same order (near 9.5 hours) as external cumulative forcing from the Baltic wind and level.

Acknowledgements

References

Calibration of HD and EU-modules of numerical model MIKE21 and simulations of annual salinity field dynamics in Vistula lagoon. Report on Vistula Lagoon Project. Book 4. 1996. P.P. Shirshov Institute of Oceanology, Atlantic Branch, Kaliningrad, Russia. (in Russian).

Chubarenko. I.P., 1996. Investigation of the Vistula Lagoon water level own oscillations after wind forcing: results of numerical modelling (MIKE21). Atlas. P.P.Shirshov Institute of Oceanology, Atlantic Branch, Kaliningrad, Russia. (in Russian).

MIKE21. Coastal Hydraulics and Oceanography. Hydrodynamic Module. Release 1.4. User Guide and Reference Manual, Danish Hydraulic Institute, Copenhagen, Denmark, 1993.

Prioritising Hot Spot Remediations in Vistula Lagoon Catchment: Environmental Assessment and Planning for the Polish and Kaliningrad parts of the lagoon (1994–1997): Report on the international project. Erik K. Rasmussen (Ed.). Water Quality Institute, Danish Hydraulic Institute, GEOMOR, Atlantic Branch of P.P. Shirshov Oceanology Institute, Hoersholm, Denmark, 1998.

DYNOCS: Status October 1996

Jacob S. Møller

Abstract

DYNOCS (Dynamics of Connecting Seas) is a CEC-sponsored MAST II research project, which runs from 1994 till 1997. The project, which is multidisciplinary, aims at a better understanding of the marine environment between connecting seas and focus on the transition area between the North Sea and the Baltic, an area characterised by complex responses of stratified flow due to changing winds and buoyancy forcing. The DYNOCS project group consists of six research institutes from northern European countries situated in the Baltic area:

- Danish Hydraulic Institute (DHI), Denmark
- Institut für Ostseeforschung Warnemünde (IOW), Germany
- Swedish Meteorological and Hydrological Institute (SMHI), Sweden
- Norwegian Hydrotechnical Laboratory (NHL), Norway
- Danish Meteorological Institute (DMI), Denmark
- Aalborg University (AUC), Denmark

The purpose of DYNOCS is to provide a sound scientific basis for the understanding and modelling of hydrodynamics and the associated transport processes of transition areas between connecting seas. This objective is pursued through an integration of numerical modelling, field campaigns and laboratory experiments. The project has been divided into the following six main tasks:

- analysis of key processes
- field measurements
- laboratory experiments
- data acquisition and dissemination
- 3D numerical modelling
- transport and ecological modelling

The project improves our general scientific knowledge of the processes studied and ends up with a 3D baroclinic eddy-resolving model of the complete marine system between the North Sea and the Baltic.

Scientific approach

Analysis of key procedures

The objective of this has been pursued through a conceptual description of the processes in the transition area, development of conceptual and analytical models, and development of subgrid-scale algorithms and parametrisation, all as part of a systematic validation of the numerical modelling of the key processes.

Field measurements

This objective has been pursued through four field campaigns with the research vessel R/V "Prof. Albrecht Penck" of IOW and with the research vessel R/V "Dana" hired by DHI from the Danish Ministry of Fisheries, and through coordination with ongoing national field programmes.

No.	Period	Area	Vessel
1	26/8–29/9, 1993	Fehmarn/Darss	R/V "Albrecht Penck" (IOW)
2	07/10–17/10, 1994	Bornholm	R/V "Dana" (DHI)
3	15/11–24/11,1994	Fehmarn/Darss	R/V "Albrecht Penck" (IOW)
4	18/07–30/07, 1995	Fehmarn/Darss Kattegat/Lillebælt	R/V "Albrecht Penck" (IOW) R/V "Dana" (DHI)

Table 1 List of DYNOCS Cruises

Laboratory experiments

Advective processes, including the natural mesoscale eddy instabilities, have been simulated in a rotating basin with the best available bathymetry of the Skagerrak–Kattegat area, vertically distorted within the realm of Froude similitude. The laboratory model was forced by controlling the density and volume fluxes of water masses from the Baltic Sea, the German Bight, the Norwegian Sea and the Central North Sea.

Tracers from chosen sources were used to identify and quantify transport routes. 3D photogrammetric tracking of neutral buoys, and in situ profiling of fluorescence provided the necessary velocity and mass distributions across chosen sections which are coincident with field measurements and numerical model boundaries. The transport routes and mesoscale mixing processes provide a windless and tideless data set for physical understanding and numerical model testing. The experiments are reported in technical notes and video.

Data acquisition and dissemination

An initialisation data set for the North Sea-Baltic region has been established on the basis of available data from the region. The data set is comprised of salinity, temperature and 10m mean wind stress and 2m temperature for the atmosphere.

Collection of time series of current, salinity, temperature, wind and water level data at selected key sites have been undertaken for a period of 12 months. This hindcast data set is based on ongoing national programmes, the field campaigns and the laboratory experiment. The hindcast period covers 12 months (15 September 1994–15 September 1995) including three of the field measurement periods. In particular, data from the ongoing programmes in the Great Belt and the Sound have been used. The database comprises currents, water levels, salinities and temperatures being measured as part of the field programme. The database sets also include (for the periods of the three field campaigns only) analysed meteorological pressure and wind fields from high resolution, limited area models of the region (HIRLAM), assimilated and interpolated to the appropriate model grids.

3D numerical modelling

(Three different primitive equation models have been applied. These three primitive equation models range from a fully nonhydrostatic grid, implicitly coupled model (the DHI 3D model) to the modified hydrostatic, free-surface version of the Bryan-Cox model, WOM (Warnemünde Ostsee Model), to the Bundesamt für Seeschiffahrt und Hydrographie (BSH) model.

A far field model is used to establish boundary and initialisation conditions for fine grid models. The DHI model has been set up to simulate the three field campaign periods using a rather large horizontal grid covering the North Sea to the Baltic. The far field grid provides boundary data to near field models which will cover the transition area or parts of this area. The boundary data have been provided using a nested grid technique with two-way coupling to enhance the resolution of narrow straits. The near field models use rather small grids in order to resolve the Rossby Radius of deformation which is a measure of the typical length scale of baroclinic eddies.

The calibration and validation of 3D baroclinic models of the transition area have placed particular emphasis on the resolution of the hydrodynamic complexities and scaling problems resulting from the irregular coastline, complex and steep topographies and stratification in the region. The performance of the different models is now (October 1996) being analysed through a direct comparison between models as well as their ability to reproduce measured data. Model intercomparison will be carried out based on hindcasts of the field experiments and the laboratory experiments. This approach will establish an independent set of measured validation data for comparison with the numerical modelled data.

Transport and ecological studies

The quantification of water masses, buffering effects and major transport routes is being pursued through simulations of passive substances and marked water masses. The hydrodynamic input for these simulations is 3D flow fields taken from the 3D numerical modelling.

In general, the temporal and spatial scales used in ecological modelling are an order of magnitude larger than in hydrodynamical modelling, due to the number of ecological components and the biological timescales involved, and this constitutes a serious problem in ecological modelling. Often the large spatial resolution in ecological models leads to excessive nonphysical diffusion of substances. The scientific challenge is to see how the time and length scales of the hydrodynamics and ecology are best combined to ensure a scientifically and economically feasible approach.

Acknowledgements

Results

A number of intensive field campaigns have been carried out under the DYNOCS project. During each campaign, selected subareas were intensively surveyed for approximately two weeks by making ADCP measurements and by frequent profiling of various parameters, primarily temperature and salinity.
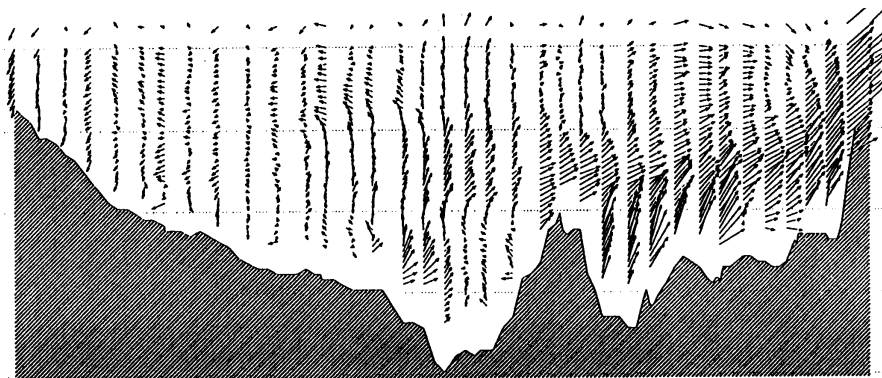

Figure 1 Example of measured current profiles along a transect crossing the Bornholm Strait at the entrance to the Baltic Sea
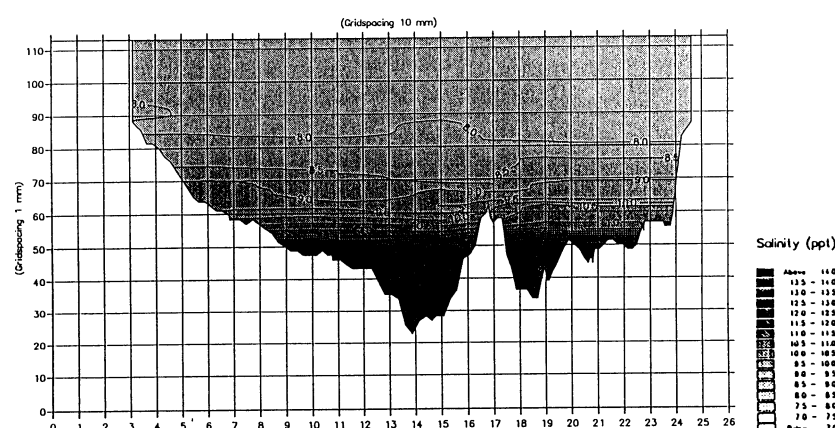

Figure 2 Example of measured salinity distributions along a transect crossing the Bornholm Strait at the entrance to the Baltic Sea

A laboratory model of a circular part of the Skagerrak–Kattegat region was built and mounted in the rotating Coriolis basin of NHL. The ocean circulation in the basin was forced by controlling the inflows of Atlantic Water from the Norwegian Sea and Brackish waters from the Baltic Sea and the German Bight, according to field data. The modelled horizontal/vertical ratio is distorted by a factor of 100. Figure 3 shows the rotating tank with three co-rotating camers;

image (x, y, z) calibration frame $(X, Y, Z)_{fr}$, model $(X, Y, Z)_{mod}$ and modified model (X', Y', Z') coordinate systems. The different coordinate systems were used in the calibration and particle tracking procedures.
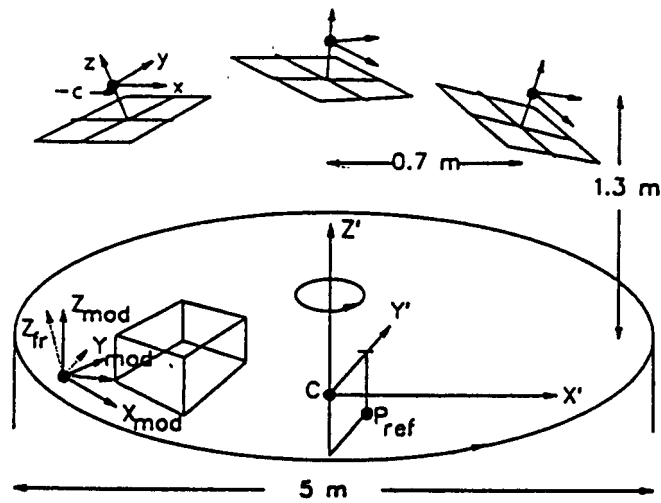
Figure 3 Laboratory model of a circular part of the Skagerrak–Kattegat region
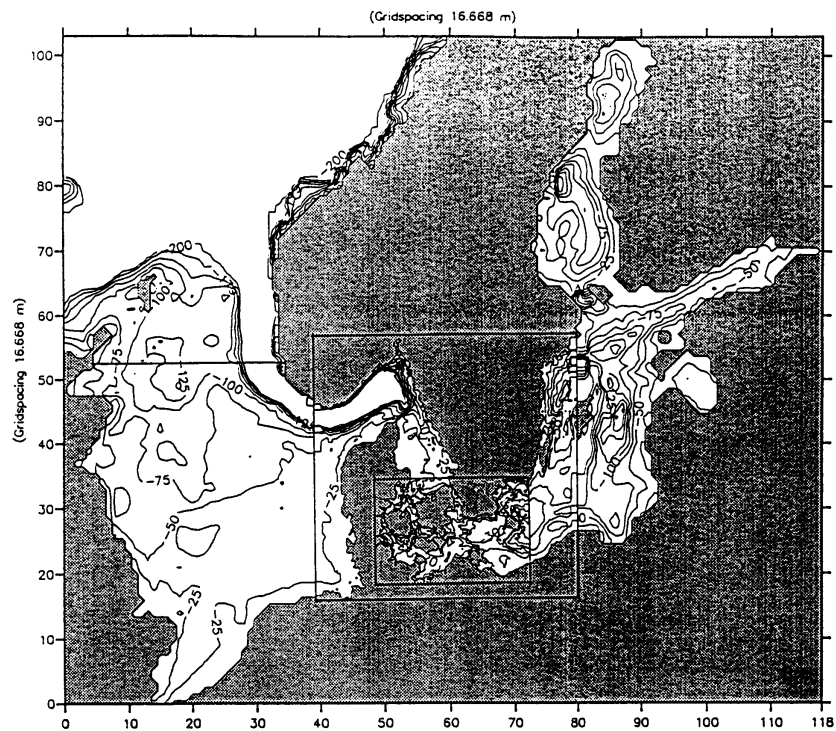
Figure 4 A numerical model bathymetry, covering the entire North Sea–Baltic Sea area has been compiled from echo sounding survey data and from navigational sea charts. The bathymetry has a resolution of one nautical mile and is based on more than 3 million data points.

List of contributors

Pekka Alenius (p 138)
Finnish Institute of Marine Research
P.O.Box 33
FIN-OO93 1 Helsinki, Finland
Phone: 358-9-613941, Fax: 358-9-61394494
e-mail: alenius@fimr.fi

Villu Astok (p 225, p 267)
Estonian Marine Institute
1 Paldiski Rd.
Tallinn
EE0001Estonia

Dagmar Benesch (p 126)
Institute of Baltic Sea Research
Seestr. 15
18119 Rostock, Germany

R. Bojanowski (p 85)
Polish Academy of Sciences
Institute of Oceanology
81-712 Sopot, Poland

Katarzyna Bradtke (p 107)
University of Gdansk, Institute of Oceanography
Al. Marszalka Pilsudskiego 46
81-378 Gdynia, Poland
ocekb@univ.gda.pl

Hans Cederwall (p 21)
Dept. of Systems Ecology
Stockholm University
S−106 91 Stockholm, Sweden

Valery Y. Chantsev (p 248)
Russian State Hydrometeorological Institute
195196 Malookhtinsky Pro 98
St. Petersburg, Russia

Maria Chomka (p 145)
Polish Academy of Sciences Institute of Oceanology
e-mail: chomka@ocean.iopan.gda.pl

Christian Christiansen (p 126)
Institute of Geography
University of Copenhagen
Øster Voldgade 10
1350 Copenhagen K, Denmark

Boris V. Chubarenko (p 151)
P. P. Shirshov Institute of Oceanology, Atlantic Branch
Prospect Mira, 1
236000, Kaliningrad, Russia
Tel: (+0112) 451574, Fax: (+0112) 272945
E-mail: chuboris@ioran.gazinter.net

Irina P. Chubarenko (p 151, p 318)
P. P. Shirshov Institute of Oceanology, Atlantic Branch
Prospect Mira, 1
236000, Kaliningrad, Russia
Tel: (+0112) 451574, Fax: (+0112) 272945
e-mail: irina@ioran.gazinter.net

Dirk Dannenberger (p 90)
Baltic Sea Research Institute Warnemünde
Now of
Research Institute for Biology of Farm Animals
Department of Muscle Biology and Growth
18196 Dummersdorf, Germany
Tel: +49 38208 68857, Fax: +49 38208 68852
e-mail: Dannenberger@fbn-dummerstorf.de

Violetta Drozdowska (p 244)
Institute of Oceanology PAS
ul.Powstancow Warszawy 55
PL-81712 Sopot, Poland

Kay-Christian Emeis (p 126, p 134, p 174)
Institute of Baltic Sea Research Warnemünde
Seestr. 15
D-19119 Rostock, Germany
Tel: +49 381 5197 370, Fax: +49 381 5197 352

Rudolf Endler (p 126, p 134)
Institute of Baltic Sea Research
Seestr. 15
D-19119 Rostock, FRG
Tel: +49 381 5197 370, Fax: +49 381 5197 352
e-mail: rudolf.endler@io-warnemuende.de

Peter Feuerpfeil (p 29)
Ernst-Moritz-Arndt-University
Institute of Ecology
Grimmer Strasse 88
D-17487 Greifswald, Germany

Stig Fonselius (p 157)
SMHI Oceanographic Laboratory
Nya Varvet Byggn. 31
S-426 71 Västra Frölunda, Sweden
Tel. 46 31 696534, Fax 46 31 690418

T. Förster (p 134)
Institute of Baltic Sea Research
Seestr. 15
D-19119 Rostock, FRG
Tel: +49 381 5197 370, Fax: +49 381 5197 352

Y.Goldfarb (p 96)
Latvian University
Riga, Latvia

N.N. Golenko (p 232)
Shirshov Institute of Oceanology
Kaliningrad/Moscow

M. Graeve (p 168)
Baltic Sea Research Institute
P. O. Box 301161
D-18112 Rostock, Germany

Eberhard Hagen (p 174, p 307)
Institute for Baltic Sea Research Warnemünde
Seestrasse 15
D-18119 Rostock, Germany

B. Henkelmann (p 121)
GSF Forschungszentrum für Umwelt und Gesundheit
Institut für Ökologische Chemie
Ingolstädter Landstr.1
D-85764 Oberschleißheim, Germany

Olaf Hennig (p 307)
Rostock University
Department of Physics
Germany

Flemming Jakobsen (p 179)
Danish Hydraulic Institute
Agern Allé 5
DK-2970 Hørsholm, Denmark
Tel: +45 45 76 95 55 Fax: +45 45 76 25 67
E-mail: flj@dhi.dk

Halina Jankowska (p 66)
Institute of Oceanography
University of Gdansk, Gdynia

H. René Jensen (p 190)
Danish Hydraulic Institute
Agern Allé 5
DK-2970 Hørsholm, Denmark

Jørn Bo Jensen (p 78)
Geological Survey of Denmark and Greenland
Thoravey 8
DK-2400 Copenhagen NV, Denmark

Vadims Jermakovs (p 21)
Institute of Aquatic Ecology
University of Latvia
Miera str. 3
LV−2169 SALASPILS, Latvia

S. Kaczmarek (p 280)
Institute of Oceanology, Polish Academy of Sciences
Sopot, Poland

Edward Kaniewski (p 118)
Gdynia Maritime Academy, Physics Department
ul. Morska 83
81–225 GDYNIA, Poland

E. Kerstan (p 13)
Baltic Sea Research Institute Warnemünde
Seestraße 15
18119 Rostock, Germany
Tel: 49 (0) 381 −5197−227, Fax: 40(0) 381−5197−440

B. Klagish (p 96)
Latvian University
Riga, Latvia

D. Knapinska-Skiba (p 85)
Polish Academy of Sciences
Institute of Oceanology,
81-712 Sopot, Poland

Vladimir P. Korovin (p 248)
Russian State Hydrometeorological Institute
195196 Malookhtinsky Pro 98
St. Petersburg, Russia

Tadeusz Krol (p 244)
Institute of Oceanology PAS
ul.Powstancow Warszawy 55
PL-81712 Sopot, Poland

Krystyna Kruczalak, (p 220)
Institute of Oceanology PAS
ul.Powstancow Warszawy 55
PL-81712 Sopot, Poland

Siegfried Krueger (p 198)
Institute for Baltic Sea Research Warnemünde
Seestrasse 15
D-18119 Rostock, Germany

Antoon Kuijpers (p 78)
Geological Survey of Denmark and Greenland
Thoravey 8
DK-2400 Copenhagen NV, Denmark

Tiit Kullas (p 225, p 267)
Estonian Marine Institute
1 Paldiski Rd.
Tallinn
EE0001Estonia

Helmar Kunzerdorf (p 126)
Risø National Laboratory
Department of Environmental Science and Technology
Postboks 49, 4000 Roskilde, Denmark

N. Kuten (p 96)
Science Technical Company "Geoprojektas"
Klaipeda, Lithuania

Birger Larsen (p 114)
Geological Survey of Denmark and Greenland (GEUS)
Thoravej 8
DK2400 Copenhagen, Denmark
Fax +4538142050
email bil@geus.dk

H.-V. Lass (p 204)
Institute for Baltic Sea Research Warnemünde
Seestrasse 15
D-18119 Rostock, Germany

Adam Latala (p 107)
University of Gdansk, Institute of Oceanography
Al. Marszalka Pilsudskiego 46,
81-378 Gdynia, Poland
ocekb@univ.gda.pl

Wolfram Lemke (p 78)
Baltic Sea Research Institute
Seestrasse 15, D-18119
Rostock-Warnemünde, Germany

Matti Lepparanta (p 299)
Department of Geophysics
P.O. Box 4
FIN-00014 University of Helsinki, Finland

Astrid Lerz (p 90)
Baltic Sea Research Institute Warnemünde
Department of Marine Chemistry
Seestraße 15
18119 Rostock, Germany
Tel: +49 381 5197-325, Fax: +49 381 5197-302

Viktoras Lujanas (p 263)
Institute of Physics
A. Gootauto 12
2600 Vilnius, Lithuania

Galina Lujaniené (p 263, p 274)
Institute of Physics
A. Gootauto 12
2600 Vilnius, Lithuania

Yuri I. Lyakhin (p 248)
Russian State Hydrometeorological Institute
195196 Malookhtinsky Pro 98
St. Petersburg, Russia

Dorota Maksymowska (p 66)
Institute of Oceanography
University of Gdansk, Gdynia

Roman Marks (p 220, p 274)
Institute of Oceanology PAS
ul.Powstancow Warszawy 55
PL-81712 Sopot, Poland

Johan Mattson (p 209)
SMHI
601 76 Norrköping, Sweden

Liongina Mickeniene (p 3)
Institute of Ecology
Akademijos g. 2
LT−2600 Vilnius, Lithuania
Tel: 72 92 41 Fax: (370−2) 72 92 57
E-mail: liong@takas lt

Jacob S. Møller, Ph.D. (p 179, p 190, p 321)
Danish Hydraulic Institute
Agern Allé 5
DK-2970 Hørsholm, Denmark
Tel.: +45 45 76 95 55 Fax: +45 45 76 25 67

Klaus Nagel (p 214)
Institute for Baltic Sea Research Warnemünde
Seestrasse 15
D-18119 Rostock, Germany

Günther Nausch (p 8)
Baltic Sea Research Institute Warnemünde
Seestraße 15
18119 Rostock, Germany

Monika Nausch (p 13)
Baltic Sea Research Institute Warnemünde
Seestraße 15
18119 Rostock, Germany
Tel: 49 (0) 381 −5197−227, Fax: 40(0) 381−5197−440
e-mail: monika.nausch@io-warnemuende.de

Dietwart Nehring (p 8)
Baltic Sea Research Institute Warnemünde
Seestraße 15
18119 Rostock, Germany

Alexei V. Nekrasov (p 248)
Russian State Hydrometeorological Institute
195196 Malookhtinsky Pro 98
St. Petersburg, Russia

Thomas Neumann (p 126)
Institut für Petrographie und Geochemie
Universität Karlsruhe
Kaiserstr. 12
76128 Karlsruhe, Germany

Bogdan Oldakowski (p 66)
Institute of Oceanography
University of Gdansk, Gdynia

M. Ostrowska (p 280)
Institute of Oceanology, Polish Academy of Sciences
Sopot, Poland

Zbigniew Otremba (p 118, p 220, p 244)
Gdynia Maritime Academy, Physics Department
ul. Morska 83,
81–225 Gdynia, Poland

Mikk Otsmann (p 225, p 267)
Estonian Marine Institute
1 Paldiski Rd.
Tallinn
EE0001Estonia

V.T. Paka (p 232)
Shirshov Institute of Oceanology
Kaliningrad/Moscow
E-mail: paka@ioran.koenig.su

Matti Pertillä (p 114)
Finnish Institute for Marine Research (FIMR)
PO 33 FIN 00931 Helsinki, Finland

Tomasz Petelski (p 145, p 263)
Institute of Oceanology of the Polish Academy of Sciences
ul. Powst. Warszawy 55
81-712. Sopot, Poland

Helmer M. Petersen (p 179)
Danish Hydraulic Institute
Agern Allé 5
DK-2970 Hørsholm, Denmark
Tel.: +45 45 76 95 55 Fax: +45 45 76 25 67

Niels H. Petersen (p 179)
Danish Hydraulic Institute
Agern Allé 5
DK-2970 Hørsholm, Denmark
Tel: +45 45 76 95 55 Fax: +45 45 76 25 67

Jacek Piskozub (p 244)
Institute of Oceanology PAS
ul.Powstancow Warszawy 55
PL-81712 Sopot, Poland

Pyotr P. Provotorov (p 248)
Russian State Hydrometeorological Institute
195196 Malookhtinsky Pro 98
St. Petersburg, Russia

Z. Radecki (p 85)
Polish Academy of Sciences
Institute of Oceanology
81-712 Sopot, Poland

Wolfgang Roeder (p 198)
Institute for Baltic Sea Research Warnemünde
Seestrasse 15
D-18119 Rostock, Germany

Arno Rosemarin PhD (p 254)
Stockholm Environment Institute
Box 2142
103 14 Stockholm, Sweden
Tel: +46 8 412 1418, Fax: +46 8 723 0348
E-mail: arno.rosemarin@sei.se

A. Rozwadowska (p 280)
Institute of Oceanology
Polish Academy of Sciences
Sopot, Poland

Grazyna Sapota (p 38)
Institute of Meteorology and Water Management, Maritime
Branch
ul. Waszyngtona 42
81−342 Gdynia, Poland
e-mail: sapota@stratus.imgw.gdynia.pl

Louise Schlüter (p 29)
Water Quality Institute
Agern Alle 11
DK-2970 Hørsholm, Denmark

Thomas Schmidt (p 179, p 204)
Institute für Ostseeforschung Warnemünde
D-2530 Rostock-Warnemünde, Germany

K. W. Schramm (p 121)
GSF Forschungszentrum für Umwelt und Gesundheit
Institut für Ökologische Chemie
Ingolstädter Landstr.1
D-85764 Oberschleißheim, Germany

Hendrik Schubert (p 29)
Ernst-Moritz-Arndt-University
Institute of Ecology
Grimmer Strasse 88
D-17487 Greifswald, Germany
Tel: +49 3834 864123, fax: +49 3834 864123
e-mail: schubh@mail.uni-greifswald.de

Ingo Schuffenhauer (p 307)
Rostock University
Department of Electrotechnics
Germany

Michael Schultz (p 274)
Institute of Inorganic and Applied Chemistry
University of Hamburg
Martin-Luther-King-Platz 6
20146 Hamburg, Germany

Torsten Seifert (p 179, p 204)
Institute für Ostseeforschung Warnemünde
D-2530 Rostock-Warnemünde, Germany

Vadim Sivkov (p 126)
Atlantic Branch Institute of Oceanology
Russian Academy of Science
Prospect Mira 1
236000 Kaliningrad, Russia

Bogdan Skwarzec (p 44)
Polish Academy of Sciences,
Institute of Oceanology, Bioradiochemistry Laboratory
81-712 Sopot, ul. Powstancow
Warszawy 55, P. O. Box 68, Poland

Krzysztof Sokolowski (p 56)
Polish Geological Institute
Branch of Marine Geology
Polna Str. 62
81-740 Sopot, Poland

Narciza Spirkauskaité (p 263, p 274)
Institute of Physics
A. Gootauto 12
2600 Vilnius, Lithuania

Klemensas Stelingis (p 263, p 274)
Institute of Physics
A. Gootauto 12
2600 Vilnius, Lithuania

Adam Stelmaszewski (p 118, p 220, p 244)
Gdynia Maritime Academy, Physics Department
ul. Morska 81
81–225 Gdynia, Poland

Piotr Stepnowski (p 44)
Polish Academy of Sciences
Institute of Oceanology, Bioradiochemistry Laboratory
81-712 Sopot, ul. Powstancow
Warszawy 55, P. O. Box 68, Poland
also
University of Gdansk
Faculty of Chemistry, Physical Chemistry Department
Radiochemistry Laboratory
80-952 Gdansk, ul. Sobieskiego 18/19, Poland.

Adolf Stips (p 307)
Joint Research Centre of the CEC
Space Applications Institute
Italy

Ulrich Struck (p 126)
Institute of Baltic Sea Research
Seestr. 15
18119 Rostock, Germany

Ülo Suursaar (p 225, p 267)
Estonian Marine Institute
1 Paldiski Rd.
Tallinn
EE0001Estonia

Janina Šyvokiene (p 3)
Institute of Ecology
Akademijos g.
LT−2600 Vilnius, Lithuania
Tel: 72 92 41 Fax: (370−2) 72 92 57
E-mail: syvo@ktl.mii.lt

Teresa Szczepanska (p 56, p 118)
Polish Geological Institute, Marine Geology Branch
ul. Polna 62
81–720 SOPOT, Poland

Nikolaj Tarasiuk (p 274)
Institute of Physics
A.Gostauto 12
2600 Vilnius, Lithuania

Jacek Urbanski (p 49)
University of Gdansk
Institute of Oceanography
Al. Pilsudskiego 46
81-378 Gdynia, Poland

S. Uscinowicz (p 85)
Polish Geological Institute
Branch of Marine Geology
81-740 Sopot, Poland

Serge V. Victorov (p 313)
State Oceanographic Institute
St.Petersburg and Russian National Institute of Remote Sensing
Methods for Geology
E-mail: vic@vniikam2.spb.su

G. Witt (p 121)
Institute of Baltic Sea Research
Seestr. 15
D-18119 Rostock, Germany

Klaus-Peter Wlost (p 198)
Institute for Baltic Sea Research Warnemünde
Seestrasse 15
D-18119 Rostock, Germany

D. Wodarg (p 168)
Baltic Sea Research Institute
P. O. Box 301161
D-18112 Rostock, Germany

B. Wozniak (p 280)
Institute of Oceanology, Polish Academy of Sciences
Sopot, Poland
also
Institute of Physics, Pedagogical University
Slupsk, Poland

S. B. Wozniak (p 280)
Institute of Oceanology, Polish Academy of Sciences
Sopot, Poland

Zhanhai Zhang (p 299)
Department of Geophysics
P.O. Box 4
FIN-00014 University of Helsinki, Finland

V.M. Zhurbas (p 232)
Shirshov Institute of Oceanology
Kaliningrad/Moscow
E-mail: zhurbas@glas.apc.org

Christoph Zülicke (p 174, p 307)
Institute for Baltic Sea Research Warnemünde
Seestrasse 15
D-18119 Rostock, Germany

List of participants

Denmark

Michael Andersen
Danmarks Fiskeriforening
Studiestræde 3
1455 København K

Ole Norden Andersen
Skov- og Naturstyrelsen
Haraldsgade 53
2100 København Ø

Hanne Bach
Vandkvalitetsinstituttet
Agern Alle 11
2970 Hørsholm

Ole Bagge
Danmarks Fiskeriundersogelser
Charlottenlund Slot
2920 Charlottenlund

Ole Bennike
Geological Survey of Denmark and
Greenland
Thoravej 8,
2400 København NV

Karsten Bolding
Danmarks Meteorologiske Institut
Lyngbyvej 100
2100 København Ø

Benny Bruhn
Storstrøms Amt
Miljøkontoret
Parkvej 37
4800 Nykøbing F

Erik Buch
Farvandsvæsenet
Overgaden O.Vandet 62B
1023 Copenhagen K

Harley Bundgard Madsen
Fyens Amt
Amtsgården
Ørbækvej 100
5220 Odense SØ

Christian Christiansen
Dept. of Earth Science
Ny Munkegade, bygn. 520
8000 Århus C

Vibeke Huess
Danmarks Meteorologiske Institut
Lyngbyvej 100
2100 København Ø

Flemming Jacobsen
Dansk Hydraulisk Institut
Agern Alle 5
2970 Hørsholm

Jørgen Norrevang Jensen
Danmarks Miljøundersøgelser
Frederiksborgvej
399 4000 Roskilde

Jørn Bo Jensen
GEUS
Thoravej 8
2400 København NV

Kurt Jensen
Vandkvalitetsinstituttet
Agern Alle 11
2970 Hørsholm

Henrik Jespersen
Bornholms Amt
Ø. Ringvej 1
3700 Rønne

Carsten Jürgensen
Fyens Amt
Amtsgården
Ørbækvej 100
5220 Odense SØ

Anton Kuipers
GEUS
Thoravej 8
2400 Copenhagen NV

Birger Larsen
GEUS
Thoravej 8
2400 København NV

Søren Larsen
Fyens Amt
Amtsgården
Ørbækvej I 00
5220 Odense SØ

Henning Matthiesen
Kemisk Institut
Århus Universitet
Langelandsgade 140
8000 Århus

Jacob Steen Møller
Dansk Hydraulisk Institut
Agern Alle 5
2970 Hørsholm

Gitte Nielsen
Teknisk Forvaltning
Roskilde Amt
Kogevej 80
4000 Roskilde

Jacob Woge Nielsen
Danmarks Meteorologiske Institut
Lyngbyvej 100
2100 København Ø

Palle Bo Nielsen
Farvandsvæsenet
Overgaden O.Vandet 62B
1023 Copenhagen K

Knud Mose Poulsen
A/S Storebælt
Vester Søgade 10
1601 København V

Erik Rasmussen
Vandkvalitetsinstituttet
Agern Alle 11
2970 Hørsholm

Mike St. John
Danrnarks Fiskeriundersøgelser
Charlottenlund Slot
2920 Charlottenlund

Gunni Ærtebjerg
Ministry of Environment and Energy, P.O.
Box 358
Frederiksborgvej 399
4000 Roskilde

Estonia

Villu Astok
Estonian Marine Institute
Paldiski St. 1,
EE0001 Tallin

Jüri Elken
Estonian Marine Institute
Paldiski St. 1,
EE0001 Tallin

Evald Ojaveer
Estonian Marine Institute
Paldiski St. 1,
EE0001 Tallin

Kaarel Orviku
Merin Ltd.
Rävala pst. 8,
EE0001 Tallin

Ulo Suursaar
Estonian Marine Institute
Paldiski St. 1,
EE0001 Tallin

Lembit Talpsepp
Estonian Marine Institute
Paldiski St. 1,
EE0001 Tallin

Tarmo Kaouts
Estonian Meteorological and Hydrological Institute,
P.O. Box 160
Kehra EE-2240

Mikk Otsmann
Estonian Marine Institute
Paldiski St. 1,
EE0001 Tallin

Siim Veski
Institute of Geology
Estonia Puistee 7
EE0001 Tallin

Urmas Lips
Estonian Marine Institute
Paldiski St. 1,
EE0001 Tallin

Urmas Raudsepp
Estonian Marine Institute
Paldiski St. 1,
EE0001 Tallin

Finland

Pekka Alenius
Finnish Institute of Marine Research
P.O. Box 33
00931 Helsinki

Ari Laine
Finnish Institute of Marine Research
P.O.Box 33
00931 Helsinki

Eija Rantajärvi
Finnish Institute of Marine Research
P.O. Box 33
00931 Helsinki

Eva Maria Blomquist
Husø Biological Station
Fin-22220 Emkarby

Kai Myrberg
Finnish Institute of Marine Research
P.O. Box 33,
00931 Helsinki

Zhang, Zhanhai
Dept. of Geophysics
P.O. Box 4
F-00014 Helsinki

Jari Haapala
University of Helsinki
Department of Geophysics
Fabianinkatu 24A, P.O. Box 4
SF-00014 Helsinki

Eeva-Liisa Poutanen
HELCOM
Katajanokanlaituri 6 B
F-00160 Helsinki

Germany

Dagmar Barthel
Düsternbrooker Weg 20
D-24105 Kiel

Eckhard Kleine
BSH
P.O. Box 301220
D-20305 Hamburg

Heye Remuhr
Inst für Meereskunde
Düsternbrooker weg 20
D-24105 Kiel

Henning Baudler
University of Rostock
Department of Biology
Muhlenstrasse 6
D-18340 Zingst

Slegfried Krüger
Institut für Ostseeforschung Warnemünde
P.O. Box 301038
D-18111 Rostock

Martin Schmidt
Institut fur Ostseeforschung Warnemünde
P.O. Box 30 10 38
D-18111 Rostock I

Claudia Bitteau
Institut fur Meereskunde
Düsternbrooker Weg 20
D-24105 Kiel

Sönke Lakaschus
Institute für Ostseeforschung
Seestr. 15
D-18119 Warnemünde

Dr. U. Schramm
Institut für Meereskunde
Düsternbrooker Weg 20
D-24105 Kiel

Dr. Dirk Dannenberger
Baltic Sea Research Institute
PF 301038, Seestr. 15
D-18119 Warnemünde

Hans Ulrich Lass
Institut für Ostseeforschung Warnemünde
P.O. Box 30 10 38
D-18111 Rostock

Hendrik Schubert
University Rostock
Freiligrathstr. 718
D-18055 Rostock

Prof Kay-Christian Emeis
Institut für Ostseeforschung Warnemünde
Seestrasse 15
D-18119 Warnemunde

Wolfgang Matthäus
Institut für Ostseeforschung Warnemünde
P.O.Box 301038
D-18111 Rostock

Sigurd Schultz
Cessingstr. 22
D-18055 Rostock

Rudolf Endler
Baltic Sea Research Institute
PF 301038, Seestr. 15
D-18119 Warnemünde

Volker Mohrholtz
Institut für Ostseeforschung Warnemünde
P.O. Box 301038
D-I8111 Rostock

Torsten Seifert
Institut für Ostseeforschung Warnemünde
P.O. Box 301038
D-18111 Rostock

Wolfgang Fennel
Institut für Ostseeforschung Warnemünde
P.O. Box 30 1038
D-I8111 Rostock

Dr. Klaus Nagel
Inst. für Ostseeforschung
Seestr. 15
D-18119 Warnemünde

Prof. Dr. Günter Weichart
Erlenweg 32
25469 Halstenbek

Martin Graeve
Inst. für Ostseeforschung
Seestr.15
D-18119 Warnemünde

Prof. Dr. Dietwart Nehring
Institute für Ostseeforschung
Seestr. 15
D-18119 Warnemünde

Dr. Gesime Witt
Baltic Sea Research Institute
PF 301038, Seestrasse 15
D-18119 Warnemünde

Andreas Jahn
Institute für Meereskunde
Düsternbrooker Weg 20
D-24105 Kiel

Thomas Neumann
Institut für Ostseeforschung Warnemünde
P.O.Box 30 10 38
D-18 III Rostock

Christoph Zülicke
Institut für Ostseeforschung Warnemünde
P.O.Box 301038
D-18 III Rostock

Eberhard Kerstan
Baltic Sea Research Institute
PF 301038, Seestr. 15
D-18119 Warnemünde

Christa Pohl
Inst. für Ostseeforschung
Seestr. 15
D-18119 Warnemünde

Lithuania

Egidijus Bemotas
Institute of Ecology
Akademijas 2 1
Vilnius 2600

N. Kuten
STC "Geoprojektas"
Danes, 23-6
5802 Klaipeda

Kestutis Joksas
Institute of Geography
Akademijos 2
2600 Vilnius

Tomas Zolubas
Fisheries Research Laboratorium
P.O. 108
Klaipda

Latvia

Vadim Jermakovs
Inst. of Aquatic Ecology
University of Latvia
Miera Str. 3
ILV-2169 Salaspils

Zinta Seisuma
University of Latvia
Inst. of Aquatic Ecology
Miera 3, LV-2169 Salaspils

Irina Kulikova
University of Latvia
Inst. of Aquatic Ecology
Miera 3, LV-2169 Salaspils

A. Yorkovskis
Marine Monitoring Centre
University of Latvia
Miera 3, LV-2169 Salaspils

Ilze Plankova
Latvian Hydrometeorological Agency
165 Maskavas Str.
LV-1019 Riga

Poland

Agnieszka Beszczynska-Möller
Powstancow Warszawy 55
817-12 Sopot

Jolanta Kusmierczyk-Michulec
Inst. of Oceanology
Polish Academy of Science
81-712 Sopot

D. Skalka
Inst. of Oceanology
Polish Academy of Science
81-712 Sopot

Bozena Bogaczericz-Adamczak
Inst. of Oceanology
University of Gdansk
81-378, Gdynia

Leszek Leczynski
Inst. of Oceanology
University of Gdansk
81-378, Gdynia

Adam Stelmaszewski
Maritime Academy
81-378 Gdynia

Katarzyna Bradtke
AI. Marzalka Pilsudskiego 46
81-378 Gdynia

Hanna Mazur
Dept. Plant Physiology
University of Gdansk
81-378 Gdynia

Piotr Stepnowski
Inst. of Oceanology
Dept. of Marine Chemistry
P.O. Box 68, Sopot

Dorota Burska
Inst. of Oceanology
University of Gdansk
81-378, Gdynia

Ksenia Pazdro
Inst. of Oceanology
Polish Academy of Science
81-712 Sopot

Joanna Szczucka
Inst. of Oceanology
Polish Academy of Science
P.O. Box 68, Sopot

Violetta Drozdowska
Inst. of Oceanology
Polish Academy of Science
81-712 Sopot

J. Pempkowiak
Inst. of Oceanology
Polish Academy of Science
P.O. Box 68, Sopot

Kazimierz Szefler
Maritime Institute Gdansk
Dlugi Torg 41/42 str.
80-830 Gdansk

Elzbieta Eysiak-Pastuzak
Institute of Metrology And Water
Management
81-378 Gdynia

Halina Piekarek-Jankowska
Inst. of Oceanography
University of Gdansk
81-378 Gdynia

Marzenna Sztobryn
ul. Waszyngtona 42
81-342 Gdynia

Lucyna Falkowska
Inst. of Oceanology
University of Gdansk
P.O. Box 37, Gdansk

Jacek Piskozub
Inst. of Oceanology
Polish Academy of Science
P.O. Box 68, Sopot

Jaroslaw Tegowski
Inst. of Oceanology
Polish Academy of Science
81-712 Sopot

Juliusz Gajewski
Maritime Institute Gdansk
Dlugi Targ 41/42 str.
80-830 Gdansk

Zbigniew Radecki
Inst. of Oceanology
Polish Academy of Science
P.O. Box 68, Sopot

Dr. Jacek Urbanski
University of Gdansk
Institute of Oceanography
Al. Pilsudskiego 46
81-378 Gdynia

Bozena Graca
Inst. of Oceanopraphy
University of Gdansk
81-378 Gdynia

J. Rokicki
University Gdansk
Al. Marzalka Pilsudskiego 46
81-378 Gdynia

Krystyna Wiktor
Institute of Oceanology
Powstancow Warszawy 55
817-12 Sopot

S. Kaczmazek
Inst. of Oceanology
Polish Academy of Science
81-712 Sopot

Stonislow Ruclowski
Maritime Institute
Dlugi Torg 41/42 str
808-30 Gdansk

Malgorzata Witak
Inst. of Oceanology
University of Gdansk
81-378, Gdynia

Alicja Kosakowska
Inst. of Oceanology
Polish Academy of Science
P.O. Box 68, Sopot

Grazyna Sapota
Inst. of Meteorology and Water
Management
Maritime Branch
81-345 Gdynia

Otremba Zbigniew
Maritime Academy
81-342 Gdynia

Dr. Adam Krezel
University of Gdansk
Institute of Oceanography
Al. Pilsudskiego 46
81-378 Gdynia

S. V. Semovski
Inst. of Oceanology
Polish Academy of Science
81-712 Sopot

Sweden

Cecilia Ambjöm
Swedish Meteorological and Hydrological
Institute
S-60 176 Norrköping

Hans Dahlin
Swedish Meteorological and Hydrological
Institute
S-601 76 Norrköping

Johan Mattsson
Swedish Meteorological and Hydrological
Institute
S-601 76 Norrköping

Elinor Andren
Dept. of Quaternary Research
University of Stockholm
S-113 22 Stockholm

Stig Fonselius
Oceanografiska Lab.
Byggn. 31, Nya Varvet
S-426 71 Vestra Frölunda

Anders Nissling
Institute of Marine Research
P.O. Box 4
S-45321 Lysekil

Thomas Andren
Dept. of Quaternary Research
University of Stockholm
S-113 22 Stockholm

Lennart Funkquist
Swedish Meteorological and Hydrological
Institute
S-601 76 Norrköping

Mats Ohlson
Swedish Meteorological and Hydrological
Institute
S-426 71 Vestra Frölunda

Bengt Erik Bengtsson

Bertil Håkansson
Swedish Meteorological and Hydrological
Institute
S-601 76 Norrköping

Dr. Arno Rosemarin
Publication and Information Manager
Stockholm Environment Institute
Box 2142
S-10314 Stockholm

Barry Broman
Swedish Meteorological and Hydrological
Institute
S-60 176 Norrköping

Ingrid Jansson
Naturvårdsverket
S-10648 Stockholm

Pauline Snoeÿs
Department of Ecological Botany
Uppsala University
Villavägen 14
S-75236 Uppsala

Hans Cederwall
Department of Systems Ecology
Stockholm University
S-106 91 Stockholm

Bemt I. Dybem
Institute of Marine Research
45321 Lysekil
P.O.Box 4

Greger Lindeberg
Geological Survey of Sweden
P.O.Box 670
S-75128 Uppsala

Eleanor Marmefelt
Swedish Meteorological and Hydrological
Institute
S-60 I 76 Norrköping

Gustav Sohlenius
Dept of Quaternary Research
University of Stockholm
S-113 22 Stockholm

Per Westman
Kvartärgeologiska Inst.
University of Stockholm
S-I 1322 Stockholm

Russia

Irina P. Chubarenko
P. P. Shirshov Institute of Oceanology
Russian Academy of Science
Pr. Mira 1
236000 Kaliningrad

Boris Czubarenko
P.P. Shirshov Institute of Oceanology
Russian Academy of Science
Pr.Mira 1
236000 Kaliningrad

Emelyan Emelyanov
P.P. Shirshov Institute of Oceanology
Russian Academy of Science
Pr. Mira 1
236000 Kaliningrad

Prof. V Galtsova
Zoological Inst.
2A, 23 linie
199026 St. Petersburg

Nikolay Golenko
Institute of Oceanology, Atlantic Branch
pr. Mira 1
236000 Kaliningrad

Alexei V. Nekrasov,
195196 Malookhtinsky pr. 98
Russian State Hydrometeorological Inst.
St. Petersburg

V. T. Paka
Institute of Oceanology, Atlantic Branch
pr. Mira 1
236000 Kaliningrad

Sergei Victorov
State Oceanographic Institute
2A, 23 linie
199026 St. Petersburg

V. Zhurbas
Institute of Oceanology, Atlantic Branch
pr. Mira 1
236000 Kaliningrad

Vladimir L Zimin
Emergency Response Centre for Radio-
logical Monitoring and Assessment
"Radium Institute"
2-nd Murinsky pr. 28,
St. Petersburg

Recent Titles Published in the *ICES Cooperative Research Report* Series

No.	Title	Price (Danish Kroner)
256	Report of the ICES Advisory Committee on the Marine Environment, 2002. 155 pp.	270
255	Report of the ICES Advisory Committee on Fishery Management, 2002. (Parts 1–3). 948 pp.	1200
254	Report of the ICES Advisory Committee on Ecosystems, 2002. 129 pp.	250
253	ICES Science 1979–1999: The View from a Younger Generation. 39 pp.	170
252	Report of the ICES/GLOBEC Workshop on the Dynamics of Growth in Cod. 97 pp. (including CD-Rom from ICES ASC 2001)	220
251	The Annual ICES Ocean Climate Status Summary 2001/2002. 27 pp.	180
250	ICES/GLOBEC Sea-going Workshop for Intercalibration of Plankton Samplers. A compilation of data, metadata and visual material, 2002. 34 pp.	190
249	Report of the ICES Advisory Committee on Ecosystems, 2001. 75 pp.	200
248	Report of the ICES Advisory Committee on the Marine Environment, 2001. 203 pp.	310
247	Effects of Extraction of Marine Sediments on the Marine Ecosystem. 80 pp.	200
246	Report of the ICES Advisory Committee on Fishery Management, 2001. (Parts 1–3). 895 pp.	1170
245	The Annual ICES Ocean Climate Status Summary 2000/2001. 21 pp.	150
244	Workshop on Gadoid Stocks in the North Sea during the 1960s and 1970s. The Fourth ICES/GLOBEC Backward-Facing Workshop. 55 pp.	160
243	Report of the 12th ICES Dialogue Meeting (First Environmental Dialogue Meeting). 28 pp.	130
242	Report of the ICES Advisory Committee on Fishery Management, 2000. (Parts 1–3). 940 pp.	1100
241	Report of the ICES Advisory Committee on the Marine Environment, 2000. 263 pp.	370
240	Report of the Young Scientists Conference on Marine Ecosystem Perspectives. 73 pp.	170
239	Report of the ICES Advisory Committee on the Marine Environment, 1999. 277 pp.	350
238	Report on Echo Trace Classification. 107 pp.	200
237	Seventh Intercomparison Exercise on Trace Metals in Sea Water. 95 pp.	190
236	Report of the ICES Advisory Committee on Fishery Management, 1999. (Part 1 and Part 2). 821 pp.	920
235	Methodology for Target Strength Measurements (With special reference to *in situ* techniques for fish and mikronekton). 59 pp.	160
234	Report of the Workshop on Ocean Climate of the NW Atlantic during the 1960s and 1970s and Consequences for Gadoid Populations. 81 pp.	180
233	Report of the ICES Advisory Committee on the Marine Environment, 1998. 375 pp.	440
232	Diets of Seabirds and Consequences of Changes in Food Supply. 66 pp.	170
231	Status of Introductions of Non-Indigenous Marine Species to North Atlantic Waters 1981–1991. 91 pp.	190
230	Working Group on Methods of Fish Stock Assessment. Reports of Meetings in 1993 and 1995. 259 pp.	330
229	Report of the ICES Advisory Committee on Fishery Management, 1998. (Part 1 and Part 2). 776 pp.	900
228	Report of the 11th ICES Dialogue Meeting on the Relationship Between Scientific Advice and Fisheries Management. 37 pp.	140

No.	Title	Price (Danish Kroner)
227	Tenth ICES Dialogue Meeting (Fisheries and Environment in the Bay of Biscay and Iberian Region: Can the Living Resources Be Better Utilized). 30 pp.	130
226	Report on the Results of the ICES/IOC/OSPARCOM Intercomparison Programme on the Determination of Chlorobiphenyl Congeners in Marine Media – Steps 3a, 3b, 4 and Assessment. 159 pp.	250
225	North Atlantic – Norwegian Sea Exchanges: The ICES NANSEN Project. 246 pp.	320
224	Ballast Water: Ecological and Fisheries Implications. 146 pp.	230
223	Report of the ICES Advisory Committee on Fishery Management, 1997. (Part 1 and Part 2). 780 pp.	760
222	Report of the ICES Advisory Committee on the Marine Environment, 1997. 210 pp.	250
221	Report of the ICES Advisory Committee on Fishery Management, 1996. (Part 1 and Part 2). 642 pp.	660
220	Guide to the Identification of North Sea Fish Using Premaxillae and Vertebrae. 231 pp (including 300 photographs)	560
219	Database Report of the Stomach Sampling Project, 1991. 422 pp.	410
218	Atlas of North Sea Benthic Infauna. 86 pp. (plus two diskettes containing relevant data)	210
217	Report of the ICES Advisory Committee on the Marine Environment, 1996. 159 pp.	210
216	Seabird/Fish Interactions, with Particular Reference to Seabirds in the North Sea. 87 pp.	140
215	Manual of Methods of Measuring the Selectivity of Towed Fishing Gears. 126 pp.	160
214	Report of the ICES Advisory Committee on Fishery Management, 1995. (Part 1 and Part 2). 636 pp.	1200
213	Report of the Results of the Fifth ICES Intercomparison Exercise for Nutrients in Sea Water. 79 pp.	125
212	Report of the ICES Advisory Committee on the Marine Environment, 1995. 135 pp.	175
211	Intercalibration Exercise on the Qualitative and Quantitative Analysis of Fatty Acids in Artemia and Marine Samples Used in Mariculture. 30 pp.	90
210	Report of the ICES Advisory Committee on Fishery Management, 1994. (Part 1 and Part 2). 534 pp.	575
209	Underwater Noise of Research Vessels: Review and Recommendations. 61 pp.	115
208	Results of the 1990/1991 Baseline Study of Contaminants in North Sea Sediments. 193 pp.	225
207	Report on the Results of the ICES/IOC/OSPARCOM Intercomparison Programme on the Analysis of Chlorobiphenyls in Marine Media – Step 2 and the Intercomparison Programme on the Analysis of PAHs in Marine Media – Stage 1. 104 pp.	150
206	Dynamics of Upwelling in the ICES Area. 73 pp.	125
205	Spawning and Life History Information for North Atlantic Cod Stocks. 150 pp.	190
204	Report of the ICES Advisory Committee on the Marine Environment, 1994. 122 pp.	165
203	Joint Report of the ICES Advisory Committee on Fishery Management and the Advisory Committee on the Marine Environment, 1994. 21 pp.	75
202	Chemicals Used in Mariculture. 100 pp.	150
201	Patchiness in the Baltic Sea (Symposium proceedings, Mariehamn, 1991). 126 pp.	150
200	Report of the Study Group on Ecosystem Effects of Fishing Activities. 120 pp.	165
199	Report of the Working Group on Methods of Fish Stock Assessments. 147 pp.	190
198	Report of the ICES Advisory Committee on the Marine Environment, 1993. 84 pp.	100

No.	Title	Price (Danish Kroner)
197	Ninth ICES Dialogue Meeting – "Atlantic Salmon: A Dialogue". 113 pp.	140
196	Reports of the ICES Advisory Committee on Fishery Management, 1993 (Part 1 and Part 2). 474 pp.	475
195	Report of the Workshop on the Applicability of Spatial Statistical Techniques to Acoustic Survey Data. 87 pp.	100
193	Reports of the ICES Advisory Committee on Fishery Management, 1992, Part 1 and Part 2. 1993. 468 pp.	425
192	Report of the Baltic Salmon Scale Reading Workshop. 1993. 71 pp.	85
191	Reports of Working Group on Methods of Fish Stock Assessment. 1993. 249 pp.	215
190	Report of the ICES Advisory Committee on Marine Pollution, 1992. 203 pp.	170
189	ICES Seventh Round Intercalibration for Trace Metals in Biological Tissue ICES 7/TM/BT (Part 2). 1992. 118 pp.	110
188	Atlantic Salmon Scale Reading Guidelines. 1992. 46 pp.	65
187	Acoustic Survey Design and Analysis Procedures: A Comprehensive Review of Current Practice. 131 pp.	125
186	Report of the Eighth Dialogue Meeting, 13–14 September 1991. 76 pp.	90
185	Report of the ICES-IOC Study Group Meeting on Models for Recruitment Processes, Paris, 7–11 May 1991. 46 pp.	50

These publications may be ordered from: ICES Secretariat, Palægade 2–4, DK-1261 Copenhagen K, Denmark, fax: +45 33 93 42 15, e-mail: ices.info@ices.dk. An invoice including the cost of postage and handling will be sent. Publications are usually dispatched within one week of receipt of payment. Further information about ICES publications, including ordering and payment by credit card, cheques and bank transfer, may be found at: www.ices.dk/pubs.htm.